UNIVERSITY OF LIVERPOOL

Dissecting host-pathogen interactions in bovine digital dermatitis

Thesis submitted in accordance with the requirements of the University of Liverpool for the degree of Doctor in Philosophy by Kerry Louise Newbrook.

September 2017

Authors Declaration

Apart from the help and advice as acknowledged, all research described within this thesis has been completed solely by the author.

…….

Kerry Louise Newbrook

September 2017

This research was carried out in the Department of Infection Biology within the Institute of Infection and Global Health, University of Liverpool

Table of Contents

Acknowledgements

This PhD would not have been possible without the contributions and support of many other people. Thank you to everyone who has offered support, help and guidance throughout my PhD journey, it really does mean everything.

First and foremost, I would like to say a huge thank you to my PhD supervisors, Dr Nicholas Evans and Professor Stuart Carter, for their unwavering support, help and advice over the last three years. You have stuck with me throughout the difficult times and never gave up hope - we made it to the end together! Thank you for everything that you have taught me and for shaping me into the scientist that I am today. Importantly, I would also like to thank the Biotechnology and Biological Sciences Research Council (BBSRC) and University of Liverpool for funding this work.

I would like to thank all members (old and new) of the Veterinary Pathobiology Research Group (aka the Treponeme Infection Team) for the amazing memories, emotional support, laughs (even when I shouldn't have been) and never-ending advice. You have honestly got me through some of the hardest times of my career so far and I will always be forever grateful for that. I couldn't have wished for a better group of people to work beside day-in day-out. Thank you to Jenny Bell, Simon Clegg, Stu Ainsworth, Hayley Crosby-Durrani, Intan Noor Aina Kamaruzaman, Jenni Mullin, Leigh Sullivan and my desk buddy, Gareth Staton!

Thank you to everyone I have had the pleasure of working alongside at the Department of Infection Biology. Special mention to the lab technicians, particularly Catherine Hartley and Jenna Dawson, who have always provided help, support and a good gossip when needed. Thank you to everyone who helped to advise and guide me through the transcriptomics analysis, particularly Professor Mark Lindsay (for the endless emails), Professor Julian Hiscox (for letting me steal your office from time to time), Dr Dong Xia and Dr Andrew Jackson. Also, thank you to Edge and Sons Abattoir for the cow feet, and the cow's themselves of course!

Finally, I would like to say a huge thank you to all of my family and friends for their endless love, support, advice and for simply listening when I needed them the most. Thank you to my mum and dad, my sister Emma, my grandparents and my best friend, Lisa. Special thank you to the best friends and collegues I could wish for - Jen, Lisa and Tess. Also to the BBSRC DTP cohort (special mention to Edd, Jess and Lisa) for making our trips to Newcastle so fun!

I have learnt more than I ever imagined during this journey and I could not have done it without each and every one of you.

Abstract

Bovine digital dermatitis (BDD) is an inflammatory infectious disease of the digital skin and is of increasing global importance for animal welfare and food security as one of the most important causes of severe lameness in dairy cattle. Whilst three phylogroups of spirochaetes of the genus *Treponema* (*Treponema medium, Treponema phagedenis* and *Treponema pedis*) are highly associated with BDD, having been consistently isolated from lesions, their individual roles in BDD pathogenesis within the bovine foot skin tissue have yet to be elucidated. The poor characterisation of BDD pathogenesis has, to-date, largely hindered development of novel therapeutics and vaccines against BDD.

The work presented within this thesis aimed to investigate host-pathogen interactions underlying BDD and determine whether individual *Treponema* phylogroups implement distinct pathogenic mechanisms upon cells of the bovine foot skin tissue. Primary fibroblast and keratinocyte cells were successfully isolated and subsequently cultured from bovine dermal and epidermal foot skin tissues, respectively, and were then characterised by immunofluorescent staining and RT-PCR, using cell markers, to provide a useful model for studying host-pathogen interactions of BDD.

The skin model was subsequently implemented to compare global transcriptional profiles of bovine foot skin fibroblasts following stimulation with representative strains of the three predominant BDD treponeme phylogroups using an RNA-Seq approach. This study is the first to report distinct differences in the dysregulation of global gene expression induced by BDD *Treponema* phylogroups in bovine fibroblasts. *T. medium* phylogroup and *T. pedis* were found to dysregulate host actin rearrangement and appeared to induce loss of cell adhesion via the *RND1* gene. Whilst *T. medium* phylogroup was profoundly less stimulatory, it also appeared to induce immune suppression through unique upregulation of the *TSC22D3* gene. *T. phagedenis* phylogroup uniquely upregulated the antimicrobial peptide precursor, β-defensin 123. Bovine fibroblasts appeared to demonstrate a strong pro-inflammatory response to Gram-negative bacterial lipopolysaccharide through the interleukin-17 signalling pathway; however, BDD treponemes specifically upregulated expression of five inflammatory mediators; most notably interleukin-8.

Commensal treponemes are commonly found within the gastrointestinal tract and provide an effective tool for comparison in host-pathogen interaction studies. In absence of a known non-pathogenic treponeme of the bovine skin, a novel spirochaete isolate of the bovine rumen was genotypically and phenotypically characterised, being proposed as novel species,

Treponema ruminis, for use as a control organism during RNA-Seq. Despite considerable genotypic and phenotypic differences, global gene expression profiles induced by *T. ruminis* and *T. phagedenis* phylogroup and *T. pedis* spirochaetes were markedly similar.

Further to this study, the molecular diversity of a putative outer membrane protein (OMP) was investigated across 121 strains representing three predominant BDD treponeme phylogroups. Gene sequencing of the novel putative OMP revealed limited intra-phylogroup diversity, suggesting that immune selection was not significantly influencing the evolution of this gene and that it may be a useful candidate for future vaccine development.

Collectively, these studies increase previously limited knowledge of the pathogenic mechanisms of BDD treponemes and provide novel insights into the host-pathogen interactions between specific treponeme phylogroups and bovine foot skin fibroblast cells during infection. Several genes identified in this study may be useful targets for the development of novel therapeutics and require further investigation.

List of figures

List of tables

List of abbreviations

ACTN1	Actinin alpha 1
ADK	Adenosine kinase
AMP	Antimicrobial peptide
BAM	Binary alignment/map
BNC2	Basonuclin
BDD	Bovine digital dermatitis
BLAST	Basic local alignment search tool
bp	Base pair
BPE	Bovine pituitary extract
BR	Broad-range
CCL	C-C motif chemokine ligand
CCR	C-C motif chemokine receptor
CDA	Cytidine deaminase
cDNA	Complementary deoxyribonucleic acid
CFB	Complement factor B
CFL1	Cofilin-1
CGR	Centre for Genomic Research
CLOCK	Clock circadian regulator
cm	Centimetre
cm^2	Square centimetre
CODD	Contagious ovine digital dermatitis
CO_2	Carbon dioxide
cpREV	General Reversible Chloroplast
CRASP	Complement regulator-acquiring surface protein
CRY	Cryptochrome circadian clock
CTLP	Chymotrypsin-like protease
CXCL	C-X-C motif chemokine ligand
C2	Complement C2
DAPI	4',6-diamidino-2-phenylindole
DC	Dendritic cell
DD	Digital dermatitis
DEFB123	Beta-defensin 123 precursor
DEJ	Dermal-epidermal junction
d_N	Non-synonymous
DNA	Deoxyribonucleic acid
dNTP	Deoxynucleoside triphosphate
DPBS-CMF	Dulbecco's phosphate buffered saline without calcium/magnesium
d_s	Synonymous
DSMZ	Leibniz-Institut Deutsche Sammlung von Mikroorganismen und Zellkulturen GmbH
E value	Expected value
ECM	Extracellular matrix
ECM1	Extracellular matrix protein 1

EDTA	Ethylenediaminetetraacetic acid
EGF	Epidermal growth factor
EGTA	Ethylene glycol-bis(2-aminoethylether)-N,N,N',N'-tetraacetic acid
ELISA	Enzyme-linked immunosorbent assay
EMT	Epithelial-to-mesenchymal transition
FAA	Fastidious anaerobe agar
FBS	Foetal bovine serum
FDR	False discovery rate
FGF	Fibroblast growth factor
FGFR2	Fibroblast growth factor receptor 2
FH	Factor H
FhbB	Factor H binding protein B
FHL-1	Factor H-like protein 1
FHL3	Four and a half LIM domains 3
FISH	Fluorescent in situ hybridization
FPKM	Fragment per kilobase of transcripts per million mapped reads
g	Centrifugal force
GAPDH	Glyceraldehyde-3-phosphate dehydrogenase
GC	Guanine-cytosine
GDH	Glutamate dehydrogenase
gDNA	Genomic deoxyribonucleic acid
GI	Gastrointestinal
GlpK	Glycerol kinase
GroEL	Heat shock protein family D member 1
GRO1	Chemokine (C-X-C motif) ligand 1
GTF	Gene transfer format
HBD-2	Human β-defensin-2
Hbp	Hemin binding protein
HBSS	Hank's balanced salt solution
HCL	Hierarchical clustering analysis
HSE	Human skin equivalent
H_2	Hydrogen
IF	Immunofluorescent
Ig	Immunoglobulin
IL	Interleukin
IPA	Ingenuity® Pathway Analysis
kbp	Kilobase pair
kDa	Kilodalton
kg	Kilograms
L	Litre
LC	Langerhans cell
LcpA	Leptospiral complement regulator-acquiring protein A
Len	Leptospiral endostatin-like
Lig	Leptospiral immunoglobulin-like
Log2	Binary logarithm

LOS	Lipooligosaccharide
LPS	Lipopolysaccharide
MAC	Membrane attack complex
MAFF	MAF bZIP transcription factor F
Mail	NF-κB inhibitor zeta
MEGA	Molecular Evolutionary Genetics Analysis
$MgCl_2$	Magnesium chloride
mg	Milligram
ml	Millilitre
MLST	Multilocus sequence typing
mm	Millimetre
mM	Millimolar
MMP	Matrix metalloproteinase
MOPS	Multifunctional Oligo Property Analysis Tool
mRNA	Messenger ribonucleic acid
Msp	Major surface protein
M scoring system	Mortellaro scoring system
NCBI	National Center for Biotechnology Information
ncRNA	Non-coding ribonucleic acid
NCTC	National Collection of Type Cultures
NDUFAF4	NADH:ubiquinone oxidoreductase complex assembly factor 4
NEXN	Nexilin F-actin binding protein
NF-κB	Nuclear factor kappa-light-chain-enhancer of activated B cells
NFKBIA	NF-κB inhibitor alpha
ng	Nano grams
NGS	Next generation sequencing
NH_4Cl	Ammonium chloride
nM	Nanomolar
NspA	Neisserial surface protein A
NUPR1	Nuclear protein 1 transcriptional regulator
N_2	Nitrogen
OCLN	Occludin
Omp	Outer membrane protein
ORF	Open reading frame
Osp	Outer surface protein
OTEB	Oral treponeme enrichment broth
PAC	Primary antibody control
PAMP	Pathogen-associated molecular pattern
PBS	Phosphate buffered saline
PCA	Principle component analysis
PCR	Polymerase chain reaction
PDGF-88	Platelet derived growth factor 88
PE	Paired-end
PER	Period circadian clock
pM	Picomolar

PRR	Pattern recognition receptor
PSMC5	Proteasome 26S subunit ATPase 5
PTGS2	Prostaglandin-endoperoxide synthase 2
PTP4A3	Protein tyrosine phosphatase type IVA member 3
PTX3	Long-pentraxin 3
p value	Probability value
PyrG	Orotidine 5'-phosphate decarboxylase
q value	FDR-adjusted *p* value
QC	Quality control
qRT-PCR	Quantitative real-time polymerase chain reaction
r	Linear correlation coefficient
recA	Recombinase A
RASL11B	Ras like family 11 member B
RGS16	Regulator of G-protein signalling 16
RHOG	Ras homolog family member G
RIN	RNA integrity number
RNA	Ribonucleic acid
RNase	Ribonuclease
RNA-Seq	Next-generation RNA sequencing
RND1	Rho family GTPase 1
RplB	Large RNA polymerase subunit
rpm	Revolutions per minute
rpo	Bacterial RNA polymerase
rRNA	Ribosomal ribonucleic acid
RS	Rabbit serum
RT-	Reverse transcription negative
RT-PCR	Reverse transcription polymerase chain reaction
R0	Singlet reads file
R1	Forward paired-end reads file
R2	Reverse paired-end reads file
r_2	Coefficient of determination
SAGE	Serial analysis of gene expression
SAA3	Serum amyloid A3
SIVA-1	SIVA-1 apoptosis-inducing factor
SLC16A12	Solute carrier family 16 member 12
SLC9A1	Solute carrier family 9 member A1
SLC9A3R2	SLC9A3 regulator 2
SNP	Single nucleotide polymorphism
snoRNA	Small nucleolar ribonucleic acid
snRNA	Small nuclear ribonucleic acid
SOD2	Superoxide dismutase 2
SOX4	SRY-box 4
SNORD22	Small nucleolar RNA
SNV	Single nucleotide variation
SS	Secondary structure

ST	Sequence type
SYNPO	Synaptopodin
TAE	Tris-acetate-EDTA
TE	Tris-EDTA
TEM	Transmission electron microscopy
TGF-β	Transforming growth factor beta
TIMP	Tissue inhibitor of metalloproteinase
TLR	Toll-like receptor
T_m	Melting temperature
TNF	Tumour necrosis factor
TNFAIP3	Tumor necrosis factor alpha-induced protein 3
TNFSF15	TNF superfamily member 15
tPA	Tissue-specific plasminogen activator
TprK	Treponema pallidum repeat protein K
Tp0751	Pallilysin
TREM1	Triggering receptor expressed on myeloid cells 1
TRITC	Tetramethylrhodamine isothiocyanante
TSC22D3	TSC22 domain family member 3
UK	United Kingdom
uPA	Urokinase-type plasminogen activator
USA	United States of America
UV	Ultraviolet
U1	U1 spliceosomal RNA
U2	U2 spliceosomal RNA
V	Volts
v/v	Volume/volume
WIPF2	WAS/WASL interacting protein family member 2
WME	William's Medium E
w/v	Weight/volume
Y_RNA	Small non-coding RNA
ZC3H12A	Zinc finger CCCH-type containing 12A
5_8S_RNA	5.8S rRNAs
α	Alpha
α2M	Alpha 2 macroglobulin
α2ML1	Alpha 2 macroglobulin-like 1
β	Beta
γδ	Gamma-delta
µg	Microgram
µl	Microlitre
µm	Micrometre
µM	Micromolar

Chapter One: Introduction

With the global human population currently exceeding seven billion, the sustainability of food production for the future is becoming an ever-growing concern worldwide. Over recent years, there has been a widespread and active move towards intensification of modern production systems in attempts to alleviate this demand. Particularly, there is now increasing reliance on dairy and beef cattle produce as a sustainable food source for the future, and this is reflected in the 9.8 million dairy and beef cattle which are currently farmed within the UK (Department for Environment Food and Rural Affairs, 2017). This profound increase in cattle production over recent years has led to concerns that it is the effective treatment and control of production animal diseases, such as mastitis and lameness in dairy cattle, that proves the largest threat to food security.

1.1 An overview of cattle lameness

Cattle lameness is now widely considered to be one of the largest unresolved challenges facing modern dairy and beef herds worldwide. It is clinically defined as an impairment of routine locomotion, most often resulting from limb injury or disease, and the most common manifestations are sole ulcers, digital dermatitis (DD) and white line disease (Amory *et al*., 2008). Lameness has a profound impact on both animal welfare and production efficiency, as the pain and discomfort typically results in an abnormal gait or uneven weight-bearing of the limbs (Whay *et al.,* 1997), which can often impact longevity (Bicalho *et al.,* 2007). Lame cattle often present with compromised reproductive performance, which is typically characterised by delayed ovarian cyclicity, irregular oestrus behaviour or conception failure (Alawneh *et al*., 2011; Garbarino *et al*., 2004; Hernandez *et al.,* 2001; Walker *et al.,* 2008). Furthermore, milk yields have been found to be reduced for up to four months before and five months after diagnosis of clinical lameness (Green *et al*., 2002). Recent estimates suggest that approximately 36.8% of the United Kingdom (UK) dairy cattle population are now clinically lame (Barker *et al.,* 2010) and, although there can be substantial inter-herd variation, the economic burden for a typical dairy herd may be up to £7,499.30 per annum (Willshire & Bell, 2009). However, with farmers considered highly prone to underestimate the incidence of lameness within their herds (Whay *et al.,* 2002), the economic implications of BDD are likely to be much higher. Lameness therefore remains one of the most significant barriers to both food security and production animal welfare and is largely thought to be attributable to the consequences of widespread intensification of modern dairy farming units (Stafford & Gregory, 2008). Body condition score and body weight, breed, milk yield,

parity and age at first calving have all been implicated (amongst others) as contributing herd-level risk factors for lameness, in addition to several farm management practices such as bedding and herd size (Alban, 1995; Chapinal *et al.,* 2014; de Vries *et al.,* 2015; Green *et al.,* 2014; Randall *et al.,* 2015; Solano *et al.,* 2015). Infectious causes of cattle lameness (such as DD) are most commonly treated either individually, through the application of topical antibiotics (including oxytetracycline or lincomycin), or through frequent whole-herd footbath treatments such as copper sulphate, formalin or antibiotics (Bell *et al.,* 2013; Blowey & Sharp, 1988; Dawson, 1998; Laven & Logue, 2006; Logue *et al.,* 2012). Such footbaths are, however, predominantly used for prevention rather than treatment of BDD. Regular hoof trimming is thought to have benefits for both the alleviation and control of infectious and non-infectious lameness (Groenevelt *et al.,* 2014; Somers *et al.,* 2005). Whilst the main emphasis for control of infectious lameness is currently placed on improving farm management and hygiene practices, non-infectious lameness is controlled through cow-comfort and nutrition. The development of novel ways to control or treat lameness, and the identification of earlier and more efficient detection systems, are each becoming increasingly important in maintaining a sustainable future for cattle production systems worldwide.

1.2 An introduction to digital dermatitis in livestock

DD is an ulcerative infectious disease of the digital skin which was first reported in dairy cattle in Italy over 40 years previously (Cheli & Mortellaro, 1974). Bovine digital dermatitis (BDD) is becoming an increasingly important cause of severe lameness in both dairy and beef cattle worldwide (Brown *et al*., 2000; Blowey & Sharp, 1988; Sullivan *et al*., 2013). It is one of several infectious diseases known to cause lameness in cattle, of which others include interdigital dermatitis (Walker *et al.,* 1995; Warnick *et al.,* 2001). DD is reportedly now endemic across dairy cattle populations in the UK, France, Germany, Denmark, Chile, the Netherlands and multiple USA states (Brown *et al*., 2000; Capion *et al*., 2008; Holzhauer *et al*., 2006a; Koenig *et al*., 2005; Laven, 2001; Nascimento *et al*., 2015; Read & Walker, 1998; Relun *et al*., 2013a; Trott *et al*., 2003; Wells *et al*., 1999). Furthermore, sporadic cases have been documented in Australia, Japan, Venezuela, Canada, Brazil, Israel, Mexico and South Africa (Argáez-Rodríguez *et al*., 1997; Borgmann *et al*., 1996; Cruz *et al*., 2001a; Hanna *et al*., 1994; McLennan & McKenzie, 1996; Shibahara *et al*., 2002; van Amstel *et al*., 1995; Villarroel-Neri *et al*., 2010; Yeruham & Perl, 1998). Although BDD is now reported to be endemic in nearly all countries that house dairy cattle, its prevalence within beef cattle is poorly documented and only a few cases have previously been reported, within the USA (Brown *et*

al., 2000), Japan (Shibahara *et al.,* 2002) and UK (Sullivan *et al.,* 2013) respectively. Similar disease manifestations have also since emerged within sheep across the UK and Ireland (Demirkan *et al.* 2001; Harwood *et al.,* 1997; Sayers *et al.,* 2009) named contagious ovine digital dermatitis (CODD). A similar pathology is reported in UK dairy goats (Groenevelt *et al.,* 2015; Sullivan *et al.,* 2015a) and most recently within wild American elk (Clegg *et al.,* 2015), collectively indicating an expanding host range beyond that initially thought. The latter two disease manifestations have yet to be investigated further and now require an assessment of their national and global prevalence, along with a wider assessment of potential spread into other domestic and wildlife species.

1.3 Bovine digital dermatitis

BDD, also commonly known as Mortellaro disease, strawberry foot or heel warts, is an inflammatory infectious foot disease of both dairy and beef cattle and is typically characterised by painful, focally-inflamed lesions on the underside of the digital skin (Blowey & Sharp, 1988; Sullivan *et al.,* 2013). BDD is widely considered one of the most important causes of severe cattle lameness and is of increasing global concern for food security, animal welfare and its associated economic burden.

1.3.1 Impact of bovine digital dermatitis

Implications for animal welfare

The alteration in gait or abnormal weight-bearing of limbs that epitomise cattle lameness are thought to often be a result of pain and discomfort caused by the lesion or disease in question (Whay *et al.,* 1997). Lame cattle suffering from BDD have specifically been shown to demonstrate a reduced nociceptive threshold when compared to non-lame cattle (Whay *et al.,* 1998), therefore suggestive of an increased sensitivity to pain. Multiple studies have also highlighted significant alterations in cattle behaviour as a result of lameness. For instance, lame cattle have a lower overall activity level when compared to non-lame cattle (O'Callaghan *et al.,* 2003) and have been specifically shown to demonstrate an increased duration of lying behaviour, less time elevated on their feet, reduced expression of oestrous behaviours and a lower bite rate and shorter grazing periods at pasture (Halsall *et al.,* 1993; Walker *et al.,* 2008). Through use of a dynamic stochastic model, Bruijnis *et al.* (2012) showed that out of seven foot disorders, BDD had the highest overall impact on animal welfare in terms of incidence, duration and pain association across both clinical and subclinical manifestations of the disease.

Implications for production

BDD has been shown to have a considerable impact on production efficiency within both dairy and beef cattle systems and is associated, through lameness, with an increased risk of premature culling (Bicalho *et al.,* 2007). The profound impact of clinical lameness on reduced milk production in dairy cattle has been widely documented (Green *et al.,* 2002; Hernandez *et al.,* 2002; Reader *et al.,* 2011) and it was recently estimated that multiparous dairy cattle suffering from moderate or severe BDD infections incurred average daily milk losses of approximately 0.50 kg and 0.75 kg respectively when compared to unaffected cattle (Relun *et al.,* 2013b). Many studies have also demonstrated a high association of BDD with poor reproductive performance in dairy cattle, particularly with respect to longer calving-to-conception intervals, increased number of days open and lower conception rates (Argáez-Rodríguez *et al.,* 1997; Gomez *et al.,* 2015; Randall *et al.,* 2016).

Economic impact

Resulting from its profound negative impacts on both animal welfare and production efficiency, BDD is a cause of substantial annual economic losses worldwide and recent estimates suggest this could exceed $190 million in the USA alone (Losinger, 2006). Largely attributable to its high clinical incidence, BDD is estimated to incur the greatest costs out of a number of infectious and non-infectious foot disorders, including sole haemorrhage, sole ulcer and interdigital dermatitis (Bruijnis *et al.,* 2010). Reduced milk yields, premature culling, prolonged calving interval and treatment expenses and their associated costs (such as veterinarian/farming labour and discarded milk) have all been implicated as significant contributors to the economic losses resulting from BDD infection (Bruijnis *et al.,* 2010; Losinger, 2006; Willshire & Bell, 2009). Cha *et al.* (2010) estimated the greatest expenses of BDD infection to be those associated with treatment, decreased fertility and then milk losses. Currently, there are few studies which attempt to estimate the exact cost of BDD to the UK cattle industry and this is further hindered by a probable underestimation of its economic importance, particularly in the detection of subclinical disease (Bruijnis *et al.,* 2010). Most recently, the Great Britain Cattle & Welfare Group (2014) estimated BDD to cost approximately £98.79 per individual case in UK dairy cattle, with an earlier estimate by Willshire & Bell (2009) of £75.57 per case. There are currently no estimates of the cost of BDD to beef cattle in the UK.

1.3.2 Prevalence of bovine digital dermatitis in dairy and beef cattle

Since being first reported in Italy over 40 years previously (Cheli & Mortellaro, 1974), BDD is now widely endemic across Europe and several USA states and has been reported in nearly

all countries in which dairy cattle are farmed. Although its prevalence can vary considerably within herds, between farms and particularly between countries, BDD is now thought to be one of the most common hoof disorders affecting global dairy cattle populations (Laven *et al.,* 2001; Solano *et al.,* 2016). BDD was first reported to have an intra-herd prevalence of 29% within Friesian dairy cattle in the UK (Blowey & Sharp, 1988). A later survey of 205 dairy farms from across England and Wales found that 79% had reported BDD cases and, of those, 39.9% of the mean lameness prevalence was attributable to BDD (Barker *et al.,* 2010). The mean intra-herd prevalence of BDD in dairy cattle across Europe and the USA is wide-ranging; from 6.1% in Chile (Rodriguez-Lainz *et al.,* 1998) to 21.6% in The Netherlands (Holzhauer *et al.,* 2006b). Whilst BDD prevalence estimates within dairy cattle are well documented, by comparison, there are currently only two published reports estimating the intra-herd prevalence of BDD within beef cattle (Brown *et al.,* 2000; Sullivan *et al.,* 2013). Brown *et al.* (2000) reported that 4% of culled beef cattle were found to have BDD lesions at slaughter within the USA, whilst prevalence estimates of approximately 0.5% and 21% have been reported within rearing and finishing beef herds, respectively, in Gloucestershire, UK (Sullivan *et al.,* 2013).

1.3.3 Clinical and pathological manifestations of bovine digital dermatitis

Lameness is the most common clinical feature associated with BDD and infected cattle are often observed to walk on their toes, redistribute the weight-bearing of their limbs or hold or shake the affected limbs in partial flexion (Blowey & Sharp, 1988; Read & Walker, 1998; Whay *et al.,* 1997). Subclinical manifestations of the disease have also been identified, however these are often difficult to diagnose as the animal might not appear to be lame despite infection (Bruijnis *et al.,* 2012). Resultantly, it is the high prevalence of this subclinical disease which is widely thought to contribute to a growing underestimation of the true impact of BDD (Bruijnis *et al.,* 2010; Bruijnis *et al.,* 2012).

Locality of bovine digital dermatitis

BDD is a focal or extensive dermatitis which is most commonly located on the hind feet (Blowey & Sharp, 1988; Holzhauer *et al.,* 2006a; Holzhauer *et al.,* 2008; Murray *et al.,* 2002; Read & Walker, 1998), on the plantar (or palmar) aspect of the bovine digit, specifically on or above the coronary band and equidistant from the heel bulbs (Blowey & Sharp, 1988; Murray *et al.,* 2002; Read & Walker, 1998). BDD lesions are primarily found on the skin surface bordering the interdigital space, and often extend locally towards the interdigital skin (Read & Walker, 1998). However, other less common sites of infection have also been identified, such as the coronary band at the abaxial wall, the skin bordering the base of the

heel bulbs and the skin surrounding the dewclaws (el-Ghoul & Shaheed, 2001; Read & Walker, 1998). BDD manifests as single or multiple lesions found either unilaterally or bilaterally, both on the plantar or palmar aspects of the foot (Blowey & Sharp, 1988; Holzhauer *et al.,* 2006a; Holzhauer *et al.,* 2008; Murray *et al.,* 2002; Read & Walker, 1998).

Clinical presentation of bovine digital dermatitis

The clinical presentation of BDD is typically that of a painful, malodorous, moist and exudative, focally-inflamed ulcerative lesion of circumscribed, raised hyperkeratotic skin which is often dark red or brown in colouration, prone to bleeding and surrounded by hypertrophied hairs (Blowey & Sharp, 1988; McLennan & McKenzie, 1996; Read & Walker, 1998). However, other clinical presentations of BDD lesions have been widely reported and these are now considered to reflect different stages in the dynamic development and healing processes of the lesion. A four-point scoring system, named the Mortellaro (M)-stage scoring system, was initially described by Döpfer *et al.* (1997) and has been widely used to categorise the principle stages of lesion development; however, over recent years this has been validated to form a more accurate five-point M-stage scoring system (Greenough *et al.,* 2008). As described in Table 1.1, the M0 stage represents normal digital skin tissue with no visible BDD lesion; the M1 stage represents a small, early-stage red or grey granulomatous lesion; the M2 stage represents the classic large, active, painful and bright red ulcerative ("strawberry-like") or granulomatous lesion; the M3 stage represents a healing lesion characterised by the formation of a dry scab-like tissue; and the M4 stage represents a late-chronic stage which may be dyskeratotic and/or proliferative. The high incidence of recurrent BDD infection is well-documented (Berry *et al.,* 2012), with 48% of dairy cattle found to have recurrent or new lesions developing 7 to 12 weeks after an initial complete therapeutic response in one study (Read & Walker, 1998). Accordingly, a further M4.1 stage is often used to represent late-stage chronic lesions which are also found to have a recurring active M1-stage component (Döpfer *et al.,* 1997). The clinical manifestations of BDD lesions associated with each M-stage score are illustrated in Figure 1.1. The inter-farm prevalence of BDD lesions within each of the developmental M-stages is known to be highly variable (Berry *et al.,* 2012; Nascimento *et al.,* 2015; Neilsen *et al.,* 2012; Relun *et al.,* 2011). Furthermore, this classification system only applies to lesions on the rear feet and does not include the increasingly common lesions on the coronary band.

Table 1.1 Description of the Mortellaro (M) scoring system used for classification of the developmental stages of bovine digital dermatitis lesions based upon their associated macroscopic and pathological changes (Döpfer et al., 1997; Greenough et al., 2008).

M-stage score	M-stage description	Description of macroscopic observations	Description of pathological observations
M0	No lesion (BDD negative)	Visibly healthy skin with no evidence of a BDD lesion.	Epithelial tissue contains approximately 5 to 35 cellular layers, with a uniform stratum corneum layer. Moderate infiltration of dermal tissue with mononuclear cells. Spirochaetes not detected within healthy tissue.
M1	Early-stage active lesion (Subclinical manifestation)	Small, focal, circumscribed granulomatous lesion (less than 2 cm in diameter) of the epithelial skin which is red or grey in colouration.	Thickening of the epithelial tissue (double or triple that of M0 stage), with a hyperplastic stratum corneum and an acanthotic stratum spinosum. Formation of rete ridges and horny columns with microabscess and haemorrhage, areas of degeneration with fibrin deposits and areas of parakeratosis with partial loss of epithelial tissue. Spirochaetes appear to penetrate stratum spinosum layer, specifically within the horny columns, and also appear within areas of degeneration. Large infiltration of neutrophils, lymphocytes and monocytes (occasionally eosinophils) within both dermal and epidermal skin tissue and perivascular infiltration of dermal tissue.
M2	Classical active-stage lesion	Large, painful ulcerative (red) or granulomatous (red or grey) lesion, over	Absence of stratum corneum across the extending lesion, with an abundance of treponemes found deep within stratum spinosum layers. Large areas of haemorrhage at the lesion interface. Predominant

		2 cm in diameter, which is prone to bleeding.	infiltration of neutrophils and eosinophils within epidermal tissue, whilst a prominent perivascular infiltration of the dermal tissue.
M3	Healing-stage lesion	Classical ulcerative lesion visibly healing and covered by a painless dry brown scab-like tissue.	No description to-date.
M4	Late-stage chronic lesion	Circumscribed dyskeratotic lesion which may also, or instead, have a proliferative hyperkeratotic component.	Epidermal tissue highly proliferative (triple the thickness of M0 stage), with extremely hyperplastic stratum corneum and acanthotic stratum spinosum. Prominent rete ridge formation and horny columns surrounded by haemorrhage and cellular detritus. Absence of keratohyaline granules. Spirochaetes identified in stratum basale. Spongy-like appearance of stratum granulosum with empty vacuoles. Predominance of neutrophils within epidermal tissue, whilst plasma cells are a prominent feature of dermal tissue.
M4.1	Late-stage chronic lesion with recurring subclinical (M1) manifestation	Circumscribed dyskeratotic lesion which may also, or instead, have a proliferative hyperkeratotic component (chronic M4-stage lesion) which also has a small, focal, circumscribed red or grey granulomatous (M1) lesion present.	No description to-date.

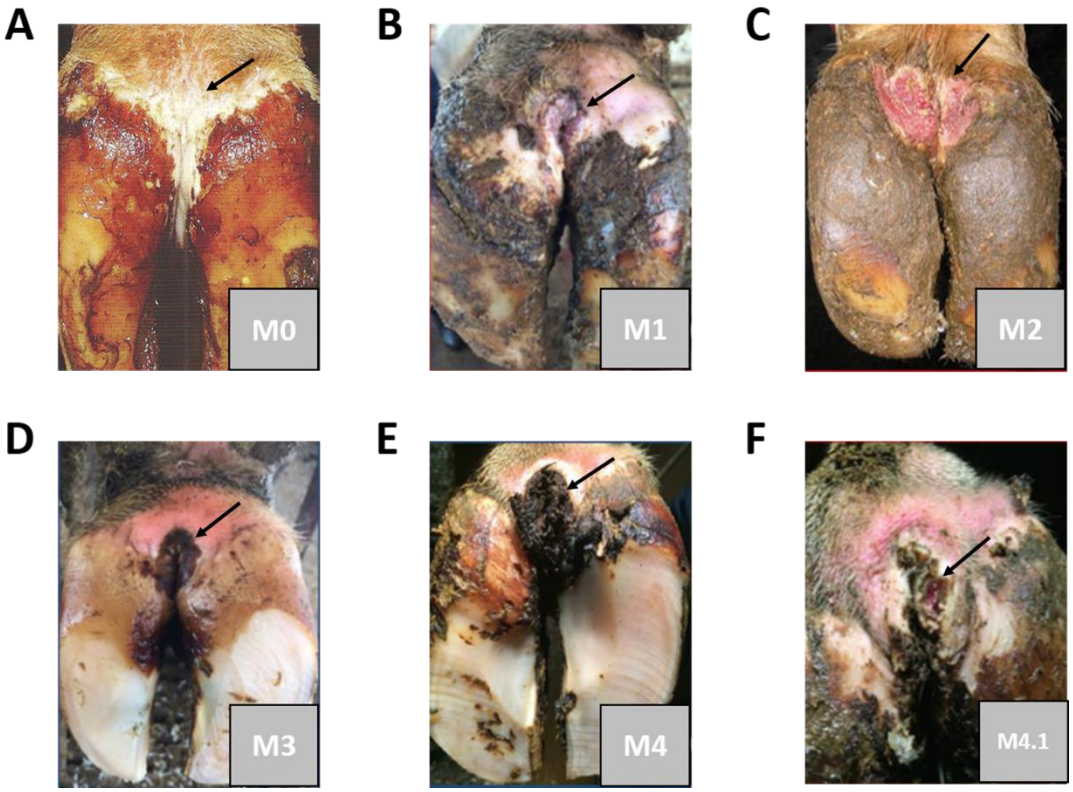

Figure 1.1 Typical manifestations of bovine digital dermatitis lesions between the heel bulbs of the hind feet of dairy cattle at various stages of development as classified by the Mortellaro (M) scoring system. *(A) M0 is visibly healthy skin with no evidence of a BDD lesion, (B) M1 is an early-stage granulomatous lesion (C) M2 is a classical, active ulcerative or granulomatous lesion, (D) M3 is a healing lesion covered by a firm brown scab, (E) M4 is a late-stage chronic lesion characterised by a dyskeratotic and/or hyperkeratotic appearance, and (F) M4.1 is a late-stage chronic M4 lesion with an additional M1 acute lesion present (Döpfer et al., 1997; Greenough, 2014; Greenough et al., 2008; Zinicola et al., 2015a).*

Pathology of bovine digital dermatitis

BDD is an acute, suppurative inflammation of the epidermis which often extends into the surrounding dermal tissues and is accompanied by observations of superficial necrosis, hyperkeratosis and often parakeratosis (Blowey & Sharp, 1988; Cruz *et al.,* 2005; Döpfer *et al.,* 1997). BDD lesions are typically characterised by a progressive degeneration of the upper epidermal layers, particularly the stratum corneum and stratum granulosum, with an abundance of highly invasive spirochaetes identified deep within the stratum spinosum and rete ridges (Cruz *et al.,* 2005; Döpfer *et al.,* 1997). There is a progressive thickening of the epidermal skin tissue between the M2 to M4 stages, significant elongation of rete ridges in M3 and M4 stages and a significantly thicker keratin layer during the M3 stage (Döpfer *et al.,* 1997; Refaai *et al.,* 2013). An abundance of inflammatory neutrophils, eosinophils and lymphocytes typically infiltrate the deeper skin layers of the reticular dermis as well as the

epidermis, with neutrophils and eosinophils reaching peak abundance at the M2 stage (Blowey & Sharp, 1988; Döpfer *et al.,* 1997; Refaai *et al.,* 2013). Lymphocytes are typically most abundant at the dermal-epidermal junction (DEJ) (Refaai *et al.,* 2013). A full description of the pathological observations across each of the lesional stages of BDD are given in Table 1.1.

1.3.4 Aetiology of bovine digital dermatitis

BDD is considered a highly infectious disease, known to spread rapidly throughout dairy cattle herds (Read & Walker, 1998). Over the last several decades, a plethora of microorganisms have been detected within BDD lesions, including spirochaetes (Blowey & Sharp, 1988; Choi *et al.,* 1997; Collighan & Woodward, 1997; Cruz *et al.,* 2005; Demirkan *et al.,* 1998; Diniz *et al.,* 2017; Döpfer *et al.,* 1997, Evans *et al.,* 2008; Moter *et al.,* 1998; Shrank *et al.,* 1995; Sullivan *et al.,* 2013), *Campylobacter faecalis* (Döpfer *et al.,* 1997), *Campylobacter jejuni* (Cruz *et al.,* 2005), *Guggenheimella bovis* (Schlafer *et al.,* 2008; Strub *et al.,* 2007; Wyss *et al.,* 2005), *Fusobacterium necrophorum* (Berry *et al.,* 2010; Cruz *et al.,* 2005), *Dichelobacter nodosus* (Capion *et al.,* 2012; Knappe-Poindecker *et al.,* 2013), *Bacteriodes* spp. (Blowey & Sharp, 1988; Collighan & Woodward, 1997), *Candidatus* Amoebophilus *asiaticus* (Zinicola *et al.,* 2015a) and *Mycoplasma* spp. (Collighan & Woodward, 1997). Several studies have consistently demonstrated no evidence for the aetiological involvement of viral or fungal infections (Borgmann *et al.,* 1996; Brandt *et al.,* 2011; Krull *et al.,* 2014) and therefore, together with the observed responsiveness of lesions to various antibiotic therapies (Berry *et al.,* 2010; Read & Walker, 1998), BDD is widely accepted to have an infectious bacterial aetiology. Despite this, the precise bacterial aetiology of BDD is still yet to be fully elucidated.

Fluorescence *in situ* hybridization (FISH) studies, amongst others, have consistently identified highly motile, helical, anaerobic spirochaetes of the *Treponema* genus to be the predominant microorganisms located deep within lesional skin tissue (Cruz *et al.,* 2005; Klitgaard *et al.,* 2008; Moter *et al.,* 1998; Rasmussen *et al.,* 2012; Santos *et al.,* 2012). Moreover, treponemes are the only microorganisms to be consistently isolated from BDD lesions whilst not present within healthy foot skin tissue (Berry *et al.,* 2010; Döpfer *et al.,* 1997; Evans *et al.,* 2009a). Resultantly, it is considered that treponemes are the likely primary causative agent of BDD, with other bacterial species considered secondary invading, opportunistic pathogens that colonise the lesion and exacerbate this initial pathology (Evans *et al.,* 2009a; Klitgaard *et al.,* 2008; Nordhoff *et al.,* 2008). The recent success of experimentally-induced BDD infection models, by exposing bovine feet to a combination of treponemes, provides further evidence

for a causative role in BDD (Gomez *et al.,* 2012). Due to the detection and isolation of multiple *Treponema* phylogroups concurrently within individual lesions, BDD is widely considered a polytreponemal disease (Evans *et al.,* 2009a; Klitgaard *et al.,* 2008; Klitgaard *et al.,* 2013; Marcatili *et al.,* 2016; Nascimento *et al.,* 2015; Nordhoff *et al.,* 2008; Sullivan *et al.,* 2013; Zinicola *et al.,* 2015a).

Through the use of 16S rRNA gene sequencing, five distinct *Treponema* phylogroups were initially identified within BDD lesions in Germany (Choi *et al.,* 1997). Three of these *Treponema* phylogroups have since been consistently isolated from BDD lesions in the UK (Evans *et al.,* 2008) and USA (Stamm *et al.,* 2002) and were also detected in lesions from Brazilian cattle (Nascimento *et al.,* 2015); namely *Treponema medium*-like/*Treponema vincentii*-like, *Treponema phagedenis*-like and *Treponema denticola*-like/*Treponema putidum*-like. The latter phylogroup has subsequently been redesignated a novel *Treponema* species, *Treponema pedis,* following taxonomical appraisal (Evans *et al.,* 2009b). Furthermore, recent multilocus sequence typing (MLST) of the three BDD-associated treponeme phylogroups has indicated a requirement for their further redesignation to *Treponema medium* phylogroup, *Treponema phagedenis* phylogroup and *Treponema pedis* respectively (Clegg *et al.,* 2016d). A molecular-based PCR survey of BDD lesions from UK dairy cattle identified *T. medium* phylogroup, *T. phagedenis* phylogroup and *T. pedis* spirochaetes within 96.1%, 98.0% and 76.5% of lesions respectively, with all three phylogroups detected concurrently within 74.5% of lesions (Evans *et al.,* 2009a). Nascimento *et al.* (2015) recently completed a parallel survey in Brazilian dairy cattle and reported near-identical results; *T. medium* phylogroup (95.5%), *T. phagedenis* phylogroup (100.0%) and *T. pedis* (86.4%) spirochaetes were found together in approximately 81.8% of BDD lesions. Several studies have now consistently reported *T. phagedenis* spirochaetes to be the most persistently found of all three phylogroups within BDD lesions (Choi *et al.,* 1997; Evans *et al.,* 2009a; Krull *et al.,* 2014; Nascimento *et al.,* 2015). Whilst the *T. phagedenis* phylogroup have been found to persist during all stages of lesion development, a recent study demonstrated profound increases in the relative abundance of *T. pedis* and *T. medium* phylogroup spirochaetes specifically during the active, ulcerative stages of lesion development (Krull *et al.,* 2014). Several metagenomics studies, and a recent metatranscriptomics study, have also recently corroborated the role of the three BDD-associated treponeme phylogroups within active and inactive BDD lesions (Marcatili *et al.,* 2016; Zinicola *et al.,* 2015a; Zinicola *et al.,* 2015b), whilst also highlighting the potential importance of several other *Treponema* species, including *Treponema maltophilum* and *Treponema paraluiscuniculi,* which were found to predominate

active BDD lesions when compared to healthy foot skin tissue (Zinicola *et al.,* 2015b). Schrank *et al.* (1999) previously isolated another novel *Treponema* taxa from a BDD lesion in Germany, however subsequent studies have largely failed to implicate it in the disease and suggest it may be a faecal contaminant (Evans *et al.,* 2011b; Nordhoff *et al.,* 2008).

Whilst treponemes are considered to have an unequivocal role in BDD pathogenesis (Nielsen *et al.,* 2016; Zinicola *et al.,* 2015a), their importance in the initial development of BDD lesions has been notably contested by several authors in recent years. Metagenomic sequencing studies have demonstrated considerable variability in the composition of microbial populations throughout the developmental stages of BDD lesions (Zinicola *et al.,* 2015a; Zinicola *et al.,* 2015b), whereby Krull *et al.* (2014) specifically identified a relatively low abundance of treponemes during the early stages of lesion development. Resultantly, whilst it is concluded that treponemes appear to be the predominant microbial constituents of advanced BDD lesions, it has been suggested that other (non-treponemal) bacterial invaders such as *Campylobacter* spp. and *Porphorymonas* spp. may have a more substantial role during early BDD infection, suggestive of a probable polymicrobial aetiology (Krull *et al.,* 2014; Marcatili *et al.,* 2016; Rasmussen *et al.,* 2012; Schlafer *et al.,* 2008; Zinicola *et al.,* 2015a; Zinicola *et al.,* 2015b).

1.3.5 Host genetics, seasonality and risk factors for bovine digital dermatitis

A number of herd-level and animal-level risk factors have been identified for BDD infection in recent years.

Herd-level risk factors for bovine digital dermatitis

The majority of herd-level risk factors for BDD are associated with housing and management practices and have often been attributed to the widespread intensification of modern dairy cattle production systems in recent years. For instance, herd size has been associated with an increased risk of BDD in several studies (Chapinal *et al.,* 2013; Rodriguez-Lainz *et al.,* 1999), with Wells *et al.* (1999) finding dairy cattle in herds of 200 or more to be 2.7 times more associated with a high incidence of BDD. Relun *et al.* (2013a) also found cattle of higher milk production to be at greater risk of BDD. The intensification of modern dairy farming has also largely prompted an increase towards housing cattle, with restricted-grazing or zero-grazing management systems becoming more common. Several studies have reported that housed dairy cattle are at increased risk of BDD infection and lameness compared to those maintained at pasture (Chapinal *et al.,* 2013; Onyiro *et al.,* 2008; Rodriguez-Lainz *et al.,* 1999; Wells *et al.,* 1999) and this is reflected in the observed seasonal trends in morbidity, whereby BDD is consistently most prevalent during the months in which cattle are housed indoors

(Blowey & Sharp, 1988; Read & Walker, 1998). Loose straw and free-stall housing systems are particularly associated with a high incidence of BDD (Rodriguez-Lainz *et al.,* 1999) and the length and width of cubicles are also known to have a significant impact (Somers *et al.,* 2005). Furthermore, flooring is also known to be an important herd-level risk factor. Whilst Wells *et al.* (1999) found that grooved concrete and smooth or slatted concrete flooring demonstrated the largest association with a high incidence of BDD, Somers *et al.* (2005) found that the use of manure scrapers with slatted flooring was found to considerably reduce the risk of BDD infection. Overall, it is widely considered that the cleanliness of the cattle and their environment is a major risk factor for BDD (Norring *et al.,* 2008; Relun *et al.,* 2013a).

One of the other most profound herd-level risk factors relates to farm biosecurity procedures, where the introduction of external replacement heifers onto dairy farms in both Chile and the USA have been consistently associated with an increased risk of BDD infection (Rodriguez-Lainz *et al.,* 1996; Wells *et al.,* 1999). Wells *et al.* (1999) also found a high incidence of BDD infection associated with the employment of hoof trimmers who work on other dairy operations. Indeed, hoof care is considered to have a profound effect on the risk of BDD infection, particularly the frequency or absence of hoof trimming and the use of unwashed trimming equipment (Becker *et al.,* 2014; Relun *et al.,* 2013a; Wells *et al.,* 1999).

Animal-level risk factors for bovine digital dermatitis

Parity is one of the most commonly reported animal-level risk factors for BDD. Primiparous dairy cattle are consistently associated with the highest risk of BDD and this is known to decrease concurrently with increasing parity (Holzhauer *et al.,* 2006a; Read & Walker, 1998; Rodriguez-Lainz *et al.,* 1999; Somers *et al.,* 2005). An increased risk of BDD infection is also consistently associated with several other claw disorders such as interdigital dermatitis (Holzhauer *et al.,* 2006a); notably, Becker *et al.* (2014) found that dairy cattle with heel-horn erosion were 4.3 times more likely to suffer from BDD infection. Dairy cattle have also been shown to have a higher risk of BDD infection during their lactation stage when compared to drying-off (Argáez-Rodríguez *et al.,* 1997); whereby, despite contradictory results, the magnitude of this risk appears to differ dependent upon their stage of lactation (Holzhauer *et al.,* 2006a; Rodriguez-Lainz *et al.,* 1999; Somers *et al.,* 2005).

Interestingly, purebred or crossbred Holstein-Friesian cattle appear to demonstrate a consistent predisposition to BDD infection and have also been associated with an increased risk of lameness when compared to other cattle breeds (Becker *et al.,* 2014; Chapinal *et al.,* 2013; Holzhauer *et al.,* 2006a; Relun *et al.,* 2013a; Rodriguez-Lainz *et al.,* 1999). Genetic studies have previously identified widespread variation in the estimated heritability of BDD

with values between 0.029 (Onyiro *et al.* 2008) to 0.40 (Oberbauer *et al.,* 2013). Aside from breed predisposition, it is considered that there may be individual host genetic factors which predispose certain animals within the same production systems to increased BDD susceptibility (Capion *et al.,* 2012). Recently, Scholey *et al.* (2012) identified 8 single nucleotide polymorphisms (SNPs) which were considered to be significantly associated with BDD-susceptible and non-susceptible dairy cattle, with suggestive involvement in skin cell proliferation and host inflammatory processes.

1.3.6 Infection reservoirs and transmission of bovine digital dermatitis

The routes of transmission for BDD have yet to be identified definitively, however a number of putative infection reservoirs have been suggested, including environmental slurry and faeces, the bovine gastrointestinal (GI) tract, bovine tissues and cattle hoof trimming equipment.

Indirect transmission: the bovine GI tract and dairy farm environment

An initial microbiological investigation into the presence of treponemes within bovine GI tract contents in the UK found that isolates were genotypically and phenotypically very different to those of BDD treponemes, forming a distinct phylogenetic cluster alongside other GI tract treponemes based upon 16S rRNA gene sequence comparisons (Evans *et al.,* 2011b). These isolates were largely considered commensal treponemes that formed part of the natural gut microbiota and differences were considered to reflect adaptation to a different host niche (Evans *et al.,* 2011b).

However, later studies indeed identified BDD treponemes within 14.3% and 14.8% of oral cavity (gingival) and rectal (recto-anal junction and rumen) tissues, respectively, during sampling of UK dairy cattle. Furthermore, during a survey of beef cattle, Sullivan *et al.* (2015b) specifically detected *T. phagedenis* phylogroup spirochaetes within 10% of gingival tissues by PCR. Taken together, these findings suggested that such host tissues may be a potential reservoir for BDD infection. More recently, BDD treponemes have been detected within bovine GI tract contents. Nascimento *et al.* (2015) found that one or more of the three BDD *Treponema* phylogroups (*T. medium, T. phagedenis* or *T. pedis*) were present within 60% of ruminal fluid samples surveyed from BDD-infected dairy cattle herds across Brazil. *T. phagedenis* phylogroup, *T. medium* phylogroup and *T. pedis* spirochaetes were present within 40.0%, 33.3% and 26.7% of samples respectively (Nascimento *et al.,* 2015). Furthermore, Zinicola *et al.* (2015a) demonstrated that several treponemes found to be of greater relative abundance within active BDD lesions (including *T. medium, T. phagedenis*

and *T. denticola*) were also almost ubiquitously found within both bovine rumen and faecal samples from Holstein dairy cattle in the USA.

Earlier PCR-based studies failed to detect or isolate BDD treponemes from the farm environment, leading to speculation that this may not be an infection reservoir for BDD (Evans *et al.,* 2012). However, through use of a highly sensitive, deep sequencing approach, Klitgaard *et al.* (2014) was able to identify 16S rRNA gene sequences of several BDD treponemes within 67.2% of environmental slurry or fresh faecal samples across six geographically diverse Danish dairy herds with recurrent BDD infection. *T. phagedenis* phylogroup and *T. pedis* spirochaetes were the most abundant within both lesions and environmental samples (Klitgaard *et al.,* 2014). Interestingly, no BDD treponeme deoxyribonucleic acid (DNA) was identified within the environment of a small free-range herd with no history of BDD infection (Klitgaard *et al.,* 2014).

Based on these observations, it is considered that the bovine tissues and bovine GI tract may act as reservoirs for BDD treponemes whereby, following defecation, treponemes will survive in the environment in slurry or faeces and will be transmitted within herds through indirect contact of the bovine foot skin tissue with slurry or faeces. Interestingly, Palmer *et al.* (2013) demonstrated that environmental slurry can increase permeability of the bovine foot skin tissue, therefore with the potential to facilitate pathogen entry.

Direct transmission: contact with hoof trimming equipment

Recently, Sullivan *et al.* (2014) detected *T. medium* phylogroup*, T. phagedenis* phylogroup and *T. pedis* spirochaetes on the metal blades of cattle hoof trimming equipment following use on BDD-infected cattle, both prior (67%, 63% and 42% respectively) and following (21%, 8%, 4%, respectively) blade disinfection. In fact, BDD treponemes were detected on 96% of blades following the hoof trimming of a BDD-positive cow, with successful isolation of a *T. phagedenis* phylogroup spirochaete, whilst none were detected on BDD-negative farms (Sullivan *et al.,* 2014). These findings may be unsurprising as several studies have identified an increased risk of BDD infection associated with hoof trimming practice (Becker *et al.,* 2014; Relun *et al.,* 2013a; Wells *et al.,* 1999).

This study provides further evidence to support direct skin contact as an alternative route of transmission for BDD; such mechanisms have previously been implicated in the transmission of yaws, a human treponemal infection (Antal *et al.,* 2002). In consideration of the frequency (once or twice per year) and wide geographical range of hoof trimming, this may be facilitating widespread transmission of BDD, both between animals within a herd and between farms, where adequate disinfection is not completed. A recent assessment of the

molecular diversity of BDD treponemes by MLST supports this hypothesis; observing apparent local and global patterns of transmission (Clegg *et al.,* 2016d).

Bovine digital dermatitis treponemes and other diseases

More recently, the three *Treponema* phylogroups associated with BDD infection (*T. medium*, *T. phagedenis* and *T. pedis*) have each been detected within a number of 'non-healing' bovine hoof disorders, including 'non-healing' white line disease, 'non-healing' sole ulcer and toe necrosis, whilst not present within healthy bovine horn from equivalent sites (Evans *et al.,* 2011a; Sykora *et al.,* 2015). Again, similar routes of indirect or direct transmission may be involved.

Furthermore, these three *Treponema* phylogroups have also been recently detected and subsequently isolated from skin lesions within a range of other production animals in the UK, including hock skin lesions in dairy cattle (Clegg *et al.,* 2016a), skin and tail lesions in pigs (Clegg *et al.,* 2016b), ischaemic teat necrosis in dairy cattle (Clegg *et al.,* 2016c) and pressure sores in UK dairy cattle (Clegg *et al.,* 2016e). *T. pedis* was also isolated from a porcine ear necrosis lesion in Sweden (Pringle *et al.,* 2009) and DD treponemes have also been detected within Canker lesions in horses in Japan and Austria (Moe *et al.,* 2010; Sykora & Brandt, 2015). The recent association of BDD treponemes with skin lesions of other host animals suggests a wider role for treponemes within production animal diseases and the possibility of an interspecies transmission mechanism, for which further investigation is still required. From available data, it is currently difficult to establish if the transmission to novel specific sites is due to tissue tropism or opportunistic infections in a farm or wildlife setting.

1.3.7 Treatment and control of bovine digital dermatitis

Currently, there is no single treatment for the elimination of BDD. Systemic antibiotics have been used previously to treat BDD infection (Laven, 2006; Read & Walker, 1998) and, particularly penicillin and macrolides (such as erythromycin) demonstrate substantial efficacy against BDD treponemes (Evans *et al.,* 2009c). However, largely due to antimicrobial stewardship, expense and its implications for milk withdrawal, systemic antibiotics are no longer commonly used to treat BDD. Currently, BDD is typically treated either individually, through the application of topical antibiotics (including oxytetracycline and lincomycin), or most commonly through frequent whole-herd footbath treatments such as copper sulphate, formalin or antibiotics (Bell *et al.,* 2013; Berry *et al.,* 2010; Blowey & Sharp, 1988; Cruz *et al.,* 2001a; Logue *et al.,* 2012). Unfortunately, these treatments often demonstrate variable efficacy and BDD lesions are commonly associated with recurrence (Berry *et al.,* 2010; Berry *et al.,* 2012; Britt *et al.,* 1996; Read & Walker, 1998; Relun *et al.,* 2012). Furthermore, many

of the novel alternative treatments, which are emerging to circumvent increasing concerns over rising antibiotic resistance, damaging milk and meat withdrawal periods and the adverse environmental (copper sulphate) and carcinogenic (formalin) effects resulting from current therapies, are not as effective (Jacobs *et al.,* 2017; Logue *et al.,* 2012).

Currently, there are no vaccines commercially available for BDD. Clinical trials were previously completed using a novel bacterin vaccine which targeted two *Treponema* phylogroups, however the vaccine demonstrated no consistent protective or therapeutic efficacy on dairy cattle in the USA (Berry *et al.,* 2004). Similarly, the clinical efficacy of a bacterin vaccine against the *Serpens* species of spirochaetes was previously evaluated in the USA (Fidler *et al.,* 2012). However, despite inducing a measurable antibody response, the vaccine demonstrated no therapeutic improvement of clinical lameness, BDD lesion size or prevalence in vaccinated Holstein dairy cattle (Fidler *et al.,* 2012). Considering its likely polytreponemal aetiology, any future vaccine would be required to target all three of the *Treponema* phylogroups and may be a reason for the poor therapeutic responses observed in previous clinical trials.

With the longevity of current and emerging therapeutics in question, and the recent emergence of similar disease manifestations in sheep (CODD; Harwood *et al.,* 1997), UK dairy goats (Groenevelt *et al.,* 2015; Sullivan *et al.,* 2015a) and wild American elk (Clegg *et al.,* 2015), there is an unequivocal urgency for the development of novel, efficacious and affordable treatments and prophylactic measures for BDD. In addition, it is evident that the improvement of farm biosecurity, cleanliness, footbathing strategies and hoof health checks would considerably reduce the risk to, or transmission of, BDD throughout herds (Cruz *et al.,* 2001b).

Unfortunately, there is currently a very limited understanding of the host-pathogen interactions and pathogenic mechanisms underlying BDD and this information will be fundamental for the identification of suitable candidates as targets for future novel therapeutics and vaccines against BDD.

1.4 An introduction to Spirochaetes

Spirochaetes are highly motile, helical, Gram-negative bacteria which may be anaerobic, aerobic, microaerophilic or facultatively anaerobic (Paster, 2011). Spirochaetes may be free-living or host-associated and a number are considered commensals living within the GI tract of animals or insects (Paster *et al.,* 2011; Smibert, 1984). However, many spirochaetes are considered pathogenic and have been highly associated with a number of infectious

diseases; including syphilis (*Treponema pallidum*), Lyme disease (*Borrelia* burgdorferi), DD (*Treponema* spp.), relapsing fever (*Borrelia* spp.), swine dysentery (*Brachyspira hyodysenteriae*), leptospirosis (*Leptospira interrogans*) and human periodontal disease (*Treponema denticola*) (Adler & de la Peña Moctezuma, 2010; Burgdorfer *et al.,* 1982; Choi *et al.,* 1997; Dewhirst *et al*., 2000; Harris *et al.,* 1972; Obermeier, 1873; Radolf *et al.,* 2006; Steere *et al.,* 1983; Taylor & Alexander, 1971).

1.4.1 Spirochaete phylogeny

The phylum Spirochaetes is taxonomically classified within the domain bacteria and currently represents one of approximately 40 different bacterial phyla which have been taxonomically characterised based upon 16S rRNA gene sequence comparisons (Hugenholz *et al.,* 1998; Woese, 1987). Spirochaetes are of the class *Spirochaetes* (Cavalier-Smith, 2002) and are found within the order *Spirochaetales* (Buchanan, 1917; Skerman *et al.,* 1980), which is presently comprised of four families; including *Spirochaetaceae, Brachyspiraceae, Leptospiraceae* and *Brevinemataceae* (Hovind-Hougen, 1979; Paster, 2011; Skerman *et al.,* 1980; Swellengrebel, 1907). More recently, Gupta *et al.* (2013) proposed the latter three families be re-classified as orders *Brachyspiriales* ord. nov., *Leptospiriales* ord. nov. and *Brevinematales* ord. nov., respectively. Furthermore, it was suggested that an additional family be added to the order *Spirochaetales,* namely *Borreliaceae* fam. nov. (Gupta *et al.,* 2013), now containing two genera, *Borrelia* and *Borreliella* (Adeolu & Gupta, 2014; Swellengrebel, 1907). Currently, there are at least seven genera within the spirochaetaceae family; including *Treponema, Spirochaeta, Cristispira, Clevelandina, Diplocalyx, Hollandina and Pillotina* (Bermudes *et al.,* 1988; Ehrenberg, 1835; Gross, 1910; Schaudinn, 1905; Skerman *et al.,* 1980). There is a single genus within each of the *Brachyspiraceae* and *Brevinemataceae* families, *Brachyspira* (Hovind-Hougen *et al.,* 1982) and *Brevinema* (Defosse *et al*., 1995) respectively, and the *Leptospiraceae* family consists of three genera, namely *Leptospira, Leptonema* and *Turneriella* (Hovind-Hougen, 1979; Levett *et al.,* 2005).

1.4.2 The *Treponema* genus

Treponema species are Gram-negative, highly motile, helical, fastidious, anaerobic (or occasionally microaerophilic) microorganisms of the phylum spirochaetes which are typically host-associated and have been identified within the GI tract, oral cavity and genital areas of animals, humans and insects (Paster, 2011; Smibert, 1984). Several *Treponema* taxa are considered commensals, living within the GI tract of animals and insects (Cwyk & Canale-Parola, 1979; Graber *et al.,* 2004; Paster & Canale-Parola, 1985). However, a number of treponemes are thought to be pathogenic and have been highly associated with a number

of infectious diseases; including DD, human periodontal disease, pinta, yaws and the venereal infection, syphilis (Choi *et al.,* 1997; Dewhirst *et al.,* 2000; Engelkens *et al.,* 1991; Mitjà *et al.,* 2013; Radolf *et al.,* 2006).

Morphological observations

Treponemes are typically between 0.10-0.70 µm in diameter, 1-20 µm in length and are helical, forming a number of regular or irregular coils (Paster, 2011). The cells possess a protoplasmic cylinder which is encased within both an inner cell membrane and a peptidoglycan-rich cell wall, as shown in Figure 1.2 (Paster, 2011). Cytoplasmic filaments are located within the protoplasmic cylinder and run parallel to the periplasmic flagella which are integral for cell motility (Paster, 2011). These periplasmic flagella consist of a core of flagellin proteins (including flagellin B1, flagellin B2 and flagellin B3) and are inserted subterminally at each end of the protoplasmic cylinder, extending along the length of the cell and overlapping in the centre in an n:2:n arrangement (Newbrook *et al.,* 2017; Norris *et al.,* 1988; Paster, 2011; Rosenberg *et al.,* 2014). The protoplasmic cylinder and periplasmic flagella are both enclosed within an outer sheath, primarily consisting of flagellin A protein, which shares several similarities with the outer membrane of other Gram-negative bacteria (Paster, 2011; Rosenberg *et al.,* 2014). The outer sheath is primarily comprised of phospholipids, glycolipids, many OMPs, carbohydrates and, often, lipooligosaccharide (LOS). Unlike those of other Gram-negative bacteria, the spirochaete outer membrane (sheath) does not contain potent antigenic lipopolysaccharide (LPS); however, an atypical form, namely LOS, has been described across several species (Hashimoto *et al.,* 2003; Paster, 2011; Rosenberg *et al.,* 2014; Schröder *et al.,* 2000; Schultz *et al.,* 1998).

Whilst this helical morphology is most typically observed in culture, treponemes are well-documented to transition between this spiral-shaped morphology and that of a spherical, encysted morphology during culture, particularly under unfavourable growth conditions (Döpfer *et al.,* 2012). Phase contrast microscopy is typically used to observe treponemes for routine culture and diagnostic purposes as treponemes are particularly difficult to visualise and distinguish by staining.

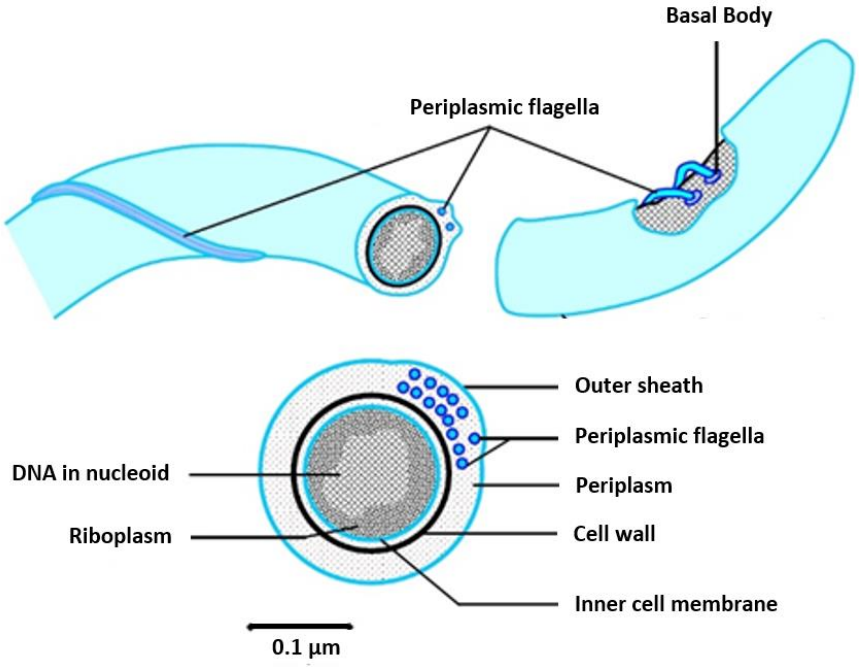

Figure 1.2 Typical morphological features of Treponema species. *Cells posses a protoplasmic cylinder which is encased within an inner cell membrane and a peptidoglycan-rich cell wall. Periplasmic flagella are essential for treponeme motility and are inserted subterminally at each end of the protoplasmic cylinder, extending along the length of the cell and overlapping in the centre in a n:2:n arrangement. The protoplasmic cylinder and periplasmic flagella are both enclosed within an outer sheath, which shares several similarities with the typical outer membranes of other Gram-negative bacteria. Illustration modified from that published by Cronodon (2017).*

Motility

Treponemes are highly motile microorganisms and their characteristic winding, serpentine-like "crawling" movements are thought to be a result of rotation and contraction of their periplasmic flagella (Paster, 2011; Rosenberg *et al.,* 2014). Several movements have been observed by treponemes in culture; including locomotion, flexing, translational movement and rotation about their longitudinal axis (Evans *et al.,* 2009b; Paster & Canale-Parola, 1985). This motility is likely to be important in their pathogenic potential.

Growth requirements

Treponemes are fastidious microorganisms and have proven extremely difficult to isolate and cultivate within culture. Nearly all treponemes are anaerobic (*T. pallidum* are microaerophilic) and do not tolerate exposure to oxygen (Cover *et al.,* 1982; Paster *et al.,* 2011). They are also extremely sensitive to temperature changes and dessication. Treponemes are chemoorganotrophs and, dependent upon the species, are known to use a variety of either carbohydrates or amino acids as a source of carbon and energy (Paster, 2011; Rosenberg *et al.,* 2014). Whilst commensals of the GI tract are typically cultivated in

ruminal fluid containing short-chain volatile fatty acids, pathogen-associated treponemes are typically cultivated in medium containing serum with long-chain fatty acids (Evans *et al.,* 2008; Paster *et al.,* 2011; Stanton & Canale-Parola, 1980).

1.5 Inflammation and the host immune response

Following infection, the host coordinates both immune and inflammatory responses in an attempt to resolve infection and reduce tissue damage to the host.

1.5.1 Inflammation

Inflammation is considered an attempted protective response to cellular injury (such as infection, toxicity, trauma or ischaemia amongst others) through both the elimination of injurious agents and the activation of wound healing and tissue repair processes (Cekici *et al.,* 2000). Although inflammation is largely considered a protective host response, it is well documented in contributing to the pathology of inflammatory diseases; particularly when in excess in response to bacterial infection (Pasparakis *et al.,* 2014). The host inflammatory response is coordinated by immune cells (particularly macrophages, monocytes, lymphocytes and neutrophils), tissue cells and a number of cytokines and chemokines, and can be split into two distinct phases; (1) the pro-inflammatory cascade and elimination of injurious agents, and (2) tissue repair and wound healing (Pasparakis *et al.,* 2014).

1.5.2 The host inflammatory response to bacterial infection

Upon cellular injury through infection, endogenous macrophages and monocytes (activated following the recognition of pathogen-associated molecular patterns (PAMPs) by pattern recognition receptors (PRRs)) are activated and together, alongside cells of the damaged tissues and microbes themselves, induce a pro-inflammatory response (Medzhitov, 2008; Newton & Dixit, 2012). This pro-inflammatory cascade leads to the recruitment and subsequent activation of neutrophils (Schleimer *et al.,* 1989), then monocytes and lymphocytes, to the site of injury as well as activation of various inflammatory mediators including chemokines and cytokines, proteolytic enzymes, eicosanoids, vasoactive amines or peptides, lipid mediators and host complement fragments (Medzhitov, 2008). The accompanying systemic response of pain, vasodilation and extravasation of fluid leads to the redness, heat and swelling which is characteristic of inflammation. Damaged host cells, microbes and apoptotic immune cells are typically destroyed and subsequently eliminated from the site of injury through host complement, the release of toxic substances (such as reactive oxygen species, elastase and cathepsin G amongst others) by activated neutrophils

and phagocytosis by activated macrophages (Medzhitov, 2008; Pasparakis *et al.,* 2014). The destruction of host tissues and release of toxic substances leads to host tissue damage.

Following the elimination of injurious agents and the removal of pro-inflammatory stimuli, the host inflammatory response progresses from an anti-bacterial, tissue-damaging response to one that promotes tissue repair and wound healing (Medzhitov, 2008). This includes the production of anti-inflammatory cytokines and chemokines, such as transforming growth factor(TGF)-beta(β) and interleukin-10 (IL-10), and matrix metalloproteinases (MMPs) (Medzhitov, 2008).

1.5.3 The host immune response to bovine digital dermatitis infection

Both humoral and cell-mediated immune responses are known to be profoundly stimulated during BDD infection of cattle (Elliot & Alt, 2009; Trott *et al.,* 2003). Although anti-treponeme antibodies develop early during BDD infection and reach high levels, particularly within active lesions, antibody levels decline substantially during convalescence and the immune response does not appear to be protective, as infection typically recurs despite treatment (Berry *et al.,* 2012; Dhawi *et al.,* 2005; Marcatili *et al.,* 2016; Trott *et al.,* 2003). A recent metatranscriptomics study hypothesised that this ineffective, unprotective host immune response may be a result of the polymicrobial nature of BDD, whereby the highly expressed antigenic epitopes are masked by an abundance of rarer, secondary "decoy" epitopes (Marcatili *et al.,* 2016). In terms of the humoral immune response, BDD infection (or BDD-associated treponemes) does not appear to stimulate an immunoglobulin M (IgM) response (Demirkan *et al.,* 1999; Dhawi *et al.,* 2005; Elliot *&* Alt, 2009; Murray *et al.,* 2002). However, whilst studies agree that the largest humoral antibody response during BDD infection is considered the immunoglobulin G (IgG) response, which reacts specifically to spirochaete LPS-like components (Trott *et al.,* 2003), the skew towards either IgG1 (Elliot & Alt, 2009) or IgG2 (Demirkan *et al.,* 1999; Murray *et al.,* 2002) remains controversial. Elliot & Alt (2009) found that the primary immune response to a range of BDD-associated *T. phagedenis* phylogroup isolates differed from that of the secondary exposure and field-exposed dairy cattle, which themselves were very similar.

1.6 An introduction to Spirochaete pathogenesis

The pathogenic mechanisms employed by various spirochaetes have been well documented over recent years and those of several important human diseases, such as Lyme disease (*B. burgdorferi*), syphilis (*T. pallidum*) and periodontal disease (*T. denticola*), have been studied in particular depth.

A primary and fundamental aspect of bacterial pathogenesis is the ability of a pathogen to initially adhere to the host cell surface, thereby facilitating the host-pathogen interactions which may then lead to successful colonisation and persistence within the host. It is the outer membrane of the spirochaetes which come into direct contact with the host and consequently, their OMP and LPS-like (LOS) components are known to have a fundamental role in the initial stages of spirochaete pathogenesis (Cullen *et al.,* 2004; Fenno *et al.,* 1996). Once in contact with the host, spirochaetes will subsequently employ a combination of pathogenic mechanisms to mediate tissue invasion (such as extracellular matrix (ECM) degradation), immune evasion (such as targeting host complement) and persistence (such as targeting wound healing and tissue repair processes) within the host. Examples for each of the fundamental spirochaetal pathogenic mechanisms are summarised in Table 1.2.

Table 1.2 Summary of the fundamental pathogenic mechanisms of spirochaetes and examples of their associated virulence factors.

Pathogenic mechanism	**Examples of spirochaetal virulence factor**	**Reference**
Adhesion to host cell surface receptors, plasma proteins or ECM components	Laminin-binding protein (*T. pallidum*)	Cameron, 2003
	Decorin-binding protein A/B (*B. burgdorferi*)	Guo *et al.,* 1998
	BBK32 (*B. burgdorferi*)	Probert & Johnson, 1998
	Major surface protein (*T. denticola*)	Fenno *et al.,* 1996; Haapasalo *et al.,* 1992
	Leptospiral immunoglobulin-like (Lig) proteins (*L. interrogans*)	Choy *et al.,* 2007
Host actin rearrangement and cytoskeletal remodelling	Major surface protein (*T. denticola*)	Wang *et al.,* 2001; Visser *et al.,* 2011
Mediation of host tissue invasion through degradation of ECM components such as collagen IV, fibronectin and laminin	Dentilisin (*T. denticola*)	Grenier *et al.,* 1990
	Extracellular serine protease, BbHTrA (*B. burgdorferi*)	Russell *et al.,* 2013; Russell & Johnson, 2013
Targeting the host fibrinolytic system to facilitate invasion and dissemination through host tissues	Outer surface protein A (OspA) (*B. burgdorferi*)	Fuchs *et al.,* 1994
	Outer surface protein C (OspC) (*B. burgdorferi*)	Önder *et al.,* 2012
	Outer membrane protein L1 (OmpL1) (*Leptospira* spp.)	Fernandes *et al.,* 2012
	Complement regulator-acquiring surface protein 1 (CRASP-1) (*B. burgdorferi*)	Hallström *et al.,* 2010
	Outer surface protein E (*B. burgdorferi*)	Hellwage *et al.,* 2001

Resistance to complement-mediated killing	CD59-like outer membrane protein (*B. burgdorferi*)	Pausa *et al.,* 2013
	BBK32 (*B. burgdorferi*)	Garcia *et al.,* 2016
	Lig proteins (*L. interrogans*)	Castiblanco-Valencia *et al.,* 2012; Meri *et al.,* 2005
	Leptospiral endostatin-like (Len) protein A/B (*L. interrogans*)	Stevenson *et al.,* 2007; Verma *et al.,* 2006
	Leptospiral complement regulator-acquiring protein A (LcpA) (*L. interrogans*)	Barbosa *et al.,* 2010
	FH binding protein B (FhbB) (*T. denticola*)	McDowell *et al.,* 2009; McDowell *et al.,* 2011
Dysregulation of the host inflammatory and immune responses	Extracellular serine protease, BbHTrA (*B. burgdorferi*)	Russell *et al.,* 2013
	Outer surface protein E (*B. burgdorferi*)	Ebnet *et al.,* 1997
Hemin binding and erythrocyte lysis	Hemin-binding protein A/B (*T. denticola*)	Scott *et al.,* 1993; Chu *et al.,* 1994
	Major surface protein (*T. denticola*)	Fenno *et al.,* 1998
Cellular detachment and cytotoxicity	Major surface protein (*T. denticola*)	Fenno *et al.,* 1998;
	Peptidoglycan component (*T. denticola*)	Grenier & Uitto, 1993

1.6.1 Spirochaete adhesion to the host cell surface

T. denticola, B. burgdorferi, L. interrogans and *T. pallidum* spirochaetes each have well-characterized adhesins (Table 1.2) on the surface of their outer membranes which are known to facilitate adherence to various host plasma proteins, ECM molecules or cell surface receptors to enable the colonisation of host tissues (Cameron, 2003; Choy *et al.,* 2007; Edwards *et al.,* 2005; Guo *et al*., 1998). For instance, the major surface protein (Msp) of *T. denticola* is known to facilitate binding to several host proteins, including collagen I, fibrinogen, laminin and fibronectin (Edwards *et al.,* 2005; Fenno *et al.,* 1996; Haapasalo *et al.,* 1992). The leptospiral immunoglobulin-like (Lig) proteins are only expressed by pathogenic *Leptospira* spp. during mammalian infection (Matsunaga *et al.,* 2003; Palaniappan *et al.,* 2002) and have been shown to bind and interact with multiple host ECM and plasma proteins; including fibronectin, collagen IV, laminin and elastin (Choy *et al.,* 2007; Lin & Chang, 2008; Lin *et al.,* 2009). Furthermore, whilst particularly known for their role in resistance to complement-mediated killing (Chapter 1.6.3), a complement regulator-acquiring surface protein (CRASP) of *B. burgdorferi,* CRASP-1, has been found to bind to host ECM proteins and plasminogen (Hallström *et al.,* 2010). Several other outer surface proteins (Osps) of *B. burgdorferi,* such as BBK32, RevA and ErpX have been identified as adhesins for mammalian fibronectin or laminin (Brissette *et al.,* 2009a; Brissette *et al.,* 2009b; Probert & Johnson, 1998).

1.6.2 Invasion, colonisation and persistence of spirochaetes within host tissues

Following initial adherence to the host, spirochaetes are thought to employ a series of pathogenic mechanisms to mediate host tissue invasion, colonisation and persistence, for instance through exploiting the host fibrinolytic system (Brissette *et al.,* 1999c), targeting host ECM components (Russell *et al.,* 2012) and exerting cytopathic effects on host cells (Uitto *et al.,* 1995). As a dynamic macromolecular network functioning to regulate cellular physiology and structural organization, the host ECM (consisting of many elements, including fibronectin, laminin, collagen, elastin and the family of matrix metalloproteinases (MMP) amongst others) is a prime target for degradation by spirochaetal pathogens in mediating tissue destruction and invasion into deeper host tissues (Russell *et al.,* 2013; Russell & Johnson, 2013). Dentilisin, a chymotrypsin-like protease (CTLP) expressed on the outer surface of *T. denticola,* is known to degrade several host ECM components (Grenier *et al.,* 1990) and can fragment fibronectin through the proteolytic activity of MMP-2 (Miao *et al.,* 2011). Furthermore, the treponemal metalloprotease pallilysin (Tp0751) is also thought to facilitate degradation of host ECM components through MMP-like proteolysis (Houston *et*

al., 2014). However, many pathogenic spirochaetes are thought to facilitate the degradation of ECM components through hijacking the host fibrinolytic system (Brissette *et al.,* 1999c; Coleman *et al.,* 1999; Fuchs *et al.,* 1994). The host fibrinolytic system is comprised of an enzymatic cascade which regulates the production of plasmin, a fundamental serine protease which itself mediates both physiological and pathological processes, such as tissue remodelling, wound healing and cellular migration (Vieira & Nascimento, 2015). Many pathogenic spirochaetes are thought to hijack this system and facilitate tissue destruction and invasion into deeper host tissues through expression of various Osps which bind the plasmin precursor, plasminogen, on their bacterial surface (Brissette *et al.,* 2009c; Fernandes *et al.,* 2012; Fuchs *et al.,* 1994; Önder *et al.,* 2012). Through the recruitment of host urokinase-type (uPA) or tissue-specific (tPA) plasminogen activators (Fuchs *et al.,* 1994), plasminogen is converted to plasmin and the plasmin-coated spirochaetes are thought to subsequently degrade host ECM components such as fibronectin, laminin and vitronectin (Coleman *et al.,* 1999). Previously, a CTLP of *T. denticola* was found to degrade a number of host protease inhibitors, such as antithrombin III and alpha 2 macroglobulin (α2M), which may therefore facilitate uncontrolled tissue destruction and favour spirochaete invasion (Grenier, 1996).

Baehni *et al.* (1992) reported phenotypic alterations of cellular cytoxicity and detachment in addition to actin rearrangement and cytoskeletal remodelling within human gingival fibroblast cells upon exposure to *T. denticola.* Furthermore, both the CTLP and Msp components of *T. denticola* have demonstrated cytotoxicity towards periodontal ligament epithelial cells and have been attributed to likely pore-forming activity (Fenno *et al.,* 1998). Interestingly, Grenier & Uitto (1993) identified the specific peptidoglycan, rather than LPS-like, components of *T. denticola* to be highly cytotoxic to epithelial cells.

Alongside these tissue-distructive mechanisms, spirochaetes possess (often multiple) periplasmic flagella which confer their characteristic high motility and likely contribute to their highly invasive and immune evasive properties. Interestingly, following experimentally-induced mutation of the flagellin B (*flaB*) gene, encoding a key protein component of periplasmic flagella, *B. burgdorferi* was rendered immotile and deficient of periplasmic flagella, with reduced viability and unable to establish infection within mammalian hosts (Motaleb *et al.,* 2000; Sultan *et al.,* 2013).

To facilitate virulence and persistence within host tissues, spirochaetes largely require mechanisms for iron acquisition to maintain growth and metabolism (Skaar, 2010), with *B. burgdorferi* and *T. pallidum* being notable exceptions (Posey & Gherardini, 2000; Posey *et*

al., 1999). Typically, bacteria may either produce iron-chelating siderophores to sequester bound iron from host iron-binding proteins, express Osps with iron-binding capabilities or sequester iron through binding heme compounds (Chu *et al.,* 1994; Scott *et al.,* 1993; Skaar, 2010; Xu *et al.,* 2001), possibly following haemolysis of host erythrocytes (Chu & Fenno *et al.,* 1998; Holt, 1994; Lee *et al.,* 2000). Interestingly, *Treponema* spp. are not thought to utilise siderophores and alternatively utilise various hemin binding proteins, such as HbpA and HbpB of *T. denticola* (Scott *et al.,* 1993; Chu *et al.,* 1994), alongside mechanisms of erythrocyte haemolysis (Chu *et al.,* 1995; Grenier, 1991), to acquire iron from the host.

1.6.3 Spirochaetes and evasion of the host immune system

Several mechanisms of spirochaetal pathogenesis are considered to have evolved to facilitate their evasion of the host immune response, including resistance to complement-mediated killing, antigen masking by host proteins, antigenic variation and suppression of the host immune response (Alderete & Baseman, 1979; Bankhead & Chaconas, 2007; McDowell *et al.,* 2011; Meri *et al.,* 2005; Zhang *et al.,* 1997; Zuerner *et al.,* 2007).

Host complement resistance

As evident from their prolonged survival in the presence of serum compared to their commensal counterparts, pathogenic spirochaetes appear to have evolved mechanisms to evade complement-mediated killing within the host environment (Barbosa *et al.,* 2009; Meri *et al.,* 2005; Stevenson *et al.,* 2007; Verma *et al.,* 2006). These mechanisms typically involve the expression of complement inhibitors, the hijacking of host complement regulators or neutralisation of components of the host complement system. The complement system is a predominant component of the host innate immune system and mediates direct killing of Gram-negative bacteria through opsonization and subsequent formation and activation of the membrane attack complex (MAC) (Janeway, 2001). *B. burgdorferi* is known to express a CD59-like OMP that binds host complement components and inhibits MAC formation (Pausa *et al.,* 2013). Several spirochaetal OMPs have been demonstrated to bind to regulatory proteins of the host complement system and likely inhibit complement activation, opsonization and formation of the MAC for the purposes of resisting complement-mediated killing (Garcia *et al.,* 2016; Hellwage *et al.,* 2001). For instance, *B. burgdorferi*, the spirochaetal pathogen of Lyme disease in humans, has been widely reported to express different lipoproteins on their cell surface, collectively known as CRASPs, which are able to bind negative regulators of the alternative complement pathway, particularly factor H (FH) and factor H-like protein 1 (FHL-1) (Seling *et al.,* 2010). An Osp of *B. burgdorferi*, OspE, has also been identified to bind to FH for this purpose (Hellwage *et al.,* 2001). More recently, a

B. burgdorferi lipoprotein (BBK32) has demonstrated inhibition of the classical complement pathway through binding to the C1 complex (Garcia *et al.,* 2016). Similarly, Lig proteins (Barbosa *et al.,* 2010; Castiblanco-Valencia *et al.,* 2012; Meri *et al.,* 2005), leptospiral endostatin-like (Len) protein A and B (Stevenson *et al.,* 2007; Verma *et al.,* 2006) and leptospiral complement regulator-acquiring protein A (LcpA) (Barbosa *et al.,* 2010) of *L. interrogans* are each known to bind and interact with complement regulators, such as FH and C4b-binding proteins. *T. denticola* is also considered to facilitate host complement evasion through binding to host FH through its FH binding protein B (FhbB) (McDowell *et al.,* 2009; McDowell *et al.,* 2011). Interestingly, however, *T. denticola* is also known to express a CTLP, namely dentilisin, upon its cell surface which has complement-degrading activity, particularly towards C3 and FH components (McDowell *et al.,* 2009; McDowell *et al.,* 2011; Yamazaki *et al.,* 2006).

Antigen masking and antigenic variation

Several studies have identified that spirochaetes are able to either mask or vary the antigenic components on their outer membrane to evade detection by the host immune system and facilitate persistence within host tissues. Alderete & Baseman (1979) previously identified several host-associated serum proteins coating the surface of *T. pallidum* spirochaetes, including α2M, immunoglobulins and albumin. Furthermore, several spirochaetes are known to coat themselves in proteolytically active host plasmin (Chapter 1.6.2) which, further to its primary role in tissue invasion, may also aid immune evasion (Hallström *et al.,* 2010).

Spirochaetes typically exist as multiple antigenic serotypes or variant strains of the same pathogenic species (Clegg *et al.,* 2016d). Antigenic variation, a rapid and sequential genetic or epigenetic alteration of surface-exposed antigens, has been reported as a key pathogenic mechanism of immune evasion and persistence of spirochaetes, particularly the borrelial pathogens of relapsing fever and Lyme disease (Giacani *et al.,* 2010; Raffel *et al.,* 2014; Trott *et al.,* 2003). For instance, *B. burgdorferi* is known to elicit antigenic variation on both Osps and variable membrane protein-like proteins and this is particularly apparent during the transition between the tick vector and mammalian host (Ohnishi *et al.,* 2000; Schwan *et al.,* 1995; Zhang *et al.,* 1997). Similarly, the borrelial pathogens of relapsing fever, particularly *Borrelia hermsii,* utilise antigenic variation of variable major proteins on their outer surface to facilitate recurrent infection within the host to avoid the efficient secondary immune response (Raffel *et al.,* 2014). These spirochaetes have also been reported to coat themselves in erythrocytes ("erythrocyte rosetting") to avoid phagocytic destruction and immune detection (Burman *et al.,* 1998). Trott *et al.* (2003) previously identified multiple antigenic

variants of *T. phagedenis* phylogroup spirochaetes isolated from BDD lesions, whilst the mechanisms of antigenic variation in *T. pallidum* have been associated with its repeat protein K (TprK) antigen (Giacani *et al*., 2010).

Dysregulation of the host inflammatory and immune response

Host inflammatory and innate immune system dysregulation is widely considered to be one of the most fundamental mechanisms of spirochaetal pathogenesis and is considered vital for both host immune evasion and the invasion, colonisation and persistence within host tissues (Evans *et al.,* 2014; Refaai *et al.,* 2013; Russell *et al.,* 2013; Scholey *et al.,* 2013; Tanabe *et al.,* 2009; Zuerner *et al.,* 2007). An extracellular serine protease of *B. burgdorferi,* BbHtrA, was found to initiate a pro-inflammatory signalling cascade in chrondrocyte cells, resulting in the upregulation of chemokine (C-X-C motif) ligand 1 (*CXCL1*), interleukin 6 (*IL6*) and several C-C chemokine ligands (*CCL1*, *CCL2* and *CCL5*) genes amongst others (Russell *et al.,* 2013). The authors suggest this response may result from pro-inflammatory fragments of host ECM components following the selective degradation of aggrecan, fibronectin and several other disease-relevant proteoglycans by BbHtrA (Russell *et al.,* 2013; Russell & Johnson, 2013). Furthermore, several pro-inflammatory chemokines and cytokines have previously been reported to be elevated in Lyme disease patient samples compared to healthy controls (Mullegger *et al.,* 2007; Zhao *et al.,* 2007). Similarly, peptidoglycans isolated from the human periodontal pathogen, *T. denticola,* were found to induce a significant and largely dose-dependent upregulation in interleukin-8 (*IL-8*), *IL6*, interleukin-1-β (*IL-1β*), matrix metalloproteinase 9 (*MMP9*), tumor necrosis factor alpha (*TNF-α*) and chemokine (C-C) motif ligand 5 (*CCL5*) gene expression in human monocyte-derived macrophage-like cells (Tanabe *et al.,* 2009). A model of Lyme disease pathogenesis reported comparable findings of *IL-8* and *CCL5* gene upregulation, in addition to an increased number of other chemokines and adhesion molecules, in primary human dermal fibroblasts exposed to *B. burgdorferi* sonicate, as attributable to the lipid moiety of its OspA (Ebnet *et al.,* 1997).

1.7 The pathogenesis of bovine digital dermatitis

To-date, there are a limited number of studies investigating the host-pathogen interactions and pathogenic mechanisms underlying BDD. However, typical of spirochaetal pathogenesis, there is evidence that dysregulation of the host inflammatory and immune response is an important mechanism of BDD pathogenesis; the spirochaete is thought to facilitate immune evasion and bacterial persistence within the host to its own advantage as a survival strategy.

1.7.1 Dysregulation of the host inflammatory and immune response

Through quantitative real-time polymerase chain reaction (qRT-PCR), Evans *et al.* (2014) investigated the dysregulation in expression of a range of inflammatory mediators within primary bovine foot skin cells, *in vitro*, following exposure to BDD-associated treponeme sonicates. Both *CCL5* and matrix metalloproteinase 12 (*MMP12*) were found to be significantly upregulated in primary bovine foot skin fibroblast cells following stimulation with sonicates of the *T. phagedenis* phylogroup and *T. pedis* (Evans *et al.,* 2014). It was suggested that this observed upregulation in *MMP12* expression within fibroblast cells may lead to degradation of the ECM component, elastin, therefore contributing to host tissue damage (Evans *et al.,* 2014). Similarly, the cell-signalling cytokine, *TNF-α*, was significantly upregulated in bovine fibroblast cells stimulated with *T. phagedenis* phylogroup sonicate. Tissue inhibitor of metalloproteinase (*TIMP3*) was also significantly upregulated in *T. pedis*-stimulated fibroblast cells, along with *TGF-β* in fibroblast cells stimulated with *T. medium* phylogroup and *T. pedis* sonicates. Although no such significant dysregulation of inflammatory mediator expression was observed in bovine foot skin keratinocytes (Evans *et al.,* 2014), Refaai *et al.* (2013) reported a significant increase in keratinocyte expression of IL-8 during both the acute (M2) and healing (M3) stages of BDD infection, as determined through qRT-PCR and immunohistochemistry. C-C motif chemokine receptor 3 (*CCR3*) and interleukin 5 were found to be significantly downregulated in healing (M3) and chronic (M4) stage lesions compared to BDD-negative tissue (Refaai *et al.,* 2013). Furthermore, interleukin 13 was significantly downregulated in M4 lesions (Refaai *et al.,* 2013).

Although knowledge of BDD pathogenesis has greatly improved through use of these targeted, gene-specific approaches to studying inflammatory dysregulation, researchers are increasingly turning to next generation sequencing (NGS) technologies to assess the global transcriptome of pathogens, infected cells or diseased lesions (Li *et al.,* 2014; Scholey *et al.,* 2013; Wu *et al.,* 2015; Zuerner *et al.,* 2007). Recently, ribonucleic acid (RNA) sequencing (RNA-Seq) analysis of global mRNA expression within BDD lesions identified the dysregulation of many mediators of fundamental bovine inflammatory and immune response signalling pathways when compared to healthy skin tissue (Scholey *et al.,* 2013). For instance, several interleukins (such as *IL24, IL19, IL6* and *IL-8*), chemokines (such as *CXCL2* and *CCL11*), matrix metalloproteinases (*MMP13*, *MMP1* and *MMP3*), the Mediterranean fever gene and secretory leukocyte peptidase inhibitor 1 gene were each highly upregulated within BDD lesions (Scholey *et al.,* 2013). Interestingly, many keratin and keratin-associated genes were highly downregulated, along with the fillagrin-2 gene (Scholey *et al.,* 2013). Each

of these contributes to either the formation or integrity of the epidermal skin cell barrier (Wu *et al.,* 2009). Alongside the previous identification of treponemes within both bovine hair follicles and sebaceous glands (Evans *et al.,* 2009a), these findings further support the hypothesis that a compromised epidermal barrier may facilitate treponemal infection. Scholey *et al.* (2013) highlighted significant enrichment of a gene network involving tissue degradation, repair and remodelling; with key mediators such as *MMP13*, *IL-1β* and alpha 2 macroglobulin-like 1 (*α2ML1*) amongst others. The significant upregulation in *α2ML1* expression within BDD lesions may suggest a potential role in host immune evasion and the promotion of treponemal growth, based upon previous findings with a related protein, α2M, in *T. denticola* (Alderete and Baseman, 1979; Scholey *et al.,* 2013; Suzuki and Loesche, 1989). Bovine macrophages have also been implicated as a likely target of BDD pathogenesis, with *T. phagedenis* phylogroup sonicate observed to have an immunosuppressive effect (Zuerner *et al.,* 2007). Serial analysis of gene expression (SAGE) previously identified the dysregulation of multiple immune mediators in bovine macrophages following exposure to *T. phagedenis* phylogroup sonicate, including *IL-8*, granulocytic chemotactic protein 2 and triggering receptor expressed on myeloid cells 1 (*TREM1*) (Zuerner *et al.,* 2007). Regulators of nuclear factor kappa-light-chain-enhancer of activated B cells (*NF-κB*) signalling, including inhibitor of NF-κB and SIVA-1 apoptosis-inducing factor (*SIVA-1*), were notably induced in bovine macrophages by stimulation with *T. phagedenis* phylogroup sonicate (Zuerner *et al.,* 2007). The antigen presentation functions of bovine macrophages also appeared a prominent target of *T. phagedenis* phylogroup spirochaetes (Zuerner *et al.,* 2007). Furthermore, whilst several genes associated with apoptosis were significantly dysregulated in bovine macrophages, many associated with wound repair functions were also downregulated by *T. phagedenis* phylogroup sonicates (Zuerner *et al.,* 2007).

There have been no studies, to-date, which have investigated the global dysregulation in gene expression of inflammatory and immune mediators within specific bovine foot skin cell types to elucidate their role in BDD pathogenesis. Furthermore, it is currently not known to what extent the three *Treponema* phylogroups share common or unique mechanisms of BDD pathogenesis.

1.7.2 Other mechanisms of bovine digital dermatitis pathogenesis

As previously discussed in Chapter 1.6, a number of other fundamental pathogenic mechanisms have now been identified for other disease-associated spirochaetes, leading to widespread speculation that these may also have a role in BDD pathogenesis. Previously, the expression of several genes associated with host cytoskeletal structure and actin

rearrangement, such as cytoskeleton-associated protein 1 and actinin alpha 1 (*ACTN1*) (fold changes of -9 and -4 respectively), were found to be downregulated by *T. phagedenis* phylogroup sonicates in bovine macrophages (Zuerner *et al.,* 2007). Several antigenic variants of BDD treponemes have recently been identified through MLST and genetic and immunological characterisation studies (Clegg *et al.,* 2016d; Trott *et al.,* 2003), however the mechanisms or pathways of antigen variation have yet to be elucidated for BDD. No further studies, as published to-date, have attempted to investigate these other pathogenic mechanisms to elucidate whether they are indeed implicated in BDD pathogenesis.

With relatively little research currently having been completed on the pathogenic mechanisms underlying BDD, further investigations are required to identify suitable candidates as targets of both novel vaccines and efficacious therapeutics for BDD in the coming years.

1.8 A role for cells of the bovine foot skin tissue in bovine digital dermatitis pathogenesis

1.8.1 Anatomy of the skin

Skin is a large well-structured organ which is comprised of two distinct layers, a thick inner layer named the dermis and a thinner outer layer named the epidermis, which are connected to underlying bone and muscle through the subcutaneous tissues (Bacha & Bacha, 2012), as shown in Figure 1.3.A. The dermal and epidermal tissues are interdependent; the robust outer epidermal tissue provides protection to the sensitive underlying tissues from physical damage and pathogens, whilst the deeper dermal tissue supplies the avascular epidermis with essential nutrients and supporting immune cells (Montagna *et al.,* 1967). The semi-permeable basement membrane which separates the dermis and epidermis, the DEJ, is known to facilitate this exchange (Burgeson & Christiano, 1997). Furthermore, the DEJ is considered important for tissue integrity and adherence and provides mechanical support and cytoskeletal organisation to cells of the epidermis (Burgeson & Christiano, 1997).

The epidermis is a dynamic, keratinized, stratified squamous epithelium which, as shown in Figure 1.3.B, is typically comprised of up to five distinct cellular layers; the stratum basale, stratum spinosum, stratum granulosum, stratum lucidum and stratum corneum (Bacha & Bacha, 2012). Keratinocytes are the predominant cell type found throughout the epidermis (Kolarsick *et al.,* 2011; Lian & Murphy, 2015) and are initially derived from the single layer of mitotic cuboidal-to-columnar keratinocytes of the stratum basale which facilitate continual

regeneration of the epidermis (Bacha & Bacha, 2012; Kolarsick *et al.,* 2011; Penneys *et al.,* 1970). These cells are typically pigmented by melanin due to their proximity to melanocytes in the stratum basale (Seiberg, 2001). From the stratum basale, keratinocytes migrate apically through the intermediate strata (stratum spinosum, stratum granulosum and, if present, stratum lucidum; which is only present within regions of thickened epidermal tissue such as the digital pads of carnivores) whilst undergoing progressive keratinization and terminal differentiation towards the uppermost superficial layer of the skin, the stratum corneum (Bacha & Bacha, 2012; Jackson *et al.,* 1993; Kolarsick *et al.,* 2011; Lian & Murphy, 2015). The keratinocytes become increasingly squamous (Lian & Murphy, 2015); their cytoplasm becomes densely packed with key intermediate filaments of the cytoskeleton, namely keratins (or cytokeratins) (Schweizer *et al.,* 2006); they accumulate irregular basophilic keratohyalin granules within the stratum granulosum and their constituents (keratin, profillagrin and loricrin) eventually form the surrounding interfibrillary matrix (Kolarsick *et al.,* 2011; Lian & Murphy, 2015); they acquire lysosomal enzymes which facilitate the dissolution of organelles towards the stratum corneum (Kolarsick *et al.,* 2011; Lian & Murphy, 2015); and they also accumulate lamellar bodies which are important for the secretion of various lipids (waterproofing and barrier function), proteases (regulation of desquamation) and antimicrobial peptides (AMPs) at the superficial epidermal surface (Braff *et al.,* 2005a; Ishida-Yamamoto *et al.,* 2004; Lian & Murphy, 2015; Menon *et al.,* 1992; Oren *et al.,* 2003). Terminally differentiated keratinocytes of the stratum corneum are large, anucleate, squamous, non-living cornified cells, often termed corneocytes, which are entirely composed of matrix-embedded keratin filaments and surrounded by an insoluble cornified envelope (marginal band) rather than a cellular membrane (Bacha & Bacha, 2012; Kolarsick *et al.,* 2011; Lian & Murphy, 2015; Watt, 1989). Involucrin, an insoluble cytoplasmic protein of the cross-linked cornified envelope, and fillagrin, a protein aggregate of keratin in corneocytes, are both typical markers of terminal differentiation within suprabasal keratinocytes of the epidermis, in addition to specific keratins (Manabe *et al.,* 1991; Watt, 1989; Yaffe *et al.,* 1993). Corneocytes form a protective barrier to the lower epidermal and dermal tissues against pathogen invasion and mechanical stresses and are continually sloughed off during desquamation and replaced by newly keratinized corneocytes as part of routine epidermal turnover (Bacha & Bacha, 2012; Jackson *et al.,* 1993; Kolarsick *et al.,* 2011). Although keratinocytes are the most abundant cells of the epidermis, other cell types located within the basal epidermal tissue include melanocytes, which protect the skin from harmful UV radiation, and Merkel cells, which have various sensory functions (Kolarsick *et al.,* 2011;

Lian & Murphy, 2015). Langerhans cells (LCs), which are fundamental antigen-presenting cells, are also found in lower abundance within the epidermis (primarily within the stratum spinosum and stratum granulosum) alongside a resident population of T lymphocytes (Hein & Dudler, 1997; Kolarsick *et al.,* 2011; Lian & Murphy, 2015; Pasparakis *et al.,* 2014).

The dermis is the thickest layer of skin tissue and is primarily comprised of loosely and densely packed connective tissue which is organised into two distinct regions; the superficial papillary dermis and the deeper reticular dermis (Bacha & Bacha, 2012; Lian & Murphy, 2015). Connective tissue is comprised of networks of collagen and elastin fibres which are embedded within an ECM consisting of ground substance; which itself comprises various glycosaminoglycans and proteoglycans (Bacha & Bacha, 2012; Lian & Murphy, 2015; Young *et al.,* 2006). The papillary dermis is a thin layer of loose connective tissue (predominantly type I and III collagen, thin elastin fibres and microvasculature) which interdigitates with the epidermis, forming dermal papillae, to provide a large surface area for anchorage and exchange (Bacha & Bacha, 2012; Lian & Murphy, 2015). In contrast, the reticular dermis is a much thicker layer of irregular, dense connective tissue with closely interlaced elastin fibres and coarse bundles of (predominantly type I) collagen which are arranged in parallel layers (Bacha & Bacha, 2012; Kolarsick *et al.,* 2011; Lian & Murphy, 2015). The reticular dermis is located much deeper within the dermis and contains blood vessels, lymphatic vessels, nerves, sensory receptors, sweat glands and hair follicles (Bacha & Bacha, 2012; Kolarsick *et al.,* 2011; Lian & Murphy, 2015). The primary function of the dermis is to provide tensile strength, pliability and elasticity to the skin; largely through its predominant component, collagen (Kolarsick *et al.,* 2011). Fibroblasts are the predominant cell type of the dermis and have a fundamental role in secreting connective tissue components such as procollagen (the protein precursor of collagen), elastin and ground substance to the dermal tissue and the DEJ (Kolarsick *et al.,* 2011; Marinkovich *et al.,* 1993; Smola *et al.,* 1998; Young *et al.,* 2006). Fibroblast cells are mesenchymal in origin and their cytoskeleton is comprised of various actin filaments and type III intermediate filaments such as vimentin (Franke *et al.,* 1978). Macrophages, mast cells, dendritic cells (DCs) and T lymphocytes are also found within the dermis, alongside a dynamic population of plasma cells and leukocytes following induction by certain stimuli, and each have a fundamental role in immune surveillance, host defence and tissue homeostasis (Hein & Dudler, 1997; Kolarsick *et al.,* 2011; Lian & Murphy, 2015).

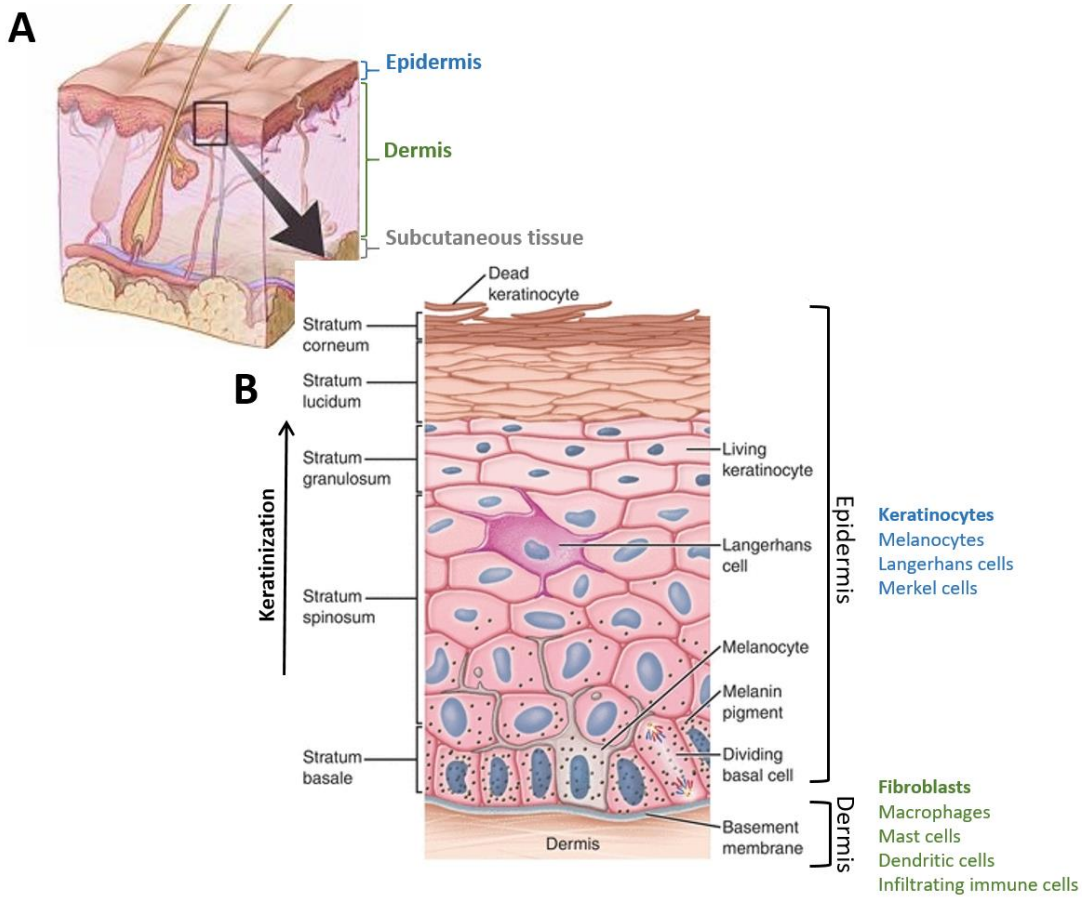

Figure 1.3 Anatomy of the skin. *(A) The skin is a large, well-structured organ which is comprised of two distinct layers, the dermis and epidermis, separated by a semi-permeable basement membrane and situated directly above the subcutaneous tissue. As the thickest layer of skin tissue, the dermis is comprised of dense and loosely packed connective tissue as a network of collagen and elastin fibres which are embedded within a proteoglycan-based matrix, ground substance. The dermis also contains a rich vascular, lymphatic and nerve supply, hair follicles, sebaceous glands and sensory receptors. Fibroblasts are the predominant cell type within the dermis, however macrophages, dendritic cells (DCs), mast cells and various immune cell populations are also present. (B) The predominant cell type within the epidermis are keratinocytes, which originate in the stratum basale and migrate apically through the intermediate strata (stratum spinosum, stratum granulosum and, if present, stratum lucidum) towards the superficial stratum corneum. Keratinocytes undergo terminal differentiation to form non-living, anucleate, squamous, keratinized cells, corneocytes, which form a protective physical barrier and continually undergo desquamation. The epidermis also contains populations of melanocyte cells, Langerhans cells (LCs) and Merkel cells. Illustration adapted from those published by Ayello et al. (2016) and National Cancer Institute (2007).*

1.8.2 The skin is a fundamental barrier to infection

The skin is a fundamental and primary aspect of the host innate immune system which provides a protective, mechanical barrier to potential microbial invaders (Campbell, 2017; Nestle *et al.,* 2009). However, the skin is also highly acidic (Fluhr *et al.,* 2001) and AMPs, such

as β-defensins and cathelicidin-derived peptides, are secreted onto the superficial epidermal surface by keratinocytes (typically from lamellar bodies) to provide a further chemical barrier to environmental pathogens (Braff *et al.,* 2005a; Braff *et al.,* 2005b; Gläser *et al.,* 2005; Harder & Schröder, 2002; Stolzenberg *et al.,* 1997). Aside from directly killing or inhibiting the growth of pathogens, AMPs are also considered to have roles in modulating the innate and adaptive host immune response (particularly through immune cell chemotaxis, apoptosis and Toll-like receptor (TLR) responsiveness) and wound repair functions such as keratinocyte migration (Bowdish *et al.,* 2005; Di Nardo *et al.,* 2007; Huang *et al.,* 1997; Ramanathan *et al.,* 2004; Tokumaru *et al.,* 2005; Veldhuizen *et al.,* 2014). Consequently, AMP dysregulation is associated with several skin diseases (Clausen *et al.,* 2013; Frohm *et al.,* 1997; Ong *et al.,* 2002) and is also considered a key target of microbial virulence (Campos *et al.,* 2004; Devine *et al.,* 1999; Jin *et al.,* 2004).

It is largely within the skin that residing and infiltrating immune and non-immune cell populations interact, both with each other and with microbial constituents, to coordinate host inflammatory and immune responses which are fundamental to maintaining effective host defence and tissue homeostasis (Epaulard *et al.,* 2014; Pasparakis *et al.,* 2014). Naik *et al.* (2015) recently epitomised the dynamic and complex nature of such host-microbe interactions through identifying that epidermal tissue-resident DCs appear to sense and subsequently respond to alterations in cytokine signatures elicited by the abundant commensal microfloral communities colonising the epidermal surface. In fact, these abundant commensal communities are thought to have a significant role in several aspects of host skin immunity, including their ability to limit opportunistic pathogen invasion (Campbell, 2017), promote effector T lymphocyte function via the interleukin-1 signalling pathway (Naik *et al.,* 2012) and maintain tissue homeostasis through regulating host inflammatory processes (Lai *et al.,* 2009).

1.8.3 Keratinocytes and fibroblasts: key players in host immune defence & wound healing

Many non-immune cell populations of the epidermis are known to facilitate alternative functions of skin tissue including its sensory, thermoregulatory and waterproofing capabilities and protection from UV radiation (Kolarsick *et al.,* 2011; Lian & Murphy, 2015). However, epidermal keratinocytes, alongside various immune cell populations, are considered key facilitators of immune surveillance, host innate immune and inflammatory responses and also have wound repair functions (Lebre *et al.,* 2007; Miller *et al.,* 2005; Tokumaru *et al.,* 2005). Epidermal keratinocytes (Lebre *et al.,* 2007; Menzies & Ingham,

2006), melanocytes (Yu *et al.,* 2009) and tissue-resident macrophages and dendritic cells (LC and dDCs) express a wide range of PRRs, such as TLRs or Nod-like receptors, upon their surface to aid the early detection of PAMPs (by invading microbes or their constituents) or damage-associated molecular patterns. In addition to the release of AMPs from activated keratinocytes and phagocytic cells (Braff *et al.,* 2005b; Selsted *et al.,* 1993; Shi *et al.,* 1996), these interactions induce a pro-inflammatory signalling cascade which is characterised by the stimulation of cytokines via the NF-κB signalling pathway (Evans *et al.,* 2014; Grossman *et al.,* 1989; Lebre *et al.,* 2007; Lee *et al.,* 2010; Refaai *et al.,* 2013; Yu *et al.,* 2009); many of which are hallmarks of inflammatory skin diseases (Grossman *et al.,* 1989; Jeong *et al.,* 2003; Scholey *et al.,* 2013). Similarly, mast cells typically degranulate upon contact with pathogens to release a cocktail of either pro-inflammatory or anti-inflammatory cytokines and chemokines and are also able to release AMPs within the dermis (Pasparakis *et al.,* 2014). Furthermore, keratinocyte cell death is also associated with the induction of pro-inflammatory responses in barrier tissues such as skin (Bonnet *et al.,* 2011; Weinlich *et al.,* 2013). Accordingly, this chemokine or cytokine signalling facilitates the chemotactic recruitment of neutrophils and, later, monocyte-derived macrophages, other DC populations and T lymphocytes through the vascular dermal tissues to sites of inflammation to eliminate offending microbes and cellular debris (Gregorio *et al.,* 2010; Sumida *et al.,* 2014).

Yao *et al.* (2015) recently identified higher expression of TLRs within human dermal fibroblasts compared to the corresponding epidermal keratinocytes, suggestive that fibroblast TLRs are highly functional and equally important for microbial recognition within skin tissues. Indeed, dermal fibroblasts are considered fundamental to the regulation and induction of pro-inflammatory responses and immune cell recruitment within the skin (Evans *et al.,* 2014; Yao *et al.,* 2015). However, fibroblasts also have a crucial role in wound healing and tissue repair processes, both directly, through the production of key connective tissue components of the dermis (Sorrell & Caplan, 2004), and indirectly, through the expression of growth factors which regulate epidermal keratinocyte proliferation (Marchese *et al.,* 2001; Rubin *et al.,* 1989; Young *et al.,* 2006). Furthermore, in the presence of an inflammatory stimulus, keratinocytes are thought to undergo a partial, reversible epithelial-to-mesenchymal transition (EMT) in which they can de-differentiate to a mesenchymal-like cell phenotype able to migrate and produce the collagen and elastin fibres required for wound healing and skin tissue repair (Arnoux *et al.,* 2005; Kalluri & Weinberg, 2009). The dysregulation of fibroblast gene expression is commonly observed in skin diseases and disorders (Byun *et al.,* 2016; Evans *et al.,* 2014).

Cells of the bovine foot skin tissue, such as fibroblasts and keratinocytes, are therefore considered to have a key role in BDD pathogenesis and require further investigation within this context.

1.9 Hypothesis, aims and objectives

Previous studies investigating BDD pathogenesis have yet to compare the individual roles of the three predominant *Treponema* phylogroups and have not specifically elucidated similarities and differences in their pathogenic potential during BDD infection.

The principle aim of this thesis is to dissect the fundamental host-pathogen interactions in BDD and investigate the following hypothesis: **"The three predominant *Treponema* phylogroups associated with BDD lesions in the UK, namely *T. medium* phylogroup, *T. phagedenis* phylogroup and *T. pedis,* implement distinct mechanisms of pathogenesis upon cells of the bovine foot skin tissue during infection."** Through elucidating specific mechanisms of host inflammatory dysregulation induced by the three predominant BDD treponeme phylogroups, and investigating the intra-phylogroup and inter-phylogroup molecular diversity of their antigenic constituents, it was hoped that this study would identify novel potential targets for future vaccine development and therapeutic intervention. The five specific objectives of this thesis are outlined in detail below.

1. **To isolate, subculture and characterise primary bovine foot skin fibroblast and keratinocyte cells for subsequent use in host-pathogen interaction studies of BDD infection.**

   To isolate primary fibroblast and keratinocyte cells from visibly healthy bovine foot skin tissue and optimise current cell purification methods to obtain pure primary cell lines for subsequent use in host-pathogen interaction studies of BDD infection. To characterise the purified primary bovine foot skin cells to confirm successful isolation of the expected lineages. Characterisations are to include morphological observation (microscopy) and the use of both immunofluorescent (IF) staining and reverse transcription polymerase chain reaction (RT-PCR) for relevant cellular markers such as vimentin, cytokeratin and involucrin.

2. **To investigate the global transcriptome of primary bovine foot skin fibroblast cells following co-incubation with treponeme sonicates to identify fundamental modulators of the host inflammatory response during BDD infection.**

   To use a next generation RNA sequencing (RNA-Seq) approach to investigate the global transcriptome profile of primary bovine foot skin fibroblast cells following co-incubation

with BDD treponeme sonicates and compare to those co-incubated with control medium, a non-specific inflammatory stimulant or treponeme sonicate produced from a bovine commensal isolate. To evaluate co-incubated cells for differential gene expression to identify fundamental mediators of the host inflammatory response during BDD infection.

3. **To investigate the molecular diversity of an outer membrane protein of BDD treponemes.**

   To identify a suitable putative OMP of BDD treponemes and develop a structural topology model for comparison across each of the three phylogroups. To develop and optimise three novel PCR assays for subsequent amplification and DNA sequencing of the putative *Omp* gene within representative isolates across each of the three BDD *Treponema* phylogroups. To assess nucleotide and amino acid diversity, selection pressures and perform phylogenetic and recombination analysis to investigate the molecular diversity of this putative *Omp* gene across each of the BDD *Treponema* phylogroups.

4. **To taxonomically characterise a novel spirochaete isolated from the bovine rumen**

   To taxonomically appraise a novel spirochaete isolated from the rumen contents of a Holstein-Friesian bull in the UK. To design and optimise a novel degenerate PCR assay for detection of the recombinase A (*recA*) gene. To perform phylogenetic analyses to compare the *16S rRNA* and *recA* gene sequences of the novel isolate to other validly named, taxonomically designated *Treponema* species. To collate phenotypic data obtained from a previous study which details the enzyme activity profile, morphological characteristics and growth requirements of the novel isolate and perform relevant comparisons to other named treponemes.

Chapter Two: Materials and methods

A detailed description of all methods performed and materials used throughout this thesis. Described chemicals and reagents are formulated and prepared according to Appendix A.

2.1 Bovine cell culture

All bovine cell isolation and culture work was performed within a Class II Microbiological Safety Cabinet under standard aseptic conditions. Bovine cell cultures were maintained within a humidified incubator (Binder KB 53/115; SciQuip Ltd, Wem, UK) at 37°C with 95% atmospheric air and 5% carbon dioxide (CO_2). Primary bovine fibroblast and keratinocyte cells were maintained for experiments until passage 8 only. Centrifugation was completed at room temperature (22°C) using a Heraeus® Multifuge® 3 S-R (Fisher Scientific UK Ltd, Loughborough, UK) for all tissue culture work, unless otherwise stated. All disposable tissue culture plates and flasks were purchased from Corning® (Appleton Woods Ltd, Kings Norton, UK).

2.1.1 Bovine cell culture media formulations

Prior to the isolation of primary fibroblast and keratinocyte cells, bovine foot skin tissue sections were initially placed within isolation media containing Williams' Medium E (WME; Sigma-Aldrich, Poole, UK) supplemented with 7.5 µg/ml Fungizone® Antimycotic (Gibco™ by Life Technologies Ltd, Paisley, UK), 300 µg/ml neomycin (Sigma-Aldrich, Poole, UK) and 150 µg/ml gentamycin (Sigma-Aldrich, Poole, UK).

Primary bovine foot skin fibroblast and keratinocyte cells were each maintained within a specific formulation of complete media, containing WME supplemented with 20% (v/v) foetal bovine serum (FBS; Gibco™ by Life Technologies Ltd, Paisley, UK; Appendix A), 2 mM L-glutamine (Gibco™ by Life Technologies Ltd, Paisley, UK), 2.5 µg/ml Fungizone® Antimycotic, 100 µg/ml neomycin, 50 µg/ml gentamycin and 10 ng/ml human recombinant epidermal growth factor (EGF 1–53, Keratinocyte-SFM supplement; Gibco™ by Life Technologies Ltd, Paisley, UK; Appendix A). Bovine keratinocyte cultures were additionally supplemented with 30 µg/ml bovine pituitary extract (BPE, Keratinocyte-SFM supplement; Gibco™ by Life Technologies Ltd, Paisley, UK), 0.4 µg/ml hydrocortisone solution (Sigma-Aldrich, Poole, UK), 5 µg/ml insulin solution from the bovine pancreas (Sigma-Aldrich, Poole, UK) and 0.1 nM cholera toxin from *Vibrio cholerae* (Sigma-Aldrich, Poole, UK; Appendix A) according to previously documented success in culturing equine keratinocyte cells (Visser & Pollitt, 2010).

2.1.2 Isolation of primary bovine foot skin cells

The hind limbs of deceased male Hereford or Red Poll beef bulls (aged between 18 and 24 months) were cut below the knee immediately following slaughter by an attendant at a local abattoir (Edge & Son Butchers, New Ferry, UK). The lower limb section was then transferred to a sterile bag and transported back to the laboratory for immediate processing. Red Poll and Hereford beef cattle were chosen for use in these studies due to the availability of bovine foot skin tissue at the local abattoir at the time of sampling – associated limitations are discussed in Chapter 3.3.3.

The sampling area was a large section of visibly healthy skin tissue found directly above (or below; initial isolation only, see Chapter 3.2.1 and 3.2.2) the dewclaws on the underside of the foot (Figure 2.1). The external surface was thoroughly disinfected twice with 2.5% (v/v) povidone iodine (Vetasept®; Animalcare Ltd, York, UK; Appendix A) and once with 70% (v/v) ethanol (molecular grade) and then gentle scraping with a sterile scalpel blade enabled the removal of hair (Figure 2.1.A). The skin tissue surface was then cleaned further with 2.5% (v/v) povidone iodine and 70% (v/v) ethanol (Figure 2.1.B). Full-thickness skin sections of approximately 4 cm x 4 cm were obtained by performing several cross-sectional cuts with a scalpel blade through the dermis and epidermis (Figure 2.1.C and 2.1.D). The bovine skin tissue sections were then placed onto a sterile 90 mm petri dish (Thermo Scientific™, Hemel Hempstead, UK) and any subcutaneous tissue found below the lower dermal skin layer was removed using a scalpel blade (Figure 2.1.E). The sections were further sterilised in 2.5% (v/v) povidone iodine and 70% (v/v) ethanol and were then rinsed and cleaned in sterile 1x Hank's Balanced Salt Solution (HBSS; Gibco™ by Life Technologies Ltd, Paisley, UK) prior to being briefly held in isolation media (Chapter 2.1.1). The tissues were again transferred to another petri dish to be further sectioned into smaller 1 cm x 1 cm biopsies using a scalpel blade (Figure 2.1.F) and placed in a 50 ml conical centrifuge tube (Starlab Ltd, Milton Keynes, UK) containing isolation media (Chapter 2.1.1) supplemented with 10 mg/ml dispase II (Sigma-Aldrich, Poole, UK; Appendix A) for digestion overnight (24 hours) at 4°C.

Primary fibroblast and keratinocyte cells were isolated from their respective dermal and epidermal layers of bovine foot skin tissue using a method previously developed for canine keratinocyte isolation (Köhler *et al.*, 2001), as recently described (Evans *et al.*, 2014). The bovine skin tissue biopsies were each transferred to a petri dish with sterile forceps and a scalpel blade was then used to partition the dermis and epidermis, while being careful to avoid the layer interface (as optimised in Chapter 3.2.3). Each layer was placed within a corresponding 7 ml Sterilin™ bijou tube (Appleton Woods Ltd, Kings Norton, UK) and

incubated with 0.25% (w/v) trypsin-ethylenediaminetetraacetic acid (trypsin-EDTA; Gibco™ by Life Technologies Ltd, Paisley, UK; Appendix A) for 30 minutes at room temperature to enable cell dissociation (as optimised in Chapter 3.2.2). An equivalent volume of WME containing 10% (v/v) FBS was subsequently added to neutralise the trypsin-EDTA and a sterile 10 ml serological pipette (VWR®, Lutterworth, UK) was used to thoroughly dissociate the cells from the primary tissue sections. The resulting cell suspension was filtered through a sterile 40 µm Falcon™ cell strainer (Fisher Scientific UK Ltd, Loughborough, UK; as optimised in Chapter 3.2.2) into a 50 ml conical centrifuge tube and the cells pelleted by centrifugation at 700 *g* for 5 minutes at room temperature. Cells were resuspended in 1 ml complete WME, with dermal and epidermal cultures maintained within fibroblast and keratinocyte cell-specific media, respectively (Chapter 2.1.1). The dermal and epidermal cell cultures were quantified and viability assessed using the trypan blue dye exclusion assay (Chapter 2.1.4) and seeded into 25 cm^2 tissue culture flasks (5 ml volume) at $2x10^4$ and $4x10^4$ cells per ml culture respectively. The primary bovine dermal and epidermal cell cultures were maintained within a humidified incubator at 37°C and remained undisturbed for an initial period of 48 and 72 hours respectively. Subsequently, the culture media was refreshed every 48 hours and cells were monitored daily using an Axiovert 25 inverted phase contrast microscope (Carl Zeiss Ltd., Cambridge, UK) with an Axiocam ERc 5s microscope camera (Carl Zeiss Ltd., Cambridge, UK) until a confluence of approximately 80% (or 90%; initial isolation only, see Chapter 3.2.1 and Chapter 3.2.2) had been achieved for initial subculture (Chapter 2.1.3).

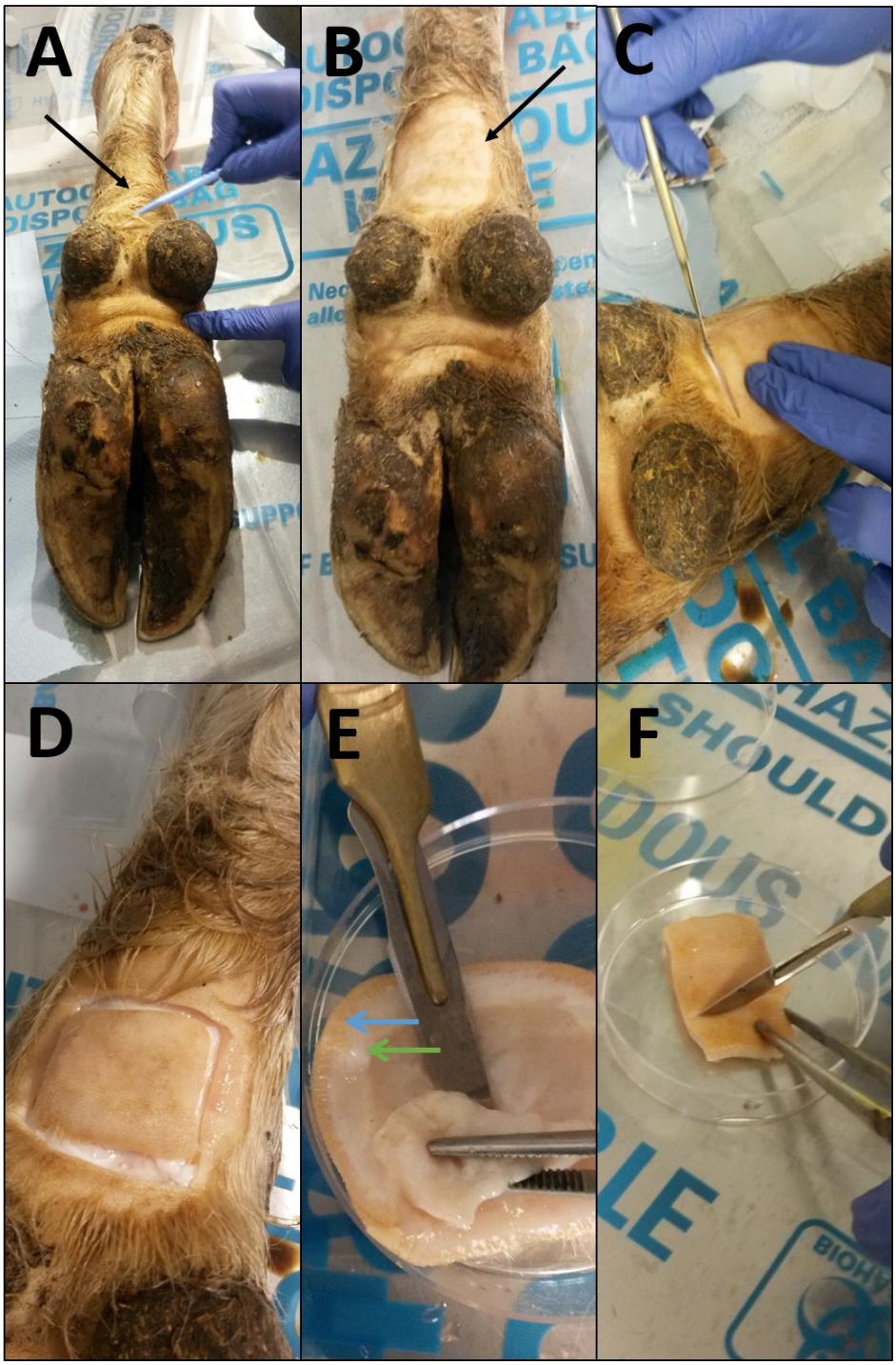

Figure 2.1 Preparation and sampling of bovine foot skin tissue for the isolation of primary fibroblast and keratinocyte cells. *(A) Visibly healthy, full-thickness (4 cm x 4 cm) skin sections were sampled from an area of tissue directly above the dewclaws on the underside of the hind feet of deceased Red Poll or Hereford beef bulls. (B) illustrates the removal of hair from the external skin surface following disinfection, (C) and (D) illustrate the cross-sectional cuts required to obtain full-thickness skin sections, (E) illustrates the removal of any remaining subcutaneous tissue directly below the dermal (green arrow) and epidermal (blue arrow) layers, and (F) represents the sectioning of skin into smaller 1 cm x 1 cm biopsies for subsequent protease digestion. Fibroblast and keratinocyte cells were subsequently dissociated from dermal and epidermal tissue sections respectively.*

2.1.3 Maintenance of primary bovine foot skin cells

Primary bovine dermal and epidermal foot skin cell cultures were each maintained within flasks containing a cell-specific formulation of complete WME (Chapter 2.1.1) for the purpose of enriching respective populations with fibroblast and keratinocyte cells. Cultures were maintained within a humidified incubator at 37°C and monitored with an Axiovert 25 inverted phase contrast microscope until subculture was required, at approximately 80% confluence (as optimised in Chapter 3.2.2). Primary bovine cells were maintained for experiments until passage eight only.

Primary bovine dermal foot skin cells were routinely subcultured as described previously (Evans *et al.*, 2014). In order to remove the inhibitory serum components prior to cell dissociation, culture medium was removed and the cell monolayer thoroughly washed three times with five volumes of sterile 1x HBSS. Following the addition of one volume of 0.025% (w/v) trypsin-EDTA (Gibco™ by Life Technologies Ltd, Paisley, UK; Appendix A), the culture was transferred to a humidified incubator at 37°C for 5 minutes to enable fibroblast dissociation. Light and phase contrast microscopy was used to monitor and confirm that the fibroblast cells had successfully rounded and detached from the flask surface. Five volumes of WME containing 10% (v/v) FBS was subsequently added to inactivate the trypsin-EDTA. A sterile serological pipette was used to thoroughly remove all cells from the flask surface and the single cell suspension was then transferred to a 50 ml conical centrifuge tube. The flask was washed a further three times with five volumes of sterile 1x HBSS to ensure that all dissociated cells were removed. Cells were subsequently pelleted by centrifugation at 180 *g* for 10 minutes at room temperature and resuspended in 1 ml fibroblast-specific complete WME (Chapter 2.1.1) for quantification using the trypan blue dye exclusion assay (Chapter 2.1.4). Cells were seeded into 25 cm^2, 75 cm^2 or 175 cm^2 tissue culture flasks in 5 ml, 15 ml or 35 ml fibroblast-specific complete WME respectively at $2x10^4$ cells per ml culture. Flasks were maintained within a humidified incubator at 37°C and were monitored daily using the Axiovert 25 inverted phase contrast microscope until subculture was required at approximately 80% confluence.

Primary bovine epidermal foot skin cell cultures were initially maintained within a cell-specific formulation of WME to enrich the population with keratinocytes. Due to the presence of a high population of contaminating fibroblasts in early culture, the epidermal foot skin cells were routinely subcultured thereafter according to the differential adherence properties of keratinocyte and fibroblast cells, a method previously described within the context of murine keratinocyte subculture (Yano & Okochi, 2005). Following removal of the

culture medium, the cell monolayer was washed three times with five volumes of sterile 1x HBSS to remove any inhibitory serum components which may interfere with cell dissociation. Weakly adherent fibroblast cells were then initially detached from the flask surface through incubation with one volume of 0.025% (w/v) trypsin-EDTA for 5 minutes at 37°C. Phase contrast microscopy was then used to ensure that the keratinocyte cells remained attached to the flask surface despite successful dissociation of the fibroblast cells. Five volumes of WME containing 10% (v/v) FBS was subsequently added to neutralise the trypsin-EDTA and a sterile serological pipette was used to thoroughly dissociate all fibroblast cells from the flask surface. The dissociated cells were discarded and the monolayer was washed a further three times with five volumes of 1x HBSS. The cell monolayer was assessed once again by phase contrast microscopy to ensure that all fibroblasts had been successfully removed. If required, the monolayer was incubated with a further one volume of 0.025% (v/v) trypsin-EDTA to allow dissociation of any remaining fibroblast cells. To dissociate the adherent keratinocytes from the flask surface, the monolayer was subsequently incubated with one volume of 0.25% (v/v) trypsin-EDTA (Appendix A) for 8 minutes at 37°C. The cell culture was monitored by phase contrast microscopy to ensure that the keratinocyte cells had detached from the flask surface prior to the addition of five volumes of WME containing 10% (v/v) FBS to inactivate the trypsin-EDTA. A sterile serological pipette was used to thoroughly detach the keratinocytes and the single cell suspension was transferred to a 50 ml conical centrifuge tube. The flask was washed a further three times with five volumes of sterile 1x HBSS and the washings were transferred to the centrifuge tube. Phase contrast microscopy was used to confirm that all dissociated keratinocyte cells had been collected. The keratinocyte cells were pelleted by centrifugation at 180 *g* for 10 minutes at room temperature and were subsequently resuspended in 1ml keratinocyte-specific complete WME (Chapter 2.1.1) for quantification using the trypan blue dye exclusion assay (Chapter 2.1.4). The cells were then seeded into 25 cm^2, 75 cm^2 or 175 cm^2 tissue culture flasks in 5 ml, 10 ml or 35 ml keratinocyte-specific complete WME respectively at $4x10^4$ cells per ml culture. Flasks were maintained within a humidified incubator at 37°C and were monitored daily using the Axiovert 25 inverted phase contrast microscope until subculture was required at approximately 80% confluence.

2.1.4 Trypan blue dye exclusion assay

Trypan blue stain has the ability to penetrate the compromised cell membranes of non-viable cells and can therefore distinguish these from viable cells which are characterised by dye exclusion (Strober, 2001). The trypan blue dye exclusion assay was used routinely during

primary cell culture in order to accurately quantify the number of viable bovine foot skin cells within suspension following trypsinization. Pelleted cells were thoroughly resuspended in 1 ml complete WME (Chapter 2.1.1) and 10 µl of the suspension was combined with 10 µl 0.4% (w/v) trypan blue solution (Sigma-Aldrich, Poole, UK). A representative 10 µl aliquot of the trypan blue-cell suspension was transferred to a single chamber of a Neubauer haemocytometer (Marienfeld-Superior, Lauda-Königshofen, Germany). The numbers of viable and non-viable cells, according to the numbers of non-stained and stained cells, respectively, were then counted under an Olympus® BH2 light microscope and the recorded values were used to calculate mean percentage viability. The haemocytometer was comprised of 9 large (1 mm) squares, with the central square containing 25 medium squares each with 16 small (0.04 mm) inner squares. The number of viable and non-viable cells within the 25 medium squares were counted and multiplied by 2 to account for the trypan blue dilution factor. This value was then multiplied by 10^4 to deduce the number of viable or non-viable cells per ml of suspension based upon a chamber depth of 0.100 mm.

2.1.5 Cryopreservation and resuscitation of bovine foot skin cells

Bovine foot skin fibroblasts and keratinocytes which required cryopreservation were initially trypsinized from tissue culture flasks and pelleted by centrifugation according to their respective standard culture maintenance protocols (Chapter 2.1.3). Cells were resuspended in 2 ml cryogenic vials (Corning®; Appleton Woods Ltd, Kings Norton, UK) containing 92% (v/v) FBS and 8% (v/v) dimethyl sulfoxide (Sigma-Aldrich, Poole, UK) at $3x10^6$ cells per ml. Vials were stored overnight at -80°C within a Mr Frosty™ freezing container (Nalgene®, Fisher Scientific UK Ltd, Loughborough, UK) to allow for slow freezing (approximately -1°C per minute) and were subsequently transferred to liquid nitrogen for long-term storage the following day.

Cells were removed from liquid nitrogen for resuscitation and were immediately thawed by placing the cryogenic vial in a water bath at 37°C. Instantly upon defrosting, cells were transferred into a 15 ml conical centrifuge tube (Starlab Ltd, Milton Keynes, UK) containing 10 ml pre-warmed (37°C) WME and the tube inverted five times. Cells were pelleted at 1,400 rpm for 5 minutes at room temperature and re-pelleted following resuspension within a further 10 ml pre-warmed WME. Bovine fibroblast and keratinocyte cells were then seeded into 25 cm^2 tissue culture flasks containing 5 ml complete WME (cell-specific) at a density of $1x10^5$ and $2x10^5$, respectively, as determined by the trypan blue dye exclusion assay (Chapter 2.1.4). Cells were maintained according to standard culture protocols and monitored daily until passage was required (Chapter 2.1.3).

2.2 Characterisation of primary bovine foot skin cells

Primary dermal and epidermal cells were characterised upon initial isolation from visibly healthy bovine foot skin tissue (Chapter 2.1.2) to confirm the successful isolation of pure fibroblast and keratinocyte cells prior to their use in host-pathogen interaction studies. Phase contrast microscopy was used to observe the characteristic spindle-shaped and cobblestone-like morphologies of fibroblasts and keratinocytes respectively. A RT-PCR assay, which was previously developed and optimised by Evans *et al.* (2014), was performed to detect an expressed marker of terminally differentiated keratinocytes, involucrin (Chapter 2.2.1). Furthermore, a novel double IF staining protocol (Chapter 2.2.2) was developed and optimised for the detection of two common epithelial cell markers, vimentin (for fibroblasts) and cytokeratin (keratinocyte cells).

2.2.1 Involucrin gene PCR assay

A previously developed (Evans *et al.,* 2014) RT-PCR assay was performed to determine whether a genetic marker of terminally differentiated keratinocytes, involucrin, was expressed within cultured primary bovine foot skin cells for the purposes of cellular characterisation. Cells were harvested for total RNA extraction as described in Chapter 2.9 and underwent cDNA synthesis according to Chapter 2.10 prior to PCR.

The involucrin gene, a keratinocyte-specific marker, was amplified from cDNA of cultured primary bovine foot skin cells by RT-PCR using *Taq* DNA polymerase (Qiagen, Manchester, UK), according to the manufacturer's instructions. The abundant bovine housekeeping gene, glyceraldehyde 3-phosphate dehydrogenase (*GAPDH*), was amplified simultaneously as a positive control. A 25 µl PCR reaction was prepared on ice with 1 µl template cDNA or reverse transcription negative (RT-) control (Chapter 2.10), 20 mM deoxynucleoside triphosphate (dNTP) mix (5 mM each of dATP, dCTP, dGTP and dTTP; Thermo Scientific™, Hemel Hempstead, UK) and 10 µM involucrin or GAPDH gene-specific forward and reverse primers (Eurofins Genomics, Ebersberg, Germany; Table 2.1). PCR thermal cycling conditions consisted of initial denaturation at 94°C for 3 minutes, 35 cycles of 94°C for 1 minute, 64°C (involucrin) or 56°C (*GAPDH*) for 3 minutes and 72°C for 1 minute, followed by a final extension step of 72°C for 7 minutes (Biometra TProfessional TRIO Thermocycler; Thistle Scientific Ltd, Glasgow, UK). To confirm assay validity, fibroblast cDNA and RNase-free water were used as negative controls, whilst keratinocyte cDNA (previously reverse transcribed by Jennifer Brown) was used as a positive control. Amplified PCR products were separated by

agarose gel electrophoresis (Chapter 2.2.2) to confirm that they were of the expected molecular weight.

Table 2.1 Primers used to detect bovine involucrin and glyceraldehyde 3-phosphate dehydrogenase genes by RT-PCR. *Forward (F) and reverse (R) primer pair sequences used to detect either the bovine involucrin or gluteraldehyde-3-phosphate dehydrogenase (GAPDH) genes by RT-PCR for characterisation of primary bovine foot skin cells. The predicted size of each amplified gene product is given in base pairs alongside the region of each gene being targeted.*

Primer specificity	Primer sequence*	Predicted size (base pairs [bp])	Region of gene targeted (positions)	Reference
Involucrin	Inv-F: 5'-ATAAGTAACCACCTGC(AG)G(AT)GTCCCAGA-3'	236	1836-1862	Evans *et al.* 2014
	Inv-R: 5'-AGGTAAAGCCTCTGGCCACCTGAGGTT-3'		2046-2072	
GAPDH	GAPDH-F: 5'-GAGTCCACTGGGGTCTTCAC-3'	117	354-373	
	GAPDH-R: 5'-TCACGCCCATCACAAACAT-3'		453-471	

*Parentheses represent degenerate nucleotides.

2.2.2 Agarose gel electrophoresis

Amplified gene products (Chapter 2.2.1) were each combined with 6x DNA loading dye (Thermo Scientific™, Hemel Hempstead, UK) and loaded onto a 1% (w/v) agarose gel containing 1x tris-acetate-EDTA (TAE) buffer (Promega UK, Southampton, UK; Appendix A) and stained with 0.5 mg/ml ethidium bromide (Fisher Scientific UK Ltd, Loughborough, UK) for separation by electrophoresis. Products were loaded alongside 100 base pair (bp) and 1 kilobase pair (kbp) DNA ladders (Promega UK, Southampton, UK; Appendix A) to estimate their molecular weight. Agarose gel electrophoresis was completed within an electrophoresis tank (GeneFlow Ltd, Staffordshire, UK) containing 1x TAE buffer at 110 V for 50 minutes using a Powerpac™ 300 electrophoresis power supply (Bio-Rad Laboratories Ltd, Hemel Hempstead, UK). DNA migration patterns were then immediately visualised through the use of an InGenius3 gel documentation system and ultraviolet (UV)-transilluminator with GeneSys software (Syngene UK, Cambridge, UK).

2.2.3 Immunofluorescent staining of cultured primary bovine foot skin cells

A novel double IF staining method was developed and subsequently optimised (Chapter 3.2.3) to detect the expression of two cellular markers, vimentin and pan cytokeratin, in

cultured primary bovine foot skin cells (Chapter 2.1.3) for the purposes of cellular characterisation. Vimentin was chosen as a key cytoskeletal intermediate filament protein of mesenchymal cells (Franke *et al.,* 1978), whereas pan cytokeratin was chosen to detect a range of the acidic and basic cytokeratins (also key intermediate filaments) which are specifically expressed in pairs through various stages of keratinocyte terminal differentiation (Schweizer *et al.,* 2006; Watt *et al.,* 1989).

IF staining was initially attempted on cultured primary bovine foot skin cells which had been grown on 13 mm cover glasses within 24-well tissue culture plates (Chapter 2.2.3.1), however was subsequently optimised for cells grown within 25 cm^3 tissue culture flasks (Chapter 2.2.3.2).

2.2.3.1 Immunofluorescent staining of primary bovine foot skin cells cultured on cover glasses

Upon initial isolation (Chapter 2.1.2), primary bovine foot skin fibroblast or keratinocyte cells were seeded into 24-well tissue culture plates containing 13 mm cover glasses (VWR®, Lutterworth, UK) at a density of $5x10^3$ (fibroblasts) or $1x10^4$ (keratinocytes) per well, each in 300 µl cell-specific complete WME (Chapter 2.1.1). The cells were maintained, as described in Chapter 2.1.3, for approximately four days until they had reached 80% confluence. The culture medium was then removed and each cell monolayer was washed three times with 300 µl Dulbecco's phosphate buffered saline without calcium and magnesium (DPBS-CMF; Sigma-Aldrich, Poole, UK) and then fixed with 4% (w/v) formaldehyde (Pierce™ by Thermo Fisher Scientific, Loughborough, UK; Appendix A) for 30 minutes at room temperature. The cells were washed a further three times each with 300 µl DPBS-CMF and were stored at 4°C in DPBS-CMF for up to 24 hours prior to IF staining.

The fixed cell monolayers were each washed five times through incubation for 5 minutes with 300 µl DPBS-CMF on a ProBlot™ 35 Deluxe Rocking Platform (Labnet International Inc., Edison, USA). To prevent non-specific staining, cell monolayers were then blocked for 1 hour at room temperature with 300 µl IF blocking buffer (Appendix A) on a rocking platform and washed five times with 300 µl DPBS-CMF. The epithelial cell markers, vimentin and pan cytokeratin (specifically those of 56.5/50/48/40 kDa [acidic subfamily] and 65-67/64/59/58/56/52 kDa [basic subfamily] molecular weights), were then detected simultaneously with a rabbit anti-vimentin polyclonal antibody (Abcam®, Cambridge, UK) and mouse anti-pan cytokeratin monoclonal antibody (Abcam®, Cambridge, UK) (both diluted 1:200 in IF blocking buffer) for 1 hour at room temperature on a rocking platform. As a negative staining control, antibodies were replaced with IF blocking buffer. Unbound

antibodies were subsequently removed by washing the cells five times with 300 µl IF washing buffer (Appendix A). Bound antibodies were simultaneously detected using a TRITC-conjugated donkey anti-rabbit immunoglobulin G (IgG) (H&L) polyclonal antibody (Abcam®, Cambridge, UK) and an Alexa Fluor® 488-conjugated donkey anti-mouse IgG (H&L) polyclonal antibody (Abcam®, Cambridge, UK), both at a 1:200 dilution in IF washing buffer, for 2 hours at room temperature on a rocking platform in the dark. Cell nuclei were counterstained with 4',6-diamidino-2-phenylindole (DAPI) by addition of 1 drop NucBlue Fixed Cell ReadyProbes Reagent (Molecular Probes™ by Thermo Fisher Scientific, Loughborough, UK) per well during the last 20 minutes of incubation. Unbound antibodies were removed by washing cells five times with 300 µl DPBS-CMF in the dark. Each cover glass (containing IF stained cells) was subsequently mounted onto a microscope slide (VWR®, Lutterworth, UK) using a single drop of hydromount® (National Diagnostics™; Thermo Fisher Scientific, Loughborough, UK). Once set, after approximately 10 minutes, the cover glasses were each sealed onto slides using nail varnish. IF stained cells were stored at 4°C in the dark for up to 24 hours prior to the detection and visualisation of fluorescent signals using an Olympus CK40 inverted phase contrast microscope (Carl Zeiss Ltd., Cambridge, UK) with a GXCAM-Eclipse (C-mount) WiFi microscope camera (GT Vision Ltd, Suffolk, UK) and Ucam Plus software. Image analysis was completed using ZEN lite 2 imaging software (Carl Zeiss Ltd., Cambridge, UK).

2.2.3.2 IF staining of primary bovine foot skin cells cultured in tissue culture flasks

Upon initial isolation (Chapter 2.1.2), primary bovine foot skin cells were seeded into 25 cm^3 tissue culture flasks at a density of $1x10^5$ (dermal cells) or $2x10^5$ (epidermal cells) in 5 ml cell-specific complete WME (Chapter 2.1.1) and were maintained to approximately 80% confluence according to their respective routine maintenance protocols (Chapter 2.1.3). Culture medium was removed and the cell monolayer was thoroughly washed three times with 1 ml sterile DPBS-CMF. Cells were then fixed with 1 ml 4% (w/v) formaldehyde (Pierce™ by Thermo Fisher Scientific, Loughborough, UK; Appendix A) for 30 minutes at room temperature. Following removal of the formaldehyde fixative, the cells were washed a further three times with 1 ml DPBS-CMF and temporarily stored at 4°C in DPBS-CMF for up to 24 hours prior to IF staining.

The fixed primary bovine foot skin cells were washed five times through incubation for 5 minutes with 1 ml DPBS-CMF on a rocking platform. To quench autofluorescence, cells were treated for 30 minutes with 1 ml 50 mM ammonium chloride (NH_4Cl; Appendix A) at room temperature on a rocking platform. Upon removal of NH_4Cl, cells were again washed a further five times with 1 ml DPBS-CMF. To prevent non-specific staining, cells were blocked

for 1 hour with 1 ml IF blocking buffer (Appendix A) at room temperature on a rocking platform. Upon removal of the blocking buffer, cells were again washed a further five times with 1 ml DPBS-CMF. The epithelial cell markers, vimentin and cytokeratin (specifically those of 56.5/50/48/40 kDa [acidic subfamily] and 65-67/64/59/58/56/52 kDa [basic subfamily] molecular weights), were then detected simultaneously with a rabbit anti-vimentin polyclonal antibody (Abcam®, Cambridge, UK) and a mouse anti-pan cytokeratin monoclonal antibody (Abcam®, Cambridge, UK) respectively, both following a 1:200 dilution in IF blocking buffer (Appendix A). Each cell monolayer underwent incubation with 1 ml of the combined antibody solution for 1 hour at room temperature on a rocking platform. As a negative staining control, each sample culture was processed alongside a primary antibody control (PAC) culture to monitor the level of non-specific IF staining and therefore instead underwent incubation with just 1 ml IF blocking buffer (Appendix A). Following removal of the incubation buffer, unbound antibodies were subsequently removed by washing the cells five times with 1 ml IF washing buffer (Appendix A). The bound anti-vimentin antibodies and anti-pan cytokeratin antibodies were then simultaneously detected using a tetramethylrhodamine isothiocyanante (TRITC)-conjugated donkey anti-rabbit immunoglobulin G (IgG) (H&L) polyclonal antibody (Abcam®, Cambridge, UK) and an Alexa Fluor® 488-conjugated donkey anti-mouse IgG (H&L) polyclonal antibody (Abcam®, Cambridge, UK), following their respective 1:200 and 1:300 dilutions (as optimised in Chapter 3.2.3) in IF washing buffer (Appendix A). Each cell monolayer underwent incubation with 1 ml of the combined antibody solution for 2 hours at room temperature on a rocking platform in the dark. Following removal of the incubation buffer, unbound antibodies were removed by washing the cells five times with 1 ml DPBS-CMF in the dark. Immunofluorescence stained cells were temporarily stored at 4°C in the dark for up to 24 hours prior to the detection and visualisation of fluorescent signals using an Olympus CK40 inverted phase contrast microscope (Carl Zeiss Ltd., Cambridge, UK) with a GXCAM-Eclipse (C-mount) WiFi microscope camera (GT Vision Ltd, Suffolk, UK) and Ucam Plus software. Image analysis was completed using ZEN lite 2 imaging software (Carl Zeiss Ltd., Cambridge, UK).

2.3 Bacterial cell culture

All bacterial cell culture work was performed under standard aseptic conditions in an anaerobic cabinet (Whitley A35 anaerobic workstation; Don Whitley, Bradford, UK) at 36°C with 85% nitrogen (N_2), 10% hydrogen (H_2) and 5% CO_2, unless otherwise stated. Cultures

were observed and monitored with phase contrast microscopy using a Diaplan Vario Orthomat-2 microscope (40x magnification; Leitz, Wetzlar, Germany).

2.3.1 Treponeme cell culture media

Treponemes were routinely cultured and maintained within oral treponeme enrichment broth (OTEB; Anaerobe Systems, Morgan Hill, USA). *T. phagedenis* phylogroup strain T320A and *T. pedis* strain T3552B^T were additionally supplemented with 10% (v/v) FBS (Appendix A), whereas *T. medium* phylogroup strain T19 was supplemented with 10% (v/v) rabbit serum (RS; GE Healthcare Life Sciences, Buckinghamshire, UK; Appendix A).

During their initial isolation, treponemes were cultured to late exponential growth phase prior to subculture on fastidious anaerobe agar (FAA) plates supplemented with rifampicin (Sigma-Aldrich, Poole, UK; see Appendix A), and enrofloxacin (Sigma-Aldrich, Poole, UK; see Appendix A), either with or without 5% (v/v) defibrinated sheep blood (TCS Biosciences Ltd, Buckingham, UK) and either no serum, 10% (v/v) FBS or 10% (v/v) RS, as previously described (Evans *et al.,* 2008). Two drops of culture were added to each plate and spread before plates were maintained at 36°C under anaerobic conditions for up to two weeks; single colonies were each reinoculated into OTEB with or without supplementation (as above) using a sterile 5 µl inoculating loop.

2.3.2 Origin of treponeme isolates

The treponemes used throughout this thesis were all initially isolated by Dr Nicholas Evans from Holstein-Friesian dairy cattle in the UK, as previously described (Evans *et al.,* 2008; Evans *et al.,* 2011b). *T. medium* phylogroup strain T19, *T. phagedenis* phylogroup strain T320A and *T. pedis* strain T3552B^T were all isolated from BDD lesion biopsies taken from the foot skin tissues of Holstein-Friesian dairy cattle in Merseyside (Evans *et al.,* 2008). *Treponema ruminis* strain Ru1^T was isolated from the rumen contents of a Holstein-Friesian bull in Cheshire (Evans *et al.,* 2011b), as described below.

Isolation and cultivation of spirochaetes from bovine ruminal contents

The collection of bovine ruminal contents and subsequent isolation of spirochaetes was completed in June 2009 by Dr Nicholas Evans as previously described (Evans *et al.,* 2011b). Briefly, the rumen of a Holstein-Friesian bull from a dairy farm in Cheshire (UK) was dissected using a sterile scalpel blade immediately after slaughter at a local abattoir. A sterile sampling container was used to collect approximately 30 ml ruminal contents from the centre of the rumen and samples were then placed on ice and transported back to the laboratory for further processing. Within an anaerobic cabinet (Whitley A35 anaerobic workstation; 36°C,

85% N_2, 10% H_2, 5% CO_2), a sterile 5 µl inoculating loop (Starlab Ltd, Milton Keynes, UK) was used to transfer three loopfuls of the ruminal contents into pre-warmed OTEB containing 25 µg/ml rifampicin (Sigma-Aldrich, Poole, UK; Appendix A), 5 µg/ml enrofloxacin (Sigma-Aldrich, Poole, UK; Appendix A) and either 10% (v/v) FBS, 10% (v/v) RS or no serum supplementation. Cultures were mixed and the lids untightened to allow gaseous exchange with the environment. Cultures were maintained at 36°C under anaerobic conditions to late exponential growth phase, as determined by phase contrast microscopy, according to Chapter 2.3.3. Phase contrast microscopy was also used to observe spirochaete motility and movement within culture. The cultures were subsequently streaked onto FAA plates (Chapter 2.3.1) which were supplemented with 25 µg/ml rifampicin and 5 µg/ml enrofloxacin, either with or without 5% (v/v) defibrinated sheep blood (TCS Biosciences Ltd, Buckingham, UK) and either no serum, 10% (v/v) FBS or 10% (v/v) RS. Plates were maintained at 36°C under anaerobic conditions for up to two weeks, whereby single colonies were each reinoculated into OTEB with or without supplementation (as above) using a sterile 5 µl inoculating loop. Cultures were then maintained at 36°C under anaerobic conditions to late exponential growth phase, as determined by phase contrast microscopy, prior to reinoculation according to Chapter 2.3.3. The cultures were purified further by again streaking onto FAA plates (Chapter 2.3.1) until pure, single-spirochaete isolates were obtained. Following their successful isolation and subsequent purification from bovine ruminal contents, spirochaetes were thereafter routinely subcultured based on the requirements determined for their optimum growth (Chapter 6.2.1), as outlined in Chapter 2.3.3. Upon successful purification, the spirochaete isolate was routinely cryopreserved (and subsequently resuscitated) according to Chapter 2.3.4.

2.3.3 Maintenance of treponeme cell cultures

Bacterial cell cultures were maintained according to specifically developed methods for the successful isolation and continual growth of treponemes (Evans *et al.,* 2008; Evans *et al.,* 2011b). Bacterial isolates were initially inoculated into 16 mm x 100 mm glass tubes containing pre-warmed OTEB and the required phylogroup-specific supplements (Chapter 2.3.1). Cultures were maintained at 36°C under anaerobic conditions (85% N_2, 10% H_2, 5% CO_2) to late exponential growth phase prior to reinoculation. Bacterial cell growth was monitored on a microscope slide (VWR®, Lutterworth, UK) with phase contrast microscopy using a Diaplan Vario Orthomat-2 microscope (Leitz, Wetzlar, Germany). Cultures typically required reinoculation after 7 days (*T. medium* phylogroup strain T19), 5 days (*T. phagedenis* phylogroup strain T320A), 4 days (*T. pedis* strain T3552B^T) or 1 day (*T. ruminis* strain Ru1^T) of

growth, dependent upon the respective treponeme phylogroup. Bacterial cell cultures were aspirated using a 150 mm plugged disposable glass Pasteur pipette (Volac, Essex, UK) and then 300 µl *T. medium* phylogroup strain T19, 120 µl *T. phagedenis* phylogroup strain T320A, 90 µl *T. pedis* strain T3552B^T or 450 µl *T. ruminis* strain Ru1^T were subsequently reinoculated into appropriately supplemented growth media (Chapter 2.3.1). The cultures were inverted five times to allow adequate mixing and the lids were then untightened to allow gaseous exchange with the anaerobic environment until reinoculation was required.

Throughout the duration of bacterial cell culture, each treponeme isolate underwent routine strain characterisation for verification prior to use in co-incubation experiments and characterisation studies. DNA was extracted intermittently from bacterial cell cultures at late exponential growth phase to enable characterisation, as described in Chapter 2.4.1. Strain characterisation was initially verified through PCR amplification of a universal bacterial *16S rRNA* gene followed by sequencing of the purified product (Chapter 2.4.2 and Chapter 2.4.6). Further to this, BDD treponeme isolates were re-verified using treponeme phylogroup-specific *16S rRNA* gene nested PCR assays (Chapter 2.4.3) and were visualised by agarose gel electrophoresis (Chapter 2.2.2).

2.3.4 Cryopreservation and resuscitation of treponeme cell cultures

Treponeme cell cultures which required cryopreservation were maintained under anaerobic conditions to late exponential growth phase, as monitored by phase contrast microscopy (Chapter 2.3.3). Thoroughly aspirated cultures were transferred into 2 ml microcentrifuge tubes (Starlab Ltd, Milton Keynes, UK) containing 10% (v/v) sterile glycerol (Sigma-Aldrich, Poole, UK). Cultures were immediately frozen at -80°C.

Treponeme cell cultures were thawed at room temperature for resuscitation. Approximately 10 to 15 drops of aspirated culture were subsequently transferred to a tube of appropriately supplemented growth medium (Chapter 2.3.1). Bacterial cell cultures were monitored by phase contrast microscopy for typically between 7 to 10 days until reinoculation was required, at late exponential growth phase, according to the routine maintenance protocol (Chapter 2.3.3).

2.3.5 Deposition of a novel spirochaete isolate in two bacterial culture collections

The novel spirochaete isolate (Chapter six) was grown to late exponential phase according to Chapter 2.3.3 and was further subcultured onto FAA plates as described in Chapter 2.3.1. The identity and purity of the novel isolate was confirmed through PCR amplification and subsequent sequencing of the *16S rRNA* and *recA* genes, as described in Chapter 2.4.2,

Chapter 2.4.4 and Chapter 2.4.6. A treponeme phylogroup-specific *16S rRNA* gene nested PCR assay (Chapter 2.4.3) was performed and the products sequenced to further confirm purity. Approximately 14 ml late exponential growth phase spirochaete culture and two FAA plates containing single colonies of the spirochaete isolate were transported by courier to the Leibniz-Institut Deutsche Sammlung von Mikroorganismen und Zellkulturen GmbH (DSMZ; Braunschweig, Germany) for strain deposition. Approximately 35 ml late exponential growth phase spirochaete culture was further transported to the National Collection of Type Cultures (NCTC; National Institute for Biological Standards and Control, South Mimms, UK) for strain deposition.

2.4 Characterisation of bacterial cell isolates

2.4.1 Genomic DNA extraction from bacterial cell cultures

Genomic DNA (gDNA) was extracted from bacterial cell cultures grown to late exponential phase (Chapter 2.3.3) using Chelex® 100 resin (Bio-Rad Laboratories Ltd, Hemel Hempstead, UK) according to a previously described method (Chua *et al.,* 2005). Bacterial cell cultures were aspirated and transferred to 1.5 ml microcentrifuge tubes (Eppendorf, Stevenage, UK) for centrifugation (Sigma 2K15 refrigerated microcentrifuge; Phillip Harris, Ashby de la Zouch, UK) at 5,000 *g* for 10 minutes (4°C). Following the removal of approximately 800 µl supernatant, the concentrated cell cultures were then resuspended and transferred to SuperLock microcentrifuge tubes (Starlab Ltd, Milton Keynes, UK) containing 250 µl 5% (w/v) chelex® 100 resin (Appendix A). Each sample was thoroughly vortexed, boiled for 10 minutes using a magnetic stirrer hotplate (Stuart Scientific, Staffordshire, UK) and then underwent centrifugation at 13,000 *g* for 10 minutes at room temperature. The bacterial supernatants containing gDNA were aliquoted and stored at -20°C until further use.

2.4.2 Universal bacterial *16S rRNA* gene PCR assay

A universal bacterial *16S rRNA* gene, previously described by Rurangirwa *et al.* (1999), was amplified by PCR using *Taq* DNA polymerase (Qiagen) according to the manufacturer's instructions. The PCR reaction was prepared on ice with 10 µM universal bacterial *16S rRNA* gene-specific forward and reverse primers (Rurangirwa *et al.,* 1999; Table 2.2), 20 mM dNTP mix (5 mM each of dATP, dCTP, dGTP and dTTP) and 1 µl gDNA (Chapter 2.4.1) to a total 25 µl volume. PCR thermal cycling conditions consisted of initial denaturation at 95°C for 5 minutes, 40 cycles of 94°C for 1 minute, 55°C for 3 minutes and 72°C for 3 minutes, with a final extension step of 72°C for 7 minutes (Biometra TProfessional TRIO Thermocycler). To confirm assay validity, water was used as a negative control. Amplified gene products were

separated by agarose gel electrophoresis and visualised using ethidium bromide, according to Chapter 2.2.2.

Table 2.2 Primers used to detect the universal bacterial 16S rRNA gene by PCR. *Forward (F) and reverse (R) primer pair sequences used to detect the universal bacterial 16S rRNA gene by PCR for characterisation of bacterial cell isolates. The predicted size of each amplified gene product is given in base pairs alongside the region of each gene being targeted.*

Primer specificity	Primer sequence	Predicted size (bp)	Region of gene targeted (positions)	Reference
Universal bacterial *16S rRNA* gene	UB16S-F: 5'-AGAGTTTGATCCTGG-3'	1526	7-26	Rurangirwa *et al.* 1999
	UB16S-R: 5'-TACCTTGTTACGACTT-3'		1491-1506	

An alternative *16S rRNA* gene PCR assay protocol (Demirkan *et al.,* 2001) was performed by Dr Nicholas Evans (Department of Infection Biology, University of Liverpool) for amplification of the universal bacterial *16S rRNA* gene sequence of the novel spirochaete isolate, represented by strain Ru1, as detailed by Evans *et al.* (2011b). Using *Taq* DNA polymerase (Roche Diagnostics Ltd, Burgess Hill, UK) according to the manufacturer's instructions, a 50 µl PCR reaction was prepared on ice with 1 µl gDNA (Chapter 2.4.1), 200 nM *16S rRNA* gene-specific forward and reverse primers (Edwards *et al.,* 1989; UB16SE-F: 5'-AGAGTTTGATCCTGGCTCAG-3', UB16SE-R: 5'-AAGGAGGTGATCCAGCCGCA-3'), 100 µM dNTPs (dATP, dCTP, dGTP, dTTP; Roche Diagnostics Ltd, Burgess Hill, UK) and 1x PCR reaction buffer (Roche Diagnostics Ltd, Burgess Hill, UK). PCR thermal cycling conditions consisted of 30 cycles of 95°C for 1 minute, 55°C for 1 minute and 72°C for 2 minutes, followed by a final extension step of 72°C for 10 minutes (GeneAmp® PCR system 2400; Applied Biosystems, Warrington, UK). To confirm assay validity, water was used as a negative control. Amplified gene products were each combined with 6x DNA loading dye and were then loaded onto a 0.7% (w/v) agarose gel containing 1x TAE buffer and stained with 0.02 mg ethidium bromide for analysis by electrophoresis. PCR products were loaded alongside 100 bp and 1 kbp DNA ladders (Appendix A) to estimate their molecular weight. Agarose gel electrophoresis was completed in an electrophoresis tank containing 1x TAE buffer at 110 V for 50 minutes using a Powerpac™ 300 electrophoresis power supply. DNA migration patterns were then immediately visualised using a Geldoc® gel documentation system and UV-transilluminator (Bio-Rad Laboratories Ltd, Hemel Hempstead, UK).

2.4.3 Treponeme phylogroup-specific *16S rRNA* gene nested PCR assays

Three treponeme phylogroup-specific *16S rRNA* gene nested PCR assays were previously developed by Evans *et al.* (2009a), targeting 300-500 bp regions within the universal bacterial *16S rRNA* gene and using primers specific for each of the BDD treponemes, *T. medium* phylogroup, *T. phagedenis* phylogroup and *T. pedis.* These nested PCR assays include a universal bacterial *16S rRNA* gene PCR step according to Chapter 2.4.2, although for 25 cycles rather than the 40 cycles described in preparation for subsequent gene sequencing. Using *Taq* DNA polymerase (Qiagen) according to the manufacturer's instructions, a 25 µl nested PCR reaction was then prepared on ice with 20 mM dNTP mix (5 mM each of dATP, dCTP, dGTP and dTTP), 10 µM treponeme phylogroup-specific forward and reverse primers (Evans *et al.,* 2009a; Table 2.3) and using 1 µl amplified *16S rRNA* gene PCR product as a template. The PCR thermal cycling conditions consisted of an initial denaturation step at 95°C for 5 minutes; 40 cycles of 95°C for 1 minute, then either 68°C for 2 minutes (*T. medium* phylogroup) or 64°C for 1 minute (*T. phagedenis* phylogroup) or 68°C for 30 seconds (*T. pedis*), and 72°C for 2 minutes; followed by a final extension step of 72°C for 10 minutes (Biometra Tprofessional TRIO Thermocycler). To confirm assay validity, water was used as a negative control and gDNA from each treponeme phylogroup was used as a positive control. Amplified gene products were separated by agarose gel electrophoresis and were subsequently visualised using ethidium bromide, according to Chapter 2.2.2.

Table 2.3. Primers used to detect T. medium phylogroup, T. phagedenis phylogroup and T. pedis spirochaetes by phylogroup-specific nested 16S rRNA gene PCR. *Following initial amplification of the 16S rRNA gene, 300-500 bp regions were then targeted using phylogroup-specific forward (F) and reverse (R) primer pair sequences. These nested 16S rRNA gene PCR assays were used to detect T. medium phylogroup, T. phagedenis phylogroup and T. pedis spirochaetes, respectively, for the characterisation of treponeme isolates. The predicted size of each amplified gene product is given in base pairs alongside the region of each gene being targeted.*

Primer specificity	Primer sequence	Predicted size (bp)	Region of gene targeted (positions)	Reference
T. medium phylogroup	Tm-F: 5'-GAATGCTCATCTGATGACGGTAATCGACG-3'	475	472-500	Evans *et al.* 2009a
	Tm-R: 5'-CCGGCCTTATCTAAGACCTTCTACTAG-3'		1001-1029	
T. phagedenis phylogroup	Tb-F: 5'-GAAATACTCAAGCTTAACTTGAGAATTGC-3'	400	612-640	Evans *et al.* 2009a

	Tb-R: 5'-CTACGCTACCATATCTCTATAATATTGC-3'		1006-1029	
T. pedis	Tp-F: 5'-GGAGATGAGGGAATGCGTCTTCGATG-3'	475	459-484	Evans *et al.* 2009a
	Tp-R: 5'-CAAGAGTCGTATTGCTACGCTGATATATC-3'		1017-1045	

2.4.4 Development and optimisation of a novel *recA* gene PCR assay

A novel degenerate PCR assay was developed and optimised to amplify the *recA* gene from treponemes of the bovine and porcine GI tract phylogenetic cluster (Evans *et al.,* 2011b). The annotated *recA* gene sequences of two relevant (porcine and bovine) GI tract treponeme isolates, *Treponema succinifaciens* DSM 2489^T (Han *et al*., 2011) and *T. brennaborense* DSM 12168^T (Lucas *et al*., 2015), were extracted from complete genome sequences from the NCBI nucleotide database (NCBI Resource Coordinators, 2017). The *recA* gene sequences were aligned within the Bioedit Sequence Alignment Editor (Hall, 2013) using CLUSTAL W (Thompson *et al*., 1994). Forward and reverse degenerate primers (Table 2.4) were then designed within conserved regions of the trimmed (1203 bp) sequence alignment, using the Multifunctional Oligo Property Analysis Tool (MOPS; Eurofins Genomics, 2016) to ensure satisfaction of specific primer design criteria (Thermo Fisher Sciencific, 2016). Primer pairs were designed to ideally be between 18-30 nucleotides in length, to have a similar guanine-cytosine (GC) content of between 40-60%, to have a melting temperature (T_m) within 5°C of each other between 65-75°C, to have a GC clamp at the 3' end, to avoid more than four nucleotide or dinucleotide repeats and to have no intra-primer or inter-primer complementarity, as determined using OligoCalc (Kibbe, 2007). A nucleotide BLAST (Altschul *et al.,* 1990) was performed against the corresponding treponeme genomes for each oligonucleotide primer sequence to ensure specificity for the target gene of interest.

Table 2.4. Degenerate primers used to detect the recA gene by PCR. *Forward (F) and reverse (R) degenerate primer pair sequences used to detect the recombinase A (recA) gene using a newly developed PCR for the characterisation of bovine gastrointestinal tract treponeme isolates. The predicted size of each amplified gene product is given in base pairs alongside the region of each gene being targeted.*

Primer specificity	Primer sequence	Predicted size (bp)	Region of gene targeted (positions)	Reference

recA	*recA*-F: 5'-GCAAC(CT)TTGTTCTTTAC(GA)-3'	574	416-433	This study
	recA-R: 5'-GAAATGTACGGTCC(CT)GAA-3'		973-990	

The *recA* gene was initially amplified from 1 µl gDNA from the spirochaete isolate (Chapter 2.4.1) in a 25 µl reaction using 10 µM degenerate *recA* gene-specific forward and reverse primers (Table 2.4), 20 mM dNTP mix (5 mM each of dATP, dCTP, dGTP, dTTP) and *Taq* DNA polymerase according to the manufacturer's instructions. Optimal PCR thermal cycling conditions were identified to be an initial denaturation step at 95°C for 5 minutes, 40 cycles of 94°C for 1 minute, 49.1°C for 3 minutes and 72°C for 3 minutes, with a final extension step of 72°C for 7 minutes (Mastercycler Gradient Thermocycler; Eppendorf, Hamburg, Germany). To confirm assay validity, water was used as a negative control. The amplified PCR products were separated by agarose gel electrophoresis to confirm that they were of the expected molecular weight (574 bp), according to Chapter 2.2.2.

2.4.5 Purification of amplified PCR products for sequencing

Amplified PCR products which were to be sent for sequencing of the universal bacterial *16S rRNA* gene (Chapter 2.4.2), *recA* gene (Chapter 2.4.4) or putative treponeme *Omp* genes (Chapter 2.8.5) were purified using a QIAquick® PCR Purification Kit (Qiagen, Manchester, UK), according to the manufacturer's instructions. Purified PCR products were temporarily stored at 4°C and sent for gene sequencing within 8 hours (Chapter 2.4.6).

2.4.6 Gene sequencing, assembly and analysis

Purified PCR products of the universal bacterial *16S rRNA* gene, *recA* gene or putative treponeme *Omp* genes (Chapter 2.4.5) were sequenced by a commercial concern (Source Bioscience, Nottingham, UK) using the Sanger DNA sequencing method. Sequences were assembled into a contiguous sequence using ChromasPro Sequence Analysis Package V2.0.0 (Technelysium Pty Ltd, South Brisbane, Australia) and were then manually curated to resolve disagreements between the nucleotide sequence chromatograms. A Basic Local Alignment Search Tool (BLAST; Altschul *et al.,* 1990) was subsequently used to compare similarities between the consensus sequence and all other nucleotide sequences within the National Center for Biotechnology Information (NCBI) database to identify the sequenced gene (NCBI Resource Coordinators, 2017).

An alternative gene sequencing, assembly and analysis protocol, as detailed by Evans *et al.* (2011b), was performed by Dr Nicholas Evans (Department of Infection Biology, University of Liverpool) for *16S rRNA* gene sequence comparisons of the novel spirochaete isolate, represented by strain Ru1 (Chapter six). Amplified gene products were purified (Chapter 2.4.5) and then sequenced commercially by Cogenics Lark Inc. (Essex, UK) using the Sanger DNA sequencing method. Sequences were assembled into a contiguous sequence using PREGAP4 within the Staden Package (Staden, 1996) and were then manually curated to resolve any disagreements between the nucleotide sequence chromatograms using GAP4. The resulting sequence was subjected to BLAST (Altschul *et al.*, 1990) which was performed to compare similarities between the obtained sequence and all other nucleotide sequences within the NCBI database to identify the sequenced gene.

Calculating sequence identitities and phylogenetic analysis

Manually curated contiguous sequences from the spirochaete isolate were subsequently aligned with corresponding (*16S rRNA* or *recA*) gene sequences of all currently recognised *Treponema* species available from the NCBI nucleotide database (NCBI Resource Coordinators, 2017) using CLUSTAL W (Thompson *et al.,* 1994) within the Bioedit Sequence Alignment Editor (Hall, 2013). The alignment was trimmed and used to produce a sequence identity matrix within the Bioedit Sequence Alignment Editor (Hall, 2013).

The most appropriate evolutionary model for phylogenetic inference of the trimmed (*16S rRNA* or *recA*) gene sequence alignment were predicted using ModelTest software in the TOPALi v2 program (Milne *et al*., 2009). This model was then used to produce a bootstrapped maximum-likelihood phylogenetic tree of the trimmed gene sequence alignment, based on 10,000 reiterations, as implemented in Molecular Evolutionary Genetics Analysis (MEGA) V6.0 (Tamura *et al.,* 2013).

2.4.7 Transmission electron microscopy

The morphological characteristics of novel spirochaete isolates were observed, identified and analysed by Brian Getty using transmission electron microscopy (TEM), as previously described (Demirkan *et al*., 2006; Evans *et al*., 2011b), for phenotypic characterisation. The spirochaete isolate was initially cultured in OTEB to late exponential growth phase according to Chapter 2.3.3. The culture broth was then directly applied to the surface of a carbon-reinforced, 400-square mesh copper grid coated with Formvar. The copper grid was air-dried and then the crystallized salts were removed by washing three times with distilled water droplets on a microscope slide. The copper grid was negatively stained with 1% (w/v)

potassium phosphotungstate (pH 7.0; Agar Scientific Ltd, Stansted, UK) and morphological characteristics were then visualised using a Philips 301 electron microscope.

2.4.8 Enzyme activity profiling

Novel spirochaete isolates underwent enzyme activity profiling using the API® ZYM system (bioMérieux UK Ltd, Basingstoke, UK), according to the manufacturer's instructions, for phenotypic characterisation. This work was performed by Dr Nicholas Evans (Department of Infection Biology, University of Liverpool) and Jennifer Brown, as described previously (Evans *et al*., 2011b). The spirochaete isolate was initially cultured to late exponential growth phase according to Chapter 2.3.3. The bacterial suspension was subsequently diluted in distilled water until its turbidity was equivalent to that of a 5 MacFarland standard (bioMérieux UK Ltd, Basingstoke, UK). The incubation chamber was humidified by adding 5 ml distilled water to the honeycombed wells. The sample reference was then recorded. The API® ZYM strip was placed into the humidified incubation chamber and 65 µl standardized spirochaete culture was added to each of the 19 reaction microwells. The negative control well received an equivalent volume of culture medium alone to account for its effect on the observed colour change. The incubation chamber was subsequently maintained at 37°C for four hours (Sanyo MCO-175 incubator). Following incubation, a single drop of ZYM A reagent and then ZYM B reagent were added to each reaction microwell and the incubation chamber was maintained at room temperature for five minutes to allow colour development. The incubation chamber was subsequently exposed to light for ten seconds to eliminate the colouration resulting from unreacted ZYM B reagent. Each enzyme reaction was observed and the colour recorded to assess positive or negative enzyme activity, with a colourless or pale yellow reaction indicative of no enzyme activity. The test was performed in triplicate as three independent experiments to confirm the isolate's enzyme activity profile. In addition, *Treponema vincentii* ATCC 35580, a treponeme with a previously determined enzyme activity profile (Schrank *et al*., 1999), was assessed alongside the spirochaete isolate to validate the API® ZYM system.

2.5 Preparation of treponeme cell sonicates

Sonication is a common method used to physically disrupt and lyse live bacterial cells through pulsing high frequency sound waves. According to a modified protocol which was originally described by Evans *et al.* (2014), treponeme cell sonicates were prepared from approximately 70 ml culture grown to late exponential phase (Chapter 2.3.3). Treponemes were initially pelleted by centrifugation (Avanti® J-E Centrifuge; Beckman Coulter Life

Sciences, Indianapolis, USA) at 4,500 *g* for 20 minutes (8°C) within 50 ml Nalgene™ Oak Ridge High-Speed centrifuge tubes (Thermo Scientific™, Hemel Hempstead, UK) and the supernatant was removed within a Class II Microbiological Safety Cabinet (Herasafe™ KS Class II Laminar Flow Cabinet; Thermo Scientific™, Hemel Hempstead, UK). Cells were washed a further two times in 30 ml 1x phosphate buffered saline (PBS, pH 7.2; Gibco™ by Life Technologies Ltd, Paisley, UK) by centrifugation at 4,500 *g* for 20 minutes (8°C). Treponemes were resuspended in 6 ml 1x PBS and transferred to a 20 ml Sterilin™ tube (Appleton Woods Ltd, Kings Norton, UK) for sonication. The cell suspension was subjected to sonication (Sonics Vibra-Cell™ VCX130 Ultrasonic Processor; VWR®, Lutterworth, UK) on ice for 4 minutes (optimal time determined) at 45% amplitude with continuous alternating 10-second cycles of sonication and resting. A small aliquot of the treponeme cell suspension (80 µl) was observed by phase contrast microscopy to verify successful cell disruption. Treponeme cell sonicate protein contents were quantified using a Qubit® Protein Assay Kit (Molecular Probes™ by Thermo Fisher Scientific, Loughborough, UK; Chapter 2.7) and then stored at -20°C until further use. For RNA-Seq, quantified treponeme cell sonicates were each diluted to an equivalent protein concentration of 10 µg/ml in control medium (WME containing 2 mM L-glutamine) for use.

2.6 Antigen preparation of treponeme cell cultures

Antigen preparations were produced from treponeme cell cultures which had been grown to late exponential phase under anaerobic conditions (Chapter 2.3.3) as previously described (Sullivan *et al.,* 2015c), based on a previously published protocol (Dhawi *et al.,* 2005). Within a Class II Microbiological Safety Cabinet, approximately 35 ml treponeme cell culture was transferred into a 50 ml Nalgene™ Oak Ridge High-Speed centrifuge tube and cells were then pelleted by centrifugation (Avanti® J-E Centrifuge; Beckman Coulter Life Sciences, Indianapolis, USA) at 12,000 rpm for 30 minutes at room temperature. Upon removal of the culture supernatant, cell pellets were resuspended in 17.5 ml 5 mM magnesium chloride ($MgCl_2$; Fisher Scientific UK Ltd, Loughborough, UK; Appendix A) and vortexed prior to the addition of and subsequent vortexing with a further 17.5 ml 5 mM $MgCl_2$. Cells were then washed by centrifugation at 12,000 rpm for 30 minutes at room temperature. Following removal of the supernatant, the cells were again resuspended and washed with 5 mM $MgCl_2$. Cells were resuspended in 3.5 ml 1x PBS (pH 7.2; Gibco™ by Life Technologies Ltd, Paisley, UK) and were then subjected to sonication using a probe (Pocklington, York, UK) on ice for 4 continuous alternating cycles of sonication (30 seconds) and resting (20 seconds). Sonicated

treponeme cell supernatants were supplemented with 70 µl Nonidet™ P 40 substitute (Sigma-Aldrich, Poole, UK) and 35 µl 100 mM ethylene glycol-bis(2-aminoethylether)-N,N,N',N'-tetraacetic acid (EGTA; Sigma-Aldrich, Poole, UK; Appendix A) and were then inverted several times to mix thoroughly. The sonicated supernatants were subsequently maintained under incubation (Sanyo MCO-175 incubator) at 36°C for 4 hours, with occasional mixing through inversion, and were then frozen (-20°C) for 1 hour. The supernatants were then thawed and underwent centrifugation at 12,000 rpm for 15 minutes at room temperature. Supernatants containing the treponeme antigens were dialysed (pre-soaked, 6.3 mm thickness dialysis tubing with a 12-14 kDa molecular weight cut-off; Medicell Membranes Ltd, London, UK) against 1 litre (L) 1x PBS (Sigma-Aldrich, Poole, UK; Appendix A) for 72 hours at 4°C, replacing the PBS approximately every 15 hours and 9 hours consecutively. Treponeme antigen preparations were quantified using a Qubit® Protein Assay Kit (Chapter 2.7) and stored at -20°C until further use. For RNA-Seq, quantified treponeme antigen preparations were each diluted to an equivalent protein concentration of 10 µg/ml in control medium (WME containing 2 mM L-glutamine) for use.

2.7 Protein quantification of treponeme cell lysate preparations

Quantification of protein in treponeme cell sonicates (Chapter 2.5) and antigen preparations (Chapter 2.6) were completed using a Qubit® Protein Assay Kit (Molecular Probes™ by Thermo Fisher Scientific, Loughborough, UK) and Qubit® 2.0 Fluorometer (Life Technologies Ltd, Paisley, UK) as per the manufacturer's instructions. A Qubit® working solution was prepared by performing a 1:200 dilution of Qubit® Protein Reagent in Qubit® Protein Buffer. Three protein standards were subsequently prepared by combining 190 µl Qubit® working solution with 10 µl of the appropriate Qubit® standard within a 0.5 ml PCR tube. Samples were prepared through addition of 1 µl treponeme preparation to 199 µl Qubit® working solution. All tubes were incubated at room temperature for 15 minutes prior to reading the protein concentration of standards and samples with the Qubit® 2.0 Fluorometer.

2.8 Investigating molecular diversity of a putative outer membrane protein of bovine digital dermatitis treponemes

2.8.1 Isolation and cultivation of treponemes

A panel of 115 treponeme isolates were investigated and comprised representatives of *T. medium* phylogroup (n = 33), *T. phagedenis* phylogroup (n = 69) and *T. pedis* (n = 13). Isolates were previously designated to a *Treponema* phylogroup or species based upon sharing over

97% *16S rRNA* gene sequence identity to one of the three representative strains, *T. medium* phylogroup strain T19, *T. phagedenis* phylogroup strain T320A and *T. pedis* strain T3552B^T (Evans *et al.,* 2008; Evans *et al.,* 2009a; Stackenbrandt & Goebel, 1994). The origin and details of the treponeme isolates belonging to each phylogroup are described in Appendix C, Table C.1, C.2 and C.3 respectively. As part of a MLST study on pathogenic treponemes, 108 of the treponeme isolates investigated here were previously re-cultured and purified for DNA extraction by Dr Simon Clegg (Department of Infection Biology, University of Liverpool), as described (Clegg *et al.,* 2016d). Further DNA preparations were required for 28 of these treponeme isolates and each underwent resuscitation and subculture for a minimum of two passages, according to Chapter 2.3, prior to DNA extraction (Chapter 2.4.1). The putative *Omp* gene sequences of a further 7 treponeme isolates (*T. medium* ATCC 700293, *T. vincentii* OMZ 838, *T. phagedenis* V1, *T. phagedenis* Reiter, *T. phagedenis* F0421, *T. phagedenis* 4A and *T. pedis* T A4; see Appendix C, Table C.1, C.2 and C.3) were taken from complete genome sequences which were available from the NCBI nucleotide database (NCBI Resource Coordinators, 2017).

2.8.2 Characterisation of treponeme isolates

The purity of each treponeme isolate was previously confirmed by Dr Simon Clegg (Clegg *et al.,* 2016d) using a treponeme phylogroup-specific 16S rRNA gene nested PCR assay, as described in Chapter 2.4.3. PCR products were visualised by agarose gel electrophoresis according to Chapter 2.2.2.

2.8.3 Identification of putative treponeme outer membrane proteins

Putative treponeme OMPs were initially identified from the complete, annotated genome sequences of *T. medium* phylogroup strain T19, *T. phagedenis* phylogroup strain T320A and *T. pedis* strain T3552B^T (Dr S.R. Clegg; unpublished) by Dr Stuart Ainsworth and Mr Gareth Staton (Department of Infection Biology, University of Liverpool) using a reverse vaccinology approach. A suitable bioinformatics pipeline was developed and subsequently used to identify putative treponeme OMPs based upon two of their most fundamental characteristics; typical β-barrel tertiary structure and presence of a signal peptide sequence (which is required for translocation to the outer membrane) (Schulz, 2002). SignalP software V4.0 (Petersen *et al.,* 2011) was initially used to predict the presence of signal peptide cleavage sites within the open reading frames (ORFs) of the *T. medium* phylogroup strain T19 genome sequence. Three independent software programmes, PRED-TMBB (Bagos *et al.,* 2004a), BOMP (Berven *et al.,* 2004) and TMBETA-NET (Gromiha, Ahmad & Suwa, 2005), were then used to screen these candidates for any predictions of the characteristic β-barrel

tertiary structure. A protein BLAST (Altschul *et al.,* 1990) was subsequently performed on each of the identified candidates against the genome sequences of both *T. phagedenis* phylogroup strain T320A and *T. pedis* strain T3552B^T to identify putative OMP candidates with homologs across each of the treponeme phylogroups, using an Expect value (E) cut-off of 1e-10.

Further selection criteria were subsequently implemented on the identified candidates to allow selection of a single putative OMP (with equivalent homologs across each of the DD treponeme phylogroups) based on a minimum cut-off value of 40% for inter-phylogroup homology. Due to the expense and time limitations of gene sequencing a large panel of treponeme isolates (n = 115), the selection of putative OMP candidates was further limited to that of a current Sanger sequence read; with a maximum gene size of 0.8 kbp. Protein homology and structural predictions were then determined, using the HHpred server (Söding, Biegert & Lupas, 2005; Alva *et al.,* 2016), to inform the final choice on a suitable putative treponeme OMP with homologs across the *T. medium* phylogroup*, T. phagedenis* phylogroup and *T. pedis* respectively.

2.8.4 Modelling the structural topology of a putative treponeme outer membrane protein

Structural topologies of the chosen putative *T. medium* phylogroup, *T. phagedenis* phylogroup and *T. pedis* OMP homologs (Chapter 5.2.1) were predicted and subsequently modelled using PRED-TMBB (Bagos *et al.,* 2004a). Using a hidden Markov model, PRED-TMBB is able to predict the transmembrane β-strands of Gram-negative bacterial OMPs to a per-residue accuracy of at least 84.2% (Bagos *et al.,* 2004b). The amino acid sequences of each putative OMP homolog were extracted from the complete, annotated genome sequences of either *T. medium* phylogroup strain T19, *T. phagedenis* phylogroup strain T320A or *T. pedis* strain T3552B^T (Dr S.R. Clegg; unpublished) using Artemis (Rutherford *et al.,* 2000). The amino acid sequences were subsequently used to generate a structural topology model for each putative OMP homolog using PRED-TMBB to predict extracellular, periplasmic and transmembrane domains (Bagos *et al.,* 2004a).

The amino acid sequences of each putative treponeme OMP homolog were aligned with amino acid sequences of the six most structurally homologous proteins (as determined using the HHPRED server; see Chapter 5.2.1), using CLUSTAL W (Thompson *et al.,* 1994) in the Bioedit Sequence Alignment Editor (Hall, 2013), to identify conserved amino acids which may confer functional significance. Sequence alignments were analysed using MEGA V6.0

(Tamura *et al*., 2013) and conserved amino acid residues were subsequently mapped onto the structural topology model.

Any non-synonymous (d_N) substitutions identified from the sequenced isolates (Chapter 2.8.9) were also mapped onto the structural topology model to determine their predicted localisation to extracellular, periplasmic or transmembrane domains.

2.8.5 Development and optimisation of novel treponeme *Omp* gene PCR assays

Three novel PCR assays were developed and optimised to each amplify one of the chosen putative treponeme *Omp* gene homologs (Chapter 5.2.1) across a range of *T. medium* phylogroup, *T. phagedenis* phylogroup and *T. pedis* isolates, as described in Chapter 2.8.1.

The gene sequences of each putative OMP homolog were extracted from the complete, annotated genome sequences of either *T. medium* phylogroup strain T19, *T. phagedenis* phylogroup strain T320A and *T. pedis* strain T3552B^T respectively (Dr S.R. Clegg; unpublished) using Artemis (Rutherford *et al.,* 2000). A nucleotide BLAST was performed to identify the nearest relatives of each putative treponeme *Omp* gene for subsequent alignment within the Bioedit Sequence Alignment Editor (Hall, 2013) using CLUSTAL W (Thompson *et al.,* 1994). Forward and reverse primers (Table 2.5) were subsequently designed within conserved regions of each trimmed (624 bp, 678 bp and 621 bp, respectively) sequence alignment for the putative *T. medium* phylogroup, *T. phagedenis* phylogroup and *T. pedis Omp* genes, using the MOPS (Eurofins Genomics, 2016) to ensure satisfaction of specific primer design criteria (Thermo Fisher Scientific, 2016), as described in Chapter 2.4.4. A nucleotide BLAST (Altschul *et al.,* 1990) was performed against the corresponding treponeme genomes (*T. medium* phylogroup strain T19, *T. phagedenis* phylogroup strain T320A or *T. pedis* strain T3552B^T; Dr S.R. Clegg; unpublished) for each oligonucleotide primer sequence to ensure specificity for the target gene of interest. Primers were synthesised by Eurofins Genomics (Ebersberg, Germany).

Table 2.5 Novel primers designed to detect putative Omp gene homologs of T. medium phylogroup, T. phagedenis phylogroup and T. pedis by PCR. *Forward (F) and reverse (R) primer pair sequences used to detect putative Omp gene homologs of the T. medium phylogroup, T. phagedenis phylogroup and T. pedis by PCR for sequencing and subsequent analysis of molecular diversity. The predicted size of each amplified gene product is given in base pairs alongside the region of each gene being targeted.*

Primer specificity	Primer sequence	Predicted size (bp)	Gene region targeted (positions)	Reference
Putative *T. medium*	TmOmp-F1: 5'-ATGAAACGTTGTTGGTTATTTT-3'	624	1-22	This study

phylogroup *Omp* gene	TmOmp-F2: 5'-TGATATGGAATACCTTTGC-3'	586	38-56	
	TmOmp-R: 5'-TTAGAAGTGATATCGGGC-3'	-	607-624	
Putative *T. phagedenis* phylogroup *Omp* gene	TphOmp-F1: 5'-CGCATATTCTTTGTTTTAATTG-3'	671	7-28	This study
	TphOmp-F2: 5'-GGTTTCTTTGCTTTACTAATC-3'	646	32-52	
	TphOmp-R: 5'-TCAAAAGTGATATCGTGCTC-3'	-	659-678	
Putative *T. pedis Omp* gene	TpeOmp-F1: 5'-GTTCTTTTGTCTAATTACCG-3'	603	18-37	This study
	TpeOmp-F2: 5'-TTTTCGTTTTCCTGTTTTGC-3'	581	40-59	
	TpeOmp-R: 5'-TTAAAAATGATACCTTGCGG-3'	-	602-621	

The three putative *Omp* gene homologs of the *T. medium* phylogroup, *T. phagedenis* phylogroup and *T. pedis* (Chapter 5.2.1) were each initially amplified from 1 µl gDNA of the representative isolate from each phylogroup, namely *T. medium* phylogroup strain T19, *T. phagedenis* phylogroup strain T320A and *T. pedis* strain T3552B^{T} (Chapter 2.8.1), for the purposes of assay optimisation by Miss Janet Wong (School of Medicine, University of Liverpool). The 25 µl reaction included 10 µM phylogroup-specific putative treponeme *Omp* gene forward and reverse primers (Table 2.5), 20 mM dNTP mix (5 mM each of dATP, dCTP, dGTP, dTTP) and Taq DNA polymerase according to the manufacturer's instructions. Optimal primer pairings and PCR thermal cycling conditions were determined with a Mastercycler Gradient Thermocycler (Eppendorf, Hamburg, Germany) using an initial denaturation step at 95°C for 5 minutes; 40 cycles of 94°C for 1 minute, either 50°C ± 5°C (*T. medium* phylogroup) or 51°C ± 5°C (*T. phagedenis* phylogroup and *T. pedis*) for 3 minutes, and 72°C for 3 minutes; and a final extension step of 72°C for 7 minutes. Water was used as a negative control. Amplified PCR products were visualised by agarose gel electrophoresis, according to Chapter 2.2.2, to confirm that they were of the expected molecular weight. PCR products with a suitable yield, and amplified at the highest annealing temperatures to ensure specificity, underwent purification and sequencing to verify their identity, as described in Chapter 2.4.6. TmOmp-F1 and TmOmp-R (*T. medium* phylogroup), TphOmp-F1 and TphOmp-R (*T. phagedenis* phylogroup) and TpeOmp-F1 and TpeOmp-R (*T. pedis*) primer pairings (Table 2.5) were found to provide the most stringent PCR conditions using annealing temperatures of 58.1°C, 54.5°C and 57°C respectively. The optimal conditions identified here for each assay were used in all future putative treponeme *Omp* gene PCRs.

2.8.6 Amplification and sequencing of putative *Omp* genes from treponeme isolates

A panel of 108 treponeme isolates of the *T. medium* phylogroup, *T. phagedenis* phylogroup and *T. pedis* (Chapter 2.8.1) each underwent amplification of a putative treponeme phylogroup-specific *Omp* gene (Chapter 5.2.1) using a novel PCR assay as developed and optimised according to Chapter 2.8.5, with the help of Miss Janet Wong (School of Medicine, University of Liverpool).

A 25 µl PCR reaction was prepared on ice with 1 µl gDNA from the treponeme isolate (Chapter 2.8.1), 10 µM of the most stringent putative treponeme phylogroup-specific *Omp* gene forward and reverse primers (Chapter 2.8.5), 20 mM dNTP mix (5 mM each of dATP, dCTP, dGTP, dTTP) and *Taq* DNA polymerase according to the manufacturer's instructions. Optimal PCR thermal cycling conditions (Chapter 2.8.5) consisted of initial denaturation at 95°C for 5 minutes; 40 cycles of 94°C for 1 minute, then either 58.1°C (*T. medium* phylogroup) or 54.5°C (*T. phagedenis* phylogroup) or 57°C (*T. pedis*) for 3 minutes, and 72°C for 3 minutes; with a final extension step of 72°C for 7 minutes (Biometra TProfessional TRIO Thermocycler). Water was used as a negative control and the three representative treponeme isolates of each phylogroup (*T. medium* phylogroup strain T19, *T. phagedenis* phylogroup strain T320A and *T. pedis* strain T3552B^T) were used as a positive control. The PCR products were separated by agarose gel electrophoresis, according to Chapter 2.2.2. Amplified PCR products of the correct molecular weight were purified according to Chapter 2.4.5 and were then sequenced commercially (Macrogen, Amsterdam, The Netherlands) using the Sanger DNA sequencing method. Each sequence was assembled into a contiguous sequence using ChromasPro Sequence Analysis Package V2.0.0 (Technelysium Pty Ltd, South Brisbane, Australia) and manually curated to resolve disagreements between nucleotide sequence chromatograms.

2.8.7 Analysis of molecular diversity within a putative outer membrane protein of bovine digital dermatitis treponemes

The contiguous putative *Omp* gene sequences from isolates of the *T. medium* phylogroup (n = 31), *T. phagedenis* phylogroup (n = 65) and *T. pedis* (n = 12) respectively, as amplified and sequenced according to Chapter 2.8.6, were each aligned within the Bioedit Sequence Alignment Editor (Hall, 2013) using CLUSTAL W (Thompson *et al.,* 1994). Putative treponeme *Omp* gene sequences of a further seven treponeme isolates taken from complete genome sequences available from the NCBI nucleotide database (Chapter 2.8.1) were also included in phylogroup-specific gene sequence alignments. Therefore, a total of 33 *T. medium*

phylogroup, 69 *T. phagedenis* phylogroup and 13 *T. pedis* putative *Omp* gene sequences were included for analysis of molecular diversity (Chapter 2.8.8 to 2.8.12). Sequence alignments were trimmed in Bioedit Sequence Alignment Editor (Hall, 2013). The length of gene and amino acid sequences were determined from trimmed sequence alignments. *Omp* alleles were designated manually from trimmed sequence alignments in MEGA V6.0 (Tamura *et al.,* 2013). The average GC content (%) of each putative *Omp* gene sequence was determined from trimmed sequence alignments using the Datamonkey web server (Pond & Frost, 2005). The mean *p*-distances (and standard error) of gene and amino acid sequence alignments, which correspond to the proportion of nucleotide or amino acid sites, respectively, at which two sequences are different, were calculated for each putative treponeme OMP homolog using MEGA V6.0 (Tamura *et al.,* 2013). The putative *Omp* gene sequences of each representative *Treponema* strain (T19, T320A and T3552B^{T} respectively) were extracted from complete, annotated genome sequences (Dr S.R. Clegg; unpublished) using Artemis (Rutherford *et al.,* 2000) and each *Omp* gene was subsequently screened for the presence of homopolymeric tracts (a repetitive sequence of consecutive nucleotides) using the Bioedit Sequence Alignment Editor (Hall, 2013).

2.8.8 Phylogenetic analysis of putative treponeme *Omp* genes

Trimmed putative *Omp* gene sequence alignments of the *T. medium* phylogroup (n = 33), *T. phagedenis* phylogroup (n = 69) and *T. pedis* (n = 13) isolates (Chapter 2.8.7) were used to produce a sequence identity matrix within the Bioedit Sequence Alignment Editor (Hall, 2013). The most appropriate evolutionary models for phylogenetic inference of each trimmed sequence alignment were then predicted using ModelTest software in the TOPALi v2 program (Milne *et al.,* 2009). The Tamura-Nei model (Tamura & Nei, 1993), Jukes-Cantor model (Jukes & Cantor, 1969) and Hasegawa-Kishino-Yano model (Hasegawa, Kishino & Yano, 1985) were each used to produce a bootstrapped maximum-likelihood phylogenetic tree (based upon 10,000 reiterations) of the trimmed putative *Omp* gene sequence alignments for the *T. medium* phylogroup, *T. phagedenis* phylogroup and *T. pedis* respectively, as implemented in MEGA V6.0 (Tamura *et al.,* 2013).

2.8.9 Analysis of the purifying and diversifying selection pressures on a putative outer membrane protein of bovine digital dermatitis treponemes

The number of variable sites within both trimmed gene and amino acid sequence alignments (Chapter 2.8.7) were determined using MEGA V6.0 (Tamura *et al.,* 2013) and the ratios of non-synonymous (d_N) to synonymous (d_S) substitutions (d_N/d_S) were calculated manually.

Whilst d_N/d_S ratios of 1 are typically considered to define evidence of no selection pressures, those below 1 are considered to provide evidence of negative or purifying selection (the elimination of d_N substitutions) and those above 1 are considered to provide evidence for positive or diversifying selection. Trimmed amino acid sequence alignments for each putative OMP homolog were also subsequently screened for positive and negative selection pressures using GARD and SLAC available through the Datamonkey web server (Pond & Frost, 2005).

2.8.10 Split decomposition analysis

The trimmed putative *Omp* gene sequence alignments for *T. medium* phylogroup, *T. phagedenis* phylogroup and *T. pedis* isolates (Chapter 2.8.7) were each screened for evidence of recombination by split decomposition analysis using SplitsTree4 V4.14.5 (Huson & Bryant, 2006). Inter-phylogroup recombination was assessed by combining the trimmed putative *Omp* gene sequence alignments.

2.8.11 Comparing putative outer membrane protein diversity with the multilocus sequence typing of bovine digital dermatitis treponemes

The designated alleles (Chapter 5.2.3) of each putative treponeme OMP homolog were comparatively analysed alongside MLST data of seven housekeeping gene loci (as previously published; Clegg *et al.,* 2016d) to determine whether the OMP was able to further delineate isolate variation across the 33 *T. medium,* 69 *T. phagedenis* and 13 *T. pedis* isolates (Chapter 2.8.1).

For each isolate, sequence data for *GroEL*, *recA*, *GlpK*, *AdK*, *GDH*, *PyrG*, *RplB* (Clegg *et al.,* 2016d) and the putative *Omp* genes (as generated during this study) were concatenated and subsequently aligned and trimmed using MEGA V6.0 (Tamura *et al.,* 2013) by Dr S.R. Clegg (Department of Infection Biology, University of Liverpool). The most appropriate evolutionary models for phylogenetic inference of each trimmed concatenated gene sequence alignment were predicted using ModelTest software in the TOPALi v2 program (Milne *et al.,* 2009) by Dr S.R. Clegg. The generalised time reversible model (Tavare, 1986) was used to produce bootstrapped maximum-likelihood phylogenetic trees (based upon 10,000 reiterations) of the trimmed concatenated gene sequence alignments for each BDD treponeme phylogroup by Dr S.R. Clegg, as implemented in MEGA V6.0 (Tamura *et al.,* 2013). Minimum spanning distance trees were drawn with the PHYLOViZ web server (Francisco *et al.,* 2012) and pie charts demonstrating species diversity within each ST were superimposed onto each node; each performed by Dr S.R. Clegg. In each case, the above analyses were

completed both including and excluding the sequence data for each corresponding putative OMP within the concatenated gene sequence alignments for comparison.

2.8.12 Comparison of putative outer membrane protein amino acid sequences of commensal and pathogenic treponemes

The amino acid sequences of each putative OMP homolog were extracted from the complete, annotated genome sequences of *T. medium* phylogroup strain T19, *T. phagedenis* phylogroup strain T320A and *T. pedis* strain T3552B^T respectively (Dr S.R. Clegg, unpublished) using Artemis (Rutherford *et al.,* 2000). A protein BLAST was performed against each of these sequences to identify and subsequently extract amino acid sequences of putative OMP homologs within other recognised *Treponema* species from the NCBI protein database (NCBI Resource Coordinators, 2017). The amino acid sequences of a further two putative OMP homologs were extracted from the complete, annotated genome sequences of commensals, *T. ruminis* and *T. rectale* (Dr S.R. Clegg, unpublished). The amino acid sequences of all putative treponeme OMPs were subsequently aligned and trimmed in the Bioedit Sequence Alignment Editor (Hall, 2013) using CLUSTAL W (Thompson *et al.,* 1994) and the 154 amino acid sequence alignment was used to produce a sequence identity matrix. The most appropriate evolutionary model for phylogenetic inference of the putative OMP amino acid sequence alignment was predicted using ModelTest software in the TOPALi v2 program (Milne *et al.,* 2009). The General Reversible Chloroplast (cpREV) model (Adachi *et al.,* 2000), specifically implementing gamma distribution and invariant sites (G+I), was subsequently used to produce a bootstrapped maximum-likelihood phylogenetic tree of the putative OMP amino acid sequence alignment, based on 10,000 reiterations, using MEGA V6.0 (Tamura *et al*., 2013).

2.9 RNA extraction, quantification and quality control

Total RNA was extracted from primary bovine foot skin cell cultures (Chapter 2.1.3) grown to approximately 80% confluence within 25 cm^3 tissue culture flasks. RNA was quantified (Chapter 2.9.3) and then further examined for adequate quality, including an assessment of integrity and purity (Chapter 2.9.4), prior to further use. RNA was either converted into cDNA (Chapter 2.10) for analysis by PCR (Chapter 2.2.1) or processed for RNA-Seq (Chapter 2.11).
All equipment and work surfaces were thoroughly disinfected with RnaseZap® ribonuclease (Rnase) decontamination solution (Ambion™ by Thermo Fisher Scientific, Loughborough, UK) prior to use. Molecular grade nuclease-free water (Ambion™ by Thermo Fisher Scientific, Loughborough, UK) and Rnase-free microcentrifuge tubes were used throughout. Unless

otherwise stated, centrifugation was completed at room temperature using a Sigma 2K15 refrigerated microcentrifuge for all RNA extractions and quality control procedures.

2.9.1 Harvesting primary bovine foot skin cell cultures for total RNA extraction

Following the removal of culture medium from 25 cm^3 tissue culture flasks, primary bovine foot skin cell monolayers were gently washed three times with 5 ml sterile 1x HBSS before the addition of 1 ml 0.025% (w/v) or 0.25% (w/v) trypsin-EDTA to facilitate the dissociation of fibroblast or keratinocyte cells respectively. Flasks were transferred to a humidified incubator (37°C, 5% CO_2) for 5 or 8 minutes until respective fibroblast or keratinocyte cells had sufficiently detached from the flask surface, as confirmed by phase contrast microscopy. Following neutralisation of the trypsin-EDTA through addition of 4 ml WME containing 10% (v/v) FBS, a serological pipette was used to thoroughly detach cells from the flask surface. The contents of each flask were transferred to a 15 ml conical centrifuge tube and each flask was washed a further two times with 5 ml sterile 1x HBSS. Cells were pelleted by centrifugation at 180 *g* for 10 minutes at room temperature and washed a further two times with 10 ml sterile 1x HBSS. The supernatants were removed and cell pellets immediately frozen at -80°C for subsequent RNA extraction.

2.9.2 Total RNA extraction from primary bovine foot skin cell cultures

Total RNA was extracted from primary bovine foot skin cells using an RNeasy® Plus Mini Kit (Qiagen, Manchester, UK) according to an optimised protocol which was modified from the manufacturer's instructions. Harvested cell pellets (Chapter 2.9.1) were thawed and subsequently dislodged from the side of the tube by flicking. Upon addition of 350 µl Buffer RLT Plus containing 1% (v/v) 2-mercaptoethanol (BDH Laboratory Supplies, Poole, UK), cell pellets were briefly vortexed for 5 seconds to mix and the disrupted cells were then homogenised by vortexing for a further 1 minute. The homogenised lysate was thoroughly mixed by pipetting and was then carefully transferred to a gDNA eliminator column placed within a 2 ml collection tube. Following centrifugation at 10,000 *g* for 30 seconds at room temperature, any residing gDNA was bound to the column for subsequent disposal, whilst RNA in the flow-through was saved for further processing. Following the addition of 350 µl 70% (v/v) molecular grade ethanol (Sigma-Aldrich, Poole, UK), the homogenised lysate was thoroughly mixed by pipetting and up to 700 µl was subsequently transferred to an RNeasy® spin column placed within a 2 ml collection tube. The column underwent centrifugation at 10,000 *g* for 15 seconds at room temperature and the resulting flow-through was carefully discarded by pipetting to avoid ethanol carryover. The RNeasy® spin column was then washed with 700 µl Buffer RW1 by centrifugation at 10,000 *g* for 15 seconds at room

temperature, again discarding the flow-through by pipetting. Following a further addition of 500 µl Buffer RPE, the column was washed by centrifugation at 10,000 *g* for 15 seconds at room temperature, and again for 2 minutes with an additional 500 µl Buffer RPE. Each time the flow-through was discarded by pipetting. The RNeasy® spin column was subsequently transferred to a new 2 ml collection tube for centrifugation at 10,000 *g* for 1 minute at room temperature to dry the membrane. The spin column was then transferred to a 1.5 ml collection tube and the membrane was allowed to air dry at room temperature for a further 15 minutes. Following the direct application of 30 µl Rnase-free water to the membrane and incubation for 1 minute at room temperature, RNA was eluted from the column by centrifugation at 10,000 *g* for 1 minute at room temperature. RNA preparations were immediately stored at -80°C in aliquots for further use to avoid unnecessary freeze-thaw cycles.

2.9.3 Quantification of total RNA preparations

Total RNA preparations (Chapter 2.9.2) were quantified using a Qubit® RNA Broad-Range (BR) Assay Kit (Invitrogen™, Loughborough, UK) and Qubit® 2.0 Fluorometer, according to the manufacturer's instructions. For RNA-Seq, a minimum concentration of 37 ng/µl (1000 ng) total RNA was required.

Initially, a Qubit® working solution was prepared by making a 1:200 dilution of the Qubit® RNA BR Reagent in Qubit® RNA BR Buffer. Two standards were then produced by combining 190 µl Qubit® working solution with 10 µl of the appropriate Qubit® standard within a 0.5 ml PCR tube, vortexing for 3 seconds to mix thoroughly. Samples were prepared through the addition of 1 µl RNA preparation to 199 µl Qubit® working solution, vortexing for 3 seconds to mix thoroughly. All tubes were subsequently allowed to incubate at room temperature for 2 minutes prior to reading the standards and samples on a Qubit® 2.0 Fluorometer.

2.9.4 Quality control of total RNA preparations

To ensure that the total RNA preparations (Chapter 2.9.2) were of sufficient quality for downstream applications, RNA integrity and purity were assessed and confirmed prior to further use.

RNA integrity was assessed with a Eukaryote Total RNA 6000 Nano Electrophoretic Assay (Agilent Technologies Inc., Santa Clara, USA) using an Agilent 2100 Bioanalyser and 2100 Expert Software VB.02.08 (Agilent Technologies Inc., Santa Clara, USA), according to the manufacturer's instructions. Following filtration of the Agilent RNA 6000 Nano gel matrix through a spin filter column by centrifugation at 1,500 *g* for 10 minutes at room temperature, 1 µl RNA Nano dye concentrate was added to a 65 µl aliquot of filtered gel. The gel-dye mix

was thoroughly vortexed and then underwent centrifugation at 13,000 *g* for 10 minutes at room temperature prior to immediate use in preparing the electrophoretic chip. An RNA Nano chip was placed onto the priming station and 9 µl gel-dye mix was loaded into the required well for subsequent priming with a syringe. Two further wells were then loaded with 9 µl gel-dye mix to complete the chip priming procedure. All sample and ladder wells were subsequently loaded with 5 µl Agilent RNA 6000 Nano Marker. RNA preparations (1 µl) were heat denatured (QBT2 dry block heater; Grant Instruments Ltd, Royston, UK) at 70°C for 2 minutes prior to loading into the corresponding sample wells of the chip to reduce the impact of secondary structures. Any unused sample wells were alternatively loaded with 1 µl Rnase-free water. The Agilent RNA 6000 ladder, previously denatured by heating at 70°C for 2 minutes, was thawed on ice and 1 µl loaded into the corresponding well. The RNA Nano chip was subsequently vortexed at 2,400 rpm for 1 minute using an IKA Vortex Mixer (Agilent Technologies Inc., Santa Clara, USA) to thoroughly mix the reagents. Upon completion, the chip was immediately inserted into the Agilent 2100 bioanalyser for analysis. Preparations with an RNA integrity number (RIN) of 9.0 or over were considered of sufficient integrity for further use in downstream applications.

RNA purity was assessed by the measurement of A260:A280 and A260:A230 ratios using a NanoDrop™ ND-2000 spectrophotometer (Thermo Fisher Scientific, Loughborough, UK), according to the manufacturer's instructions. The spectrophotometer was blanked against 1 µl Rnase-free water and RNA purity was subsequently assessed from a single 1 µl aliquot of well-mixed RNA preparation. Values equal to or above 1.80 for both ratios were considered sufficient for further use in downstream applications.

2.10 cDNA production by reverse transcription

Total RNA preparations of sufficient quantity and quality (Chapter 2.9), which were extracted from primary bovine foot skin cell cultures (Chapter 2.1.3), were reverse transcribed to synthesise first-strand cDNA using SuperScript® III Reverse Transcriptase (Invitrogen™, Loughborough, UK) according to the manufacturer's instructions. All incubation steps were completed using a QBT2 dry block heater. Firstly, 500 ng total RNA was combined with 1 µl 0.5 µg/µl oligo(dT)$_{12\text{-}18}$ primer (Invitrogen™, Loughborough, UK), 1 µl 10 mM dNTP mix (Invitrogen™, Loughborough, UK) and up to 11 µl nuclease-free water within a 1.5 ml microcentrifuge tube. Preparations were mixed thoroughly by pipetting and then underwent incubation at 65°C for 5 minutes before being placed on ice for a further 5 minutes. Upon brief centrifugation to collect the tube contents, preparations were combined with 1 µl

RNaseOUT™ Recombinant RNase Inhibitor (Invitrogen™, Loughborough, UK), 4 µl 5x first-strand buffer, 1 µl 0.1M dithiothreitol and 1 µl SuperScript® III reverse transcriptase. First-strand cDNA was synthesised by incubating the preparations at 50°C for 60 minutes and the reaction was then inactivated by incubation at 70°C for 15 minutes. Until further use, cDNA preparations were stored at -20°C.

Prior to the use of RNA preparations in sensitive downstream applications, such as RNA-Seq, it is important to confirm that any contaminating gDNA was successfully eliminated during the RNA extraction procedure (Chapter 2.9.2). Contaminating gDNA can be indiscriminately amplified alongside cDNA and is therefore a potential source of false positive data. Alongside the production of first-strand cDNA by reverse transcription, RNA preparations were also used to produce an equivalent RT- control for the purposes of monitoring each preparation for gDNA. The RT- controls were prepared in an identical manner to the cDNA preparations, except that 1 µl Rnase-free water replaced the addition of 1 µl SuperScript® III reverse transcriptase. In the absence of reverse transcriptase within the RT- control preparations, gDNA was identified by visible amplification of the abundant housekeeping gene, *GAPDH*, as determined by PCR (Chapter 2.2.1). RNA preparations which were confirmed to be contaminated with gDNA were not used for further downstream applications.

2.11 RNA sequencing analysis

2.11.1 Co-incubation of primary bovine foot skin fibroblast cell monolayers with treponeme constituents

Whilst the use of live bacterial preparations can be far more representative of the host-pathogen interactions observed *in vivo*, it is the specific molecular components of treponemes which are likely to come into direct contact with the host and such interactions can greatly inform key mechanisms of BDD pathogenesis. Initial co-incubation experiments were attempted with antigen preparations purified from live treponeme cultures (Chapter 4.2.2), however were later attempted (and successfully analysed by RNA-Seq) using cell lysate prepared by sonication of live treponeme cultures (Chapter 4.2.3).

Primary bovine foot skin fibroblasts were seeded at a cell density of $1x10^5$ into 25 cm^3 tissue culture flasks in 5 ml fibroblast-specific complete WME (Chapter 2.1.1). Cultures were maintained within a humidified incubator (37°C, 5% CO_2) for approximately four days, according to Chapter 2.1.3, until the cell monolayer reached 80% confluence. Cell monolayers were washed three times with five volumes of sterile 1x HBSS and subsequently each co-incubated with either 3 ml control medium (WME containing 2 mM L-glutamine), 3

ml (10 µg/ml) purified LPS from *Salmonella enterica* serotype Typhimurium (Sigma-Aldrich, Poole, UK; Appendix A) as a non-specific inflammatory stimulant control, 3 ml (10 µg/ml) treponeme antigen preparation (Chapter 2.6) or 3 ml (10 µg/ml) treponeme cell sonicate/lysate (Chapter 2.5). Phase contrast microscopy was used to confirm that cell monolayers remained intact. Cells were then maintained within a humidified incubator (37°C, 5% CO_2) for six hours. Following incubation, phase contrast microscopy was again used to confirm monolayers remained intact. Treatments were subsequently removed and cell monolayers immediately harvested for total RNA extraction, as described in Chapter 2.9.1. To confirm successful removal of gDNA contaminants during RNA extraction, a representative preparation for each independent experimental replicate (designated "QC") was reverse transcribed to cDNA, alongside an equivalent RT- control, for RT-PCR analysis according to Chapter 2.10.

Three independent experimental replicates were performed on different days and each experiment included three technical replicates for each parameter under study. The experimental design of this study was limited by the large economic costs of RNA-Seq. Accordingly, the number of experimental replicates chosen was not based upon any specific sample size calculations but rather based upon economic limitations of this study.

2.11.2 RNA-Seq analysis of bovine foot skin fibroblasts following treponeme challenge

Total RNA preparations of sufficient quantity and quality (Chapter 2.4.3 and 2.4.4) were processed for RNA-Seq by Dr Nichola Rockliffe and Dr Anita Lucaci at the Centre for Genomic Research (CGR), University of Liverpool. Dr Richard Gregory (CGR) then assessed the quality of sequenced reads and trimmed these accordingly (Chapter 2.11.3). All subsequent downstream data processing and analysis (Chapter 2.11.4 to 2.11.8) was completed solely by the author unless otherwise stated.

A reference-based assembly approach was chosen to implement transcriptional profiling. Trimmed, sequenced reads for each sample were mapped to the *Bos taurus* genome (UMD 3.1.1/bosTau8; GenBank Assembly Accession Number GCA_000003055.5) and were then assembled into transcripts for comparative analysis of differential gene expression and assessment of replicate quality. Each stage of the analyses was implemented using the Galaxy platform's main public server, http://usegalaxy.org (Afgan *et al.,* 2016).

Ribosomal RNA depletion

Upon submission to the CGR, each total RNA preparation underwent further quantification and quality control assessment to later allow direct comparisons between total RNA and corresponding ribosomal RNA (rRNA)-depleted RNA preparations. For this, a Eukaryote Total RNA 6000 Pico Electrophoretic Assay was performed using an Agilent 2100 Bioanalyser (Agilent Technologies Inc., Santa Clara, USA), as per manufacturer's instructions.

Total RNA preparations (1000 ng) were subsequently rRNA-depleted using a Ribo-Zero™ Gold rRNA removal (human/mouse/rat) kit (Illumina®; San Diego, USA), as per manufacturer's instructions. Purified rRNA-depleted RNA was eluted in 8.5 µl RNase-free water and samples immediately placed on ice for quality assessment with the Eukaryote Total RNA 6000 Pico Electrophoretic Assay, as above.

To determine whether rRNA depletion had been successful enough for use in the preparation of cDNA libraries for NGS, the quantity (ng) of each corresponding total RNA and rRNA-depleted RNA preparation was used to calculate percentage RNA recovery. Purified rRNA-depleted RNA was considered sufficient quality if the RNA recovery percentage upon depletion was <10% of the input total RNA. Bioanalyzer traces of total RNA and rRNA-depleted RNA were overlaid using 2100 Expert Software (Agilent Technologies Inc., Santa Clara, USA) to confirm absence of all previously observed rRNA peaks and new peaks (indicating RNA degradation) upon Ribo-Zero™ depletion. All total RNA preparations submitted to the CGR were considered to have been successfully depleted of rRNA, except one sample which required a further round of rRNA depletion (Chapter 4.2.3, Table B.1).

Preparation of cDNA libraries for RNA-Seq

The purified rRNA-depleted RNA preparations (5 µl) were used to prepare cDNA libraries for subsequent NGS using a NEBNext® Ultra™ Directional RNA Library Prep Kit for Illumina® (New England Biolabs (UK) Ltd, Hertfordshire, UK), according to the manufacturer's instructions. PCR-enriched, adaptor ligated cDNA libraries were eluted in 23 µl 0.1x Tris-EDTA (TE) buffer and stored at -20°C.

The cDNA libraries underwent quantification and quality assessment prior to multiplexing (pooling). Each cDNA library (2-3 µl) was diluted (1:4) in 0.1 x TE buffer and then 1 µl was used for quantification using a Qubit® dsDNA High Sensitivity (HS) Assay Kit (Invitrogen™, Loughborough, UK) and Qubit® 2.0 Fluorometer, according to manufacturer's instructions. A further 1 µl of each diluted cDNA library was used to assess quality using an Agilent High Sensitivity DNA Kit using an Agilent 2100 Bioanalyser and 2100 Expert Software VB.02.08 (Agilent Technologies Inc., Santa Clara, USA), as per manufacturer's instructions. The cDNA libraries were expected, and confirmed, to have an electropherogram peak size of ~300 bp

and a narrow distribution to be of sufficient quality for RNA-Seq. The average fragment size (bp) of each cDNA library was determined.

Multiplexing, qRT-PCR and RNA-Seq

The cDNA libraries were pooled (two pools of 10 samples) in equimolar amounts, as calculated using the quantification (Qubit) and quality (Agilent) data. Quantity and quality of pooled cDNA libraries were further assessed using the Qubit® dsDNA HS Assay Kit and Agilent High Sensitivity DNA Kit.

Subsequently, a qRT-PCR assay designed to specifically amplify cDNA flanked by Illumina® adaptors was performed, using an Illumina® KAPA Library Quantification Kit (Kapa Biosystems, Wilmington, USA) as per manufacturer's instructions. This assay specifically quantifies the number of cDNA templates containing adaptor sequences at both ends and, therefore, those that could successfully form clusters on a flowcell for sequencing. The PhiX Control V3 (Illumina®, San Diego, USA) was quantified and subsequently prepared alongside the pooled cDNA libraries as a positive internal control library. Thermal cycling was completed using a LightCycler® LC48011 (Roche Diagnostics Ltd, Burgess Hill, UK).

Prior to sequencing, clustering of the cDNA templates was performed using a HiSeq® 3000/4000 Paired-End (PE) Cluster Kit with a cBot™ Cluster Generation System (Illumina®, San Diego, USA), according to manufacturer's instructions. Denatured template cDNA (alongside a 1% spike of PhiX Control library) was diluted to a 3 nM stock concentration, using qPCR and bioanalyser data to calculate molarity, and 5 µl used to achieve a loading concentration of 300 pM in a 50 µl final reaction volume on the flow cell for clustering. During clustering, the templates were immobilized onto a proprietary flow cell surface, designed to present the DNA in such a manner to facilitate access to enzymes whilst maintaining high stability of surface-bound template and low non-specific binding of fluorescently labelled nucleotides. Up to 1000 identical copies of each single template molecule were created through exclusion amplification cluster amplification that ensures only a single DNA template binds and forms a cluster within a single well of the patterned flow cell.

Following cluster generation, libraries were sequenced on an Illumina® HiSeq™4000 (Illumina®, San Diego, USA) with version 1 chemistry using sequencing by synthesis technology to generate 2 x 150 bp paired-end reads. This allowed the sequencing of tens of millions of clusters on the flow cell surface in parallel.

2.11.3 Quality control and trimming of raw sequencing reads

Raw sequencing reads (FASTQ format) obtained for each sample (Chapter 2.11.2) were trimmed using option -O 3 in Cutadapt V1.2.1 (Martin, 2011) to exclude those matching

Illumina adaptor sequences (≥3 bp) at the 3' end. Reads were further trimmed to exclude those of poor quality, implementing a minimum window quality score of 20, and those less than 10 bp after trimming, using Sickle V1.200 (Joshi & Fass, 2011). Trimmed sequenced reads were included within their corresponding R1 and R2 files (forward and reverse reads respectively) if both reads from a pair were of sufficient quality. Where only one read of a pair was of sufficient quality, the unpaired read was included in the R0 (singlet) file; however, this was not used in downstream analysis.

2.11.4 Read mapping to the *Bos taurus* genome

FASTQ files containing the trimmed forward (R1) and reverse (R2) paired-end reads for each RNA-Seq sample (Chapter 2.11.3) were uploaded onto the Galaxy platform's main public server, http://usegalaxy.org (Afgan *et al.,* 2016), through a local file transfer protocol client, FileZilla (http://filezilla-project.org/index.php). Each FASTQ file was converted into the standard Sanger quality score format (required for downstream analysis in Galaxy tools) using FASTQ Groomer (Galaxy tool V1.0.4; Blankenberg, 2010). Trimmed forward and reverse read pairs (groomed R1 and R2 files) for each sample were mapped to the *Bos taurus* reference genome (UMD 3.1.1/bosTau8; GenBank Assembly Accession Number GCA_000003055.5) using the fast splice junction mapper, TopHat2 (Galaxy tool V2.1.0; Daehwan *et al.,* 2013). Paired-end mapping parameters remained as default, allowing a maximum of two read mismatches. However, altered parameters included a mean inner distance between mate pairs of 160 bp ± 60 bp standard deviation, a FR firststrand library type and a maximum of one read alignment to the bovine genome to avoid multiple alignment biases. An overall read mapping rate of 70% to 90% was expected for successful read mapping. The Integrative Genome Viewer was used to inspect each output binary alignment/map (BAM) file to ensure reads were correctly mapped to exons of the *Bos taurus* reference genome (Robinson *et al.,* 2011; Thorvaldsdóttir *et al.,* 2013).

2.11.5 Normalisation of expression data

To assess quality and variation within experimental replicates, Cuffnorm (Galaxy tool V2.2.1.1; Trapnell *et al.,* 2010) was implemented by Galaxy (Afgan *et al.,* 2016) to provide normalised expression data on each individual replicate.

Initially, a master transcriptome assembly was prepared for accurate and uniform comparative expression profiling between treatment groups. Mapped reads for each sample (Chapter 2.11.4) were assembled into transcripts by Cufflinks (Galaxy tool V2.2.1; Trapnell *et al.,* 2010), using a gene transfer format (GTF) file of the annotated *Bos taurus* genome (UMD 3.1.1/bosTau8; ftp://ftp.ensembl.org/pub/release-88/gtf/bos_taurus; GenBank Assembly

Accession Number GCA_000003055.5) as a reference. This genome assembly was manually curated by Professor Mark Lindsay (University of Bath), through the addition of chromosome identifiers ("Chr"), to circumvent initial incompatabilities with the assembled transcripts. Transcript assembly was completed using default parameters; however, bias correction and multi-read correct were also enabled. Cuffmerge (Galaxy tool V2.2.1.0; Trapnell *et al.,* 2010) was subsequently used (default parameters) to combine all assembled transcripts (GTF) with the annotated *Bos taurus* genome (as above) to produce the final transcriptome assembly. Mapped read (BAM) files corresponding to replicates for each treatment group were uploaded into Cuffnorm, alongside the master transcriptome assembly (GTF), to generate normalised gene expression profiles for each replicate using default parameters.

2.11.6 Analysis of variance in normalised expression data

Fragment per kilobase of transcripts per million mapped reads (FPKM) expression data (Chapter 2.11.5) for the 20 most upregulated and downregulated genes across each treatment group (Chapter 2.11.7) were displayed as heatmaps, using Genesis V1.8.1 (Sturn *et al.,* 2002), to compare variation across each experimental replicate.

2.11.7 Analysis of differential gene expression

Global differential gene expression profiles of bovine foot skin fibroblasts were generated for each treatment group under comparison (each compared to the media control) through implementation of Cuffdiff in Galaxy (Galaxy tool V2.2.1.3; Trapnell *et al.* 2010). Each profile represented mean FPKM gene expression across three experimental replicates (and an additional technical replicate if applicable). Mapped read (BAM) files (Chapter 2.11.4) corresponding to replicates for each treatment and control group comparison were uploaded into Cuffdiff alongside the master transcriptome assembly (GTF) (Chapter 2.11.5) and the resulting expression profiles extracted for further analysis. Cuffdiff parameters largely remained as default; including the use of geometric library normalisation, pooled dispersion estimation method and a false discovery rate (FDR) of 0.05. However, again, multi-read correct and bias correction were enabled. Differentially expressed genes with a p value ≤ 0.05 and an adjusted p value (q value or FDR) ≤ 0.05 were considered statistically significant. To establish the most appropriate log2 fold change cut-off values, which were both inclusive yet stringent, both lower stringency (≥ 1 and ≤ -1) and higher stringency (≥ 2 and ≤ -2) strategies were initially implemented (Chapter 4.2.4.3).

Venn diagrams were produced using the online omics tool, Venny V2.0 (Oliveros, 2007), to compare unique or commonly shared significant differentially expressed genes across each

treatment group. Ensembl stable gene identifiers corresponding to statistically significant differentially expressed genes ($p \leq 0.05$, $q \leq 0.05$) for each treatment group, with a log2 fold change ≥ 1 or ≤ -1, were uploaded to Venny as individual lists for comparison. For simplicity, due to the high number of treatment groups under comparison, the LPS control data was not included in the comparison.

Expression heatmaps were generated in Genesis V1.8.1 (Sturn *et al.,* 2002) for comparison of the 20 most significantly upregulated and downregulated genes in primary bovine foot skin fibroblasts across each of the treatment groups compared to the media control. Log2 fold change values corresponding to each of the 20 greatest upregulated or downregulated genes identified across all treatment groups were collated and subsequently uploaded to Genesis (Sturn *et al.,* 2002) alongside corresponding gene identifiers to produce traditional expression heatmap images. For relevance, expression scales were adjusted within the limits of the observed expression.

2.11.8 Ingenuity Pathway Analysis

IPA (Qiagen Bioinformatics, Denmark) software was used to investigate and compare specific canonical pathways, diseases and biological functions and upstream regulators which were significantly enriched within each stimulated fibroblast population. Enrichment was measured by comparing differential expression observed within each dataset to that of associated genes found within the ingenuity knowledge base and the significance and relevance of such enrichment was measured two-fold. The right-tailed Fisher Exact Test calculated the probability (p) that an observed under- or over-representation of genes associated with a particular pathway, disease or biological function within the dataset (compared to the IPA knowledge base) was due to chance; with $p \leq 0.05$ denoting statistical significance. IPA also computed a z-score; the probability that observed parameters were activated (orange colour), inhibited (blue colour) or had an unknown or undetermined activity (grey and white colour respectively).

Initially, all statistically significant or insignificant differentially expressed genes, which had been successfully tested using Cuffdiff (therefore excluding genes designated “NOTEST” or “HIDATA”), were assigned to a corresponding Ensembl stable bovine gene identifier based upon gene name and chromosome number and position, if required, using the UMD 3.1.1 *Bos taurus* reference genome assembly of the Ensembl genome browser release 88 (Aken *et al.,* 2017). In cases where Cuffdiff had annotated a differentially expressed mRNA transcript with multiple bovine gene identifiers (Appendix B3, Table B.4), each identifier was manually inspected using the UMD 3.1.1 *Bos taurus* reference genome (Ensembl genome browser

release 88; Aken *et al.,* 2017). Upon mapping their genomic positions relatively to that of the corresponding mRNA transcript, the gene identifiers furthest to the 5' end were consistently found (with few exceptions) to map to the near-complete or complete mRNA transcript and so this criterion was subsequently chosen to manually curate all ambiguous cases.

As IPA currently only supports human (*Homo sapiens*), mouse (*Mus musculus*) or rat (*Rattus norvegicus*) species within its knowledge database, the bovine gene identifiers were subsequently converted to an equivalent, putative orthologous human gene using the Ensembl gene database release 88 in Ensembl BioMart (Aken *et al.,* 2017; Kinsella *et al.,* 2011). Where a bovine gene mapped to multiple putative orthologous human genes (approximately 3.83% genes across each treatment group; Table B.5, Appendix B3), a reciprocal nucleotide BLAST was performed through Ensembl (Aken *et al.*, 2017; Altschul *et al.,* 1990) to predict putative gene orthology (approximately 51.85% cases resolved). Where reciprocal BLAST was not able to confirm putative orthology to a human gene (approximately 48.15% of cases across each treatment group; Table B.5, Appendix B3), the bovine gene was subsequently excluded.

Ensembl stable gene identifiers, corresponding to human genes successfully identified as putative orthologs of both statistically significant and insignificant differentially expressed bovine genes, were subsequently uploaded into IPA alongside their corresponding log2 fold change (log ratio), *p* value and *q* value (FDR) for each treatment group. Core analysis was performed on each individual treatment group dataset, applying the following non-default analyses parameters: ingenuity knowledge base (genes only), direct and indirect relationships, including endogenous chemicals and filtering for molecules and/or relationships which had been experimentally observed within human species only. Expression value cut-offs were applied to produce a set of "analysis-ready" molecules, including the use of $p \leq 0.05$, $q \leq 0.05$ and a log2 fold change ≥ 1 or ≤ -1. Comparative analysis was subsequently performed across the core analyses to identify uniquely and commonly enriched canonical pathways, diseases or biological functions and upstream regulators across each of the treatment groups.

2.12 Statistical analyses

2.12.1 Principle component analysis

Principle component analysis (PCA) is a multivariate statistical analysis procedure. It is used to extract observations from an inter-correlated dataset (typically described by several dependent variables) and represents these as a set of novel orthogonal, linearly uncorrelated

variables, named principle components; whereby the first principle component accounts for the largest variability in the dataset, followed by successive components (Abdi & Williams, 2010). Through visualising data from its point of highest variance, PCA analysis provides a comprehensive insight into internal structure and variance across a dataset. This can be viewed in relation to variables of interest, such as treatment group, to determine if this does indeed explain the observed variance (Abdi & Williams, 2010).

Supervised PCA was used to analyse variance in the normalised RNA-Seq expression dataset (Chapter 2.11.5). As PCA is highly sensitive to the relative scaling of original variables, FPKM expression data for each replicate (Chapter 2.11.5) underwent normalisation prior to PCA, using Genesis V1.8.1 (Sturn *et al.,* 2002), to establish the quality and variation in replicate samples within each treatment group.

2.12.2 Hierarchical clustering analysis

Hierarchical clustering (HCL) analysis attempts to build a hierarchical tree to visualise clusters of similar grouping within a dataset, with branch length directly correlating to the similarity between each cluster (Eisen *et al.,* 1998). HCL was used to analyse variance in the normalised RNA-Seq expression dataset (Chapter 2.11.5). FPKM expression data for each experimental replicate (Chapter 2.11.5) underwent normalisation and HCL analysis, using the average linkage WPGMA method in Genesis V1.8.1 (Sturn *et al.,* 2002), to establish replicate clustering patterns within the dataset.

2.12.3 Linear regression analysis

Linear regression analysis was performed on log2 fold change expression data for the 20 most significantly upregulated and downregulated fibroblast genes across each treatment group of the RNA-Seq dataset (Chapter 2.11.7) using GraphPad Prism V5 (San Diego, California, USA). Through performing pairwise comparisons between each treatment group, the resulting linear correlation coefficient (r) and coefficient of determination (r^2) values were able to determine whether there was a significant ($p \leq 0.05$) correlation between the differential gene expression observed in bovine fibroblasts following co-incubation with one treatment and another. Indicating strength and direction of correlation between each pairwise treatment group comparison, a positive r value indicates a positive correlation (up to +1), a negative r value indicates a negative correlation (down to -1) and an r value of 0 indicates no correlation. The r^2 value indicates the proportion of variance induced by one treatment group which can predict that of another.

2.13 Ethics statement

All sampling described within this thesis was conducted in accordance with UK legislation. Furthermore, all sampling was approved by the University of Liverpool Ethical Review Process with approved ethics application number, VREC137.

Chapter Three: Isolation, subculture and characterisation of primary bovine foot skin fibroblasts and keratinocytes.

3.1 Introduction

BDD is an inflammatory infectious disease of the bovine digital skin which is typically characterised by painful, focally-inflamed, ulcerative lesions and often accompanied by necrosis, hyperkeratosis and parakeratosis of the affected skin tissue (Blowey & Sharp, 1988; McLennan & McKenzie, 1996; Read & Walker, 1998). Highly motile, helical, anaerobic spirochaetes of the genus *Treponema* have been consistently isolated from deep within lesional tissue and are considered to have a predominant role in BDD pathogenesis (Evans *et al.,* 2008; Moter *et al.,* 1998; Rasmussen *et al.,* 2012). Indeed, previous studies have implicated these BDD treponemes in inflammatory dysregulation of both bovine macrophages (Zuerner *et al.,* 2007) and cells of the bovine foot skin tissue (Evans *et al.,* 2014; Refaai *et al.,* 2013). However, to-date, the specific interactions between invading treponemes and key cell lineages of the bovine foot skin tissue, which likely underpin BDD pathogenesis, remain largely unknown.

With an essential role in host immune defence and wound healing processes, and as the predominant cell lineages within dermal and epidermal foot skin tissue respectively (as discussed in Chapter 1.8), fibroblasts and keratinocytes are considered to play a significant role in BDD pathogenesis. However, little is currently known about the specific interactions with invading treponemes that contribute to BDD pathogenesis. To investigate the host-pathogen interactions and pathogenic mechanisms which underly BDD infection, an appropriate disease model would be advantageous. Although previous studies investigating the inflammatory dysregulation within complete BDD lesions (Refaai *et al.,* 2013; Scholey *et al.,* 2013) have been highly informative, they are not able to elucidate the individual contributions and interactions of specific treponemes or host cell lineages in disease pathogenesis. In such cases, monolayer cell culture models of host-pathogen interactions are often valuable despite their simplicity (Inagaki *et al.,* 2016; Naresh *et al.,* 2009; Ramesh *et al.,* 2013). Such studies have previously implicated the inflammatory dysregulation of bovine macrophages (Zuerner *et al.,* 2007) and cells of the bovine foot skin tissue (Evans *et al.,* 2014; Refaai *et al.,* 2013) in BDD pathogenesis.

Therefore, this study aimed to successfully isolate, subculture and characterise primary fibroblast and keratinocyte cells from bovine foot skin tissue for subsequent use as a model for host-pathogen interaction studies of BDD infection.

The primary objectives of this chapter are outlined below:

1) Isolate primary fibroblast and keratinocyte cells from visibly healthy bovine foot skin tissue and successfully subculture these to obtain pure primary cell lines for subsequent use in host-pathogen interaction studies of BDD infection.
2) Characterise primary bovine foot skin cells by morphological observation (microscopy) and the use of both IF staining and RT-PCR for relevant cellular markers (vimentin, pan cytokeratin, involucrin) to confirm successful isolation of the expected lineages.

3.2 Results

3.2.1 Initial attempts at the isolation and subculture of primary bovine foot skin fibroblast and keratinocyte cells

Upon initial attempts, primary bovine cells were successfully isolated from both the dermal and epidermal foot skin tissues of a male, 18-month old Red Poll beef bull immediately following slaughter, as described in Chapter 2.1.2.

Primary bovine dermal foot skin cells were initially rounded on isolation; however, following adherence they developed the characteristic spindle-shaped morphology which is typical of fibroblasts in culture (Figure 3.1.A). The cells became increasingly elongated through the first few days post-isolation (Figure 3.1.B) and prominent cytoplasmic projections were also subsequently seen extending from the cell body (Figure 3.1.C). Cells were found to reach 90% confluence, for initial passage, after approximately six to seven days in culture and were accordingly subcultured and then maintained as described in Chapter 2.1.3. Upon subculture, cells retained their characteristic fibroblast-like morphology (Figure 3.1.D, 3.1.E and 3.1.F) and continued to do so until approximately passage number eight or nine. On occasion, two other cellular morphologies were observed within the fibroblast-like cell monolayer; one with a darker-coloured teardrop-shaped nucleus (Figure 3.1.G) and the other with a rounded lipocyte-like structure (Figure 3.1.H and 3.1.I). As these morphologies were only ever observed within dermal cultures from the initial isolation attempt, they were believed to be contamination due to poor initial tissue dissection and, where observed, these cultures were discarded.

The primary bovine epidermal foot skin cells were initially rounded and non-adherent following isolation. However, they began to form small, compact, three-dimensional,

adherent rosette-like structures (Figure 3.2.A) within approximately three to four days of culture. Over the following days, these rosette-like structures were then observed to extend outwards, radially, into the surrounding spaces (Figure 3.2.B) to form larger, compact "islands" of small, rounded cobblestone-shaped cells with prominent nuclei (Figure 3.2.C and 3.2.D), which are characteristic of keratinocytes in culture. Cells with a fibroblast-like morphology were also observed within these cultures and were found to increasingly surround the keratinocyte-like cell islands with confluence (Figure 3.2.E and 3.2.F). The epidermal cells were found to reach 90% confluence after approximately seven to eight days in culture and were accordingly subcultured and then maintained as described in Chapter 2.1.3. The contaminating fibroblast-like cells were almost completely removed through initial trypsinization with 0.025% (w/v) trypsin-EDTA, with a small number remaining closely around the perimeter of the keratinocyte-like cell islands (Figure 3.2.G), following which the remaining keratinocyte-like cells were then detached for subculture with 0.25% (w/v) trypsin-EDTA. Upon subculture, epidermal foot skin cell cultures demonstrated a lack of the rosette-like adherent structures and subsequent keratinocyte-like cell islands which appeared to be characteristic of the cultures following initial isolation. Again, cultures appeared to be increasingly populated with fibroblast-like cells. Following eight days in culture, the contaminating fibroblast-like cells were over 90% confluent and a large number of non-viable (confirmed using the trypan blue dye exclusion assay, Chapter 2.1.4) and non-adherent cells, particularly those that appeared to be keratinocyte-like cell islands, were observed within the media. Two keratinocyte-like cell islands were observed within just one of the epidermal cultures after eight days (Figure 3.2.H and 3.2.I); however, these were lost during subsequent passage attempts. It was considered the keratinocyte-like cell islands may have remained as a single confluent monolayer, rather than individual cells, during trypsinisation; therefore, leading to non-adherence and an opportunity for contaminating fibroblast-like cells to outgrow the keratinocyte-like cells. Subsequently, further attempts were made to optimise the keratinocyte-like cell isolation and subculture techniques (Chapter 3.2.2).

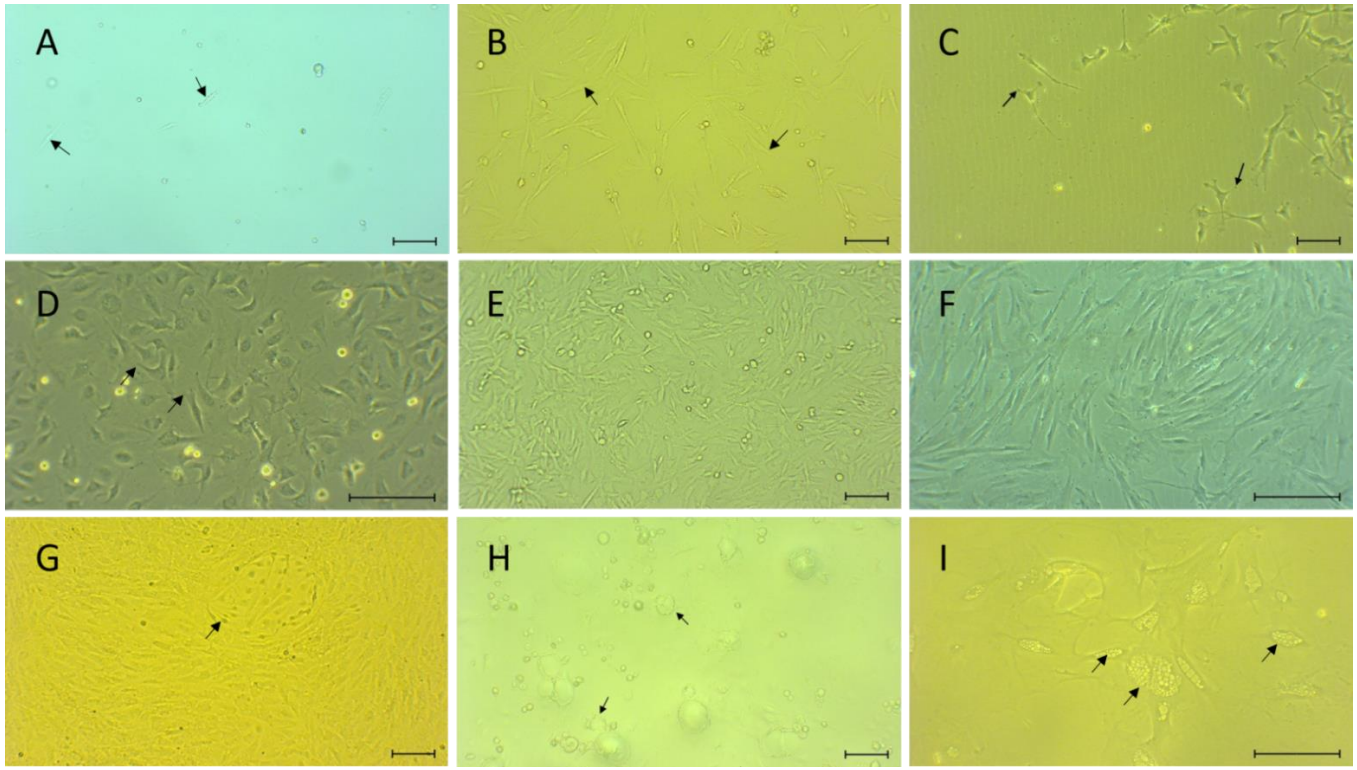

Figure 3.1 Morphology of cultured primary bovine dermal foot skin cells. *Primary cells were isolated from the dermal foot skin tissue of a male Red Poll beef bull in attempts to isolate and subculture bovine fibroblast cells. The morphology of these cultured primary bovine dermal foot skin cells was observed by both light microscopy and phase contrast microscopy. (A) Following their initial isolation, the dermal foot skin cells began to adhere and elongate, (B) developing the characteristic spindle-shaped morphology and (C) cytoplasmic projections (as indicated by arrows) which are characteristic of fibroblasts in culture. Upon subculture, the cells were found to retain their fibroblast-like morphology, as shown here at passage number (D) two, (E) three and (F) four respectively. On occasion, cells with both a (G) darker-coloured, teardrop-shaped nucleus and (H, I) lipocyte-like structure (as indicated by arrows) were observed amongst the fibroblast-like cell monolayers. Each panel corresponds to one field of view which is representative of the observations within each cell culture. Bars represent 100 µm.*

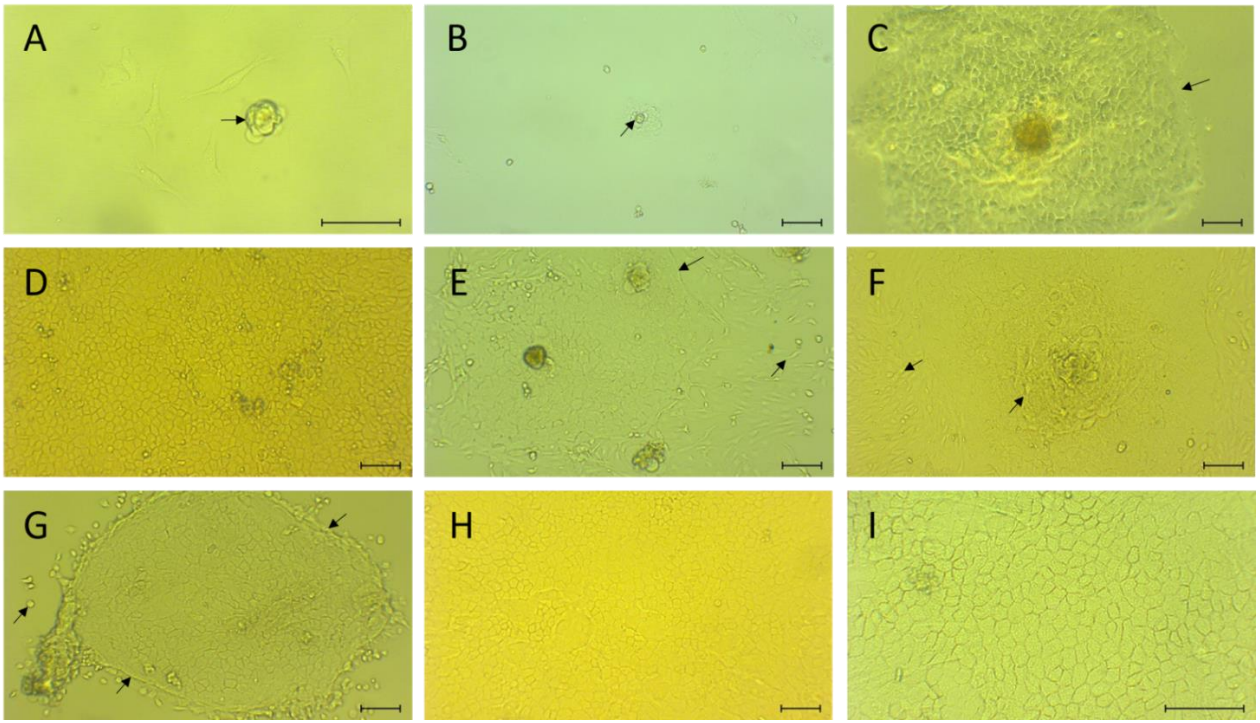

Figure 3.2 Morphology of cultured primary bovine epidermal foot skin cells. *Primary cells were isolated from the epidermal foot skin tissue of a male Red Poll beef bull in attempts to isolate and subculture bovine keratinocyte cells. The morphology of these cultured primary bovine epidermal foot skin cells was observed by both light microscopy and phase contrast microscopy. (A) Following their initial isolation, the epidermal foot skin cells began to adhere and form three-dimensional, rosette-like structures, (B) gradually extending outwards, radially, into the surrounding spaces (C, D) to form larger, compact "islands" of small, rounded, cobblestone-shaped keratinocyte-like cells. (E, F) Fibroblast-like cells were found to surround these keratinocyte-like cell islands with increasing confluence. (G) The epidermal foot skin cell cultures were subcultured using two different concentrations of trypsin-EDTA to initially remove contaminating fibroblast-like cells prior to re-seeding the keratinocyte-like cells. (H, I) Upon subculture, keratinocyte-like cell islands were initially observed within just one of the epidermal cell cultures, however these were lost upon subsequent passage attempts. Each panel corresponds to one field of view which is representative of the observations within each cell culture.Bars represent 100 µm.*

3.2.2 Optimisation of the isolation and subculture techniques for primary bovine foot skin keratinocytes

Despite the successful isolation of primary keratinocyte-like cells from epidermal foot skin tissue of a Red Poll bull, initial attempts to further subculture these cells ultimately proved unsuccessful (Chapter 3.2.1). Non-viable, non-adherent cells, which were typically in the form of cell monolayers and thought to be the keratinocyte-like cell islands, were observed in abundance within the medium of passaged cultures. Furthermore, it appeared that fibroblast-like cells had rapidly overgrown the few remaining adherent keratinocyte-like cells. However, it was unclear whether this outcome was due to poor isolation efficiency of the keratinocyte-like cells, therefore providing a potential opportunity for overgrowth by fibroblast-like cells, or whether specific isolation or subculture conditions had led to poor re-adherence of the keratinocyte-like cells. Resultantly, as summarised in Table 3.1, attempts were made to optimise various stages of both the cell isolation and culture procedures (Chapter 2.1.2 and 2.1.3) to improve the initial isolation yield and enable successful subculture of primary keratinocyte-like cells from bovine foot skin tissue.

Tissue locality

To determine whether bovine foot skin tissue locality influenced the yield of primary keratinocyte-like cells obtained from the epidermis, full-thickness skin tissue sections were taken from either directly below (as previously) or above the dewclaws on the underside of the foot and epidermal cell isolation and subculture was then attempted, as described previously (Chapter 2.1.2 and 2.1.3). Primary keratinocyte-like cells and contaminating fibroblast-like cells, which were both morphologically alike those described during the initial isolation attempt (Chapter 3.2.1), were observed within cultures from both tissue sections. However, a greater number of keratinocyte-like cell islands were observed within cultures taken from the bovine foot skin tissue directly above the dewclaws. Upon subculture, the cells from each culture were found to retain their characteristic keratinocyte-like and fibroblast-like morphologies, however a larger number of keratinocyte-like cells were again observed in cultures from tissue taken directly above the dewclaws. Keratinocyte-like cells were successfully subcultured up to passage number six without any observed alterations in cellular morphology. Resultantly, all future keratinocyte cell isolation attempts were completed using bovine epidermal foot skin tissue taken from directly above the dewclaws on the underside of the foot.

Dissociation of keratinocytes from bovine epidermis

Identifying an appropriate cell dissociation method is an important consideration when working with adherent cell lines and previous studies have highlighted the benefit of more gentle and efficient dissociation reagents (such as TrypLE) when compared to the slow action of non-enzymatic reagents or the poor cell viability and loss of surface antigen expression obtained when using trypsin (Tsuji *et al.,* 2017). Accordingly, attempts were made to optimise the reagents and conditions used for the dissociation of primary cells from the epidermis in the hope of improving the yield or subsequent adherence of epidermal keratinocyte-like cells in culture. Primary cells were isolated from the epidermal foot skin tissue of a beef cow, as described in Chapter 2.1.2, through dissociation with either (1) 0.25% (w/v) trypsin-EDTA for 30 minutes at room temperature (as previously), or (2) 37°C using a water bath, (3) 1 x TrypLE™ express enzyme (Gibco™ by Life Technologies Ltd, Paisley, UK) for 30 minutes at room temperature, or (4) at 37°C using a water bath. Cell cultures were maintained as described in Chapter 2.1.2 and 2.1.3. Primary keratinocyte-like cells and contaminating fibroblast-like cells were observed within cultures following isolation by each of the dissociation conditions after 10 days and were morphologically like those described during the initial isolation attempt. There were no distinct differences observed in the yield of keratinocyte-like cells obtained upon isolation, or their ability for re-adherence following subculture, between the conditions. Resultantly, the original protocol was used for all future keratinocyte cell isolation attempts.

Cell strainers

To determine whether primary keratinocyte-like cells were being lost through exclusion by the 40 µm Falcon™ cell strainers during the initial isolation attempt (Chapter 3.2.1), epidermal cells were isolated from bovine foot skin tissue using either 40 µm or 70 µm Falcon™ cell strainers (Fisher Scientific UK Ltd, Loughborough, UK). Primary keratinocyte-like and fibroblast-like cells were successfully isolated using both 40 µm and 70 µm Falcon™ cell strainers and were morphologically alike those described previously (Chapter 3.2.1). Although there were no obvious differences in cell isolation or subsequent culture efficiency of the keratinocyte-like cells, there was an observed increase in tissue debris found initially within cell cultures isolated using the 70 µm Falcon™ cell strainers. Resultantly, all future isolation attempts were completed using 40 µm Falcon™ cell strainers, as previously.

Cell culture surface

Previous studies of murine, equine and human keratinocyte cell culture have documented the requirement of collagen-coated tissue culture surfaces for the successful isolation and subculture of keratinocytes (Liu and Karasek, 1978; Visser & Pollitt, 2010; Yano & Okochi,

2005). To determine whether collagen-coated tissue culture surfaces similarly enhanced the plating efficiencies of primary bovine foot skin keratinocyte-like cells upon isolation or subsequent culture, un-coated and collagen-coated plastic culture surfaces were compared. Accordingly, epidermal cells were isolated from bovine foot skin tissue as described in Chapter 2.1.2 and were subsequently seeded into 25 cm^3 plastic tissue culture flasks which were either un-coated (as previously) or pre-coated with 1 ml (100 µg/ml) PureCol® bovine type I collagen solution (Advanced BioMatrix Inc., Carlsbad, USA; Appendix A) or 1 ml (100 µg/ml) rat tail collagen type I (First Link UK Ltd, Wolverhampton, UK; Appendix A), as per the manufacturer's instructions. Cultures were maintained as previously described (Chapter 2.1.2 and 2.1.3). Unlike previous studies of murine, equine and human keratinocytes, primary bovine keratinocyte-like cells demonstrated poor adherence and growth after 10 days when cultured on the collagen-coated plastic surfaces examined here (bovine and rat tail type I collagen). Conversely, large numbers of keratinocyte-like cell islands were observed upon equivalent un-coated culture surfaces. Resultantly, primary bovine epidermal cells were thereafter isolated and cultured, as previously, on un-coated plastic surfaces.

Composition of culture medium

The composition of culture medium is crucial to balancing the proliferation and differentiation capacity of primary keratinocyte cells in culture and many variations have been described. The composition of culture medium used upon initial attempts to isolate and subculture primary bovine foot skin cells was informed by a previous study (Evans *et al.,* 2014). However, alternative medium formulations were subsequently trialled in attempts to improve the yield or subsequent growth of primary keratinocyte-like cells in culture: (1) keratinocyte-specific complete WME (as previously), (2) keratinocyte-specific complete WME (2% FBS), (3) keratinocyte-specific WME minus BPE and (4) fibroblast-specific complete WME. Each of the three alternative media compositions were found to profoundly reduce the number of keratinocyte-like cells obtained upon subculture when compared to the original formulation. The medium without BPE supplementation resulted in particularly poor cell viability and growth and the fibroblast-specific formula resulting in a higher contamination with fibroblast-like cells. To determine whether supplementation with an alternative origin or (v/v) concentration of FBS would be beneficial, several alternatives were tested: (1) 20% (v/v) (as previously) or (2) 10% (v/v) FBS (South American origin; Gibco™ by Life Technologies Ltd), (3) 20% (v/v) FBS (USA origin; Gibco™), (4) 20% (v/v) FBS (USA origin; Sigma-Aldrich) and (5) 20% (v/v) FBS (Hyclone™ USA origin; GE Healthcare Life Sciences). The original medium formulation was again found to provide the highest yield of keratinocyte-

like cells upon isolation and subsequent culture, although keratinocyte-like cells were observed with all formulations. Accordingly, the original composition of keratinocyte-specific complete WME was used for all future keratinocyte isolation and subculture attempts.

Cell confluence for subculture

The unsuccessful initial attempt to subculture primary bovine foot skin keratinocyte-like cells following isolation appeared to suggest overgrowth by fibroblast-like cells but also that keratinocyte-like cell islands may have detached as a confluent sheet rather than individual cells during trypsinisation. Accordingly, primary cells were isolated from bovine epidermal foot skin tissue as previously (Chapter 2.1.2) and were then subsequently maintained to either 90% (as previously) or 80% confluence prior to subculture to determine whether plating efficiency could be improved. The reduction in cell confluency prior to subculture, from 90% to 80%, was found to greatly improve the number of keratinocyte-like cells observed in culture after passage and also appeared to reduce the number of contaminating fibroblast-like cells. Resultantly, all future subculture attempts were completed using cell cultures with a maximum confluence of 80%.

Cloning cylinders

Cloning cylinders are considered a useful tool in tissue culture for the isolation of specific cell populations and have been used previously to obtain pure primary bovine foot skin fibroblast and keratinocyte cell cultures (Evans *et al.,* 2014). Primary epidermal cells were initially isolated from bovine foot skin tissue, according to Chapter 2.1.2, and were seeding into 6-well tissue culture plates and maintained until approximately 80% confluent. Cloning cylinders were subsequently placed over keratinocyte-like cell islands within confluent cultures and these cellular subsets then subcultured according to Chapter 2.1.3. Despite multiple attempts, there were no obvious improvements in the yield of keratinocyte-like cells obtained when using the cloning cylinders and no reductions were observed in the number of contaminating fibroblast-like cells. Cloning cylinders were therefore not used in future subculture attempts.

Table 3.1 Optimisation strategies for the isolation and culture of primary keratinocyte cells from bovine epidermal foot skin tissue. *Summary of the strategies used to optimise procedures for the isolation and subculture of primary keratinocyte cells from bovine epidermal foot skin tissue of beef cattle. Original strategies are given alongside the alternative strategies chosen in attempts for optimisation. Optimal conditions as determined by this study are highlighted in green.*

Optimisation strategy	Original condition	Alternative conditions attempted		
		1	2	3
Isolation				
Locality of bovine foot skin tissue sections	Below the dewclaws	**Above the dewclaws**	-	-
Section of epidermal tissue for cellular dissociation*	Complete epidermis	**Avoid DEJ interface**	-	-
Dissociation reagent and incubation temperature	**Trypsin-EDTA, 22°C (RT)**	Trypsin-EDTA, 37°C	TrypLE™, 22°C (RT)	TrypLE™, 37°C
Size of cell strainers (µm)	**40**	70	-	-
Culture				
Coating of cell culture surface (25 cm^3, plastic)	**Un-coated**	Bovine type I collagen	Rat tail type I collagen	-
Composition of complete WME	**Kerat-specific (20% FBS)**	Kerat-specific (2% FBS)	Kerat-specific (no BPE)	Fibro-specific (20% FBS)
FBS composition and origin	**Gibco™ South American**	Gibco™ USA	Sigma-Aldrich USA	Hyclone™ USA
Cell confluence for subculture (%)	90	**80**	-	-
Use of cloning cylinders	**No**	Yes	-	-

**Further optimal condition identified later (Chapter 3.2.3).*

Figure 3.3 illustrates the successful isolation and continued subculture of primary bovine foot skin keratinocyte-like cells across several passages following protocol optimisation. Bovine keratinocyte-like cells were observed within culture for up to six passages without any observed changes to cellular morphology.

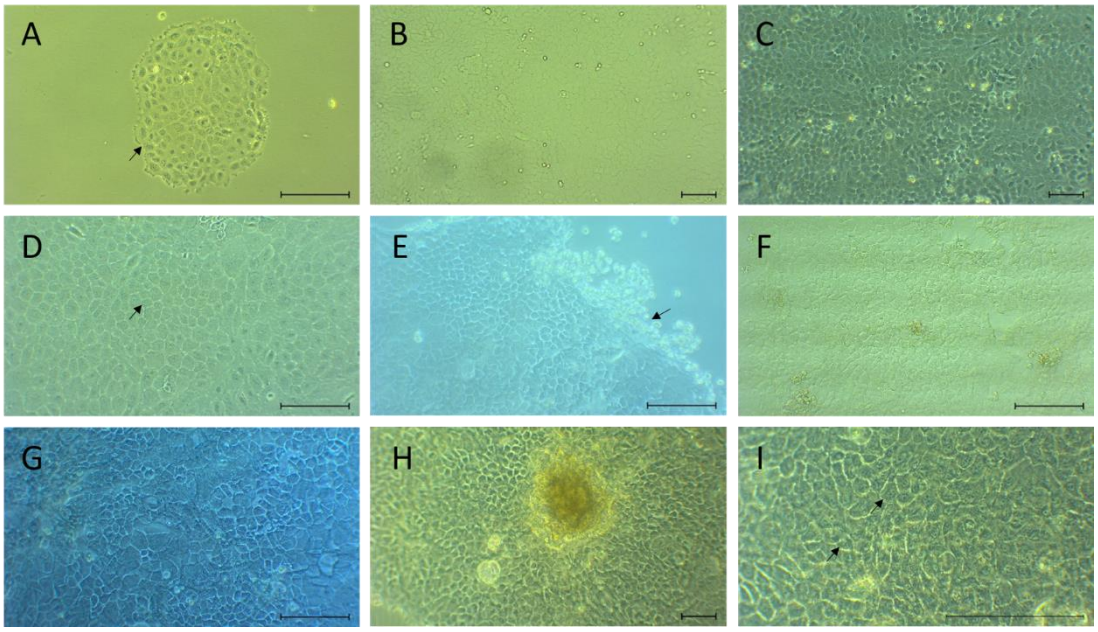

Figure 3.3 Morphological observations of cultured primary keratinocyte-like cells from bovine foot skin epidermis across several passages following successful optimisation of isolation and subculture procedures. *Initial procedures were optimised for the successful isolation and subculture of primary keratinocyte-like cells from bovine foot skin epidermis. Cellular morphology was observed by both light microscopy and phase contrast microscopy. (A) Cobblestone-shaped, keratinocyte-like cells adhere and form a compact island within the first seven days post-isolation, which upon subculture (passage number 1) were successfully maintained to form larger sheets of cobblestone-shaped cells, as observed by (B) light or (C, D) phase contrast microscopy. (E) Upon trypsinisation, the contaminating fibroblast-like cells present were successfully removed and (F, G) large sheets of keratinocyte-like cells were observed with similar morphology to those seen previously at approximately seven days post-seeding. (H) Upon further subculture, keratinocyte-like cells retained their morphology and what appeared to be (I) desmosomes were seen at high magnification which connected the keratinocyte-like cells together. Each panel corresponds to one field of view which is representative of the observations within each cell culture. Bars represent 100 µm.*

3.2.3 Characterisation of primary bovine foot skin cells

Following the successful isolation and subculture of primary fibroblast-like and keratinocyte-like cells from bovine foot skin tissue (Chapter 3.2.1 and 3.2.2 respectively), cultures subsequently underwent both RT-PCR (Chapter 2.2.1) and a novel double IF staining protocol

(Chapter 2.2.3) to detect several common cellular markers of fibroblasts (vimentin) and keratinocytes (involucrin and pan cytokeratin) for the purposes of cellular characterisation.

RT-PCR to detect the bovine involucrin gene

Primary bovine foot skin fibroblast-like and keratinocyte-like cells were initially characterised by RT-PCR, according to Chapter 2.2.1, to detect expression of the involucrin gene, a marker of terminal differentiation of keratinocyte cells. As shown in Figure 3.4.A, primary bovine epidermal foot skin cell cultures were found to strongly express the involucrin gene, suggesting the presence of terminally differentiating keratinocytes, as previously indicated by morphological observations. Cells within the primary bovine dermal cultures which, morphologically, appeared to contain fibroblast-like cells were also found to weakly express the involucrin gene and suggested likely contamination with epidermal keratinocytes. In both instances, cells were found to express the *GAPDH* gene (positive control). Accordingly, attempts were made to prevent future contamination of dermal cultures with epidermal keratinocytes through adapting the previously optimised cell isolation protocol (Chapter 3.2.2) to avoid tissue of the immediate DEJ when separating tissue for cell dissociation. As shown by Figure 3.4.B, this strategy was found to circumvent the contamination problem and subsequent dermal cell cultures were found to not express the involucrin gene. Interestingly, this optimisation strategy was also found to positively impact the keratinocyte cell isolation procedure and was found to greatly improve the yield of keratinocyte-like cells, whilst also reducing the number of contaminating fibroblast cells, obtained within epidermal cell cultures. This strategy was therefore incorporated into all future isolation attempts.

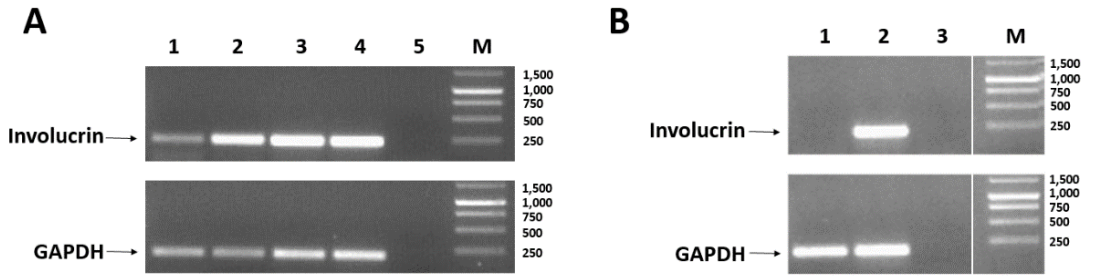

Figure 3.4 Detection of involucrin gene expression in primary bovine foot skin dermal and epidermal cell cultures by RT-PCR for cellular characterisation. *Following their isolation from dermal and epidermal sections of bovine foot skin tissue, primary fibroblast-like and keratinocyte-like cell cultures were harvested and subjected to RNA extraction and cDNA synthesis to assess their expression of the involucrin gene, a marker of terminally differentiated keratinocytes, by RT-PCR, for the purposes of cellular characterisation. (A) The expression of involucrin and housekeeping (positive control) gene, glyceraldehyde 3-phosphate dehydrogenase (GAPDH), were assessed in (1) dermal and (2) epidermal cDNA preparations, with (3, 4) keratinocyte cDNA and (5) water used as positive and negative*

controls, respectively, for validation. Products were visualised by agarose gel electrophoresis, as shown, using a 1kb DNA marker (M) to validate PCR product sizes (bp). Dermal cell cultures were found to be contaminated with involucrin-expressing keratinocyte cells and so the cell isolation protocol was optimised further to prevent epidermal keratinocyte contamination. (B) Dermal cell cultures were re-assessed for involucrin gene expression by RT-PCR following optimisation of the isolation procedure, and (1) confirmed the absence of contaminating epidermal keratinocytes, using (2) keratinocyte cDNA and (3) water as positive and negative controls respectively.

A novel double IF staining procedure to detect vimentin and pan cytokeratin

It was necessary to confirm the presence or absence of other fibroblast and keratinocyte cell markers within dermal and epidermal cultures for characterisation. A novel double IF staining protocol was developed and subsequently optimised (as described in Chapter 2.2.3) for this purpose, whereby the cytoskeletal intermediate filament proteins, vimentin and pan cytokeratin, were chosen as suitable markers for fibroblast and keratinocyte cells respectively. Initially, IF staining was attempted on cultured primary bovine foot skin cells which had been grown on 13 mm cover glasses within 24-well tissue culture plates (Chapter 2.2.3.1) to determine (1) if the use of a paraformaldehyde fixation method was effective, and (2) if the routine culture system using 25 cm^3 tissue culture flasks could be successfully scaled down. Whilst the fixation method was found to be effective, these initial IF staining attempts resulted in poor growth and staining of the keratinocyte-like cell islands. This was thought to result from an inadequate surface area for effective cell proliferation, leading to rapid overgrowth by contaminating fibroblast-like cells. A profound improvement in growth and subsequent IF staining was achieved when keratinocyte-like cells were cultured within their routine 25 cm^3 plastic tissue culture flasks (Chapter 2.2.3.2) and so all further optimisation attempts for IF staining were completed within this system. Optimal antibody dilutions were subsequently determined, each starting from an initial dilution of 1:200. The optimised IF staining method, as described in Chapter 2.2.3.2, was used for all future characterisation of primary bovine foot skin cells.

As shown in Figure 3.5.A, the fibroblast-like cells within dermal cultures were found to demonstrate strong cytoplasmic staining for the mesenchymal cell marker, vimentin, whilst demonstrating no staining for the keratinocyte intermediate filament protein, pan cytokeratin. Conversely, keratinocyte-like cells within epidermal cultures were found to demonstrate a profound cytoplasmic staining for the keratinocyte intermediate filament protein, pan cytokeratin and no staining for vimentin (Figure 3.5.B). On occasion, typically upon initial isolation, contaminating fibroblast-like cells located at the periphery of

keratinocyte-like cell islands within epidermal cultures were found to demonstrate positive staining for the mesenchymal cell marker, vimentin.

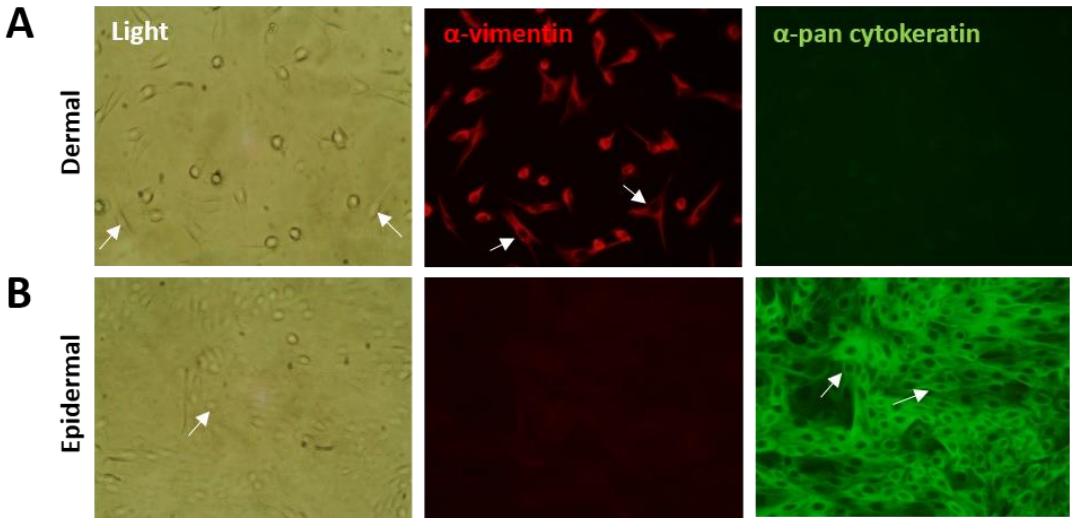

Figure 3.5 Double immunofluorescent staining of primary bovine foot skin fibroblast-like and keratinocyte-like cell cultures against anti-vimentin and anti-pan cytokeratin for the purposes of cellular characterisation. *Following their isolation from bovine foot skin tissue of a Red Poll beef bull, (A) dermal and (B) epidermal cell cultures were stained against known mesenchymal cell marker, vimentin (red), and the keratinocyte intermediate filament protein, pan cytokeratin (green), for characterisation. Fibroblast-like cells within dermal cell cultures were found to express vimentin and not pan cytokeratin, whilst keratinocyte-like cells within epidermal cell cultures were found to express pan cytokeratin and not vimentin. Together these observations further indicated the successful isolation and subculture of pure primary bovine foot skin fibroblast and keratinocyte cells, respectively. Each panel corresponds to one field of view which is representative of triplicate images taken for each sample. Scale, x10 magnification.*

3.3 Discussion

BDD is an inflammatory infectious disease of the bovine digital skin and previous studies have suggested a significant role for the predominant dermal and epidermal cellular constituents, fibroblasts and keratinocytes respectively, in disease pathogenesis (Evans *et al.,* 2014; Refaai *et al.,* 2013). However, to study the host-pathogen interactions and pathogenic mechanisms associated with BDD infection, an appropriate disease model was required. Accordingly, through the isolation, routine subculture and characterisation of primary bovine foot skin fibroblast and keratinocyte cells, this study has successfully validated suitable models for subsequent and future host-pathogen interaction studies of BDD infection.

3.3.1 Primary fibroblast and keratinocyte cells were successfully isolated and cultured from bovine foot skin tissue

During this study, primary fibroblast and keratinocyte cells were successfully isolated from bovine foot skin tissue and were thereafter routinely subcultured for a further eight (fibroblasts) or six (keratinocytes) passages without any observed morphological alterations in cellular phenotype. Eight passages are typical of the lifespan of primary fibroblast cells in culture (Moulin *et al.,* 2011). The isolation protocol used here was adapted from that previously described by Evans *et al.* (2014) and to the author's knowledge is, to-date, one of only three published protocols describing the isolation of primary bovine fibroblast cells (Akkoc *et al.,* 2016; Green & Kerr, 2014), and the only published protocol describing primary keratinocyte cell isolation, from bovine foot skin tissue.

Despite successful isolation of primary keratinocyte-like cells from bovine epidermal foot skin tissue, attempts to further subculture these cells were initially unsuccessful and required further optimisation. The difficulties of maintaining primary epidermal keratinocyte cells in culture beyond initial isolation are notorious. In recent years, successful culture attempts have been described for primary human (Kaviani *et al.,* 2015), murine (Yano & Okochi, 2005), ovine (Watkins *et al.,* 2009), caprine (Islam & Zhou, 2007), porcine (van den Bogaerdt *et al.,* 2004), equine (Dahm *et al.,* 2002; Visser & Pollitt, 2010) and canine (Köhler *et al.,* 2001; Wilkinson *et al.,* 1987) epidermal keratinocytes. The successful isolation and subculture of primary bovine epidermal keratinocytes has, to-date, only been described on two occasions (Evans *et al.,* 2014; McBride *et al.,* 2000). The reason as to why the protocol described by Evans *et al.* (2014) did not result in the successful subculture of primary bovine foot skin keratinocytes in this study, despite multiple attempts, remains unknown. The contamination of primary cell cultures with *Mycoplasma* spp. was ruled out by use of a routine diagnostic PCR; however, alternative explanations may be differences in specific cell culture reagents (particularly batch differences in FBS), tissue culture plates, equipment or even technical variation between each study (Baker, 2016; Rheinwald & Green, 1975). Due to time constraints within the scope of this study, several strategies were subsequently employed in attempt to optimise the published isolation and subculture protocol to enable successful and routine subculture of primary bovine foot skin keratinocytes. Based upon morphological observations, the initial keratinocyte isolation attempt was considered to have been unsuccessful due to either (1) a sub-optimal keratinocyte isolation yield, (2) poor adherence to the culture surface, (3) poor growth, (4) fibroblast overgrowth or (5) overconfluence.

Interestingly, the locality of bovine foot skin tissue was found to have a profound impact on the yield of primary keratinocyte cells obtained following both isolation and subculture. This finding may be unsurprising as the epidermis is well known to be much thicker within areas of greater mechanical stress and trauma or those lacking a protective barrier of hair (Mauldin & Peters-Kennedy, 2016). Indeed, the bovine skin tissue located on the underside of the foot was observed to be visibly much thicker below, than above, the dewclaws; which is in keeping with its greater weight-bearing load and the increased risk of trauma due to direct contact with hard surfaces. With a larger number of keratinocytes interlinked by desmosomal attachment, the digestion of thicker epidermal tissue is likely to be less efficient and therefore result in poorer keratinocyte dissociation from the tissue. Interestingly, the area of tissue dissected for cell dissociation was also found to significantly influence the yield and purity of primary keratinocyte and fibroblast cells upon isolation from bovine foot skin. Avoidance of the tissue immediately surrounding the DEJ was found to profoundly reduce the observed cellular contamination of respective cultures and resulted in pure keratinocyte and fibroblast cell cultures. This may be unsurprising as the chance for contamination between dermal and epidermal tissue would be greatly reduced by avoiding the tissue interface; furthermore, any cross contamination would likely be in much lower numbers, thereby reducing the chance for overgrowth by opposing cell lineages.

Although primary keratinocyte cells have previously been successfully and routinely cultured on uncoated plastic surfaces (Evans *et al.,* 2014; Köhler *et al.,* 2001; van den Bogaerdt *et al.,* 2004; Watkins *et al.,* 2009), several studies of primary murine, equine and human epidermal keratinocyte cell culture have reported the benefit or requirement of using collagen- or, more recently, gelatin-coated culture surfaces (Kaviani *et al.,* 2015; Liu and Karasek, 1978; Rahsaz *et al.,* 2015; Visser & Pollitt, 2010; Yano & Okochi, 2005). Indeed, Liu and Karasek (1978) found that significantly higher plating efficiencies (over 70%) were achieved following initial isolation when seeding primary human epidermal keratinocytes onto collagen- or collagen gel-coated plastic culture surfaces compared to un-coated glass (2.8%) or plastic (14%). However, despite trialling both bovine and rat tail (type I) collagen-coated culture surfaces upon isolation and subculture, primary bovine foot skin keratinocytes grew most efficiently when seeded onto uncoated plastic culture surfaces. Furthermore, keratinocytes were found to adhere poorly to collagen when compared to uncoated plastic, an observation which was also previously demonstrated by equine keratinocytes (Dahm *et al.,* 2002). It is likely that the complex growth medium used within this protocol, as previously developed by Evans *et al.* (2014), is optimised to support growth without the requirement for further

ECM support. Several studies, most notably that of the other known bovine keratinocyte culture system (McBride *et al.,* 2000), have also reported successful *in vitro* keratinocyte cell culture using immortalised 3T3 or mitomycin C-treated fibroblast cell lines as feeder cell layers (Dahm *et al.,* 2002; Islam & Zhou, 2007; Rheinwald & Green, 1975); often also circumventing requirements for many additional growth factor supplements (Islam & Zhou, 2007). However, due to the eventual requirement of a pure, uncontaminated keratinocyte cell lineage for host-pathogen interaction studies of BDD (Rheinwald & Green, 1975), this strategy was not attempted as part of the protocol optimisation described here.

Although published protocols for the isolation of primary keratinocytes are generally well conserved, the basal growth medium and further addition of supplementary growth factors or serum can be highly variable. Indeed, several growth factors, including insulin, BPE and EGF, have been reported to improve keratinocyte proliferation *in vitro* and are often routinely added to culture medium (Evans *et al.,* 2014; Islam & Zhou, 2015; Köhler *et al.,* 2001; Papini *et al.,* 2003; Sun & Green, 1976; van den Bogaerdt *et al.,* 2004). Therefore, maybe unsurprisingly, the use of keratinocyte-specific growth medium without BPE supplementation or fibroblast-specific complete WME (which does not contain insulin, BPE, hydrocortisone or cholera toxin) was found to result in poor growth of primary bovine foot skin keratinocytes and, often, fibroblast overgrowth. Calcium is also considered a key physiological regulator of keratinocyte maturation, with greater calcium concentrations inducing greater keratinocyte differentiation *in vitro* (Li *et al.,* 1996). Interestingly, Köhler *et al.* (2001) found that canine keratinocytes required reduced calcium and serum concentrations within their medium at later passages to maintain monolayer growth in culture. The majority of published protocols describe the use of culture medium supplemented with either 5% (McBride *et al.,* 2000), 10% (Islam & Zhou, 2007; Kaviani *et al.,* 2015; van den Bogaerdt *et al.,* 2004; Watkins *et al.,* 2009) or 20% (Dahm *et al.,* 2002; Evans *et al.,* 2014) (v/v) FBS. Whilst successful primary keratinocyte isolation attempts have been described using serum-free culture medium, notably often with the use of ECM coating or feeder layers (Papini *et al.,* 2003; Rahsaz *et al.,* 2015), others have suggested serum-free conditions lead to a rapid deterioration in cell viability in culture (Kaviani *et al.,* 2015) and an inability to form stratified, mature epidermis (Lamb & Ambler, 2013). Here, primary bovine foot skin keratinocytes were not able to be successfully maintained in culture under low serum concentrations and were, interestingly, found to demonstrate poorer growth than those cultured in medium containing 20% (v/v) FBS. The culture medium described by Evans *et al.* (2014) appeared to be optimal for use in this skin model.

Although an improvement in cell viability and surface antigen expression has been described when using alternative cell dissociation agents to trypsin, such as TrypLE (Tsuji *et al.,* 2017), no such benefits were observed during this study. However, the degree of cell confluence prior to subculture was found to have a profound impact on the plating efficiency of primary keratinocytes, with 80% rather than 90% confluence resulting in much higher keratinocyte yields upon subculture. Whilst many studies concerning primary keratinocyte cell culture typically passage at between 80% to 100% confluence, two previous studies have described an optimal confluence of 70% for successful subculture (Islam & Zhou, 2007; McBride *et al.,* 2000). These results are largely not surprising. Indeed, the detriment of culturing cells beyond optimal confluence is well documented, with overconfluent cultures typically resulting in a reduced or non-proliferative state, poor reattachment, atypical morphology, contact inhibition and the release of excessive metabolic products resulting in cellular toxicity (Balint *et al.,* 2015; Islam & Zhou, 2007). Poumay & Pittelkow (1995) previously highlighted cell confluence as a key factor in regulating keratinocyte differentiation; with fully confluent keratinocyte cultures initiating terminal differentiation through contact inhibition-like mechanisms. Whilst nutrient deprivation is considered to initiate a reversible process of keratinocyte differentiation, cell confluence is thought to result in irreversible growth arrest and terminal differentiation. Therefore, within the more confluent (90%) bovine foot skin keratinocyte colonies, it is likely that an increased number of terminally differentiated corneocyte cells may be present; which are much more robust and insoluble due to their natural barrier function (Sun & Green, 1976). Therefore, overconfluent keratinocyte cell cultures are likely to be less amenable to cellular dissociation and equally less likely to re-attach upon subculture; both due to the lack of a single cell suspension and also the fact that an increasing proportion of the culture may be non-living corneocytes. Under these conditions, and due to their comparatively greater proliferation rate (Islam & Zhou, 2007), fibroblasts are more likely to have overgrown the keratinocyte cultures. It is likely that the reduction in cell confluence prior to subculture allowed effective dissociation and provided a single cell suspension for subsequent reseeding and attachment, therefore reducing the opportunity for fibroblast overgrowth.

3.3.2 Characterisation of primary bovine foot skin fibroblasts and keratinocytes

The primary bovine dermal foot skin cells isolated and subsequently expanded within culture were found to demonstrate the typical elongated, spindle-shaped morphology and prominent cytoplasmic projections consistent with previous observations of bovine foot skin fibroblasts in culture (Evans *et al.,* 2014). A further two alternative cell morphologies were

observed within primary bovine dermal foot skin cultures during the initial isolation attempt. Cells with darker-coloured, teardrop-shaped nuclei were consistent with previous morphological observations of dermal endothelial cells in culture (Monsuur *et al.,* 2016) and likely arose from the presence of small blood or lymphatic capillaries within dermal tissue. Cells with a rounded, lipocyte-like morphology are of unknown origin, however their adipocyte-like appearance (Huber *et al.,* 2016) was suggestive of contamination by cells of the underlying subcutaneous tissue, likely due to a poor initial dissection technique.

Primary bovine epidermal foot skin cells were found to form the small polygonal, cobblestone-shaped cell colonies which are typical of keratinocytes in monolayer culture (Evans *et al.,* 2014; Sun & Green, 1976). As described previously (Islam & Zhou, 2007), contaminating fibroblast-like cells were often observed within keratinocyte cultures upon initial isolation, however were successfully eliminated by differential trypsinisation at early subculture. These fibroblast-like cells may have been of dermal origin or, due to the susceptibility of cell monolayer de-differentiation *in vitro,* may have been epidermal keratinocytes undergoing EMT (Arnoux *et al.,* 2005). It should be remembered that keratinocyte and fibroblast cells are interdependent *in vivo* and a complex signalling cascade regulates barrier function of the skin; attempts to culture pure keratinocyte cells *in vitro,* in the absence of fibroblast cells, is a highly artificial environment and cell lineage must be routinely confirmed prior to use.

For this reason, it was imperative to confirm the presence of pure primary fibroblast and keratinocyte cell lineages within respective dermal and epidermal cultures for validation prior to use as a model for subsequent and future host-pathogen interaction studies. Previous studies have characterised skin cell models using a variety of immunological and molecular-based techniques against a range of relevant cellular markers (Dahm *et al.,* 2002; Evans *et al.,* 2014; Jin *et al.,* 2013; Watkins *et al.,* 2009). For instance, Jin *et al.* (2013) performed IF staining against the mesenchymal cell marker, vimentin, and various keratinocyte-specific cytokeratins to determine the cell lineages present within primary dolphin skin explant cultures. Watkins *et al.* (2009) performed immunohistochemical staining against the keratinocyte-specific marker, involucrin, for the characterisation of cultured primary ovine keratinocytes and corresponding skin tissue sections; whilst further using haemotoxylin and eosin staining to confirm cellular morphology. Similarly, Dahm *et al.* (2002) reported the characterisation of primary equine keratinocytes through immunohistochemical staining of skin tissue and cell cultures against several cellular markers, including pan-keratin, cytokeratins, vimentin and the cell proliferation marker, Ki-

67. The characterisation of primary bovine foot skin fibroblast and keratinocyte cell lineages have been described previously, whereby, alongside routine morphological observations, Evans *et al.* (2014) developed a novel RT-PCR to detect expression of the bovine involucrin gene, a common marker of terminally differentiated keratinocytes, within dermal and epidermal cell cultures. This RT-PCR was used as a method of characterisation for the bovine foot skin cell cultures in the present study. However, although the combined morphological observations and involucrin expression detected within primary bovine epidermal foot skin cell cultures strongly indicated the presence of some terminally differentiating keratinocytes, this did not confirm lineage purity. Furthermore, despite observations of a consistent fibroblast-like morphology, negative involucrin expression by cells of the primary bovine dermal foot skin cultures did not confirm the presence (or, definitively, the purity) of fibroblast cells. The present study has successfully advanced the methods of characterisation currently described for primary bovine foot skin fibroblast and keratinocyte cells to more definitively confirm the presence of keratinocyte and fibroblast cell lineages within such cultures.

Accordingly, a novel double IF staining protocol was developed and optimised to detect the mesenchymal cell marker, vimentin, and various keratinocyte-specific cytokeratins (pan cytokeratin) within primary bovine foot skin cell cultures and, therefore, provides an extremely useful tool for future characterisation of primary bovine skin cells in culture.

Vimentin is the most abundant intermediate filament protein within the cytoskeleton of fibroblast cells and is also expressed by many other mesenchymal cell lineages (Franke *et al.,* 1978; Goodpaster *et al.,* 2008). Due to the current lack of available fibroblast-specific markers, vimentin is arguably the most commonly used marker for the characterisation of dermal fibroblast cells within skin models, despite its lack of fibroblast specificity, and is typically used alongside morphological observation and the detection of markers of other common cell lineages (Akkoc *et al.,* 2016; Dahm *et al.,* 2002; Jin *et al.,* 2013). In the present study, primary bovine dermal foot skin fibroblast-like cells were found to strongly express vimentin. In combination with morphological observations and a lack of detectable expression of the keratinocyte-specific markers, involucrin and pan cytokeratin, this would suggest a mesenchymal lineage consistent with fibroblast cells. However, whilst often considered the current "gold standard" for fibroblast characterisation, vimentin is far from a definitive cell marker. Notably, keratinocytes undergoing EMT to a mesenchymal cell phenotype are known to express vimentin (Nakamura & Tokura, 2011). Furthermore, cultured human keratinocytes have been shown to co-express vimentin and cytokeratin

intermediate filaments under low calcium, serum-free conditions and have a likely role in epidermal motility at wound edges (Biddle & Spandau, 1996; Castro-Muñozledo *et al.,* 2015; Velez-delValle *et al.,* 2016). Here, primary bovine epidermal foot skin keratinocyte-like cells were found to not express vimentin, as would typically be expected. Vimentin expression was detected by several contaminating fibroblast-like cells around the periphery of keratinocyte-like cell colonies upon initial isolation, believed to be dermal tissue contaminants. Although vimentin was considered to sufficiently distinguish the respective dermal and epidermal cell lineages within this model, the limitations of this marker should be considered when used in such models for host-pathogen interaction studies. Several other dermal fibroblast cell markers have been identified including fibroblast-specific protein 1 (Strutz *et al.,* 1995), fibroblast cell surface antigens (Singer *et al.,* 1989) and collagen-associated proteins such as heat-shock protein 47 (Kuroda & Tajima, 2004). However, many have also demonstrated evidence of poor specificity (Goodpaster *et al.,* 2008; Singer *et al.,* 1989). TE-7 has been identified as a specific marker of human dermal fibroblasts in formalin-fixed, paraffin-embedded dermal tissues and monolayer cultures for application in immunofluorescence studies, enzyme-linked immunosorbent assay (ELISA) and immunohistochemistry (Goodpaster *et al.,* 2008), however there are currently no such antibodies available for use in bovine species.

Whilst dermal fibroblasts lack specific cellular markers, there are many specific cellular markers available for the characterisation of epidermal keratinocytes *in vitro* and many of these correspond to specific stages of terminal differentiation. Such markers include transcription factors such as p63 and basonuclin (BNC2) (Green *et al.,* 2003); the type I (acidic) and type II (basic) cytokeratins (Akkoc *et al.,* 2016; Green *et al.,* 2003; Schweizer *et al.,* 2006); precursors of the cornified envelope such as involucrin (Evans *et al.,* 2014; Green *et al.,* 2003; Tharakan *et al.,* 2010; Watkins *et al.,* 2009), loricrin (Tharakan *et al.,* 2010) and transglutaminases 1, 3 and 5 (Tharakan *et al.,* 2010) and filaggrin (Watt *et al.,* 1989). As with the well-characterised human cytokeratins, bovine cytokeratins are highly abundant, water-insoluble, intermediate filament proteins which form the cytoskeletal tonofilaments of epidermal keratinocytes (Cooper & Sun, 1986; Fuchs & Green, 1980; Moll *et al.,* 1982; Tseng *et al.,* 1982). Acidic and basic cytokeratins are expressed as pairs to enable filament formation; whilst cytokeratins 5 (58 kDa) and 14 or 15 (50 kDa) are typically expressed concomitantly in basal keratinocytes of the stratum basale, cytokeratins 1 (68 kDa) and 10 (56.5 kDa) are common markers of keratinocytes of the suprabasal layers during terminal differentiation (Cooper & Sun, 1986; Fuchs & Green, 1980; Moll *et al.,* 1982; Schweizer *et al.,*

2006; Tseng *et al.,* 1982). As the specific stage of keratinocyte differentiation was unknown in this model, a pan cytokeratin antibody able to detect multiple key cytokeratins of acidic (10, 14, 15, 16 and 19) and basic (1, 2, 4, 5, 6, 9 and 11) pairing, inclusive of those likely to be expressed by epidermal keratinocytes in culture, was chosen (Moll *et al.,* 1982). Primary bovine epidermal foot skin keratinocyte-like cells were found to express pan cytokeratin, whilst primary bovine dermal foot skin fibroblast-like cells were found to not express pan cytokeratin; each further confirming the likely presence of respective keratinocyte and fibroblast cell lineages within culture. Although the use of cytokeratin-specific antibodies would have provided more information on the specific keratinocyte subpopulations isolated and routinely maintained within culture, the primary aim within the context of this study was to distinguish between fibroblast and keratinocyte cell lineages. Indeed, the pan cytokeratin antibody appeared to successfully distinguish between such skin cell lineages within this model.

3.3.3 Suitability as a model for host-pathogen interaction studies of BDD infection

BDD is an inflammatory infectious disease of the bovine digital skin (Blowey & Sharp, 1988) and therefore cells of the bovine foot skin tissue will be involved, to some degree, in the initial or subsequent host-pathogen interactions that facilitate the underlying pathogenesis and deeper invasion of treponemes within bovine foot skin tissue. Host immune cells are also likely to be involved and a previous study has implicated the dysregulation of bovine macrophages in BDD pathogenesis (Zuerner *et al.,* 2007). As the predominant cell lineages within dermal and epidermal foot skin tissue, respectively, and with a well-characterised functional role in immune defence and wound healing, fibroblast and keratinocyte cells are likely at the forefront of such host-pathogen interactions. Previous studies have implicated the dysregulation of inflammatory mediator expression of both keratinocytes and fibroblasts in BDD pathogenesis (Evans *et al.,* 2014; Refaai *et al.,* 2013). Currently, however, relatively little is known about the individual contributions of bovine foot skin cells and the specific interactions with invading treponemes which underly BDD pathogenesis. To investigate such host-pathogen interactions and pathogenic mechanisms which underly BDD infection, an appropriate disease model would be advantageous.

Previous studies of BDD pathogenesis have attempted to elucidate the dysregulation in host inflammatory and immune responses within complete BDD lesions and therefore provide an informative snapshot of disease pathogenesis at a particular stage of lesion development (Refaai *et al.,* 2013; Scholey *et al.,* 2013). However, although highly informative, such disease models are not able to elucidate the role of specific host cell lineages or individual

Treponema phylogroups in disease pathogenesis. Although yet to be used within this setting, the recent development of *in vivo* infection models for BDD may provide a useful tool for such studies of pathogenesis in the near future (Gomez *et al.,* 2012; Krull *et al.,* 2016).

Recent advances in *in vitro* cell culture techniques have seen the development of elegant skin models for application to studies of therapeutic efficacy, infection and inflammation and disease pathogenesis. For instance, Wufuer *et al.* (2016) recently reported the development of a microfluidic human "skin-on-a-chip" model which is able to recapitulate a realistic cellular environment (with epidermal, dermal and endothelial components) and a functional skin barrier. Although in their infancy, and currently only described for human species (Atac *et al.,* 2013; Wufuer *et al.,* 2016), these microfluidic skin models will likely revolutionize future understanding of mammalian host-pathogen interactions. Nevertheless, it is important to consider that even these more advanced skin models currently remain unable to model the interactions of bovine foot skin with the microbiome environment or its associated impact on the progression of infectious disease, such as BDD.

Classically, skin models for host-pathogen interaction studies were previously focused around less advanced, static, two-dimensional or three-dimensional organotypic culture systems, with either a single epidermal component or full-thickness skin models which combine dermal and epidermal components (Reijnders *et al.,* 2015; Rosdy & Clauss, 1990). These "human skin equivalent" (HSE) models may use primary cells, immortalized cells or a combination of the two (Reijnders *et al.,* 2015; Thakoersing *et al.,* 2012). Although these culture systems are useful, they are unable to elucidate the specific cellular interactions which are often crucial for functional analysis; particularly within a pathogenic setting. For these studies, single monolayer cultures are the most effective and have been used extensively to study host-treponeme interactions in a range of disease states and cell lines (Nakao *et al.,* 2014; Zuerner *et al.,* 2007). Indeed, using such models, Evans *et al.* (2014) previously identified a likely role for primary bovine foot skin fibroblasts in BDD pathogenesis and highlighted a number of key inflammatory mediators which were differentially expressed by BDD treponeme sonicates.

One of the major disadvantages of such models are that they are extremely simplistic. As discussed previously (Chapter 1.8), the skin is a dynamic organ which requires complex interactions between the non-immune cells of the epidermis and dermis in addition to immune cells, located both within and outside of the skin tissue, to maintain its protective barrier function, amongst others. Although such simplistic models are extremely useful for functional analysis, it must be noted that they do not account for the complexity of

interactions occurring within the skin tissue and are therefore not representative of the *in vivo* skin environment; this is an important consideration when interpreting data obtained from such models. Nevertheless, such classical models are still widely used in host-pathogen interaction studies of the skin tissue and only serves to emphasise their importance within the field. Within the present study, a simplistic model for use in investigating the host-pathogen interactions of BDD infection has been validated and may provide further application to other diseases of the bovine foot skin tissue.

It is also important to consider that this simplistic bovine foot skin model has been characterised using tissues from Red Poll beef bulls. Red Poll beef cattle were chosen for use in this study due to the availability of bovine foot skin tissue at the local abattoir at the time of sampling. The use of such beef breeds arguably present a limitation of this model as it is dairy cattle breeds, such as Holstein-Friesian, which are most commonly affected and susceptible to BDD. However, whilst the use of bovine foot skin tissue sections from Holstein-Friesian cattle would undoubtedly have been more representative in identifying host-pathogen interactions that are typically observed during BDD infection within the field, beef cattle are known to be susceptible to BDD and therefore such models remain highly informative for elucidating its pathogenesis.

3.3.4 Conclusions

Primary fibroblast and keratinocyte cells have been successfully isolated from bovine foot skin tissue and were, thereafter, routinely subcultured under optimal conditions. A novel double IF staining protocol was developed for characterisation of fibroblast and keratinocyte cell lineages and has advanced the limited range of methods currently described for the characterisation of bovine foot skin cells. Overall, this study provides a useful model for subsequent and future host-pathogen interaction studies of BDD infection.

Chapter Four: RNA sequencing analysis of bovine foot skin fibroblasts following co-incubation with digital dermatitis treponemes.

4.1 Introduction

The transcriptome of a cell is the complete, quantitative and qualitative subset of protein-coding and non-protein-coding RNA transcripts expressed at a particular developmental stage, under specific physiological conditions. Transcriptome profiling can therefore inform cellular function and the dynamic complexities of developmental and disease processes. With host transcriptional regulation widely considered a fundamental driver of pathogenesis, transcriptome data is increasingly used in host-pathogen interaction studies to elucidate underlying disease mechanisms (Blomström *et al.,* 2015; Dillon *et al.,* 2015; Reeder *et al.,* 2017; Zuerner *et al.,* 2007).

Early studies used northern blotting, *in situ* hybridisation or qRT-PCR techniques to investigate mRNA transcript expression on an individual gene basis (Abler *et al.,* 2011; Bhardwaj *et al.,* 2012; Refaai *et al.,* 2013). Evans *et al.* (2014) developed novel qRT-PCR assays to investigate dysregulation of inflammatory mediators in primary bovine foot skin cells following stimulation with BDD treponeme sonicates; finding significant upregulation in *CCL5*, *MMP12*, *TNF-α*, *TIMP3* and *TGF-β* gene expression in fibroblasts. Although these targeted methods have greatly advanced understanding of disease pathogenesis and transcriptional processes, their gene-by-gene approach is limited and not feasible for large comparative studies.

High-throughput methods have since been developed to enable global transcriptome analysis. Collectively termed “transcriptomics”, these broadly encompass the study of transcriptomes and their function, commonly involving characterisation of: (1) transcriptional species including messenger RNA (mRNA), non-coding RNA (ncRNA), small nuclear RNA (snRNA) and small nucleolar RNA (snoRNA), (2) transcript structures (splice variants, post-translational modifications) and (3) differential expression of RNA transcripts at particular stages of development, physiology or disease (Wang *et al.,* 2009).

Relatively inexpensive, hybridization-based microarrays (using fluorescently-conjugated cDNA) were developed for transcriptional profiling studies, however demonstrate high background expression due to cross-hybridisation and are not suitable for organisms with

poorly annotated genomes (Okoniewski & Miller, 2006). Sequenced cDNA or expressed sequence tag library methods were subsequently replaced with more quantitative and higher throughput tag-based methods, such as SAGE and massively parallel signature sequencing. Zuerner *et al.* (2007) used SAGE to investigate global differential gene expression in bovine macrophages exposed to *T. phagedenis* phylogroup sonicate and identified dysregulation of innate immune and wound repair functions. Despite dominating genomic and molecular biology studies in past decades, such "first generation" sequencing technologies (Sanger DNA sequencing; Sanger *et al.,* 1977) are no longer considered as cost-effective for global transcriptomics and are often unable to map short tag sequences uniquely to reference genomes (Wang *et al.,* 2009).

NGS technology provides a comparatively inexpensive platform for high-throughput, parallel sequencing of fragmented and clonally amplified DNA or RNA and has been increasingly favoured for whole genome sequencing, targeted genome and exon sequencing and transcriptomic studies in recent years. The use of NGS technology for transcriptomic profiling, namely RNA-Seq, has revolutionized our understanding of the complexity of transcriptomes during host-pathogen interactions. Currently, RNA-Seq is arguably the most advanced technique for providing unparalleled high resolution and deep coverage of the transcriptional changes that occur during pathogenesis and is highly reproducible by other quantitative methods such as qRT-PCR (Blomström *et al.,* 2015; Jing *et al.,* 2016). RNA-Seq requires very small sample volumes, detects a higher dynamic range, allows discovery of novel transcripts and splice variants and is much more cost-effective than alternatives (Nookaew *et al.,* 2012). Scholey *et al.* (2013) recently used RNA-Seq technology to comparatively analyse global mRNA expression within BDD lesions and healthy bovine foot skin tissue, identifying 1371 significantly differentially expressed genes. This was the first reported global transcriptomics study of BDD pathogenesis using RNA-Seq and provided a profound insight into global patterns of transcription occurring within BDD lesions. NGS technology has yet to be used to investigate the role of individual bovine foot skin cell types in BDD pathogenesis.

The overall aim of this study was to use an RNA-Seq approach to investigate dysregulation of global mRNA expression in primary bovine foot skin fibroblasts following stimulation with representative strains of three predominant BDD *Treponema* phylogroups and a commensal treponeme. Through elucidating key genes, canonical pathways and biological functions associated with inflammatory and immune system dysregulation in the fibroblasts, this approach hoped to highlight possible mechanisms of BDD pathogenesis and identify

important candidates as potential future targets of therapeutic intervention and vaccines against BDD. The primary objectives of this chapter are outlined below:

1) Perform RNA-Seq using the Illumina HiSeq4000 platform to generate differential gene expression profiles for primary bovine foot skin fibroblasts exposed to either LPS from *S. enterica* serotype Typhimurium or sonicates from *T. medium* phylogroup, *T. phagedenis* phylogroup, *T. pedis* or *T. ruminis* (commensal).
2) Compare differential gene expression profiles for each treatment group and use IPA to elucidate key genes, canonical pathways and biological functions that are influenced by each of the three BDD treponemes or commensal treponeme to induce inflammatory and immune system dysregulation within bovine fibroblasts.
3) Identify which of these targets were unique to or commonly shared across each of the treponemes (both pathogenic and commensal) to build on the limited knowledge of BDD pathogenesis and to further dissect the role of connective tissue cells in BDD.

4.2 Results

4.2.1 Isolation, subculture and characterisation of primary bovine foot skin fibroblast cells

Primary bovine fibroblast cells were successfully isolated and subsequently cultured from the dermal layer of visibly healthy, full-thickness foot skin tissue obtained from the underside of the foot (directly above the dewclaws) of a male Red Poll beef bull (24 months of age), immediately at slaughter, as described in Chapter 2.1.2 and 2.1.3. Foot skin tissue from a male Hereford beef bull (20 months of age) was used to isolate primary bovine fibroblast cells for the initial co-incubation experiment using treponeme antigen preparations (Chapter 4.2.2). The choice of cattle breed used to obtain bovine foot skin tissue for this study was based upon the availability of tissues from the abattoir at the time of sampling, as discussed in Chapter 3.3.3. Upon initial subculture, the primary cells underwent characterisation, as described in Chapter 2.2, to confirm the successful isolation of pure primary bovine foot skin fibroblast cells prior to experimental use. By phase contrast microscopy, cells exhibited prominent cytoplasmic projections and the elongated, spindle-shaped morphology characteristic of fibroblasts in culture (Figure 4.1). IF staining confirmed their expression of the cellular marker, vimentin, which is a key intermediate filament of fibroblast cells (Figure 4.1). Cells did not express any of the acidic (56.5/50/48/40 kDA) or basic (65-67/64/59/58/56/52 kDa) cytokeratins, which constitute key intermediate filaments of epidermal keratinocytes, that were examined by IF staining (Figure 4.1). An RT-PCR assay

confirmed absence of an expressed marker of terminally differentiated keratinocytes, involucrin, within primary cultures (Figure 4.2). These observations strongly indicate an absence of contaminating epidermal keratinocytes within the primary bovine foot skin fibroblast cultures.

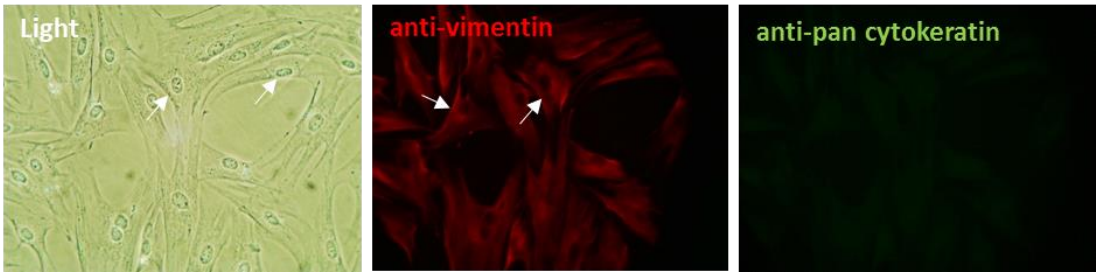

Figure 4.1 Double immunofluorescent staining of primary bovine foot skin fibroblast-like cells against anti-vimentin and anti-pan cytokeratin to validate cell lineage prior to use in RNA sequencing analysis. *Following isolation from bovine foot skin tissue of a Red Poll beef bull, a primary dermal cell culture, representative of the cells used for RNA sequencing, were stained against a known mesenchymal cell marker, vimentin (red), and the keratinocyte intermediate filament protein, pan cytokeratin (green), to validate cell lineage prior to use. The fibroblast-like cells were confirmed to express vimentin, whilst not expressing keratinocyte intermediate filament proteins, pan cytokeratin, and were therefore considered suitable for use in RNA sequencing analysis as pure primary bovine foot skin fibroblast cells. The panel corresponds to one field of view which is representative of triplicate images taken across three experimental replicates. Scale, x20 magnification.*

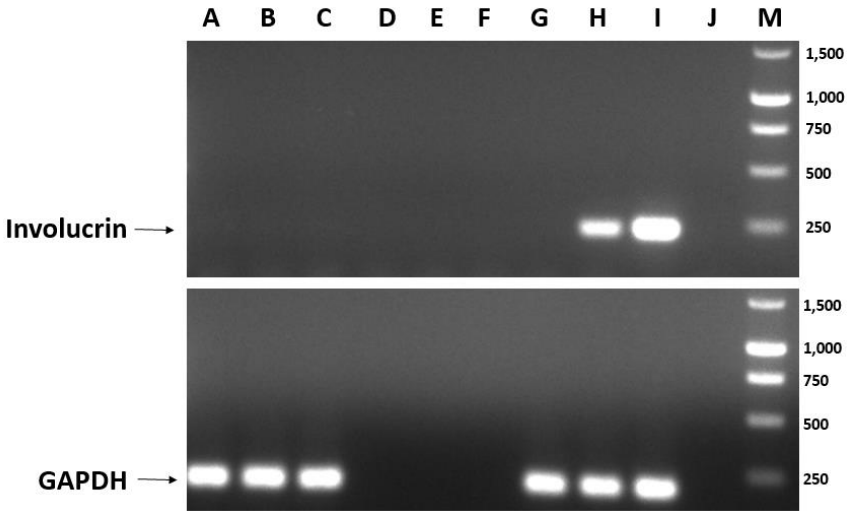

Figure 4.2 Detection of involucrin gene expression in primary bovine dermal foot skin cell cultures by RT-PCR to validate their fibroblast cell lineage prior to RNA sequencing analysis and confirm absence of contaminating gDNA in corresponding total RNA preparations. *Following isolation from bovine dermal foot skin tissue of a Red Poll beef bull, primary fibroblast-like cell cultures corresponding to those prepared for each experimental replicate during RNA sequencing, (A) day one, (B) day two and (C) day three respectively, were subjected to RNA extraction and reverse transcription to produce cDNA. Involucrin gene*

expression was determined by RT-PCR, alongside that of the housekeeping gene, glyceraldehyde 3-phosphate dehydrogenase (GAPDH), to validate their pure fibroblast cell lineage prior to use in RNA sequencing. Products were visualised by agarose gel electrophoresis, as shown, using a 1kb DNA marker (M) to identify correct product sizes. (G) Fibroblast cell cDNA and (H, I) keratinocyte cell cDNA were used as positive controls, with (J) water used as a negative control. Appropriate reverse transcription negative (RT-) controls, (D) day one, (E) day two and (F) day three respectively, were prepared and analysed simultaneously to confirm the absence of involucrin and GAPDH expression which would otherwise suggest gDNA contamination of RNA preparations.

4.2.2 Co-incubation of primary bovine foot skin fibroblasts with treponeme antigen

Whilst the use of live bacterial preparations can be far more representative of the host-pathogen interactions observed *in vivo*, it is the specific molecular components of treponemes which likely come into direct contact with the host. Studying such interactions can greatly inform key mechanisms of BDD pathogenesis and so initial attempts were made to study the interactions between bovine foot skin fibroblast cells and treponeme antigen preparations. Despite several attempts to co-incubate primary bovine foot skin fibroblast cells with *T. medium* phylogroup strain T19, *T. phagedenis* phylogroup strain T320A and *T. pedis* strain T3552B^{T} antigen preparations (Chapter 2.6) for the purposes of RNA-Seq analysis, according to Chapter 2.11.1, this was unsuccessful. It was apparent that, unlike the relevant control cultures (control media and LPS from *S. enterica* serotype Typhimurium), incubation of the fibroblasts with each treponeme antigen preparation caused complete cell lysis within minutes of contact.

To determine whether the observed cell cytotoxicity was due to pathogenic effects of treponeme antigen, fibroblast cells were co-incubated with *T. medium* phylogroup antigen before or after heat-inactivation (105°C, 15 minutes, QBT2 dry block heater). Both inactive and active antigen preparations caused fibroblast cell lysis within minutes of contact, suggesting the observed cytotoxicity is unlikely a result of treponeme pathogenesis.

To determine whether this cytotoxic effect was dose-dependent, fibroblast cells underwent co-incubation with either control medium, a Nonidet™ P 40 substitute control (an equivalent concentration of the detergent without treponeme antigen) or serial dilutions (neat, 1:10, 1:50, 1:100, 1:500 and 1:1000) of the *T. phagedenis* phylogroup antigen in control media. Within minutes of contact, fibroblast cell lysis was observed within cultures incubated with the Nonidet™ P 40 substitute control and neat, 1:10 and 1:50 dilutions of treponeme antigen, whilst the control medium cell culture remained intact. Fibroblasts co-incubated with 1:100 dilution of treponeme antigen began detaching and lysing after 15 minutes and reached

complete lysis after 80 minutes; whilst 1:500 and 1:1000 dilutions remained largely unaffected, however minor morphological changes were observed. As detergents are known to solubilise cellular membranes, the cytotoxicity was considered due to residual Nonidet™ P 40 substitute within the antigen preparations due to insufficient removal during dialysis. Due to time constraints within the scope of this project, it was considered most appropriate to continue co-incubation experiments with non-detergent-based preparations of treponeme lysate rather than proceed with optimising the antigen preparation protocol. Sonication is a common method used to physically disrupt and lyse live bacterial cells through pulsing high frequency sound waves, without the requirement for detergents which may be incompatible with downstream applications. This was the chosen method to prepare treponemes for co-incubation for subsequent RNA-Seq analysis (Chapter 2.5).

4.2.3 RNA sequencing of primary bovine foot skin fibroblast cells following co-incubation with treponeme cell sonicates

Primary bovine foot skin fibroblast cells were successfully co-incubated for 6 hours with control media, LPS from *S. enterica* serotype Typhimurium and sonicated (cell lysate) preparations of *T. medium* phylogroup strain T19, *T. phagedenis* phylogroup strain T320A, *T. pedis* strain T3552B^{T} and *T. ruminis* strain Ru1^{T} (Chapter 2.3 and 2.5), as detailed in Chapter 2.11.1. Fibroblasts exhibited no observed changes in morphological characteristics (by light and phase contrast microscopy) following co-incubation with each of the treatments and subsequently all underwent total RNA preparation, according to Chapter 2.9. An assessment of the quantity and quality (both purity and integrity) of each total RNA preparation was performed according to Chapter 2.9.3 and 2.9.4, as summarised in Appendix B1, Table B.1. To confirm successful removal of gDNA contaminants during RNA extraction, a representative preparation for each independent experimental replicate (designated "QC" in Table B.1) was reverse transcribed to cDNA, alongside an equivalent RT- control, for RT-PCR analysis (Chapter 2.10). As shown in Figure 4.2, RT-PCR confirmed an absence of contaminating gDNA within the three representative total RNA preparations across each experimental replicate.

Twenty total RNA preparations (Appendix B1, Table B.1) of highest quantity and quality, representative of each co-incubation treatment across triplicate experimental replicates, were submitted to the CGR for RNA-Seq analysis (Chapter 2.11). Resultantly, an additional two total RNA preparations were able to be submitted, providing two technical replicates for an experimental replicate of the *T. phagedenis* and *T. ruminis* sonicate treatment groups. On occasion, RNA preparations with the required RIN and A260:A280 ratio were found to have

an A260:A230 ratio marginally below optimal for RNA-Seq, however had to be chosen where a greater quality sample was not available. Due to insufficient rRNA depletion of several total RNA preparations carried out by the CGR, three were replaced (Table B.1 qualifies these samples).

4.2.4 RNA sequencing analysis of the fibroblast transcriptome following challenge with treponeme sonicates

RNA-Seq analysis was used to generate a transcriptome profile of primary bovine foot skin fibroblast cells to identify global changes in gene expression following challenge for 6 hours with sonicated preparations of *T. medium* phylogroup strain T19, *T. phagedenis* phylogroup strain T320A, *T. pedis* strain T3552B^T and *T. ruminis* strain Ru1^T alongside a non-specific inflammatory stimulant, LPS from *S. enterica* serotype Typhimurium. RNA-Seq was also completed on equivalent non-bacterial challenge (control media) samples for comparison. Details of the RNA-Seq pipeline are described in Chapter 2.11.

4.2.4.1 Processing of raw sequenced reads

An average of 66,911,863 (range of 44,401,794 to 102,256,288) raw sequenced reads were obtained per sample. Following the identification and subsequent exclusion of any reads with poor quality or adaptor contamination, and therefore any resulting singlet reads, an average of 66,333,535 (range of 44,104,369 to 101,608,258) sequenced reads per sample remained for further analysis. Details of the total numbers of sequenced reads for each individual sample, before and after quality control procedures, are provided in Appendix B1, Figure B.1.

Trimmed sequence reads for each individual sample (Chapter 2.11.3) were subsequently mapped to the *Bos taurus* genome (UMD 3.1.1/bosTau8) using TopHat2 (Kim *et al.,* 2013), according to Chapter 2.11.4, achieving an average overall read mapping rate of 85.74% (range 78.00% to 90.30%). Average aligned reads per mate pair across each of the treatment groups were 27,693,481 (medium control), 26,783,104 (LPS control), 34,342,019 (*T. medium* phylogroup sonicate), 24,471,173 (*T. phagedenis* phylogroup sonicate), 27,498,649 (*T. pedis* sonicate) and 29,489,722 (*T. ruminis* sonicate). Further details of mapping rates for each individual sample are provided in Appendix B1, Table B.2. Mapped reads for each sample were subsequently used both to investigate the impact of various treponeme sonicates (or LPS control) on differential gene expression in fibroblast cells compared to the media control group (Chapter 2.11.7) and also used to investigate the quality and variation of experimental replicates through normalised gene expression (Chapter 2.11.5 and 2.11.6).

4.2.4.2 Analysis of global differential gene expression

Total numbers of significantly differentially expressed genes ($p \leq 0.05$, $q \leq 0.05$) identified in primary bovine foot skin fibroblast cells, based on log2 fold change, are summarised for each co-incubation treatment in Table 4.1. Use of a log2 fold change cut-off of ≥ 2 for upregulation and ≤ -2 for downregulation in gene expression (higher stringency strategy) was found to exclude the majority of significantly differentially expressed genes in the dataset. A log2 fold change cut-off of ≥ 1 and ≤ -1 (lower stringency strategy) was considered to provide a much more appropriate and relevant balance of inclusion and stringency and was used with $p \leq 0.05$ and $q \leq 0.05$ (FDR-adjusted *p* value) to define significantly differentially expressed genes for all subsequent analyses, unless otherwise stated. A complete list of the significantly differentially expressed genes ($p \leq 0.05$, $q \leq 0.05$, log2 fold change ≥ 1 and ≤ -1) for each treatment group are detailed in Appendix B2, Table B.3.

The fibroblast cells demonstrated a substantial host response to the positive control, LPS from *S. enterica* serotype Typhimurium. Sonicate of the GI tract isolate, *T. ruminis* strain Ru1^T, induced the most global changes in gene expression across the fibroblast transcriptome (Table 4.1). Comparatively, *T. medium* phylogroup strain T19 sonicate was least stimulatory of all co-incubation treatment groups, with just 58 genes significantly differentially expressed (54 were upregulated) when compared to the media control. Unlike this largely upregulatory host response, sonicates of the other two BDD treponemes, *T. phagedenis* phylogroup strain T320A and *T. pedis* strain T3552B^T, induced a greater overall downregulation in the expression of bovine fibroblast genes. These comparisons highlighted differences in host response to each treponeme phylogroup and were explored in more detail.

Table 4.1 Summary of global differential gene expression identified by RNA sequencing in bovine fibroblasts challenged with treponeme sonicates. *Primary bovine foot skin fibroblast cells were co-incubated for 6 hours with either a media control, LPS from S. enterica serotype Typhimurium (positive inflammatory stimulant control), BDD treponeme sonicates (either T. medium phylogroup, T. phagedenis phylogroup or T. pedis) or T. ruminis sonicate. Three independent experimental replicates were performed on different days and each experiment included three technical replicates for each parameter under study. Each cell replicate was subsequently harvested for total RNA extraction and those of best quantity and quality (purity and integrity), representative of each co-incubation treatment across triplicate experimental replicates, were processed for RNA sequencing. Sequenced reads for each co-incubation treatment group were analysed using Cuffdiff to determine global changes in differential gene expression compared to the media control group. Total numbers of significantly differentially expressed fibroblast genes for each co-incubation treatment group, with significance defined during this study as a p value ≤ 0.05 and an FDR-adjusted p value (q value) ≤ 0.05, are given in log2 fold change and are expressed as a mean of three or four (T. phagedenis and T. ruminis) experimental replicates. Total numbers of significantly upregulated and downregulated genes are also given for each co-incubation treatment.*

Co-incubation treatment group	**Total number of significantly differentially expressed genes ($p \leq 0.05$, $q \leq 0.05$)**			**Total number of significantly upregulated genes ($p \leq 0.05$, $q \leq 0.05$, log2 fold change ≥ 1)**	**Total number of significantly downregulated genes ($p \leq 0.05$, $q \leq 0.05$, log2 fold change ≤ -1)**
	All log2 fold changes	**Log2 fold change ≥ 2 or ≤ -2**	**Log2 fold change ≥ 1 or ≤ -1**		
LPS from *S. enterica* serotype Typhimurium [control]	817	41	246	227	19
T. medium phylogroup sonicate strain T19	88	22	58	54	4
T. phagedenis phylogroup sonicate strain T320A	1338	15	398	134	264
T. pedis sonicate strain T3552B^T	670	39	395	38	357
T. ruminis sonicate strain Ru1^T	3185	61	1469	763	706

Shared and unique differentially expressed genes

A Venn diagram was used to visualise and identify the number of these significantly differentially expressed genes which were commonly or uniquely expressed across the fibroblast transcriptome upon stimulation with the different treponeme sonicates (Figure 4.3). A complete list of all uniquely and commonly significantly differentially expressed genes are summarised in Appendix B2, Table B.3.

Interestingly, only ten of the total number of significantly differentially expressed genes were found to be commonly stimulated (each being highly upregulated) by all four of the treponeme sonicates; *IL6*, complement factor B (*CFB*), NF-κB inhibitor zeta (*Mail*), TNF superfamily member 15 (*TNFSF15*), cytidine deaminase (*CDA*), superoxide dismutase 2 (mitochondrial; *SOD2*) and several members of the C-X-C and C-C motif chemokine subfamilies (*CXCL2, CXCL3, CXCL5* and *CCL2*). Furthermore, the three pathogenic BDD treponeme (*T. medium* phylogroup*, T. phagedenis* phylogroup and *T. pedis*) sonicates shared significant differential expression of just 5 additional genes; regulator of G-protein signalling 16 (*RGS16*), MAF bZIP transcription factor F (*MAFF*), zinc finger CCCH-type containing 12A (*ZC3H12A*) and the pro-inflammatory chemokines, *IL-8* and chemokine (C-X-C motif) ligand 1 (*GRO1*). Notably, all 15 of these genes were also significantly upregulated by the LPS control (Appendix B2, Table B.3).

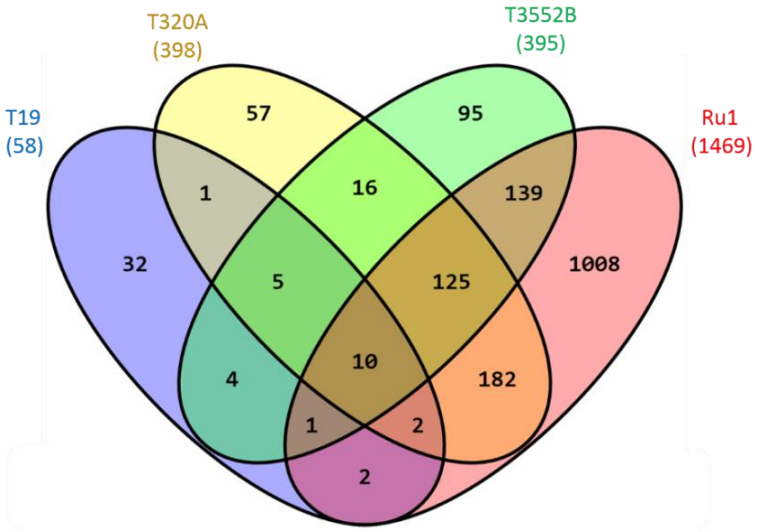

Figure 4.3 Comparison of commonly and uniquely significantly differentially expressed genes in primary bovine foot skin fibroblast cells exposed to treponeme sonicates. *Primary bovine foot skin fibroblast cells were co-incubated for 6 hours with sonicates of T. medium phylogroup strain T19 (blue), T. phagedenis phylogroup strain T320A (yellow), T. pedis strain T3552B^T (green) and T. ruminis strain Ru1^T (red) and total RNA preparations subsequently processed for RNA sequencing. Global differential gene expression in primary bovine foot skin fibroblasts were analysed for each co-incubation treatment group compared to a media control group using Cuffdiff, with each representing the mean of three independent*

experimental replicates performed on different days. Numbers of significantly differentially expressed genes, as defined with a p value ≤ 0.05, an FDR-adjusted p value (q value) ≤ 0.05 and a log2 fold change ≥ 1 or ≤ -1, which were commonly or uniquely expressed in primary bovine foot skin fibroblast cells of each treatment group are illustrated by Venn diagram. The total numbers of significantly differentially expressed genes under comparison for each treatment group are given in parentheses.

A large proportion of the significantly differentially expressed genes in bovine fibroblasts each exposed to sonicates of the *T. medium* phylogroup (55.17%) and *T. ruminis* (68.62%) were uniquely expressed; however, a considerably lower proportion (14.32% and 24.05% respectively) were uniquely expressed following stimulation with *T. phagedenis* phylogroup and *T. pedis* sonicates. Accordingly, the majority of these significantly differentially expressed genes resulting from *T. phagedenis* phylogroup (45.73%) and *T. pedis* (35.19%) stimulation were instead found to be shared with those of the commensal GI treponeme, *T. ruminis*, and then between all three of these groups (~31%).

Interestingly, *T. medium* phylogroup sonicate was the only treponeme treatment, in addition to the LPS control, which stimulated a significant upregulation (+1.085 log2 fold change) of complement C2 (*C2*) in bovine foot skin fibroblast cells. *T. medium* phylogroup sonicate also uniquely stimulated significant upregulation in the expression of TSC22 domain family member 3 (*TSC22D3*; +1.484 log2 fold change), kruppel-like factor 9 (+1.326 log2 fold change), colony stimulating factor 1 (+1.784 log2 fold change), FK506 binding protein 5 (+3.623 log2 fold change), glutamate-ammonia ligase (+1.731 log2 fold change) and phosphoglucomutase 5 (+1.629 log2 fold change).

Whilst found to induce a significant upregulation (+1.221 log2 fold change) in the expression of ISG15 ubiquitin-like modifier alongside the LPS control, *T. phagedenis* phylogroup sonicate also uniquely induced a significant downregulation in expression of mitochondrial ferrochelatase (-1.242 log2 fold change), PHD finger protein 11 (-1.037 log2 fold change), protein GPR107 (-1.104 log2 fold change), regulator of calcineurin 1 (-1.135 log2 fold change) and BCL2 associated athanogene (-1.286 log2 fold change) in bovine foot skin fibroblasts.

Bovine foot skin fibroblast cells were found to demonstrate a significant downregulation in the expression of Cbl proto-oncogene like 1 (-1.423 log2 fold change), ferritin heavy chain (-1.195 log2 fold change), protocadherin gamma subfamily A5 (-1.185 log2 fold change), coagulation factor II thrombin receptor like 2 (-1.390 log2 fold change) and several genes involved in regulating the host immune response such as TRAF3 interacting protein 2 (-1.213 log2 fold change), nuclear factor of activated T-cells 3 (-1.403 log2 fold change) and tripartite motif containing 14 (-1.812 log2 fold change), however only upon stimulation with *T. pedis*

sonicate. This treatment group also uniquely induced a significant upregulation of interleukin 36 alpha (*IL36A*; +1.549 log2 fold change) and, alongside the LPS control, proteasome subunit β9 (+1.066 log2 fold change).

Interestingly, *T. ruminis* was found to induce a significant downregulation in calcineurin binding protein 1 (-1.271 log2 fold change), basal cell adhesion molecule (-1.032 log2 fold change) and several genes associated with cell adhesion, including claudin 15 (-1.272 log2 fold change), kirre like nephrin family adhesion molecule 1 (-1.592 log2 fold change), leucine-rich repeat and fibronectin type III domain-containing protein 3 (-1.662 log2 fold change) and armadillo repeat gene deleted in velocardiofacial syndrome (-1.120 log2 fold change). Microfibril-associated glycoprotein 4, MTSS1L I-BAR domain containing and tenascin C were also each found to be significantly downregulated by only *T. ruminis* sonicate (log2 fold changes of -1.592, -2.847 and -1.977 respectively), whilst annexin A3 and IL-1 receptor associated kinase 4 were found to be significantly upregulated (+1.301 and +1.317 log2 fold changes respectively).

A number of genes within the bovine fibroblast transcriptome, as summarised in Table 4.2, were solely found to have detectable significant expression levels, measured as FPKM, within either the control or treatment group under pairwise comparison. These genes were excluded from subsequent analyses due to the absence of a reportable log2 fold change and will instead be discussed separately. The majority of these genes were found to be non-coding RNAs, including 5.8S rRNAs (*5_8S_rRNA*), small non-coding RNAs (*Y_RNA*), small nuclear RNAs (*U1* and *U2* spliceosomal RNA) and a small nucleolar RNA (*SNORD22*). Several protein-coding genes were also identified, including a novel bovine gene encoding mammary serum amyloid A3.2 (ENSBTAG00000010433) which was only expressed in the control group. Interestingly, the β-defensin 123 precursor (*DEFB123*) was found to be expressed (2.3227 FPKM) in bovine fibroblast cells co-incubated with *T. phagedenis* phylogroup sonicate, but not in the media control. Furthermore, long-pentraxin 3 (*PTX3*) was found to be expressed (1.25328 FPKM) in bovine fibroblast cells only following co-incubation with *T. medium* phylogroup sonicate.

Table 4.2 Summary of significantly expressed genes across the bovine fibroblast transcriptome without detectable expression within both control and treatment comparison groups. *Primary bovine foot skin fibroblast cells were co-incubated for 6 hours with either a media control, LPS from S. enterica serotype Typhimurium (positive inflammatory stimulant control), BDD treponeme sonicates (either T. medium phylogroup, T. phagedenis phylogroup or T. pedis) or T. ruminis sonicate and total RNA preparations subsequently processed for RNA sequencing. Global differential gene expression was analysed in primary bovine foot skin fibroblasts exposed to each co-incubation treatment group and compared to a media control group using Cuffdiff, with each representing the mean log2 fold change across three independent experimental replicates performed on different days. The dataset presented several genes with detectable expression, measured as fragments per kilobase of transcipts per million mapped reads (FPKM), solely in bovine foot skin fibroblasts exposed to either the media control or treatment group under pairwise comparison. In such cases, a log2 fold change of differential gene expression was unable to be calculated and FPKM values were instead analysed on an individual basis.*

Gene	Gene expression (FPKM) in co-incubation treatment					
	Media control	LPS from *S. enterica* serotype Typhimurium	*T. medium* phylogroup sonicate	*T. phagedenis* phylogroup sonicate	*T. pedis* sonicate	*T. ruminis* sonicate
ENSBTAG00000038735	0.669	0.000	-	-	-	0.000
ENSBTAG00000010433	0.000	0.637	-	-	-	-
ENSBTAG00000046013	0.646	-	0.000	0.000	-	0.000
DEFB123	0.000	-	-	2.323	-	-
MIXL1	0.531	-	0.000	-	-	-
PTX3	0.000	-	1.253	-	-	-
U1	0.000	-	-	-	-	16.341
U2	4.351	-	-	0.000	-	-
Y_RNA	0.000	4466.040	3448.030	4082.640	-	5247.090
SNORD22	90.476	-	-	-	0.000	-
5_8S_rRNA	214.783	-	-	-	0.000	-
5_8S_rRNA	119.780	-	-	-	0.000	-
5_8S_rRNA	233.162	-	-	-	0.000	-
5_8S_rRNA	220.805	-	-	-	0.000	-
5_8S_rRNA	217.597	-	-	-	0.000	-

The most upregulated and downregulated genes

To help further dissect these specific host responses on an individual gene basis, the 20 most upregulated and 20 most downregulated genes expressed in primary bovine foot skin fibroblasts resulting from stimulation with the different treatment groups, compared to the media control, were collated and summarised (Figures 4.4 to 4.8).

The bovine fibroblasts demonstrated a marked upregulation in gene expression following stimulation with each treatment, with the largest positive log2 fold changes observed within the LPS control group. Several chemokines and cytokines were consistently some of the most upregulated genes across the fibroblast expression profiles of all treatment groups; particularly *IL6* (+2.774 to +5.726 log2 fold change), *CCL2* (+4.772 to +6.651 log2 fold change) and several chemokine (C-X-C motif) ligands including *CXCL3*, *CXCL5* and particularly *CXCL2* (+5.019 to +7.702 log2 fold change). Several apoptotic mediators, including caspase 4 (*CASP4*) and baculoviral IAP repeat-containing protein 3 (*BIRC3*), were also highly upregulated in fibroblasts across the majority of treatment groups, although notably not following stimulation with sonicate of the *T. medium* phylogroup. Interestingly, bovine fibroblasts stimulated with control LPS and sonicates of *T. medium* phylogroup and *T. pedis* each demonstrated significant upregulation of occulin (*OCLN*) and Rho family GTPase 1 (*RND1*), in addition to the inflammatory mediators, NF-κB inhibitor alpha (*NFKBIA*) and tumor necrosis factor alpha-induced protein 3 (*TNFAIP3*). Furthermore, *CFB* and *SOD2* were both highly upregulated in fibroblasts following stimulation with each of the treatments, demonstrating log2 fold changes of between +2.876 to +4.763 and +2.181 to +4.124 respectively.

The greatest overall downregulation in gene expression was observed in fibroblast cells that had been stimulated with sonicates of *T. pedis* and *T. ruminis*. FUS RNA-binding protein (*FUS*) and protein tyrosine phosphatase type IVA member 3 (*PTP4A3*) were both highly downregulated in these treatment groups. Interestingly, these sonicates were also both found to significantly downregulate the expression of several genes associated with actin rearrangement, including *ACTN1*, synaptopodin (*SYNPO*) and WAS/WASL interacting protein family member 2 (*WIPF2*). Furthermore, several other genes associated with actin rearrangement and cytoskeletal structure were found to be significantly differentially expressed upon stimulation with *T. pedis* sonicate only, including four and a half LIM domains 3 (*FHL3*), nexilin F-actin binding protein (*NEXN*), cofilin-1 (*CFL1*) and Ras homolog family member G (*RHOG*). Notably, *T. medium* phylogroup sonicate was found to stimulate significant downregulation in the expression of just 4 genes, namely fibroblast growth factor

18 (*FGF18*; -1.482 log2 fold change), regulatory factor X2 (*RFX2;* -1.116 log2 fold change) and two *5.8S rRNAs* (-2.422 and -2.917 log2 fold changes respectively). With exception of the *T. pedis* sonicate, the expression of *FGF18* was also consistently downregulated across the remaining treatment groups and demonstrated the greatest (-2.688) log2 fold change following stimulation with *T. ruminis* sonicate. TATA-box binding protein associated factor 15 (*TAF15*) and proteasome 26S subunit ATPase 5 (*PSMC5*) were found to be the most highly downregulated genes of *T. phagedenis* phylogroup sonicate-stimulated fibroblasts (-2.143 and -2.114 log2 fold changes respectively); however, these were also significantly downregulated to a lesser extent in both *T. pedis* and *T. ruminis* sonicate-stimulated cells. Interestingly, extracellular matrix protein 1 (*ECM1*) was found to be significantly downregulated in fibroblasts exposed to sonicates of BDD treponemes, *T. phagedenis* phylogroup strain T320A and *T. pedis* strain T3552B^{T}, and most substantially by that of the GI tract isolate, *T. ruminis* (-2.857 log2 fold change). The expression of this gene was, however, not significantly dysregulated in fibroblasts stimulated with the LPS control or *T. medium* phylogroup sonicate.

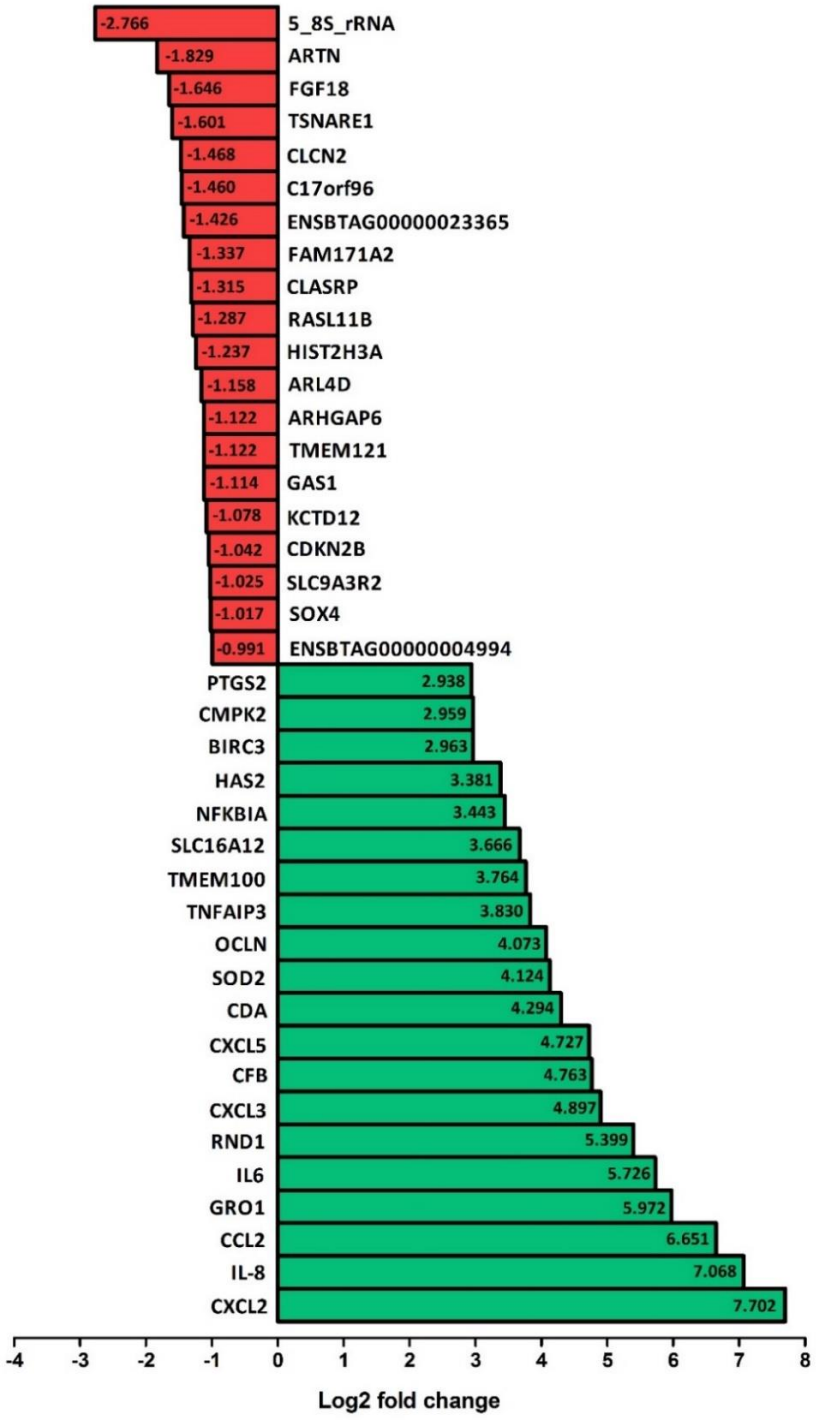

Figure 4.4 The 20 greatest upregulated and downregulated genes expressed in primary bovine foot skin fibroblasts following co-incubation with LPS from S. enterica serotype Typhimurium. *Primary bovine foot skin fibroblast cells were co-incubated for 6 hours with LPS from S. enterica serotype Typhimurium or a media control and total RNA preparations processed for RNA sequencing for comparison of global differential gene expression between the treatment and control group using Cuffdiff. The 20 significantly differentially expressed genes, as defined by a p value ≤ 0.05 and an FDR-adjusted p value (q value) ≤ 0.05, each with the greatest increased (green) and decreased (red) log2 fold changes are provided and represent the mean of three independent experimental replicates performed on different days. Log2 fold change values are provided within each bar for clarity.*

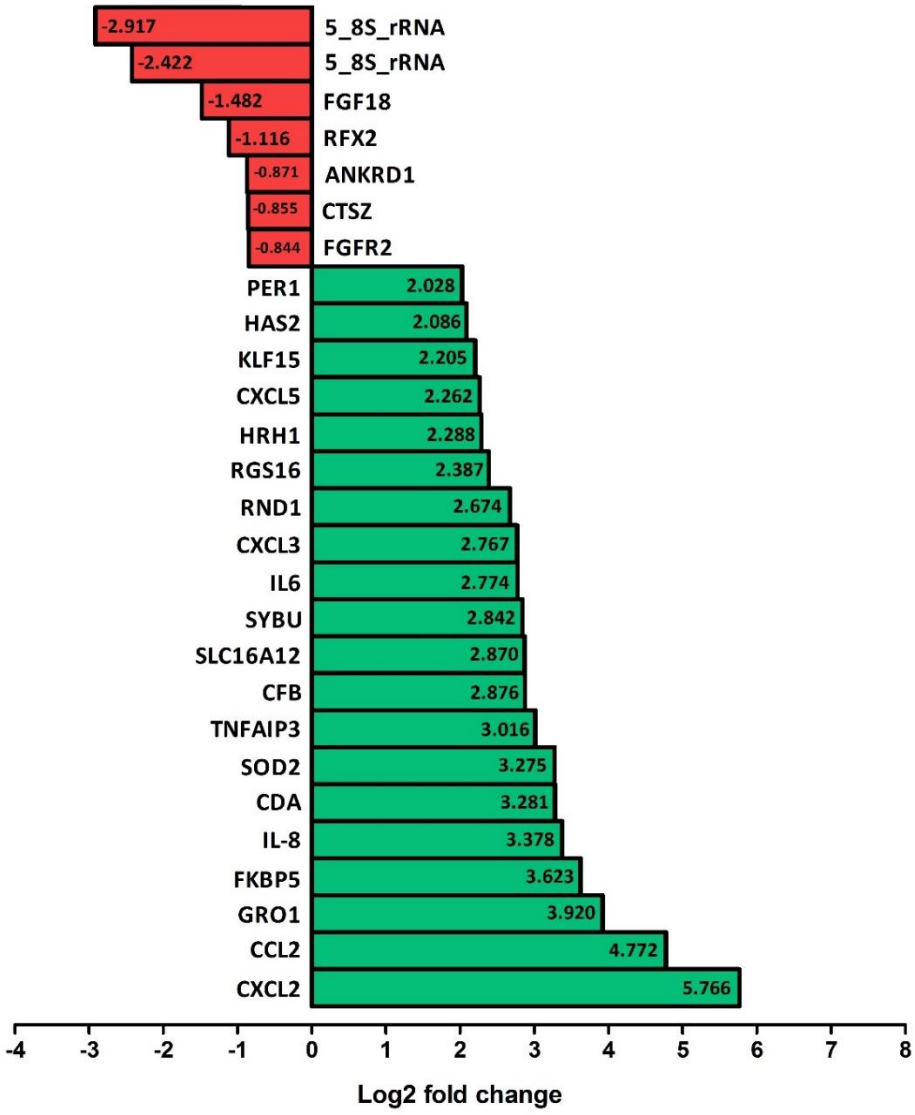

Figure 4.5 The 20 greatest upregulated and 7 downregulated genes expressed in primary bovinefoot skin fibroblasts following co-incubation with T. medium phylogroup strain T19 sonicate. *Primary bovine foot skin fibroblast cells were co-incubated for 6 hours with T. medium phylogroup strain T19 sonicate or a media control and total RNA preparations processed for RNA sequencing for comparison of global differential gene expression between the treatment and control group using Cuffdiff. The 20 and 7 significantly differentially expressed genes, as defined by a p value ≤ 0.05 and an FDR-adjusted p value (q value) ≤ 0.05, each with the greatest increased (green) and decreased (red) log2 fold changes are provided and represent the mean of three independent experimental replicates performed on different days. Log2 fold change values are provided within each bar for clarity.*

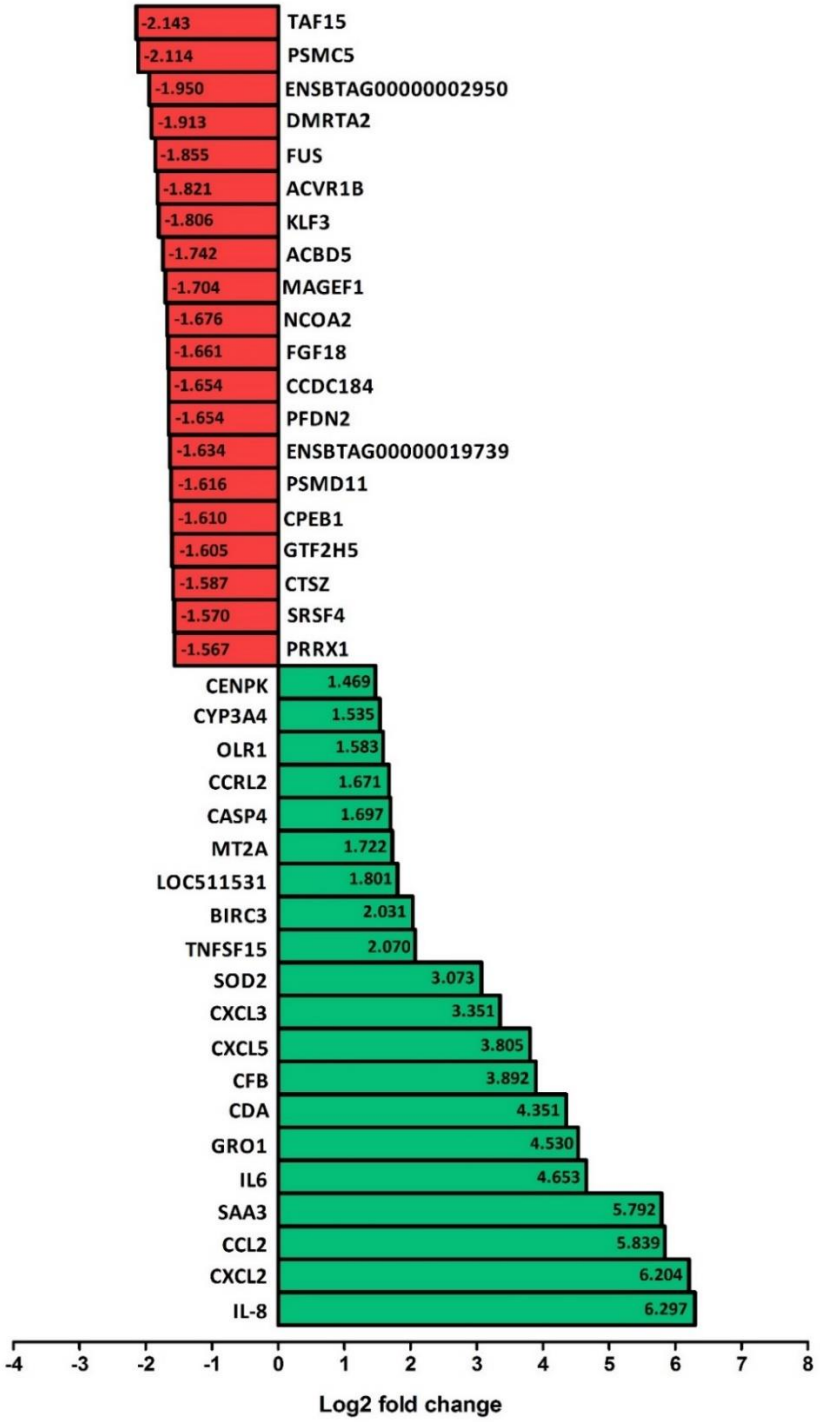

Figure 4.6 The 20 greatest upregulated and downregulated genes expressed in primary bovine foot skin fibroblasts following co-incubation with T. phagedenis phylogroup strain T320A sonicate. *Primary bovine foot skin fibroblast cells were co-incubated for 6 hours with T. phagedenis phylogroup strain T320A or a media control and total RNA preparations processed for RNA sequencing for comparison of global differential gene expression between the treatment and control group using Cuffdiff. The 20 significantly differentially expressed genes, as defined by a p value ≤ 0.05 and an FDR-adjusted p value (q value) ≤ 0.05, each with the greatest increased (green) and decreased (red) log2 fold changes are provided and represent the mean of three independent experimental replicates performed on different days. Log2 fold change values are provided within each bar for clarity.*

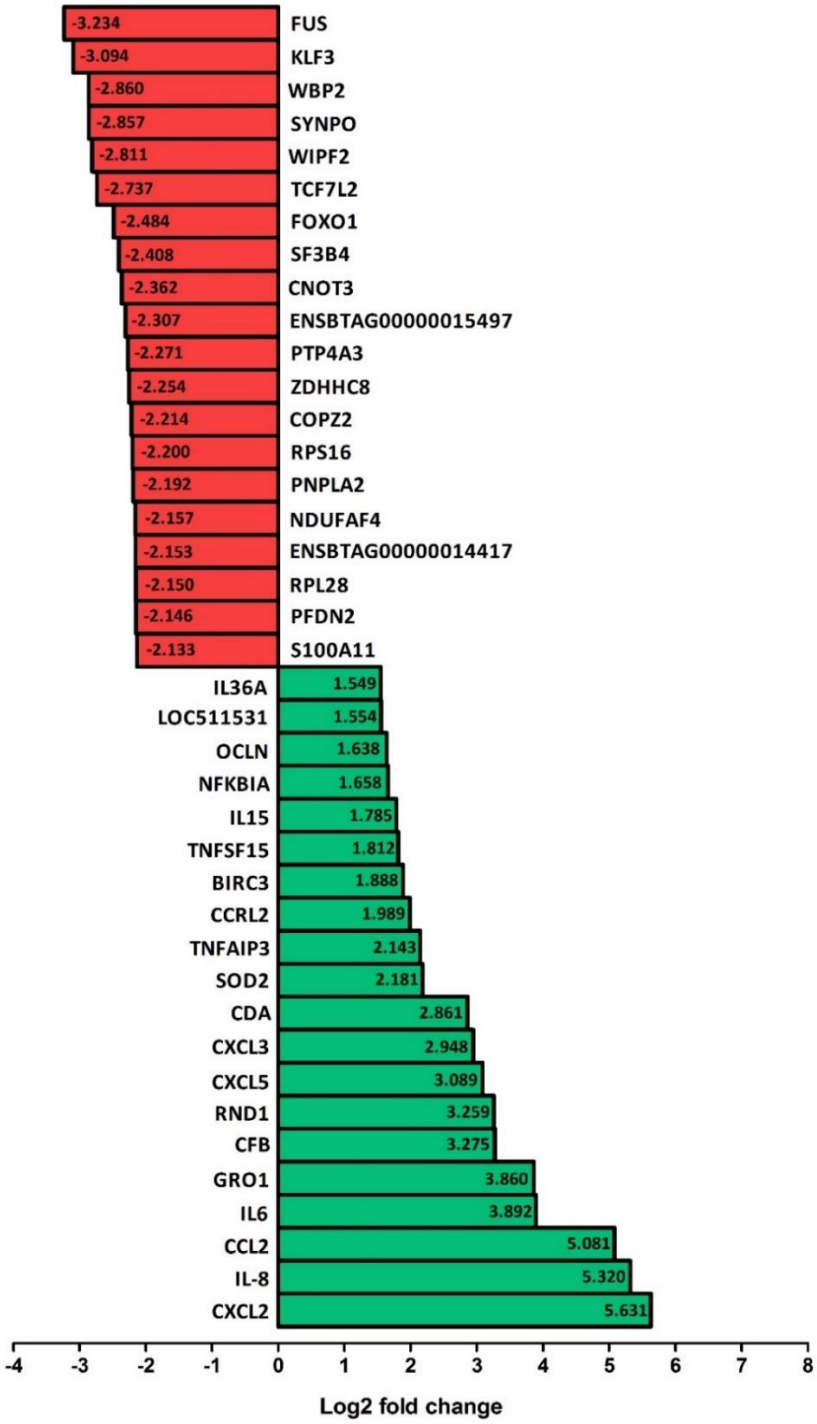

Figure 4.7 The 20 greatest upregulated and downregulated genes expressed in primary bovine foot skin fibroblasts following co-incubation with T. pedis strain T3552B^T sonicate. *Primary bovine foot skin fibroblast cells were co-incubated for 6 hours with T. pedis strain T3552B^T or a media control and total RNA preparations processed for RNA sequencing for comparison of global differential gene expression between the treatment and control group using Cuffdiff. The 20 significantly differentially expressed genes, as defined by a p value ≤ 0.05 and an FDR-adjusted p value (q value) ≤ 0.05, each with the greatest increased (green) and decreased (red) log2 fold changes are provided and represent the mean of three independent experimental replicates performed on different days. Log2 fold change values are provided within each bar for clarity.*

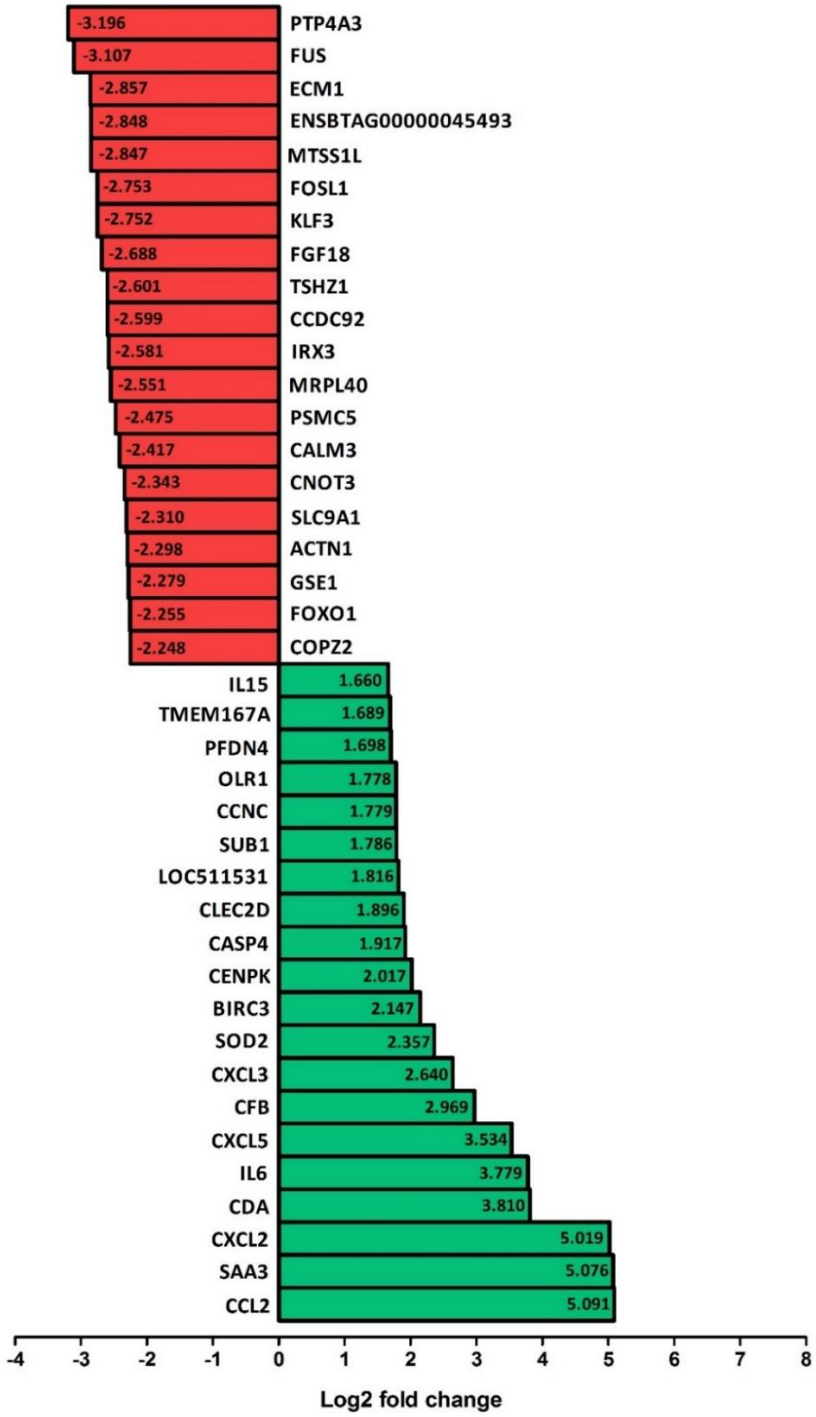

Figure 4.8 The 20 greatest upregulated and downregulated genes expressed in primary bovine foot skin fibroblasts following co-incubation with T. ruminis strain Ru1^T sonicate. *Primary bovine foot skin fibroblast cells were co-incubated for 6 hours with T. ruminis strain Ru1^T or a media control and total RNA preparations processed for RNA sequencing for comparison of global differential gene expression between the treatment and control group using Cuffdiff. The 20 significantly differentially expressed genes, as defined by a p value ≤ 0.05 and an FDR-adjusted p value (q value) ≤ 0.05, each with the greatest increased (green) and decreased (red) log2 fold changes are provided and represent the mean of three independent experimental replicates performed on different days. Log2 fold change values are provided within each bar for clarity.*

Comparative analysis of the most upregulated and downregulated genes

Subsequently, these most significantly upregulated and downregulated bovine genes were each collated into heatmaps (Figure 4.9), according to Chapter 2.11.7, in order to provide a clearer comparison of the observed differential gene expression across each of the treatment groups.

Interestingly, whilst *IL-8* expression was highly upregulated within bovine fibroblasts stimulated with sonicates of each of the BDD treponemes (+3.378 to +6.297 log2 fold change) and the LPS control, it was noticeably not differentially expressed following stimulation with the GI tract isolate, *T. ruminis.* An identical pattern of expression was also observed across the treatment groups for the chemokine, *GRO1*, with log2 fold changes of between +3.860 and +5.972. These particular chemokine expression profiles are in direct contrast to the consistent upregulation observed across all treatment groups for the majority of other significantly differentially expressed cytokines and chemokines. Exceptions to this include interleukin 15 and the immune mediator, serum amyloid A3 (*SAA3*) which were found to be significantly upregulated in fibroblasts stimulated with *T. pedis* and *T. ruminis* sonicates and *T. phagedenis* phylogroup and *T. ruminis* sonicates respectively.

Perhaps the most striking expression profile was found to be that of the period circadian clock 1 (*PER1*) gene, which was found to be significantly upregulated in bovine fibroblasts following *T. medium* phylogroup sonicate stimulation (+2.028 log2 fold change); however, by contrast *PER1* was significantly downregulated following stimulation with *T. phagedenis* phylogroup sonicate (-1.462 log2 fold change). Interestingly, similarities were observed between the gene expression profiles of fibroblasts stimulated with *T.* medium phylogroup sonicate and the LPS control, whereby hyaluronan synthase 2 (*HAS2*), solute carrier family 16 member 12 (*SLC16A12*) and prostaglandin-endoperoxide synthase 2 (*PTGS2*) were each significantly upregulated within these treatments alone. Furthermore, the transcription factor associated with keratinocyte proliferation, *BNC2,* was found to significantly downregulated by both *T. phagedenis* phylogroup and *T. pedis* sonicates.

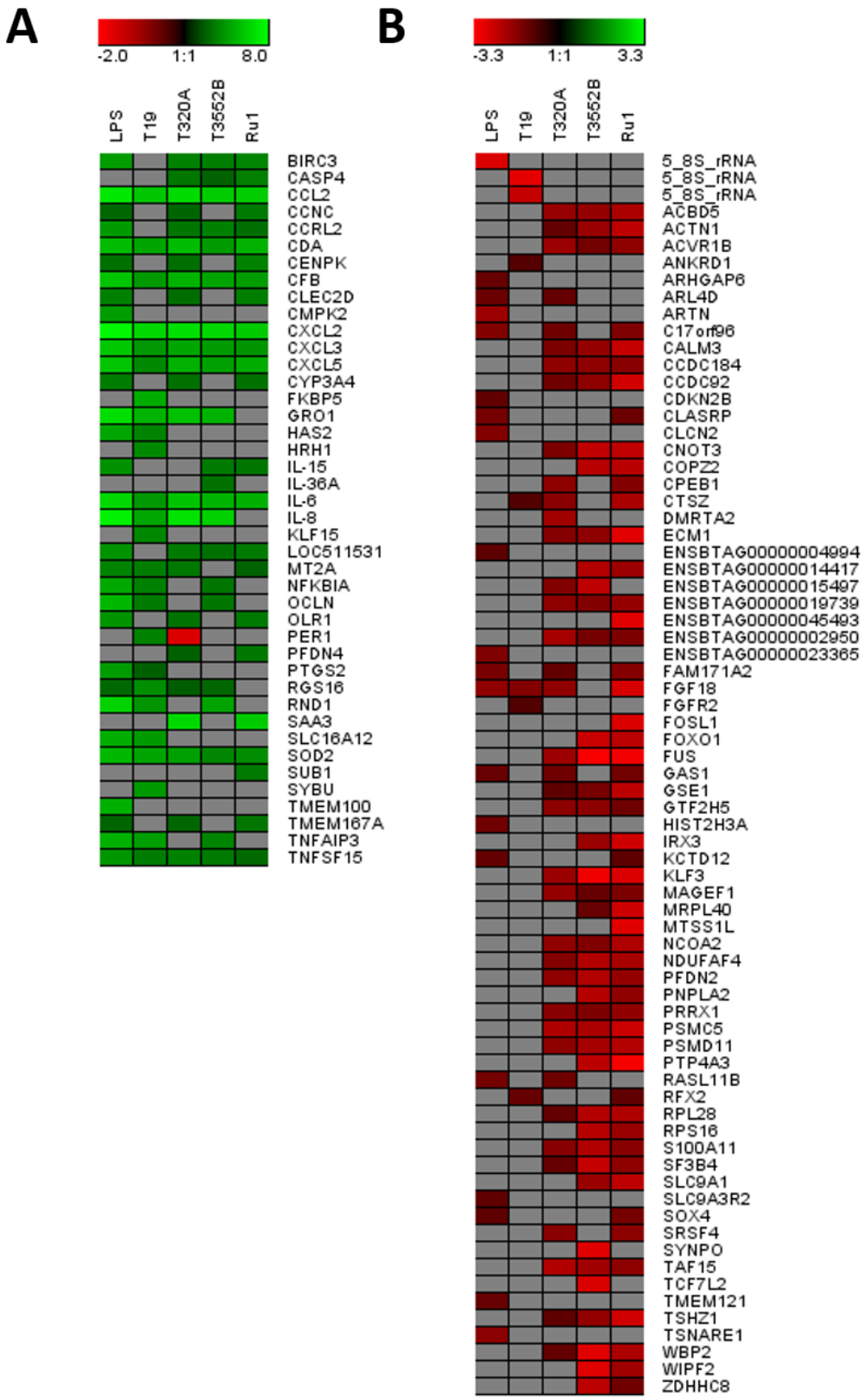

Figure 4.9 Comparison of the greatest upregulated and downregulated significantly differentially expressed genes in primary bovine foot skin fibroblast cells challenged with treponeme cell sonicates. *Primary bovine foot skin fibroblast cells were co-incubated for 6 hours with either a media control, LPS from S. enterica serotype Typhimurium (positive inflammatory stimulant control), BDD treponeme sonicates (either T. medium phylogroup*

strain T19, T. phagedenis phylogroup strain T320A or T. pedis strain T3552B^T) or T. ruminis strain Ru1^T sonicate and total RNA preparations processed for RNA sequencing. Global differential gene expression was analysed in primary bovine foot skin fibroblasts exposed to each co-incubation treatment group compared to the media control using Cuffdiff, with each representing the mean log2 fold change of three independent experimental replicates performed on different days. The 20 significantly differentially expressed genes, defined as a p value ≤ 0.05, an FDR-adjusted p value (q value) ≤ 0.05 and a log2 fold change ≥ 1 or ≤ -1, with the greatest (A) increased (green) and (B) decreased (red) log2 fold changes in primary bovine foot skin fibroblast cells across each treatment group, compared to the media control, are summarised by heatmap. Grey squares indicate that no significant differential gene expression was identified.

In contrast to the upregulatory expression profile of Figure 4.9.A, the most noticeable features of the downregulatory expression profile (Figure 4.9.B) were the striking differences observed between the LPS control and *T. medium* phylogroup sonicate compared to the other remaining treatment groups. The primary bovine foot skin fibroblasts were shown to have a fairly distinct downregulatory expression pattern resulting from stimulation with the LPS control, including the unique downregulation of rho GTPase activating protein 6 (*ARHGAP6*), artemin (*ARTN*) and SLC9A3 regulator 2 (*SLC9A3R2*). There were, however, some similarities observed between this control group and those of the other treponemes, including the downregulation of Ras like family 11 member B (*RASL11B*) and SRY-box 4 (*SOX4*) by the LPS control and sonicates of the *T. phagedenis* phylogroup and *T. ruminis* respectively. As previously observed, Figure 4.9.B highlights the comparatively small number of significantly downregulated genes identified within bovine fibroblasts of the *T. medium* phylogroup sonicate treatment group. Furthermore, many of these significantly downregulated genes appeared to be uniquely expressed within this treatment group, such as the -0.844 log2 fold change in fibroblast growth factor receptor 2 (*FGFR2*). The expression of a considerably large proportion of significantly downregulated genes (identified in Figure 4.9.B) were shared between the *T. phagedenis* phylogroup, *T. pedis* and *T. ruminis* sonicate treatment groups including S100 calcium binding protein A11 (*S100A11*), activin A receptor type 1B (*ACVR1B*), calmodulin 3 (*CALM3*) and NADH:ubiquinone oxidoreductase complex assembly factor 4 (*NDUFAF4*). Despite *T. ruminis* being considered a commensal treponeme of the GI tract, it was found to share dysregulatory gene expression patterns with several of the BDD treponemes; including the consistently significant downregulation of both forkhead box O1 (FOXO1) and solute carrier family 9 member A1 (*SLC9A1*) with *T. pedis*. Furthermore, *T. ruminis, T. phagedenis* phylogroup and *T. medium* phylogroup sonicates were each found

to induce significant downregulation (-2.009, -1.587 and -0.855 log2 fold changes respectively) of the cathepsin Z (*CTSZ*) gene within fibroblast cells.

4.2.4.3 Ingenuity Pathway Analysis

By analysis of orthologous human genes, IPA was used to provide an insight into the specific canonical pathways, diseases and biological functions and upstream regulators predicted to be significantly enriched in bovine foot skin fibroblasts upon stimulation with different treponeme sonicates or the control LPS, as described in Chapter 2.11.8. The number of orthologous human genes successfully mapped or unmapped to the IPA knowledge base are summarised in Table 4.3. Both high (data not shown) and low stringency (Table 4.3) significance cut-off values were assessed to determine which provided an optimal number of "analysis-ready" genes across each of the treatment groups for subsequent IPA (Chapter 2.11.8). The upper cut-off limit was largely defined by the *T. ruminis* sonicate treatment; the 1372 significantly differentially expressed "analysis-ready" genes of the low stringency cut-off (log2 fold change ≥ 1 or ≤ -1) were considered more optimal than the much greater number (2945 genes) identified using the more stringent (log2 fold change ≥ 2 or ≤ -2) cut-off. By contrast, the lower cut-off limit was largely defined by the comparatively poorly stimulating *T. medium* phylogroup sonicate. As shown in Table 4.3, fibroblast cells stimulated with *T. medium* phylogroup sonicate were found to have a sub-optimal number of significantly differentially expressed "analysis-ready" genes (48) when compared to the other treatment groups (ranging from 207 to 1372), particularly despite having an equivalent number of mapped human orthologous genes (Table 4.3). Even when removing the log2 fold change cut-off filter, the number of its "analysis-ready" genes were found to increase to just 74, whilst increasing the number of "analysis-ready" genes within the other treatment groups to between 616 and 2945 (data not shown). Resultantly, the initial log2 fold change cut-off of ≥ 1 or ≤ -1 was considered, overall, to be the most stringent yet inclusive for further analysis by IPA.

Table 4.3 Summary of significantly differentially expressed genes in bovine foot skin fibroblast cells exposed to treponeme cell sonicates whose putative human gene orthologs were successfully mapped, unmapped or "analysis-ready" for Ingenuity Pathway Analysis. *Primary bovine foot skin fibroblast cells were co-incubated for 6 hours with either a media control, LPS from S. enterica serotype Typhimurium (positive inflammatory stimulant control), BDD treponeme sonicates (either T. medium phylogroup strain T19, T. phagedenis phylogroup strain T320A or T. pedis strain T3552B^T) or T. ruminis strain Ru1^T sonicate and total RNA preparations processed for RNA sequencing. Global differential gene expression was analysed in primary bovine foot skin fibroblasts exposed to each co-incubation treatment group compared to the media control using Cuffdiff, with each representing the mean of three independent experimental replicates performed on different days. Equivalent putative human gene orthologs of all significantly or insignificantly differentially expressed genes were identified, where possible, to enable Ingenuity Pathway Analysis (IPA). Those orthologous genes that were successfully mapped to the IPA database are given, alongside those that were not able to be mapped and were therefore excluded from subsequent analysis. The number of "analysis-ready" molecules, mapped orthologous genes which passed the significance cut-off values implemented for further analysis in IPA, including a p value ≤ 0.05, an FDR-adjusted p value (q value) ≤ 0.05 and a log2 fold change ≥ 1 or ≤ -1.*

Co-incubation treatment group	**Total number of differentially expressed human orthologous genes**	**Number of differentially expressed human orthologous genes mapped to the IPA knowledge database**	**Number of differentially expressed human orthologous genes unmapped to the IPA knowledge database**	**Total number of "analysis-ready" human orthologous genes (*p* ≤ 0.05, q ≤ 0.05, log2 fold change ≥ 1 or ≤ 1)**
LPS from *S. enterica* serotype Typhimurium [control]	10162	9935	227	207
T. medium phylogroup sonicate	10191	9964	227	48
T. phagedenis phylogroup sonicate	10188	9964	224	370
T. pedis sonicate	10188	9963	225	365
T. ruminis sonicate	10188	9962	226	1372

Heatmaps each depicting a comparison of the 20 most significantly enriched canonical pathways (A and B), diseases or biological functions (C and D) and upstream regulators (E and F) across each of the treatment groups are summarised (Figure 4.10) by significance according to both *p* values and z scores. Furthermore, bar charts each depicting the most enriched canonical pathways or diseases and biological functions for individual treatment groups (core analysis) can be found in Appendix B2, Figure B2 to B6.

Enriched canonical pathways

Few canonical pathways were predicted to be significantly enriched in bovine foot skin fibroblasts commonly upon stimulation across all treatment groups; however, glucocorticoid receptor signalling and several interleukin-17 (*IL-17*) signalling and disease-associated pathways were notable exceptions. Interestingly, the role of *IL-17* in psoriasis, a chronic human inflammatory skin disease, was predicted to be significantly enriched within bovine fibroblasts stimulated by the three BDD treponemes and the LPS control. The *TREM1* signalling pathway was also significantly activated in fibroblast cells across each of the pathogenic treatment groups, although to a lesser extent with *T. pedis* sonicate; however, *TREM1* was not activated following stimulation with the GI tract treponeme, *T. ruminis.* Interestingly, several canonical pathways associated with cell adhesion, proliferation and cytoskeletal structure were predicted to be inhibited by the *T. ruminis, T. phagedenis* phylogroup and *T. pedis* sonicates such as integrin signalling, integrin-linked kinase signalling and actin cytoskeletal signalling pathways. Notably, whilst the LPS control was found to predictably induce activation of B cell receptor signalling, *T. ruminis, T. phagedenis* phylogroup and *T. pedis* sonicates were found to inhibit this signalling pathway.

Enriched diseases and biological functions

Cell death and survival were prominent and highly significant features of fibroblasts upon stimulation with each of the treponeme sonicates and the non-specific inflammatory LPS control. In particular, necrotic and apoptotic functions were significantly increased across all treatment groups with notable exception to the decreased activity observed by cells stimulated with *T. ruminis* sonicate. Furthermore, while most treponeme sonicates induced a decrease in cell viability and survival, fibroblasts stimulated with both the *T. medium* phylogroup sonicate and LPS control increased these functions. Unsurprisingly, infectious disease, immunological disease and inflammatory disease pathways were all significantly enriched in fibroblasts across each of the treatment groups, alongside that of the host inflammatory response. Gene expression was significantly enriched across all treatment groups, being the most significantly enriched biological function in cells stimulated with both

T. pedis and *T. ruminis* sonicates ($p \geq 3.5 \times 10^{-13}$ and $p \geq 3.9 \times 10^{-10}$ respectively). Stimulated fibroblasts were each significantly associated with organismal injury and abnormalities in addition to connective tissue disorders, the latter being a particularly prominent feature of stimulation by *T. medium* phylogroup sonicate ($p \geq 7.11 \times 10^{-10}$). Furthermore, skeletal and muscular disorder pathways significantly featured across all treatment groups ($1.45 \times 10^{-4} \geq p \geq 7.11 \times 10^{-10}$), although most prominently for the *T. medium* phylogroup and LPS control groups. Interestingly, GI disease was one of the most significantly enriched diseases or biological functions ($p \geq 4.47 \times 10^{-9}$) within fibroblast cells stimulated with the GI tract treponeme, *T. ruminis,* whilst its significance across the other treatment groups was markedly lower ($p \geq 1.69 \times 10^{-6}$). Although the majority of significantly enriched diseases and biological functions identified were commonly shared across each of the treatment groups, several were found to be uniquely enriched. For instance, the cell-mediated immune response and hypersensitivity response were both significantly associated with only pathogens, including sonicates of the three BDD treponemes and the control LPS. Furthermore, genes associated with the humoral immune response were only significantly enriched in fibroblasts stimulated with either *T. pedis* or *T. ruminis* sonicate and the LPS control. Interestingly, only *T. medium* phylogroup sonicate was found to significantly induce the dysregulation of genes associated with energy production and nutritional disease, whilst all treatment groups except for *T. pedis* sonicate induced functions associated with carbohydrate metabolism and metabolic disease. Furthermore, *T. phagedenis* phylogroup sonicate was found to be uniquely associated with dental disease. Interestingly, RNA damage and repair was a significantly enriched feature of only the *T. pedis* sonicate treatment, and whilst enriched across all treatment groups, the expression and transcription of RNA was also a particularly pronounced biological function within this group. Whilst protein degradation was a prominent feature of only *T. pedis* and *T. ruminis* sonicate-stimulated cells, protein synthesis was a feature of all but the *T. medium* phylogroup sonicate treatment group.

Although the majority of significantly enriched diseases and biological functions were commonly shared in fibroblasts among treatment groups, there was a marked dichotomy in the form of dysregulation observed across these groups (Figure 4.10.D). Although there was a widespread inhibition of key biological functions observed by fibroblast cells stimulated with the *T. phagedenis* phylogroup, *T. pedis* and *T. ruminis* sonicates, by contrast, stimulation by *T. medium* phylogroup sonicate and the LPS control largely induced activation. For example, all treatment groups were found to significantly induce both cellular movement and growth and proliferation in the fibroblast cells, with immune cell migration (phagocytes)

and chemotaxis (leukocytes, especially neutrophils) found to be particularly pertinent to *T. medium* phylogroup and *T. phagedenis* phylogroup sonicate groups. However, whilst a significant increase was observed by *T. medium* phylogroup sonicate and the LPS control, sonicates of the remaining pathogenic and commensal treponeme groups (particularly that of *T. pedis*) were found to largely inhibit cell movement and migration. Cellular assembly and organisation was found to be significantly altered in fibroblast cells particularly following stimulation with either *T. pedis* or *T. ruminis* sonicates and to a lesser extent, *T. medium* phylogroup sonicate. Specifically, both *T. pedis* and *T. ruminis* sonicates induced a significant decrease in microtubule dynamics and in the organisation of both the cytoskeleton and cytoplasm whereas, conversely, *T. medium* phylogroup sonicate significantly increased the organisation of the cytoskeleton and microtubule dynamics. However, whilst stimulation with *T. pedis* sonicate induced a significant reduction in the quantity of focal adhesions, actin stress fibres and actin filaments, stimulation with *T. ruminis* sonicate induced a marked increase.

Enriched upstream regulators

Featuring at the centre of one of the most significantly enriched canonical pathways in the dataset, it was unsurprising that *TREM1* was predicted to be a significantly enriched upstream regulator in bovine foot skin fibroblasts across all treatment groups. Its activation was predicted for the LPS control and *T. medium* phylogroup sonicate groups. Similarly, *IL-17* was predicted to be significantly enriched across all treatment groups, with activation predicted for the LPS control, *T. medium* phylogroup and *T. pedis* sonicate groups. Several cytokines, including TNF, interleukin-1-alpha (*IL-1α*) and *IL-1β*, were also predicted to be highly activated across all treatment groups (particularly the LPS control, *T. medium* phylogroup and *T. pedis* sonicates) with the exception of *TNF* in the *T. ruminis* sonicate treatment group. Notably, whilst *T. ruminis, T. phagedenis* phylogroup and *T. pedis* sonicates were predicted to inhibit platelet derived growth factor 88 (*PDGF-88*), both *T. medium* phylogroup sonicate and the LPS control were predicted to induce its activation.

Interestingly, Figure 4.10.E highlights the profound differences in upstream regulator profile predictions observed between the pathogenic and commensal bacterial treatment groups. Many significantly enriched upstream regulators of the pathogenic treatment groups were not shared (or at least not to the same magnitude) by *T. ruminis* sonicate. Notably, the NF-κB complex was found to be significantly activated in bovine foot skin fibroblast cells exposed to constituents of the bacterial pathogens, however notably not by the commensal treponeme, *T. ruminis.* Furthermore, whilst the pathogenic treatment groups were each

predicted to activate nuclear protein 1 transcriptional regulator (*NUPR1*), the commensal treponeme was predicted to inhibit the expression of this upstream regulator.

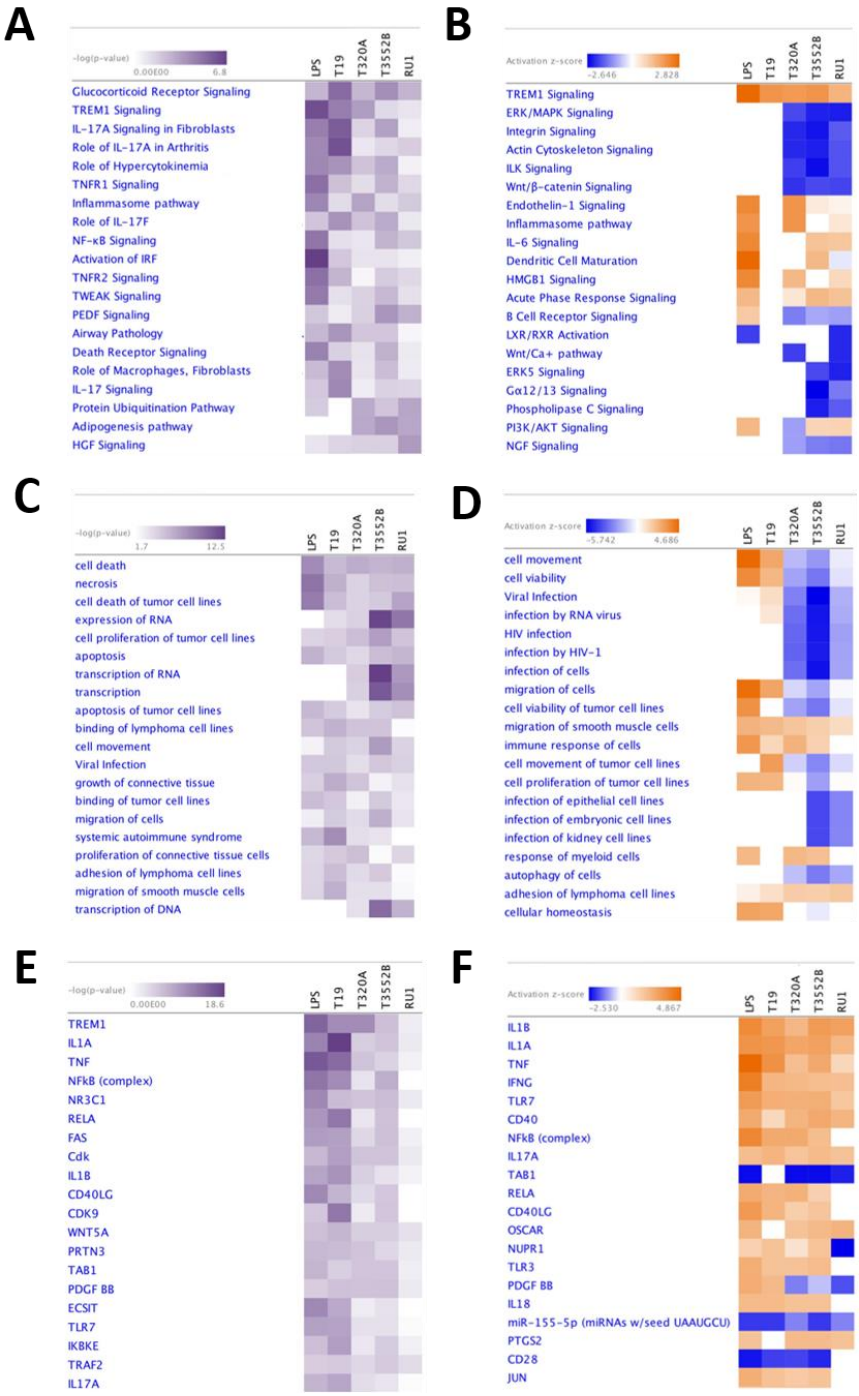

Figure 4.10 Summary of the most enriched canonical pathways, diseases and biological functions and upstream regulators in primary bovine foot skin fibroblast cells exposed to treponeme cell sonicates by Ingenuity Pathway Analysis. *Primary bovine foot skin fibroblast cells were co-incubated for 6 hours with either a media control, LPS from S. enterica serotype Typhimurium (positive inflammatory stimulant control), BDD treponeme sonicates (either T. medium phylogroup strain T19, T. phagedenis phylogroup strain T320A or T. pedis strain T3552B^T) or T. ruminis strain Ru1^T sonicate and total RNA preparations processed for RNA sequencing. Global differential gene expression in primary bovine foot skin fibroblasts were*

analysed for each co-incubation treatment group compared to the media control using Cuffdiff, with each representing the mean of three independent experimental replicates performed on different days. Ingenuity Pathway Analysis (IPA) identified the most significantly enriched (A) canonical pathways, (C) diseases and biological functions or (E) upstream regulators in primary bovine foot skin fibroblast cells exposed to each treatment group, with a right-tailed Fisher Exact Test used to calculate the probability of enrichment compared to the IPA database, denoted as –log(p value) with $p \leq 0.05$ for statistical significance. The most activated (orange) or inhibitid (blue) (B) canonical pathways, (D) diseases and biological functions and (F) upstream regulators, were calculated based upon the IPA z-score algorithm. The greater the z-score beyond 2 the greater the prediction for activation, whereas the greater the z score below -2 the greater the prediction for inhibition. For simplicity, heatmaps documented only the 20 most enriched canonical pathways, diseases and biological functions or upstream regulators for each parameter.

4.2.4.4 Elucidating the correlation in global differential gene expression induced in bovine foot skin fibroblasts by treponemes

Linear regression analysis was performed on log2 fold change expression data for the 20 most significantly upregulated and downregulated fibroblast genes across each treatment group, according to Chapter 2.12.3. Pairwise comparisons were used to determine whether there was significant correlation in differential gene expression of bovine fibroblast cells following stimulation with each treatment group. Each pairwise treatment group comparison (Figure 4.11) was found to demonstrate a statistically significant, strong positive correlation, with a *p* value ≤ 0.001 and an r value > 0.75 in each case. The strongest positive correlation was between that of the LPS control and *T. phagedenis* phylogroup sonicate (r = 0.9531; Figure 4.11.B); followed by the *T. phagedenis* phylogroup and *T. ruminis* sonicates (r = 0.9483; Figure 4.11.I) and then the *T. pedis* and *T. ruminis* sonicates (r = 0.9192; Figure 4.11.J). The least strong positive correlation was between the *T. medium* phylogroup and *T. ruminis* sonicates (r = 0.7611; Figure 4.11.G) and then the *T. medium* phylogroup and *T. pedis* sonicates (r = 0.7727; Figure 4.11.F). These observations mirrored the r^2 values in the degree to which each treatment group reflected predictions for that of the other group during pairwise comparison.

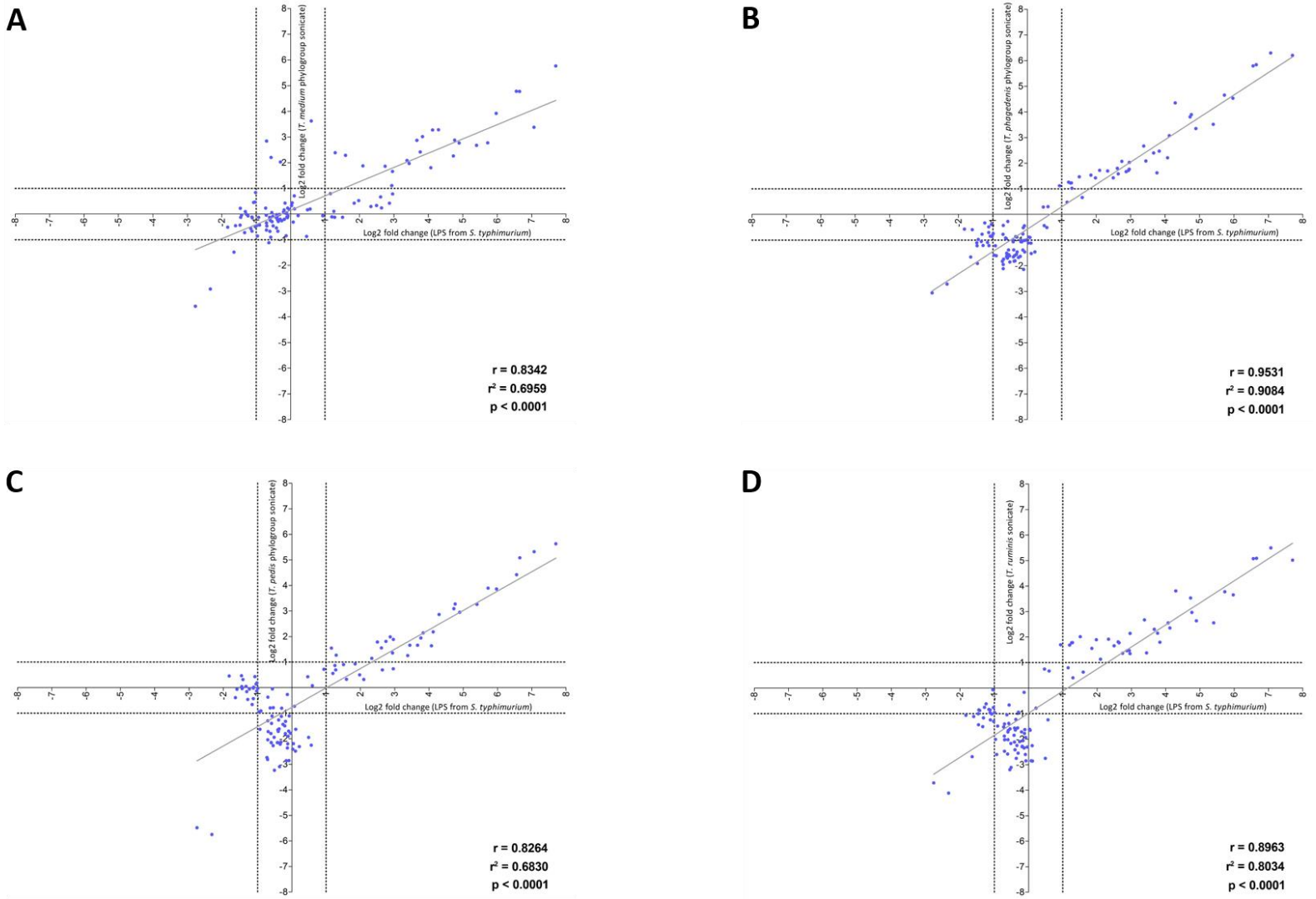
A
Log2 fold change (T. medium phylogroup sonicate)
Log2 fold change (LPS from S. typhimurium)
r = 0.8342
r² = 0.6959
p < 0.0001
B
Log2 fold change (T. phagedenis phylogroup sonicate)
Log2 fold change (LPS from S. typhimurium)
r = 0.9531
r² = 0.9084
p < 0.0001
C
Log2 fold change (T. pedis phylogroup sonicate)
Log2 fold change (LPS from S. typhimurium)
r = 0.8264
r² = 0.6830
p < 0.0001
D
Log2 fold change (T. ruminis sonicate)
Log2 fold change (LPS from S. typhimurium)
r = 0.8963
r² = 0.8034
p < 0.0001

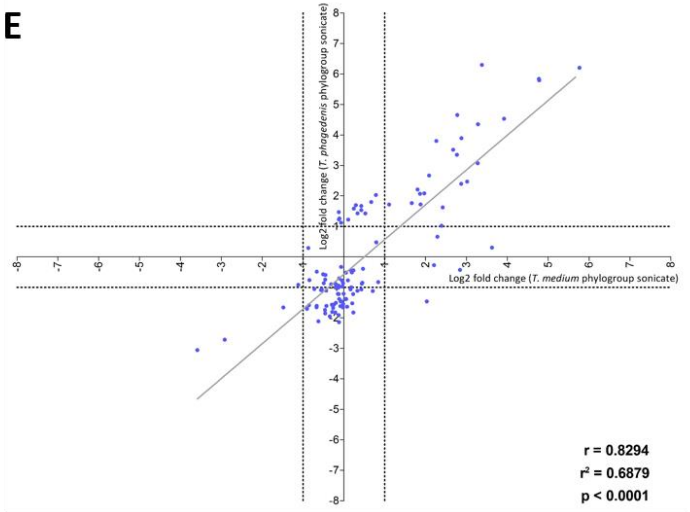
E
Log2 fold change (T. phagedenis phylogroup sonicate)
Log2 fold change (T. medium phylogroup sonicate)
r = 0.8294
r² = 0.6879
p < 0.0001

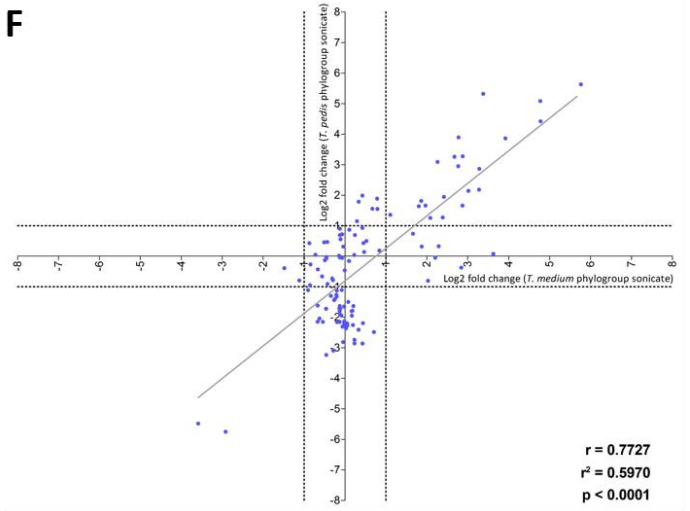
F
Log2 fold change (T. pedis phylogroup sonicate)
Log2 fold change (T. medium phylogroup sonicate)
r = 0.7727
r² = 0.5970
p < 0.0001

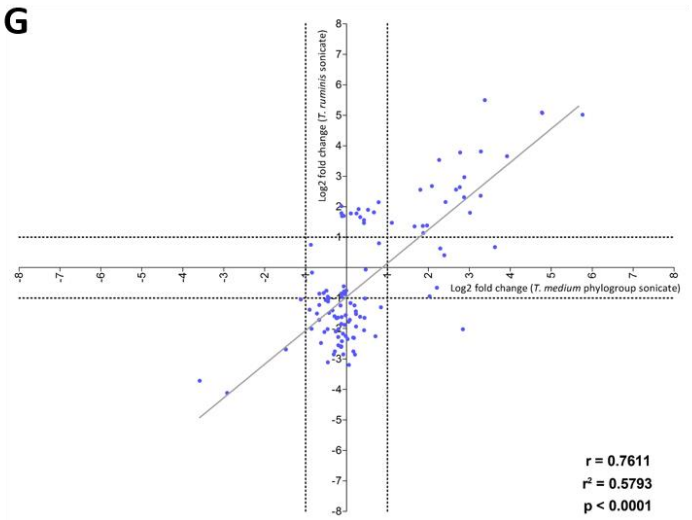
G
Log2 fold change (T. ruminis sonicate)
Log2 fold change (T. medium phylogroup sonicate)
r = 0.7611
r² = 0.5793
p < 0.0001

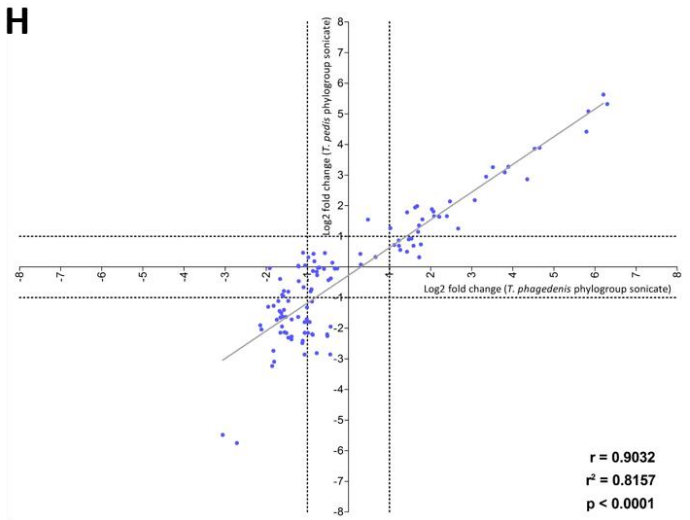
H
Log2 fold change (T. pedis phylogroup sonicate)
Log2 fold change (T. phagedenis phylogroup sonicate)
r = 0.9032
r² = 0.8157
p < 0.0001

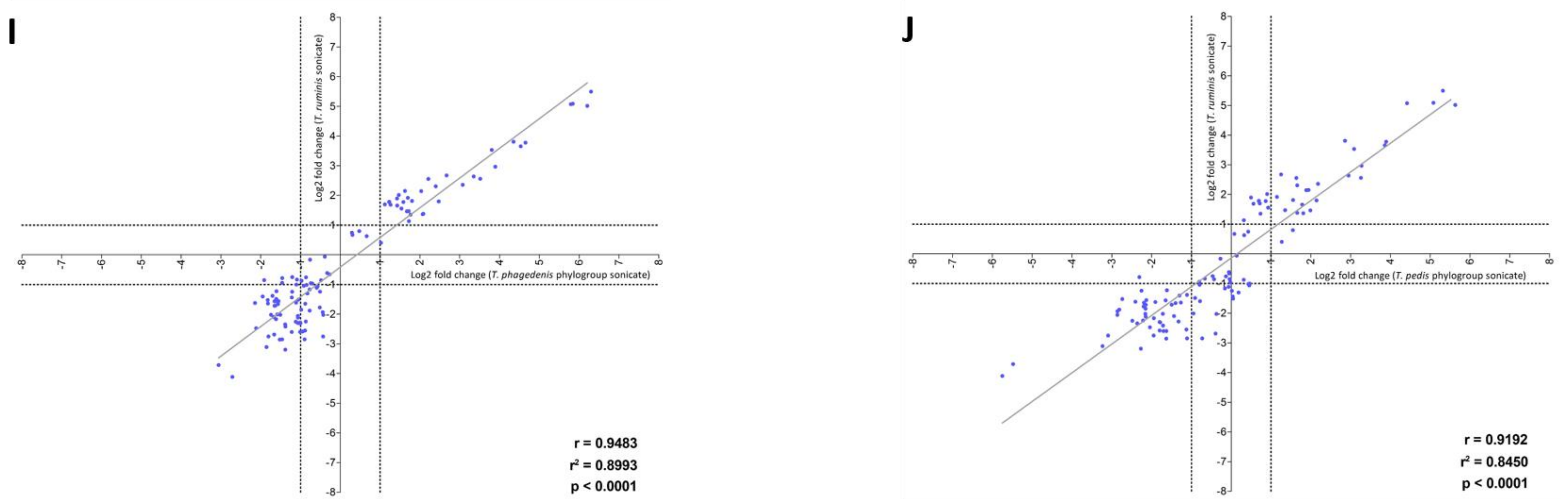

Figure 4.11 Correlation of the differential gene expression profiles of primary bovine foot skin fibroblast cells exposed to treponeme cell sonicates using linear regression analysis. *Primary bovine foot skin fibroblast cells were co-incubated for 6 hours with either a media control, LPS from S. enterica serotype Typhimurium (positive inflammatory stimulant control), BDD treponeme sonicates (either T. medium phylogroup strain T19, T. phagedenis phylogroup strain T320A or T. pedis strain T3552B^T) or T. ruminis strain Ru1^T sonicate and total RNA preparations processed for RNA sequencing. Global differential gene expression (p value ≤ 0.05, an FDR-adjusted p value (q value) ≤ 0.05 and a log2 fold change ≥ 1 or ≤ -1) in primary bovine foot skin fibroblasts were analysed for each co-incubation treatment group compared to the media control using Cuffdiff, with each representing the mean of three independent experimental replicates performed on different days. Correlation of global differential gene expression, represented as log2 fold change of the 20 greatest upregulated and downregulated genes, was determined by linear regression analysis, between the following pairwise comparisons: (A) LPS from S. enterica serotype Typhimurium versus T. medium phylogroup sonicate, (B) LPS from S. enterica serotype Typhimurium versus T. phagedenis phylogroup sonicate, (C) LPS from S. enterica serotype Typhimurium versus T. pedis sonicate, (D) LPS from S. enterica serotype Typhimurium versus T. ruminis sonicate, (E) T. medium phylogroup sonicate versus T. phagedenis phylogroup sonicate, (F) T. medium phylogroup sonicate versus T. pedis sonicate, (G) T. medium phylogroup sonicate versus T. ruminis sonicate, (H) T. phagedenis phylogroup sonicate versus T. pedis sonicate, (I) T. phagedenis phylogroup sonicate versus T. ruminis sonicate, (J) T. pedis sonicate versus T. ruminis sonicate. The regression line (grey) for each pairwise treatment comparison is shown alongside its corresponding linear correlation coefficient (r), coefficient of determination (r^2) and p value (p), where p ≤ 0.05 represents statistical significance.*

4.2.4.5 Analysing the variance between experimental replicates

Upon analysis of differential gene expression, several multivariate analyses were undertaken to identify whether the observed differential gene expression (Chapter 4.2.4.2) and predicted enrichment of specific biological functions and canonical pathways (Chapter 4.2.4.3) in bovine fibroblasts were likely a result of true biological variation, due to treatment stimulation, or a result of confounding experimental variation. These analyses included PCA (Chapter 2.12.1), heatmap expression profiling (Chapter 2.11.7) and HCL analysis (Chapter 2.12.2).

Principle component analysis

PCA was performed by comparing normalised FPKM expression data for each of the 20 experimental replicates. The quality and variance of these replicates across each treatment group were displayed as a series of principle component plots, as shown in Figure 4.12. The first principle component plot (Figure 4.12.A) illustrated that 82.50% of variation within the dataset can be explained by the first principle component, with the second and third principle component accounting for a further 4.67% and 3.13% of variation respectively. With over 90% of the variation within the dataset accounted for by principle component 1 (PC1), principle component 2 (PC2) and principle component 3 (PC3), there was high confidence that the 3 corresponding principle component plots (Figure 4.12.B, Figure 4.12.C and Figure 4.12.D) were representative of the observed variation across the dataset.

The plots of both PC1 versus PC2 (Figure 4.12.B) and PC2 and PC3 (Figure 4.12.D) both appeared to demonstrate that the experimental replicates formed two distinct variant clusters across the dataset. Since the clustering pattern did not appear to correspond to particular treatments, as experimental replicates of each treatment group were found to occupy both distinct clusters, this suggested a likely experimental batch effect. PCA also revealed that three of the experimental replicates, each belonging to a different treatment group (sample numbers 11, 18 and 38), consistently clustered independently of the two predominant variant groups when comparing variation across PC1 versus PC2 (Figure 4.12.B), PC1 versus PC3 (Figure 4.12.C) and PC2 versus PC3 (Figure 4.12.D). Resultantly, these three experimental replicates appear to be likely outliers. To determine whether the presence of these putative outliers were skewing the observed variance across the dataset, the three experimental replicates were removed and the PCA repeated. The resulting principle component plots (Figure B.7, Appendix B3) displayed an even more prominent divide of the experimental replicates across the two variant clusters than that displayed in Figure 4.12. Interestingly, the removal of these three outliers also highlighted another potential outlier

within the media control group as sample number 52 (Figure B.7, Appendix B3). That said, the variance pattern was largely unchanged.

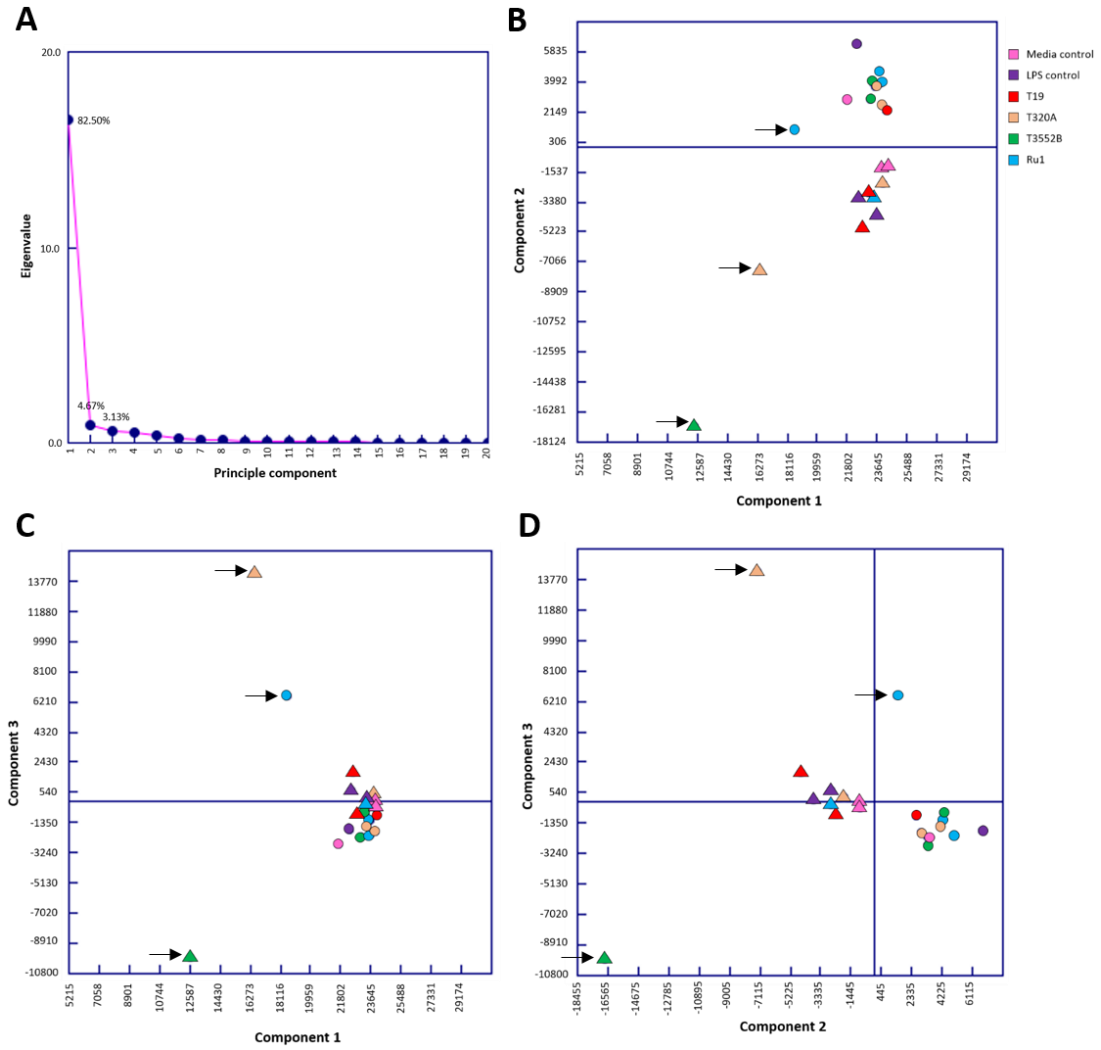

Figure 4.12 Principle component analysis demonstrating the variance of normalised gene expression in primary bovine foot skin fibroblast cells exposed to treponeme cell sonicates, across all experimental replicates, by RNA sequencing. *Primary bovine foot skin fibroblast cells were co-incubated for 6 hours with either a media control, LPS from S. enterica serotype Typhimurium (positive inflammatory stimulant control), BDD treponeme sonicates (either T. medium phylogroup strain T19, T. phagedenis phylogroup strain T320A or T. pedis strain T3552B^T) or T. ruminis strain Ru1^T sonicate and total RNA preparations processed for RNA sequencing. Normalised gene expression values, measured as fragments per kilobase of transcipts per million mapped reads (FPKM), for primary bovine foot skin fibroblast cells exposed to each co-incubation treatment group were further normalised for principle component analysis (PCA) to determine the quality and variation in each of the 20 experimental replicates. PCA plots illustrate (A) the percentage (%) of variation explained by each of the 20 principle components, variation observed by comparison of (B) principle component 1 and principle component 2, (C) principle component 1 and principle component 3, (D) principle component 2 and principle component 3. The circular and triangular nodes*

each represent two distinct variant clusters within the dataset, which correspond to the two pools of cDNA libraries processed during sequencing. Experimental replicates that were considered likely outliers are highlighted with a black arrow.

Heatmaps for normalised expression profiling

Heatmaps of normalised FPKM expression data were produced to further assess variance across each of the 20 experimental replicates for the 20 most upregulated and downregulated genes (Chapter 4.2.4.2). As shown in Figures B8 to B12 (Appendix B3), these heatmaps highlighted several experimental replicates whose gene expression profile differed from others of the same treatment group, suggesting they may be outliers. One of these outliers, sample number 52 (medium control), was also highlighted as a likely outlier by PCA following the exclusion of three putative outliers (Figure B.7, Appendix B3).

Hierarchical clustering analysis

The clustering patterns and variance of normalised FPKM expression across the complete dataset for each of the 20 experimental replicates were assessed by HCL analysis. The HCL dendrogram in Figure 4.13 presents these clustering patterns, however only the gene expression patterns for the 20 most significantly upregulated and downregulated genes (Chapter 4.2.4.2) have been shown for simplicity. Interestingly, the HCL dendrogram revealed a consistent pattern of variance across the experimental replicates to those demonstrated by PCA analysis in Figure 4.12. The three likely outliers (samples 11, 18 and 38) were again found to cluster independently from the other two main clusters. Within both clusters, there does appear to be some clustering of replicates from the same treatment groups (particularly samples 8 and 33 from the media control group and samples 51 and 57 from the *T. ruminis* sonicate treatment group).

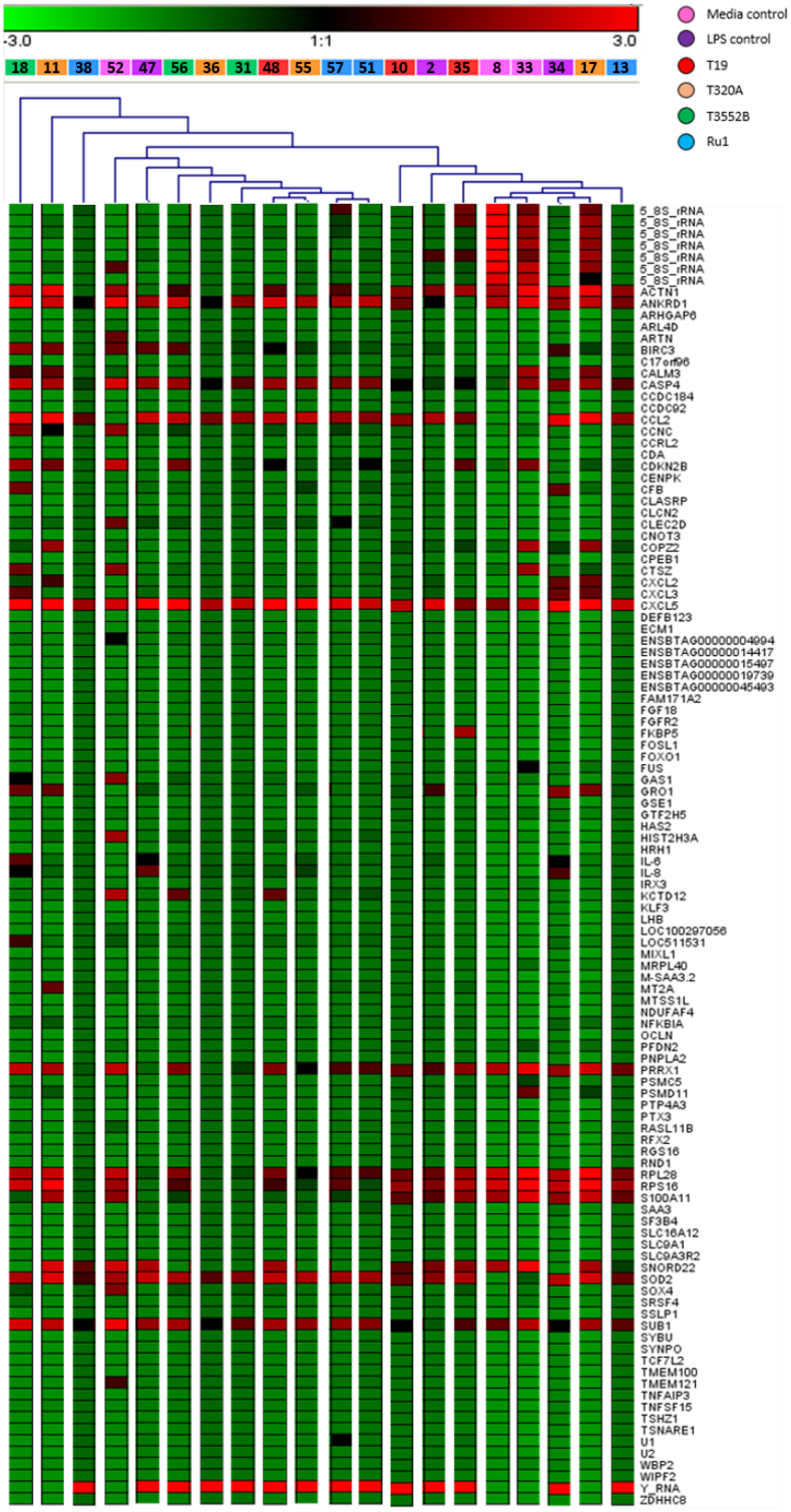

Figure 4.13 Hierarchical clustering dendrogram illustrating the clustering patterns and variance of normalised gene expression in primary bovine foot skin fibroblast cells exposed to treponeme cell sonicates, across all experimental replicates, by RNA sequencing. *Primary bovine foot skin fibroblast cells were co-incubated for 6 hours with either a media control, LPS from S. enterica serotype Typhimurium (positive inflammatory stimulant control), BDD treponeme sonicates (either T. medium phylogroup strain T19, T. phagedenis phylogroup*

strain T320A or T. pedis strain T3552B^T) or T. ruminis strain Ru1^T sonicate and total RNA preparations processed for RNA sequencing. Normalised gene expression values, measured as fragments per kilobase of transcipts per million mapped reads (FPKM), for primary bovine foot skin fibroblast cells exposed to each co-incubation treatment group were further normalised for hierarchical clustering analysis, using the average linkage WPGMA method. Normalised expression profiles of only the 20 most significantly upregulated and downregulated genes were presented here for simplicity, with sample numbers and corresponding treatment groups (represented by different colours) indicated for each experimental replicate. Branch length directly correlates to the similarity between clusters.

4.3 Discussion

BDD is an inflammatory infectious disease of the bovine digital skin highly associated with spirochaetal bacteria of the genus *Treponema* (Blowey & Sharp, 1988; Evans *et al.,* 2008; Evans *et al.,* 2009a). Although *T. medium* phylogroup, *T. phagedenis* phylogroup and *T. pedis* spirochaetes have each been consistently isolated from lesions in the UK (Evans *et al.,* 2008), their individual roles in the underlying pathogenesis of BDD have yet to be elucidated and will be essential in identifying novel targets for future vaccines and therapeutics. RNA-Seq has become an increasingly valuable tool for transcriptomic analysis in recent years and is a particularly valid approach for investigating the host-pathogen interactions that underly disease pathogenesis. An RNA-Seq approach was recently used to elucidate global changes in mRNA expression within BDD lesions compared to healthy bovine foot skin tissue (Scholey *et al.,* 2013). However, most transcriptome studies of BDD pathogenesis have largely focused on either a targeted gene approach (Refaai *et al.,* 2013) or the role of specific cell populations (Evans *et al.,* 2014; Zuerner *et al.,* 2007). These approaches have yet to be combined in host-pathogen interaction studies of BDD pathogenesis. Accordingly, this study has used an RNA-Seq approach to investigate global transcriptional changes in a specific bovine foot skin cell population, following exposure to BDD treponeme constituents, to elucidate fundamental mechanisms of BDD pathogenesis and the individual role of each *Treponema* phylogroup.

4.3.1 An appropriate model for investigating host-pathogen interactions of BDD

A simplistic monolayer cell culture model was considered most appropriate for investigating the specific host-pathogen interactions between bovine foot skin cell populations and specific *Treponema* phylogroups, as previously discussed in Chapter 3.3.3. The monolayer cell culture model used in this study was successfully validated in Chapter 3. Bovine foot skin fibroblasts were chosen as the initial target host cell population for this study; with the intention to subsequently repeat such experiments using the keratinocyte model. As

previously discussed (Chapter 3), fibroblast and keratinocyte cells are both considered to have a fundamental role in host immune defence and wound healing processes within the skin tissue. However, Evans *et al.* (2014) recently hypothesised a greater role for bovine foot skin fibroblasts, rather than keratinocytes, as a target of pathogenesis for BDD treponemes. Unfortunately, due to time constraints within the scope of this study, it was ultimately not possible to complete further experiments using the keratinocyte model as originally intended. One of the limitations of the model used within this study was the choice of a Red Poll beef bull, rather than a more susceptible breed such as Holstein-Friesian, to isolate the primary bovine foot skin fibroblast cells for studying host-pathogen interactions of BDD, as discussed during Chapter 3.3.3. This breed was chosen due to the availability of bovine tissues at the abattoir at the time of sampling and, whilst the use of Holstein-Friesian tissues would have been more representative of the interactions occurring during BDD infection within the field, beef cattle are also susceptible and are a useful tool for informing such interactions within equivalent tissues of dairy cattle breeds.

Whilst host-pathogen interaction studies using live bacterial preparations can be highly informative and often more representative of such interactions *in vivo,* it is the specific molecular components of invading treponemes which are considered to induce the characteristic inflammatory and immune responses within host tissues during BDD infection. Therefore, initial attempts were made to investigate the host-pathogen interactions between bovine foot skin fibroblast cells and treponeme antigen; however, despite multiple attempts, these were unsuccessful due to complete fibroblast cell lysis. After eliminating cytopathic effect as a possible explanation, it was concluded that the observed dose dependent effect, alongside the known ability of detergent to lyse cells, was suggestive of residual Nonidet™ P 40 substitute within the antigen preparations. The method of antigen preparation was chosen as previously described in producing BDD treponeme antigen for serological ELISA (Dhawi *et al.,* 2005; Sullivan *et al.,* 2015c). However, upon closer inspection it was found that Nonidet™ P 40 detergent is not readily dialyzable due to the high molecular weight of its detergent micelles (Pierce, 2004) and is, therefore, unable to be efficiently removed from solution by this method. Within the scope of this study, it was considered more time effective to continue the co-incubation experiment using treponeme proteins prepared using an alternative, non-detergent-based method, rather than attempt optimisation of the antigen preparation protocol and risk further detergent-based effects. Treponeme sonicates have been successfully used in many previous host-pathogen studies of BDD pathogenesis *in vitro* (Evans *et al.,* 2014; Zuerner *et al.,* 2007) and this is likely due to

the difficulties of coordinating large host-pathogen interaction studies using fastidious microorganisms. For these reasons, treponeme sonicates were chosen as the preferred alternative here. Importantly, Ebnet *et al.* (1997) previously demonstrated that *B. burgdorferi* sonicates induced an inflammatory profile which was representative of that induced by equivalent viable spirochaete preparations in human skin cells. Furthermore, Naresh *et al.* (2009) previously highlighted the importance of using spirochaete sonicate preparations, in addition to viable cells and culture supernatants, to elucidate the specific pathogenic mechanisms of *Brachyspira pilosicoli* in cultured Caco-2 cells. Whilst treponeme sonicates were therefore considered appropriate for elucidating the key host-pathogen interactions between bovine fibroblasts and BDD treponeme phylogroups, it should be noted that a previous study did identify greater host responses with sonicated, rather than live, bacterial preparations (Nixon *et al.,* 2000) and data interpretation should therefore be carefully considered.

The co-incubation experiment itself was largely modelled on that previously described for investigating host-pathogen interactions in bovine foot skin fibroblasts using qRT-PCR (Evans *et al.,* 2014). *T. medium* phylogroup strain T19, *T. phagedenis* phylogroup strain T320A and *T. pedis* strain T3552B^{T} were chosen representatives of the three BDD treponeme phylogroups as they have each been used previously in this capacity (Evans *et al.,* 2009b; Evans *et al.,* 2014), are frequently isolated from BDD lesions (Evans *et al.,* 2008; Stamm, 2002) and are highly associated with lesion pathogenesis (Evans *et al.,* 2008; Evans *et al.,* 2009a; Klitgaard *et al.,* 2013; Marcatili *et al.,* 2016). Although it would have been interesting to compare additional BDD-associated treponeme isolates, the expense of RNA-Seq was a limiting factor and the three predominant BDD treponemes of UK lesions were considered most relevant to this study. The recently characterised bovine commensal, *T. ruminis* strain Ru1^{T} (Newbrook *et al.,* 2017; Chapter six), was also included to provide a comparison between commensal and pathogenic treponemes; particularly as the function of such commensals are currently unknown. Although several other bovine commensal treponemes have been characterised (Paster & Canale-Parole, 1985; Staton *et al.,* 2017), it was not possible to investigate more representatives due to the expense of RNA-Seq. LPS from the Gram-negative anaerobe, *S. enterica* serotype Typhimurium, was included to provide a representative positive control for inflammatory stimulation, as previously by Evans *et al.* (2014). Similarly to Evans *et al.* (2014), the LPS control was found to demonstrate a transcriptional profile which was largely distinct from that of the BDD treponemes. Due to the expense of RNA-Seq, fibroblast transcriptome profiles were investigated at a single time

point following treatment co-incubation. Evans *et al.* (2014) previously reported 6 hours to be an optimal post-challenge time point for the detection of mRNA expression within treponeme-stimulated bovine foot skin fibroblasts and so this time point was chosen.

4.3.2 Interpretation of global differential gene expression analysis

Upon analysis of global differential gene expression, transcriptome profiles clearly revealed significant dysregulation in a number of expressed genes of bovine foot skin fibroblasts stimulated by each of the treponeme sonicates or control LPS when compared to unstimulated cells.

Gram-negative bacterial LPS appears to stimulate a panel of host pro-inflammatory cytokines and chemokines in bovine foot skin tissue via the IL-17 signalling pathway

Several pro-inflammatory cytokines and chemokines were found to be universally upregulated in bovine foot skin fibroblasts upon stimulation with each of the pathogenic BDD treponeme and commensal treponeme sonicates and the control LPS from *S. enterica* serotype Typhimurium. These included the inducible inflammatory cytokine, *IL6* (Kent *et al.,* 1998), and chemoattractants for both neutrophils, such as *CXCL2, CXCL3* and *CXCL5* (Lahouassa *et al.,* 2008; Rainard *et al.,* 2008), and monocytes, such as CCL2 (also known as monocyte chemoattractant protein-1) (Leonard & Yoshimura, 1990; Wempe *et al.,* 1994). Interestingly, both *IL6* (6.6 log2 fold change) and *CXCL2* (7.3 log2 fold change) were previously found to be significantly upregulated within BDD lesions when compared to healthy bovine foot skin tissue by RNA-Seq (Scholey *et al.,* 2013); *IL6* expression peaking within M2-stage lesions (Refaai *et al.,* 2013). Such findings are unsurprising, as BDD is an inflammatory disease of bovine foot skin which is typically accompanied by an abundance of infiltrating immune cells (particularly neutrophils) within deeper layers of the reticular dermis and epidermis (Blowey & Sharp, 1988; Döpfer *et al.,* 1997; Refaai *et al.,* 2013). Many of these pro-inflammatory cytokines and chemokines (including *CCL2, CXCL2* and *IL6*) were also significantly upregulated in human dermal fibroblasts stimulated with three prominent pathogenic spirochaetes of Lyme disease, namely *B. burgdorferi* sensu stricto*, Borrelia afzelii* and *Borrelia garinii* (Meddeb *et al*., 2016; Schramm *et al*., 2012). Furthermore, *IL6* and *CCL2* were both significantly upregulated in human gingival fibroblasts stimulated with the periodontal pathogens, *T. pectinovorum* and *T. denticola* (Nixon *et al.,* 2000; Tanabe *et al.,* 2009). Taken together with observations that the commensal treponeme, *T. ruminis,* and Gram-negative bacterial pathogen, *S. enterica* serotype Typhimurium, induced similar responses, it is likely that such pro-inflammatory cytokines and chemokines are a host response to Gram-negative bacterial LPS (Skovbjerg *et al.,* 2010).

Interestingly, the expression of several of these profoundly upregulated pro-inflammatory cytokines and chemokines (particularly *IL6, CCL2* and *IL-8*, as mentioned below) are mediated via the IL-17 signalling pathway (Brembilla *et al.,* 2013; Fossiez *et al.,* 1996; Hymowitz *et al.,* 2001; Park *et al.,* 2005; Yao *et al.,* 1995). *IL-17* is considered a fundamental cytokine mediator of host inflammatory and immune responses for defence against Gram-negative pathogens, including *T. pallidum* and *B. burgdorferi*, in barrier tissues such as skin (Burchill *et al.,* 2003; Cruz *et al.,* 2012; Infante-Duarte *et al.,* 2000; Ishigame *et al.,* 2009). *IL-17*-mediated pro-inflammatory responses have been linked to skin disease pathologies such as psoriasis and the arthritic pathology of Lyme disease (Burchill *et al.,* 2003; Cruz *et al.,* 2012; Krueger *et al.,* 2012; Oosting *et al.,* 2011) and, therefore, it would be plausible to predict a likely role for IL-17 signalling in BDD pathogenesis in bovine foot skin tissue. Here, IPA predicted the upstream regulation and significant enrichment of IL-17 signalling in bovine foot skin fibroblasts stimulated with each of the bacterial treatments, whilst, as expected, only the pathogenic bacterial treatments were predicted to stimulate disease-associated IL-17 pathways such as those for arthritis and psoriasis. The data presented here is the first to predict a role for IL-17 signalling in BDD pathogenesis and further work would now be required to determine to what extent this pathway is involved. Interestingly, *IL-17* and *IL-17* receptor inhibitors appear to be promising future targets for novel therapeutics in psoriasis (Lebwohl *et al.,* 2015; Leonardi *et al.,* 2012) and may provide novel therapeutic targets for BDD.

In addition to these pro-inflammatory cytokines and chemokines, several other genes were significantly upregulated within bovine foot skin fibroblasts universally across each of the treatment groups; including *SOD2*, *CDA, Mail, TNFSF15* and *CFB*.

SOD2 encodes a mitochondrial enzyme which functions to convert harmful superoxide anions, induced by pro-inflammatory cytokines (such as *TNF-α*) or bacterial LPS, to hydrogen peroxide and therefore protect cells from oxidative stress whilst facilitating the elimination of invading pathogens, for example through the neutrophil burst (Meyrick & Magnuson, 1994; Skalerič *et al.,* 2000; Visner *et al.,* 1990). The upregulation of *SOD2* expression across this dataset is therefore unsurprising and, agreeably, *SOD2* expression was also found to be significantly upregulated by human gingival fibroblasts upon stimulation with *B. burgdorferi* sensu stricto (Schramm *et al.,* 2012). Furthermore, Skalerič *et al.* (2000) previously found LPS to induce greater *SOD2* expression than equivalent bacterial preparations and the same observations were true here.

With a central role in the activation of the alternative pathway of the complement cascade (Janeway *et al.,* 2001), it was also unsurprising that *CFB* was significantly induced by each of

the treatments. Kaczorowski *et al.* (2010) previously reported a significant upregulation of *CFB* in murine macrophages upon stimulation of TLR4 by *E. coli* LPS. The predicted upstream activation and enrichment of *TNF* and IL-17 signalling pathways, respectively, may offer plausible mechanisms for mediation of the observed upregulation in *CFB* in bovine foot skin fibroblasts (Katz *et al.,* 2000). Interestingly, only *T. medium* phylogroup sonicate was found to significantly upregulate the expression of classical complement component, *C2*. Furthermore, Hofman *et al.* (2007) reported an upregulation in both *CFB* and *C2* within gastric biopsies infected with Gram-negative bacterial pathogen, *Helicobacter pylori.* To the authors' knowledge, the dysregulation of both *CFB* and *C2* complement components have yet to be described in BDD pathogenesis and further work will be required to elucidate whether the phylogroup-specific upregulation of *C2* observed here represents a distinct mechanism of *T. medium* spirochaete pathogenesis.

The NF-κB signalling pathway is a key mediator of host immune and inflammatory responses, cellular proliferation, survival and differentiation and has been shown to be activated by inflammatory cytokines, treponemal OMP components or through PAMP-mediated TLR activation (Brozovic *et al.,* 2006; Lawrence, 2009; Wooten *et al.,* 1996). It is therefore unsurprising that the *NF-κB* complex was predicted to be induced by the pathogenic bacterial treatments in bovine fibroblasts; however, it was interestingly not activated by commensal, *T. ruminis*. NF-κB signalling is tightly regulated by a number of *NF-κB* inhibitors. One of these, *Mail,* was significantly upregulated within this dataset across all treatment groups and therefore, together with the predicted activation of *NF-κB*, likely suggests induction of the negative feedback loop controlling NF-κB signalling. Notably, Xue *et al.* (2013) also identified a significant upregulation in both NF-κB inhibitor alpha and *Mail* expression within human peripheral blood monocytes upon *Leptospira interrogans* infection. Furthermore, Zuerner *et al.* (2007) identified a significant six-fold and five-fold upregulation in the expression of *NF-κB* inhibitors, *IκB* and *SIVA-1* respectively, in bovine macrophages upon stimulation with *T. phagedenis* phylogroup sonicate. The observed significant upregulation of cytokine, *TNFSF15*, universally across bovine fibroblasts of all treatment groups also further supports a significant role for NF-κB signalling in BDD pathogenesis (Marsters *et al.,* 1996). *TNFSF15* is in fact multifunctional and was suggested to be a Th1-polarising cytokine which correlated to severity of inflammatory diseases such as Crohn's disease (Bamias *et al.,* 2003); therefore, suggestive that its observed upregulation likely correlates to the inflammatory pathology of BDD infection.

The universal upregulation of *CDA* expression observed in bovine fibroblasts across each treatment group correlated with findings of enriched RNA expression and transcription by IPA. *CDA* is known to have a key role in scavenging cytidine for uridine monophosphate synthesis, a key monomer of RNA, for pyrimidine salvaging and nucleotide metabolism (Nygaard *et al.,* 1986; Zimin *et al.,* 2009).

BDD treponemes commonly dysregulate the expression of five genes in bovine foot skin fibroblasts

Only five significantly differentially expressed genes of bovine foot skin fibroblasts were commonly stimulated (upregulated) by all three BDD treponemes and not the commensal treponeme; *IL-8*, *RGS16*, *GRO1*, *MAFF* and *ZC3H12A*. Notably, these genes were also dysregulated by the LPS of Gram-negative pathogen, *S. enterica* serotype Typhimurium, and are therefore not considered BDD-specific. Nevertheless, such pathogen-specific gene dysregulation may provide useful targets for future novel therapeutics and vaccines against BDD infection.

As neutrophil infiltration is a key characteristic of BDD pathology (Blowey & Sharp, 1988; Döpfer *et al.,* 1997; Refaai *et al.,* 2013), it may be unsurprising that expression of the key neutrophil chemoattractant, *GRO1,* was found to be upregulated by BDD treponemes and not the commensal, *T. ruminis.* Although there is not a definitive human ortholog to bovine *GRO1* (*CXCL1*), the human *CXCL1* gene was reported to be significantly upregulated by *B. burgdorferi* and its BbHtrA protease in human dermal fibroblasts and chondrocytes respectively (Russell *et al.,* 2013; Schramm *et al.,* 2012), which may suggest shared pathogenic mechanisms to Lyme disease.

ZC3H12A, encoding MCP-induced protein 1, is known to regulate host immune and inflammatory responses through inhibitory RNase activity on mRNA targets such as *IL6* and *IL-17* (Garg *et al.,* 2015; Koga *et al.,* 2011; Ruiz-Romeu *et al.,* 2016). *ZC3H12A* expression is known to be upregulated in inflammatory psoriatic lesions, inflammatory-mediated keratinocytes and in murine macrophages exposed to live *B. burgdorferi* (Guatam *et al.,* 2011; Ruiz-Romeu *et al.,* 2016) and is therefore suggestive of a role in BDD pathogenesis.

RGS16 encodes a GTPase-activating protein which negatively regulates G protein-coupled receptor signalling pathways; such as those of chemokine receptors which mediate host inflammatory responses (Lippert *et al.,* 2003; Shankar *et al.,* 2012). Resultantly, *RGS16* inhibits pro-inflammatory cytokine production (*IL6, IL-8* and *TNF-α*) in monocytes and modulates the chemotaxis of immune cells, such as T lymphocytes (Lippert *et al.,* 2003; Shankar *et al.,* 2012; Suurväli *et al.,* 2015). However, Suurväli *et al.* (2015) also previously

suggested an anti-inflammatory role for *RGS16* involving a "feed-forward loop" with pro-inflammatory cytokines and the anti-inflammatory cytokine, IL-10. *RGS16* dysregulation has also been implicated in chronic inflammatory skin diseases, such as psoriasis and atopic dermatitis, and as a pathogenic target of porcine circovirus (Choi *et al.,* 2015; Li *et al.,* 2013; Timmusk *et al.,* 2009). *RGS16* likely, therefore, has a significant role in BDD pathogenesis.

MAFF is an important transcriptional regulator which, through its association with various cap 'n' collar basic region-leucine zipper (bZIP) transcription factors, is thought to have a fundamental regulatory role in the inflammatory response and cellular stress response of mammalian cells (Ishii *et al.,* 2000; Massrieh *et al.,* 2006; Motohashi & Yamamoto, 2004).

GRO1, ZC3H12A, RGS16 and *MAFF* have each yet to be implicated in BDD pathogenesis; further work is now warranted to elucidate their functional importance.

Bovine foot skin fibroblasts also appear to be a source of *IL-8* in BDD infection

IL-8 has been consistently linked to BDD pathogenesis in previous studies. *T. phagedenis* phylogroup spirochaetes upregulated *IL-8* expression within bovine macrophages (Zuerner *et al.,* 2007). Furthermore, whilst *IL-8* was also found to be significantly upregulated (+6.5 log2 fold change) within BDD lesions compared to healthy bovine foot skin tissue, with greatest upregulation observed at the M2-stage (+328.0 log fold change), bovine foot skin keratinocytes were previously implicated as the source of *IL-8* dysregulation (Refaai *et al.,* 2013; Scholey *et al.,* 2013). Interestingly, the data presented here reports for the first time that bovine foot skin fibroblasts also contribute to this observed upregulation of *IL-8* expression within BDD lesions. *IL-8* is an inflammatory chemokine which is expressed at low levels in unstimulated fibroblasts (Nixon *et al.,* 2000), however is known to have a fundamental role in neutrophil chemotaxis during the host immune response (Caswell *et al.,* 1999). Invading treponemes likely induce *IL-8* upregulation in fibroblasts and keratinocytes of lesional foot skin tissue as part of the host innate immune response to infection; likely resulting in AMP production, phagocytosis and neutrophil infiltration which is characteristic to BDD pathology. *IL-8* dysregulation has previously been implicated in the pathogenesis of human periodontal disease, with findings that *T. medium* and *T. vincentii* spirochaetes induce *IL-8* expression within human gingival epithelial cells in a cell- and dose-dependent manner (Asai *et al.,* 2003). Furthermore, both human skin fibroblasts and keratinocytes have been shown to express *IL-8* following stimulation with *B. burgdorferi* N40 (infected tick) in a dose-dependent manner, peaking 12 hours post-challenge (Marchal *et al.,* 2009). Disease-associated treponemes therefore likely share this same mechanism of pathogenesis and the

lack of *IL-8* dysregulation induced by *T. ruminis* only further highlights its importance as a target of pathogenesis.

BDD treponemes appear to stimulate distinct differential gene expression profiles in bovine foot skin fibroblasts

With just 58 significantly differentially expressed genes, *T. medium* phylogroup sonicate was profoundly less stimulatory to bovine foot skin fibroblasts than equivalent concentrations of the other BDD treponeme sonicates, *T. phagedenis* phylogroup and *T. pedis* (with 398 and 395 genes respectively). Linear regression analysis further supported this finding, with least correlation observed between transcriptional profiles of fibroblasts stimulated with sonicates of *T. medium* phylogroup and either *T. ruminis* or *T. pedis*.

These observations were likely not attributable to excessive stimulation by *T. phagedenis* phylogroup and *T. pedis* sonicates as the control LPS from *S. enterica* serotype Typhimurium demonstrated comparable (although, notably, slightly lower) numbers of significantly differentially expressed genes to these phylogroups. Neither were these observations likely due to poor sequencing depth as the 34,342,019 average aligned reads per mate-pairs are considered more than sufficient for differential expression analysis (The ENCODE Consortium, 2011). Interestingly, Evans *et al.* (2014) previously reported comparatively smaller fold changes in the gene expression of four of the seven inflammatory mediators investigated in bovine foot skin fibroblasts stimulated with *T. medium* phylogroup sonicate when compared to *T. phagedenis* phylogroup and *T. pedis* sonicates. Furthermore, *T. vincentii* sonicate was previously shown to be comparatively less inhibitory to murine fibroblast proliferation than *T. denticola* sonicates (Boehringer *et al.,* 1984), which may suggest a similar pattern for their role in the pathogenesis of human periodontal disease. Notably, *T. medium* phylogroup spirochaetes are also known to have profoundly different growth requirements to that of the other BDD treponemes; with optimal growth being much slower and achieved through supplementation with rabbit serum rather than FBS (Evans *et al.,* 2008; Evans *et al.,* 2009b). The reasons for this are currently unclear, however these distinct growth and nutrient requirements further suggest possible disparate mechanisms of pathogenesis for this phylogroup.

Many of the pro-inflammatory cytokines and chemokines stimulated in bovine foot skin fibroblast cells by other BDD treponemes (and the LPS control) were also stimulated by the *T. medium* phylogroup sonicate, which would suggest this phylogroup still has inflammatory capabilities. However, much of the gene dysregulation (particularly downregulation) associated with actin rearrangement and apoptosis observed here by other BDD treponemes

was not induced by *T. medium* phylogroup sonicate. The data presented here may suggest that *T. medium* phylogroup is not as pathogenic to bovine foot skin fibroblasts when compared to the other BDD treponemes or, equally, may instead operate through very distinct pathogenic mechanisms to those of the other BDD treponemes. Notably, Krull *et al.* (2014) recently highlighted distinct variation in the *Treponema* phylogroups present at various stages of lesion development and such observations must be considered when interpreting host-pathogen interaction studies under specific conditions *in vitro*. Further work would be required to elucidate whether similar expression patterns emerge at other time points, with other cell lineages (such as bovine foot skin keratinocytes) and, most importantly, within more complex and representative skin models.

Although there is currently no published data to definitively support a predominating role for one of the *Treponema* phylogroups in BDD pathogenesis, several studies have consistently highlighted *T. phagedenis* phylogroup spirochaetes to be the most consistently found within BDD lesions (Choi *et al.,* 1997; Evans *et al.,* 2009a; Krull *et al.,* 2014), suggesting a possibly greater role for this phylogroup in BDD pathogenesis. Interestingly, the present study identified a near-identical number of significantly differentially expressed genes in bovine foot skin fibroblasts upon stimulation with either *T. phagedenis* phylogroup or *T. pedis* sonicates and suggests they likely both play a fundamental role in BDD pathogenesis. Whilst the majority of these significantly differentially expressed genes were downregulated (66.3% and 90.4% for *T. phagedenis* phylogroup and *T. pedis* respectively), the *T. medium* phylogroup sonicate and control LPS largely induced upregulation (93.1% and 92.3% respectively) of their significantly differentially expressed genes. Many of the dysregulated fibroblast genes induced here by the positive control, LPS from *S. enterica* serotype Typhimurium, were agreeably dysregulated in cultured human epithelial cells by live cultures using RNA-Seq (Hannemann & Galán, 2017). In keeping with the observations of *T. phagedenis* phylogroup and *T. pedis* sonicates, Scholey *et al.* (2013) identified the majority of significantly differentially expressed genes (79.6%) to be downregulated within complete BDD lesions. Again, these observations highlight the apparent differences in pathogenic mechanisms of the BDD treponeme phylogroups and notably contradict their earlier reported similarities when inducing dysregulation in the gene expression of seven inflammatory mediators in bovine foot skin fibroblasts (Evans *et al.,* 2014). Indeed, this perfectly epitomises the value of high-throughput transcriptomics studies, in enabling comparisons of global differential gene expression, rather than more targeted, lower-throughput studies which are unable to detect such broader patterns of expression.

BDD treponemes elicit distinct dysregulatory mechanisms in bovine foot skin fibroblasts

One of the most interesting and novel findings is the unique upregulation in *TSC22D3* gene expression observed within bovine foot skin fibroblasts by *T. medium* phylogroup sonicate. The human *TSC22D3* gene, which encodes the glucocorticoid-induced leucine zipper (GILZ) protein, has a well-characterised anti-inflammatory and immunosuppressive potential. It is known to inhibit the activation of several key inflammatory mediators, such as transcription factors *NF-κB* and activator protein-1, and is thought to regulate T lymphocyte activation and inhibit inflammatory responses in a number of cell lineages including epithelial cells, macrophages and T lymphocytes (Ayroldi *et al.,* 2001; Berrebi *et al.,* 2003; Eddleston *et al.,* 2007; Mittelstadt & Ashwell, 2001). Whilst the glucocorticoid receptor signalling pathway was predicted to be significantly enriched in bovine foot skin fibroblasts across all treatment groups, it was only the *T. medium* phylogroup which upregulated the expression of this anti-inflammatory gene. It is likely that *T. medium* phylogroup spirochaetes may facilitate their immune evasion, prolonged survival and persistence deep within bovine foot skin tissue through upregulating host expression of such anti-inflammatory genes. These observations support a role for *T. medium* phylogroup in the pathogenesis of bovine foot skin cells during BDD infection despite their apparent poor stimulatory potential and, again, suggest BDD treponemes employ distinct mechanisms of pathogenesis during infection. Such differences may be accountable to the distinct variation in tissue distribution observed between *Treponema* phylogroups in BDD lesions (Moter *et al.,* 1998).

Interestingly, gene expression of the pro-inflammatory cytokine, *IL36A*, was found to be uniquely upregulated by *T. pedis* sonicate in bovine foot skin fibroblast cells. *IL36A* is predominantly expressed in epithelial tissues such as the skin and is considered to have a significant role in the initiation and regulation of host immune and inflammatory responses through the induction of AMPs and pro-inflammatory mediators (such as *IL-8* and *IL6*) via IL-17, TNF-α and NF-κB signalling pathways (Blumberg *et al.,* 2007; Carrier *et al.,* 2011; Conde *et al.,* 2015; Frey *et al.,* 2013; Towne *et al.,* 2004). *IL36A* gene and protein expression has been found to be upregulated within psoriatic lesions, psoriatic-like murine skin models and osteoarthritic chondrocytes (Blumberg *et al.,* 2007; Carrier *et al.,* 2011; Conde *et al.,* 2015; Frey *et al.,* 2013). Notably, Blumberg *et al.* (2007) demonstrated an inflammatory murine skin phenotype characterised by hyperkeratosis, acanthosis, increased cytokine and chemokine expression and a prominent dermal inflammatory cell infiltrate in transgenic mice expressing *IL36A* in basal keratinocytes. Accordingly, the specific upregulation in *IL36A*

expression by *T. pedis* sonicate observed here may suggest a significant role in BDD pathogenesis, particularly as such phenotypes are characteristic of BDD lesions.

Several circadian clock genes were dysregulated by BDD treponemes in bovine fibroblasts. The mammalian circadian clock is responsible for synchronising circadian activities including body temperature, metabolism and immune function and its dysregulation has been associated with impaired innate immune responses and inflammatory diseases (Ando *et al.,* 2015; Bellet *et al.,* 2013; Gibbs *et al.,* 2014; Hand *et al.,* 2016). It is predominantly driven by a negative feedback loop involving clock circadian regulator (*CLOCK*) and aryl hydrocarbon receptor nuclear translocator like, and its inhibitors period circadian clock (*PER*) and cryptochrome circadian clock (*CRY*) (Mohawk *et al.,* 2012). Ando *et al.,* (2015) recently identified the *CLOCK* gene to be a likely key regulator of psoriasis-like inflammation in murine skin through modulation of interleukin-23 receptor signalling in T lymphocytes; implicating *PER2* mutations in increased lesion severity. Interestingly, here, the gene expression of negative regulators, *PER1* and *CRY2*, were significantly upregulated in bovine foot skin fibroblasts only by *T. medium* phylogroup sonicate, whilst *PER1* was notably downregulated by *T. phagedenis* phylogroup sonicate. Interestingly, *CRY1* and *CRY2* were recently found to suppress local inflammatory responses in fibroblast-like synoviocytes (Hand *et al.,* 2016) and, therefore, further support a likely anti-inflammatory role for *T. medium* phylogroup dysregulation within bovine foot skin tissue. The dysregulation of the circadian clock has yet to be reported for BDD pathogenesis and further work will now be required to elucidate the role of treponemes in such changes.

***T. phagedenis* phylogroup spirochaetes induce β-defensin AMP in bovine fibroblasts**

The β-defensins are a predominant family of skin AMPs which demonstrate significant antimicrobial activity and therefore constitute a prominent chemical barrier to invading microbes (Cormican *et al.,* 2008; Liu *et al.,* 2002; Ong *et al.,* 2002; Yang *et al.,* 1999), as discussed in Chapter 1.8. Here, *DEFB123* was found to be expressed (2.323 FPKM) in bovine foot skin fibroblasts only upon stimulation with *T. phagedenis* phylogroup. The data presented here may be unsurprising as human *DEFB123* has been found to demonstrate profound antimicrobial activity against a number of Gram-negative bacteria (Motzkus *et al.,* 2006) and β-defensins are commonly upregulated within inflamed skin or following stimulation with microbial constituents or inflammatory cytokines (Liu *et al.,* 1998; Liu *et al.,* 2002). The absence of *DEFB123* expression by fibroblasts stimulated with other bacterial preparations likely represents disparate pathogenic mechanisms between BDD treponeme phylogroups and, agreeably, Evans *et al.* (2014) previously identified variable antigenic

constituent profiles of the three BDD treponemes which may account for such differences. However, it is important to consider that this may also represent a limit of mRNA detection. Interestingly, Marchal *et al.* (2009) demonstrated a greater role for primary human epidermal keratinocytes, than dermal fibroblasts, in the expression of human β-defensin-2 following stimulation with the spirochaete, *B. burgdorferi.* Accordingly, targeted studies would be warranted to determine whether *T. phagedenis* phylogroup have a similar impact on β-defensin dysregulation in bovine foot skin keratinocytes.

The specific dysregulation of acute phase proteins by BDD treponemes

The acute phase response, consisting of both positive and negative acute phase reactants, is a fundamental arm of the innate immune response and is stimulated by inflammatory cytokines for the purposes of host defence (Gruys *et al.,* 2005). Several acute phase reactants were dysregulated by BDD treponemes in bovine foot skin fibroblasts. Most notably, the bovine *PTX3* gene, encoding a soluble pattern recognition receptor, was universally induced upon stimulation, however, only significantly (1.25328 FPKM) by *T. medium* phylogroup sonicate. Interestingly, *B. burgdoferi* was also found to upregulate *PTX3* gene expression in human dermal fibroblasts, which may suggest shared pathogenic mechanisms with Lyme disease spirochaetes (Meddeb *et al.,* 2016). Bevelacqua *et al.* (2006) also previously demonstrated strong immunohistochemical staining of *PTX3* in fibroblasts, endothelial cells and macrophages from severe psoriatic lesional skin and further suggest a potentially important role for *PTX3* dysregulation in BDD pathogenesis.

***T. medium* phylogroup and *T. pedis* sonicates appear to induce actin rearrangement and loss of cell adhesion in bovine foot skin fibroblasts**

The actin cytoskeleton is a key component of cellular physiology which is essential for maintaining cell morphology and tissue integrity, intracellular transport, phagocytosis and for facilitating fibroblast migration during wound healing and tissue repair (Tojkander *et al.,* 2012). These dynamic cellular processes are mediated through both actin polymerisation (and depolymerisation) and contractile force. The primary contractile unit of mammalian cells are stress fibres, which typically consist of bundles of actin and myosin II filaments which are cross-linked by alpha-actinin and are commonly attached to the ECM by focal adhesions, which themselves are important for cell adhesion and migration (Geiger *et al.,* 2009; Parsons *et al.,* 2010). With a fundamental role in cellular physiology, it may be unsurprising that the actin cytoskeleton components themselves, alongside their regulatory signalling counterparts, are often key targets of pathogenesis for Gram-negative bacterial pathogens;

and treponemes are no exception to this (Baehni *et al.,* 1992; Fullner & Mekalanos, 2000; Yang *et al.,* 1998; Zuerner *et al.,* 2007).

Several studies have previously reported the cytotoxic effect of *T. denticola* in perturbing actin rearrangement, cytoskeletal structure and even causing the detachment of human gingival fibroblasts; suggesting a likely role in the pathogenesis of human periodontal disease through inhibition of wound repair function (Baehni *et al.,* 1992; Visser *et al.,* 2011; Yang *et al.,* 1998). Indeed, *T. denticola* and its OMP constituents were found to significantly reduce filamentous actin and increase rearrangement of stress fibres through depletion of local inositol phosphate (Yang *et al.,* 1998). More recently, the downregulation of several structural genes, including *ACTN1* and cytoskeletal-associated protein 1 (-4.0 and -9.0 fold changes respectively), have been described for bovine macrophages exposed to *T. phagedenis* phylogroup spirochaetes and may suggest a role in BDD pathogenesis (Zuerner *et al.,* 2007).

The present study appears to again confirm a role for actin rearrangement in BDD pathogenesis and implicates *T. pedis*. Actin and cytoskeleton signalling pathways (and the associated integrin-linked kinase signalling pathways; Graness *et al.,* 2006) were predicted to be significantly inhibited by *T. pedis* sonicates in bovine fibroblasts; with reduced organisation of the cytoskeleton, cytoplasm and microtubules and reduced quantities of focal adhesions, stress fibres and actin filaments. Several F-actin-associated proteins (*ACTN1, WIP2, SYNPO* and *NEXN*) (Aspenström, 2002; Wang *et al.,* 2005; Zimin *et al.,* 2009), the Rho family GTPase, *RHOG* (Gauthier-Rouviére *et al.,* 1998), a regulator of wound healing (*FHL3*; Coghill *et al.,* 2003), and *CFL1*, which has a well-characterised function in actin polymerization (Maciver & Hussey, 2002), were also each downregulated by *T. pedis.* Interestingly, *T. medium* phylogroup sonicate was predicted to (opposingly) stimulate an increase in cytoskeletal organisation. Furthermore, both *T. medium* phylogroup and *T. pedis* sonicates were found to profoundly upregulate the expression of *RND1* in bovine fibroblasts, alongside the LPS control. RND1 is known to localise to adherens junctions of confluent fibroblasts and its upregulation is associated with inhibition of actin stress fibre formation and loss of integrin-based focal adhesions leading to cell rounding (Nobes *et al.,* 1998).

The data presented in this study suggests that both *T. medium* phylogroup and *T. pedis* spirochaetes, however notably not *T. phagedenis* phylogroup, are able to facilitate the loss of fibroblast cell-cell adhesion within bovine foot skin tissue and, therefore, promote deeper invasion and persistence through tissue damage and destruction. *T. pedis* spirochaetes appear to have a particularly prominent role in pathogenic actin rearrangement in bovine

fibroblasts. With previous studies linking the structural cytotoxicity of *T. denticola* to its well-characterised Msp component (Visser *et al.,* 2011; Wang *et al.,* 2001), it would seem plausible to suggest that there may be a similar OMP of *T. pedis* spirochaetes mediating the dysregulation of actin rearrangement in bovine foot skin cells during BDD infection. By contrast to the pathogenic BDD treponemes, *T. ruminis* sonicate was found to increase the quantity of focal adhesions, stress fibres and actin filaments in bovine fibroblast cells. Such rearrangements are typically associated with wound healing and cell migration and, as a commensal treponeme, may be suggestive of a host response to commensal infection.

A role for fibroblast growth factor ligand and receptor dysregulation in BDD pathogenesis

Fibroblast growth factor (FGF) ligands and their receptors have a key role in tissue repair and wound healing in the skin and demonstrate cell-specific action within the dermis and epidermis. Whilst FGF7 is expressed in dermal fibroblasts and stimulates DNA synthesis and proliferation in keratinocytes, with an observed 3.5-fold upregulation after wounding in mice (Komi-Kuramochi *et al.,* 2005), FGF18 is associated with the proliferation of fibroblasts themselves whilst maintaining the skin and regulating hair growth (Hu *et al.,* 1998; Kawano *et al.,* 2005). In this study, *FGF18* gene expression was significantly downregulated in bovine fibroblasts by all bacterial treatments with the notable exception of *T. pedis;* meanwhile its receptor (Ornitz *et al.,* 1996; Eswarakumar *et al.,* 2005; Zhang *et al.,* 2006), FGF receptor 2 (*FGFR2*) was also significantly downregulated by *T. medium* and *T. phagedenis* phylogroup sonicates. Together, this may suggest an important role for particularly *T. medium* and *T. phagedenis* phylogroup in impairing the host wound repair function of fibroblasts within dermal tissues and may therefore result in deeper tissue penetration and facilitate persistence. Interestingly, *FGF7* gene expression was found to be significantly upregulated in fibroblasts stimulated by the LPS control, *T. phagedenis* and *T. ruminis* sonicates, similarly to its upregulation in human dermal fibroblasts by *B. burgdorferi* as previously described (Schramm *et al.,* 2012). These observations correlate to the observed pathology of BDD lesions within skin and suggest dysregulation of FGF ligands and receptors may be important for spirochaete pathogenesis.

Commensal treponeme sonicate stimulates the most significantly differentially expressed genes in fibroblasts

Maybe most surprisingly, it was sonicate of the commensal treponeme, *T. ruminis,* which induced the greatest dysregulation; with approximately three to four times greater the number of significantly differentially expressed genes (1469) compared to *T. phagedenis* phylogroup and *T. pedis* sonicates and the control LPS (398, 395 and 246 genes respectively).

Notably, a recent study of secondary syphilis correlated robust pro-inflammatory immune responses with favourable host outcome and more effective bacterial clearance (Pastuszczak *et al.,* 2017). A plausible explanation for the observed large host response to *T. ruminis* may be that commensal treponemes of the GI tract induce such profound responses when in contact with bovine foot skin tissue and are subsequently, therefore, rapidly cleared and unable to persist within host tissues. In contrast, it may be that BDD treponemes, particular *T. medium* phylogroup according to this data, are able to induce a substantially smaller host response and may allow for host immune evasion and persistence within BDD lesions. However, the distinct difference in natural host niches of commensal (natural bovine GI flora) and pathogenic BDD (bovine foot skin) treponemes must also be considered (Evans *et al.,* 2008; Evans *et al.,* 2011b; Newbrook *et al.,* 2017). Cellular constituents of *T. ruminis* are likely to induce a stronger host dermal fibroblast responses compared to that of resident BDD treponemes, as the latter are likely more adapted to the foot skin tissue environment.

Commensal treponeme sonicate stimulates many of the same host genes as *T. phagedenis* and *T. pedis* phylogroup sonicates.

One of the most intriguing findings from the dataset was that sonicates of the BDD treponemes, *T. phagedenis* phylogroup and *T. pedis*, were found to induce dysregulation in many of the same host genes as the commensal treponeme, *T. ruminis.* Indeed, both linear regression analysis and the observations of shared and unique genes from Venn diagrams confirmed these findings. Furthermore, Evans *et al.* (2008) previously reported greater *16S rRNA* gene sequence similarity between *T. phagedenis* phylogroup and *T. pedis* than *T. medium* phylogroup spirochaetes. Notably, however, whilst stimulating many common genes, *T. ruminis* was not predicted to regulate many of the upstream genes that BDD treponemes were, including many inflammatory and immune cytokines such as *TREM1*. The data presented here provides further evidence for the apparent distinct pathogenic mechanisms of *T. medium* phylogroup spirochaetes and may suggest that, whilst commensal treponemes are able to dysregulate many of the same host genes as BDD treponemes, the uniquely dysregulated genes of BDD treponeme phylogroups likely confer their pathogenicity.

4.3.3 Interpretation of canonical pathway and biological function enrichment

Unsurprisingly, the TREM1 signalling pathway was predicted to be significantly enriched in bovine foot skin fibroblasts upon stimulation with each of the pathogenic bacterial preparations. TREM1 is part of the immunoglobulin superfamily which is typically activated following microbial stimulation (commonly via TLR signalling) and is known to induce a pro-

inflammatory signalling cascade (Colonna, 2003; Sharif & Knapp, 2008). Zuerner *et al.* (2007) previously implicated *T. phagedenis* phylogroup-induced upregulation of *TREM1* expression in bovine macrophages in BDD pathogenesis and *TREM1* was predicted to be significantly enriched upstream in fibroblasts stimulated with each BDD treponeme sonicate here. Bouquet *et al.* (2016) recently reported the TREM1 signalling pathway to be one of the most significantly enriched and activated pathways during acute Lyme disease and also within *in vitro* co-incubation experiments of primary microglial cells and *B. burgdorferi* (Myers *et al.,* 2009)*;* suggestive that spirochaetes indeed commonly induce inflammation in host tissues via TREM1 signalling pathways.

In line with the inflammatory nature of BDD infection, it was unsurprising to observe the predicted upstream activation of a number of pro-inflammatory cytokines such as *TNF, IL-1α* and *IL-1β*. Indeed, several studies have previously identified a significant upregulation in *IL-1β* expression within BDD lesions (Scholey *et al.,* 2013), human monocyte-derived macrophage-like cells stimulated with peptidoglycans from the human periodontal pathogen, *T. denticola,* and Caco-2 cells stimulated with *Brachyspira pilosicoli* sonicate (Naresh *et al.,* 2009). A number of observed diseases and biological functions enriched in BDD treponeme-stimulated fibroblasts correlated to disease pathology, including necrosis and apoptosis; whilst the commensal treponeme sonicate, in keeping with its symbiotic nature in the bovine GI tract, did not. The enrichment of cell death and survival functions, inflammatory responses and infectious, immunological and inflammatory disease functions in fibroblasts stimulated by each of the treatment groups was typical of the characteristic host response to bacterial infection. The predicted disparate changes in fibroblast viability and survival stimulated by *T. medium* phylogroup (increased) versus other treponeme sonicates (decreased) further demonstrates possible distinct mechanisms of pathogenesis between the BDD treponemes.

Interestingly, whilst gene expression was predicted to be elevated in fibroblasts stimulated by each of the bacterial preparations as would be expected during infection, *T. ruminis and T. pedis* sonicates appeared to induce the greatest transcription within host cells. Previous FISH studies have demonstrated that whilst *T. pedis* (previously described as *T. denticola*-like) spirochaetes are typically found within the superficial skin layers (stratum spinosum) of BDD lesions, both *T. medium* phylogroup and *T. phagedenis* phylogroup spirochaetes were typically found much deeper within the skin tissue (Moter *et al.,* 1998; Nordhoff *et al.,* 2008). This may explain the observed prominence of connective tissue and skeletal and muscular disorder functions particularly in *T. medium* phylogroup-stimulated fibroblasts.

Furthermore, the distinct tissue distribution of BDD treponemes may also explain the observed enrichment of immune cell migration and chemotaxis (particularly neutrophils) within fibroblasts by *T. medium* and *T. phagedenis* phylogroup spirochaetes, as *T. pedis* are considered to not typically be found within deeper skin tissues such as the dermis. Interestingly, whilst *T. pedis* spirochaetes are considered most closely related to the human periodontal pathogens, *T. denticola* and *T. putidum* (Evans *et al.,* 2008), it was *T. phagedenis* phylogroup spirochaetes which instead appeared to be associated with dental disease; indeed, this may be due to differences in tissue locality of *T. phagedenis* and the typically superficial location of *T. pedis* spirochaetes *in vivo.*

The predicted enrichment of gene dysregulation associated with energy production and nutritional disease in only *T. medium* phylogroup-stimulated fibroblasts may suggest a greater role for this phylogroup in exploiting the host for nutritional and energy benefit. Furthermore, it was *T. pedis* sonicate which induced carbohydrate metabolism and metabolic disease which again may suggest distinct mechanisms of pathogenesis within bovine foot skin fibroblasts during BDD.

4.3.4 Validity and true biological relevance of the RNA-Seq dataset

The comparative analysis of significantly differentially expressed genes and enriched canonical pathways and biological functions across transcriptome profiles of bovine foot skin fibroblasts stimulated with different treponeme sonicates identified interesting and seemingly biologically relevant findings for BDD pathogenesis. As essential tools for analysis of variation across large transcriptomic datasets (Bouquet *et al.,* 2016; Dillon *et al.,* 2015; Lee *et al.,* 2014; Liu *et al.,* 2017; Scholey *et al.,* 2013), multivariate analyses were employed here to determine whether these observations were attributable to true biological variation or potentially confounding experimental variation. Agreeably, both PCA and HCL analysis consistently identified two distinct variant clusters across the dataset which did not correspond to variation attributable to specific treatment groups; therefore, suggesting that experimental variation may be involved. Indeed, the experimental replicates occupying each cluster directly correspond to the two distinct cDNA library pools which were processed independently for RNA-Seq analysis (Chapter 2.11.2). There do not appear to be any further distinctions between the experimental replicates comprising each cluster which account for these distinct groupings. Accordingly, the multivariate data presented here does suggest the influence of a prominent batch effect across the dataset due to pooled sequencing and the presence of such effects are, unfortunately, likely to have reduced the statistical power of the data obtained (Nygaard & Rødland, 2016). Importantly, the experimental replicates

belonging to each batch were found to be evenly balanced across the treatment groups and, unlike unbalanced batch effects, are less likely to have a significant confounding effect on the dataset (Nygaard & Rødland, 2016). Furthermore, the significant differentially expressed genes, canonical pathways and biological functions present within the dataset were identified despite the presence of a potentially confounding batch effect and so, alongside relevant supporting literature, are still likely to be biologically significant. Nevertheless, batch effects are an important consideration of transcriptomics datasets (Dillon *et al.,* 2015; Goh *et al.,* 2017) and it is crucial to determine their influence on such datasets to confirm biological assumptions. Unfortunately, due to time constraints within the scope of this study, it was not possible to complete further global differential gene expression analysis and IPA on the dataset following necessary adjustments for the batch effect.

PCA and HCL analysis also identified three likely outliers which were consistently found to cluster independently from replicates of these two main groupings within the dataset; a further fourth outlier was identified upon their exclusion. The outliers demonstrated somewhat distinct gene expression profiles to that of others within their treatment group by heatmap analysis. However, there did not appear to be a commonality between these outliers; they were each representatives of a different treatment group, they were of good quality and quantity of RNA and they were not samples of poorer sequencing quality. There is still considerable debate about whether the exclusion of potential outliers within large transcriptomics datasets is best practice. Whilst some argue the exclusion of outliers prevents skewing of the dataset, others argue that excluding particular samples may bias the dataset to an "optimal" outcome without accounting for natural variation (Bøvelstad *et al.,* 2017). Here, global differential gene expression analysis was completed by comparison of all 20 experimental replicates to sufficiently account for the natural experimental and technical variation observed when performing experiments over different days. However, PCA analysis indicated that, upon removal of such outliers from the dataset, there were no major changes to the variant groupings across the dataset, with just a more visible division of the two (batch effect) clusters. Time permitting, it would have been advantageous to repeat the global differential gene expression analysis and IPA following the exclusion of likely outliers to determine their true impact on the dataset and this will form part of future work.

The data presented here, whilst demonstrating a number of similar gene expression changes to the previously limited number of studies on BDD pathogenesis, has also identified a large number of novel potential targets of BDD pathogenesis. A number of important gene targets identified by previous studies of BDD pathogenesis (Refaai *et al.,* 2013; Scholey *et al.,* 2013)

were not identified here. However, such findings are likely due to target cell specificity and these changes being mediated within skin tissue as a whole rather than specific cell types and by a range of bacterial and environmental stimuli beyond those observed *in vitro* within this simple host-pathogen model.

4.3.5 Conclusions

The novel transcriptomics dataset generated during this study has provided a unique insight into the distinct pathogenic mechanisms of three predominant BDD treponeme phylogroups in bovine foot skin fibroblasts and serve to further highlight the complexities of BDD pathogenesis. This study has highlighted the important role of connective tissue cells in BDD pathogenesis. The data present here is suggestive that particularly *T. medium* phylogroup spirochaetes may avoid bacterial clearance and host immune evasion through promoting anti-inflammatory gene expression. By contrast, commensal treponemes may be unable to elicit pathogenesis when in contact with bovine foot skin tissue due to their strong induction of host pro-inflammatory responses. This study has highlighted a significant role for both *T. medium* and *T. pedis* in tissue damage through promoting the loss of cell adhesion and actin rearrangement. Conclusively, this study has identified a number of pathogenic gene targets which require further investigation as potential candidates for the development of vaccines and therapeutics in the coming years.

Chapter Five: Investigating the molecular diversity of a putative outer membrane protein of DD treponemes.

5.1 Introduction

Despite previous difficulties in isolation, subculture and purification of these fastidious Gram-negative microorganisms, there have now been a number of treponemes isolated from BDD lesions in the UK (Evans *et al.,* 2008; Evans *et al.,* 2009a). These BDD treponemes exist as multiple antigenic serotypes or variant strains and typically cluster, both genotypically and phenotypically, into three distinct groupings; *T. medium* phylogroup*, T. phagedenis* phylogroup and *T. pedis* (Evans *et al.,* 2008, Evans *et al.,* 2009b; Clegg *et al.,* 2016d). A further two *Treponema* phylogroups have been identified in BDD lesions in Germany (Choi *et al.,* 1997). These spirochaetes have also now been isolated from hoof and skin lesions in a range of livestock species, including wildlife (Clegg *et al.,* 2015; Clegg *et al.,* 2016a-c; Groenevelt *et al.,* 2015; Harwood *et al.,* 1997; Sullivan *et al.,* 2015a). However, whilst known to share wide-ranging geographical and host niches, little is known about the intra-phylogroup or inter-phylogroup molecular diversity of BDD treponemes and their antigenic or OMP constituents, or its involvement in disease pathogenesis.

Evans *et al.* (2008) previously reported diversity between the three BDD treponeme phylogroups based upon *16S rRNA* gene sequence identity; however, there appeared to be little variation within these phylogroups. Agreeably, Clegg *et al.* (2016d) identified a low level of diversity between representative strains of the three BDD phylogroups across seven housekeeping loci by MLST. BDD treponeme OMPs have yet to be identified or characterised and their molecular diversity between and within these phylogroups remains unknown.

An understanding of the molecular diversity of antigenic and OMP constituents of BDD treponemes is essential for elucidating mechanisms of disease pathogenesis and in the development of novel therapeutics and vaccines.

Antigenic variation is a key pathogenic mechanism employed by spirochaetes, such as *Borrelia* spp. (Raffel *et al.,* 2014; Zhang *et al.,* 1997), *T. pallidum* (Trott *et al.,* 2003) and *T. denticola* (Giacani *et al.,* 2010), to facilitate host immune evasion and persistence (as previously discussed, Chapter 1.6.3). Arguably the best-characterised example of antigenic variation in spirochaetes is *B. burgdorferi,* which has multiple antigenic variants (notably OspA and OspC) that are considered relevant to its pathogenicity. The host immune system is considered a major driving force for the selection of antigenic diversity in both pathogenic

and commensal treponemes to promote survival and persistence within their host. Indeed, various studies have identified diversifying selection pressures to be driving non-synonymous (d_N) substitutions on surface-exposed antigenic components of bacterial pathogens such as *Neisseria meningitidis* (Urwin *et al.,* 1998).

Elucidating the molecular diversity of antigenic constituents of BDD treponemes, such as OMPs, should be fundamental in enabling the development of novel multi-valent vaccines which confer effective cross-protection (Evans *et al.,* 2010; Morgan *et al.,* 2003). Previous attempts at trialling a bacterin vaccine against BDD, targeting only two *Treponema* phylogroups, were unsuccessful (Berry *et al.,* 2004), however, considering the known genotypic diversity amongst the three *Treponema* phylogroups this is unsurprising (Evans *et al.,* 2008). As BDD treponeme OMPs have yet to be publicly characterised or their molecular diversity assessed, those of other pathogenic treponemes currently serve as useful models (Gaibani *et al.,* 2010; Houston *et al.,* 2015).

The aim of this study was to investigate the molecular diversity of a putative OMP across the three predominant BDD *Treponema* phylogroups. This study hoped to provide novel insights into whether such potential antigenic targets of future therapeutics and vaccines are well conserved or variable both within and between the BDD treponeme phylogroups.

The primary objectives of this chapter are:

1) Identify a suitable putative OMP which is shared across *T. medium* phylogroup, *T. phagedenis* phylogroup and *T. pedis* spirochaetes for use in molecular diversity studies.
2) Compare structural topology of the putative treponeme OMP across three *Treponema* phylogroups and identify conserved and unique regions of sequence diversity.
3) Develop and optimise three novel PCR assays to enable amplification and sequencing of the putative *Omp* gene from representative treponeme isolates of each phylogroup.
4) Assess nucleotide and amino acid diversity, selection pressures and perform phylogenetic and recombination analysis to investigate the molecular diversity of this putative *Omp* gene across each of the BDD *Treponema* phylogroups.
5) Compare amino acid sequences of the putative OMP to those of homologous proteins from other pathogenic and commensal treponemes to assess its molecular diversity across other *Treponema* species.

5.2 Results

5.2.1 Identifying a suitable putative outer membrane protein of digital dermatitis treponemes for molecular diversity studies

Putative treponeme OMPs were initially identified from the complete, annotated genome sequences of *T. medium* phylogroup strain T19, *T. phagedenis* phylogroup strain T320A and *T. pedis* strain T3552B^T using a reverse vaccinology-based approach with a suitable bioinformatics pipeline, as described in Chapter 2.8.3. Reverse vaccinology identified 14 putative treponeme OMPs predicted to have characteristic β-barrel tertiary structure, signal peptide cleavage site and also equivalent homologs across all three DD phylogroups (Table 5.1). Four of these identified putative treponeme OMP candidates (Omp_34, Omp_694, Omp_2390; Omp_480, Omp_1722, Omp_2267; Omp_2427, Omp_2465, Omp_976; and Omp_2501, Omp_1243, Omp_2625) were found to fulfil the specific requirements of this study (Chapter 2.8.3), with a maximum gene size of 0.8 kbp and a minimum of 40% inter-phylogroup amino acid sequence homology.

The protein domain and structural homology predictions of HHPRED software, as shown in Table 5.2, Table 5.3 and Table 5.4, were subsequently used to inform the final choice of a suitable putative treponeme OMP candidate for molecular diversity studies. Of the four remaining candidates, Omp_34, Omp_694 and Omp_2390 were the only homologs found to share strong structural similarities and protein domain homology to other recognised OMPs of organisms within the HHPRED database, including *Escherichia coli* and *Pseudomonas auruginosa*. Each of their six most homologous protein domains were OMPs, typically of an eight-stranded β-barrel structure which formed hydrophobic channels to mediate molecular transport across bacterial outer membranes (Hong *et al.,* 2006; Pautsch and Schulz, 2000; Vandeputte-Rutten *et al.,* 2003). In contrast, the putative treponeme OMP homologs Omp_480, Omp_1722 and Omp_2267 shared homology with several protein domains of an alpha-helix structure which are known to have variable functions in protein binding, hydrolysis and the regulation of ubiquitination pathways (Guo & Xu, 2015; Jeong *et al.,* 2016; Lüthy, Grutter & Mittl, 2002; Yeh *et al.,* 2011). Resultantly, this particular putative OMP candidate did not appear to be suitable for our study. The putative treponeme OMP homologs Omp_2427, Omp_2465 and Omp_976 shared most homology to the carbohydrate binding modules of several xylanases and endoglucanases (Carvalho *et al*., 2004; Charnock *et al.,* 2000). Furthermore, putative treponeme OMP homologs Omp_2501, Omp_1243 and Omp_2625 shared protein domain homology with several members of the SurA-like

peptidyl-prolyl cis-trans isomerase family; molecular chaperones which facilitate correct folding of OMPs (Bitto and McKay, 2002; Naveen *et al.,* 2016).

In conclusion to these predictions of structural similarity and protein domain homology, the putative treponeme OMP homologs Omp_34 (*T. medium* phylogroup), Omp_694 (*T. phagedenis* phylogroup) and Omp_2390 (*T. pedis*) were chosen as the most suitable candidates for further studies of molecular diversity across our range of treponeme isolates.

Table 5.1 Details of the 14 putative treponeme OMP candidates identified using a reverse vaccinology pipeline. *Putative OMP candidates were initially identified from the genome sequence of T. medium phylogroup strain T19 based upon the presence of a signal peptide cleavage sequence (SignalP software) and prediction of a characteristic β-barrel tertiary structure (BOMP, PRED-TMBB and TMBETA-NET software). A protein BLAST was used to identify whether any putative OMP candidates had homologs within the genome sequences of T. phagedenis phylogroup strain T320A and T. pedis T3552B^T, using an E value cut-off of 1e-10. Of the 14 putative treponeme OMPs identified to have homologs across all three BDD phylogroups, only four candidates (highlighted in green) had a minimum inter-phylogroup homology of 40% and maximum gene size of 0.8 kbp to satisfy study requirements.*

Putative OMPs of *T. medium* phylogroup strain T19	**Putative *Omp* gene size (kbp)**	**Signal peptide cleavage site**	**Prediction of β-barrel tertiary structure**			**Identification of putative OMP candidate homologs by protein BLAST**							
						***T. phagedenis* phylogroup strain T320A**				***T. pedis* strain T3552B^T**			
			BOMP	**PRED-TMBB**	**TMBETA-NET**	**Candidate Omp**	**Query cover (%)**	**E-value**	**Identity (%)**	**Candidate Omp**	**Query cover (%)**	**E-value**	**Identity (%)**
Omp_19	1.80	Yes	Yes	No	No	Omp_3090	100	0.00	53	Omp_1724	100	0.00	55
Omp_20	1.60	Yes	Yes	No	No	Omp_3089	98	4.00e-166	45	Omp_1723	95	2.00e-157	44
Omp_34	0.62	Yes	No	Yes	Yes	Omp_694	100	2.00e-84	50	Omp_2390	80	8.00e-71	57
Omp_148	1.40	Yes	No	Yes	Yes	Omp_1978	98	1.00e-134	43	Omp_2169	91	4.00e-99	37
Omp_480	0.60	Yes	Yes	No	No	Omp_1722	98	8.00e-115	74	Omp_2267	99	1.00e-105	72
Omp_483	2.40	Yes	Yes	Yes	Yes	Omp_1725	100	0.00	63	Omp_2260	100	0.00	58
Omp_489	0.70	Yes	Yes	Yes	Yes	Omp_654	99	3.00e-17	28	Omp_1350	100	7.00e-25	29
Omp_740	1.50	Yes	Yes	Yes	No	Omp_1728	29	1.00e-04	23	Omp_1694	77	1.00e-170	62
Omp_914	1.60	Yes	Yes	Yes	Yes	Omp_103	73	9.00e-97	37	Omp_983	70	7.00e-55	30
Omp_1472	0.70	Yes	Yes	Yes	Yes	Omp_2637	74	3.00e-15	34	Omp_683	99	5.00e-35	32
Omp_1497	1.20	Yes	Yes	Yes	Yes	Omp_2649	98	2.00e-115	43	Omp_904	93	2.00e-137	50
Omp_2427	0.70	Yes	Yes	No	No	Omp_2465	99	1.00e-128	70	Omp_976	99	6.00e-140	72
Omp_2501	0.70	Yes	Yes	No	No	Omp_1243	99	2.00e-127	50	Omp_2625	100	8.00e-99	43
Omp_2582	0.94	Yes	Yes	Yes	No	Omp_892	100	4.00e-87	41	Omp_2391	96	3.00e-40	29

Table 5.2 Predictions of structural and protein domain homology for the four putative T. medium phylogroup OMP candidates to inform selection for molecular diversity studies. *The four suitable putative OMP candidates of the T. medium phylogroup were assessed by HHPRED software to predict their structural and protein domain homology and inform selection of a single putative treponeme OMP candidate for further studies of molecular diversity. The six most homologous protein domains and their corresponding identifiers (in parentheses) are provided for each putative treponeme OMP candidate alongside the organism from which they were identified. Protein homology is represented using several parameters: sequence identity (%); the probability of true local or global homology; expected (E)-value or average number of false-positive hits; the p value or pairwise comparison of the E-value; the raw score in similarity of amino acid distribution; and the secondary structure (SS) score, a measure of SS similarity.*

Putative treponeme OMP	**Predictions of structural and protein domain homology using HHPRED**							
	Homologous domain and ID	**Organism**	**Identity (%)**	**Probability**	**E-value**	***p* value**	**Raw score**	**SS score**
Omp_34	Outer membrane protein A, OmpA (3nb3_A)	*Escherichia coli*	13	99.78	1.1e-16	2.9e-21	129.76	22.6
	Outer membrane protein OprG (2x27_X)	*Pseudomonas aeruginosa*	15	99.68	1.0e-14	2.6e-19	110.46	19.2
	Neisserial Surface Protein A, NspA (1p4t_A)	*Neisseria meningitidis*	11	99.67	9.2e-14	2.4e-18	99.37	22.1
	Outer membrane porin F (4rlc_A)	*Pseudomonas aeruginosa*	9	99.66	1.1e-13	2.8e-18	101.69	22.5
	Outer membrane protein A, OmpA (1qjp_A)	*Escherichia coli*	11	99.63	3.9e-13	9.9e-18	97.77	22.1
	Outer membrane protein W, OmpW (2f1v_A)	*Escherichia coli* K12	19	99.61	2.8e-13	7.3e-18	100.90	20.4
Omp_480	*Helicobacter pylori* cysteine-rich protein B, HcpB (1klx-A)	*Helicobacter pylori*	17	81.57	3.7	9.4e-05	28.09	5.0
	Spartin, Microtubule Interacting and Trafficking (2dl1_A)	*Homo sapiens*	6	52.23	27.0	0.00069	26.43	4.6
	Spartin (4u7i_A)	*Homo sapiens*	6	46.75	43.0	0.0011	23.84	4.8
	Nuclear import adaptor, Nro1 (3msv_A)	*Schizosaccharomyces pombe*	7	41.93	1.9e+02	0.0049	25.31	8.9

	Helicobacter pylori cysteine-rich protein C, HcpC (1ouv_A)	*Helicobacter pylori*	20	30.65	32.0	0.00081	26.76	2.0
	Protein Sel-1 homolog 1 (5b26_A)	*Mus musculus*	18	29.16	19.0	0.00048	25.34	0.5
Omp_2427	Endoglucanase H (1v0a_A)	*Clostridium thermocellum*	12	98.33	8.7e-05	2.2e-09	61.65	18.4
	Chondroitinase (2q1f_A)	*Bacteroides thetaiotaomicron*	14	98.10	6.4e-05	1.6e-09	78.25	15.4
	Chondroitin ABC lyase I (1hn0_A)	*Proteus vulgaris*	14	97.71	0.00100	2.6e-08	69.31	16.4
	Endo-1,4-beta-xylanase C (4xuo_A)	*Paenibacillus barcinonensis*	12	97.51	0.02100	5.3e-07	44.94	17.9
	Endo-beta-1,4-mannanase (1wky_A)	*Bacillus* sp. strain JAMB-602	11	97.29	0.01100	2.9e-07	55.09	16.1
	Non-catalytic protein 1, Ncp1 (1gwm_A)	*Piromyces equi*	8	97.04	0.01100	2.8e-07	48.33	11.6
Omp_2501	Hypothetical protein LIC12922 (3nrk_A)	*Leptospira interrogans*	16	100.0	8.6e-33	2.2e-37	250.49	30.2
	Survival protein A, SurA (1m5y_A)	*Escherichia coli*	12	100.0	2.3e-30	6.0e-35	241.86	29.6
	Cell-binding factor 2 (3rfw_A)	*Campylobacter jejuni*	15	99.97	6.9e-30	1.8e-34	222.89	25.4
	Possible periplasmic protein, chaperone (3rgc_A)	*Campylobacter jejuni*	15	99.97	7.0e-30	1.8e-34	222.91	24.2
	Putative peptidyl-prolyl cis-trans isomerase HP_0175 (5ez1_A)	*Helicobacter pylori*	18	99.97	5.5e-30	1.4e-34	226.81	18.4
	Foldase protein PrsA (5tvl_A)	*Streptococcus pneumoniae*	19	99.97	3.2e-29	8.2e-34	223.04	23.3

Table 5.3 Predictions of structural and protein domain homology for the four putative T. phagedenis phylogroup OMP candidates to inform selection for molecular diversity studies. *The four suitable putative OMP candidates of the T. phagedenis phylogroup were assessed by HHPRED software to predict their structural and protein domain homology and inform selection of a single putative treponeme OMP candidate for further studies of molecular diversity. The six most homologous protein domains and their corresponding identifiers (in parentheses) are provided for each putative treponeme OMP candidate alongside the organism from which they were identified. Protein homology is represented using several parameters: sequence identity (%); the probability of true local or global homology; expected (E)-value or average number of false-positive hits; the p value or pairwise comparison of the E-value; the raw score in similarity of amino acid distribution; and the secondary structure (SS) score, a measure of SS similarity.*

Putative treponeme OMP	**Predictions of structural and protein domain homology using HHPRED**							
	Homologous domain and ID	**Organism**	**Identity (%)**	**Probability**	**E-value**	***p* value**	**Raw score**	**SS score**
Omp_694	Outer membrane protein A, OmpA (3nb3_A)	*Escherichia coli*	11	99.78	7.6e-17	1.9e-21	138.60	22.8
	Outer membrane protein OprG (2x27_X)	*Pseudomonas aeruginosa*	13	99.77	5.2e-17	1.3e-21	130.53	18.7
	Neisserial Surface Protein A, NspA (1p4t_A)	*Neisseria meningitidis*	12	99.75	1.1e-15	2.9e-20	115.62	22.2
	Outer membrane porin F (4rlc_A)	*Pseudomonas aeruginosa*	11	99.74	2.3e-15	6.0e-20	117.35	23.7
	Outer membrane protein A, OmpA (1qjp_A)	*Escherichia coli*	10	99.71	8.0e-15	2.0e-19	112.85	22.7
	Outer membrane protein W, OmpW (2f1v_A)	*Escherichia coli* K12	13	99.71	2.7e-15	6.8e-20	118.43	19.7
Omp_1722	*Helicobacter pylori* cysteine-rich protein B, HcpB (1klx-A)	*Helicobacter pylori*	16	83.58	3.1	8.0e-05	28.44	5.2
	Spartin, Microtubule Interacting and Trafficking (2dl1_A)	*Homo sapiens*	8	49.80	29.0	0.00074	26.24	4.4
	Spartin (4u7i_A)	*Homo sapiens*	9	43.87	48.0	0.00120	23.61	4.6

	Nuclear import adaptor, Nro1 (3msv_A)	*Schizosaccharomyces pombe*	4	42.49	1.7e+02	0.00440	25.54	8.7
	Helicobacter pylori cysteine-rich protein C, HcpC (1ouv_A)	*Helicobacter pylori*	17	34.96	28.0	0.00071	27.05	2.3
	Protein Sel-1 homolog 1 (5b26_A)	*Mus musculus*	15	34.58	16.0	0.00041	25.67	0.9
Omp_2465	Endoglucanase H (1v0a_A)	*Clostridium thermocellum*	12	98.20	0.00021	5.3e-09	59.69	17.8
	Chondroitinase (2q1f_A)	*Bacteroides thetaiotaomicron*	13	97.68	0.00099	2.5e-08	69.80	15.7
	Chondroitin ABC lyase I (1hn0_A)	*Proteus vulgaris*	15	97.52	0.00190	4.9e-08	67.69	15.2
	Endo-beta-1,4-mannanase (1wky_A)	*Bacillus* sp. strain JAMB-602	13	97.32	0.01400	3.7e-07	54.65	17.2
	Endo-1,4-beta-xylanase C (4xuo_A)	*Paenibacillus barcinonensis*	8	97.07	0.08900	2.3e-06	41.41	18.2
	Non-catalytic protein 1, Ncp1 (1gwm_A)	*Piromyces equi*	8	96.72	0.04100	1.0e-06	45.15	12.5
Omp_1243	Hypothetical protein LIC12922 (3nrk_A)	*Leptospira interrogans*	15	100.0	1.3e-32	3.5e-37	250.09	33.9
	Survival protein A, SurA (1m5y_A)	*Escherichia coli*	11	99.97	1.7e-29	4.2e-34	236.92	31.4
	Cell-binding factor 2 (3rfw_A)	*Campylobacter jejuni*	15	99.97	7.1e-30	1.8e-34	223.55	26.6
	Possible periplasmic protein, chaperone (3rgc_A)	*Campylobacter jejuni*	18	99.97	4.8e-30	1.2e-34	224.74	24.9
	Foldase protein PrsA (5tvl_A)	*Streptococcus pneumoniae*	18	99.97	1.2e-28	3.1e-33	220.14	25.5
	Putative peptidyl-prolyl cis-trans isomerase HP_0175 (5ez1_A)	*Helicobacter pylori*	17	99.97	1.8e-29	4.6e-34	224.31	16.8

Table 5.4 Predictions of structural and protein domain homology for the four putative T. pedis OMP candidates to inform selection for molecular diversity studies. *The four suitable putative OMP candidates of T. pedis were assessed by HHPRED software to predict their structural and protein domain homology and inform selection of a single putative treponeme OMP candidate for further studies of molecular diversity. The six most homologous protein domains and their corresponding identifiers (in parentheses) are provided for each putative treponeme OMP candidate alongside the organism from which they were identified. Protein homology is represented using several parameters: sequence identity (%); the probability of true local or global homology; expected (E)-value or average number of false-positive hits; the p value or pairwise comparison of the E-value; the raw score in similarity of amino acid distribution; and the secondary structure (SS) score, a measure of SS similarity.*

Putative treponeme OMP	**Predictions of structural and protein homology using HHPRED**							
	Homologous domain and ID	**Organism**	**Identity (%)**	**Probability**	**E-value**	***p* value**	**Raw score**	**SS score**
Omp_2390	Outer membrane protein A, OmpA (3nb3_A)	*Escherichia coli*	13	99.80	4.3e-17	1.1e-21	125.70	22.5
	Outer membrane protein OprG (2x27_X)	*Pseudomonas aeruginosa*	15	99.72	1.6e-15	4.0e-20	109.22	18.2
	Neisserial Surface Protein A, NspA (1p4t_A)	*Neisseria meningitidis*	12	99.72	1.4e-14	3.7e-19	98.68	22.1
	Outer membrane porin F (4rlc_A)	*Pseudomonas aeruginosa*	10	99.71	2.9e-14	7.5e-19	99.51	23.3
	Outer membrane protein W, OmpW (2f1v_A)	*Escherichia coli* K12	15	99.67	4.4e-14	1.1e-18	100.20	19.9
	Outer membrane protein A, OmpA (1qjp_A)	*Escherichia coli*	11	99.66	2.4e-13	6.1e-18	94.15	22.5
Omp_2267	*Helicobacter pylori* cysteine-rich protein B, HcpB (1klx-A)	*Helicobacter pylori*	15	82.64	3.6	9.2e-05	28.02	5.2
	Spartin, Microtubule Interacting and Trafficking (2dl1_A)	*Homo sapiens*	10	52.28	25.0	0.00065	26.52	4.4
	Spartin (4u7i_A)	*Homo sapiens*	11	46.69	41.0	0.00110	23.90	4.6

	Nuclear import adaptor, Nro1 (3msv_A)	*Schizosaccharomyces pombe*	5	43.86	1.7e+02	0.00430	25.54	8.9
	Protein Sel-1 homolog 1 (5b26_A)	*Mus musculus*	15	32.13	18.0	0.00046	25.33	0.8
	Spastin (3eab_A)	*Homo sapiens*	13	26.90	64.0	0.00170	22.74	2.9
Omp_976	Endoglucanase H (1v0a_A)	*Clostridium thermocellum*	15	98.13	0.00034	8.8e-09	58.42	17.9
	Chondroitinase (2q1f_A)	*Bacteroides thetaiotaomicron*	12	97.77	0.00066	1.7e-08	71.22	16.1
	Chondroitin ABC lyase I (1hn0_A)	*Proteus vulgaris*	15	97.69	0.00079	2.0e-08	70.62	15.1
	Endo-beta-1,4-mannanase (1wky_A)	*Bacillus* sp. strain JAMB-602	13	97.35	0.00970	2.5e-07	55.83	16.4
	Endo-1,4-beta-xylanase C (4xuo_A)	*Paenibacillus barcinonensis*	11	97.28	0.05200	1.3e-06	42.79	18.0
	Endo-1,4-beta-xylanase Y (1dyo_A)	*Clostridium thermocellum*	14	96.63	0.19000	4.9e-06	38.73	15.9
Omp_2625	Hypothetical protein LIC12922 (3nrk_A)	*Leptospira interrogans*	15	100.0	3.4e-32	8.8e-37	247.80	31.2
	Survival protein A, SurA (1m5y_A)	*Escherichia coli*	12	99.97	4.9e-29	1.2e-33	234.10	30.6
	Cell-binding factor 2 (3rfw_A)	*Campylobacter jejuni*	14	99.97	4.8e-28	1.2e-32	212.23	26.9
	Possible periplasmic protein, chaperone (3rgc_A)	*Campylobacter jejuni*	17	99.96	3.7e-28	9.5e-33	213.09	24.0
	Foldase protein PrsA (5tvl_A)	*Streptococcus pneumoniae*	16	99.96	1.2e-27	3.0e-32	214.09	26.0
	Putative peptidyl-prolyl cis-trans isomerase HP_0175 (5ez1_A)	*Helicobacter pylori*	17	99.95	5.5e-28	1.4e-32	215.07	15.8

5.2.2 Modelling the predicted structural topology of a putative treponeme outer membrane protein

Upon identification of a suitable putative treponeme OMP candidate for molecular diversity studies (Chapter 5.2.1), the structural topologies of the *T. medium* phylogroup (Omp_34), *T. phagedenis* phylogroup (Omp_694) and *T. pedis* (Omp_2390) homologs were predicted and subsequently modelled according to Chapter 2.8.4 using reference strains T19, T320A and T3552B^{T} respectively, as illustrated in Figure 5.1, 5.2 and 5.3.

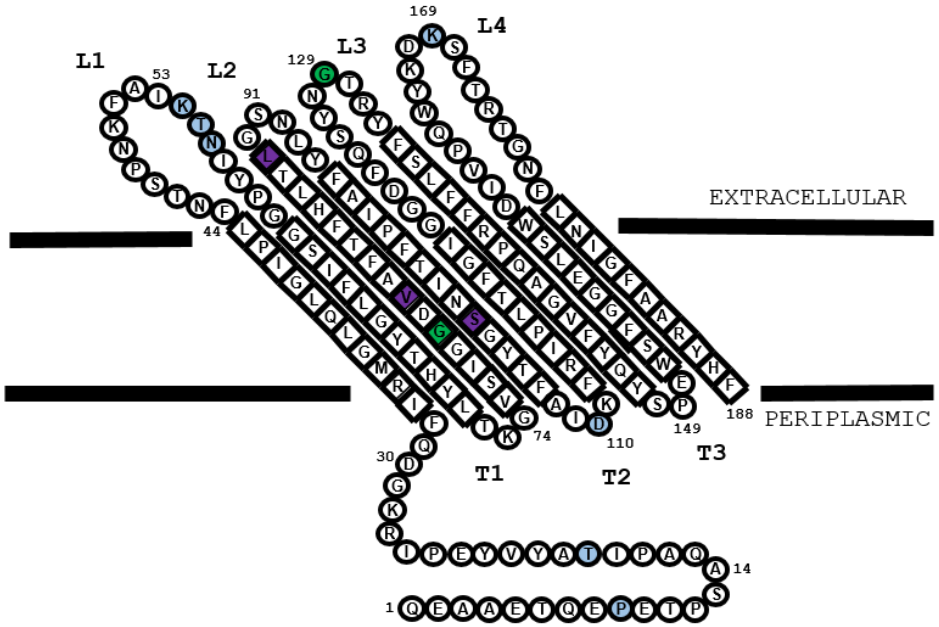

Figure 5.1 Predicted structural topology model of the putative T. medium phylogroup OMP indicating both variable and conserved regions. *Following identification of a putative treponeme OMP with homologs across all three BDD treponeme phylogroups, structural topology was predicted and subsequently modelled using PRED-TMBB software. The predicted putative T. medium phylogroup OMP is a 188 amino acid sequence consisting of eight anti-parallel β-strands (squares), four extracellular loops (L1, L2, L3 and L4) and three short periplasmic turns (T1, T2 and T3). The molecular diversity of this putative OMP was investigated across 33 T. medium phylogroup isolates and non-synonymous substitutions were identified within extracellular loops (blue), a periplasmic turn (blue) and the transmembrane β-strands (purple). When compared to its six most homologous proteins (Chapter 5.2.1), two conserved glycine residues were identified across all homologs (green).*

The putative OMP homologs of *T. medium* phylogroup, *T. phagedenis* phylogroup and *T. pedis* were 188, 206 and 186 amino acids in length and were each predicted to consist of eight anti-parallel β-strands (each consistently between eight and 15 amino acids in length), four extracellular loops (L1 to L4) and three small periplasmic turns (T1 to T3), alongside a short initial 28 to 69 amino acid sequence. The extracellular loop, L2, was consistently of much shorter length (5 or 9 amino acids) compared to L1, L3 and L4 (on average, 15 amino

acids), with L1 consistently the longest across each of the phylogroups. Whilst each of the small periplasmic turns were found to be of identical length across OMP homologs of the three BDD treponeme phylogroups, with three (T1 and T3) or four (T2) amino acids respectively, the extracellular loops were far more variable. Interestingly, the putative *T. medium* phylogroup OMP had the largest L4 extracellular loop, however the smallest L2 extracellular loop. Furthermore, the putative *T. phagedenis* phylogroup OMP was found to have the largest L1 and L3 extracellular loops.

Few amino acid residues were found to be conserved amongst the sequences of putative OMP homologs of *T. medium* phylogroup*, T. phagedenis* phylogroup or *T. pedis* and those of their six most homologous protein relatives (Chapter 5.2.1; Table 5.2, 5.3 and 5.4). Only *T. medium* phylogroup isolates were found to have conserved amino acid residues within all proteins and these were single glycine residues within the extracellular loop and transmembrane domain respectively (Figure 5.1).

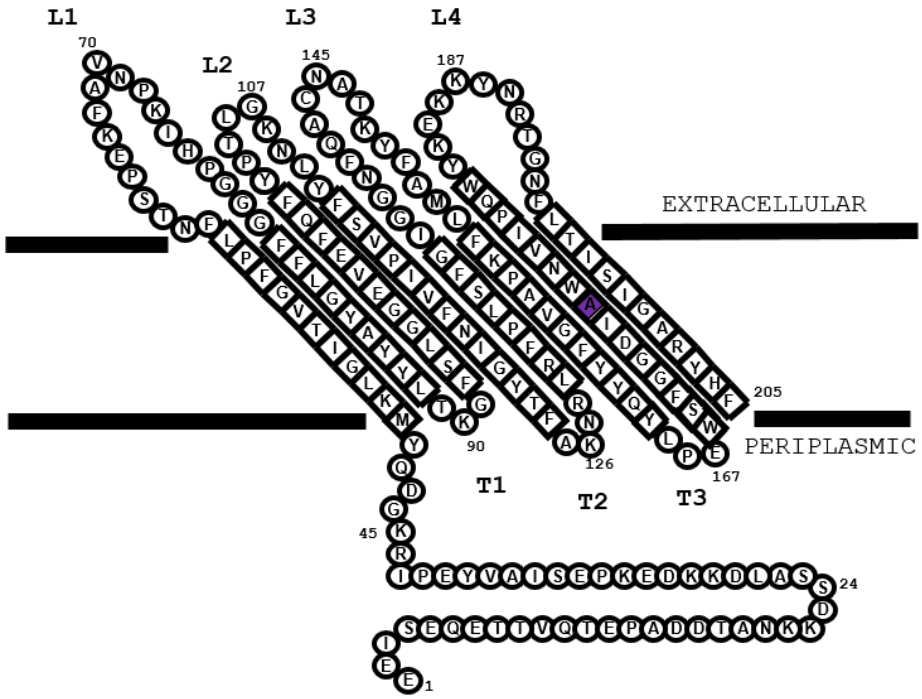

Figure 5.2 Predicted structural topology model of the putative T. phagedenis phylogroup OMP indicating both variable and conserved regions. *Following identification of a putative treponeme OMP with homologs across all three BDD treponeme phylogroups, structural topology was predicted and subsequently modelled using PRED-TMBB software. The predicted putative T. phagedenis phylogroup OMP is a 205 amino acid sequence consisting of eight anti-parallel β-strands (squares), four extracellular loops (L1, L2, L3 and L4) and three short periplasmic turns (T1, T2 and T3). The molecular diversity of this putative OMP was investigated across 69 T. phagedenis phylogroup isolates and only a single non-synonymous substitution was identified within a transmembrane β-strand (purple).*

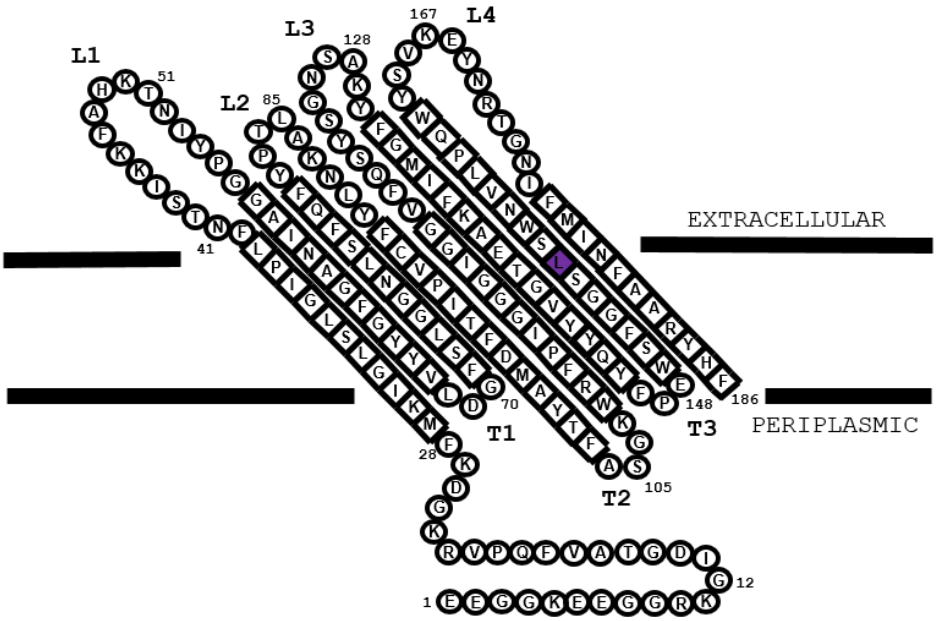

Figure 5.3 Predicted structural topology model of the putative T. pedis OMP indicating both variable and conserved regions. *Following identification of a putative treponeme OMP with homologs across all three BDD treponeme phylogroups, structural topology was predicted and subsequently modelled using PRED-TMBB software. The predicted putative T. pedis OMP is a 186 amino acid sequence consisting of eight anti-parallel β-strands (squares), four extracellular loops (L1, L2, L3 and L4) and three short periplasmic turns (T1, T2 and T3). The molecular diversity of this putative OMP was investigated across 13 T. pedis isolates and only a single non-synonymous substitution was identified within a transmembrane β-strand (purple).*

5.2.3 Investigating molecular diversity of a putative treponeme outer membrane protein

Following the successful development and optimisation of three novel PCR assays to enable amplification of each putative treponeme phylogroup-specific *Omp* gene homolog (Chapter 2.8.5), the assays were used to enable amplification and subsequent sequencing of the putative *Omp* gene homologs across a panel of 108 treponeme isolates of the *T. medium* phylogroup, *T. phagedenis* phylogroup and *T. pedis* (Chapter 2.8.1), according to Chapter 2.8.6.

The near-complete gene sequences of putative OMP homologs, Omp_34 (504 bp), Omp_694 (547 bp) and Omp_2390 (480 bp), were obtained from 33 *T. medium* phylogroup, 69 *T. phagedenis* phylogroup and 13 *T. pedis* isolates respectively and both nucleotide and amino acid sequence diversity was subsequently assessed (Table 5.5). Purifying and diversifying selection pressures, recombination and phylogenetic relationships were also investigated, as described in Chapter 2.8.7 to 2.8.12.

Nucleotide and amino acid sequence diversity

The average identity between putative OMP nucleotide and amino acid sequences of *T. medium* phylogroup strain T19, *T. phagedenis* phylogroup strain T320A and *T. pedis* strain T3552B^T were 58.5% and 49.1% respectively.

Despite consisting of a much larger representative sample of isolates by comparison to the other treponeme phylogroups, the putative OMP homolog of *T. phagedenis* phylogroup isolates was found to be highly conserved; with just two allelic variants across all 69 treponeme isolates. The average putative *Omp* gene sequence similarity across isolates of the *T. phagedenis* phylogroup was 99.97%, with a range of between 99.80% and 100.0%. These two variants were found to result from a single nucleotide variation (SNV) (C → T) of allele 1 at bp 512, resulting in a d_N substitution from alanine to valine at residue 171 (allele 2). The vast majority (92.75%) of *T. phagedenis* phylogroup isolates were identified as allele 1, whilst the SNV of allele 2 was identified in all of the isolates from man and, notably, also one isolate from a wild American elk. Such variation did not appear to be influenced by geographical location or temporal isolation.

By contrast, the putative OMP homologs of *T. medium* phylogroup and *T. pedis* were found to have four and five different allelic variants across their respective 33 and 13 isolates. Allele 1 and allele 4 were most commonly identified amongst *T. medium* phylogroup (60.61%) and *T. pedis* (38.46%) isolates respectively. The average putative *Omp* gene sequence similarity across isolates of the *T. medium* phylogroup was 98.27% (range 90.6% and 100.0%), whilst that of *T. pedis* isolates was 98.6% (range 96.0% and 100.0%). A greater number of variable nucleotide sites were identified across *T. medium* phylogroup isolates (n = 53) compared to those of *T. pedis* (n = 21). However, whilst these variants translated into an observably large proportion of amino acid substitutions (d_N) for the *T. medium* phylogroup homolog (with 10 variable sites), those of the putative *T. pedis* OMP did not and were largely d_S substitutions. Whilst its occurrence did not appear to demonstrate geographical, temporal or host specificity, the most frequently occurring d_N substitution of the *T. medium* phylogroup OMP homolog (12 of 33 isolates) was a SNV (C → A) at position 19, resulting in a threonine rather than proline residue (position 7) and giving rise to allele 2. Interestingly, it was the putative OMP sequence of the human isolate, *T. vincentii* OMZ 838, which demonstrated the most variation within this phylogroup; with 40 nucleotide variants and seven d_N substitutions when compared to the bovine reference strain, T19. Excluding this highly variable *T. vincentii* isolate, the remaining d_N substitutions of this phylogroup were almost exclusively found within the central region of the amino acid sequence, between positions 79 and 108, and

were also commonly shared by treponeme isolates of wild American elk (EL024 R, EL022R and EL023 aR), humans and the notable bovine (dairy) isolate, DD3F(1); each of allelic variants 3 or 4. Nucleotide substitutions were also largely observed within the central sequence region, between position 183 to 260 and 301 to 363.

Both G9JD and G3ST1, *T. pedis* isolates of caprine and ovine species respectively, commonly shared 15 SNVs between nucleotide position 207 and 430 and gave rise to the only d_N substitution (leucine to phenylalanine) observed within the putative OMP sequence of 13 *T. pedis* isolates; a T → C substitution at position 430 leading to a phenylalanine rather than leucine residue at position 144. Resultantly, these isolates, forming allelic variant 2, had the most divergent putative OMP sequence of the *T. pedis* isolates investigated. The pig isolate, *T. pedis* T A4, had a unique d_S SNV (A → G) at position 33 and shared a further two d_S SNVs (position 63 and 435) with the dairy cattle isolate, 9185 Med Ag 2; forming allelic variants 5 and 3, respectively. Notably, each of the *T. pedis* ST5 isolates shared the same d_S substitutions at position 135 (C → T) and 246 (A → G) and formed a distinct fourth allele. Allele 1 resulted from SNVs of the putative OMP sequence at nucleotide positions 150 and 246, respectively.

The *p*-distance values calculated for both nucleotide and amino acid sequences of the putative OMP homologs of *T. medium* phylogroup*, T. phagedenis* phylogroup and *T. pedis* isolates were consistent with above observations (Table 5.5). The putative OMP of *T. medium* phylogroup had the highest percentage of both nucleotide and amino acid sites at which sequences were different, with mean *p*-distances of 1.70% and 1.20% respectively. The putative OMP of *T. pedis* was found to have a mean nucleotide *p*-distance of 1.20%, but varied very little at different sites across the amino acid sequence (0.20%). In contrast, as previously identified, the putative *T. phagedenis* phylogroup OMP was found to have very little nucleotide and sequence diversity, with mean nucleotide and amino acid *p*-distances of 0.00% and 0.10%, respectively.

Evidence of homopolymeric tracts

There was evidence of long homopolymeric tracts within the putative *Omp* gene sequences of all three BDD treponeme phylogroups. Whilst the *T. phagedenis* phylogroup gene sequence contained an eight bp polyA tract between nucleotide position 614 and 621, the *T. medium* phylogroup and *T. pedis* sequences each had a seven bp homopolymeric tract (polyT and polyA, respectively) within the first 32 nucleotides of the sequence (Table 5.5). These seven bp and eight bp homopolymeric tracts were not found in the trimmed sequences of

the treponeme isolates; however, a number of six bp polyT and polyA tracts were identified throughout the length of the sequence.

Table 5.5 Nucleotide and amino acid sequence diversity among the putative Omp gene homologs of T. medium* phylogroup*, T. phagedenis* phylogroup *and T. pedis isolates. *The near-complete gene sequences of novel putative treponeme Omp homologs were obtained from 33 T. medium phylogroup (504 bp), 69 T. phagedenis phylogroup (547 bp) and 13 T. pedis (480 bp) isolates to investigate intra-phylogroup and inter-phylogroup molecular diversity across BDD treponemes. The contiguous putative treponeme Omp gene sequences of each phylogroup were aligned and trimmed prior to analysis of: their average GC content (%) using the Datamonkey web server; their number of Omp alleles (designated manually using MEGA); the number of nucleotide or amino acid variable sites; the presence of homopolymeric tracts; the mean p-distances (% ± standard error) or proportion of nucleotide or amino acid sites at which two sequences are different (as determined using MEGA); and the ratio of non-synonymous (d_N) and synonymous (d_S) substitutions to indicate the presence of purifying (ratio < 1) or diversifying (ratio > 1) selection pressures.*

	***T. medium* phylogroup**	***T. phagedenis* phylogroup**	***T. pedis***
Putative *Omp* gene diversity			
Number of sequences	33	69	13
Length of sequences (bp)	504	547	480
Average GC content (%)	45.08	40.21	40.83
Number of alleles	4	2	5
Number of variable sites	53	1	21
Mean *p*-distance (% ± SE)	1.70 ± 0.30	0.00 ± 0.00	1.30 ± 0.30
d_N/d_S	0.29	ND	0.05
Homopolymeric tract	8 bp polyA	7 bp polyT	7 bp polyA
Putative OMP protein diversity			
Number of amino acid sequences	4	2	2
Length of amino acid sequences (residues)	167	182	159
Number of variable sites	10	1	1
Mean *p*-distance (% ± SE)	1.20 ± 0.40	0.10 ± 0.10	0.20 ± 0.20

ND; not able to be determined.

Purifying and diversifying selection pressures

Purifying (negative) and diversifying (positive) selection pressures were assessed across the putative *Omp* gene sequences of treponeme isolates; however, no significant pressures were identified at a *p* value of 0.05. *T. medium* phylogroup isolates were found to be under negative selection pressures at codon 34, 74 and 82 at a non-significant *p* value of 0.15 and, agreeably, a d_N/d_S ratio of 0.29 was calculated. Similarly, negative selection pressures were

identified at codon 82 of the *T. pedis* isolates, again only at a non-significant *p* value of 0.15. A d_N/d_S ratio of 0.05 was calculated. No selection pressures were able to be predicted, neither a d_N/d_S ratio calculated, across the *T. phagedenis* phylogroup isolates due to insufficient sequence diversity.

All d_N substitutions identified were mapped onto the structural topology models of the *T. medium* phylogroup (Figure 5.1), *T. phagedenis* phylogroup (Figure 5.2) and *T. pedis* (Figure 5.3) putative OMP homologs to determine their predicted locality within the protein structure. The single amino acid variants of *T. phagedenis* phylogroup and *T. pedis* isolates were each predicted to be in the transmembrane domains of the putative OMP on the seventh anti-parallel β-strand, at residue positions 175 and 155 respectively. In contrast, a large number of amino acid variants were observed within the putative OMP sequence across isolates of the *T. medium* phylogroup. Three of these were found within the transmembrane domains; including valine to isoleucine (position 81) and leucine to arginine (position 89) substitutions on the third anti-parallel β-strand and a serine to alanine (position 103) substitution on the fourth strand. Notably, the three consecutive d_N substitution sites identified on the L1 extracellular loop (lysine, threonine and asparagine residues to asparagine, proline and lysine residues respectively) and the d_N substitution site on loop L4 (lysine to serine) were each altered only within the putative OMP sequence of human periodontal isolate, *T. vincentii.* Unlike the putative OMP homologs of *T. phagedenis* phylogroup and *T. pedis, T. medium* phylogroup isolates also demonstrated d_N variants in the amino acid sequence upstream of the first N terminal β-strand, at residue sites 9 and 19, respectively, and within the periplasmic turn, T2.

Analysis of phylogenetic relatedness based upon the putative treponeme *Omp* gene

Phylogeny was inferred from each of the putative *Omp* gene sequence alignments of *T. medium* phylogroup, *T. phagedenis* phylogroup and *T. pedis* isolates as shown in Figure 5.4, Figure 5.5 and Figure 5.6 respectively. Phylogenetic reconstruction generally agreed with previous observations of *Omp* allelic variants (as above), whereby each of the allelic variants formed distinct clusters within each of the phylogenies.

Interestingly, allelic variants 1 and 2 of the putative OMP homolog of *T. medium* phylogroup isolates were most similar and solely contained isolates of domesticated production animals (Figure 5.4). By contrast, allele 4 was largely found to consist of wild American elk isolates, that of the dairy cattle isolate, DD3F(1), and the human isolate *T. medium* ATCC 700293. Most notably, the human periodontal isolate, *T. vincentii* OMZ 838, was found to form a

distinct allele which was noticeably divergent from all others of the *T. medium* phylogroup. Isolates did not appear to cluster based upon geographical or temporal parameters; however, with the exception of ST7 and ST6, isolate Omp sequences of the same ST (as designated by MLST; Clegg *et al.,* 2016d) did appear to form distinct clusters within the *T. medium* phylogeny.

Phylogenetic inference of the *T. phagedenis* phylogroup OMP homolog identified two distinct clusters corresponding to allele 1 and allele 2 isolates respectively. Allele 1 isolates formed the predominant cluster, whilst the minor cluster of allele 2 contained all of the human isolates and the wild American elk isolate of ST1, EL022 F. Interestingly, the ST1 isolates from sheep and dairy species were found within the predominant allele 1 cluster. Isolates did not cluster by geographical location.

One of the most striking observations of the *T. pedis* phylogeny of putative *Omp* gene sequence comparisons is that the isolates of G9JD and G3ST1 (allele 2) clustered distinctly from those of the other alleles. However, whilst both of ST2, these isolates did not share similarity with the other *T. pedis* isolate of ST2, G3T1. The other predominant cluster of the phylogeny was found to contain representatives of the four remaining alleles, which each formed a distinct grouping. Whilst isolates of allele 4 (and coincidentally ST5) clustered most distinctly, those of the pig isolate, *T. pedis* T A4*,* and the dairy isolate, 9185 Med Ag 2, were quite similar.

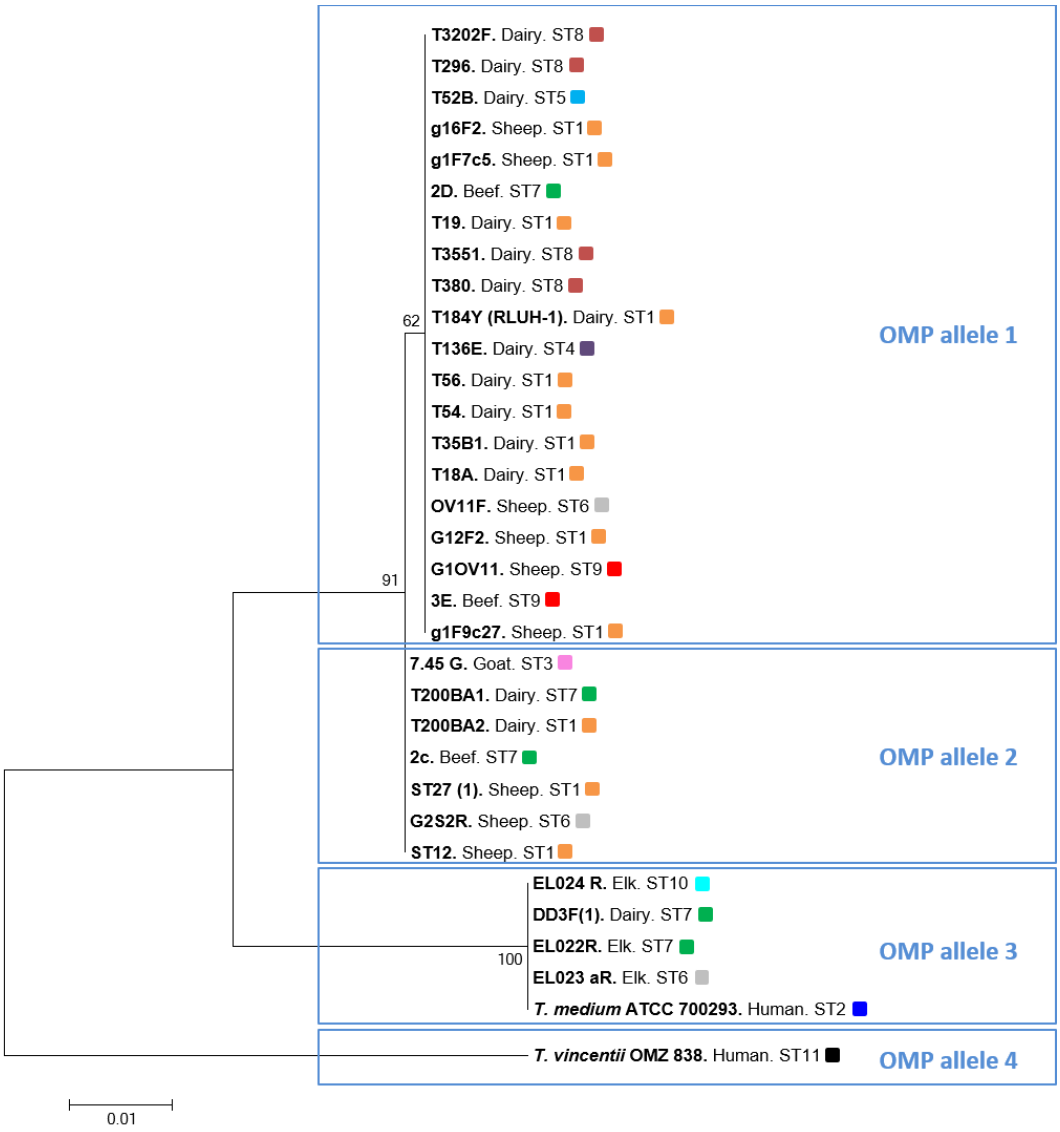

Figure 5.4 Phylogenetic tree of maximum-likelihood illustrating putative Omp gene sequence comparisons over 504 aligned bases across a panel of 33 T. medium phylogroup isolates. *The near-complete gene sequences (504 bp) of a novel putative treponeme Omp homolog were compared across a panel of 33 T. medium phylogroup isolates. Phylogeny was inferred from the trimmed sequence alignment using the Tamura-Nei model to produce a bootstrapped phylogenetic tree of maximum-likelihood, based upon 10,000 reiterations. T. medium phylogroup isolate names are given in bold type, alongside the host from which they were isolated and their respective sequence type (ST; colour-coded blocks) based upon a previous MLST study (Clegg et al. 2016d). The four designated Omp alleles are shown in blue. Bootstrap confidence intervals are shown as percentages at the nodes. Bar, 0.01 nucleotide substitutions per site.*

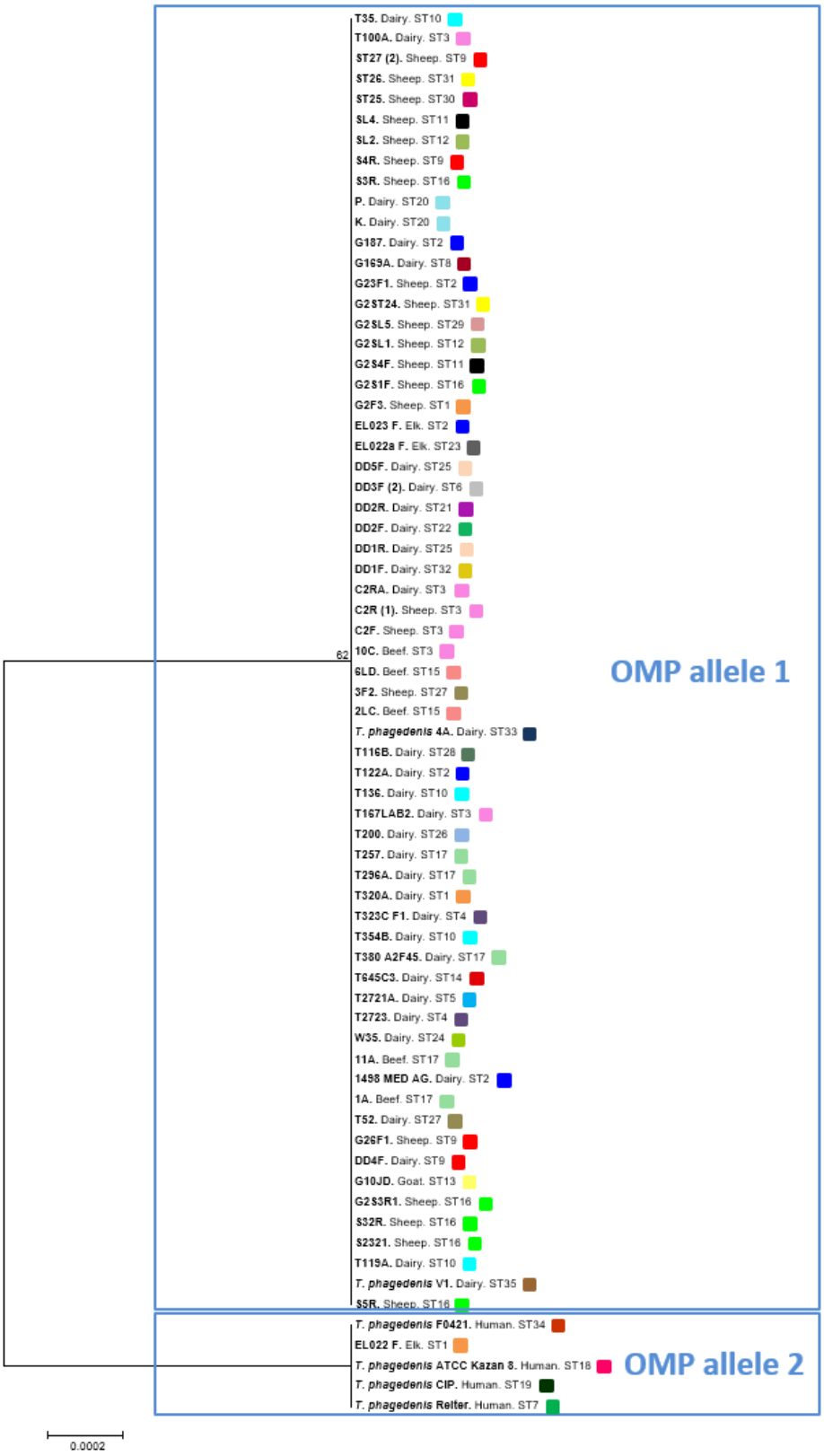

Figure 5.5 Phylogenetic tree of maximum-likelihood illustrating putative Omp gene sequence comparisons over 547 aligned bases across a panel of 69 T. phagedenis phylogroup isolates. *The near-complete gene sequences (547 bp) of a novel putative treponeme Omp homolog were compared across a panel of 69 T. phagedenis phylogroup isolates. Phylogeny was inferred from the trimmed sequence alignment using the Jukes-*

Cantor model to produce a bootstrapped phylogenetic tree of maximum-likelihood, based upon 10,000 reiterations. T. phagedenis phylogroup isolate names are given in bold type, alongside the host from which they were isolated and their respective sequence type (ST; colour-coded blocks) based upon a previous MLST study (Clegg et al. 2016d). The two designated Omp alleles are shown in blue. Bootstrap confidence intervals are shown as percentages at the nodes; values below 40% were removed for clarity. Bar, 0.0002 nucleotide substitutions per site.

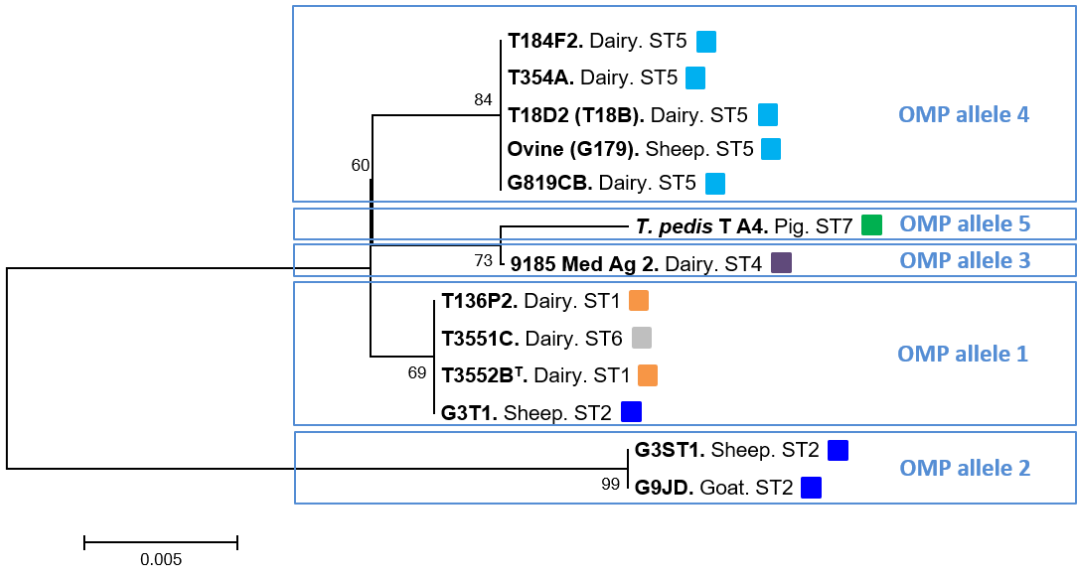

Figure 5.6 Phylogenetic tree of maximum-likelihood illustrating putative Omp gene sequence comparisons over 480 aligned bases across a panel of 13 T. pedis isolates. *The near-complete gene sequences (480 bp) of a novel putative treponeme Omp homolog were compared across a panel of 13 T. pedis isolates. Phylogeny was inferred from the trimmed sequence alignment using the Hasegawa-Kishino-Yano model to produce a bootstrapped phylogenetic tree of maximum-likelihood, based upon 10,000 reiterations. T. pedis isolate names are given in bold type, alongside the host from which they were isolated and their respective sequence type (ST; colour-coded blocks) based upon a previous MLST study (Clegg et al. 2016d). The five designated Omp alleles are shown in blue. Bootstrap confidence intervals are shown as percentages at the nodes. Bar, 0.005 nucleotide substitutions per site.*

Evidence of *Omp* gene recombination within and between bovine digital dermatitis treponeme phylogroups

Split decomposition analysis of the putative *Omp* gene homologs identified evidence of recombination within the *T. medium* phylogroup (Figure 5.7) and *T. pedis* isolates (Figure 5.9, but not within the *T. phagedenis* phylogroup isolates (Figure 5.8). No evidence of recombination was identified between the putative *Omp* gene sequences of these three *Treponema* phylogroups (Figure 5.10).

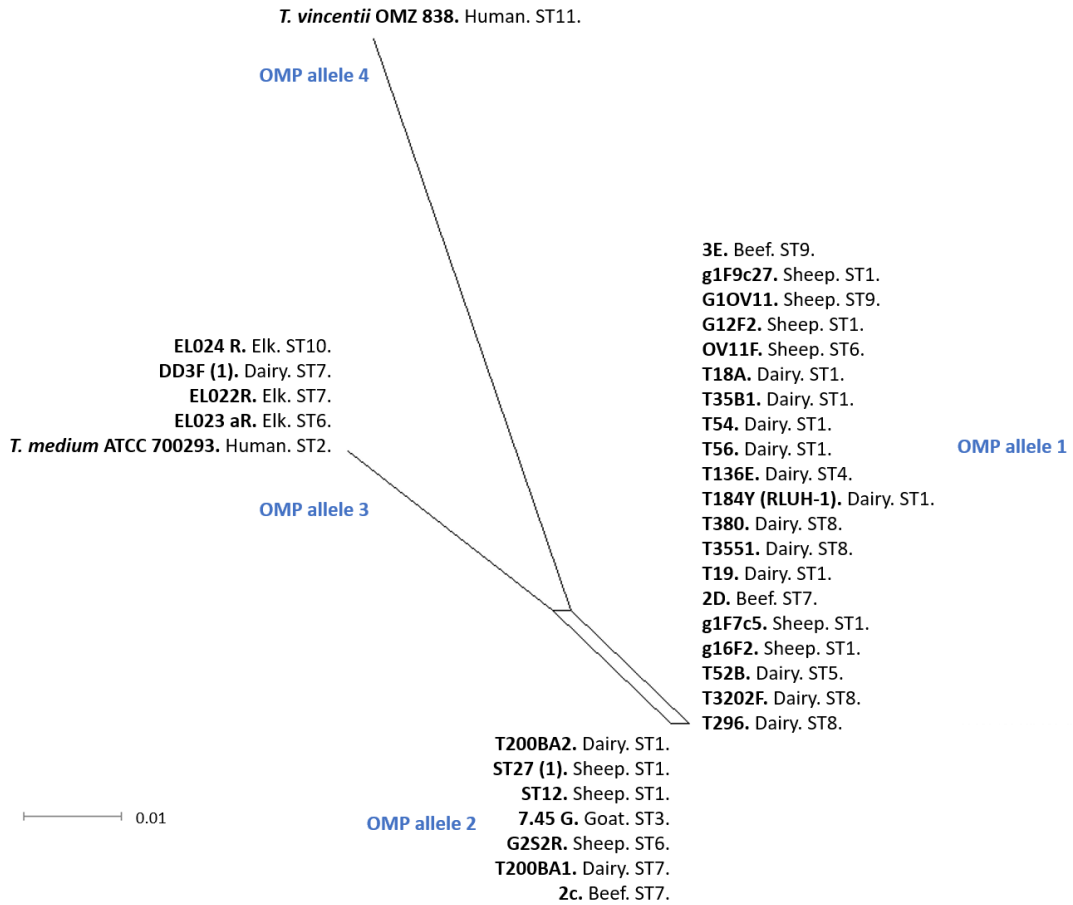

Figure 5.7 Evidence of recombination between the putative treponeme Omp genes of 33 T. medium phylogroup isolates. *Split decomposition analysis was performed using SplitsTree4 software to determine whether recombination is predicted to have occurred between the putative treponeme Omp genes of the 33 T. medium phylogroup isolates investigated during this study. T. medium phylogroup isolate names are given in bold type, alongside the host from which they were isolated and their respective sequence type (ST) based upon a previous MLST study (Clegg et al. 2016d). The four designated Omp alleles are shown in blue. Bar, 0.01 relative sequence disimilarity.*

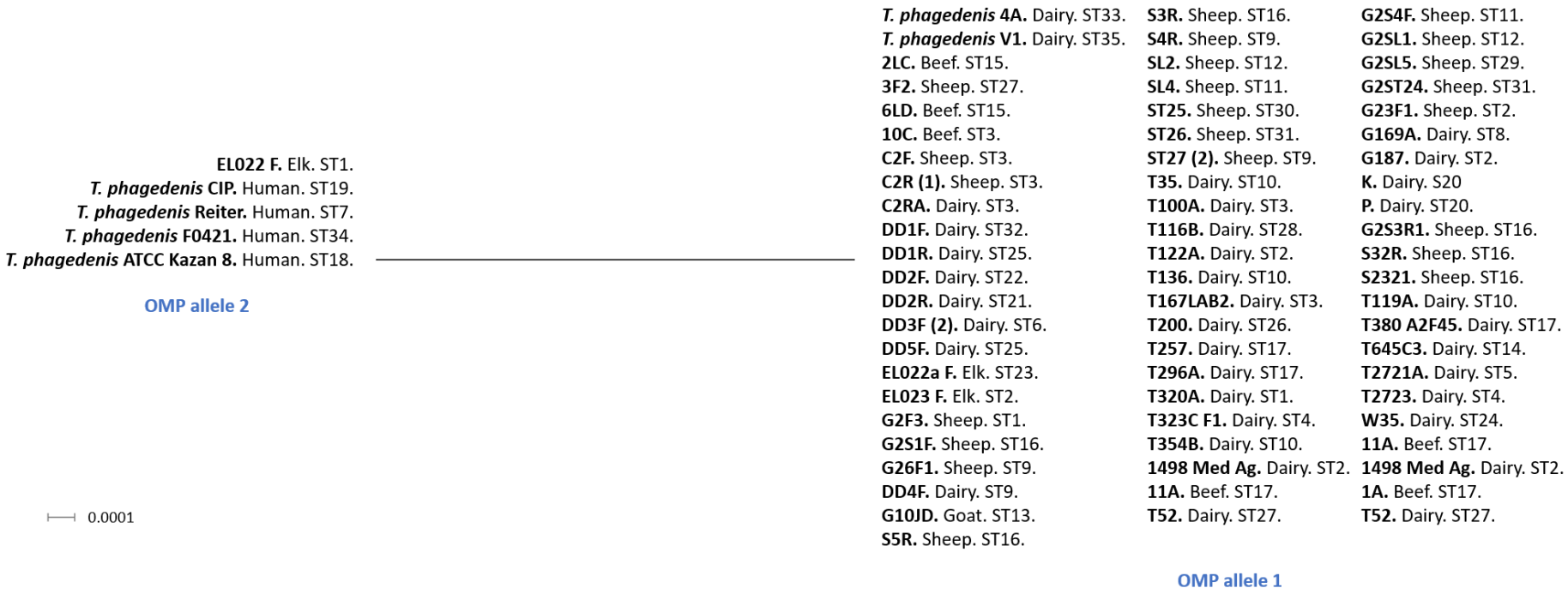

Figure 5.8 Evidence of recombination between the putative treponeme Omp genes of 69 T. phagedenis phylogroup isolates. *Split decomposition analysis was performed using SplitsTree4 software to determine whether recombination is predicted to have occurred between the putative treponeme Omp genes of the 69 T. phagedenis phylogroup isolates investigated during this study. T. phagedenis phylogroup isolate names are given in bold type, alongside the host from which they were isolated and their respective sequence type (ST) based upon a previous MLST study (Clegg et al. 2016d). The two designated Omp alleles are shown in blue. Bar, 0.0001 relative sequence disimilarity.*

Figure 5.9 Evidence of recombination between the putative treponeme Omp genes of 13 T. pedis isolates. *Split decomposition analysis was performed using SplitsTree4 software to determine whether recombination is predicted to have occurred between the putative treponeme Omp genes of the 13 T. pedis isolates investigated during this study. T. pedis isolate names are given in bold type, alongside the host from which they were isolated and their respective sequence type (ST) based upon a previous MLST study (Clegg et al. 2016d). The five designated Omp alleles are shown in blue. Bar, 0.001 relative sequence disimilarity.*

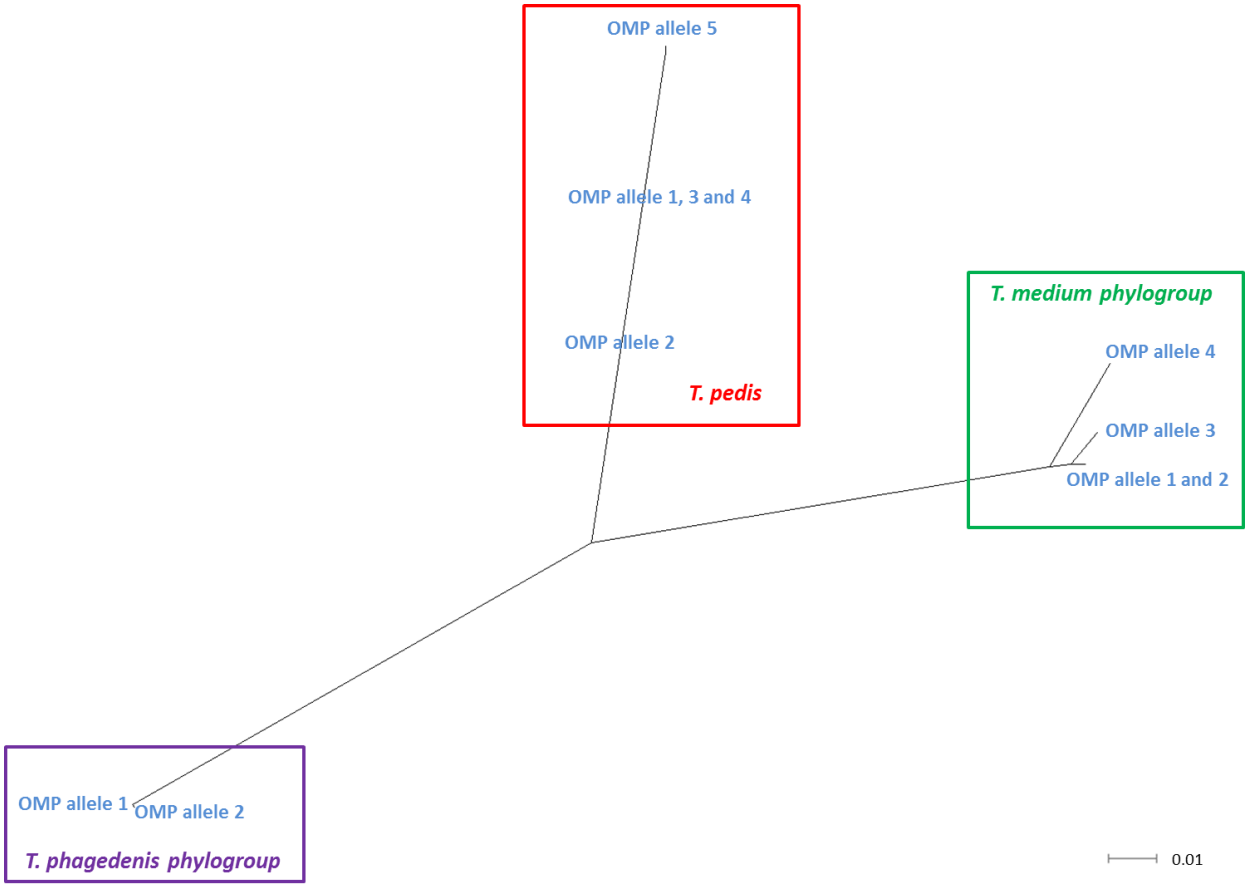

Figure 5.10 Evidence of recombination between the putative treponeme Omp genes of T. medium phylogroup, T. phagedenis phylogroup and T. pedis isolates. *Split decomposition analysis was performed using SplitsTree4 software to determine whether recombination is predicted to have occurred between the putative treponeme Omp genes of T. medium phylogroup (green), T. phagedenis phylogroup (purple) and T. pedis (red) isolates investigated during this study. Designated Omp alleles for each Treponema phylogroup are given in blue and correspond to treponeme isolates of Table C.1, C.2 and C.3 in Appendix C. Bar, 0.01 relative sequence disimilarity.*

5.2.4 Delineation of bovine digital dermatitis treponeme isolates based upon the molecular diversity of putative treponeme *Omp* gene homologs

Gene sequences of the three putative OMP homologs of *T. medium* phylogroup (Omp_34), *T. phagedenis* phylogroup (Omp_694) and *T. pedis* (Omp_2390) isolates were compared to corresponding MLST data (Clegg *et al.,* 2016d) to determine whether the observed OMP diversity enabled further delineation of these isolates. Phylogenies were inferred from concatenated gene sequence alignments of the seven housekeeping genes, with or without further addition of the putative *Omp* gene. Bootstrapped maximum-likelihood phylogenetic trees, based on 10,000 reiterations, were produced for *T. medium* phylogroup (Figure 5.11), *T. phagedenis* phylogroup (Figure C.1, Appendix C) and *T. pedis* (Figure C.2, Appendix C) isolates respectively. Minimum spanning trees were also produced to compare the relatedness amongst isolates of different STs and host species within the *T. medium* phylogroup (Figure 5.12A and 5.12B), *T. phagedenis* phylogroup (Figure 5.12C and 5.12D) and *T. pedis* (Figure 5.12E and 5.12F).

Interestingly, the EL022 F isolate from wild American elk formed a small cluster amongst other ST1 isolates of the *T. phagedenis* phylogroup based upon MLST data (Clegg *et al.,* 2016d; Figure C.1 and 5.12C). However, its possession of the human-specific d_N substitution at position 512 of the putative *Omp* gene sequence here meant its delineation as a distinct ST (ST36) within this phylogroup (Figure C.1 and 5.12D). Similarly, only a single *T. pedis* isolate, namely G3T1, was further delineated by the putative *Omp* gene and formed a novel ST, namely ST8 (Figure 5.12F). The phylogenetic groupings were not changed by the addition of the putative OMP to the MLST comparisons (Figure C.2, Appendix C). Notably, several STs were not altered by observed diversity within the putative *Omp* gene of *T. pedis* isolates due to being singletons.

Whilst little further delineation was achieved for isolates of the *T. phagedenis* phylogroup and *T. pedis,* several profound alterations were observed across isolates of the *T. medium* phylogroup when enrolling the putative *Omp* gene into the MLST scheme and analysis. The STs of nine isolates of the *T. medium* phylogroup were further delineated on the basis of putative *Omp* gene diversity (Figure 5.11). The dairy and sheep isolates, T200BA2, ST12 and ST27 respectively, clustered within a novel ST, designated ST12, within this new scheme. Whilst previously found to cluster within ST1 alongside other sheep isolates from the same farm (Farm C, Conwy, Wales; see Table C.1, Appendix C), isolate ST27 now clustered amongst isolates from different farms (Wales and England) based upon its differing gene sequence of the putative OMP. Four isolates of ST7 formed two novel STs, namely ST14 (EL022R and DD3F

(1)) and ST15 (T200BA1 and 2c). The elk and sheep isolates, EL023 aR and G2S2R respectively, were also each found to form a novel ST. Indeed, several of the *T. medium* phylogroup isolates able to be further delineated by the observed putative *Omp* gene diversity were of elk species and formed a distinct phylogenetic cluster; with the EL023 aR isolate now clustering independently of its previous isolate cluster (Figure 5.11B). Notably, such delineation of the elk isolates was not previously possible when using the seven housekeeping genes of the MLST study alone. Aside from the above-mentioned observations, further species or geographical delineations were not apparent.

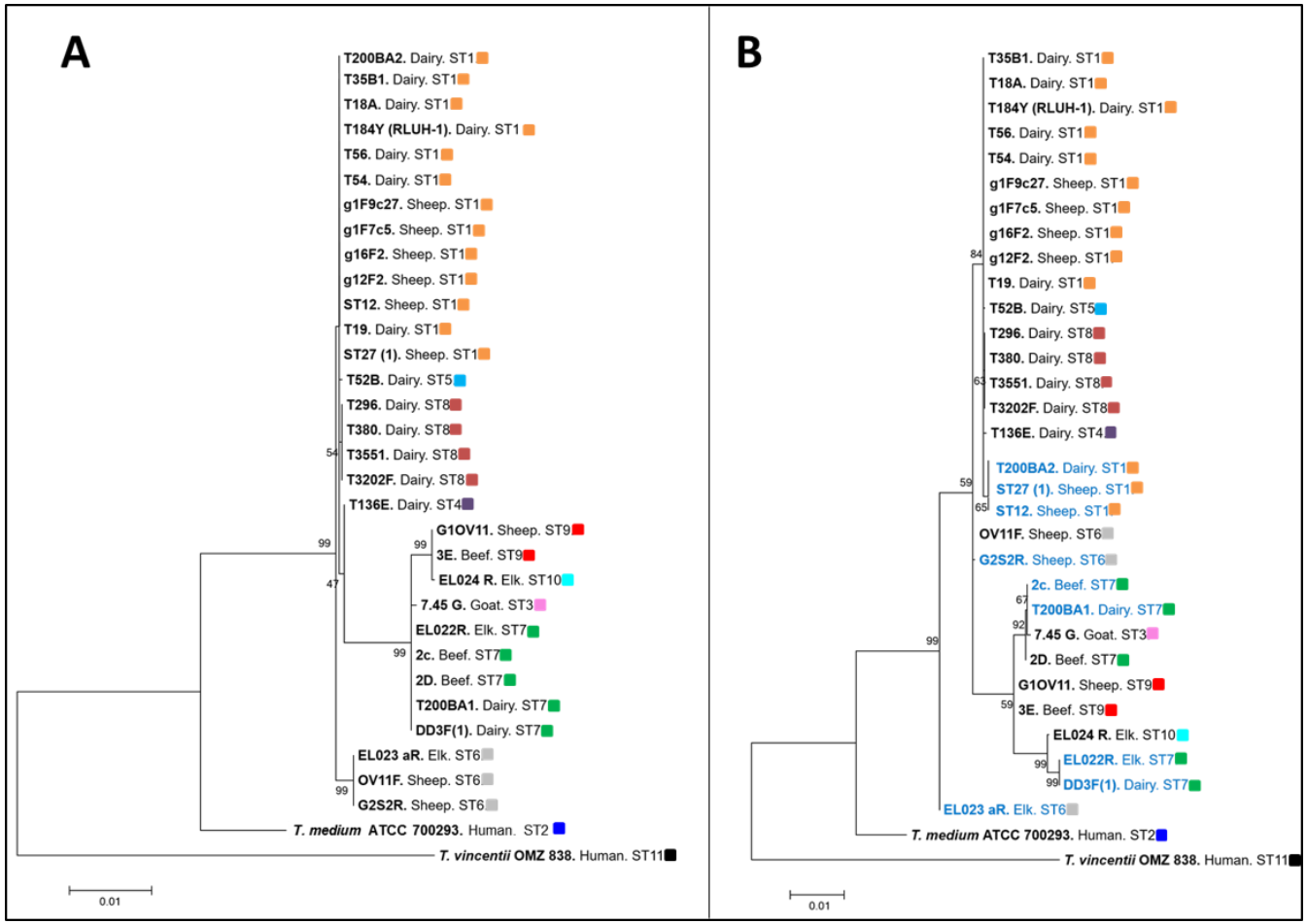

Figure 5.11 Delineation of T. medium phylogroup isolates based upon molecular diversity of the putative Omp gene. *Phylogenetic tree of maximum-likelihood comparing concatenated gene sequences of (A) seven housekeeping genes alone (data from Clegg et al., 2016d) with (B) further addition of the putative treponeme Omp gene homolog (identified during this study) across 3215 and 3719 aligned bases, respectively, for 33 T. medium phylogroup isolates, to determine if molecular diversity of the putative Omp gene homolog enabled further isolate delineation. T. medium phylogroup isolate names are given in bold type, alongside the host from which they were isolated and their respective sequence type (ST; colour-coded blocks) based upon a previous MLST study (Clegg et al. 2016d). Treponeme isolates with an altered relationship based upon the addition of putative Omp_34 are in blue. Bootstrap confidence intervals, based on 10,000 reiterations, are shown as percentages at the nodes. Bar, 0.01 nucleotide substitutions per site.*

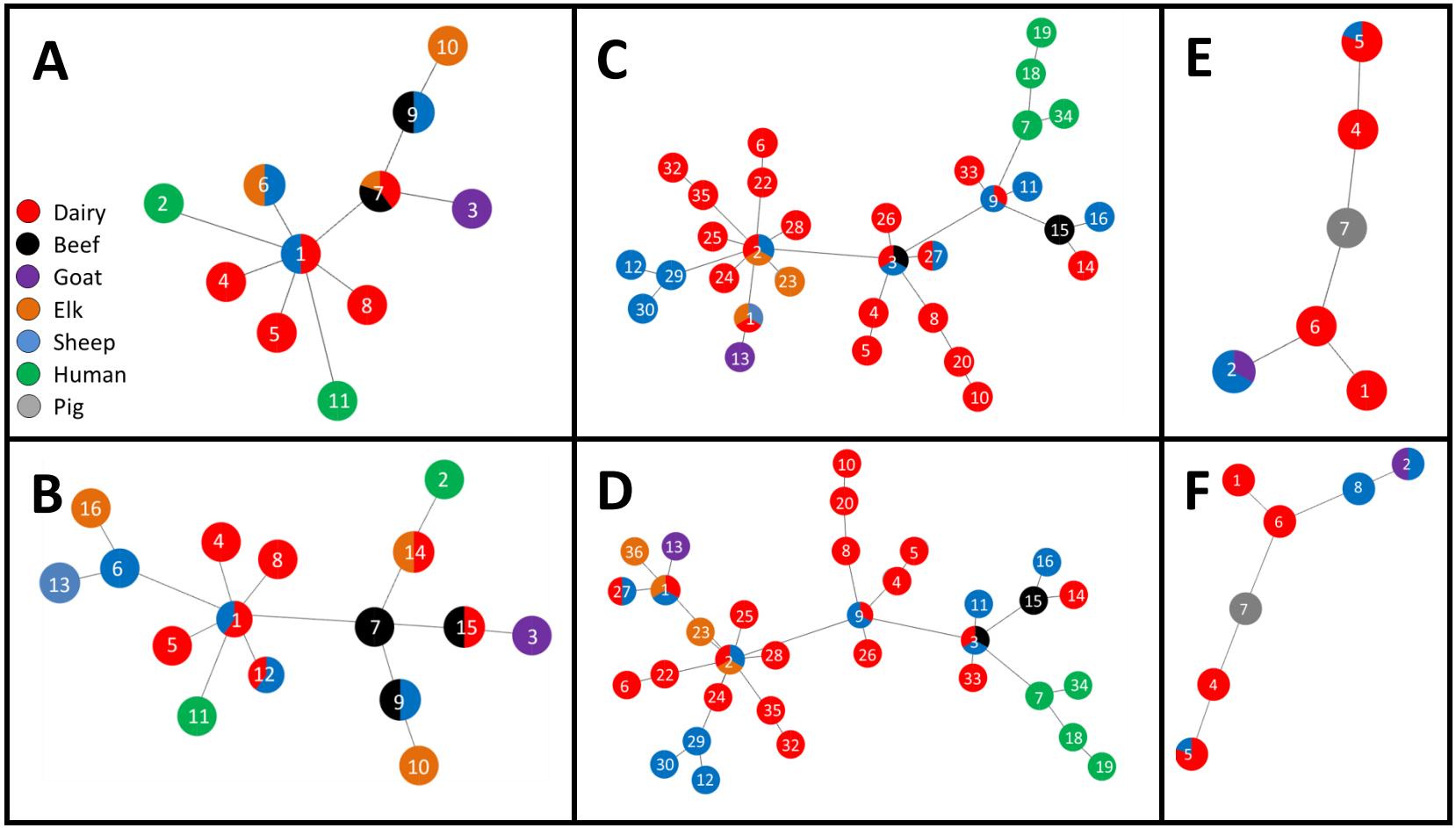

Figure 5.12 Delineation of T. medium phylogroup isolate sequence types based upon molecular diversity of the putative Omp gene using minimum spanning distance trees. *Minimum spanning distance trees comparing sequence type (ST) designations of (A, B) 33 T. medium phylogroup, (C, D) 69 T. phagedenis phylogroup and (E, F) 13 T. pedis isolates across seven housekeeping genes (A, C, E) excluding and (B, D, F) including the putative Omp gene alleles. Each node illustrates the proportion of sequences within a sequence type (as given by the numbers; see Appendix C; Table C.1, C.2 and C.3) which were isolated from each host species.*

5.2.5 Investigating the diversity of putative outer membrane protein homologs within recognised commensal and pathogenic treponemes

A recent proteomics experiment carried out at the University of Liverpool on BDD (*T. medium* phylogroup strain T19, *T. phagedenis* phylogroup strain T320A, *T. pedis* strain T3552B^T), human periodontal (*T. phagedenis* strain Reiter and *T. medium* strain ATCC 700293) and bovine commensal (*T. ruminis* strain Ru1^T and *T. rectale* strain CHPA^T) treponeme isolates identified the putative OMP of *T. medium* and *T. phagedenis* phylogroup to be expressed within the membrane-associated and total fractions and total fractions only, respectively (Dr Stuart Armstrong, University of Liverpool; personal communication).

Following investigation of the gene and protein sequence diversity of this putative OMP across the three predominant BDD treponemes, it was considered timely to investigate the protein diversity of this OMP across other pathogenic and commensal treponemes. Accordingly, amino acid sequences of the putative OMP homologs, Omp_34 (*T. medium* phylogroup), Omp_694 (*T. phagedenis* phylogroup) and Omp_2390 (*T. pedis*), were compared over 154 aligned residues to homologous proteins of other recognised pathogenic and commensal treponemes (Chapter 2.8.12). A summary of amino acid sequence identities between the putative OMPs of the three BDD treponemes and those of homologous proteins within other recognised *Treponema* isolates are provided in Table C.4, Appendix C. Whilst Omp_34 and Omp_694 shared highest sequence similarity with the human periodontal pathogens, *T. medium* (96.2%) and *T. phagedenis* (100.0%) respectively, Omp_2390 was most similar to the pig isolate, *T. pedis* T A4 (100.0%). Interestingly, putative OMPs of the three BDD treponemes shared, on average, 33.0% sequence similarity with bovine GI tract commensals, *T. ruminis* strain Ru1^T and *T. rectale* strain CHPA^T.

Phylogeny was inferred from this amino acid sequence alignment using the cpREV model (Adachi *et al.,* 2000), as the predicted best-fit evolutionary model, to produce a bootstrapped maximum-likelihood phylogenetic tree, based upon 10,000 reiterations (Figure 5.13). Interestingly, phylogenetic inference identified two distinct, deep-rooted clusters which largely appeared to distinguish the pathogenic treponeme isolates (namely designated the "pathogenic cluster") from those of the commensal treponemes ("commensal cluster"). The *T. medium* phylogroup (Omp_34), *T. phagedenis* phylogroup (Omp_694) and *T. pedis* (Omp_2390) putative OMPs were found to form distinct groupings within the "pathogenic cluster" alongside homologous proteins of human periodontal treponemes; *T. medium and T. vincentii, T. phagedenis* and *T. denticola and T. putidum* respectively. Protein homologs of both *T. pallidum* and *T. paraluiscuniculi* formed a distinct grouping within this "pathogenic

cluster." All of the recognised commensal treponemes with identified protein homologs to the putative OMPs of the BDD treponemes clustered within the so-called "commensal cluster." The termite GI tract treponemes clustered distinctly from the porcine and bovine GI tract treponemes. Interestingly, several periodontal pathogens such as *T. socranskii* and *T. maltophilum and T. lecithinolyticum* were in this largely commensal-containing cluster.

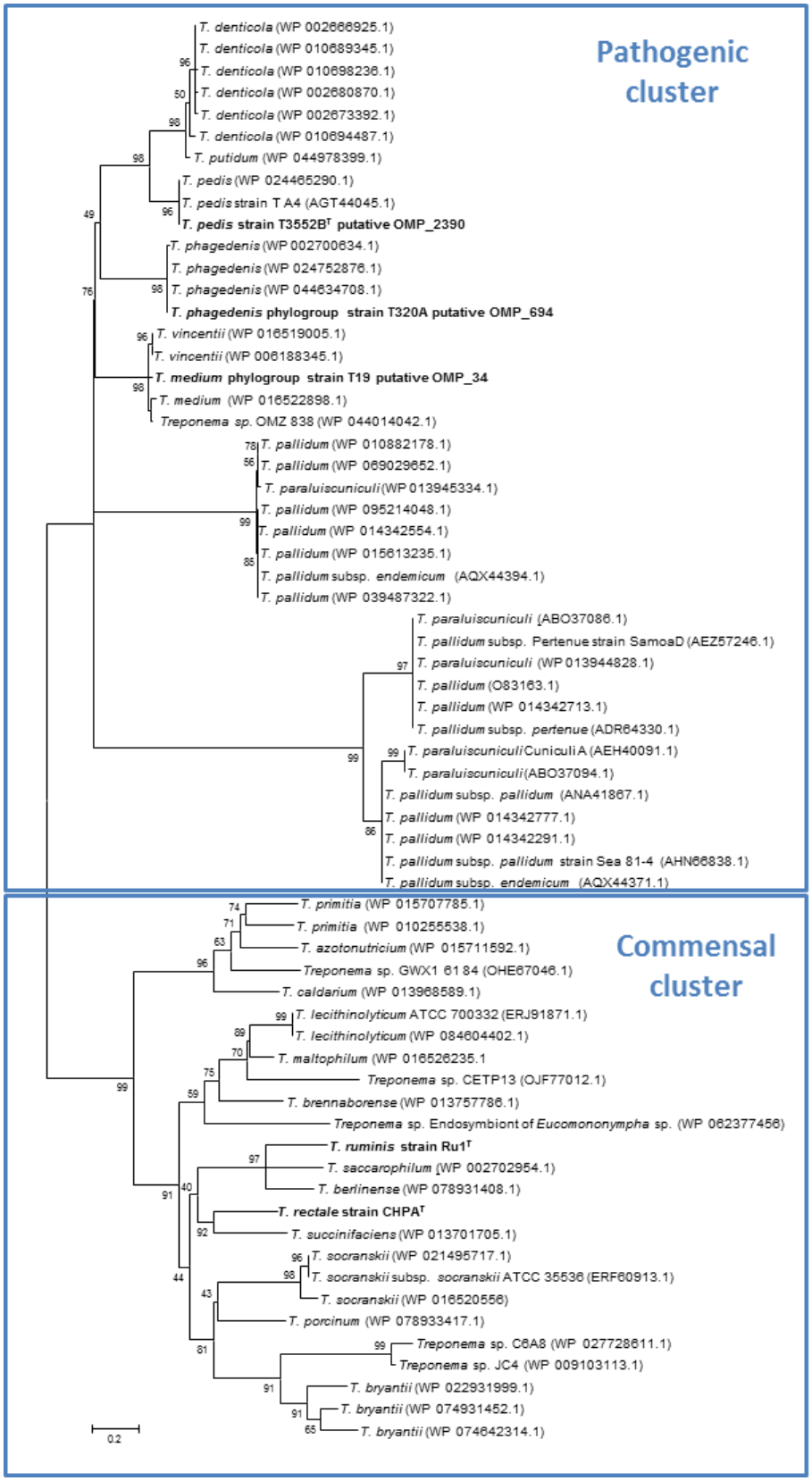

Figure 5.13 Phylogenetic tree of maximum-likelihood illustrating relatedness between the putative treponeme Omp gene homologs of BDD treponemes and those of homologous proteins within other pathogenic and non-pathogenic treponeme isolates. *Phylogenetic tree of maximum-likelihood illustrating amino acid sequence comparisons, over 154 aligned residues, of the putative outer membrane protein homologs of T. medium phylogroup strain*

T19, T. phagedenis phylogroup strain T320A and T. pedis strain T3552B^T with those of homologous proteins within other pathogenic and non-pathogenic (commensal) treponeme isolates. Phylogeny was inferred from the trimmed sequence alignment using the General Reversible Chloroplast (cpREV) model. Bootstrap confidence intervals, based on 10,000 reiterations, are shown as percentages at the nodes; values below 40% were removed for clarity. Accession numbers are given in parentheses next to each strain. Bar, 0.2 amino acid substitutions per site.

5.3 Discussion

A number of treponemes have now been isolated from BDD lesions of dairy and beef cattle, CODD in sheep, hoof lesions of wild American elk and UK goats and skin lesions on a range of domestic production animals (Clegg *et al.,* 2015; Clegg *et al.,* 2016a, 2016b, 2016c, 2016e; Evans *et al.,* 2008; Groenevelt *et al.,* 2015; Harwood *et al.,* 1997; Sullivan *et al.,* 2015a). Several *Treponema* species have also been implicated in the pathogenesis of human periodontal disease and syphilis (Dewhirst *et al.,* 2000; Engelkens *et al.,* 1991; Radolf *et al.,* 2006). BDD treponemes have been found to exist as multiple antigenic serotypes or variant strains and although those of the representative strains, *T. medium* phylogroup strain T19, *T. phagedenis* phylogroup strain T320A and *T. pedis* strain T3552B^T, are generally well studied, those of other isolates have been poorly characterised to-date (Evans *et al.,* 2008; Evans *et al.,* 2009b). A recent MLST study attempted to delineate the diversity amongst isolates of the *T. medium* phylogroup, *T. phagedenis* phylogroup and *T. pedis* on the basis of seven housekeeping genes (Clegg *et al.,* 2016d). However, the molecular diversity of important, potentially antigenic OMPs, both within and amongst these three BDD treponeme phylogroups, have yet to be investigated. This study has successfully identified a novel putative OMP of BDD treponemes and has subsequently elucidated both its intra-phylogroup and inter-phylogroup molecular diversity at both a nucleotide and amino acid level.

5.3.1 BDD treponeme outer membrane protein is homologous to other Gram-negative bacterial outer membrane proteins

The chosen putative OMP was predicted to consist of eight anti-parallel β-strands, four extracellular loops and four short periplasmic turns; its recent identification within the membrane-associated fraction of *T.* medium phylogroup (and total fraction of *T. phagedenis* phylogroup) by proteomics (Chapter 5.2.5) lends further support to this OMP-like topology. Based upon its predicted structure and protein domains, the novel OMP was found to demonstrate most significant homology to previously characterised OMP domains of *E. coli*

(OmpA and OmpW), an outer membrane porin (OprF) of *P. aeruginosa* and a surface protein (NspA) of *N. meningitidis*; each possessing a similar eight-stranded anti-parallel β-barrel structure (Brinkman *et al.,* 2000; Hong *et al.,* 2006; Pautsch & Schulz, 1998; Straatsma & Soares, 2008; Vandeputte-Rutten *et al.,* 2003). Notably, OmpA of *E. coli* is a comparatively larger protein; with an amino acid sequence of 417 residues (Pautsch & Schulz, 1998) compared to that of the treponemal OMP identified here (< 205 residues). Interestingly, the *T. pallidum* OMP, tpn50*,* is also known to have significant amino acid sequence homology, although notably much higher, to *E. coli* OmpA (43.2%) and to the OprF of *Pseudomonas* sp. (47.4%) (Hardham & Stamm, 1994), which may suggest similar functionality between these treponemal OMPs.

Many of these OMPs, which are homologous to the novel treponeme OMP described here, have been well-characterised and are known to perform a variety of functions. Unlike larger 12 to 22 β-stranded OMPs which typically span the outer membrane of Gram-negative bacteria to facilitate the essential transport of nutrients or secreted proteins, smaller eight to ten-stranded anti-parallel β-barrel OMPs are often considered to have more predominant roles in stabilising bacterial outer membranes (OmpA), host cell adhesion (NspA) and disease pathogenesis through, for example, resistance to phagocytosis (OmpW) (Manning *et al.,* 1977; Vandeputte-Rutten *et al.,* 2003; Weiser & Gotschlich, 1991; Wu *et al.,* 2013). Several treponeme OMPs have previously been identified; such as the 16-stranded OMP associated with OMP biogenesis*,* Tp0326 (Desrosiers *et al.,* 2011; Luthra *et al.,* 2015), and the eight-stranded putative OmpW-like porin, Tp0126 (Giacani *et al.,* 2015), each of *T. pallidum*. The novel OMP identified as part of this study appears to possess structural and protein domain homology to these smaller OMP families and may therefore share similar functions, however further work is now required to characterise this novel OMP.

Whilst the novel OMP of BDD treponemes demonstrated homology to OmpW of *E. coli*, a small OMP thought to function as a hydrophobic channel (Hong *et al.,* 2006), it was found to lack key structural motifs of this unusual small OMP family. The novel OMP lacked the specific leucine and tryptophan residues of position 56 and 155, respectively, thought to form the "hydrophobic gate" (Hong *et al.,* 2006), suggesting that the novel OMP identified here may not function in a similar manner. Interestingly, another of its homologs, NspA, is known to have significant homology to the adhesive opacity (Opa) proteins of *Neisseria* sp. (Martin *et al.,* 1997), which mediate entry into host epithelial cells (Chen & Gotschlich, 1996). A similar function may therefore be plausible for the novel OMP in mediating BDD treponemal entry into bovine foot skin tissue. The novel OMP was consistently most similar to OmpA of *E. coli.*

OmpA is known to be well conserved across Gram-negative bacteria, typically sharing 60 to 70% similarity (Beher *et al.,* 1980; Pautsch & Schulz, 1998). With OmpA-like homologs of *T. pallidum* (such as *tpn50* and Tp0624) already recognised (Hardham & Stamm, 1994; Parker *et al.,* 2016), this novel OMP may represent a similar OmpA homolog of BDD treponemes.

5.3.2 Novel outer membrane protein highly conserved within bovine digital dermatitis treponeme phylogroups with some inter-phylogroup diversity

Whilst the novel OMP demonstrated high intra-phylogroup homology (98.27%, 99.27% and 98.6% gene sequence identity for *T. medium* phylogroup, *T. phagedenis* phylogroup and *T. pedis* respectively), there was considerably more diversity observed between isolates of the three BDD *Treponema* phylogroups; with an average nucleotide and amino acid sequence identity of 58.5% and 49.1% respectively. Notably, this lack of molecular diversity generally extended across treponeme isolates of distinct species, geographical locations and STs (as designated based upon housekeeping gene diversity), which may be somewhat surprising; particular as OMPs are often in direct contact with host cells and the external environment. This lack of diversity does suggest it may have an important function within the outer membrane of these BDD treponemes and also is unlikely to be involved in the antigenic variation observed by other treponemal OMPs (Centurion-Lara *et al.,* 2000a).

Notably, this study elucidated molecular diversity of the novel putative treponeme OMP across just three representative BDD treponeme phylogroups and, whilst these are predominantly found within BDD lesions in the UK, there are five currently reported in Germany (Choi *et al.,* 1997). Furthermore, whilst the treponeme isolates chosen for this study were based on those available within our comprehensive strain collection, matching those examined by MLST by Clegg *et al.* (2016d) to enable later comparison for isolate delineation purposes, both *T. medium* phylogroup (n = 33) and particularly *T. pedis* (n = 13) were found to lack available strains for comparablility. This was notably one of the greater limitations of this study and with further time, expense and resources would be a welcome addition to the experimental design.

Previous studies investigating the molecular diversity of BDD treponemes based upon housekeeping gene sequence comparisons identified similar intra-phylogroup and inter-phylogroup trends. Whilst demonstrating complete or near-complete homology of 16S rRNA gene sequences from isolates within the *T. medium* phylogroup (100.0%), *T. phagedenis* phylogroup (99.9%) or *T. pedis* (99.7%) respectively, the sequence homology amongst these phylogroups was notably lower (90.1 to 92.3% identity) (Evans *et al.,* 2008). Similarly, Clegg

et al. (2016d) identified little intra-phylogroup or inter-phylogroup diversity amongst seven housekeeping genes by MLST.

Whilst it may be expected that such housekeeping genes are highly conserved between related treponemes, this study is the first to report strong intra-phylogroup homology of an OMP of BDD treponemes. A previous study of the OmpW-like protein, Tp0126, similarly found high conservation across subspecies of *T. pallidum* (Giacani *et al.,* 2015). Furthermore, the *T. pallidum* metalloprotease, pallilysin, and its associated protein, Tp0750, were each found to be highly conserved across several pathogenic *Treponema* species, with a single amino acid difference and no difference, respectively, in the orthologous sequences of two *T. phagedenis* spirochaetes across human and bovine species (Houston *et al.,* 2015). However, a notable exception to this are several highly heterologous members of the *T. pallidum* OMP family, Tpr; including TprK, which has seven variable sites and nearly all strains are known to have multiple allelic variants (Centurion-Lara *et al.,* 2000a; Centurion-Lara *et al.,* 2000b; Centurion-Lara *et al.,* 2004; Sun *et al.,* 2004). There are currently very few studies describing within-species variation of treponemal OMPs and further studies are therefore warranted to assess this further.

Interestingly, the novel OMP demonstrated some molecular diversity between the three BDD phylogroups, however was still fairly well-conserved. Jun *et al.* (2008) previously identified similar levels of homology (41.6 to 71.6% identity) between the OMP, Tp92, of oral treponemes such as *T. denticola, T. lecithinolyticum, T. socranskii* subsp. *socranskii* and *T. maltophilum.* Notably, Clegg *et al.* (2016d) found much greater sequence diversity amongst housekeeping gene loci of the *T. medium* phylogroup than those of the *T. phagedenis* phylogroup or *T. pedis;* the same was found to be true of the novel OMP investigated here. Whilst the reasons for this are currently unknown, it should be noted that isolates of the *T. medium* phylogroup have distinct growth requirements to those largely shared by *T. phagedenis* phylogroup and *T. pedis* isolates.

Notably, it was the human periodontal pathogen, *T. vincentii,* which demonstrated most *Omp* gene sequence diversity by comparison to other isolates of the *T. medium* phylogroup; a finding which has also been emulated by a comparison of housekeeping genes using MLST (Clegg *et al.,* 2016d). This finding may be somewhat unsurprising as a recent MLST study proposed the human oral spirochaete, *T. vincentii,* to be a novel species to that of *T. medium* (Huo *et al.,* 2017).

5.3.3 Bovine digital dermatitis treponeme outer membrane protein sequences diverge markedly from those of commensal treponemes

One of the most notable findings from this study was that the OMP sequences of many pathogenic treponemes (such as those associated with DD, human periodontal disease and syphilis) were found to be markedly different to those of commensal treponemes of the GI tract. Interestingly, previous phylogenetic studies have identified a similar divergence between pathogenic BDD and commensal treponemes based upon 16S rRNA gene sequence comparisons (Evans *et al.,* 2011b). Furthermore, Parker *et al.* (2016) recently identified this similar distinct evolutionary split between the pathogenic and non-pathogenic treponemes for the *T. pallidum* OMP, Tp0624. Parker *et al.* (2016) concluded that it was the presence of its three domains, collectively, which formed this evolutionary split from non-pathogenic treponemes, themselves lacking the D3 domain, and therefore correlates with pathogenesis. Further work would now be required to determine whether these novel OMP homologs of BDD treponemes behave in a similar manner; the greater homology observed amongst other pathogenic treponemes may suggest a shared role in disease pathogenesis. Such differences may also reflect the distinct host niches of commensal (GI tract) and pathogenic (bovine foot tissues, oral tissues, venereal tissues) treponemes, however the close clustering of pathogenic treponemes of distinct host niches suggests this may not have a major role.

5.3.4 Molecular diversity of the novel outer membrane protein demonstrates some species specificity

Interestingly, the molecular diversity of this novel OMP amongst treponeme isolates of all three BDD phylogroups demonstrated considerable host species specificity. The novel OMP successfully delineated *T. phagedenis* phylogroup isolates of man from those of production animals, with the further allelic variant of a wild American elk isolate suggestive of possible treponemal transmission between man and wild elk in the USA. Unfortunately, the sample sizes of isolates of both human and wild American elk species were limited in this study. Further investigations would be required to determine the true extent of diversity across a larger population and elucidate whether this amino acid substitution confers functional significance in disease pathogenesis of man. Similarly, diversity of the novel OMP largely delineated elk isolates of the *T. medium* phylogroup, which is something not possible on the basis of housekeeping gene diversity (Clegg *et al.,* 2016d). Notably, even isolates from the same farm, previous categorised as the same ST based upon housekeeping gene diversity, were found to have variations in their *Omp* gene sequences. Although this may be suggestive of specific selection pressures from the host, none were detected to be significant as part of

this study. Indeed, the non-significant purifying selection pressures of *T. medium* and *T. pedis* were found to occur within the transmembrane domains of the β-barrel structure, which is unsurprising.

A particularly interesting finding from this study was that the molecular diversity of this novel OMP across *T. medium* phylogroup spirochaetes was almost exclusively found within the central region of the amino acid sequence. Interestingly, when investigating the molecular diversity of Msp (the porin-like virulence factor of *T. denticola)* obtained from 17 clinical periodontal samples, Giabani *et al.* (2010) also identified profound diversity within central regions of the gene and amino acid sequences. These differences were only identified within particular strains of *T. denticola* (Giabani *et al.,* 2010) and may also explain why such patterns of molecular diversity were not seen within other BDD treponeme phylogroups here. Such molecular diversity was predicted to lead to antigenic modifications of the surface-exposed portion and may account for differences in pathogenicity, invasiveness and persistence within host tissues between different strains.

The relative lack of molecular diversity observed both within and between BDD treponeme phylogroups may indeed correlate to the presence of homopolymeric tracts within the coding region of this locus for each of these phylogroups. Homopolymeric DNA tracts are typically a repetitive sequence of identical consecutive nucleotides which result in incomplete DNA replication due to "replication slippage" by a DNA polymerase. Such tracts are typically between seven and ten nucleotides in length (Dechering *et al.,* 1998; Zhou *et al.,* 2004). Treponemes and other spirochaetes are known to contract or expand homopolymeric tracts which resultantly, through change in reading frame, may turn the expression of the encoded proteins "phase off" and therefore alter the expression of antigens on their surface as a mechanism of pathogenesis (Gogol *et al.,* 2007). Such mechanisms may explain this lack of diversity and further investigations are now required.

5.3.5 The well-conserved treponemal outer membrane protein may be a useful vaccine candidate

The novel, highly conserved OMP identified as part of this study is likely to have an important role within the outer membrane of BDD treponemes and its high conservation particularly across other pathogenic treponemes suggests an important role in disease pathogenesis. Such well-conserved OMPs are often prime targets for vaccine development and many homologs of this novel treponemal OMP, including OmpW and NspA, have been proposed as candidates recently (Li *et al.,* 2016; Vandeputte-Rutten *et al.,* 2003). This novel treponemal

OMP may be a useful candidate for vaccine and therapeutic development against BDD, however further work is required to determine its use in such a capacity.

5.3.6 Conclusions

The present study has identified a novel treponemal OMP which is structurally homologous to the small OMPs of other Gram-negative bacteria. This novel OMP demonstrated very little molecular diversity within BDD isolates of the *T. medium* phylogroup, *T. phagedenis* phylogroup and *T. pedis,* with only a small amount of diversity observed between these phylogroups. A notable difference was observed in the OMP sequence diversity between pathogenic and commensal treponemes. In combination, this highly conserved treponemal OMP may be a potentially valuable candidate as a target for future therapeutic intervention and vaccine development against BDD. Further studies are now warranted to elucidate its functional importance in *Treponema* species and, particularly, to identify whether it has a significant role in mediating the host-pathogen interactions of BDD infection.

Chapter Six: Taxonomic characterisation of a spirochaete isolated from the bovine rumen

6.1 Introduction

Species of the genus *Treponema* are fastidious, highly motile, Gram-negative, anaerobic microorganisms of the phylum Spirochaetes which have been identified within the GI tract, oral cavity and genital areas of humans, animals and insects (Smibert, 1984). Some treponemes are highly associated with infectious diseases, including DD, human periodontal disease, yaws, pinta and syphilis (Choi *et al.,* 1997; Dewhirst *et al.,* 2000; Engelkens *et al.,* 1991; Mitjà *et al.,* 2013; Radolf *et al.,* 2006). In contrast, several treponeme taxa are considered commensal symbionts living within the GI tract of animals and insects (Graber *et al.,* 2004; Nordhoff *et al.,* 2005; Paster & Canale-Parola, 1985). Currently, the nature of this symbiotic relationship and their functional importance within the GI tract have yet to be elucidated. Pathogenic and commensal treponemes do appear to possess distinct genotypic and phenotypic characteristics (Evans *et al.,* 2011b) and therefore further taxonomic appraisals may inform their functional importance and characteristics conferring pathogenicity.

The successful isolation, purification and subculture of *Treponema* species has proven notoriously difficult, likely due to their highly fastidious nature, and only a handful of GI treponemes have been characterized to-date (Cwyk & Canale-Parola, 1979; Dröge *et al.,* 2008; Graber *et al.,* 2004; Nordhoff *et al.,* 2005; Paster & Canale-Parola, 1985; Stanton & Canale-Parola, 1980). Metagenomic studies focusing on sequencing of the *16S rRNA* gene, amongst others, have identified a diverse variety of spirochaetes within the bovine rumen (Edwards *et al.,* 2004; Paster & Canale-Parola, 1982; Tajima *et al.,* 1999; Zinicola *et al.,* 2015a). Although several spirochaetes have been successfully isolated from the bovine rumen (Evans *et al.,* 2011b; Ziolecki, 1979; Ziolecki & Wojciechowicz, 1980) there are currently only two that have been formally proposed as novel treponeme taxa, namely *Treponema bryantii* and *Treponema saccharophilum* (Paster & Canale-Parola, 1985; Stanton & Canale-Parola, 1980). Further work is required to understand the true extent in diversity of treponemes within the bovine GI tract.

Previously, Evans *et al.* (2011b) attempted to isolate and characterize spirochaetes from the GI tract of Holstein-Friesian cattle in the UK for comparison with BDD treponemes. Isolates were obtained from regions of the bovine rumen (strain Ru1 and Ru2), omasum (strain OC1),

abomasum (strain AC3), colon (strain CC2) and rectum (strain CHPA and Re1) which, based upon 16S rRNA gene sequence comparisons, were found to cluster into four novel phylotypes within the genus *Treponema* (Evans *et al.,* 2011b). Phylotype 1 (OC1, CC2, Re1 and Ru2), phylotype 2 (CHPA), phylotype 3 (AC3) and phylotype 4 (Ru1) each demonstrated distinct genotypic diversity and shared less than 97% *16S rRNA* gene sequence identity to extant species of the genus *Treponema,* suggesting these isolates represent novel taxa (Evans *et al.,* 2011b; Stackebrandt & Goebel, 1994). However, comprehensive taxonomic appraisals are required to elucidate whether these GI isolates are indeed novel species within the genus *Treponema.*

The taxonomic characterisation of microbial populations is fundamental for understanding host-pathogen interactions, disease pathogenesis and transmission and for identifying novel targets for vaccine development and therapeutics (Emerson *et al.,* 2008). Bacterial characterisation typically involves a biphasic approach with both genotypic and phenotypic appraisal. Whilst genotypic characterisation typically involves comparing phylogenetic relatedness within a bacterial genus using conserved housekeeping genes (16S rRNA being most common), phenotypic characterisation often involves a combined appraisal of morphological and biochemical characteristics (Evans *et al.,* 2009b; Cwyk & Canale-Parola, 1979). Interestingly, spirochaetes are one of few bacterial families whose phylogenetic relationships reflect their observed phenotypic characteristics (Paster *et al.,* 1984).

The aim of this study was to further taxonomically characterise a novel spirochaete isolated from the rumen contents of a Holstein-Friesian bull in the UK, represented by strain Ru1 (Evans *et al.,* 2011b; Chapter 2.3.2). Characterisation of a novel bovine GI tract treponeme, as described here, may provide new insights into the functional roles of such commensal symbionts and will constitute an important control organism for future host-pathogen interaction studies in elucidating key mechanisms of treponeme pathogenesis.

The primary objectives of this chapter are:

1) To develop and optimise a novel degenerate PCR assay for detection of the *recA* gene and subsequently perform phylogenetic analyses to compare *16S rRNA* and *recA* gene sequences of the novel isolate to other validly named, taxonomically designated *Treponema* species for its genotypic characterisation.
2) To phenotypically characterise the novel treponeme isolate through collating phenotypic data on its enzyme activity profile, morphology and growth requirements and comparing to other validly named, taxonomically designated *Treponema* species.

6.2 Results

The novel spirochaete isolate, represented by strain Ru1, underwent genotypic and phenotypic analysis, including a comparison with all recognised *Treponema* species, for its taxonomic appraisal. Phenotypic characterisation included an assessment of growth characteristics, observations of bacterial morphology (Chapter 2.4.7) and enzyme activity profiling (Chapter 2.4.8), whereas genotypic characterisation was based upon the use of *16S rRNA* (Chapter 2.4.2) and *recA* (Chapter 2.4.4) gene sequence comparisons to determine its degree of similarity and phylogenetic relatedness to other recognised treponemes (Chapter 2.4.6).

6.2.1 Growth characteristics

The novel spirochaete was initially isolated in OTEB supplemented with 25 µg/ml rifampicin, 5 µg/ml enrofloxacin and either 10% (v/v) FBS, 10% (v/v) RS or no serum according to Chapter 2.3.2. The isolate initially reached late exponential growth phase after two to three days in culture at 36°C under anaerobic conditions (85% N_2, 10% H_2, 5% CO_2) and was found to demonstrate equivalent growth with or without serum supplementation. The spirochaete was found to sediment at the bottom of the culture tube. The novel spirochaete isolate was subsequently purified through subculture onto FAA plates supplemented with 25 µg/ml rifampicin, 5 µg/ml enrofloxacin, with or without 5% (v/v) defibrinated sheep blood and either 10% (v/v) FBS, 10% (v/v) RS or no serum. Single-spirochaete colonies were obtained following two successive rounds of subculture onto FAA plates and colonies were found to reach optimal growth after ten days at 36°C under anaerobic conditions. The isolate demonstrated equivalent colony growth with or without serum supplementation and the addition of defibrinated sheep blood did not enhance colony growth or size. In conclusion, the novel spirochaete isolate did not require serum for growth and was therefore considered to be serum independent. Upon initial isolation, the single-spirochaete colonies were thereafter routinely subcultured in OTEB without serum or antibiotic supplementation and were found to reach optimal growth after one day in liquid culture. The isolate was successfully stored (-80°C) in growth medium containing 10% (v/v) glycerol according to Chapter 2.3.4.

The novel spirochaete isolate was found to have a distinct colony morphology. Circular, translucent, convex and punctiform colonies with a diameter of between 0.2-0.5 mm were observed on unsupplemented FAA plates after ten days of growth. The colonies did not exhibit a metallic sheen or local haemolysis.

6.2.2 Bacterial cell morphology and motility

Morphological characteristics of the novel spirochaete isolate were observed, identified and analysed by TEM, according to Chapter 2.4.7. The novel isolate was found to be a very small-sized, helically coiled spirochaete which was approximately 5-9 µm in length, 0.4-0.5 µm in width and typically had between three to five regular coils (Figure 6.1). Each cell possessed eight periplasmic flagella; four originating at each end and overlapping in the centre of the cell in a 4:8:4 arrangement (Figure 6.1).

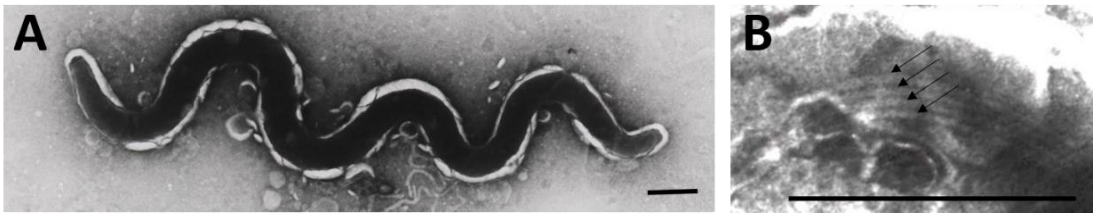

Figure 6.1 Electron micrograph of negatively stained cells of the novel spirochaete isolate represented by strain Ru1 for assessment of its morphological characteristics. *Transmission electron microscopy was used to assess morphological characteristics of the novel spirochaete isolate of the bovine rumen, represented by strain Ru1. The novel spirochaete isolate was found to have (A) eight periplasmic flagella, (B) with four originating at each end (arrows) and overlapping in the centre of the cell in a 4:8:4 arrangement. Bar, 0.5µm.*

The cells were found to exhibit rotational and translational movement, jerky flexing and high motility by phase contrast microscopy.

6.2.3 Enzyme activity profiling

The novel spirochaete isolate underwent enzyme activity profiling using the API® ZYM system, according to Chapter 2.4.8. The novel spirochaete isolate was found to exhibit C8 esterase lipase, leucine arylamidase, β-galactosidase and β-glucosidase activity. Furthermore, the API® ZYM system identified that the isolate did not possess enzyme activity for alkaline phosphatase, C4 esterase, C14 lipase, valine arylamidase, cysteine arylamidase, trypsin, chymotrypsin, acid phosphatase, naphthol-AS-BI-phosphohydrolase, α-galactosidase, β-glucuronidase, α-glucosidase, N-acetyl-β-glucosaminidase, α-mannosidase and α-fucosidase. The enzyme activity profile of the novel spirochaete isolate was subsequently compared to profiles available for all other recognised *Treponema* species, as shown in Table 6.1. The novel isolate was found to exhibit a unique API® ZYM enzyme activity profile which was dissimilar to those previously reported for other recognised treponemes.

Table 6.1. Comparison of the enzyme activity profiles of the novel spirochaete isolate and those available for all other recognised Treponema species as determined by the API® ZYM system. *The novel spirochaete isolate of the bovine rumen, represented by strain Ru1, was analysed by API® ZYM and the resulting enzyme activity profile was compared to those available for all other recognised Treponema species. Profiling was performed in triplicate as three independent experiments. The enzyme activity profile of Treponema vincentii ATCC 35580 (Schrank et al., 1999) was assessed alongside the novel isolate for test validation. Enzymes tested: 1, alkaline phosphatase; 2, C4 esterase; 3, C8 esterase lipase; 4, C14 lipase; 5, leucine arylamidase; 6, valine arylamidase; 7, cysteine arylamidase; 8, trypsin; 9, chymotrypsin; 10, acid phosphatase; 11, naphthol-AS-BI-phosphohydrolase; 12, α-galactosidase; 13, β-galactosidase; 14, β-glucuronidase; 15, α-glucosidase; 16, β-glucosidase; 17, N-acetyl-β-glucosaminidase; 18, α- mannosidase; 19, α-fucosidase. +, positive; -, negative.*

***Treponema* species**	**Presence of enzyme activity**																		
	1	**2**	**3**	**4**	**5**	**6**	**7**	**8**	**9**	**10**	**11**	**12**	**13**	**14**	**15**	**16**	**17**	**18**	**19**
Treponema spp. strain Ru1[‡]	-	-	+	-	+	-	-	-	-	-	-	-	+	-	-	+	-	-	-
Treponema porcinum ATCC BAA-908[T†]	-	+	-	-	-	-	-	-	-	+	+	-	-	-	+	-	-	-	-
Treponema berlinense ATCC BAA-909[T†]	-	-	-	-	-	-	-	-	-	+	+	-	-	-	-	-	-	-	-
Treponema pedis DSM 18691[T*]	-	+	+	-	-	-	-	+	+	-	-	-	-	-	-	-	-	-	-
Treponema brennaborense CIP 105900[T§]	+	+	+	-	-	-	-	-	-	+	+	-	+	-	+	-	+	-	-
Treponema pectinovorum ATCC 33768[T#]	-	+	+	-	-	-	-	-	-	+	+	-	-	-	-	-	-	-	-
Treponema socranskii subsp. *socranskii* ATCC 35536[T#]	+	+	-	-	-	-	-	-	-	+	+	-	-	-	-	-	-	-	-
Treponema maltophilum ATCC 51939[T#]	+	+	+	-	-	-	-	-	-	+	+	+	-	-	+	-	-	-	+
Treponema amylovorum ATCC 700288[T|]	+	+	-	-	-	-	-	-	-	+	+	-	-	-	-	-	-	-	+
Treponema medium ATCC 700293[T*]	+	+	+	-	+	-	-	-	-	-	-	-	+	-	-	-	-	-	-
Treponema putidum ATCC 700334[T+]	+	+	+	-	+	-	-	+	+	+	+	+	+	-	+	+	-	-	-
Treponema denticola ATCC 35405[T+]	-	+	-	-	-	-	-	+	+	-	-	-	-	-	-	-	-	-	-
Treponema parvum ATCC 700770[Tα]	+	+	+	-	-	-	-	-	-	+	+	-	-	+	-	-	-	-	-
Treponema lecithinolyticum OMZ 684[Tβ]	+	+	+	-	-	-	-	-	-	+	+	-	+	+	-	-	+	-	+

API® ZYM profile reported previously by [‡]Evans *et al.,* 2011b, [†]Nordhoff *et al.,* 2005, [*]Evans *et al*., 2009b, [§]Schrank *et al*., 1999, [#]Wyss *et al*., 1996, [|]Wyss *et al*., 1997, [+]Wyss *et al*., 2004, [α]Wyss *et al*., 2001, [β]Wyss *et al*., 1999.

6.2.4 Phylogenetic analysis of the *16S rRNA* gene of the novel spirochaete isolate

The near-complete (1,312 bp) *16S rRNA* gene sequence of the spirochaete isolate, which was initially amplified, sequenced and subsequently assembled according to Chapter 2.4.2, was aligned with the *16S rRNA* gene sequences of all currently recognised *Treponema* species for genotypic comparison, as described in Chapter 2.4.6. The degree of sequence similarity between the novel isolate and all other recognised extant *Treponema* species are given in Table 6.2. Interestingly, the novel bovine spirochaete isolate was found to share highest *16S rRNA* gene sequence identity (86.1%) with *Treponema porcinum* ATCC BAA-908^T, a spirochaete previously isolated from the faecal contents of a porcine GI tract (Nordhoff *et al.,* 2005). Furthermore, the novel isolate was found to share considerable *16S rRNA* gene sequence identity with a further two porcine GI tract isolates, namely *T. succinifaciens* ATCC 33096^T (85.8%) and *Treponema berlinense* ATCC BAA-909^T (84.8%) (Cwyk & Canale-Parola, 1979; Nordhoff *et al.,* 2005). Perhaps surprisingly, the novel bovine GI tract isolate was found to share comparatively lower *16S rRNA* gene sequence similarity with two extant *Treponema* species of the bovine rumen, *T. saccharophilum* ATCC 43261^T (84.1%) and *T. bryantii* ATCC 33254^T (84.0%) (Paster & Canale-Parola, 1985; Stanton & Canale-Parola, 1980). The novel isolate was found to share approximately 82% *16S rRNA* gene sequence similarity each with three treponeme taxa isolated from termite GI tract contents, namely *Treponema primitia* ATCC BAA-887^T, *Treponema azotonutricium* ATCC BAA-888^T and *Treponema isoptericolens* DSM 18056^T (Dröge *et al.,* 2008; Graber *et al.,* 2004). A large number of recognised *Treponema* species which are associated with human periodontal disease were found to share an average of 82.4% *16S rRNA* gene sequence identity (range 80.5% to 84.5%) with the novel isolate and the BDD-associated treponeme, *T. pedis* DSM 18691^T (Evans *et al.,* 2009b), was found to share just 80.6% sequence identity.

Notably, aside from extant *Treponema* species, the spirochaete isolate was found to demonstrate 99% sequence identity to an uncultured bovine rumen bacterium *16S rRNA* gene clone, R-ACA152, from Japan (Y. Kobayashi, unpublished; Genbank accession number AB614799). This gene clone was not included in further phylogenetic analyses as it was deemed relevant to compare the novel spirochaete isolate only to those of taxonomically designated *Treponema* species.

Table 6.2 Sequence identities between the novel spirochaete isolate and other recognised Treponema spp. based upon 16S rRNA gene sequence comparisons. *Upon amplification and sequencing of the 16S rRNA gene from the novel spirochaete isolate, represented by strain Ru1, the 16S rRNA gene sequences of other extant Treponema species were aligned by CLUSTAL W and their sequence identities (%) subsequently compared.*

***Treponema* species**	***16S rRNA* gene sequence identity shared with the novel spirochaete isolate (%)**
Treponema porcinum ATCC BAA-908^T	86.1
Treponema succinifaciens ATCC 33096^T	85.8
Treponema berlinense ATCC BAA-909^T	84.8
Treponema amylovorum ATCC 700288^T	84.5
Treponema saccharophilum ATCC 43261^T	84.1
Treponema bryantii ATCC 33254^T	84.0
Treponema parvum ATCC 700770^T	83.9
Treponema caldarium ATCC 51460^T	83.8
Treponema pectinovorum ATCC 33768^T	83.8
Treponema stenostreptum ATCC 25083^T	83.8
Treponema socranskii subsp. *paredis* ATCC 35535^T	83.3
Treponema socranskii subsp. *socranskii* ATCC 35536^T	83.2
Treponema isoptericolens DSM 18056^T	82.8
Treponema socranskii subsp. *buccale* ATCC 35534^T	82.8
Treponema azotonutricium ATCC BAA-888^T	82.3
Treponema brennaborense CIP 105900^T	82.2
Treponema primitia ATCC BAA-887^T	82.0
Treponema zuelzerae ATCC 19044^T	81.7
Treponema putidum ATCC 700334^T	81.6
Treponema pallidum subsp. *pertenue* strain Gauthier	81.4
Treponema denticola ATCC 35405^T	81.2
Treponema medium ATCC 700293^T	80.6
Treponema pedis DSM 18691^T	80.6
Treponema lecithinolyticum OMZ 684^T	80.5
Treponema maltophilum ATCC 51939^T	80.5

Phylogeny was inferred from the alignment of *16S rRNA* gene sequences according to Chapter 2.4.6 and, based upon predictions of the best-fit evolutionary model in TOPALi v2, the Tamura-Nei model (Tamura & Nei, 1993) was chosen to produce a bootstrapped maximum-likelihood tree based on 10,000 reiterations, as shown in Figure 6.2. Phylogenetic reconstruction revealed that the novel spirochaete isolate formed a distinct phylotype within a wider, deep-branched region of porcine and bovine GI tract treponemes. The novel bovine isolate was found to cluster specifically with *T. succinifaciens* ATCC 33096^T (Cwyk & Canale-Parola, 1979) and then *T. saccharophilum* ATCC 43261^T (Paster & Canale-Parola, 1985) in agreement with the observed *16S rRNA* gene sequence identities of 85.8% and 84.1% respectively. *T. porcinum* ATCC BAA-908^T (Nordhoff *et al.,* 2005), the porcine GI tract

treponeme which was identified as the novel spirochaete isolates' closest relative based upon *16S rRNA* gene sequence identity, was also found within this deep-rooted cluster of GI tract treponemes alongside the bovine rumen isolate, *T. bryantii* ATCC 33254^{T} (Stanton & Canale-Parola, 1980). The novel isolate also clustered more loosely with a number of the treponemes associated with human periodontal disease which were found to demonstrate high *16S rRNA* gene sequence identity, including *T. amylovorum* ATCC 700288^{T} and *T. parvum* ATCC 700770^{T} (Wyss *et al.,* 1997; Wyss *et al.,* 2001). Furthermore, the isolate also demonstrated a clear phylogenetic diversity to the *16S rRNA* gene sequences of two taxonomic representatives isolated from BDD lesions, namely *T. pedis* (Evans *et al.,* 2009b) and *T. brennaborense* (Schrank *et al.,* 1999).

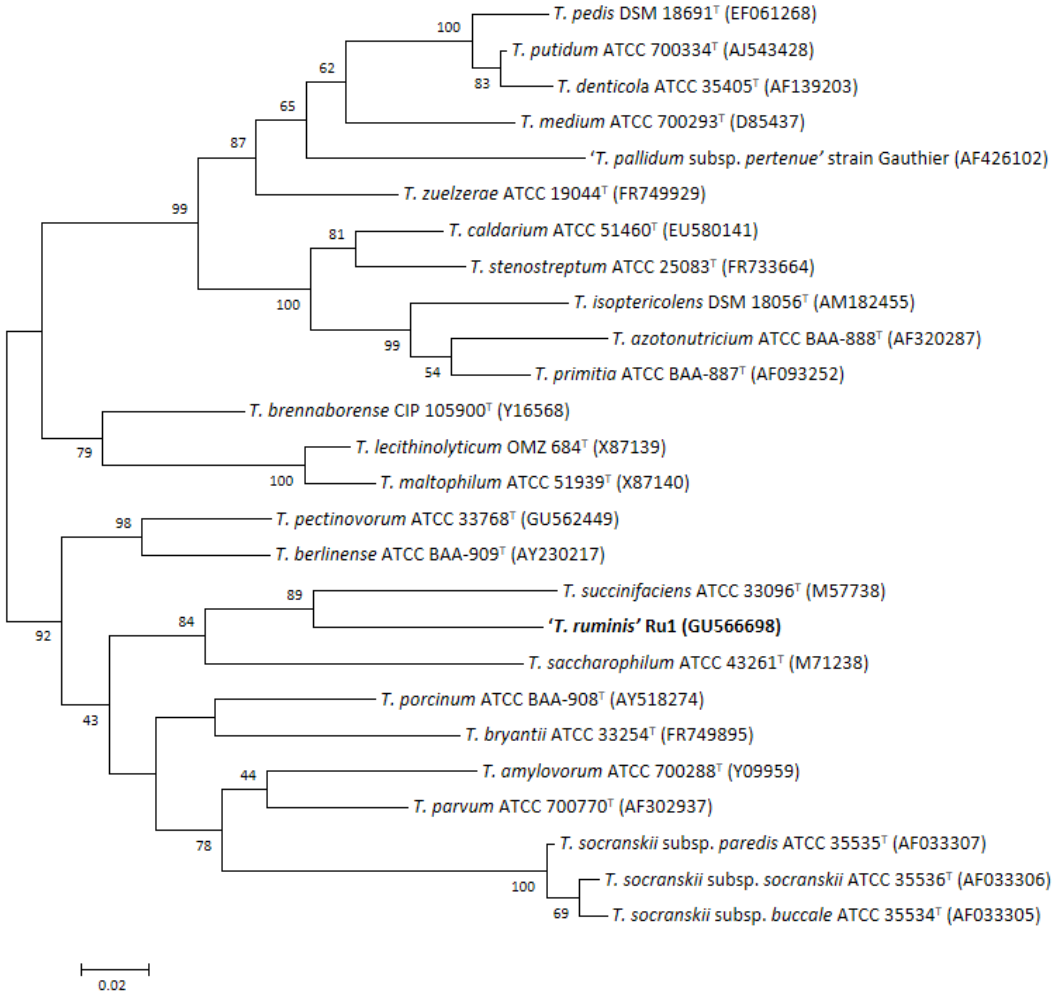

Figure 6.2 Phylogenetic relatedness of the novel spirochaete isolate to other recognised Treponema spp. based upon 16S rRNA gene sequence comparisons. *Phylogenetic tree of maximum-likelihood illustrating 16S rRNA gene sequence comparisons, over 1,312 aligned bases, between the bovine gastrointestinal tract isolate, represented by strain Ru1 (bold type), and all other recognised Treponema spp. The novel spirochaete isolate was found to*

cluster within a wider, deep-branched region of bovine and porcine gastrointestinal tract treponemes. Bootstrap confidence intervals, based on 10,000 reiterations, are shown as percentages at the nodes; values below 40% were removed for clarity. Genbank accession numbers are given in parentheses next to each strain. Bar, 0.02 nucleotide substitutions per site.

6.2.5 Development and optimisation of a novel degenerate *recA* gene PCR assay

A novel degenerate PCR assay was successfully developed and subsequently optimised by gradient PCR, as described in Chapter 2.4.4, for amplification of the *recA* gene from the novel spirochaete isolate for phylogenetic comparisons with those sequences available for other GI treponeme isolates. The mean inter-species *recA* gene sequence similarity was determined to provide an indication of the variation in *recA* gene sequence identity across currently recognised species of the genus *Treponema* for this novel assay. The available *recA* gene sequences for 17 *Treponema* species were found to differ from each other markedly, with a mean gene sequence similarity of 64.3% between extant species of the genus *Treponema* (ranging from 56.3% to 93.8%). The mean intra-species *recA* gene sequence similarities for two recognised species of the genus *Treponema* (with *recA* data available for a range of isolates) were calculated as 99.1% and 97.4% for *T. medium* and *T. pedis* respectively (Clegg *et al.,* 2016d).

6.2.6 Phylogenetic analysis of the *recA* gene of the novel spirochaete isolate

Approximately 479 bp of the *recA* gene sequence of the novel spirochaete isolate was compared to all available *recA* gene sequences of extant *Treponema* species, as described in Chapter 2.4.6, to determine their degree of sequence identity, as shown in Table 6.3. The novel bovine spirochaete isolate was found to have highest *recA* gene sequence similarity (76.8%) with the porcine GI tract isolate, *T. succinifaciens* ATCC 33096^T (Cwyk & Canale-Parola, 1979). *T. saccharophilum* ATCC 43261^T was found to share 74.3% *recA* gene sequence identity to the novel isolate, which may be unsurprising as both are isolates of the bovine rumen. Equally, the treponeme thought to be a derivative of bovine faecal contamination, *T. brennaborense* CIP 105900^T, was found to share 75.3% *recA* gene sequence identity with the novel isolate. Similar to observations based upon *16S rRNA* gene sequence comparisons, the novel spirochaete also demonstrated a wide-ranging identity (between 71.3% and 75.3%) to the *recA* gene sequences of several human periodontal disease-associated treponemes. Importantly, it should be noted that *recA* gene sequences were not available for several of the isolates which were found to cluster most closely with the novel spirochaete isolate based upon 16S rRNA gene sequence comparison, notably *T. porcinum* ATCC BAA-908^T.

Table 6.3 Sequence identities between the novel spirochaete isolate and other recognised Treponema spp. based upon recA gene sequence comparisons. *Upon amplification and sequencing of the recombinase A (recA) gene from the novel spirochaete isolate, represented by strain Ru1, those recA gene sequences of other extant Treponema species were aligned by CLUSTAL W and their sequence identities (%) subsequently compared.*

***Treponema* species**	***recA* gene sequence identity shared with the novel spirochaete isolate (%)**
Treponema succinifaciens ATCC 33096^T	76.8
Treponema brennaborense CIP 105900^T	75.3
Treponema socranskii subsp. *paredis* ATCC 35535^T	75.3
Treponema maltophilum ATCC 51939^T	74.5
Treponema saccharophilum ATCC 43261^T	74.3
Treponema socranskii subsp. *socranskii* ATCC 35536^T	74.3
Treponema azotonutricium ATCC BAA-888^T	73.0
Treponema caldarium ATCC 51460^T	72.8
Treponema lecithinolyticum OMZ 684^T	72.6
Treponema primitia ATCC BAA-887^T	72.6
Treponema putidum ATCC 700334^T	71.3
Treponema denticola ATCC 35405^T	70.9
Treponema medium ATCC 700293^T	70.7
Treponema pallidum subsp. *pertenue* strain Gauthier	65.7

Phylogeny was inferred from the alignment of *recA* gene sequences using the Tamura-Nei model (Tamura & Nei, 1993), according to Chapter 2.4.6, as determined to be the most appropriate evolutionary model by TOPALi v2, to produce a bootstrapped phylogenetic tree of maximum-likelihood based upon 10,000 reiterations, as shown in Figure 6.3. Phylogenetic reconstruction revealed that the novel isolate again formed a distinct phylotype clustering specifically amongst the porcine and bovine GI tract treponemes, *T. succinifaciens* ATCC 33098^T and *T. saccharophilum* ATCC 43261^T (Cwyk & Canale-Parola, 1979; Paster & Canale-Parola, 1985). Alongside this GI tract treponeme cluster, the novel isolate was found to cluster more loosely with *T. brennaborense* CIP 105900^T and several of the treponemes associated with human periodontal disease.

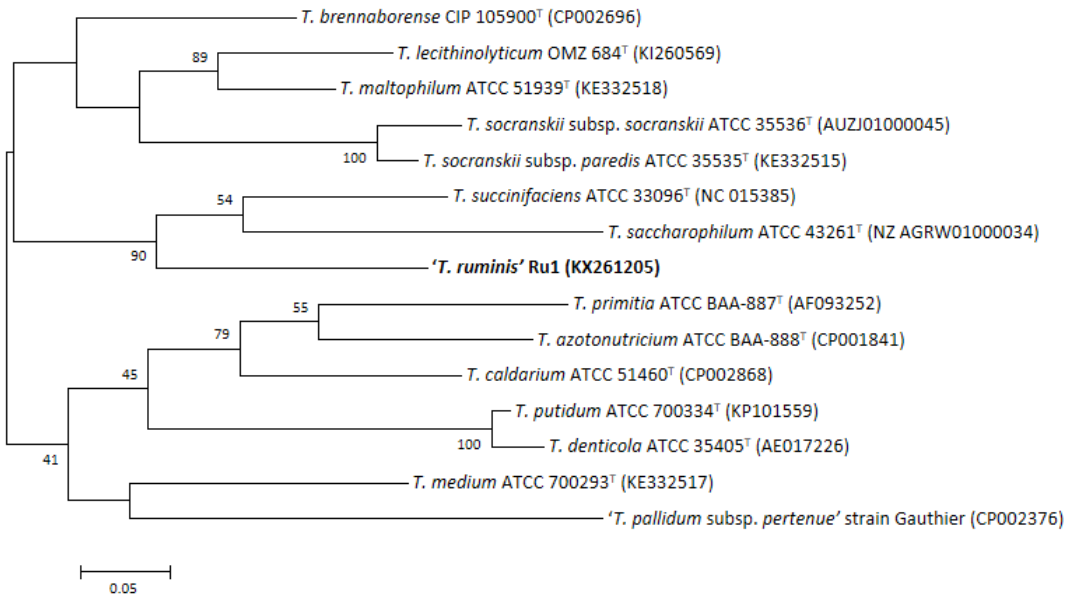

Figure 6.3 Phylogenetic relatedness of the novel spirochaete isolate to other recognised Treponema spp. based upon recombinase A gene sequence comparisons. *Phylogenetic tree of maximum-likelihood illustrating recombinase A (recA) gene sequence comparisons, across 479 aligned bases, between the bovine gastrointestinal tract isolate, represented by strain Ru1 (bold type), and all other recognised Treponema spp. The novel spirochaete isolate was found to cluster with other bovine and porcine gastrointestinal tract treponemes. Bootstrap confidence intervals, based on 10,000 reiterations, are shown as percentages at the nodes; values below 40% were removed for clarity. Genbank accession numbers are given in parentheses next to each strain. Bar, 0.05 nucleotide substitutions per site.*

6.2.7 Deposition of *Treponema ruminis* strain Ru1^T into two bacterial culture collections

The novel spirochaete isolate (designated *Treponema ruminis* sp. nov.) was successfully deposited as type strain Ru1^T into the DSMZ (Braunschweig, Germany) under the culture accession number DSM 103462^T and into the National Collection of Type Cultures (NCTC; National Institute for Biological Standards and Control, South Mimms, UK) under the culture accession number NCTC 13847^T, as described in Chapter 2.3.5.

6.2.8 Nucleotide sequence accession numbers for *16S rRNA* and *recA* genes of *T. ruminis*

The *16S rRNA* gene nucleotide sequence of *Treponema* spp. strain Ru1 (designated *Treponema ruminis* strain Ru1^T) was previously deposited in GenBank by Dr Nicholas Evans (Department of Infection Biology, University of Liverpool) under the accession number GU566698 (Evans *et al*., 2011b). The *recA* gene nucleotide sequence of *Treponema ruminis*

strain Ru1^T, as determined during this study, was deposited in GenBank under the accession number KX261205.

6.3 Discussion

Several treponeme taxa are considered commensal symbionts living within the GI tract of animals and insects; however, their functional importance has yet to be elucidated. Treponeme inhabitants of the bovine GI tract have been poorly characterised to-date and further taxonomic appraisals are currently required to elucidate the true extent of their diversity within this host niche. Through taxonomic characterisation of a novel spirochaete isolated from the bovine rumen, it was hoped that this study would provide a useful control organism for future host-pathogen interaction studies and would therefore facilitate the identification of functional importance in addition to possible mechanisms of treponeme pathogenesis.

6.3.1 Strain Ru1 shares key phenotypic characteristics of the *Treponema* genus

Phenotypic characterisation confirmed that the novel spirochaete isolate (Ru1) shared many of the common morphological and growth characteristics in keeping with spirochaetes of the genus *Treponema,* but particularly those of other recognised GI treponemes.

For instance, as typical of nearly all *Treponema* species, the novel isolate was found to grow anaerobically and at a temperature (36°C) generally in keeping with that of its natural host niche. The novel isolate demonstrated a typical spiral morphology with regular coils and its relatively small size and dimensions (5-9 µm long, 0.4-0.5 µm wide) fell within those expected for members of the genus *Treponema* (Paster, 2011). The isolate possessed a protoplasmic cylinder with a number of periplasmic flagella which originated at each end and, notably unlike *Leptospira* spp. (Birch-Andersen, 1973), typically overlapped in the centre in a classical n:2:n arrangement (Norris *et al.,* 1988; Paster, 2011; Rosenberg *et al.,* 2014). The isolate was also found to exhibit rotational and translational movement, jerky flexing and the high motility characteristic of treponemes in culture (Paster, 2011; Rosenberg *et al.,* 2014).

Interestingly, the novel isolate displayed a distinctive, serum-independent growth pattern which was near-identical to that of a newly-proposed *Treponema* species isolated from the bovine rectum, *Treponema rectale* DSM 103679^T (Staton *et al.,* 2017), and similar to the serum-independent culture conditions of other bovine, porcine and termite GI treponemes (Dröge *et al.,* 2008; Graber *et al.,* 2004; Nordhoff *et al.,* 2005; Paster & Canale-Parola, 1985; Stanton & Canale-Parola, 1980). Interestingly, the growth profile of the novel isolate was profoundly different to those of several pathogenic treponemes, such as *T. medium* ATCC

700293^T (Umemoto *et al.,* 1997) and *T. pedis* DSM 18691^T (Evans *et al.,* 2009b), which alternatively achieve optimal growth in the presence of serum. These observed differences in optimal growth conditions are likely due to respective pathogenic or functional adaptations to these physiologically distinct host niches; as further demonstrated by the ruminal fluid supplementation required for optimal growth of several GI treponemes (Cwyk & Canale-Parola, 1979; Piknova *et al.,* 2008; Stanton & Canale-Parola, 1980). It is not currently known if ruminal fluid supplementation improves growth of the novel spirochaete isolate, as this was beyond the scope of the present study; however, the isolate did demonstrate sufficient growth for reinoculation without such supplementation.

6.3.2 Strain Ru1 demonstrates several unique phenotypic traits

Whilst displaying key phenotypic characteristics in keeping with those of currently recognised *Treponema* species, the novel isolate displayed several distinct morphological characteristics, growth requirements and a unique enzyme activity profile which have not yet been reported for other species of the genus *Treponema.*

Cell and colony morphologies

The novel spirochaete isolate is a small-sized treponeme (5-9 µm long, 0.4-0.5 µm wide) which was distinguishable although probably most similar, morphologically, to that of the ovine rumen isolate, unofficially named *T. zioleckii* (Piknova et al., 2008), the bovine rumen isolate, *T. bryantii* ATCC 33254^T (Stanton & Canale-Parola, 1980), and then the porcine GI treponeme isolates (Cwyk & Canale-Parola, 1979; Nordhoff et al., 2005). Interestingly, other bovine GI tract isolates have shown great variation in size, with *T. saccharophilum* ATCC 43261^T typically 12-20 µm long and 0.6-0.7 µm wide (Paster & Canale-Parola, 1985), whereby the newly proposed rectal isolate, *T. rectale* DSM 103679^T*,* is typically just 1-5 µm long and 0.15-0.25 µm wide (Staton *et al.,* 2017).

The novel isolate was also found to have a distinct colony morphology which was very different to those reported for several other recognised *Treponema* species. For instance, *T. succinifaciens* ATCC 33096^T and *T. saccharophilum* ATCC 43261^T form spherical, opaque colonies with a diameter of 4-8 mm and 3-4 mm respectively, whereas colonies of *T. porcinum* ATCC BAA-908^T and *T. berlinense* ATCC BAA-909^T exhibit a 1-2 mm diameter and are irregular and greyish in colouration (Cwyk & Canale-Parola, 1979; Nordhoff *et al.,* 2005; Paster & Canale-Parola, 1985). Furthermore, the colonies did not exhibit a metallic sheen or the local haemolysis which is typical of several pathogenic treponemes (Evans *et al.,* 2008; Evans *et al.,* 2009b). Notably, the observed differences in growth characteristics between species of the genera *Treponema* may result from variable culture systems, particularly

growth conditions and agar concentration (Mitchell & Wimpenny, 1997), and therefore these comparisons are somewhat subjective. However, the novel isolate still maintained several key differences in colony morphology to the novel rectal isolate, *T. rectale* DSM 103679^T, despite identical culture conditions (Staton *et al.,* 2017).

Arrangement of periplasmic flagella

The novel isolate was found to have a unique periplasmic flagella arrangement (4:8:4) which has not yet been described for other recognised *Treponema* species. With notable exception to the 16:32:16 arrangement observed by the bovine rumen isolate, *T. saccharophilum* ATCC 43261^T (Paster & Canale-Parola, 1985), GI treponemes (and in fact many pathogenic species) commonly display a 1:2:1 or 2:4:2 flagella arrangement (Cwyk & Canale-Parola, 1979; Graber *et al*., 2004; Nordhoff *et al*., 2005; Stanton & Canale-Parola, 1980; Staton *et al*., 2017). It is currently not known whether these differences confer a functional importance; however, there does not appear to be a correlation between the number or arrangement of periplasmic flagella and treponeme pathogenicity. The larger sized treponemes, however, do tend to have more periplasmic flagella (Paster & Canale-Parola, 1985; Umemoto et al., 1997) which likely result from the more demanding motility requirements of larger spirochaetes.

Rapid growth in culture

In contrast to the much slower growth of other treponemes, particularly pathogenic species such as *T. pedis* DSM 18691^T (Evans *et al.,* 2009b) and *T. socranskii* subsp. *socranskii* ATCC 35536^T (Smibert *et al.,* 1984), the novel isolate required strict daily subculture to achieve optimal growth. Another bovine GI tract treponeme, *T. rectale* DSM 103679^T, which was recently proposed as a novel species, also required daily subculture for optimal growth (Staton *et al.,* 2017). Both the novel isolate and *T. rectale* DSM 103679^T were both cultured within OTEB and therefore alternative media formulations such as OMIZ-pat medium used to subculture *T. porcinum* ATCC BAA-908^T and *T. berlinense* ATCC BAA-909^T (Nordhoff *et al.,* 2005) or medium MVTY used to subculture *T. saccharophilum* ATCC 43261^T (Paster & Canale-Parola, 1985) may account for such differences in the observed growth patterns. Notably, the minimal medium requirements for the novel spirochaete isolate were not determined as this was beyond the scope of the present study.

Unique enzyme activity profile

Interestingly, among species of the genus *Treponema,* the novel isolate was found to have a unique API® ZYM profile, suggestive of its involvement in the metabolism of lipids (C8

esterase lipase activity), proteins (leucine arylamidase activity) and carbohydrates (β-galactosidase and β-glucosidase activity). Apart from the β-galactosidase activity also recently reported to be active in the bovine rectal isolate, *T. rectale* DSM 103679^T (Staton *et al.,* 2017), the enzyme activities detected in the novel isolate have not previously been associated with those of other recognised GI treponemes with published profiles to-date, including *T. porcinum* ATCC BAA-908^T, *T. berlinense* ATCC BAA-909^T and *T. rectale* DSM 103679^T (Nordhoff *et al.,* 2005; Staton *et al.,* 2017). Although likely highlighting different nutritional and, therefore, metabolic requirements between different host species (porcine versus bovine) and in different GI localities (bovine rumen versus rectum), it remains to be seen whether other treponemes of the bovine rumen (for example *T. saccharophilum* ATCC 43261^T and *T. bryantii* ATCC 33254^T) possess a similar enzyme activity. Interestingly, the novel isolate does share common enzyme activities with the human periodontal pathogens, *T. putidum* ATCC 700334^T, *T. medium* ATCC 700293^T and *T. lecithinolyticum* OMZ 684^T (Umemoto *et al.,* 1997; Wyss *et al.,* 1999; Wyss *et al.,* 2004), and a probable faecal contaminant, *T. brennaborense* CIP 105900^T (Evans *et al.,* 2011b; Schrank *et al.,* 1999). Indeed, these periodontal treponemes are commonly found to occupy phylogenetic clusters associated with both commensal and pathogenic treponemes (Evans *et al.,* 2011b) and further work is required to elucidate the reason for this.

6.3.3 Strain Ru1 is separated by phylogenetic distances akin to those observed amongst extant *Treponema* species

Although phenotypic traits are valuable for the characterisation of novel bacterial isolates, genotypic appraisals provide important information regarding their evolutionary relationships to other recognised species of relevant genera and therefore aid in distinguishing novel bacterial species. Bacterial phylogeny and taxonomy studies typically involve comparisons of well-conserved housekeeping gene sequences across recognised species of a relevant genus to determine sequence identity and phylogenetic relatedness. The *16S rRNA* gene is the predominant housekeeping gene used for taxonomic characterisation of novel bacterial species as it is well-conserved within nearly all bacterial species and is considered a good representation of evolutionary change rather than functional adaptation (Janda & Abbott, 2007; Stackebrandt & Goebel, 1994). Other housekeeping genes, such as DNA gyrase subunit B and the bacterial RNA polymerase (*rpo*) gene family, are considered good candidates for taxonomic characterisation of novel bacterial isolates (Rowland *et al.,* 1993; Wang *et al.,* 2007) and the *recA* gene has been cited as a useful housekeeping gene for distinguishing species of the *Burkholderia* genus (Payne *et*

al., 2005). In the present study, both the *16S rRNA* gene and the *recA* gene were used to perform genotypic characterisation of the novel spirochaete isolate.

Through comparison to the *16S rRNA* and *recA* gene sequences of extant *Treponema* species, genotypic characterisation identified that the novel spirochaete isolate formed a distinct phylotype within a wider and deep-branched region of both bovine and porcine GI treponemes. As an isolate of the bovine rumen, it was not surprising that the novel spirochaete clustered most closely with extant *Treponema* species of the GI tract as it is likely that they share similar functional adaptations to enable colonisation of this host niche. In corroboration, the isolate displayed clear phylogenetic diversity to the *16S rRNA* gene sequence of a taxonomic representative previously isolated from BDD lesions, *T. pedis* DSM 18691^T (Evans *et al.,* 2009b) and also demonstrated comparatively lower sequence identity to several periodontal treponemes. It is likely that these observations are due to functional adaptations to distinct host niches (the bovine digit and oral cavity) and to adaptations in virulence of these treponemal pathogens. Interestingly, however, the novel bovine isolate was found to share highest *16S rRNA* gene (86.1%) and *recA* gene (76.8%) sequence identities with the porcine GI tract isolates, *T. porcinum* ATCC BAA-908^T and *T. succinifaciens* ATCC 35535^T respectively, with the latter species also sharing 85.8% *16S rRNA* gene sequence identity to the novel isolate. It might have been expected that the novel bovine isolate would share highest phylogenetic relatedness with treponemes of the bovine GI tract; however, its consistently high identity to several porcine GI treponemes may suggest relatively low phylogenetic diversity between treponemes of the bovine and porcine GI tract. Indeed, Nordhoff *et al.* (2005) previously found that the porcine GI treponeme, *T. berlinense* ATCC BAA-909^T, clustered closely alongside the bovine GI tract isolate, *T. saccharophilum* ATCC 43261^T. Interestingly, based upon *recA* gene sequence similarities, the novel isolate did share second highest similarity (75.3%) with the probable bovine faecal contaminant, *T. brennaborense* CIP 105900^T, and comparatively much lower identity to the bovine rumen isolate, *T. saccharophilum* ATCC 43261^T. However, based upon the distinct and considerably diverse phenotypic characteristics of *T. saccharophilum,* particularly its much larger size and number of periplasmic flagella (Paster & Canale-Parola, 1985), this may not be too surprising. Whilst clustering closely to the porcine and bovine GI tract treponemes, the novel spirochaete isolate had diverged markedly from them such that they were separated by phylogenetic distances akin to those observed among extant *Treponema* species. The novel isolate was found to share a maximum of 86.1% 16S rRNA gene sequence identity to the porcine GI tract isolate, *T. porcinum* ATCC BAA-908^T, and 76.8% *recA* gene sequence similarity

to another porcine GI tract isolate, *T. succinifaciens* ATCC 33096^T. More recently, a newly-proposed *Treponema* species of the bovine rectum, *T. rectale* DSM 103679^T, was found to share 87.0% *16S rRNA* gene sequence identity and 77.4% *recA* gene sequence identity with the novel spirochaete isolate (Staton *et al.,* 2017). However, these sequence similarities are each well below the proposed threshold of less than 97% identity required for species delineation (Stackebrandt & Goebel, 1994) and suggest that the isolate represents a novel species within the genus *Treponema.*

The genotypic characterisation of *Treponema* species through the use of the *recA* gene has been described here for the first time. Although sequence variation of the *16S rRNA* gene provided sufficient evidence for the proposal of a novel species of the genus *Treponema,* the *recA* gene provided further indication of the phylogenetic relatedness between species. The family of recombinase genes have previously been used to identify inter-species variation (Everest *et al.,* 2011) and this assay may therefore be an important application for future bacterial classification of *T. ruminis* strains. In fact, recently, Staton *et al.* (2017) used this novel *recA* gene PCR assay for the genotypic characterisation of a novel *Treponema* species, *T. rectale* DSM 103679^T.

Interestingly, the observation that the novel spirochaete isolate shares 99% *16S rRNA* gene sequence identity with an uncultured bovine rumen bacterium *16S rRNA* gene clone, R-ACA152 (Y. Kobayashi, unpublished; GenBank accession number AB614799), suggests that this uncultured clone likely represents another strain within the same species as the novel spirochaete isolate, sharing over 97% sequence identity (Stackebrandt & Goebel, 1994). This uncultured clone was not included in further genotypic comparisons as, within the scope of this taxonomic study, it was deemed important to only include relevant, currently recognised *Treponema* species for comparison.

Within this study, pure cultures of the novel spirochaete isolate were genotypically characterised by comparison of specific housekeeping genes (*16S rRNA* and *recA*) to those of other recognised treponemes and this approach has commonly been used for the characterisation of other novel treponeme isolates (Cwyk & Canale-Parola, 1979; Nordhoff *et al.,* 2005; Paster & Canale-Parola, 1985; Stanton & Canale-Parola, 1980). However, increasing advancements in NGS technology in recent years have made high-throughput, whole genome sequencing of pure bacterial isolates, mixed bacterial populations and even infected tissues far more affordable and realistic. Indeed, metagenomics studies have already provided a wealth of information regarding spirochaete populations within the GI tract of ruminants (Edwards *et al.,* 2004; Paster & Canale-Parola, 1982; Tajima *et al.,* 1999;

Zinicola *et al.,* 2015a) which are often lost by cultivation-based approaches such as those used here. Accordingly, the novel spirochaete isolate recently underwent whole genome sequencing as part of a separate genomics project within the research group; however, this information was unavailable at the time of this study. When available, the whole genome sequence of this novel GI tract treponeme isolate will provide an undoubtedly important source of information for further genotypic characterisation and will hope to inform the functional importance of such isolates. Arguably one of the biggest unanswered questions from this study is the role for the novel spirochaete isolate, and other isolates of a similar nature, within the bovine rumen. Treponeme isolates of the GI tract are generally considered to be commensal symbionts, however, as discussed previously there is currently very little evidence to specifically validate this. The evidence provided in this study suggests that the novel spirochaete isolate, represented by Ru1, is genotypically and phenotypically very similar to other treponemes found within the GI tract of ruminants, suggesting they may have a similar role. This requires further investigation in future studies.

6.3.4 Conclusions

Based upon the comparative genotypic and phenotypic data presented in this study, strain Ru1^T is considered to represent a novel species within the *Treponema* genus, for which the name *Treponema ruminis* sp. nov. has subsequently been proposed (Newbrook *et al.,* 2017). *Treponema ruminis* is now available as type strain Ru1^T within two recognised culture collections, the DSMZ (DSM 103462^T) and the NCTC (NCTC 13847^T).

Description of *Treponema ruminis* spp. nov.

Treponema ruminis (ru'mi.nis. L. neut. gen. n. *ruminis*, of the rumen). Anaerobic, gram-negative, helically coiled, motile and very small-sized treponemes. Cells are approximately 5-9 µm long and 0.4-0.5 µm wide, have between three to five even windings and each have eight periplasmic flagella in a 4:8:4 arrangement. Cells typically reach optimal growth following anaerobic incubation at 36°C for one day within oral treponeme enrichment broth without serum supplementation. Cells exhibit translational movement, rotation and jerky flexing in culture and typically sediment towards the bottom of the tube. Circular, translucent, convex, punctiform colonies of 0.2-0.5 mm diameter are observed after 10 days when streaked onto unsupplemented fastidious anaerobic agar plates. Colonies do not have a metallic sheen or exhibit local hemolysis. Cells can be stored at -80°C in growth medium containing 10% (v/v) glycerol. The API® ZYM system identified enzyme activity for C8 esterase lipase, leucine arylamidase, β-galactosidase and β-glucosidase, while detecting no activity for alkaline phosphatase, C4 esterase, C14 lipase, valine arylamidase, cysteine arylamidase,

trypsin, chymotrypsin, acid phosphatase, naphthol-AS-BI-phosphohydrolase, α-galactosidase, β-glucuronidase, α-glucosidase, N-acetyl-β-glucosaminidase, α-mannosidase and α-fucosidase.

The type strain, Ru1^T (=DSM 103462^T=NCTC 13847^T), was isolated from the rumen contents of a Holstein-Friesian bull from a Cheshire farm in the UK.

Chapter Seven: General discussion

7.1 The importance of understanding more about BDD pathogenesis

With increasing concerns over the future sustainability of global food production, the health and well-being of domestic production animals such as dairy and beef cattle, as a major food-source, are becoming of increasing importance. Cattle lameness is now widely considered one of the largest unresolved challenges facing modern dairy and beef herds worldwide. Its profound implications for animal welfare (Whay *et al.,* 1997), production efficiency (Bicalho *et al.,* 2007; Green *et al.,* 2002; Hernandez *et al.,* 2001) and its economic burden (Willshire & Bell, 2009) should make it a key priority in veterinary research over the coming years.

As one of the most common causes of severe cattle lameness, BDD is of high global importance. The expanding host range (both wild and domestic species) and emergence of similar disease pathologies associated with its primary aetiological agent, treponemes, alongside the broader association of treponemes with other well-characterised human and animal diseases, only serves to emphasise its importance further (Clegg *et al.,* 2015; Clegg *et al.,* 2016c; Clegg *et al.,* 2016b; Harwood *et al.,* 1997; Sullivan *et al.,* 2015a; Sykora & Brandt, 2015). A large body of research has already been undertaken to elucidate the prevalence, risk factors and impact, complex aetiology and most efficacious treatment and control strategies of BDD. Despite this, however, there is currently a relative lack of understanding of BDD pathogenesis; with just a handful of papers having previously attempted to elucidate key mechanisms of BDD treponeme pathogenesis (Evans *et al.,* 2014; Refaai *et al.,* 2013; Scholey *et al.,* 2013; Zuerner *et al.,* 2007).

With an increasing drive for antibiotic stewardship, as antimicrobial resistance continues to emerge globally across many bacterial species, there is an ever-present demand for the development of alternative therapeutics and efficacious vaccines in veterinary and also human medicine. The unsuitability of antibiotics for use in domestic production animals entering the food chain, and the environmental toxicity of many alternatives, make novel therapeutics and vaccines a significant priority for BDD. A deeper understanding of the key pathogenic mechanisms of BDD treponemes are now at the forefront of advancing such developments. For instance, the higher abundance in expression of genes associated with copper and antibiotic resistance within acute and healing BDD lesions recently identified by Zinicola *et al.* (2015b) provides a plausible explanation for the current failures in many therapeutics used to treat BDD and will also act to inform selection and development of

novel therapeutics going forward. A comprehensive understanding of the shared and unique pathogenic mechanisms of each BDD treponeme phylogroup, both globally and across different species, will also be crucial for developing the most efficacious vaccines with maximal coverage and global impact. The significant advances in isolation, culture and characterisation of these highly fastidious, anaerobic treponemes in recent years (Evans *et al.,* 2008; Evans *et al.,* 2011b), alongside the development of sophisticated *in vivo* models of BDD infection (Gomez *et al.,* 2012; Krull *et al.,* 2016), should now pave the way for progression within the field of BDD pathogenesis and, ultimately, development of the first vaccine against BDD infection.

7.2 An overview of the principle findings

Developing a valuable model for future host-pathogen interaction studies of bovine digital dermatitis

To investigate the host-pathogen interactions and pathogenic mechanisms underlying BDD, an appropriate disease model was required. A simple monolayer cell culture model was chosen to enable analysis of the individual contributions and interactions of specific treponemes and host cell lineages in disease pathogenesis. In Chapter three, previously published protocols (Evans *et al.,* 2014) were implemented and subsequently optimised to enable the successful isolation and prolonged subculture (eight and six passages respectively) of primary fibroblast and keratinocyte cells from bovine foot skin tissue; as predominant cell lineages of the dermis and epidermis respectively. Reduced confluence to passage (80% rather than 90%), avoidance of the DEJ and tissue taken from above, rather than below, the dewclaws were each found to improve the final cell isolation and subculture yields. Currently, a major limitation of fibroblast identification is a lack of known and validated fibroblast-specific markers; therefore, fibroblast characterisation is typically performed by eliminating the expression of other cellular markers. A novel IF staining method was successfully developed and optimised to advance characterisation methods of bovine foot skin cells (Evans *et al.,* 2014). Staining with anti-pan cytokeratin antibody confirmed the presence of keratinocytes within only epidermal cell cultures, whilst dual staining with anti-vimentin antibody confirmed the presence of a fibroblast-like cell lineage within dermal cultures (in the absence of keratinocytes). These newly characterised bovine foot skin cell culture models provide a valuable tool for future host-pathogen interaction studies of BDD as well as studies of other disruptions or pathologies of normal bovine skin physiology.

Elucidating profound differences in the pathogenic mechanisms of bovine digital dermatitis treponemes

The fibroblast monolayer cell culture model was used in Chapter four to investigate dysregulation of global mRNA expression in bovine foot skin fibroblasts following stimulation with representative strains of the three predominant BDD treponeme phylogroups (*T. medium, T. phagedenis* and *T. pedis*), a commensal treponeme (*T. ruminis*) or a Gram-negative bacterial LPS control. A next generation RNA-Seq approach was taken to harness high resolution and unparalleled coverage of the expressed fibroblast transcriptome. This study is the first to report profound differences between the mechanisms of inflammatory dysregulation of bovine foot skin cells induced by the three BDD treponeme phylogroups; with *T. medium* phylogroup found to markedly contrast other phylogroups by being less stimulatory, although potentially immunosuppressive. Furthermore, in light of its distinct growth requirements compared to other BDD treponemes (Evans *et al.,* 2008), *T. medium* phylogroup isolates urgently warrant further functional and taxonomic characterisations. In agreement with previous findings for the human periodontal pathogen, *T. denticola* (Baehni *et al.,* 1992), both *T. medium* phylogroup and *T. pedis* (however, notably, not *T. phagedenis* phylogroup) appeared to dysregulate host actin arrangement and cytoskeletal structure. A novel finding from this study further appeared to implicate these same treponemes in tissue disruption through loss of host cell adhesion via *RND1* dysregulation; this is strongly suggestive of a direct role for these organisms in observed BDD pathology. Interestingly, the GI tract treponeme, *T. ruminis,* compared to BDD treponemes, stimulated over four times more differentially expressed genes in bovine fibroblasts. A recent study of secondary syphilis correlated robust host pro-inflammatory immune responses with favourable host outcome and more effective bacterial clearance (Pastuszczak *et al.,* 2017). This host outcome may, therefore, explain why *T. ruminis,* eliciting a large fibroblast response, is unable to survive within and contribute to BDD pathogenesis despite likely exposure to the foot surface. This bovine GI tract treponeme was considered a relevant control for this study, although it might be argued that, in the future, alternative more relevant commensals of the bovine foot may be identified, characterised and surveyed within this system. IPA highlighted a number of common canonical signalling pathways to be predictably activated by the treponemes, including many associated with the host inflammatory response and bacterial-induced activation. Several, often novel, pathogenic treponeme host gene targets were highlighted during this study, including *IL-8*, *DEFB123* and *TSC22D3*, and may inform future developments of novel, efficacious therapeutics and vaccines against BDD; these now

warrant immediate further investigation. Furthermore, the similarities drawn between the host cell responses of BDD infection here and those of psoriasis in humans may suggest that psoriatic treatments may also be of value in treating BDD. Notably, salicylic acid was recently found to demonstrate significant efficacy in the treatment of BDD lesions (Schultz & Capion, 2013) and warrants further investigation.

Identification of a well-conserved treponemal outer membrane protein with potential as a vaccine candidate

The OMPs of BDD treponemes come into direct contact with bovine foot skin cells and are therefore almost certainly involved in the initial host-pathogen interactions which underly BDD infection and lead to their persistence within the host. Importantly, BDD treponeme OMPs have yet to be identified characterised or their molecular diversity across the three predominant phylogroups assessed. This was due, at least in part, to the considerable difficulties in the isolation, subculture and characterisation of these fastidious microorganisms. Chapter five attempted to identify a putative OMP homolog expressed by BDD treponemes and subsequently characterise its molecular diversity. A predicted eight-stranded anti-parallel β-barrel OMP with homologs across each of the three BDD treponeme phylogroups was identified, sharing significant homology to OMPs (OmpA, OmpW and NspA) of other Gram-negative bacterial pathogens. The novel OMP was found to be highly conserved within each phylogroup, whilst demonstrating only limited diversity amongst the three treponeme phylogroups, and was not under significant evolutionary selection pressures. Whilst strongly implying that the novel OMP is not involved in mechanisms of antigenic modulation in BDD treponemes, its high conservation is suggestive of an important functional role; potentially in treponeme pathogenesis. The marked divergence observed in its protein homology between pathogenic and commensal treponemes only serves to further highlight its potential importance as a valuable candidate in the future development of novel therapeutics and vaccines; warranting functional characterisation of this treponemal protein.

Characterisation of a novel *Treponema* spp. as a useful control organism in future studies

When attempting to understand mechanisms of disease pathogenesis, it can be extremely valuable to draw comparisons between the host-pathogen interactions of both pathogenic and relevant commensal species. In the absence of relevant commensal treponemes of the bovine foot skin tissue itself, other well-characterised commensal treponemes undoubtedly provide a useful alternative. Detailed taxonomic characterisation of the novel bovine rumen isolate (Ru1) in Chapter six identified this likely commensal treponeme as a useful future tool

for comparative studies of treponeme pathogenesis and we have deposited this novel treponemal species in relevant international culture collections. Whilst found to share many of the typical phenotypic characteristics of commensal GI tract treponemes, its unique flagella arrangement and enzyme activity profile have begun to delineate further functional roles for these poorly studied treponemes. Whilst genotypically most similar to other recognised porcine and bovine GI tract treponemes, the rumen isolate was considered to represent a novel species, designated *T. ruminis* (Newbrook *et al.,* 2017). Whilst the findings from this study go a long way in informing functional importance of commensal treponemes and highlighting the merits of taxonomic characterisation, further work is now required to complete detailed taxonomic and functional characterisation on a wider range of commensal treponemes to provide further control organisms for studying mechanisms of pathogenesis.

7.3 Forward perspectives

The work presented within this thesis represents a major milestone in delineating mechanisms of BDD pathogenesis and also providing important tools for future host-pathogen interaction studies; each using a wide range of approaches. However, these studies have also highlighted some significant gaps to be addressed which, with further time and resources, would have been considerably beneficial and complimentary to the outcomes of this work. These offer significant opportunities for future work within this field.

As discussed in Chapter three, there are now a number of sophisticated *in vitro* skin cell culture models being developed for application to studies of therapeutic efficacy, infection and inflammation and disease pathogenesis (Reijnders *et al.,* 2015; Wufuer *et al.,* 2016). Whilst previous host-pathogen interaction studies of BDD (and that presented here) were completed using simple bovine monolayer cell culture models, largely due to their simplicity in elucidating the interactions of single cell lineages, these are not directly representative of the *in vivo* skin environment. As this novel comparative transcriptomics study has identified a wide range of novel potential gene targets of BDD pathogenesis, it is important that future work sees their application to more complex and representative bovine skin models, such as skin-on-a-chip and skin-equivalent models. Whilst it is hoped that the most recent and sophisticated advances in human skin-on-a-chip models (Wufuer *et al.,* 2016) will be translated to equivalent bovine models in the near future, I am somewhat doubtful. The work completed as part of this thesis has highlighted significant gaps within bovine research (particularly in the availability of species-specific antibodies, suitable and representative bovine skin models, research tools and methods and advancements in detailed annotation

of the bovine genome), which severely hinder the capabilities of researchers working on bovine infectious diseases, such as BDD. Whilst significant improvements have been made in recent years, more needs to be done to close this gap between bovine and human research over the coming years to allow further significant advancements in the development of novel therapeutics and vaccines against bovine infectious diseases. Although *in vitro* models are extremely useful, the recent development of novel *in vivo* models of BDD infection (Gomez *et al.,* 2012; Krull *et al.,* 2016) certainly serve to provide novel models for host-pathogen interaction studies in the near future; particularly in the current absence of more representative *in vitro* bovine skin models.

One of the great advantages of using such *in vivo* models for studies of host-pathogen interactions during disease is that, unlike other simplistic and complex *in vitro* or *ex-vivo* skin models, *in vivo* models are realistic and representative of the true skin environment. One of the greatest differences is that *in vivo* models enable consideration of important interactions between the skin tissue and its abundant microbiome. Unfortunately, the nature of the simplistic skin model chosen for studies of host-pathogen interactions throughout this thesis meant an inability to account for the dynamic interactions occurring with the skin microbiome during BDD infection. As previously discussed, such omissions must be considered during interpretation of the dataset presented in Chapter four. As discussed in Chapter 1.8.2, host-microbe interactions on the epidermal skin surface are complex and extremely dynamic (Naik *et al.,* 2015), both during health and disease. These abundant commensal communities are thought to have a significant role in host skin immunity, including an ability to limit opportunistic invasion (Campbell, 2017). Zinicola *et al.* (2015a) previously found that the microbiomes of healthy skin and acute and chronic BDD lesions are each profoundly distinct. For instance, a plethora of pathogenic treponemes, including *T. denticola, T. maltophilum, T. medium* and *T. phagedenis*, were found to be markedly increased within acute BDD lesions alongside a previously unassociated bacterium, *Candidatus Amoebophilus asiaticus,* when compared to healthy skin (Zinicola *et al.,* 2015a). Krull *et al.* (2014) also highlighted the true complexity of the skin microbiome during BDD infection and revealed significant changes in the microbiome community of bovine skin throughout lesion development. For instance, whilst treponemes appeared to predominate during acute BDD infection, they had a relatively low abundance within early-stage lesions (Krull *et al.,* 2014). Such studies are now paving the way for further research within this area of significant interest and hope to elucidate more about the complexities of the skin

microbiome during BDD infection and the potential role of these microbial communities in pathogenesis.

Whilst transcriptomics analysis is an extremely valuable tool for the identification of global differential gene expression under specific pathological conditions or following interaction between different cell types, further functional characterisations are required to elucidate true biological and functional importance. Whilst low-throughput functional studies using, for instance, western blotting are useful, the recent application of high-throughput proteomic approaches in the analysis of protein expression provides novel opportunities to confirm whether such changes in the transcriptome are translated into protein function within the cell. Such approaches have yet to be described in studies of host-pathogen interactions of BDD, however will be crucial for determining the true biological significance of observed changes, such as those of Chapter four, in the future.

The studies presented within this thesis have highlighted the potential value of two profoundly distinct targets in the future development of novel therapeutics and vaccines, namely treponemal LPS and OMPs, which now warrant further investigation.

A reverse vaccinology approach was recently applied in the development of a novel meningococcus serogroup B vaccine, targeting three highly immunogenic OMPs, which has now been licensed for use (Serruto *et al.,* 2012). Bacterial OMPs also appear to be promising targets for application to veterinary vaccines and a number have shown substantial efficacy (Meenakshi *et al.,* 1999; Pasquevich *et al.,* 2009). Further studies are now warranted to characterise the remaining OMPs of BDD treponemes and, together with the novel OMP identified in Chapter five, consider their potential in this promising avenue of vaccine development to prevent BDD.

The significant host cell response to Gram-negative bacterial LPS observed by transcriptomics analysis in Chapter four highlights a promising avenue in the development of novel therapeutics and vaccines against BDD treponemes. Whilst it is known that treponemes have an atypical LPS-like component, LOS, in contrast to their Gram-negative bacterial counterparts, this has yet to be characterised and presents a significant opportunity for future work. The work presented in this thesis highlights an urgent need for the biochemical characterisation of BDD treponeme LOS and to assess its intra-phylogroup and inter-phylogroup antigenic diversity. The host-pathogen interactions of specific treponemal LOS components also warrant further characterisation to elucidate which specific treponemal antigenic components elicit the observation transcriptional changes identified in Chapter four. Such studies could be facilitated by sophisticated allelic replacement

mutagenesis techniques, using the characterised bovine foot skin cell models of Chapter three to study host-pathogen interactions.

Interestingly, the distinct inter-phylogroup variation highlighted during this thesis, both in terms of molecular diversity of the novel OMP and their dysregulation of inflammatory mediators during host-pathogen interactions, further confirm the likely requirement of a multivalent vaccine against BDD, targeting each of the three predominant treponeme phylogroups. As the first study to report significant differences between the three treponeme phylogroups associated with BDD infection, this work should form a strong platform to encourage more detailed investigations into such inter-phylogroup variation.

7.4 Future studies

7.4.1 Developing a realistic model for studying host-pathogen interactions of bovine digital dermatitis

As discussed previously, one of the major limitations, and indeed benefits, of the bovine foot skin model characterised during this study (Chapter three) is its simplicity. Following the identification of key pathogenic mechanisms of BDD infection using this model, it will be imperative to investigate whether such mechanisms appear to be important within more realistic skin models which are more representative of the *in vivo* skin environment. Accordingly, the development of more complex bovine foot skin models (such as HSE or skin-on-a-chip) will undoubtedly be of great benefit to advancing current knowledge of BDD pathogenesis; particularly in light of the current lack of such bovine skin models described within the literature. Further to this, the recent development of *in vivo* infection models for BDD (Gomez *et al.,* 2012; Krull *et al.,* 2016) may provide a useful tool for application within this setting, particularly for its considerations of the dynamic complexity of the skin and interactions with the skin microbiome.

Due to time constraints within the scope of this study, further keratinocyte cell-specific markers were not investigated for use in the characterisation of primary bovine fibroblast and keratinocyte cell lineages within this model. Due to the susceptibility of monolayer de-differentiation *in vitro,* it would be beneficial to characterise the primary bovine foot skin fibroblast and keratinocyte cell lineages throughout each stage of subculture to confirm their suitability throughout subculture. As discussed previously, it would also be beneficial to further validate the model using cytokeratin-specific markers (rather than pan cytokeratin), amongst others, to characterise the particular stages of keratinocyte differentiation represented within this model as this equates to keratinocytes of specific epidermal strata.

7.4.2 Elucidating the extent and true importance of these novel pathogenic mechanisms of bovine digital dermatitis treponemes in host inflammatory dysregulation

Through the use of an RNA-Seq approach, Chapter four has unearthed a considerable amount of data, helping to delineate the pathogenesis of BDD and identify profound differences between the mechanisms of inflammatory dysregulation of cells of the bovine foot skin tissue induced by the three predominant BDD treponeme phylogroups. However, as with all studies, the dataset points us in several directions.

Many of the novel gene targets identified within this study, as highlighted in Chapter 4.3, require further investigation to determine their true biological importance within BDD pathogenesis; in particular, those which appeared to be dysregulated within a pathogen-specific manner.

Following the experiments of Baehni *et al.* (1992), it would be of interest to visualise the changes in actin rearrangement within bovine foot skin fibroblasts as identified during this study and the novel IF staining method developed in Chapter three would likely be of use here with some adaptations.

One of the major limitations of this study is that although the differential expression profiles of bovine foot skin fibroblasts provide key information, they are solely based upon the host responses of a single animal and provide just a single biological replicate and, therefore, no information on the biological variation across bovine populations. Further work would be required to perform a much larger scale experiment to account for such likely biological variation and avoid such biases within the dataset. As BDD susceptibility was previously shown to be influenced by cattle breed, it would be of interest to determine whether breed influences such host-pathogen interactions.

As previously discussed in Chapter three, the model chosen for this study has several limitations and, whilst such simplistic monolayer co-culture models are extremely beneficial for dissecting specific host-pathogen interactions in disease pathogenesis, they only provide a single snap-shot of the pathogenesis occurring at a particular moment in time. Such models also do not account for the dynamic complexities of bovine foot skin tissue observed *in vivo.* It would be of interest to determine whether the interactions highlighted during this study are representative of those at other co-incubation time points, within other host cell lineages (particularly keratinocytes) and also within more representative skin models.

In addition, it would be beneficial to further assess the dataset to confirm whether the observed batch effect (as previously mentioned) and possible outliers identified within this

dataset are indeed having a confounding effect on the dataset observed. More recently, RNA-Seq analysis programmes, such as DESeq2 (Love *et al.,* 2014), have been developed to account for such batch effects which are not able to be accounted for with Cuffdiff, as used in this study. In light of the observed batch effect, such programmes may be more beneficial for the analysis of this dataset.

7.4.3 Identifying functional importance of the novel conserved outer membrane protein of bovine digital dermatitis treponemes

Following the identification of a well-conserved OMP of BDD treponemes in Chapter five, it is now imperative to elucidate its functional importance within *Treponema* species to determine its potential as a future target of novel therapeutics or vaccine development. It is pertinent to determine whether its function within pathogenic treponemes is similar or different to that within the GI tract of animals and insects; particularly due to its distinct sequence diversity.

To aid in such functional studies it would also be important to elucidate the true structure of this novel OMP using protein crystallography and confirm our predictions of an 8-stranded anti-parallel β-barrel.

Although this study specifically aimed to investigate molecular diversity within a single putative treponeme *Omp* gene and its corresponding homologs across BDD treponemes, it would be pertinent to perform whole genome sequencing on the treponeme isolates in order to allow greater investigation of their molecular diversity across a number of *Omp* genes.

As the first study to identify and subsequently characterise the molecular diversity of a BDD treponeme OMP, it would be timely to further investigate some of the other larger *Omp* genes (where time and cost would be permitting) identified as part of this study to determine whether other OMPs of BDD treponemes are as highly conserved as the novel OMP homologs examined here.

7.4.4 Further functional characterisation of *T. ruminis* and other bovine gastrointestinal tract treponemes

Within Chapter six, a novel spirochaete isolate, represented by strain Ru1^T, was successfully taxonomically characterised and proposed as a novel *Treponema* species, namely *Treponema ruminis.* Although the distinguishable genotypic and phenotypic characteristics presented here unequivocally validate the spirochaete isolate as a novel species within the genus *Treponema,* one of the major limitations of this study is that this proposal is based upon a single isolate (strain Ru1^T) within a single cow. Treponemes are highly fastidious,

anaerobic microorganisms which are notoriously difficult to isolate, cultivate and purify and consequently only a handful of GI treponemes have been successfully characterised to-date (Cwyk & Canale-Parola, 1979; Dröge *et al.,* 2008; Graber *et al.,* 2004; Newbrook *et al.,* 2017; Nordhoff *et al.,* 2005; Paster & Canale-Parola, 1985; Stanton & Canale-Parola, 1980; Staton *et al.,* 2017). Despite multiple surveys of the bovine GI tract, encompassing 12 bovine rumen samples and 29 faecal samples, this novel *Treponema* species (represented here by strain Ru1^T) has only ever been successfully isolated from one bovine rumen sample (Evans *et al.,* 2011b; Evans *et al.,* 2012). Constraints of time and the cost of expensive culture conditions have precluded further investigations beyond the scope of this study. Further work would therefore be required to investigate the presence of *T. ruminis* across a larger number of bovine GI tract samples and to subsequently identify any potential inter-species strain variation. As previously discussed, an uncultured bovine rumen bacterium *16S rRNA* gene clone, R-ACA152 (Y. Kobayashi, unpublished; Genbank accession number AB614799) appears to represent another strain of *T. ruminis* and so further genotypic and phenotypic characterisations would be required to determine whether this is indeed the case.

Due to time constraints beyond the scope of this project, the minimal medium required for sufficient growth of *T. ruminis* strain Ru1^T could not be determined. Further work is required to determine the minimal medium requirements of *T. ruminis* and, in particular, it would be of interest to determine whether OMIZ-pat medium, which is commonly used for the growth of other GI treponemes (Nordhoff *et al.,* 2005; Schrank *et al.,* 1999), would support *T. ruminis* growth. The present study also determined that the addition of serum supplementation was not required for treponeme growth; however, it is not known if the addition of ruminal fluid (which is commonly used to supplement growth of GI treponemes) or other nutrients, beyond those found within OTEB, would enhance growth.

Although beyond the scope of the current study, analysis of the genome and proteome of *T. ruminis* would provide a more detailed characterisation of this novel species and would hope to elucidate a functional role for treponemes within the bovine GI tract. These studies are currently part of on-going projects within the research group and hope to inform genotypic and functional characterisation of *T. ruminis* in the future.

The novel spirochaete characterised as part of this study was one of seven isolated from the bovine GI tract (Evans *et al.,* 2011b); however, aside from strain CHPA, which has recently been proposed as *T. rectale* DSM 103679^T, these have yet to be formally characterised. Further characterisation of these spirochaete isolates would be highly beneficial for determining phenotypic and genotypic variation between species of the bovine GI tract as

currently there are very few that have been fully characterised (Newbrook *et al.,* 2017; Paster & Canale-Parola, 1985; Stanton & Canale-Parola, 1980; Staton *et al.,* 2017). Furthermore, such studies would provide further indication and evidence of the functional of these treponemes within the bovine GI tract.

7.5 Final conclusions

The studies presented in this thesis have made significant advances in increasing previously limited knowledge of the pathogenic mechanisms underlying BDD and provide promising new avenues for future research within this field. The novel bovine fibroblast and keratinocyte monolayer cell culture models characterised during this study are a valuable tool for future host-pathogen interaction studies of BDD. This study is the first to report significant differences between the inflammatory dysregulation of bovine foot skin cells induced by the three predominant phylogroups of BDD treponemes. Furthermore, the characterisation of a novel commensal treponeme provides a useful tool for important comparisons between commensal and pathogenic treponemes; both in terms of elucidating pathogenic mechanisms and for informing functionality of these relatively unstudied GI tract treponemes. Finally, many of the novel gene targets identified by comparative transcriptomics, and the highly conserved novel OMP identified during this study, each present as potentially important future targets for the development of novel therapeutics and vaccines against BDD infection.

References

Abdi, H. and Williams, L.J. (2010) 'Principle component analysis', *Wiley Interdisciplinary Reviews: Computational Statistics,* 2(4), pp. 433-459.

Abler, L.L., Mehta, V., Keil, K.P., Joshi, P.S., Flucus, C.L., Hardin, H.A., Schmitz, C.T. and Vezina, C.M. (2011) 'A high throughput *in situ* hybridization method to characterize mRNA expression patterns in the fetal mouse lower urogenital tract', *Journal of Visualized Experiments,* 54, pp. 2912.

Adachi, J., Waddell, P.J., Martin, W. and Hasegawa, M. (2000) 'Plastid genome phylogeny and a model of amino acid substitution for proteins encoded by chloroplast DNA', *Journal of Molecular Evolution,* 50(4), pp. 348-358.

Adeolu, M. and Gupta, R.S. (2014) 'A phylogenomic and molecular marker based proposal for the division of the genus *Borrelia* into two genera: the emended genus *Borrelia* containing only the members of the relapsing fever *Borrelia,* and the genus *Borreliella* gen. nov. containing members of the Lyme disease *Borrelia* (*Borrelia burgdorferi* sensu lato complex)', *Antonie van Leeuwenhoek,* 105, pp. 1049-1074.

Adler, B. and de la Peña Moctezuma, A. (2010) 'Leptospira and leptospirosis', *Veterinary Microbiology,* 140, pp. 287-296.

Afgan, E., Baker, D., van den Beek, M., Blankenberg, D., Bouvier, D., Čech, M., Chilton, J., Clements, D., Coraor, N., Eberhard, C., Grüning, B., Guerler, A., Hillman-Jackson, J., Von Kuster, G., Rasche, E., Soranzo, N., Turaga, N., Taylor, J., Nekrutenko, A. and Goecks, J. (2016) 'The Galaxy platform for accessible, reproducible and collaborative biomedical analyses: 2016 update', *Nucleic Acids Research*, 44(W1), pp. W3-W10.

Aken, B.L., Achuthan, P., Akanni, W., Amode, M.R., Bernsdorff, F., Bhai, J., Billis, K., Carvalho-Silva, D., Cummins, C., Clapham, P., Gil, L., Girón, C.G., Gordon, L., Hourlier, T., Hunt, S.E., Janacek, S.H., Juettemann, T., Keenan, S., Laird, M.R., Lavidas, I., Maurel, T., McLaren, W., Moore, B., Murphy, D.N., Nag, R., Newman, V., Nuhn, M., Ong, C.K., Parker, A., Patricio, M., Riat, H.S., Sheppard, D., Sparrow, H., Taylor, K., Thormann, A., Vullo, A., Walts, B., Wilder, S.P., Zadissa, A., Kostadima, M., Martin, F.J., Muffato, M., Perry, E., Ruffier, M., Staines, D.M., Trevanion, S.J., Cunningham, F., Yates, A., Zerbino, D.R. and Flicek, P. (2017) 'Ensembl 2017', *Nucleic Acids Research,* 45(D1), pp. D635-D642.

Akkoc, A., Kahraman, M.M., Vatansever, A., Gunaydin, E. and Akdesir, E. (2016) 'Lipopolysaccharide (LPS) induces matrix metalloproteinase-2 and -9 (MMP-2 and MMP-9) in bovine dermal fibroblasts', *Pakistan Veterinary Journal,* 36(2), pp. 189-193.

Alawneh, J.I., Laven, R.A. and Stevenson, M.A. (2011) 'The effect of lameness on the fertility of dairy cattle in a seasonally breeding pasture-based system', *Journal of Dairy Science*, 94(11), pp. 5487-5493.

Alban, L. (1995) 'Lameness in Danish dairy cows: frequency and possible risk factors', *Preventive Veterinary Medicine,* 22(3), pp. 213-225.

Alderete, J.F. and Baseman, J.B. (1979) 'Surface-associated host proteins on virulent *Treponema pallidum*', *Infection and Immunity,* 26(3), pp. 1048-1056.

Altschul, S.F., Gish, W., Miller, W., Myers, E.W. and Lipman, D.J. (1990) 'Basic local alignment search tool', *Journal of Molecular Biology*, 215(3), pp. 403-410.

Alva, V., Nam, S.Z., Söding, J., Lupas, A.N. (2016) 'The MPI bioinformatics toolkit as an integrative platform for advanced protein sequence and structure analysis', *Nucleic Acids Research,* 44(W1), W410-W415.

Amory, J.R., Barker, Z.E., Wright, J.L., Mason, S.A., Blowey, R.W. and Green, L.E. (2008) 'Associations between sole ulcer, white line disease and digital dermatitis and the milk yield of 1824 dairy cows on 30 dairy cow farms in England and Wales from February 2003-November 2004', *Preventive Veterinary Medicine*, 83(3-4), pp. 381-391.

Ando, N., Nakamura, Y., Aoki, R., Ishimaru, K., Ogawa, H., Okumura, K., Shibata, S., Shimada, S. and Nakao, A. (2015) 'Circadian gene *clock* regulates psoriasis-like skin inflammation in mice', *Journal of Investigative Dermatology,* 135(12), pp. 3001-3008.

Antal, G.M., Lukehart, S.A. and Meheus, A.Z. (2002) 'The endemic treponematoses', *Microbes and Infection,* 4(1), pp. 83-94.

Argáez-rodríguez, F.J., Hird, D.W., Hernández de Anda, J., Read, D.H. and Rodríguez-Lainz, A. (1997) 'Papillomatous digital dermatitis on a commercial dairy farm in Mexicali, Mexico: incidence and effect on reproduction and milk production', *Preventive Veterinary Medicine*, 32(3-4), pp. 275-286.

Arnoux, V., Côme, C., Kusewitt, D.F., Hudson, L.G. and Savagner, P. (2005) 'Cutaneous wound reepithelialization: a partial and reversible EMT.' In: Savagner, P. Rise and Fall of Epithelial Phenotype: concepts of epithelial-mesenchymal transition, Molecular Biology Intelligence Unit, 2005 edition, Boston, MA: Springer, pp. 111-134.

Asai, Y., Jinno, T. and Ogawa, T. (2003) 'Oral treponemes and their outer membrane extracts activate human gingival epithelial cells through Toll-like receptor 2', *Infection and Immunity,* 71(2), pp. 717-725.

Aspenström, P. (2002) 'The WASP-binding protein WIRE has a role in the regulation of the actin filament system downstream of the platelet-derived growth factor receptor', *Experimental Cell Research,* 279(1), pp. 21-33.

Atac, B., Wagner, I., Horland, R., Lauster, R., Marx, U., Tonevitsky, A.G., Azar, R.P. and Lindner, G. (2013) 'Skin and hair on-a-chip: *in vitro* skin models versis *ex vivo* tissue maintenance with dynamic perfusion', *Lab Chip,* 13(18), pp. 3555-3561.

Ayello, E.A., Levine, J.M., LeBlanc, K. and Tomic-Canic, M. (2016) 'Skin anatomy and physiology.' [Online] Available at https://nursekey.com/skin-an-essential-organ/ (Accessed: 21st July 2017).

Ayroldi, E., Migliorati, G., Bruscoli, S., Marchetti, C., Zollo, O., Cannarile, L., D'Adamio, F. and Riccardi, C. (2001) 'Modulation of T-cell activation by the glucocorticoid-induced leucine zipper factor via inhibition of nuclear factor κB', *Blood,* 98(3), pp. 743-753.

Baehni, P.C., Song, M., McCulloch, C.A.G. and Ellen, R.P. (1992) '*Treponema denticola* induces actin rearrangement and detachment of human gingival fibroblasts', *Infection and Immunity,* 60(8), pp. 3360-3368.

Bacha, W.J., and Bacha, L.M. (2012) 'Colour atlas of veterinary histology.' 3rd edition. Basel, Switzerland: John Wiley and Sons, pp. 105-106.

Bagos, P.G., Liakopoulos, T.D., Spyropoulos, I.C. and Hamodrakas, S.J. (2004a) 'PRED-TMBB: a web server for predicting the topology of beta-barrel outer membrane proteins', *Nucleic Acids Research,* 32(web server issue), pp. W400-W404.

Bagos, P.G., Liakopoulos, T.D., Spyropoulos, I.C. and Hamodrakas, S.J. (2004b) 'A hidden Markov model method, capable of predicting and discriminating beta-barrel outer membrane proteins', *BMC Bioinformatics,* 5(29), pp. 1-13.

Baker, M. (2016) 'Reproducibility: respect your cells', *Nature,* 537, pp. 433-435.

Balint, R., Richardson, S.M. and Cartmell, S.H. (2015) 'Low-density subculture: a technical note on the importance of avoiding cell-to-cell contact during mesenchymal stromal cell expansion', *Journal of Tissue Engineering and Regenerative Medicine,* 9(10), pp. 1200-1203.

Bamias, G., Martin, C., Marini, M., Hoang, S., Mishina, M., Ross, W.G., Sachedina, M.A., Friel, C.M., Mize, J., Bickston, S.J., Pizarro, T.T., Wei, P. and Cominelli, F (2003) 'Expression, localization, and functional activity of TL1A, a novel Th1-polarizing cytokine in inflammatory bowel disease', *The Journal of Immunology,* 171(9), pp. 4868-4874.

Bankhead, T. and Chaconas, G. (2007) 'The role of VlsE antigenic variation in the Lyme disease spirochete: persistence through a mechanism that differs from other pathogens, 65(6), pp. 1547-1558.

Barbosa, A.S., Abreu, P.A.E., Vasconcellos, S.A., Morais, Z.M., Gonçales, A.P., Silva, A.S., Daha, M.R. and Isaac, L. (2009) 'Immune evasion of *Leptospira* species by acquisition of human complement regulator C4BP', *Infection and Immunity,* 77(3), pp. 1137-1143.

Barbosa, A.S., Monaris, D., Silva, L.B., Morais, Z.M., Vasconcellos, S.A., Cianciarullo, A.M., Isaac, L. and Abreu, P.A.E. (2010) 'Functional characterisation of LcpA, a surface-exposed protein of *Leptospira* spp. that binds the human complement regulator C4BP', *Infection and Immunity,* 78(7), pp. 3207-3216.

Barker, Z.E., Leach, K.A., Whay, H.R., Bell, N.J. and Main, D.C.J. (2010) 'Assessment of lameness prevalence and associated risk factors in dairy herds in England and Wales', *Journal of Dairy Science*, 93(3), pp. 932-941.

Becker, J., Steiner, A., Kohler, S., Koller-Bähler, A., Wüthrich, M. and Reist, M. (2014) 'Lameness and foot lesions in Swiss dairy cows: II. Risk factors', *Schweizer Archiv fur Tierheilkunde*, 156(2), pp. 79-89.

Beher, M.G., Schnaitman, C.A. and Pugsley, A.P. (1980) 'Major heat-modifiably outer membrane protein in Gram-negative bacteria: comparison with the OmpA protein of *Escherichia coli', Journal of Bacteriology,* 143(2), pp. 906-913.

Bell, N.J., Blowey, R.W., Reader, J.D., Laven, R.A. and Smith, R. (2013) 'Clinical Forum: Digital dermatitis: treatment and control', *Livestock,* 18(2), pp. 6-12.

Bellet, M.M., Beriu, E., Liu, J.Z., Grimaldi, B., Blaschitz, C., Zeller, M., Edwards, R.A., Sahar, S., Dandekar, S., Baldi, P., George, M.D., Raffatellu, M. and Sassone-Corsi, P. (2013) 'Circadian clock regulates the host response to *Salmonella', Proceedings of the National Academy of Sciences of the United States of America,* 110(24), pp. 9897-9902.

Bermudes, D., Chase, D. and Margulis, L. (1988) 'Morphology as a basis for taxonomy of large spirochetes symbiotic in wood-eating cockroaches and termites: *Pillotina* gen. nov., nom. rev.; *Pillotina calotermitidis* sp. nov., nom. rev.; *Diplocalyx* gen. nov., nom. rev.; *Diplocalyx calotermitidis* sp. nov., nom. rev.; *Hollandina* gen. nov., nom. rev.; *Hollandina pterotermitidis* sp. nov., nom. rev.; and *Clevelandina reticulitermitidis* gen. nov., sp. nov.', *International Journal of Systematic and Evolutionary Microbiology,* 38, pp. 291-302.

Berrebi, D., Bruscoli, S., Cohen, N., Foussat, A., Migliorati, G., Bouchet-Delbos, L., Maillot, M.C., Portier, A., Couderc, J., Galanaud, P., Peuchmaur, M., Riccardi, C. and Emilie, D. (2003)

'Synthesis of glucocorticoid-induced leucine zipper (GILZ) by macrophages: an anti-inflammatory and immunosuppressive mechanism shared by glucocorticoids and IL10', *Blood,* 101(2), pp. 729-738.

Berry, S.L., Ertze, R.A., Read, D.H., Hird, D.W. (2004) 'Field evaluaton of prophylactic and therapeutic effects of a vaccine against (papillomatous) digital dermatitis of dairy cattle in two Californian dairies.' In: *Proceedings of the 13th International Symposium and Conference on Lameness in Ruminants.* Maribor, Slovenija, pp. 147.

Berry, S.L., Read, D.H., Famula, T.R., Mongini, A. and Döpfer, D. (2012) 'Long-term observations on the dynamics of bovine digital dermatitis lesions on a California dairy after topical treatment with lincomycin HCl', *The Veterinary Journal,* 193(3), pp. 654-658.

Berry, S.L., Read, D.H., Walker, R.L. and Famula, T.R. (2010) 'Clinical, histologic, and bacteriologic findings in dairy cows with digital dermatitis (footwarts) one month after topical treatment with lincomycin hydrochloride or oxytetracycline hydrochloride', *Journal of the American Veterinary Medical Association,* 237(5), pp. 555-560.

Berven, F.S., Flikka, K., Jensen, H.B. and Eidhammer, I. (2004) 'BOMP: a program to predict integral beta-barrel outer membrane proteins encoded within genomes of Gram-negative bacteria', *Nucleic Acids Research,* 32(web server issue), pp. W394-W399.

Bevelacqua, V., Libra, M., Mazzarino, M.C., Gangemi, P., Nicotra, G., Curatolo, S., Massimino, D., Plumari, A., Merito, P., Valente, G., Stivala, F., La Greca, S. and Malaponte, G. (2006) 'Long pentraxin 3: a marker of inflammation in untreated psoriatic patients', *International Journal of Molecular Medicine,* 18(3), pp. 415-423.

Bhardwaj, A.R., Pandey, R., Agarwal, M. and Katiyar-Agarwal, S. (2012) 'Northern blot analysis for expression profiling of mRNAs and small RNAs', *Methods in Molecular Biology,* 883, pp. 19-45.

Bicalho, R.C., Vokey, F., Erb, H.N. and Guard, C.L. (2007) 'Visual locomotion scoring in the first seventy days in milk: impact on pregnancy and survival', *Journal of Dairy Science,* 90(10), pp. 4586-4591.

Biddle, D. and Spandau, D.F. (1996) 'Expression of vimentin in cultured human keratinocytes is associated with cell-extracellular matrix junctions', *Archives of Dermatological Research,* 288(10), pp. 621-624.

Birch-Andersen, A., Hovind Hougen, K., Borg-Petersen, C. (1973) 'Electron microscopy of *Leptospira*', APMIS, 81B(6), pp. 665-676.

Bitto, E. and McKay, D.B. (2002) 'Crystallographic structure of SurA, a molecular chaperone that facilitates folding of outer membrane porins', *Structure,* 10(11), pp. 1489-1498.

Blankenberg, D., Gordon, A., Von Kuster, G., Coraor, N., Taylor, J., Nekrutenko, A. and the Galaxy Team. (2010) 'Manipulation of FASTQ data with Galaxy', *Bioinformatics,* 26(14), pp. 1783-1785.

Blomström, A.L., Gu, Q., Barry, G., Wilkie, G., Skelton, J.K., Baird, M., McFarlane, M., Schnettler, E., Elliott, R.M., Palmarini, M. and Kohl, A. (2015) 'Transcriptome analysis reveals the host response to Schmallenberg virus in bovine cells and antagonistic effects of the NSs protein', *BMC Genomics,* 16, pp. 324.

Blowey, R.W. and Sharp, M.W. (1988) 'Digital dermatitis in dairy cattle', *Veterinary Record*, 122(21), pp. 505-508.

Blumberg, H., Dinh, H., Trueblood, E.S., Pretorius, J., Kugler, D., Weng, N., Kanaly, S.T., Towne, J.E., Willis, C.R., Kuechle, M.K., Sims, J.E. and Peschon, J.J. (2007) 'Opposing activities of two novel members of the IL-1 ligand family regulates skin inflammation', *The Journal of Experimental Medicine,* 204(11), pp. 2603-2614.

Boehringer, H., Taichman, N.S. and Shenker, B.J. (1984) 'Suppression of fibroblast proliferation by oral spirochaetes', *Infection and Immunity,* 45(1), pp. 155-159.

Bonnet, M.C., Preukschat, D., Welz, P.S., van Loo, G., Ermolaeva, M.A., Bloch, W., Haase, I. and Pasparakis, M. (2011) 'The adaptor protein FADD protects epidermal keratinocytes from necroptosis *in vivo* and prevents skin inflammation', *Immunity,* 35(4), pp. 572-582.

Borgmann, I.E., Bailey, J. and Clark, E.G. (1996) 'Spirochete-associated bovine digital dermatitis', *The Canadian Veterinary Journal*, 37(1), pp. 35-37.

Bouquet, J., Soloski, M.J., Swei, A., Cheadle, C., Federman, S., Billaud, J.N., Rebman, A.W., Kabre, B., Halpert, R., Boorgula, M., Aucott, J.N. and Chiu, C.Y. (2016) 'Longitudinal transcriptome analysis reveals a sustained differential gene expression signature in patients treated for acute Lyme disease', *MBio,* 7(1), pp. e00100-e00116.

Bowdish, D.M.E., Davidson, D.J., Scott, M.G. and Hancock, R.E.W. (2005) 'Immunomodulatory activities of small host defense peptides', *Antimicrobial Agents and Chemotherapy,* 49(5), pp. 1727-1732.

Bøvelstad, H.M., Holsbø, E., Bongo, L.A. and Lund, E. (2017) 'A standard operating procedure for outlier removal in large-sample epidemiological transcriptomics datasets', *Cold Spring Harbor Laboratory*, In Press.

Braff, M.H., Di Nardo, A. and Gallo, R.L. (2005a) 'Keratinocytes store the antimicrobial peptide cathelicidin in lamellar bodies', *Journal of Investigative Dermatology,* 124(2), pp. 394-400.

Braff, M.H., Zaiou, M., Fierer, J., Nizet, V. and Gallo, R.L. (2005b) 'Keratinocyte production of cathelicidin provides direct activity against bacterial skin pathogens', *Infection and Immunity,* 73(10), pp. 6771-6781.

Brandt, S., Apprich, V., Hackl, V., Tober, R., Danzer, M., Kainzbauer, C., Gabriel, C., Stanek, C. and Kofler, J. (2011) 'Prevalence of bovine papillomavirus and *Treponema* DNA in bovine digital dermatitis lesions', *Veterinary Microbiology,* 148(2-4), pp. 161-167.

Brembilla, N.C., Montanari, E., Truchetet, M.E., Raschi, E., Meroni, P. and Chizzolini, C. (2013) 'Th17 cells favour inflammatory responses while inhibiting type I collagen deposition by dermal fibroblasts: differential effects in healthy and systemic sclerosis fibroblasts', *Arthritis Research and Therapy,* 15(5), pp. R151.

Brinkman, F.S.L., Bains, M. and Hancock, R.E.W. (2000) 'The amino acid terminus of *Pseudomonas aeruginosa* outer membrane protein OprF forms channels in lipid bilayer membranes: correlation with a three-dimensional model', *Journal of Bacteriology,* 182(18), pp. 5251-5255.

Brissette, C.A., Bykowski, T., Cooley, A.E., Bowman, A. and Stevenson, B. (2009a) '*Borrelia burgdorferi* RevA antigen binds host fibronectin', *Infection and Immunity,* 77(7), pp. 2802-2812.

Brissette, C.A., Haupt, K., Barthel, D., Cooley, A.E., Bowman, A., Skerka, C., Wallich, R., Zipfel, P.F., Kraiczy, P. and Stevenson, B. (2009c) '*Borrelia burgdorferi* infection-associated surface

proteins ErpP, ErpA, and ErpC bind human plasminogen', *Infection and Immunity,* 77(1), pp. 300-306.

Brissette, C.A., Verma, A., Bowman, A., Cooley, A.E. and Stevenson, B. (2009b) 'The *Borrelia burgdorferi* outer-surface protein ErpX binds mammalian laminin', *Microbiology,* 155(Pt3), pp. 863-872.

Britt, J.S., Gaska, J., Garrett, E.F., Konkle, D. and Mealy, M. (1996) 'Comparison of topical application of three products for treatment of papillomatous digital dermatitis in dairy cattle', *Journal of the American Veterinary Medical Association,* 209(6), pp. 1134-1136.

Brozovic, S., Sahoo, R., Barve, S., Shiba, H., Uriarte, S., Blumberg, R.S. and Kinane, D.F. (2006) '*Porphyromonas gingivalis* enhances FasL expression via up-regulation of NF-κB-mediated gene transcription and induces apoptotic cell dealth in human gingival epithelial cells', *Microbiology,* 152, pp. 797-806.

Brown, C.C., Kilgo, P.D. and Jacobsen, K.L. (2000) 'Prevalence of papillomatous digital dermatitis among culled adult cattle in the southeastern United States', *American Journal of Veterinary Research*, 61(8), pp. 928-930.

Bruijnis, M.R.N., Beerda, B., Hogeveen, H. and Stassen, E.N. (2012) 'Assessing the welfare impact of foot disorders in dairy cattle by a modelling approach', *Animal,* 6(6), pp. 962-970.

Bruijnis, M.R.N., Hogeveen, H. and Stassen, E.N. (2010) 'Assessing economic consequences of foot disorders in dairy cattle using a dynamic stochastic simulation model', *Journal of Dairy Science,* 93(6), pp. 2419-2432.

Buchanan, R.E. (1917) 'Studies in the nomenclature and classification of the bacteria. II. The primary subdivisions of the *Schizomycetes*', *Journal of Bacteriology,* 2(2), pp. 155-164.

Burchill, M.A., Nardelli, D.T., England, D.M., DeCoster, D.J., Christopherson, J.A., Callister, S.M. and Schell, R.F. (2003) 'Inhibition of interleukin-17 prevents the development of arthritis in vaccinated mice challenged with *Borrelia burgdorferi', Infection and Immunity,* 71(6), pp. 3437-3442.

Burgdorfer, W., Barbour, A.G., Hayes, S.F., Benach, J.L., Grunwaldt, E. and Davis, J.P. (1982) 'Lyme disease-a tick-borne spirochetosis?', *Science,* 216(4552), pp. 1317-1319.

Burgeson, R.E. and Christiano, A.M. (1997) 'The dermal-epidermal junction', *Current Opinion in Cell Biology,* 9(5), pp. 651-658.

Burman, N., Shamaei-Tousi, A. and Bergström, S. (1998) 'The spirochete *Borrelia crocidurae* causes erythrocyte resetting during relapsing fever', *Infection and Immunity,* 66(2), pp. 815-819.

Byun, J.W., Park, I.S., Choi, G.S. and Shin, J. (2016) 'Role of fibroblast-derived factors in the pathogenesis of melasma', *Clinical and Experimental Dermatology,* 41(6), pp. 601-609.

Cameron, C.E. (2003) 'Identification of a *Treponema pallidum* laminin-binding protein', *Infection and Immunity,* 71(5), pp. 2525-2533.

Campbell, I. (2017) 'Protective mechanisms of the body', *Anaesthesia and Intensive Care Medicine,* 18(3), pp. 138-140.

Campos, M.A., Vargas, M.A., Regueiro, V., Llompart, C.M., Albertí, S. and Bengoechea, J.A. (2004) 'Capsule polysaccharide mediates bacterial resistance to antimicrobial peptides', *Infection and Immunity,* 72(12), pp. 7107-7114.

Capion, N., Boye, M., Ekstrøm, C.T. and Jensen, T.K. (2012) 'Infection dynamics of digital dermatitis in first-lactation Holstein cows in an infected herd', *Journal of Dairy Science,* 95(11), pp. 6457-6464.

Capion, N., Thamsborg, S.M. and Enevoldsen, C. (2008) 'Prevalence of foot lesions in Danish Holstein cows', *Veterinary Record*, 163(3), pp. 80-86.

Carrier, Y., Ma, H.L., Ramon, H.E., Napierata, L., Small, C., O'Toole, M., Young, D.A., Fouser, L.A., Nickerson-Nutter, C., Collins, M., Dunussi-Joannopoulos, K. and Medley, Q.G. (2011) 'Inter-regulation of Th17 cytokines and the IL-36 cytokines *in vitro* and *in vivo:* implications in psoriasis pathogenesis', *Journal of Investigative Dermatology,* 131(12), pp. 2428-2437.

Carvalho, A.L., Goyal, A., Prates, J.A.M., Bolam, D.N., Gilbert, H.J., Pires, V.M.R., Ferreira, L.M.A., Planas, A., Romão, M.J. and Fontes, C.M.G.A. (2004) 'The family 11 carbohydrate-binding module of *Clostridium thermocellum* Lic26A-Cel5E accommodates β-1,4- and β-1,3-1,4-mixed linked glucans at a single binding site', *The Journal of Biological Chemistry,* 279(33), pp. 34785-34793.

Castro-Muñozledo, F., Velez-delValle, C., Marsch-Moreno, M., Hernández-Quintero, M. and Kuri-Harcuch, W. (2015) 'Vimentin is necessary for colony growth of human diploid keratinocytes', *Histochemistry and Cell Biology,* 143(1), pp. 45-57.

Caswell, J.L., Middleton, D.M. and Gordon, J.R. (1999) 'Production and functional characterization of recombinant bovine interleukin-8 as a specific neutrophil activator and chemoattractant', *Veterinary Immunology and Immunopathology,* 67(4), pp. 327-340.

Cavalier-Smith, T. (2002) 'The neomuran origin of archaebacteria, the negibacterial root of the universal tree and bacterial megaclassification', *International Journal of Systematic and Evolutionary Microbiology,* 52, pp. 7-76.

Cekici, A., Kantarci, A., Hasturk, H. and van Dyke, T.E. (2014) 'Inflammatory and immune pathways in the pathogenesis of periodontal disease', *Periodontal 2014,* 64(1), pp. 57-80.

Centurion-Lara, A., Godornes, C., Castro, C., Van Voorhis, W.C. and Lukehart, S.A. (2000a) 'The tprK gene is heterogeneous among *Treponema pallidum* strains and has multiple alleles', *Infection and Immunity,* 68(2), pp. 824-831.

Centurion-Lara, A., Sun, E.S., Barrett, L.K., Castro, C., Lukehart, S.A. and van Voorhis, W.C. (2000b) 'Multiple alleles of *Treponema pallidum* repeat gene D in *Treponema pallidum* isolates', *Journal of Bacteriology,* 182(8), pp. 2332-2335.

Centurion-Lara, A., LaFond, R.E., Hevner, K., Godornes, C., Molini, B.J., Van Voorhis, W.C. and Lukehart, S.A. (2004) 'Gene conversion: a mechanism for generation of heterogeneity in the tprK gene of *Treponema pallidum* during infection', *Molecular Microbiology,* 52(6), pp. 1579-1596.

Cha, E., Hertl, J.A., Bar, D. and Gröhn, Y.T. (2010) 'The cost of different types of lameness in dairy cows calculated by dynamic programming', *Preventive Veterinary Medicine,* 97(1), pp. 1-8.

Chapinal, N., Liang, Y., Weary, D.M., Wang, Y. and von Keyserlingk, M.A.G. (2014) 'Risk factors for lameness and hock injuries in Holstein herds in China', *Journal of Dairy Science,* 97(7), pp. 4309-4316.

Chapinal, N., Barrientos, A.K. von Keyserlingk, M.A.G., Galo, E. and Weary, D.M. (2013) 'Herd-level risk factors for lameness in freestall farms in the NorthEastern United States and California', *Journal of Dairy Science,* 96(1), pp. 318-328.

Charnock, S.J., Bolam, D.N., Turkenburg, J.P., Gilbert, H.J., Ferreira, L.M.A., Davies, G.J. and Fontes, C.M.G.A. (2000) 'The X6 "thermostabilizing" domains of xylanases are carbohydrate-binding modules: structure and biochemistry of the *Clostridium thermocellum* X6b domain', *Biochemistry,* 39(17), pp. 5013-5021.

Cheli, R. and Mortellaro, C. (1974) 'Digital dermatitis in cattle.' In: *Proceedings of the 8th International Conference on Diseases of Cattle.* Milan, Italy, pp. 208-213.

Chen, T. and Gotschlich, E.C. (1996) 'CGM1a antigen of neutrophils, a receptor of gonococcal opacity proteins', *Proceedings of the National Academy of Sciences of the United States of America,* 93(25), pp. 14851-14856.

Choi, B.K., Nattermann, H., Grund, S., Haider, W. and Göbel, U.B. (1997) 'Spirochetes from digital dermatitis lesions in cattle are closely related to treponemes associated with human periodontitis', *International Journal of Systematic and Evolutionary Bacteriology*, 47(1), pp. 175-181.

Choi, C.Y., Rho, S.B., Kim, H.S., Han, J., Bae, J., Lee, S.J., Jung, W.W. and Chun, T. (2015) 'The ORF3 protein of porcine circovirus type 2 promotes secretion of IL-6 and IL-8 in porcine epithelial cells by facilitating proteasomal degradation of regulator of G protein signalling 16 through physical interaction', *Journal of General Virology,* 96(Pt5), pp. 1098-1108.

Choy, H.A., Kelley, M.M., Chen, T.L., Møller, A.K., Matsunaga, J. and Haake, D.A. (2007) 'Physiological osmotic induction of *Leptospira interrogans* adhesion: LigA and LigB bind extracellular matrix proteins and fibrinogen', *Infection and Immunity,* 75(5), pp. 2441-2450.

Chu, L., Burgum, A., Kolodrubetz, D. and Holt, S.C. (1995) 'The 46-kilodalton-hemolysin gene from *Treponema denticola* encodes a novel hemolysin homologous to aminotransferases', *Infection and Immunity,* 63(11), pp. 4448-4455.

Chu, L., Song, M. and Holt, S.C. (1994) 'Effect of iron regulation on expression and hemin-binding function of outer-sheath proteins from *Treponema denticola', Microbial Pathogenesis,* 16(5), pp. 321-335.

Chua, P.K., Corkill, J.E., Hooi, P.S., Cheng, S.C., Winstanley, C. and Hart, C.A. (2005) 'Isolation of *Waddlia malaysiensis*, a novel intracellular bacterium, from fruit bat (*Eonycteris spelaea*)', *Emerging Infectious Diseases*, 11(2), pp. 271-277.

Clausen, M.L., Jungersted, J.M., Andersen, P.S., Slotved, H.C., Krogfelt, K.A. and Agner, T. (2013) 'Human β-defensin-2 as a marker for disease severity and skin barrier properties in atopic dermatitis', *The British Journal of Dermatology,* 169(3), pp. 587-593.

Clegg, S.R., Bell, J., Ainsworth, S., Blowey, R.W., Bell, N.J., Carter, S.D. and Evans, N.J. (2016a) 'Isolation of digital dermatitis treponemes from cattle hock skin lesions', *Veterinary Dermatology,* 27(2), pp. 106-e30

Clegg, S.R., Carter, S.D., Birtles, R.J., Brown, J.M., Hart, C.A. and Evans, N.J. (2016d) 'Multilocus sequence typing of pathogenic treponemes isolated from cloven-hoofed animals and comparison to treponemes isolated from humans', *Applied and Environmental Microbiology,* 82(15), pp. 4523-4536.

Clegg, S.R., Carter, S.D., Stewart, J.P., Amin, D.M., Blowey, R.W. and Evans, N.J. (2016c) 'Bovine ischaemic teat necrosis: a further potential role for digital dermatitis treponemes', *The Veterinary Record,* 178(3), pp.71.

Clegg, S.R., Crosby-Durrani, H.E., Bell, J., Blundell, R., Blowey, R.W., Carter, S.D. and Evans, N.J. (2016e) 'Detection and isolation of digital dermatitis treponemes from bovine pressure sores', *Journal of Comparative Pathology,* 154(4), pp. 273-282.

Clegg, S.R., Mansfield, K.G., Newbrook, K., Sullivan, L.E., Blowey, R.W., Carter, S.D. and Evans, N.J. (2015) 'Isolation of digital dermatitis treponemes from hoof lesions in wild North American elk (*Cervus elaphus*) in Washington State, USA', *Journal of Clinical Microbiology*, 53(1), pp. 88-94.

Clegg, S.R., Sullivan, L.E., Bell, J., Blowey, R.W., Carter, S.D. and Evans, N.J. (2016b) 'Detection and isolation of digital dermatitis treponemes from skin and tail lesions in pigs', *Research in Veterinary Science,* 104, pp. 64-70.

Clements, D.N., Vaughan-Thomas, A., Peansukmanee, S., Carter, S.D., Innes, J.F., Ollier, W.E.R. and Clegg, P.D. (2006) 'Assessment of the use of RNA quality metrics for the screening of articular cartilage specimens from clinically normal dogs and dogs with osteoarthritis', *American Journal of Veterinary Research,* 67(8), pp. 1438-1444.

Coghill, I.D., Brown, S., Cottle, D.L., McGrath, M.J., Robinson, P.A., Nandurkar, H.H., Dyson, J.M. and Mitchell, C.A. (2003) 'FHL3 is an actin-binding protein that regulates α-actinin-mediated actin bundling: FHL3 localizes to actin stress fibres and enhances cell spreading and stress fiber disassembly', *Journal of Biological Chemistry,* 278(26), pp. 24139-24152.

Coleman, J.L., Roemer, E.J. and Benach, J.L. (1999) 'Plasmin-coated *Borrelia burgdorferi* degrades soluble and insoluble components of the mammalian extracellular matrix', *Infection and Immunity,* 67(8), pp. 3929-3936.

Collighan, R.J. and Woodward, M.J. (1997) 'Spirochaetes and other bacterial species associated with bovine digital dermatitis', *FEMS Microbiology Letters,* 156(1), pp. 37-41.

Colonna, M. (2003) 'TREMS in the immune system and beyond', *Nature Reviews,* 3(6), pp. 445-453.

Conde, J., Scotece, M., Abella, V., Lois, A., López, V., García-Caballero, T., Pino, J., Gómez-Reino, J.J., Gómez, R., Lago, F. and Gualillo, O. (2015) 'IL-36α: a novel cytokine involved in the catabolic and inflammatory response in chondrocytes', *Scientific Reports,* 5(16674), pp. 1-8.

Cooper, D. and Sun, T.T. (1986) 'Monoclonal antibody analysis of bovine epithelial keratin', *The Journal of Biological Chemistry,* 261(10), pp. 4646-4654.

Cormican, P., Meade, K.G., Cahalane, S., Narciandi, F., Chapwanya, A., Lloyd, A.T. and O'Farrelly, C. (2008) 'Evolution, expression and effectiveness in a cluster of novel bovine β-defensins, *Immunogenetics,* 60(3-4), pp. 147-156.

Cover, W.H., Norris, S.J. and Miller, J.N. (1982) 'The microaerophilic nature of *Treponema pallidum:* enhanced survival and incorporation of tritiated adenine under microaerobic conditions in the presence or absence of reducing compounds', *Sexually Transmitted Diseases,* 9(1), pp. 1-8.

Cronodon (2017) 'Spirochaetes.' [Online] Available at http://cronodon.com/BioTech/Bacteria_motility3.html (Accessed: 15th June 2017).

Cruz, A.R., Ramirez, L.G., Zuluanga, A.V., Pillay, A., Abreu, C., Valencia, C.A., La Vake, C., Cervantes, J.L., Dunham-Ems, S., Cartun, R., Mavilio, D., Radolf, J.D. and Salazar, J.C. (2012) 'Immune evasion and recognition of the syphilis spirochete in blood and skin of secondary syphilis patients: two immunologically distinct compartments', *PLoS Neglected Tropical Diseases,* 6(7), pp. e1717.

Cruz, C., Driemeier, D., Cerva, C. and Corbellini, L.G. (2001a) 'Bovine digital dermatitis in southern Brazil', *Veterinary Record*, 148(18), pp. 576-577.

Cruz, C., Driemeier, D., Cerva, C. and Corbellini, L.G. (2001b) 'Clinical and epidemiological aspects of bovine digital lesions in southern Brazil', *Arquivo Brasileiro de Medicina Veterinária e Zootecnia,* 53(6), pp. 654-657.

Cruz, C.E.F., Pescador, C.A., Nakajima, Y. and Driemeier, D. (2005) 'Immunopathological investigations on bovine digital epidermitis', *The Veterinary Record,* 157(26), pp. 834-840.

Cullen, P.A., Haake, D.A. and Adler, B. (2004) 'Outer membrane proteins of pathogenic spirochetes', *FEMS Microbiology Reviews,* 28, pp. 291-318.

Cwyk, W.M. and Canale-Parola, E. (1979) '*Treponema succinifaciens* sp. nov., an anaerobic spirochete from the swine intestine', *Archives of Microbiology,* 122(3), pp. 231-239.

Daehwan, K., Pertea, G., Trapnell, C., Pimentel, H., Kelley, R. and Salzberg, S.L. (2013) 'TopHat2: accurate alignment of transcriptomes in the presence of insertions, deletions and gene fusions', *Genome Biology,* 14(4), pp. R36.

Dahm, A.M., de Bruin, A., Limat, A., von Tscharner, C., Wyder, M. and Suter, M.M. (2002) 'Cultivation and characterisation of primary and subcultured equine keratinocytes', *Equine Veterinary Journal,* 34(2), pp. 114-120.

Dawson, J.C. (1998) 'Digital dermatitis - survey and debate.' In: *Proceedings of the 20th World Buiatrics Congress*. Sydney, Australia, pp. 91-93.

Dechering, K.J., Cuelenaere, K., Konings, R.N.H. and Leunissen, J.A.M. (1998) 'Distinct frequency-distributions of homopolymeric DNA tracts in different genomes', *Nucleic Acids Research,* 26(17), pp. 4056-4062.

Defosse, D.L., Johnson, R.C., Paster, B.J., Dewhirst, F.E. and Fraser, G.J. (1995) '*Brevinema andersonii* gen. nov., sp. nov., an infectious spirochete isolated from the short-tailed shrew (*Blarina brevicauda*) and the white-footed mouse (*Peromyscus leucopus*)', *International Journal of Systematic Bacteriology,* 45(1), pp. 78-84.

Desrosiers, D.C., Anand, A., Luthra, A., Dunham-Ems, S.M., LeDoyt, M., Cummings, M.A., Eshghi, A., Cameron, C.E., Cruz, A.R., Salazar, J.C., Caimano, M.J. and Radolf, J.D. (2011) 'TP0326, a *Treponema pallidum* β-barrel assembly machinery A (BamA) orthologue and rare outer membrane protein', *Molecular Microbiology,* 80(6), pp. 1496-1515.

de Vries, M., Bokkers, E.A.M., van Reenen, C.G., Engel, B., van Schaik, G., Dijkstra, T. and de Boer, I.J.M. (2015) 'Housing and management factors associated with indicators of dairy cattle welfare', *Preventive Veterinary Medicine,* 118(1), pp. 80-92.

Demirkan, I., Carter, S.D., Murray, R.D., Blowey, R.W. and Woodward, M.J. (1998) 'The frequent detection of a treponeme in bovine digital dermatitis by immunocytochemistry and polymerase chain reaction', *Veterinary Microbiology,* 60(2-4), pp. 285-292.

Demirkan, I., Carter, S.D., Winstanley, C., Bruce, K.D., McNair, N.M., Woodside, M. and Hart, C.A. (2001) 'Isolation and characterisation of a novel spirochaete from severe virulent ovine foot rot', *Journal of Medical Microbiology,* 50(12), pp. 1061-1068.

Demirkan, I., Walker, R.L., Murray, R.D., Blowey, R.W. and Carter, S.D. (1999) 'Serological evidence of spirochaetal infections associated with digital dermatitis in dairy cattle', *The Veterinary Journal,* 157(1), pp. 69-77.

Demirkan, I., Williams, H.F., Dhawi, A., Carter, S.D., Winstanley, C., Bruce, K.D. and Hart, C.A. (2006) 'Characterization of a spirochaete isolated from a case of bovine digital dermatitis', *Journal of Applied Microbiology,* 101(4), pp. 948-955.

Department for Environment Food and Rural Affairs (2017) 'Farming statistics - livestock populations at 1 December 2016, UK', *National Statistics*. [Online] Available at: https://www.gov.uk/government/statistics/farming-statistics-livestock-populations-at-1-december-2016-uk (Accessed 28th May 2017).

Devine, D.A., Marsh, P.D., Percival, R.S., Rangarajan, M. and Curtis, M.A. (1999) 'Modulation of antibacterial peptide activity by products of *Porphyromonas gingivalis* and *Prevotella* spp.', *Microbiology,* 145(Pt4), pp. 965-971.

Dewhirst, F.E., Tamer, M.A., Ericson, R.E., Lau, C.N., Levanos, V.A., Boches, S.K., Galvin, J.L. and Paster, B.J. (2000) 'The diversity of periodontal spirochetes by 16S rRNA analysis', *Oral Microbiology and Immunology,* 15(3), pp. 196-202.

Dhawi, A., Hart, C.A., Demirkan, I., Davies, I.H. and Carter, S.D. (2005) 'Bovine digital dermatitis and severe virulent ovine foot rot: a common spirochaetal pathogenesis', *The Veterinary Journal,* 169(2), pp. 232-241.

Di Nardo, A., Braff, M.H., Taylor, K.R., Na, C., Granstein, R.D., McInturff, J.E., Krutzik, S., Modlin, R.L. and Gallo, R.L. (2007) 'Cathelicidin antimicrobial peptides block dendritic cell TLR4 activation and allergic contact sensitization', *Journal of Immunology,* 178(3), pp. 1829-1834.

Dillon, L.A., Suresh, R., Okrah, K., Corrada Bravo, H., Mosser, D.M. and El-Sayed, N.M. (2015) 'Simultaneous transcriptional profiling of *Leishmania major* and its murine macrophage host cell reveals insights into host-pathogen interactions', *BMC Genomics,* 16, pp. 1108.

Diniz, S. Sandes, S.H.C., Bomfim, M.R.Q., Santos, P.C., Cruz, F.D., Moreira, T.F., Carvalho, M.R.S., Cisalpino, P.S. and Moreira, E.S.A. (2017) 'Culture and molecular identification of microorganisms from digital dermatitis lesions in diary cattle: *Leptospira,* an unexpected finding', *Arquivo Brasileiro Medicina Veterinária* e *Zootecnia,* 69(3), pp. 559-569.

Döpfer, D., Anklam, K., Mikheil, D. and Ladell, P. (2012) 'Growth curves and morphology of three *Treponema* subtypes isolated from digital dermatitis in cattle', *The Veterinary Journal,* 193(3), pp. 685-693.

Döpfer, D., Koopmans, A., Meijer, F.A., Szakáll, I., Schukken, Y.H., Klee, W., Bosma, R.B., Cornelisse, J.L., van Asten, A.J. and ter Huurne, A.A. (1997) 'Histological and bacteriological evalutation of digital dermatitis in cattle, with special reference to spirochaetes and *Campylobacter faecalis*', 140(24), pp. 620-623.

Dröge, S., Rachel, R., Radek, R. and König, H. (2008) '*Treponema isoptericolens* sp. nov., a novel spirochaete from the hindgut of the termite *Incisitermes tabogae*', *International Journal of Systematic and Evolutionary Microbiology,* 58(5), pp. 1079-1083.

Ebnet, K., Brown, K.D., Siebenlist, U.K., Simon, M.M. and Shaw, S. (1997) '*Borrelia burgdorferi* activates nuclear factor-kappa B and is a potent inducer of chemokine and adhesion molecule gene expression in endothelial cells and fibroblasts', *The Journal of Immunology,* 158(7), pp. 3285-3292.

Eddleston, J., Herschbach, J., Wagelie-Steffen, A.L., Christiansen, S.C. and Zuraw, B.L. (2007) 'The anti-inflammatory effect of glucocorticoids is mediated by glucocorticoid-induced

leucine zipper in epithelial cells', *The Journal of Allergy and Clinical Immunology,* 119(1), pp. 115-122.

Edwards, A.M., Jenkinson, H.F., Woodward, M.J. and Dymock, D. (2005) 'Binding properties and adhesion-mediating regions of the major sheath protein of *Treponema denticola* ATCC 35405', *Infection and Immunity,* 73(5), pp. 2891-2898.

Edwards, J.E., McEwan, N.R., Travis, A.J. and Wallace, R.J. (2004) '16S rDNA library-based analysis of ruminal bacterial diversity', *Antonie van Leeuwenhoek,* 86(3), pp. 263-281.

Edwards, U., Rogall, T., Blöcker, H., Emde, M. and Böttger, E.C. (1989) 'Isolation and direct complete nucleotide determination of entire genes. Characterization of a gene coding for 16S ribosomal RNA', *Nucleic Acids Research,* 17(19), pp. 7843-7853.

Ehrenberg, C.G. (1835) 'Dritter beitrag zur erkenntniss grosser organisation in der Richtung des kleinsten raumes', *Abhandlungen der Preussischen Akademie der Wissenschaften (Berlin) aus den Jahre*, pp. 143-336.

Eisen, M.B., Spellman, P.T., Brown, P.O. and Botstein, D. (1998) 'Cluster analysis and display of genome-wide expression patterns', *Proceedings of the National Academy of Sciences of the United States of America,* 95(25), pp. 14863-14868.

El-Ghoul, W. and Shaheed, B.I. (2001) 'Ulcerative and papillomatous digital dermatitis of the pastern region in dairy cattle: clinical and histopathological studies', *Deutsche tierarztliche Wochenschrift*, 108(5), pp. 216-222.

Elliot, M.K. and Alt, D.P. (2009) 'Bovine immune response to papillomatous digital dermatitis (PDD)-associated spirochetes is skewed in isolate reactivity and subclass elicitation', *Veterinary Immunology and Immunopathology,* 130(3-4), pp. 256-261.

Emerson, D., Agulto, L., Liu, H. and Liu, L. (2008) 'Identifying and characterizing bacteria in an era of genomics and proteomics', *Bioscience,* 58(10), pp. 925-936.

Engelkens, H.J., Niemel, P.L., van der Sluis, J.J., Megheus, A. and Stolz, E. (1991) 'Endemic treponematoses. Part II. Pinta and endemic syphilis', *International Journal of Dermatology,* 30(4), pp. 231-238.

Epaulard, O., Adam, L., Poux, C., Zurawski, G., Salabert, N., Rosenbaum, P., Dereuddre-Bosquet, N., Zurawski, S., Flamar, A.L., Oh, S., Romain, G., Chapon, C., Banchereau, J., Lévy, Y., Le Grand, R. and Martinon, F. (2014) 'Macrophage- and neutrophil-derived TNF-α instructs skin Langerhans cells to prime antiviral immune responses', *The Journal of Immunology,* 193(5), pp. 2416-2426.

Eswarakumar, V.P., Lax, I. and Schlessinger, J. (2005) 'Cellular signalling by fibroblast growth factor receptors', *Cytokine and Growth Factor Reviews,* 16, pp. 139-149.

Eurofins Genomics (2016) *The multifunctional oligo calculator* [Online] Ebersberg, Germany: Eurofins Genomics. Available from http://www.eurofinsgenomics.eu/en/dna-rna-oligonucleotides/oligo-design-more/oligo-property-scan.aspx (Accessed: 07 March 2016).

Evans, N.J., Blowey, R.W., Timofte, D., Isherwood, D.R., Brown, J.M., Murray, R., Paton, R.J. and Carter, S.D. (2011a) 'Association between bovine digital dermatitis treponemes and a range of 'non-healing' bovine hoof disorders', *The Veterinary Record,* 168(8), pp. 214.

Evans, N.J., Brown, J.M., Demirkan, I., Birtles, R., Hart, C.A. and Carter, S.D. (2009c) '*In vitro* susceptibility of bovine digital dermatitis associated spirochates to antimicrobial agents', *Veterinary Microbiology,* 136, pp. 115-120.

Evans, N.J., Brown, J.M., Demirkan, I., Murray, R.D., Birtles, R.J., Hart, C.A. and Carter, S.D. (2009b) '*Treponema pedis* sp. nov., a spirochaete isolated from bovine digital dermatitis lesions', *International Journal of Systematic and Evolutionary Microbiology,* 59(Pt5), pp. 987-991.

Evans, N.J., Brown, J.M., Demirkan, I., Murray, R.D., Vink, W.D., Blowey, R.W., Hart, C.A. and Carter, S.D. (2008) 'Three unique groups of spirochetes isolated from digital dermatitis lesions in UK cattle', *Veterinary Microbiology*, 130(1-2), pp. 141-150.

Evans, N.J., Brown, J.M., Demirkan, I., Singh, P., Getty, B., Timofte, D., Daan Vink, W., Murray, R.D., Blowey, R.W., Birtles, R.J., Hart, C.A. and Carter, S.D. (2009a) 'Association of unique, isolated treponemes with bovine digital dermatitis lesions', *Journal of Clinical Microbiology*, 47(3), pp. 689-696.

Evans, N.J., Brown, J.M., Murray, R.D., Getty, B., Birtles, R.J., Hart, C.A. and Carter, S.D. (2011b) 'Characterization of novel bovine gastrointestinal tract *Treponema* isolates and comparison with bovine digital dermatitis treponemes', *Applied and Environmental Microbiology*, 77(1), pp. 138-147.

Evans, N.J., Brown, J.M., Scholey, R., Murray, R.D., Birtles, R.J., Hart, C.A. and Carter, S.D. (2014) 'Differential inflammatory responses of bovine foot skin fibroblasts and keratinocytes to digital dermatitis treponemes', *Veterinary Immunology and Immunopathology*, 161(1-2), pp. 12-20.

Evans, N.J., Harrison, O.B., Clow, K., Derrick, J.P., Feavers, I.M. and Maiden, M.C.J. (2010) 'Variation and molecular evolution of HmbR, the *Neisseria meningitidis* haemoglobin receptor', *Microbiology,* 156, pp. 1384-1393.

Evans, N.J., Timofte, D., Isherwood, D.R., Brown, J.M., Williams, J.M., Sherlock, K., Lehane, M.J., Murray, R.D., Birtles, R.J., Hart, C.A. and Carter, S.D. (2012) 'Host and Environmental reservoirs of infection for bovine digital dermatitis treponemes', *Veterinary Microbiology,* 156(1-2), pp. 102-109.

Everest, G.J., Cook, A.E., Kirby, B.M. and Meyers, P.R. (2011) 'Evaluation of the use of *recN* sequence analysis in the phylogeny of the genus *Amycolatopsis', Antonie van Leeuwenhoek,* 100(4), pp. 483-496.

Fenno, J.C., Hannam, P.M., Leung, W.K., Tamura, M., Uitto, V.J. and McBride, C. (1998) 'Cytopathic effects of the major surface protein and the chymotrypsinlike protease of *Treponema denticola',* 66(5), pp. 1869-1877.

Fenno, J.C., Müller, K.H. and McBride, B.C. (1996) 'Sequence analysis, expression, and binding activity of recombinant major outer sheath protein (Msp) of *Treponema denticola', Journal of Bacteriology,* 178(9), pp. 2489-2497.

Fernandes, L.G.V., Vieira, M.L., Kirchgatter, K., Alves, I.J., de Morais, Z.M., Vasconcellos, S.A., Romero, E.C. and Nascimento, A.L.T.O. (2012) 'OmpL1 is an extracellular matrix- and plasminogen-interacting protein of *Leptospira* spp.', *Infection and Immunity,* 80(10), pp. 3679-3692.

Fidler, A.P., Alley, M.L. and Smith, G.W. (2012) 'Evaluation of a *Serpens* species bacterin for treatment of digital dermatitis in dairy cattle', *Research in Veterinary Science,* 93, pp. 1258-1260.

Fluhr, J.W., Kao, J., Jain, M., Ahn, S.K., Feingold, K.R. and Elias, P.M. (2001) 'Generation of free fatty acids from phospholipids regulates stratum corneum acidification and integrity', *Journal of Investigative Dermatology,* 117(1), pp. 44-51.

Fossiez, F., Djossou, O., Chomarat, P., Flores-Romo, L., Ait-Yahia, S., Maat, C., Pin, J.J., Garrone, P., Garcia, E., Saeland, S., Blanchard, D., Gaillard, C., Mahapatra, B.D., Rouvier, E., Golstein, P., Banchereau, J. and Lebecque, S. (1996) 'T cell interleukin-17 induces stromal cells to produce proinflammatory and hematopoietic cytokines', *The Journal of Experimental Medicine,* 183(6), pp. 2593-2603.

Francisco, A.P., Vaz, C., Monteiro, P.T., Melo-Cristino, J., Ramirez, M. and Carriço, J.A. (2012) 'PHYLOViZ: phylogenetic inference and data visualization for sequence based typing methods', *BMC Bioinformatics,* 13(87), pp. 1-10.

Franke, W.W., Schmid, E., Osborn, M. and Weber, K. (1978) 'Different intermediate-sized filaments distinguished by immunofluorescence microscopy', *Proceedings of the National Academy of Sciences of the United States of America,* 75(10), pp. 5034-5038.

Frey, S., Derer, A., Messbacher, M.E., Baeten, D.L.P., Bugatti, S., Montecucco, C., Schett, G. and Hueber, A.J. (2013) 'The novel cytokine interleukin-36α is expressed in psoriatic and rheumatoid arthritis synovium', *Annals of the Rheumatic Diseases,* 72(9), pp. 1569-1574.

Frohm, M., Agerberth, B., Ahangari, G., Stâhle-Bäckdahl, M., Lidén, S., Wigzell, H. and Gudmundsson, G.H. (1997) 'The expression of the gene coding for the antibacterial peptide LL-37 is induced in human keratinocytes during inflammatory disorders', *The Journal of Biological Chemistry,* 272(24), pp. 15258-15263.

Fuchs, E. and Green, H. (1980) 'Changes in keratin gene expression during terminal differentiation of the keratinocyte', *Cell,* 19(4), pp. 1033-1042.

Fuchs, H., Wallich, R., Simon, M.M. and Kramer, M.D. (1994) 'The outer surface protein A of the spirochete *Borrelia burgdorferi* is a plasmin(ogen) receptor', *Proceedings of the National Academy of Sciences of the United States of America*, 91(26), pp. 12594-12598.

Fullner, K.J. and Mekalanos, J.J. (2000) '*In vivo* covalent cross-linking of cellular actin by the *Vibrio cholerae* RTX toxin', *The EMBO Journal,* 19(20), pp. 5315-5323.

Gaibani, P., Pellegrino, M.T., Rossini, G., Alvisi, G., Miragliotta, L., Prati, C. and Sambri, V. (2010) 'The central region of the Msp gene of *Treponema denticola* has sequence heterogeneity among clinical samples, obtained from patients with periodontitis', *BMC Infectious Diseases,* 10(345), pp. 1-8.

Garbarino, E.J., Hernandez, J.A., Shearer, J.K., Risco, C.A. and Thatcher, W.W. (2004) 'Effect of lameness on ovarian activity in postpartum Holstein cows', *Journal of Dairy Science*, 87(12), pp. 4123-4131.

Garcia, B.L., Zhi, H., Wager, B., Höök, M. and Skare, J.T. (2016) '*Borrelia burgdorferi* BBK32 inhibits the classical pathway by blocking activation of the C1 complement complex', *PLoS Pathogens,* 12(1), pp. e1005404.

Garg, A.V., Amatya, N., Chen, K., Cruz, J.A., Grover, P., Whibley, N., Conti, H.R., Mir, G.H., Sirakova, T., Childs, E.C., Smithgall, T.E., Biswas, P.S., Kolls, J.K., McGeachy, M.J., Kolattukudy, P.E. and Gaffen, S.L. (2015) 'MCPIP1 endoribonuclease activity negatively regulates interleukin-17-mediated signalling and inflammation', *Immunity,* 43(3), pp. 475-487.

Gauthier-Rouviére, C., Vignal, E., Mériane, M., Roux, P., Montcourier, P. and Fort, P. (1998) 'RhoG GTPase controls a pathway that independently activates Rac1 and Cdc42Hs', *Molecular Biology of the Cell,* 9(6), pp. 1379-1394.

Geiger, B., Spatz, J.P. and Bershadsky, A.D. (2009) 'Environmental sensing through focal adhesions', *Nature Reviews. Molecular Cell Biology,* 10(1), pp. 21-33.

Giacani, L., Brandt, S.L., Ke, W., Reid, T.B., Molini, B.J., Iverson-Cabral, S., Ciccarese, G., Drago, F., Lukehart, S.A., Centurion-Lara, A. (2015) 'Transcription of TP0126, *Treponema pallidum* putative OmpW homolog, is regulated by the length of a homopolymeric guanosine repeat', *Infection and Immunity,* 83(6), pp. 2275-2289.

Gibbs, J., Ince, L., Matthews, L., Mei, J., Bell, T., Yang, N., Saer, B., Begley, N., Poolman, T., Pariollaud, M., Farrow, S., Demayo, F., Hussell, T., Worthen, G.S., Ray, D. and Louden, A. (2014) 'An epithelial circadian clock controls pulmonary inflammation and glucocorticoid action', *Nature Medicine,* 20(8), pp. 919-926.

Gläser, R., Harder, J., Lange, H., Bartels, J., Christophers, E. and Schröder, J.M. (2005) 'Antimicrobial psoriasin (S100A7) protects human skin from *Escherichia coli* infection', *Nature Immunology,* 6(1), pp. 57-64.

Goh, W.W.B., Wang, W. and Wong, L. (2017) 'Why batch effects matter in Omics data, and how to avoid them', *Trends in Biotechnology,* 35(6), pp. 498-507.

Gomez, A, Cook, N.B., Bernardoni, N.D., Rieman, J., Dusick, A.F., Hartshorn, R., Socha, M.T., Read, D.H. and Döpfer, D. (2012) 'An experimental infection model to induce digital dermatitis infection in cattle', *Journal of Dairy Science,* 95(4), pp. 1821-1830.

Gomez, A., Cook, N.B., Socha, M.T. and Döpfer, D. (2015) 'First-lactation performance in cows affected by digital dermatitis during the rearing period', *Journal of Dairy Science,* 98(7), pp. 4487-4498.

Goodpaster, T., Legesse-Miller, A., Hameed, M.R., Aisner, S.C., Randolph-Habecker, J. and Coller, H.A. (2008) 'An immunohistochemical method for identifying fibroblasts in formalin-fixed, paraffin-embedded tissue', *Journal of Histochemistry and Cytochemistry,* 56(4), pp. 347-358.

Graber, J.R., Leadbetter, J.R. and Breznak, J.A. (2004) 'Description of *Treponema azotonutricium* sp. nov. and *Treponema primitia* sp. nov., the first spirochetes isolated from termite guts', *Applied and Environmental Microbiology*, 70(3), pp. 1315-1320.

Graness, A., Giehl, K. and Goppelt-Struebe, M. (2006) 'Differential involvement of the integrin-linked kinase (ILK) in RhoA-dependent rearrangement of F-actin fibers and induction of connective tissue growth factor (CTGF)', *Cellular Signalling,* 18(4), pp. 433-440.

Great Britain Cattle & Welfare Group, 2014 Second report. Great Britain Cattle Health and Welfare group (2014) [Online] Available at: http://beefandlamb.ahdb.org.uk/wp-content/uploads/2013/06/CHAWG-Annual-Report-2014.pdf (Accessed: 15th May 2017)

Green, B.B. and Kerr, D.E. (2014) 'Epigenetic contribution to individual variation in response to lipopolysaccharide in bovine dermal fibroblasts', *Veterinary Immunology and Immunopathology,* 157(1-2), pp. 49-58.

Green, H., Easley, K. and Luchi, S. (2003) 'Marker succession during development of keratinocytes from cultured human embryonic stem cells', *Proceedings of the National Academy of Sciences of the United States of America,* 100(26), pp. 15625-15630.

Green, L.E., Hedges, V.J., Schukken, Y.H., Blowey, R.W. and Packington, A.J. (2002) 'The impact of clinical lameness on the milk yield of dairy cows', *Journal of Dairy Science*, 85(9), pp. 2250-2256.

Green, L.E., Huxley, J.N., Banks, C. and Green, M.J. (2014) 'Temporal associations between low body condition, lameness and milk yield in a UK dairy herd', *Preventive Veterinary Medicine,* 113(1), pp. 63-71.

Greenough, P.R. (2014) 'Dairy Cattle Hoof Lesion Severity Guide', *Hoof Lesion Severity Guide.* [Online] Available at http://dairyhoofhealth.info/LesionSeverityGuide/index.html (Accessed: 06th June 2017).

Greenough, P.R., Muelling, C.K.W., Döpfer, D. and Tomlinson, D.J. (2008) 'International atlas of lesions of cattle feet', Nomenclature and atlas update.' In: *Proceedings of the 15th International Symposium and the 7th Conference on Lameness in Ruminants*. Kuopio, Finland, pp. 40.

Gregorio, J., Meller, S., Conrad, C., Nardo, A.D., Homey, B., Lauerma, A., Arai, N., Gallo, R.L., DiGiovanni, J. and Gilliet, M. (2010) 'Plasmacytoid dendritic cells sense skin injury and promote wound healing through type I interferons', *The Journal of Experimental Medicine,* 207(13), pp. 2921-2930.

Grenier, D. (1991) 'Characteristics of haemolytic and hemagglutinating activities of *Treponema denticola', Molecular Oral Microbiology,* 6(4), pp. 246-249.

Grenier, D. (1996) 'Degradation of host protease inhibitors and activation of plasminogen by proteolytic enzymes from *Porphyromonas gingivalis* and *Treponema denticola', Microbiology,* 142, pp. 955-961.

Grenier, D. and Uitto, V.J. (1993) 'Cytotoxic effect of peptidoglycan from *Treponema denticola', Microbial Pathogenesis,* 15(5), pp. 389-397.

Grenier, D., Uitto, V.J. and McBride, B.C. (1990) 'Cellular location of a *Treponema denticola* chymotrypsonlike protease and importance of the protease in migration through the basement membrane', *Infection and Immunity,* 58(2), pp. 347-351.

Groenevelt, M., Anzuino, K., Langton, D.A. and Grogono-Thomas, R. (2015) 'Association of treponeme species with atypical foot lesions in goats', *Veterinary Record*, 176(24), pp. 626.

Groenevelt, M., Main, D.C.J., Tisdall, D., Knowles, T.G. and Bell, N.J. (2014) 'Measuring the response to therapeutic foot trimming in dairy cows with fortnightly lameness scoring', *The Veterinary Journal,* 201(3), pp. 283-288.

Gromiha, M.M., Ahmad, S. and Suwa, M. (2005) 'TMBETA-NET: discrimination and prediction of membrane spanning beta-strands in outer membrane proteins', *Nucleic Acids Research,* 33(web server issue), pp. W164-167.

Gross, J. (1910) '*Cristispira* nov. gen. ein beitragzur spirachätenfrage', *Mitteilungen aus der Zoologischen Station zu Neapel,* 20, pp. 41-93.

Grossman, R.M., Krueger, J., Yourish, D., Granelli-Piperno, A., Murphy, D.P., May, L.T., Kupper, T.S., Sehgal, P.B. and Gottlieb, A.B. (1989) 'Interleukin 6 is expressed in high levels in psoriatic skin and stimulates proliferation of cultured human keratinocytes', *Proceedings of the National Academy of Sciences of the United States of America,* 86(16), pp. 6367-6371.

Gruys, E., Toussaint, M.J.M., Niewold, T.A. and Koopmans, S.J. (2005) 'Acute phase reaction and acute phase proteins', *Journal of Zhejiang University Science B,* 6(11), pp. 1045-1056.

Guatam, A., Dixit, S., Philipp, M.T., Singh, S.R., Morici, L.A., Kaushal, D. and Dennis, V.A. (2011) 'Interleukin-10 alters effector functions of multiple genes induced by *Borrelia burgdorferi* in macrophages to regulate Lyme disease inflammation', *Infection and Immunity,* 79(12), pp. 4876-4892.

Guo, B.P., Brown, E.L., Dorward, D.W., Rosenberg, L.C. and Höök, M. (1998) 'Decorin-binding adhesins from *Borrelia burgdorferi*', *Molecular Microbiology,* 30(4), pp. 711-723.

Guo, E.Z. and Xu, Z. (2015) 'Distinct mechanisms of recognizing Endosomal Sorting Complex Required for Transport III (ESCRT-III) protein IST1 by different Microtubule Interacting and Trafficking (MIT) domains', *The Journal of Biological Chemistry,* 290(13), pp. 8396-8408.

Gupta, R.S., Mahmood, S. and Adeolu, M. (2013) 'A phylogenomic and molecular signature based approach for characterization of the phylum Spirochaetes and its major clades: proposal for a taxonomic revision of the phylum', *Frontiers in Microbiology,* 4(217), 1-18.

Haapasalo, M., Müller, K.H., Uitto, V.J., Leung, W.K. and McBride, B.C. (1992) 'Characterization, cloning, and binding properties of the major 53-kilodalton *Treponema denticola* surface antigen', *Infection and Immunity,* 60(5), pp. 2058-2065.

Hall, T. (2013) *Bioedit: Biological sequence alignment editor for Win95/98/NT/2K/XP/7* [Online] Carlsbad, USA: Ibis Biosciences. Available from http://www.mbio.ncsu.edu/bioedit/bioedit.html (Accessed: 08 January 2016).

Hallström, T., Haupt, K., Kraiczy, P., Hortschansky, P., Wallich, R., Skerka, C. and Zipfel, P.F. (2010) 'Complement regulator-acquiring surface protein 1 of *Borrelia burgdorferi* binds to human bone morphogenic protein 2, several extracellular matrix proteins and plasminogen', *The Journal of Infectious Diseases,* 202(3), pp. 490-498.

Halsall, S.A., Ward, W.R. and Murray, R.D. (1993) 'Effects of lameness on the behaviour of cows during the summer', *The Veterinary Record,* 132(23), pp. 578-580.

Hand, L.E., Hopwood, T.W., Dickson, S.H., Walker, A.L., Loudon, A.S., Ray, D.W., Bechtold, D.A. and Gibbs, J.E. (2016) 'The circadian clock regulates inflammatory arthritis', *FASEB Journal,* 30(11), pp. 3759-3770.

Hanna, P., Lofstedt, J. and Duivenvoorden, P. (1994) 'Prince Edward Island. Papillomatous digital dermatitis in a Canadian dairy herd', *The Canadian Veterinary Journal*, 35(10), pp. 657.

Hannemann, S. and Galán, J.E. (2017) '*Salmonella enterica* serovar-specific transcriptional reprogramming of infected cells', *PLoS Pathogens,* 13(7), pp. e1006532.

Harder, J. and Schröder, J.M. (2002) 'RNase 7, a novel innate immune defense antimicrobial protein of healthy human skin', *The Journal of Biological Chemistry,* 277(48), pp. 46779-46784.

Hardham, J.M. and Stamm, L.V. (1994) 'Identification and characterization of the *Treponema pallidum tpn50* gene, an *ompA* homolog', *Infection and Immunity,* 62(3), pp. 1015-1025.

Harris, D.L., Glock, R.D., Christensen, C.R. and Kinyon, J.M. (1972) 'Inoculation of pigs with *Treponema hyodysenteriae* (new species) and reproduction of the disease', *Veterinary Medicine, Small Animal Clinician,* 67(1), pp. 61-64.

Harwood, D.G., Cattell, J.H., Lewis, C.J. and Naylor, R. (1997) 'Virulent foot rot in sheep', *The Veterinary Record,* 140(26), pp. 687.

Hasegawa, M., Kishino, H. and Yano, T. (1985) 'Dating of the human-ape splitting by a molecular clock of mitochondrial DNA', *Journal of Molecular Evolution,* 22(2), pp. 160-174.

Hashimoto, M., Asai, Y., Jinno, T., Adachi, S., Kushomoto, S. and Ogawa, T., (2003) 'Structural elucidation of polysaccharide part of glycoconjugate from *Treponema medium* ATCC 700293', *The European Journal of Biochemistry,* 270(12), pp. 2671-2679.

Hein, W.R. and Dudler, L. (1997) 'TCR cd+ cells are prominent in normal bovine skin and express a diverse repertoire of antigen receptors', *Immunology,* 91, pp. 58-64.

Hellwage, J., Meri, T., Heikkilä, T., Alitalo, A., Panelius, J., Lahdenne, P., Seppälä, I.J. and Meri, S. (2001) 'The complement regulator factor H binds to the surface protein OspE of *Borrelia burgdorferi', The Journal of Biological Chemistry*, 276(11), pp. 8427-8435.

Hernandez, J., Shearer, J.K. and Webb, D.W. (2001) 'Effect of lameness on the calving-to-conception interval in dairy cows', *Journal of the American Veterinary Medical Association,* 218(10), pp. 1611-1614.

Hofman, V.J., Moreilhon, C., Brest, P.D., Lassalle, S., Brigand, K.L., Sicard, D., Raymond, J., Lamarque, D., Hébuterne, X.A., Mari, B., Barbry, P.J.P. and Hofman, P.M. (2007) 'Gene expression profiling in human gastric mucosa infected with *Helicobacter pylori', Modern Pathology,* 20(9), pp. 974-989.

Holzhauer, M., Bartels, C.J.M., van den Borne, B.H.P. and van Schaik, G. (2006b) 'Intra-class correlation attributable to claw trimmers scoring common hind-claw disorders in Dutch dairy herds', *Preventive Veterinary Medicine,* 75(1-2), pp. 47-55.

Holzhauer, M., Hardenberg, C., Bartels, C.J.M. and Frankena, K. (2006a) 'Herd- and cow-level prevalence of digital dermatitis in the Netherlands and associated risk factors', *Journal of Dairy Science*, 89(2), pp. 580-588.

Hong, H., Patel, D.R., Tamm, L.K. and van den Berg, B. (2006) 'The outer membrane protein OmpW forms an eight-stranded β-barrel with a hydrophobic channel', *The Journal of Biological Chemistry,* 281(11), pp. 7568-7577.

Houston, S., Taylor, J.S., Denchev, Y., Hof, R., Zuerner, R.L. and Cameron, C.E. (2015) 'Conservation of the host-interacting proteins Tp0750 and pallilysin among treponemes and restriction of proteolytic capacity to *Treponema* pallidum', *Infection and Immunity,* 83(11), pp. 4204-4216.

Hovind-Hougen, K. (1979) 'Leptospiraceae, a new family to include *Leptospira noguchi* 1917 and *Leptonema* gen. nov.', *International Journal of Systematic and Evolutionary Microbiology,* 29(3), pp. 245-251.

Hovind-Hougen, K., Birch-Andersen, A., Henrik-Nielsen, R., Orholm, M., Pedersen, J.O., Teglbjaerg, P.S. and Thaysen, E.H. (1982) 'Intestinal spirochetosis: morphological characterization and cultivation of the spirochete *Brachyspira aalborgi* gen. nov., sp. nov.', *Journal of Clinical Microbiology,* 16(6), pp. 1127-1136.

Hu, M.C.T., Qiu, W.R., Wang, Y.P., Hill, D., Ring, B.D., Scully, S., Bolon, B., DeRose, M., Luethy, R., Simonet, W.S., Arakawa, T. and Danilenko, D.M. (1998) 'FGF-18, a novel member of the fibroblast growth factor family, stimulates hepatic and intestinal proliferation', *Molecular and Cellular Biology,* 18(10), pp. 6063-6074.

Huang, H.J., Ross, C.R. and Blecha, F. (1997) 'Chemoattractant properties of PR-39, a neutrophil antibacterial peptide', *Journal of Leukocyte Biology,* 61(5), pp. 624-629.

Huber, B., Link, A., Linke, K., Gehrke, S.A., Winnefeld, M. and Kluger, P.J. (2016) 'Integration of mature adipocytes to build-up a functional three-layered full-skin equivalent', *Tissue Engineering. Part C, Methods,* 22(8), pp. 756-764.

Hugenholtz, P., Goebel, B.M. and Pace, N.R. (1998) 'Impact of culture-independent studies on the emerging phylogenetic view of bacterial diversity', *Journal of Bacteriology,* 180(18), pp. 4765-4774.

Huo, Y.B., Chan, Y., Lacap-Bugler, D.C., Mo, S., Woo, P.C.Y., Leung, W.K. and Watt, R.M. (2017) 'Multilocus sequence analysis of phylogroup 1 and 2 oral treponeme strains', *Applied and Environmental Microbiology,* 83(3), pp. e02499-e02516.

Huson, D.H., and Bryant, D. (2006) 'Application of phylogenetic networks in evolutionary studies', *Molecular Biology and Evolution,* 23(2), pp. 254-267.

Hymowitz, S.G., Filvaroff, E.H., Yin, J.P., Lee, J., Cai, L., Risser, P., Maruoka, M., Mao, W., Foster, J., Kelley, R.F., Pan, G., Gurney, A.L., de Vos, A.M. and Starovasnik, M.A. (2001) 'IL-17s adopt a cysteine knot fold: structure and activity of a novel cytokine, IL-17F, and implications for receptor binding', *The EMBO Journal,* 20(19), pp. 5332-5341.

Inagaki, S., Kimizuka, R., Kokubu, E., Saito, A. and Ishihara, K. (2016) '*Treponema denticola* invasion into human gingival epithelial cells', *Microbial Pathogenesis,* 94, pp. 104-111.

Infante-Duarte, C., Horton, H.F., Byrne, M.C. and Kamradt, T. (2000) 'Microbial lipopeptides induce the production of IL-17 in Th cells', *Journal of Immunology,* 165(11), pp. 6107-6115.

Ishida-Yamamoto, A., Simon, M., Kishibe, M., Miyauchi, Y., Takahashi, H., Yoshida, S., O'Brien, T.J., Serre, G. and Iizuka, H. (2004) 'Epidermal lamellar granules transport different cargoes as distinct aggregates', *Journal of Investigative Dermatology,* 122(5), pp. 1137-1144.

Ishigame, H., Kakuta, S., Nagai, T., Kadoki, M., Nambu, A., Komiyama, Y., Fujikado, N., Tanahashi, Y., Akitsu, A., Kotaki, H., Sudo, K., Nakae, S., Sasakawa, C., Iwakura, Y. (2009) 'Differential roles of interleukin-17A and -17F in host defense against mucoepithelial bacterial infection and allergic responses', *Immunity,* 30(1), pp. 108-119.

Ishii, T., Itoh, K., Takahashi, S., Sato, H., Yanagawa, T., Katoh, Y., Bannai, S. and Yamamoto, M. (2000) 'Transcription factor Nrf2 coordinately regulates a group of oxidative stress-inducible genes in macrophages', *The Journal of Biological Chemistry,* 275(21), pp. 16023-16029.

Islam, M.S. and Zhou, H.M. (2007) 'Isolation and propagation of keratinocytes derived from Cashmere goat fetus', *Tissue and Cell,* 39(6), pp. 377-385.

Jackson, S.M., Williams, M.L., Feingold, K.R. and Elias, P.M. (1993) 'Pathobiology of the stratum corneum', *The Western Journal of Medicine,* 158(3), pp. 279-285.

Jacobs, C., Orsel, K., Mason, S., Gray, K. and Barkema, H.W. (2017) 'Comparison of the efficacy of a commercial footbath product with copper sulfate for the control of digital dermatitis', *Journal of Dairy Science*, 100(7), pp. 5628-5641.

Janda, J.M. and Abbott, S.L. (2007) '16S rRNA gene sequencing for bacterial identification in the diagnostic laboratory: pluses, perils and pitfalls', *Journal of Clinical Microbiology,* 45(9), pp. 2761-2764.

Janeway, C.A., Travers, P., Walport, M. and Shlomchik, M.J. (2001) 'Innate Immunity: The complement system and innate immunity. The Immune System in Health and Disease.' [E-Book] In: *Immunobiology,* 5th Edition, New York: Garland Science. Available from: https://www.ncbi.nlm.nih.gov/books/NBK10757/ (Accessed: 15th June 2017).

Jeong, C.W., Ahn, K.S., Rho, N.K., Park, Y.D., Lee, D.Y., Lee, J.H., Lee, E.S. and Yang, J.M. (2003) 'Differential *in vivo* cytokine mRNA expression in lesional skin of intrinsic vs. extrinsic atopic

dermatitis patients using semiquantitative RT-PCR', *Clinical and Experimental Allergy,* 33(12), pp. 1717-1724.

Jeong, H., Sim, H.J., Song, E.K., Lee, H., Ha, S.C., Jun, Y., Park, T.J. and Lee, C. (2016) 'Crystal structure of SEL1L: insights into the roles of SLR motifs in ERAD pathways', *Scientific Reports,* 9, pp. 20261.

Jin, T., Bokarewa, M., Foster, T., Mitchell, J., Higgins, J. and Tarkowski, A. (2004) '*Staphylococcus aureus* resists human defensins by production of staphylokinase, a novel bacterial evasion mechanism', *The Journal of Immunology,* 172(2), pp. 1169-1176.

Jin, W., Jia, K., Yang, L., Chen, J., Wu, Y. and Yi, M. (2013) 'Derivation and characterization of cell cultures from the skin of the Indo-Pacific humpback dolphin *Sousa chinensis', In Vitro Cellular and Developmental Biology; Animal,* 49(6), pp. 449-457.

Jing, C.E., Du, X.J., Ping, L. and Wang, S. (2016) 'Transcriptome analysis of *Cronobacter sakazakii* ATCC BAA-894 after interaction with human intestinal epithelial cell line HCT-8', *Applied Microbiology and Biotechnology,* 100(1), pp. 311-322.

Joshi, N.A. and Fass, J.N. (2011) 'Sickle: a sliding-window, adaptive, quality-based trimming tool for FastQ files (version 1.33).' [Software] Available at https://github.com/najoshi/sickle (Accessed 5th March 2017).

Jukes, T.H., and Cantor, C.R. (1969) 'Evolution of protein molecules', In: Munro, H.N., *Mammalian Protein Metabolism.* New York: Academic Press, pp. 21-132.

Jun, H.K., Kang, Y.M., Lee, H.R., Lee, S.H. and Choi, B.K. (2008) 'Highly conserved surface proteins of oral spirochetes as adhesins and potent inducers of proinflammatory and osteoclastogenic factors', *Infection and Immunity,* 76(6), pp. 2428-2438.

Kaczorowski, D.J., Afrazi, A., Scott, M.J., Kwak, J.H., Gill, R., Edmonds, R.D., Liu, Y., Fan, J. and Billiar, T.R. (2010) 'Pivotal advance: the pattern recognition receptor ligands lipopolysaccharide and polyinosine-polycytidylic acid stimulate factor B synthesis by the macrophage through distinct but overlapping mechanisms', *Journal of Leukocyte Biology,* 88(4), pp. 609-618.

Kalluri, R. and Weinberg, R.A. (2009) 'The basics of epithelial-mesenchymal transition', *The Journal of Clinical Investigation,* 119(6), pp. 1420-1428.

Katz, Y., Nadiv, O., Rapoport, M.J. and Loos, M. (2000) 'IL-17 regulates gene expression and protein synthesis of the complement system, C3 and factor B, in skin fibroblasts', *Clinical and Experimental Immunology,* 120(1), pp. 22-29.

Kaviani, M., Geramizadeh, B., Rahsaz, M. and Marzban, S. (2015) 'Considerations in the improvement of human epidermal keratinocyte culture *in vitro', Experimental and Clinical Transplantation,* 13, pp. 366-370.

Kawano, M., Komi-Kuramochi, A., Asada, M., Suzuki, M., Oki, J., Jiang, J. and Imamura, T. (2005) 'Comprehensive analysis of FGF and FGFR expression in skin: FGF18 is highly expressed in hair follicles and capable of inducing anagen from telogen stage hair follicles', *Journal of Investigative Dermatology,* 124, pp. 877-885.

Kent, L.W., Rahemtulla, F., Hockett Jr., R.D., Gilleland, R.C. and Michalek, S.M. (1998) 'Effect of lipopolysaccharide and inflammatory cytokines on interleukin-6 production by healthy human gingival fibroblasts', *Infection and Immunity,* 66(2), pp. 608-614.

Kibbe, W.A. (2007) 'OligoCalc: an online oligonucleotide properties calculator', *Nucleic Acids Research*, 35(webserver issue), pp. W43-W46.

Kim, D., Pertea, G., Trapnell, C., Pimentel, H., Kelley, R. and Salzberg, S.L. (2013) 'TopHat2: accurate alignment of transcriptomes in the presence of insertions, deletions and gene fusions', *Genome Biology*, 14(4), pp. R36.

Kinsella, R.J., Kähäri, A., Haider, S., Zamora, J., Proctor, G., Spudich, G. Almeida-King, J., Staines, D., Derwent, P., Kerhornou, A., Kersey, P. and Flicek, P. (2011) 'Ensembl BioMarts: a hub for data retrieval across taxonomic space', *Database,* 2011, pp. bar030.

Klitgaard, K., Boye, M., Capion, N. and Jensen, T.K. (2008) 'Evidence of multiple *Treponema* phylotypes involved in bovine digital dermatitis as shown by 16S rRNA gene analysis and fluorescence in situ hybridization', *Journal of Clinical Microbiology,* 46(9), pp.3012-3020.

Klitgaard, K., Foix Bretó, A., Boye, M. and Jensen, T.K. (2013) 'Targeting the treponemal microbiome of digital dermatitis infections by high-resolution phylogenetic analyses and comparison with fluorescent *in situ* hybridization', *Journal of Clinical Microbiology,* 51(7), pp. 2212-2219.

Klitgaard, K., Nielsen, M.W., Ingerslev, H.C., Boye, M. and Jensen, T.K. (2014) 'Discovery of bovine digital dermatitis-associated *Treponema* spp. in the dairy herd environment by a targeted deep-sequencing approach, *Applied and Environmental Microbiology,* 80(14), pp. 4427-4432.

Knappe-Poindecker, M., Gilhuus, M., Jensen, T.K., Klitgaard, K., Larssen, R.B. and Fjeldaas, T. (2013) 'Interdigital dermatitis, heel horn erosion, and digital dermatitis in 14 Norwegian dairy herds', *Journal of Dairy Science,* 96(12), pp. 7617-7629.

Koenig, S., Sharifi, A.R., Wentrot, H., Landmann, D., Eise, M. and Simianer, H. (2005) 'Genetic parameters of claw and foot disorders estimated with logistic models', *Journal of Dairy Science*, 88(9), pp. 3316-3325.

Koga, T., Yamasaki, S., Migita, K., Kita, J., Okada, A., Kawashiri, S., Iwamoto, N., Tamai, M., Arima, K., Origuchi, T., Nakamura, H., Osaki, M., Tsurumoto, T., Shindo, H., Eguchi, K. and Kawakami, A. (2011) 'Post-transcriptional regulation of IL-6 production by Zc3h12a in fibroblast-like synovial cells', *Cell and Experimental Rheumatology,* 29, pp. 906-912.

Köhler, H.B.K., Huchzermeyer, B., Martin, M., De Bruin, A., Meier, B. and Nolte, I. (2001) 'TNF-α dependent NF-κB activation in cultured canine keratinocytes is partly mediated by reactive oxygen species', *Veterinary Dermatology*, 12(3), pp. 129-137.

Kolarsick, P.A.J., Kolarsick, M.A. and Goodwin, C. (2011) 'Anatomy and physiology of the skin', *Journal of the Dermatology Nurses' Association,* 3(4), pp. 203-213.

Komi-Kuramochi, A., Kawano, M., Oda, Y., Asada, M., Suzuki, M., Oki, J. and Imamura, T. (2005) 'Expression of fibroblast growth factors and their receptors during full-thickness skin wound healing in young mice and aged mice', *Journal of Endocrinology,* 186, pp. 273-289.

Krueger, J.G., Fretzin, S., Suárez-Fariñas, M., Haslett, P.A., Phipps, K.M., Cameron, G.S., McColm, J., Katcherian, A., Cueto, I., White, T., Banerjee, S. and Hoffman, R.W. (2012) 'IL-17A is essential for cell activation and inflammatory gene circuits in subjects with psoriasis', *Journal of Allergy and Clinical Immunology,* 130(1), pp. 145-154.

Krull, A.C., Cooper, V.L., Coatney, J.W., Shearer, J.K., Gorden, P.J. and Plummer, P.J. (2016) 'A highly effective protocol for the rapid and consistent induction of digital dermatitis in Holstein calves', *PLoS ONE,* 11(4): e0154481.

Krull, A.C., Shearer, J.K., Gorden, P.J., Cooper, V.L., Phillips, G.J. and Plummer, P.J. (2014) 'Deep sequencing analysis reveals temporal microbiota changes associated with development of bovine digital dermatitis', *Infection and Immunity,* 82(8), pp. 3359-3373.

Kuroda, K. and Tajima, S. (2004) 'HSP47 is a useful marker for skin fibroblasts in formalin-fized, paraffin-embedded tissue specimens', *Journal of Cutaneous Pathology,* 31(3), pp. 241-246.

Lahouassa, H., Rainard, P., Caraty, A. and Riollet, C. (2008) 'Identification and characterization of a new interleukin-8 receptor in bovine species', *Molecular Immunology,* 45(4), pp. 1153-1164.

Lai, Y., Di Nardo, A., Nakatsuji, T., Leichtle, A., Yang, Y., Cogen, A.L., Wu, Z.R., Hooper, L.V., von Aulock, S., Radek, K.A., Huang, C.M., Ryan, A.F. and Gallo, R.L. (2009) 'Commensal bacteria regulate TLR3-dependent inflammation following skin injury', *Nature Medicine,* 15(12), pp. 1377-1382.

Lamb, R. and Ambler, C.A. (2013) 'Keratinocytes propagated in serum-free, feeder-free culture conditions fail to form stratified epidermis in a reconstituted skin model', *PLoS ONE,* 8(1), pp. e52494.

Laven, R. (2001) 'Control of digital dermatitis in cattle', *In Practice*, 23(6), pp. 336-341.

Laven, R.A. and Logue, D.N. (2006) 'Treatment strategies for digital dermatitis for the UK', *The Veterinary Journal,* 171(1), pp. 79-88.

Lawrence, T. (2009) 'The nuclear factor NF-kappaB pathway in inflammation', *Cold Spring Harbour Perspectives in Biology,* 1(6), pp. a001651.

Lebre, M.C., van der Aar, A.M.G., van Baarsen, L., van Capel, T.M.M., Schuitemaker, J.H.N., Kapsenberg, M.L. and de Jong, E.C. (2007) 'Human keratinocytes express functional Toll-like receptor 3, 4, 5, and 9', *Journal of Investigative Dermatology,* 127(2), pp. 331-341.

Lebwohl, M., Strober, B., Menter, A., Gordon, K., Weglowska, J., Puig, L., Papp, K., Spelman, L., Toth, D., Kerdel, F., Armstrong, A.W., Stingl, G., Kimball, A.B., Bachelez, H., Wu, J.J., Crowley, J., Langley, R.G., Blichardski, T., Paul, C., Lacour, J.P., Tyring, S., Kircik, L., Chimenti, S., Duffin, K.C., Bagel, J., Koo, J., Aras, G., Li, J., Song, W., Milmont, C.E., Shi, Y., Erongu, N., Klekotka, P., Kotzin, B. and Nirula, A. (2015) 'Phase 3 studies comparing brodalumab with ustekinumab in psoriasis', *The New England Journal of Medicine,* 373(14), pp. 1318-1328.

Lee, K.J., Yin, W., Arafat, D., Tang, Y., Uppal, K., Tran, V., Cabrera-Mora, M., Lapp, S., Moreno, A., Meyer, E., DeBarry, J.D., Pakala, S., Nayak, V., Kissinger, J.C., Jones, D.P., Galinski, M., Styczynski, M.P. and Gibson, G. (2014) 'Comparative transcriptomics and metabolomics in a rhesus macaque during drug administration study', *Frontiers in Cell and Developmental Biology,* 2(54), pp. 1-19.

Lee, S.H., Kim, K.A., Park, Y.G., Seong, I.W., Kim, M.J. and Lee, Y.J. (2000) 'Identification and partial characterization of a novel hemolysin from *Leptospira interrogans* serovar *lai', Gene,* 254(1-2), pp. 19-28.

Lee, Y., Kim, H., Kim, S., Kim, K. and Chung, J.H. (2010) 'Activation of toll-like receptors 2, 3 or 5 induces matrix metalloproteinase-1 and -9 expression with the involvement of MAPKs and NF-κB in human epidermal keratinocytes', *Experimental Dermatology,* 19(8), pp. e44-e49.

Leonard, E.J. and Yoshimura, T. (1990) 'Human monocyte chemoattractant protein-1 (MCP-1)', *Immunology Today,* 11(3), pp. 97-101.

Leonardi, C., Matheson, R., Zachariae, C., Cameron, G., Li, L., Edson-Heredia, E., Braun, D. and Banerjee, S. (2012) 'Anti-interleukin-17 monoclonal antibody ixekizumab in chronic plaque psoriasis', *The New England Journal of Medicine,* 366(13), pp. 1190-1199.

Levett, P.N., Morey, R.E., Galloway, R., Steigerwalt, A.G. and Ellis, W.A. (2005) 'Reclassification of *Leptospira parva* Hovind-Hougen *et al.* 1982 as *Turneriella parva* gen. nov., comb. nov.', 55, pp. 1497-1499.

Li, B., Tsoi, L.C., Swindell, W.R., Gudjonsson, J.E., Tejasvi, T., Johnston, A., Ding, J., Stuart, P.E., Xing, X., Kochkodan, J.J., Voorhees, J.J., Kang, H.M., Nair, R.P., Abecasis, G.R. and Elder, J.T. (2014) 'Transcriptome analysis of psoriasis in a large case-control sample: RNA-Seq provides insights into disease mechanisms', *Journal of Investigative Dermatology,* 134, pp. 1828-1838.

Li, L., Tennenbaum, T., Yuspa, S.H. (1996) 'Suspension-induced murine keratinocyte differentiation is mediated by calcium', *Journal of Investigative Dermatology,* 106(2), pp. 254-260.

Li, W., Wen, L., Li, C., Chen, R., Ye, Z., Zhao, J. and Pan, J. (2016) 'Contribution of the outer membrane protein OmpW in *Escherichia coli* to complement resistance from binding to factor H', *Microbial Pathogenesis,* 98, pp. 57-62.

Li, X., Li, J., Yang, Y., Hou, R., Liu, R., Zhao, Z., Yan, X., Yin, G., An, P., Wang, Y. and Zhang, K. (2013) 'Differential gene expression in peripheral blood T cells from patients with psoriasis, lichen planus, and atopic dermatitis', *Journal of the American Academy of Dermatology',* 69(5), pp. e235-e243.

Lian, C.G. and Murphy, G.F. (2015) 'Histology of the skin.' In: Elder, D.E., Elenitas, R., Rosenbach, M., Murphy, G.F., Rubin, A.I. and Xu, X. Lever's Histopathology of the skin, 11th edition, London, UK: Wolters Kluwer, pp. 8-76.

Lin, Y.P. and Chang, Y.F. (2008) 'The C-terminal variable domain of LigB from *Leptospira* mediates binding to fibronectin', *Journal of Veterinary Science,* 9(2), pp. 133-144.

Lin, Y.P., Lee, D.W., McDonough, S.P., Nicholson, L.K., Sharma, Y. and Chang, Y.F. (2009) 'Repeated domains of leptospira immunoglobulin-like proteins interact with elastin and tropoelastin', The *Journal of Biological Chemistry,* 284(29), pp. 19380-19391.

Lippert, E., Yowe, D.L., Gonzalo, J.A., Justice, J.P., Webster, J.M., Fedyk, E.R., Hodge, M., Miller, C., Gutierrez-Ramos, J.C., Borrego, F., Keane-Myers, A. and Druey, K.M. (2003) 'Role of regulator of G protein signaling 16 in inflammation-induced T lymphocyte migration and activation', *The Journal of Immunology,* 171(3), pp. 1542-1555.

Liu, A.Y., Destoumieux, D., Wong, A.V., Park, C.H., Valore, E.V., Liu, L. and Ganz, T. (2002) 'Human β-defensin-2 production in keratinocytes is regulated by interleukin-1, bacteria, and the state of differentiation', Journal of *Investigative Dermatology,* 118(2), pp. 275-281.

Liu, L., Wang, L., Jia, H.P., Zhao, C., Heng, H.H.Q., Schutte, B.C., McCray (Jr), P.B. and Ganz, T. (1998) 'Structure and mapping of the human β-defensin HBD-2 gene and its expression at sites of inflammation', *Gene,* 222(2), pp. 237-244.

Liu, S.C. and Karasek, M. (1978) 'Isolation and growth of adult human epidermal keratinocytes in cell culture', *The Journal of Investigative Dermatology,* 71(2), pp. 157-162.

Liu, X., Speranza, E., Muñoz-Fontela, C., Haldenby, S., Rickett, N.Y., Garcia-Dorival, I., Fang, Y., Hall, Y., Zekeng, E.G., Lüdtke, A., Xia, D., Kerber, R., Krumkamp, R., Duraffour, S., Sissoko, D., Kenny, J., Rockliffe, N., Williamson, E.D., Laws, T.R., N'Faly, M., Matthews, D.A., Günther, S., Cossins, A.R., Sprecher, A., Connor, J.H., Carroll, M.W. and Hiscox, J.A. (2017)

'Transcriptomic signatures differentiate survival from fatal outcomes in humans infected with Ebola virus', *Genome Biology,* 18(1), pp. 4.

Logue, D.N., Gibert, T., Parkin, T., Thomson, S. and Taylor, D.J. (2012) 'A field evaluation of a footbathing solution for the control of digital dermatitis in cattle', *The Veterinary Journal,* 193(3), pp. 664-668.

Losinger, W.C. (2006) 'Economic impacts of reduced milk production associated with papillomatous digital dermatitis in dairy cows in the USA', *Journal of Dairy Research*, 73(2), pp. 244-256.

Love, M.I., Huber, W. and Anders, S. (2014) 'Moderated estimation of fold change and dispersion for RNA-Seq data with DESeq2', *Genome Biology,* 15(550), pp. 1-21.

Lucas, S., Han, J., Lapidus, A., Bruce, D., Goodwin, L., Pitluck, S., Peters, L., Kyrpides, N., Mavromatis, K., Ivanova, N., Mikhailova, K., Pagani, I., Teshima, H., Detter, J.C., Tapia, R., Han, C., Land, M., Hauser, L., Markowitz, V., Cheng, J.F., Hugenholtz, P., Woyke, T., Wu, D., Gronow, S., Wellnitz, S., Brambilla, E., Klenk, H.P. and Eisen, J.A. (2015) 'The complete genome of *Treponema brennaborense* DSM 12168.' [Unpublished] Available at: https://www.ncbi.nlm.nih.gov/nuccore/NC_015500.1 (Accessed: 29th February 2016).

Luthra, A., Anand, A., Hawley, K.L., LeDoyt, M., La Vake, C.J., Caimano, M.J., Cruz, A.R., Salazar, J.C. and Radolf, J.D. (2015) 'A homology model reveals novel structural features and an immunominant surface loop/opsonic target in the *Treponema pallidum* BamA ortholog TP_0326', *Journal of Bacteriology,* 197(11), pp. 1906-1920.

Lüthy, L., Grutter, M.G. and Mittl, P.R.E. (2002) 'The crystal structure of *Helicobacter pylori* cysteine-rich protein B reveals a novel fold for a penicillin-binding protein', *The Journal of Biological Chemistry,* 277(12), pp. 10187-10193.

Maciver, S.K. and Hussey, P.J. (2002) 'The ADF/cofilin family: actin-remodeling proteins', *Genome Biology,* 3(5), pp. 3007.1-3007.12.

Manabe, M., Sanchez, M., Sun, T.T. and Dale, B.A. (1991) 'Interaction of filaggrin with keratin filaments during advanced stages of normal human epidermal differentiation and in Ichthyosis vulgaris', *Differentiation,* 48(1), pp. 43-50.

Manning, P.A., Pugsley, A.P. and Reeves, P. (1977) 'Defective growth functions in mutants of *Escherichia coli* K12 lacking a majour outer membrane protein, *Journal of Molecular Biology,* 116(2), pp. 285-300.

Marcatili, P., Nielsen, M.W., Sicheritz-Pontén, T., Jensen, T.K., Schafer-Nielsen, C., Boye, M., Nielsen, M. and Klitgaard, K. (2016) 'A novel approach to probe host-pathogen interactions of bovine digital dermatitis, a model of a complex polymicrobial infection', *BMC Genomics,* 17, pp. 987.

Marchal, C.M.P., Luft, B.J., Yang, X., Sibilia, J., Jaulhac, B. and Boulanger, N.M. (2009) 'Defensin is suppressed by tick salivary gland extract during the *in vitro* interaction of resident skin cells with *Borrelia burgdorferi', Journal of Investigative Dermatology,* 129(10), pp. 2515-2517.

Marchese, C., Felici, A., Visco, V., Lucania, G., Igarashi, M., Picardo, M., Frati, L. and Torrisi, M.R. (2001) 'Fibroblast growth factor 10 induces proliferation and differentiation of human primary cultured keratinocytes', *The Journal of Investigative Dermatology,* 116(4), pp. 623-628.

Marinkovich, M.P., Keene, D.R., Rimberg, C.S. and Burgeson, R.E. (1993) 'Cellular origin of the dermal-epidermal basement membrane', *Developmental Dynamics,* 197(4), pp. 255-267.

Marsters, S.A., Sheridan, J.P., Donahue, C.J., Pitti, R.M., Gray, C.L., Goddard, A.D., Bauer, K.D. and Ashkenazi, A. (1996) 'Apo-3, a new member of the tumor necrosis factor receptor family, contains a death domain and activates apoptosis and NF-κB', *Current Biology,* 6(12), pp. 1669-1676.

Martin, D., Cadieux, N., Hamel, J. (1997) 'Highly conserved *Neisseria meningitidis* surface protein confers protection against experimental infection', *Journal of Experimental Medicine,* 185(7), pp. 1173-1183.

Martin, M. (2011) 'Cutadapt removes adapter sequences from high-throughput sequencing reads', *EMBnet.journal,* 17(1), pp. 10-12.

Massrieh, W., Derjuga, A., Doualla-Bell, F., Ku, C.Y., Sanborn, B.M. and Blank, V. (2006) 'Regulation of the MAFF transcription factor by proinflammatory cytokines in myometrial cells', *Biology of Reproduction,* 74(4), pp. 699-705.

Matsunaga, J., Barocchi, M.A., Croda, J., Young, T.A., Sanchez, Y., Siqueira, I., Bolin, C.A., Reis, M.G., Riley, L.W., Haake, D.A. and Ko, A.I. (2003) 'Pathogenic *Leptospira* species express surface-exposed proteins belonging to the bacterial immunoglobulin superfamily', *Molecular Microbiology,* 49(4), pp. 929-946.

Mauldin, E.A. and Peters-Kennedy, J. (2016) 'Integumentary System.' In: Maxie, G. Jubb, Kennedy and Palmer's Pathology of Domestic Animals (Volume 1), 6th Edition, St Louis, Missouri: Elsevier, pp. 511-518.

McBride, A.A., Dlugosz, A. and Baker, C.C. (2000) 'Production of infectious bovine papillomavirus from cloned viral DNA by using an organotypic raft/xenograft technique', *Proceedings of the National Academy of Sciences of the United States of America,* 97(10), pp. 5533-5539.

McDowell, J.V., Frederick, J., Miller, D.P., Goetting-Minesky, M.P., Goodman, H., Fenno, J.C. and Marconi, R.T. (2011) 'Identification of the priumary mechanism of complement evasion by the periodontal pathogen, *Treponema denticola', Molecular Oral Microbiology,* 26(2), pp. 140-149.

McDowell, J.V., Huang, B., Fenno, J.C., Marconi, R.T. (2009) 'Analysis of a unique interaction between the complement regulatory protein factor H and the periodontal pathogen *Treponema denticola',* Infection and Immunity, 77(4), pp. 1417-1425.

McLennan, M.W. and McKenzie, R.A. (1996) 'Digital dermatitis in a Friesian cow', *Australian Veterinary Journal*, 74(4), pp. 314-315.

Meddeb, M., Carpentier, W., Cagnard, N., Nadaud, S., Grillon, A., Barthel, C., De Martino, S.J., Jaulhac, B., Boulanger, N. and Schramm, F. (2016) 'Homogeneous inflammatory gene profiles induced in human dermal fibroblasts in response to the three main species of *Borrelia burgdorferi* sensu lato', *PLoS ONE,* 11(10), pp. e0164117.

Medzhitov, R. (2008) 'Origin and physiological roles of inflammation', *Nature,* 454, pp. 428-435.

Meenakshi, M., Bakshi, C.S., Butchaiah, G., Bansal, M.P., Siddiqui, M.Z. and Singh, V.P. (1999) 'Adjuvanted outer membrane protein vaccine protects poultry against infection with *Salmonella enteritidis', Veterinary Research Communications,* 23(2), pp. 81-90.

Menon, G.K., Ghadially, R., Williams, M.L. and Ellias, P.M. (1992) 'Lamellar bodies as delivery systems of hydrolytic enzymes: implications for normal and abnormal desquamation', *British Journal of Dermatology,* 126(4), pp. 337-345.

Menzies, M. and Ingham, A. (2006) 'Identification and expression of Toll-like receptors 1-10 in selected bovine and ovine tissues', *Veterinary Immunology and Immunopathology,* 109(1-2), pp. 23-30.

Merhej, V., Georgiades, K. and Raoult, D. (2013) 'Postgenomic analysis of bacterial pathogens repertoire reveals genome reduction rather than virulence factors', *Briefings in Functional Genomics,* 12(4), pp. 291-304.

Merhej, V., Royer-Carenzi, M., Pontarotti, P. and Raoult, D. (2009) 'Massive comparative genomic analysis reveals convergent evolution of specialized bacteria', *Biology Direct,* 4(13), pp. 1-25.

Meri, T., Murgia, R., Stefanel, P., Meri, S. and Cinco, M. (2005) 'Regulation of complement activation at the C3-level by serum resistant leptospires', *Microbial Pathogenesis,* 39(4), pp. 139-147.

Meyrick, B., and Magnuson, M.A. (1994) 'Identification and functional characterization of the bovine manganous superoxide dismutase promoter', *American Journal of Respiratory Cell and Molecular Biology,* 10(1), pp. 113-121.

Miao, D., Fenno, J.C., Timm, J.C., Joo, N.E. and Kapila, Y.L. (2011) 'The *Treponema denticola* chymotrypsin-like protease dentilisin induces matrix metalloproteinase-2-dependent fibronectin fragmentation in periodontal ligament cells', *Infection and Immunity,* 79(2), pp. 806-811.

Miller, L.S., Sørensen, O.E., Liu, P.T., Jalian, H.R., Eshtiaghpour, D., Behmanesh, B.E., Chung, W., Starner, T.D., Kim, J., Sieling, P.A., Ganz, T. and Modlin, R.L. (2005) 'TGF-α regulates TLR expression and function on epidermal keratinocytes', *The Journal of Immunology,* 174(10), pp. 6137-6143.

Milne, I., Lindner, D., Bayer, M., Husmeier, D., McGuire, G., Marshall, D.F. and Wright, F. (2009) 'TOPALi v2: a rich graphical interface for evolutionary analyses of multiple alignments on HPC clusters and multi-core desktops', *Bioinformatics,* 25(1), pp. 126-127.

Mitchell, A.J. and Wimpenny, J.W.T. (1997) 'The effects of agar concentration on the growth and morphology of submerged colonies of motile and non-motile bacteria', *Journal of Applied Microbiology,* 83(1), pp. 76-84.

Mitjà, O., Asiedu, K. and Mabey, D. (2013) 'Yaws', *Lancet*, 381, pp. 763-773.

Mittelstadt, P.R. and Ashwell, J.D. (2001) 'Inhibition of AP-1 by the glucocorticoid-inducible protein GILZ', *The Journal of Biological Chemistry,* 276(31), pp. 29603-29610.

Moe, K.K., Yano, T., Kuwano, A., Sasaki, S. and Misawa, N. (2010) 'Detection of treponemes in canker lesions of horses by 16S rRNA clonal sequencing analysis', *The Journal of Veterinary Medical Science,* 72(2), pp. 235-239.

Mohawk, J.A., Green, C.B. and Takahashi, J.S. (2012) 'Central and peripheral circadian clocks in mammals', *Annual Review of Neuroscience,* 35, pp. 445-462.

Moll, R. Franke, W.W., Schiller, D.L., Geiger, B. and Krepler, R. (1982) 'The catalog of human cytokeratins: patterns of expression in normal epithelia, tumors and cultured cells', *Cell,* 31(1), pp. 11-24.

Monsuur, H.N., Weijers, E.M., Niessen, F.B., Gefen, A., Koolwijk, P., Gibbs, S. and van den Broek, L.J. (2016) 'Extensive characterisation and comparison of endothelial cells derived from dermis and adipose tissue: potential use in tissue engineering', *PLoS ONE,* 11(11), pp. e0167056.

Montagna, W. (1967) 'Comparative anatomy and physiology of the skin', *Archives in Dermatology,* 96, pp. 357-363.

Morgan, C.A., Lukehart, S.A. and Van Voorhis, W.C. (2003) 'Protection against syphilis correlates with specificity of antibodies to the variable regions of *Treponema pallidum* repeat protein K', *Infection and Immunity,* 71(10), pp. 5605-5612.

Motaleb, M.A., Corum, L., Bono, J.L., Elias, A.F., Rosa, P., Samuels, D.S. and Charon, N.W. (2000) '*Borrelia burgdorferi* periplasmic flagella have both skeletal and motility functions', *Proceedings of the National Academy of Sciences of the United States of America,* 97(20), pp. 10899-10904.

Moter, A., Leist, G., Rudolph, R., Schrank, K., Choi, B.K., Wagner, M. and Göbel, U.B. (1998) 'Fluorescence *in situ* hydridization shows spatial distribution of as yet uncultured treponemes in biopsies from digital dermatitis lesions', *Microbiology,* 144(Pt 9), pp. 2459-2467.

Motohashi, H. and Yamamoto, M. (2004) 'Nrf2-Keap1 defines a physiologically important stress response mechanism', *TRENDS in Molecular Medicine,* 10(11), pp. 549-557.

Motzkus, D., Schulz-Maronde, S., Heitland, A., Schulz, A., Forssmann, W.G., Jübner, M. and Maronde, E. (2006) 'The novel β-defensin DEFB123 prevents lipopolysaccharide-mediated effects *in vitro* and *in vivo', The Federation of American Societies for Experimental Biology Journal*, 20(10), pp. 1701-1702.

Müellegger, R.R., Means, T.K., Shin, J.J., Lee, M., Jones, K.L., Glickstein, L.J., Luster, A.D. and Steere, A.C. (2007) 'Chemokine signatures in the skin disorders of Lyme borreliosis in Europe: predominance of CXCL9 and CXCL10 in erthyema migrans and acrodermatitis and CXCL13 in lymphocytoma', *Infection and Immunity,* 75(9), pp. 4621-4628.

Murray, R.D., Downham, D.Y., Demirkan, I. and Carter, S.D. (2002) 'Some relationships between spirochaete infections and digital dermatitis in four UK dairy herds', *Research in Veterinary Science,* 73(3), pp. 223-230.

Myers, T.A., Kaushal, D., Philipp, T. (2009) 'Microglia are mediators of *Borrelia burgdorferi*-induced apoptosis in SH-SY5Y neuronal cells', *PLoS Pathogens,* 5(11), pp. e1000659.

Naik, S., Bouladoux, N., Linehan, J.L., Han, S.J., Harrison, O.J., Wilhelm, C., Conlan, S., Himmelfarb, S., Byrd, A.L., Deming, C., Quinones, M., Brenchley, J.M., Kong, H.H., Tussiwand, R., Murphy, K.M., Merad, M., Segre, J.A. and Belkaid, Y. (2015) 'Commensal-dendritic-cell interaction specifies a unique protective skin immune signature', *Nature,* 520(7545), pp. 104-108.

Naik, S., Bouladoux, N., Wilhelm, C., Molloy, M.J., Salcedo, R., Kastenmuller, W., Deming, C., Quinones, M., Koo, L., Conlan, S., Spencer, S., Hall, J.A., Dzutsev, A., Kong, H., Campbell, D.J., Trinchieri, G., Segre, J.A. and Belkaid, Y. (2012) 'Compartmentalized control of skin immunity by resident commensals', *Science,* 337(6098), pp. 1115-1119.

Nakamura, M. and Tokura, Y. (2011) 'Epithelial-mesenchymal transition in the skin', *Journal of Dermatological Science,* 61(1), pp. 7-13.

Nakao, R., Takashiba, S., Kosono, S., Yoshida, M., Watanabe, H., Ohnishi, M. and Senpuku, H. (2014) 'Effect of *Porphyromonas gingivalis* outer membrane vesicles on gingipain-mediated detachment of cultured oral epithelial cells and immune responses', *Microbes and Infection,* 16(1), pp. 6-16.

Naresh, R., Song, Y., Hampson, D.J. (2009) 'The intestinal spirochete *Brachyspira pilosicoli* attaches to cultured Caco-2 cells and induces pathological changes', *PLoS ONE,* 4(12), pp. e8352.

Nascimento, L.V., Mauerwerk, M.T., dos Santos, C.L., Barros Filho, I.R.D., Birgel Júnior, E.H., Sotomaior, C.S., Madeira, H.M.F. and Ollhoff, R.D. (2015) 'Treponemes detected in digital dermatitis lesions in Brazilian dairy cattle and possible host reservoirs of infection', *Journal of Clinical Microbiology*, 53(6), pp. 1935-1937.

National Cancer Institute (2007) 'Layers of the skin.' [Online] Available at: https://visualsonline.cancer.gov/details.cfm?imageid=4366 (Accessed: 21st July 2017).

Naveen, V., Chu, C.H., Chen, B.W., Tsai, Y.C., Hsiao, C.D. and Sun, Y.J. (2016) '*Helicobacter pylori* cell binding factor 2: insights into domain motion', *Journal of Structural Biology,* 194(1), pp. 90-101.

NCBI Resource Coordinators (2017) 'Database resources of the National Center for Biotechnology Information', *Nucleic Acids Research,* 45(D1), pp. D12-D17.

Neilsen, B.H., Thomsen, P.T., Green, L.E., Kaler, J. (2012) 'A study of the dynamics of digital dermatitis in 742 lactating dairy cows', *Preventive Veterinary Medicine,* 104(1-2), pp. 44-52.

Nestle, F.O., Meglio, P.D., Qin, J.Z. and Nickoloff, B.J. (2009) 'Skin immune sentinels in health and disease', *Nature Reviews Immunology,* 9(10), pp. 679-691.

Newbrook, K., Staton, G.J., Clegg, S.R., Birtles, R.J., Carter, S.D. and Evans, N.J. (2017) '*Treponema ruminis* sp. Nov., a spirochaete isolated from the bovine rumen', *International Journal of Systematic and Evolutionary Microbiology,* 67, pp. 1349-1354.

Newton, K. and Dixit, V.M. (2012) 'Signaling in innate immunity and inflammation', *Cold Springs Harbour Perspectives in Biology,* 4, pp. a006049.

Nielsen, M.W., Strube, M.L., Isbrand, A., Al-Medrasi, W.D.H.M., Boye, M., Jensen, T.K. and Klitgaard, K. (2016) 'Potential bacterial core species associated with digital dermatitis in cattle herds identified by molecular profiling of interdigital skin samples', *Veterinary Microbiology,* 186, pp. 139-149.

Nixon, C.S., Steffen, M.J. and Ebersole, J.L. (2000) 'Cytokine responses to *Treponema pectinovorum* and *Treponema denticola* in human gingival fibroblasts', *Infection and Immunity,* 68(9), pp. 5284-5292.

Nobes, C.D., Lauritzen, I., Mattei, M.G., Paris, S., Hall, A. and Chardin, P. (1998) 'A new member of the Rho family, Rnd1, promotes disassembly of actin filament structures and loss of cell adhesion', *The Journal of Cell Biology,* 141(1), pp. pp. 187-197.

Nookaew, I., Papini, M., Pornputtapong, N., Scalcinati, G., Fagerberg, L., Uhlén, M. and Nielsen, J. (2012) 'A comprehensive comparison of RNA-Seq-based transcriptome analysis from reads to differential gene expression and cross-comparison with microarrays: a case study in *Saccharomyces cerevisiae', Nucleic Acids Research,* 40(20), pp. 10084-10097.

Nordhoff, M., Moter, A., Schrank, K. and Wieler, L.H. (2008) 'High prevalence of treponemes in bovine digital dermatitis-a molecular epidemiology', *Veterinary Microbiology,* 131(3-4), pp. 293-300.

Nordhoff, M., Taras, D., Macha, M., Tedin, K., Busse, H.J. and Wieler, L.H. (2005) '*Treponema berlinense* sp. nov. and *Treponema porcinum* sp. nov., novel spirochaetes isolated from porcine faeces', *International Journal of Systematic and Evolutionary Microbiology,* 55(4), pp. 1675-1680.

Norring, M., Manninen, E., de Passillé, A.M., Rushen, J., Munksgaard, L. and Saloniemi, H. (2008) 'Effects of sand and straw bedding on the lying behaviour, cleanliness, and hoof and hock injuries of dairy cows', *Journal of Dairy Science,* 91(2), pp. 570-576.

Norris, S.J., Charon, N.W., Cook, R.G., Fuentes, M.D. and Limberger, R.J. (1988) 'Antigenic relatedness and N-terminal sequence homology define two classes of periplasmic flagellar proteins of *Treponema pallidum* subsp. *pallidum* and *Treponema phagedenis', Journal of Bacteriology,* 170(9), pp. 4072-4082.

Nygaard, P. (1986) 'On the role of cytidine deaminase in cellular metabolism', *Advances in Experimental Medicine and Biology,* 195(Pt B), pp. 415-420.

Nygaard, V. and Rødland, E.A. (2016) 'Methods that remove batch effects while retaining group differences may lead to exaggerated confidence in downstream analyses', *Biostatistics,* 17(1), pp. 29-39.

Obermeier, O. (1973) 'Vorkommen, feinster eine Eigenbewegung zeigender Fäden im Blute von Recurrenskranken', *Zentralblatt für die Medizinischen Wissenschaften,* 11, pp. 145-147.

O'Callaghan, K.A., Cripps, P.J., Downham, D.Y. and Murray, R.D. (2003) 'Subjective and objective assessment of pain and discomfort due to lameness in dairy cattle', *Animal Welfare,* 12(4), pp. 605-610.

Ohnishi, J., Piesman, J., de Silva, A.M. (2000) 'Antigenic and genetic heterogeneity of *Borrelia burgdorferi* populations transmitted by ticks', *Proceedings of the National Academy of Sciences of the United States of America,* 98(2), pp. 670-675.

Okoniewski, M.J. and Miller, C.J. (2006) 'Hybridization interactions between probesets in short oligo microarrays lead to spurious correlations', *BMC Bioinformatics,* 7, pp. 276.

Oliveros, J.C. (2007-2015) 'Venny. An interactive tool for comparing lists with Venn's diagrams.' Available at: http://bioinfogp.cnb.csic.es/tools/venny/ (Accessed: 10th February 2017).

Ong, P.Y., Ohtake, T., Brandt, C., Strickland, I., Boguniewicz, M., Ganz, T., Gallo, R.L. and Leung, D.Y.M. (2002) 'Endogenous antimicrobial peptides and skin infections in atopic dermatitis', *The New England Journal of Medicine,* 347(15), pp. 1151-1160.

Onyiro, O.M., Andrews, L.J. and Brotherstone, S. (2008) 'Genetic parameters for digital dermatitis and correlations with locomotion, production, fertility traits, and longevity in Holstein-Friesian dairy cows', *Journal of Dairy Science,* 91(10), pp. 4037-4046.

Oosting, M., ter Hofstede, H., van de Veerdonk, F.L., Sturm, P., Kullberg, B.J., van der Meer, J.W.M., Netea, M.G. and Joosten, L.A.B. (2011) 'Role of interleukin-23 (IL-23) receptor

signalling for IL-17 responses in human Lyme disease', *Infection and Immunity,* 79(11), pp. 4681-4687.

Oren, A., Ganz, T., Liu, L., Meerloo, T. (2003) 'In human epidermis, β-defensin 2 is packaged in lamellar bodies', *Experimental and Molecular Pathology,* 74(2), pp. 180-182.

Ornitz, D.M., Xu, J., Colvin, J.S., McEwen, D.G., MacArthur, C.A., Coulier, F., Gao, G. and Goldfarb, M. (1996) 'Receptor specificity of the fibroblast growth factor family', *The Journal of Biological Chemistry,* 271(25), pp. 15292-15297.

Palaniappan, R.U.M, Chang, Y.F., Jusuf, S.S.D., Artiushin, S., Timoney, J.F., McDonough, S.P., Barr, S.C., Divers, T.J., Simpson, K.W., McDonough, P.L. and Mohammed, H.O. (2002) 'Cloning and molecular characterization of an immunogenic LigA protein of *Leptospira interrogans', Infection and Immunity,* 70(11), pp. 5924-5930.

Palmer, M.A., Donnelly, R.F., Garland, M.J., Majithiya, R. and O'Connell, N.E. (2013) 'The effect of slurry on skin permeability to methylene blue dye in dairy cows with and without a history of digital dermatitis', *Animal,* 7(10), pp. 1731-1737.

Papini, S., Cecchetti, D., Campani, D., Fitzgerald, W., Grivel, J.C., Chen, S., Margolis, L. and Revoltella, R.P. (2003) 'Isolation and clonal analysis of human epidermal keratinocyte stem cells in long-term culture', *Stem Cells,* 21(4), pp. 481-494.

Park, H., Li, Z., Yang, Z.O., Chang, S.H., Nurieva, R., Wang, Y.H., Wang, Y., Hood, L., Zhu, Z., Tian, Q. and Dong, C. (2005) 'A distinct lineage of CD4 T cells regulates tissue inflammation by producing interleukin 17', *Nature Immunology,* 6(11), pp. 1133-1141.

Parker, M.L., Houston, S., Wetherell, C., Cameron, C.E. and Boulanger, M.J. (2016) 'The structure of *Treponema pallidum* Tp0624 reveals a modular assembly of divergently functionalized and previously uncharacterised domains', *PLoS ONE,* 11(11), pp. e0166274.

Parsons, J.T., Horwitz, A.R. and Schwartz, M.A. (2010) 'Cell adhesion: integrating cytoskeletal dynamics and cellular tension', *Nature Reviews Molecular Cellular Biology,* 11(9), pp. 633-643.

Pasparakis, M., Haase, I. and Nestle, F.O. (2014) 'Mechnisms regulating skin immunity and inflammation', *Nature Reviews Immunology,* 14(5), pp. 289-301.

Pasquevich, K.A., Estein, S.M., Samartino, C.G., Zwerdling, A., Coria, L.M., Barrionuevo, P., Fossati, C.A., Giambartolomei, G.H. and Cassataro, J. (2009) 'Immunization with recombinant *Brucella* species outer membrane protein Omp16 or Omp19 in adjuvant induces specific CD4+ and CD8+ T cells as well as systemic and oral protection against *Brucella abortus* infection', *Infection and Immunity,* 77(1), pp. 436-445.

Paster, B.J. (2011) 'Phylum XV. Spirochaetes Garrity and Holt 2001.' In: Krieg, N.R., Staley, J.T., Brown, D.R., Hedlund, B.P., Paster, B.J., Ward, N.L., Ludwig, W. and Whitman, W.B. *Bergey's Manual of Systematic Bacteriology* (Volume 4), 2nd edition, New York: Springer, pp. 471-563.

Paster, B.J. and Canale-Parola, E. (1982) 'Physiological diversity of rumen spirochetes', *Applied and Environmental Microbiology,* 43(3), pp. 686-693.

Paster, B.J. and Canale-Parola, E. (1985) '*Treponema saccharophilum* sp. nov., a large pectinolytic spirochete from the bovine rumen', *Applied and Environmental Microbiology,* 50(2), pp. 212-219.

Paster, B.J., Stackebrandt, E., Hespell, R.B., Hahn, C.M. and Woese, C.R. (1984) 'The phylogeny of the spirochaetes', *Systematic and Applied Microbiology*, 5(3), pp. 337-351.

Pastuszczak, M., Gozdzialska, A., Jakiela, B., Obtulowicz, A., Jaskiewicz, J., Wojas-Pelc, A. (2017) 'Robust pro-inflammatory immune response is associated with serological cure in patients with syphilis: an observational study', *Sexually Transmitted Infections,* 93(1), pp. 11-14.

Pautsch, A., and Schulz, G.E. (1998) 'Structure of the outer membrane protein A transmembrane domain', *Nature,* 5(11), pp. 1013-1017.

Pautsch, A. and Schulz, G.E. (2000) 'High-resolution structure of the OmpA membrane domain', *Journal of Molecular Biology,* 298(2), pp. 273-282.

Payne, G.W., Vandamme, P., Morgan, S.H., LiPuma, J.J., Coenye, T., Weightman, A.J., Jones, T.H. and Mahenthiralingam, E. (2005) 'Development of a *recA* gene-based identification approach for the entire *Burkholderia* genus', *Applied and Environmental Microbiology,* 71(7), pp. 3917-3929.

Penneys, N.S., Fulton, J.E.(Jr), Weinstein, G.D. and Frost, P. (1970) 'Location of proliferating cells in human epidermis', *Archives of Dermatology,* 101(3), pp. 323-327.

Petersen, T.N., Brunak, S., von Heijne, G. and Nielsen, H. (2011) 'SignalP 4.0: discriminating signal peptides from transmembrane regions', *Nature Methods,* 8(10), pp. 785-786.

Pierce (2004) 'Remove detergent from protein samples.' [Online] Available at: https://fscimage.fishersci.com/webimages_FSC/downloads/pierce_detergent.pdf (Accessed: 1st July 2017).

Piknova, M., Guczynska, W., Miltko, R., Javorsky, P., Kasperowicz, A., Michalowski, T. and Pristas, P. (2008) '*Treponema zioleckii* sp. nov., a novel fructan-utilizing species of rumen treponemes', *FEMS Microbiology Letters,* 289(2), pp. 166-172.

Pond, S.L. and Frost, S.D. (2005) 'Datamonkey: rapid detection of selection pressure on individual sites of codon alignments', *Bioinformatics,* 21(10), pp. 2531-2533.

Posey, J.E. and Gherardini, F.C. (2000) 'Lack of a role for iron in the Lyme disease pathogen', *Science,* 288(5471), pp. 1651-1653.

Posey, J.E., Hardham, J.M., Norris, S.J. and Gherardini, F.C. (1999) 'Characterization of a manganese-dependent regulatory protein, TroR, from *Treponema pallidum', Proceedings of the National Academy of Sciences of the United States of America,* 96(19), pp. 10887-10892.

Poumay, Y. and Pittelkow, M.R. (1995) 'Cell density and culture factors regulate keratinocyte commitment to differentiation and expression of suprabasal K1/K10 keratins', *Journal of Investigative Dermatology,* 104(2), pp. 271-276.

Pringle, M., Backhans, A., Otman, F., Sjölund, M. and Fellström, C. (2009) 'Isolation of spirochaetes of genus *Treponema* from pigs with ear necrosis', 139(3-4), pp. 279-283.

Probert, W.S. and Johnson, B.J.B. (1998) 'Identification of a 47 kDa fibronectin-binding protein expressed by *Borrelia burgdorferi* isolate B31', *Molecular Microbiology,* 30(5), pp. 1003-1015.

Radolf, J.D., Hazlett, K.R.O. and Lukehart, S.A. (2006) 'Pathogenesis of syphilis.' In: Radolf, J.D. and Lukehart, S.A. *Pathogenic Treponema: Molecular and Cellular Biology,* Norfolk, UK: Caister Academic Press, pp. 197-236.

Raffel, S.J., Battisti, J.M., Fischer, R.J. and Schwan, T.G. (2014) 'Inactivation of genes for antigenic variation in relapsing fever spirochete *Borrelia hermsii* reduces infectivity in mice and transmission by ticks, *PLoS Pathogens,* 10(4), pp. e1004056.

Rahsaz, M., Geramizadeh, B., Kaviani, M. and Marzban, S. (2015) 'Gelatin for purification and proliferation of primary keratinocyte culture for use in chronic wounds and burns', *Experimental and Clinical Transplantation,* 13(Suppl 1), pp. 361-365.

Rainard, P., Riollet, C., Berthon, P., Cunha, P., Fromageau, A., Rossignol, C. and Gilbert, F.B. (2008) 'The chemokine CXCL3 is responsile for the constitutive chemotactic activity of bovine milk for neutrophils', *Molecular Immunology,* 45(15), pp. 4020-4027.

Ramanathan, B., Wu, H., Ross, C.R. and Blecha, F. (2004) 'PR-39, a porcine antimicrobial peptide, inhibits apoptosis: involvement of caspase-3', *Developmental and Comparative Immunology,* 28(2), pp. 163-169.

Ramesh, G., Santana-Gould, L., Inglis, F.M., England, J.D. and Philipp, M.T. (2013) 'The Lyme disease spirochete *Borrelia burgdorferi* induces inflammation and apoptosis in cells from dorsal root ganglia', *Journal of Neuroinflammation,* 10(88), pp. 1-14.

Randall, L.V., Green, M.J., Chagunda, M.G.G., Mason, C., Archer, S.C., Green, L.E. and Huxley, J.N. (2015) 'Low body condition predisposes cattle to lameness: an 8-year study of one dairy herd', *Journal of Dairy Science,* 98(6), pp. 3766-3777.

Rasmussen, M., Capion, N., Klitgaard, K., Rogdo, T., Fjeldaas, T., Boye, M. and Jensen, T.K. (2012) 'Bovine digital dermatitis: possible pathogenic consortium consisting of *Dichelobacter nodosus* and multiple *Treponema* species', *Veterinary Microbiology,* 160(1-2), pp. 151-161.

Read, D.H. and Walker, R.L. (1998) 'Papillomatous digital dermatitis (footwarts) in California dairy cattle: clinical and gross pathologic findings', *Journal of Veterinary Diagnostic Investigation*, 10(1), pp. 67-76.

Read, D.H., Walker, R.L., Castro, A.E., Sundberg, J.P. and Thurmond, M.C. (1992) 'An invasive spirochaete associated with interdigital papillomatosis of dairy cattle', *The Veterinary Record,* 130, pp. 59-60.

Reader, J.D., Green, M.J., Kaler, J., Mason, S.A. and Green, L.E. (2011) 'Effect of mobility score on milk yield and activity in dairy cattle', *Journal of Dairy Science,* 94(10), pp. 5045-5052.

Reeder, S.M., Palmer, J.M., Prokkola, J.M., Lilley, T.M., Reeder, D.M. and Field, K.A. (2017) '*Pseudogymnoascus destructans* transcriptome changes during white-nose syndrome infections', *Virulence,* In Press.

Refaai, W., Ducatelle, R., Geldhof, P., Mihi, B., El-shair, M. and Opsomer, G. (2013) 'Digital dermatitis in cattle is associated with an excessive innate immune response triggered by the keratinocytes', *BMC Veterinary Research,* 9, pp. 193.

Reijnders, C.M., van Lier, A., Roffel, S., Kramer, D., Scheper, R.J. and Gibbs, S. (2015) 'Development of a full-thickness human skin equivalent *in vitro* model derived from TERT-immortalized keratinocytes and fibroblasts', *Tissue Engineering Part A,* 21(17-18), pp. 2448-2459.

Relun, A., Guatteo, R., Roussel, P. and Bareille, N. (2011) 'A simple method to score digital dermatitis in dairy cows in the milking parlor', *Journal of Dairy Science,* 94(11), pp. 5424-5434.

Relun, A., Lehebel, A., Bareille, N. and Guatteo, R. (2012) 'Effectiveness of different regimens of a collective topical treatment using a solution of copper and zinc chelates in the cure of digital dermatitis in dairy farms under field conditions', *Journal of Dairy Science,* 95, pp. 3722-3735.

Relun, A., Lehebel, A., Bruggink, M., Bareille, N. and Guatteo, R. (2013a) 'Estimation of the relative impact of treatment and herd management practices on prevention of digital dermatitis in French dairy herds', *Preventive Veterinary Medicine*, 110(3-4), pp. 558-562.

Relun, A., Lehebel, A., Chesnin, A., Guatteo, R. and Bareille, N. (2013b) 'Association between digital dermatitis lesions and test-day milk yield of Holstein cows from 41 French dairy farms', *Journal of Dairy Science*, 96(4), pp. 2190-2200.

Rheinwald, J.G. and Green, H. (1975) 'Serial cultivation of strains of human epidermal keratinocytes: the formation of keratinizing colonies from single cells', *Cell,* 6(3), pp. 331-344.

Robinson, J.T., Thorvaldsdóttir, H., Winckler, W., Guttman, M., Lander, E.S., Getz, G. and Mesirov, J.P. (2011) 'Integrative Genomics Viewer', *Nature Biotechnology,* 29(1), pp. 24-26.

Rodriguez-Lainz, A., Melendez-Retamal, P., Hird, D.W., Read, D.H. and Walker, R.L. (1999) 'Farm- and host-level risk factors for papillomatous digital dermatitis in Chilean dairy cattle', *Preventive Veterinary Medicine,* 42(2), pp. 87-97.

Rosdy, M. and Clauss, L.C. (1990) 'Terminal epidermal differentiation of human keratinocytes grown in chemically defined medium on inert filter substrates at the air-liquid interface', *The Journal of Investigative Dermatology,* 95(4), pp. 409-414.

Karami, A., Sarshar, M., Ranjbar, R. and Zanjani, R.S. (2014) 'The Phylum Spirochaetaceae.' In: Rosenberg, E., DeLong, E.F., Lory, S., Stackebrandt, E. and Thompson, F. The prokaryotes: other major lineages of bacteria and the archaea. 4th edition, Heidelberg, Berlin: Springer, pp. 915-931.

Rowland, G.C., Aboshkiwa, M. and Coleman, G. (1993) 'Comparative sequence analysis and predicted phylogeny of the DNA-dependent RNA polymerase beta subunits of *Staphylococcus aureus* and other eubacteria', *Biochemical Society Transactions,* 21(1), pp. 40S.

Rubin, J.S., Osada, H., Finch, P.W., Taylor, W.G., Rudikoff, S. and Aaronson, S.A. (1989) 'Purification and characterization of a newly identified growth factor specific for epithelial cells', *Proceedings of the National Academy of Sciences of the United States of America,* 86(3), pp. 802-806.

Ruiz-Romeu, E., Ferran, M., Giménez-Arnau, A., Bugara, B., Lipert, B., Jura, J., Florencia, E.F., Prens, E.P., Celada, A., Pujol, R.M. and Santamaria-Babí, L.F. (2016) 'MCPIP1 RNase is aberrantly distributed in psoriatic epidermis and rapidly induced by IL-17a', *Journal of Investigative Dermatology,* 136(8), pp. 1599-1607.

Rurangirwa, F.R., Dilbeck, P.M., Crawford, T.B., McGuire, T.C. and McElwain, T.F. (1999) 'Analysis of the 16S rRNA gene of micro-organism WSU 86-1044 from an aborted bovine foetus reveals that it is a member of the order *Chlamydiales*: proposal of *Waddliaceae* fam. nov., *Waddlia chondrophilia* gen. nov., sp. nov.', *International Journal of Systematic Bacteriology,* 49(Pt2), pp. 577-581.

Russell, T.M., Delorey, M.J. and Johnson, B.J.B. (2013) '*Borrelia burgdorferi* BbHtrA degrades host ECM proteins and stimulates release of inflammatory cytokines *in vitro*', *Molecular Medicine,* 90(2), pp. 241-251.

Russell, T.M. and Johnson, B.J.B. (2013) 'Lyme disease spirochaetes possess an aggrecan-binding protease with aggrecanase activity', *Molecular Microbiology,* 90(2), pp. 228-240.

Rutherford, K., Parkhill, J., Crook, J., Horsnell, T., Rice, P., Rajandream, M.A. and Barrell, B. (2000) 'Artemis: sequence visualization and annotation', *Bioinformatics*, 16(10), pp. 944-945.

Sanger, F., Nicklen, S. and Coulson, A.R. (1977) 'DNA sequencing with chain-terminating inhibitors', *Proceedings of the National Academy of Sciences of the United States of America,* 74(12), pp. 5463-5467.

Santos, T.M.A., Pereira, R.V., Caixeta, L.S., Guard, C.L. and Bicalho, R.C. (2012) 'Microbial diversity in bovine papillomatous digital dermatitis in Holstein dairy cows from upstate New York', *FEMS Microbiology Ecology,* 79(2), pp. 518-529.

Schaudinn, F. (1905) 'Korrespondenzen', *Deutsche Medizinische Wochenschrift,* 31, pp. 1728.

Schlafer, S., Nordhoff, M., Wyss, C., Strub, S., Hübner, J., Gescher, D.M., Petrich, A., Göbel, U.B. and Moter, A. (2008) 'Involvement of *Guggenheimella bovis* in digital dermatitis lesions of dairy cows', *Veterinary Microbiology,* 128(1-2), pp. 118-125.

Schleimer, R.P., Freeland, H.S., Peters, S.P., Brown, K.E. and Derse, C.P. (1989) 'An assessment of the effects of glucocorticoids on degranulation, chemotaxis, binding to vascular endothelium and formation of leukotriene B4 by purified human neutrophils', *The Journal of Pharmacology and Experimental Therapeutics,* 250(2), pp. 598-605.

Scholey, R.A., Blowey, R.W., Murray, R.D., Smith, R.F., Cameron, J., Massey, J.P., Ollier, W.R. and Carter, S.D. (2012) 'Investigating host genetic factors in bovine digital dermatitis', *The Veterinary Record,* 171(24), pp. 624.

Scholey, R.A., Evans, N.J., Blowey, R.W., Massey, J.P., Murray, R.D., Smith, R.F., Ollier, W.E. and Carter, S.D. (2013) 'Identifying the host pathogenic pathways in bovine digital dermatitis by RNA-Seq analysis', *The Veterinary Journal,* 197(3), pp. 699-706.

Schramm, F., Kern, A., Barthel, C., Nadaud, S., Meyer, N., Jaulhac, B. and Boulanger, N. (2012) 'Microarray analyses of inflammation response of human dermal fibroblasts to different strains of *Borrelia burgdorferi* sensu stricto', *PLoS ONE,* 7(6), pp. e40046.

Schrank, K., Choi, B.K, Grund, S., Moter, A., Heuner, K., Nattermann, H. and Göbel, U.B. (1999) '*Treponema brennaborense* sp. nov., a novel spirochaete isolated from a dairy cow suffering from digital dermatitis', *International Journal of Systematic Bacteriology,* 49(Pt1), pp. 43-50.

Schröder, N.W., Opitz, B., Lamping, N., Michelsen, K.S., Zähringer, U., Göbel, U.B. and Schumann, R.R. (2000) 'Involvement of lipopolysaccharide binding protein, CD14, and Toll-like receptors in the initiation of innate immune responses by *Treponema* glycolipids', *Journal of Immunology,* 165(5), pp. 2683-2693.

Schulz, G.E. (2002) 'The structure of bacterial outer membrane proteins', *Biochimica et Biophysica Acta,* 1565, pp. 308-317.

Schultz, C.P., Wolf, V., Lange, R., Mertens, E., Wecke, J., Naumann, D. and Zähringer, U. (1998) 'Evidence for a new type of outer membrane lipid in oral spirochete *Treponema denticola.* Functioning permeation barrier without lipopolysaccharides', *Journal of Biological Chemistry,* 273(25), pp. 15661-15666.

Schultz, N. and Capion, N. (2013) 'Efficacy of salicylic acid in the treatment of digital dermatitis in dairy cattle', *The Veterinary Journal,* 198(2), pp. 518-523.

Schwan, T.G., Piesman, J., Golde, W.T., Dolan, M.C. and Rosa, P.A. (1995) 'Induction of an outer surface protein on *Borrelia burgdorferi* during tick feeding', *Proceedings of the National Academy of Sciences of the United States of America,* 92(7), pp. 2909-2913.

Schweizer, J., Bowden, P.E., Coulombe, P.A., Langbein, L., Lane, E.B., Magin, T.M., Maltais, L., Omary, M.B., Parry, D.A.D., Rogers, M.A. and Wright, M.W. (2006) 'New consensus nomenclature for mammalian keratins', *The Journal of Cell Biology,* 174(2), pp. 169-174.

Scott, D., Siboo, I.R., Chan, E.C., Klitorinos, A. and Siboo, R. (1993) 'Binding of hemin and congo red by oral haemolytic spirochetes', *Oral Microbiology and Immunology,* 8(4), pp. 245-250.

Seiberg, M. (2001) 'Keratinocyte-melanocyte interactions during melanosome transfer', *Pigment Cell and Melanoma Research,* 14(4), pp. 236-242.

Seling, A., Siegel, C., Fingerle, V., Jutras, B.L., Brissette, C.A., Skerka, C., Wallich, R., Zipfel, P.F., Stevenson, B. and Kraixzy, P. (2010) 'Functional characterization of *Borrelia spielmanii* outer surface proteins that interact with distinct members of the human factor H protein family and with plasminogen', *Infection and Immunity,* 78(1), pp. 39-48.

Selsted, M.E., Tang, Y.Q., Morris, W.L., McGuire, P.A., Novotny, M.J., Smith, W., Henschen, A.H. and Cullor, J.S. (1993) 'Purification, primary structures, and antibacterial activities of β-defensins, a new family of antimicrobial peptides from bovine neutrophils', *Journal of Biological Chemistry,* 268(9), pp. 6641-6648.

Serruto, D., Bottomley, M.J., Ram, S., Giuliani, M.M. and Rappuoli, R. (2012) 'The new multicomponent vaccine against meningococcal serogroup B, 4CMenB: immunological, functional and structural characterization of the antigens', *Vaccine,* 30(Suppl 2), pp. B87-B97.

Shankar, S.P., Wilson, M.S., DiVietro, J.A., Mentink-Kane, M.M., Xie, Z., Wynn, T.A. and Druey, K.M. (2012) 'RGS16 attenuates pulmonary Th2/Th17 inflammatory responses', *The Journal of Immunology,* 188(12), pp. 6347-6356.

Sharif, O. and Knapp, S. (2008) 'From expression to signalling: roles of TREM-1 and TREM-2 in innate immunity and bacterial infection', *Immunobiology,* 213, pp. 701-713.

Shi, J., Ross, C.R., Leto, T.L. and Blecha, F. (1996) 'PR-39, a proline-rich antibacterial peptide that inhibits phagocyte NADPH oxidase activity by binding to Src homology 3 domains of p47 phox', *Proceedings of the National Academy of Sciences of the United States of America,* 93(12), pp. 6014-6018.

Shibahara, T., Ohya, T., Ishii, R., Ogihara, Y., Maeda, T., Ishikawa, Y. and Kadota, K. (2002) 'Concurrent spirochaetal infections of the feet and colon of cattle in Japan', *Australian Veterinary Journal*, 80(8), pp. 497-502.

Singer, K.H., Scearce, R.M., Tuck, D.T., Whichard, L.P., Denning, S.M. and Haynes, B.F. (1989) 'Removal of fibroblasts from human epithelial cell cultures with use of a complement fixing monoclonal antibody reactive with human fibroblasts and monocytes/macrophages', *The Journal of Investigative Dermatology,* 92(2), pp. 166-170.

Skaar, E.P. (2010) 'The battle for iron between bacterial pathogens and the vertebrate host', *PLoS Pathogens,* 6(8), pp. e1000949.

Skalerič, U., Manthey, C.M., Mergenhagen, S.E., Gašpirc, B. and Wahl, S.M. (2000) 'Superoxide release and superoxide dismutase expression by human gingival fibroblasts', *European Journal of Oral Sciences,* 108(2), pp. 130-135.

Skerman, V.B.D., McGowan, V. and Sneath, P.H.A. (1980) 'Approved lists of bacterial names', *International Journal of Systematic Bacteriology,* 30, pp. 225-420.

Skovbjerg, S., Martner, A., Hynsjö, L., Hessle, C., Olsen, I., Dewhirst, F.E., Tham, W. and Wold, A.E. (2010) 'Gram-positive and Gram-negative bacteria induce different patterns of cytokine production in human mononuclear cells irrespective of taxonomic relatedness', *Journal of Interferon and Cytokine Research,* 30(1), pp. 23-32.

Smibert, R.M. (1984) 'Genus III *Treponema.*' In: Krieg, N.R. and Holt, J.G. *Bergey's Manual of Systematic Bacteriology* (Volume 1)*,* 2nd edition, Baltimore: Williams and Wilkins, pp. 49-57.

Smibert, R.M., Johnson, J.L. and Ranney, R.R. (1984) '*Treponema socranskii* sp. nov., *Treponema socranskii* subsp. *socranskii* subsp. nov., *Treponema socranskii* subsp. *buccale* subsp. nov., and *Treponema socranskii* subsp. *paredis* subsp. nov. isolated from the human periodontia', *International Journal of Systematic Bacteriology,* 34(4), pp. 457-462.

Smola, H., Stark, H.J., Thiekötter, G., Mirancea, N., Krieg, T. and Fusenig, N.E. (1998) 'Dynamics of basement membrane formation by keratinocyte-fibroblast interactions in organotypic skin culture', *Experimental Cell Research,* 239(2), pp. 399-410.

Söding, J., Biegert, A. and Lupas, A.N. (2005) 'The HHpred interactive server for protein homology detection and structure prediction', *Nucleic Acids Research,* 33(web server issue), pp. W244-W248.

Solano, L., Barkema, H.W., Pajor, E.A., Mason, S., LeBlanc, S.J., Zaffino Heyerhoff, J.C., Nash, C.G.R., Haley, D.B., Vasseur, E., Pellerin, D., Rushen, J., de Passillé, A.M. and Orsel, K. (2015) 'Prevalence of lameness and associated risk factors in Canadian Holstein-Friesian cows housed in freestall barns', *Journal of Dairy Science,* 98(10), pp.6978-6991.

Somers, J.G.C.J., Frankena, K., Noordhuizen-Stassen, E.N. and Metz, J.H.M. (2005) 'Risk factors for digital dermatitis in dairy cows kept in cubicle houses in The Netherlands', *Preventive Veterinary Medicine,* 71(1-2), pp. 11-21.

Sorrell, J.M. and Caplan, A.I. (2004) 'Fibroblast heterogeneity: more than skin deep', *Journal of Cell Science,* 117, pp. 667-675.

Stackebrandt, E. and Goebel, B.M. (1994) 'Taxonomic note: a place for DNA-DNA reassociation and 16S rRNA sequence analysis in the present species definition in bacteriology', *International Journal of Systematic Bacteriology,* 44(4), pp. 846-849.

Staden, R. (1996) 'The Staden sequence analysis package', *Molecular Biotechnology,* 5(3), pp. 233-241.

Stafford, K.J. and Gregory, N.G. (2008) 'Implications of intensification of pastoral animal production on animal welfare', *New Zealand Veterinary Journal,* 56(6), pp. 274-280.

Stamm, L.V., Bergen, H.L. and Walker, R.L. (2002) 'Molecular typing of papillomatous digital dermatitis-associated *Treponema* isolates based on analysis of 16S-23S ribosomal DNA intergenic spacer regions', *Journal of Clinical Microbiology,* 40(9), pp. 3463-3469.

Stanton, T.B. and Canale-Parola, E. (1980) '*Treponema bryantii* sp. nov., a rumen spirochete that interacts with cellulolytic bacteria', *Archives of Microbiology*, 127(2), pp. 145-156.

Staton, G.J., Newbrook, K., Clegg, S.R., Birtles, R.J., Evans, N.J. and Carter, S.D. (2017) '*Treponema rectale* sp. nov., a spirochete isolated from the bovine rectum', *International Journal of Systematic and Evolutionary Microbiology,* 67(7), pp. 2470-2475.

Steere, A.C., Grodzicki, R.L., Kornblatt, A.N., Craft, J.E., Barbour, A.G., Burgdorfer, W., Schmid, G.P., Johnson, E. and Malawista, S.E. (1983) 'The spirochetal etiology of Lyme disease', *The New England Journal of Medicine,* 308, pp. 733-740.

Stevenson, B., Choy, H.A., Pinne, M., Rotondi, M.L., Miller, M.C., DeMoll, E., Kraiczy, P., Cooley, A.E., Creamer, T.P., Suchard, M.A., Brissette, C.A., Verma, A. and Haake, D.A. (2007) '*Leptospira interrogans* endostatin-like outer membrane proteins bind host fibronectin, laminin and regulators of complement', *PLoS ONE,* 2(11), pp. e1188.

Stolzenberg, E.D., Anderson, G.M., Ackermann, M.R., Whitlock, R.H. and Zasloff, M. (1997) 'Epithelial antibiotic induced in states of disease', *Proceedings of the National Academy of Sciences of the United States of America,* 94(16), pp. 8686-8690.

Straatsma, T.P. and Soares, T.A. (2008) 'Characterization of the outer membrane protein OprF of *Pseudomonas aeruginosa* in a lipopolysaccharide membrane by computer simulation', *Proteins,* 74(2), pp. 475-488.

Strober, W. (2001) 'Trypan blue exclusion test of cell viability', *Current Protocols in Immunology,* 21(3B), A.3B.1-A.3B.2.

Strub, S., van der Ploeg, J.R., Nuss, K., Wyss, C., Luginbühl, A. and Steiner, A. (2007) 'Quantitation of *Guggenheimella bovis* and treponemes in bovine tissues related to digital dermatitis', *FEMS Microbiology Letters,* 269(1), pp. 48-53.

Strutz, F., Okada, H., Lo, C.W., Danoff, T., Carone, R.L., Tomaszewski, J.E. and Nielson, E.G. (1995) 'Identification and characterization of a fibroblast marker: FSP1', *The Journal of Cell Biology,* 130(2), pp. 393-405.

Sturn, A., Quackenbush, J., Trajanoski, Z. (2002) 'Genesis: cluster analysis of microarray data', *Bioinformatics,* 18(1), pp. 207-208.

Sullivan, L.E. (2015c) 'Identifying digital dermatitis infection reservoirs in beef cattle and sheep', PhD Thesis, University of Liverpool, Liverpool, UK.

Sullivan, L.E., Blowey, R.W., Carter, S.D., Duncan, J.S., Grove-White, D.H., Page, P., Iveson, T., Angell, J.W. and Evans, N.J. (2014) 'Presence of digital dermatitis treponemes on cattle and sheep hoof trimming equipment', *The Veterinary Record,* 175(8), pp. 201.

Sullivan, L.E., Carter, S.D., Blowey, R., Duncan, J.S., Grove-White, D. and Evans, N.J. (2013) 'Digital dermatitis in beef cattle', *Veterinary Record*, 173(23), pp. 582.

Sullivan, L.E., Carter, S.D., Duncan, J.S., Grove-White, D.H., Angell, J.W. and Evans, N.J. (2015b) 'The gastrointestinal tract as a potential infection reservoir of digital dermatitis-associated treponemes in beef cattle and sheep', *Applied and Environmental Microbiology,* 81(21), pp. 7460-7469.

Sullivan, L.E., Evans, N.J., Clegg, S.R., Carter, S.D., Horsfield, J.E., Grove-White, D. and Duncan, J.S. (2015a) 'Digital dermatitis treponemes associated with a severe foot disease in dairy goats', *Veterinary Record*, 176(11), pp. 283.

Sultan, S.Z., Manne, A., Stewart, P.E., Bestor, A., Rosa, P.A., Charon, N.W. and Motaleb, M.A. (2013) 'Motility is crucial for the infectious life cycle of *Borrelia burgdorferi*', *Infection and Immunity,* 81(6), pp. 2012-2021.

Sumida, H., Yanagida, K., Kita, Y., Abe, J., Matsushima, K., Nakamura, M., Ishii, S., Sato, S. and Shimizu, T. (2014) 'Interplay between CXCR2 and BLT1 facilitates neutrophil infiltration and resultant keratinocyte activation in a murine model of imiquimod-induced psoriasis', *The Journal of Immunology,* 192(9), pp. 4361-4369.

Sun, E.S., Molini, B.J., Barrett, L.K., Centurion-Lara, A., Lukehart, S.A. and van Voorhis, W.C. (2004) 'Subfamily I *Treponema pallidum* repeat protein family: sequence variation and immunity', *Microbes and Infection,* 6(8), pp. 725-737.

Sun, T.T. and Green, H. (1976) 'Differentiation of the epidermal keratinocyte in cell culture: formation of the cornified envelope', *Cell,* 9(4), pp. 511-521.

Suurväli, J., Pahtma, M., Saar, R., Paalme, V., Nutt, A., Tiivel, T., Saaremäe, M., Fitting, C., Cavaillon, J.M. and Boudinot, R. (2015) 'RGS16 restricts the pro-inflammatory response of monocytes', *Scandinavian Journal of Immunology,* 81(1), pp. 23-30.

Suzuki, M. and Loesche, W.J. (1989) 'Ceruloplasmin can substitute for rabbit serum in stimulating the growth of *Treponema denticola*', *Infection and Immunity,* 57(2), pp. 643-644.

Swellengrebel, N.H. (1907) 'Sur la cytologie compare des spirochetes et des spirilles', *Annales de l'Institut Pasteur (Paris),* 21, pp. 562-586.

Sykora, S. and Brandt, S. (2015) 'Occurrence of *Treponema* DNA in equine hoof canker and normal hoof tissue', *Equine Veterinary Journal,* 47(5), pp. 627-630.

Sykora, S., Kofler, J., Glonegger-Reichert, J., Dietrich, J., Auersperg, G. and Brandt, S. (2015) '*Treponema* DNA in bovine 'non-healing' versus common sole ulcers and white line disease', *The Veterinary Journal,* 205(3), pp. 417-420.

Tajima, K., Aminov, R.I., Nagamine, T., Ogata, K., Nakamura, M., Matsui, H. and Benno, Y. (1999) 'Rumen bacterial diversity as determined by sequence analysis of 16S rDNA libraries', *FEMS Microbiology Ecology*, 29(2), pp. 159-169.

Tamura, K. and Nei, M. (1993) 'Estimation of the number of nucleotide substitutions in the control region of mitochondrial DNA in humans and chimpanzees', *Molecular Biology and Evolution*, 10(3), pp. 512-526.

Tamura, K., Stecher, G., Peterson, D., Filipski, A. and Kumar, S. (2013) 'MEGA6: Molecular Evolutionary Genetics Analysis version 6.0', *Molecular Biology and Evolution,* 30(12), pp. 2725-2729.

Tanabe, S.I., Bodet, C. and Grenier, D. (2009) '*Treponema denticola* peptidoglycan induces the production of inflammatory mediators and matrix metalloproteinase 9 in macrophage-like cells', *Journal of Periodontal Research,* 44(4), pp. 503-510.

Tavaré, S. (1986) 'Some probabilistic and statistical problems in the analysis of DNA sequences', *American Mathematical Society: Lectures on Mathematics in the Life Sciences,* 17, pp. 57-86.

Taylor, D.J. and Alexander, T.J. (1971) 'The production of dysentery in swine by feeding cultures containing spirochaete', *The British Veterinary Journal,* 127(11), pp. 58-61.

Thakoersing, V.S., Danso, M.O., Mulder, A., Gooris, G., Ghalbzouri, A.E. and Bouwstra, J.A. (2012) 'Nature versus nurture: does human skin maintain its stratum corneum lipid properties *in vitro', Experimental Dermatology,* 21(11), pp. 865-870.

Tharakan, S., Pontiggia, L., Biedermann, T., Böttcher-Haberzeth, S., Schiestl, C., Reichmann, E. and Meuli, M. (2010) 'Transglutaminases, involucrin, and loricrin as markers of epidermal

differentiation in skin substitutes derived from human sweat gland cells', *Pediatric Surgury International,* 26(1), pp. 71-77.

The ENCODE consortium (2011) 'Standards, guidelines and best practices for RNA-Seq: 2010/2011. *RNA-Seq: RNA standards v1.0.'* [Online] Available at: https://www.encodeproject.org/about/experiment-guidelines/experiment-guidelines-previous/ (Accessed 29th February 2016).

Thompson, J.D., Higgins, D.G. and Gibson, T.J. (1994) 'CLUSTAL W: improving the sensitivity of progressive multiple sequence alignment through sequence weighting, position-specific gap penalties and weight matrix choice', *Nucleic Acids Research*, 22(22), pp. 4673-4680.

Thorvaldsdóttir, H., Robinson, J.T. and Mesirov, J.P. (2013) 'Integrative Genomics Viewer (IGV): high-performance genomics data visualization and exploration', *Briefings in Bioinformatics,* 14(2), pp. 178-192.

Timmusk, S., Merlot, E., Lövgren, T., Järvekülg, L., Berg, M. and Fossum, C. (2009) 'Regulator of G protein signalling 16 is a target for a porcine circovirus type 2 protein', *Journal of General Virology,* 90(10), pp. 2425-2436.

Tojkander, S., Gateva, G. and Lappalainen, P. (2012) 'Actin stress fibers – assembly, dynamics and biological roles', *Journal of Dairy Science,* 125(Pt8), pp. 1-10.

Tokumaru, S., Sayama, K., Shirakata, Y., Komatsuzawa, H., Ouhura, K., Hanakawa, Y., Yahata, Y., Dai, X., Tohyama, M., Nagai, H., Yang, L., Higashiyama, S., Yoshimura, A., Sugai, M. and Hashimoto, K. (2005) 'Induction of keratinocyte migration via transactivation of the epidermal growth factor receptor by the antimicrobial peptide LL-37', *The Journal of Immunology,* 175(7), pp. 4662-4668.

Towne, J.E., Garka, K.E., Renshaw, B.R., Virca, G.D. and Sims, J.E. (2004) 'Interleukin (IL)-1F6, IL-1F8, and IL-1F9 signal through IL-1Rrp2 and IL-1RAcP to activate the pathway leading to NF-κB and MAPKs', *The Journal of Biological Chemistry,* 279(14), pp. 13677-13688.

Trapnell, C., Williams, B.A., Pertea, G., Mortazavi, A., Kwan, G., van Baren, M.J., Salzberg, S.L., Wold, B.J. and Pachter, L. (2010) 'Transcript assembly and quantification by RNA-Seq reveals unannotated transcripts and isoform switching during cell differentiation', *Nature Biotechnology,* 28(5), pp. 511-515.

Trott, D.J., Moeller, M.R., Zuerner, R.L., Goff, J.P., Waters, W.R., Alt, D.P., Walker, R.L. and Wannemuehler, M.J. (2003) 'Characterization of *Treponema phagedenis*-like spirochetes isolated from papillomatous digital dermatitis lesions in dairy cattle', *Journal of Clinical Microbiology*, 41(6), pp. 2522-2529.

Tseng, S.C.G., Jarvinen, M.J., Nelson, W.G., Huang, J.W., Woodcock-Mitchell, J. and Sun, T.T. (1982) 'Correlation of specific keratins with different types of epithelial differentiation: monoclonal antibody studies', *Cell,* 30(2), pp. 361-372.

Tsuji, K., Ojima, M., Otabe, K., Horie, M., Koga, H., Sekiya, I. and Muneta, T. (2017) 'Effects of different cell-detaching methods on the viability and cell surface antigen expression of synovial mesenchymal stem cells', *Cell Transplantation,* 26(6), pp. 1089-1102.

Uitto, V.J., Pan, Y.M., Leung, W.K., Larjava, H., Ellen, R.P., Finlay, B.B. and McBride, B.C. (1995) 'Cytopathic effects of *Treponema denticola* chymotrypsin-like proteinase on migrating and stratified epithelial cells', *Infection and Immunity,* 63(9), pp. 3401-3410.

Umemoto, T., Nakazawa, F., Hoshino, E., Okada, K., Fukunaga, M. and Namikawa, I. (1997) '*Treponema medium* sp. nov., isolated from human subgingival dental plaque', *International Journal of Systematic and Evolutionary Microbiology*, 47(1), pp. 67-72.

Urwin, R., Feavers, I.M., Jones, D.M., Maiden, M.C.J. and Fox, A.J. (1998) 'Molecular variation of meningococcal serotype 4 antigen genes', *Epidemiology and Infection,* 121(1), pp. 95-101.

van Amstel, S.R., van Vuuren, S. and Tutt, C.L. (1995) 'Digital dermatitis: report of an outbreak', *Journal of the South African Veterinary Association*, 66(3), pp. 177-181.

van den Bogaerdt, A.J., Ulrich, M.M.W., van Galen, M.J.M., Reijnen, L., Verkerk, M., Pieper, J., Lamme, E.N. and Middelkoop, E. (2004) 'Upside-down transfer of porcine keratinocytes from a porous, synthetic dressing to experimental full-thickness wounds', *Wound Repair and Regeneration,* 12(2), pp. 225-234.

Vandeputte-Rutten, L., Bos, M.P., Tommassen, J. and Gros, P. (2003) 'Crystal structure of Neisserial surface protein A (NspA), a conserved outer membrane protein with vaccine potential', *The Journal of Biological Chemistry,* 278(27), pp. 24825-24830.

Veldhuizen, E.J.A., Schneider, V.A.F., Agustiandari, H., van Dijk, A., Tjeerdsma-van Bokhoven, J.L.M., Bikker, F.J. and Haagsman, H.P. (2014) 'Antimicrobial and immunomodulatory activities of PR-39 derived peptides', *PLoS ONE,* 9(4), pp. e95939.

Velez-delValle, C., Marsch-Moreno, M., Castro-Muñozledo, F., Galván-Medoza, I.J. and Kuri-Harcuch, W. (2016) 'Epithelial cell migration requires the interaction between the vimentin and keratin intermediate filaments', *Scientific Reports,* 6, pp. 24389.

Verma, A., Hellwage, J., Artiushin, S., Zipfel, P.F., Kraiczy, P., Timoney, J.F. and Stevenson, B. (2006) 'LfhA, a novel factor H-binding protein of *Leptospira interrogans*', *Infection and Immunity,* 74(5), pp. 2659-2666.

Vieira, M.L. and Nascimento, A. (2015) 'Interactions of spirochetes with the host fibrinolytic system and potential roles in pathogenesis', *Critical Reviews in Microbiology,* 42(4), pp. 1-15.

Villarroel-Neri, R., Pino-Ramírez, D., Sánchez-Villalobos, A., García-Bracho, D., Boscán-Ocando, J. and González-Martín, J. (2010) 'Descripción de un brote de dermatitis digital bovina en el municipio Miranda del estado Zulia, Venezuela (primer reporte)', *Revista Científica*, 20(6), pp. 600-607.

Visner, G.A., Dougall, W.C., Wilson, J.M., Burr, I.A. and Nick, H.S. (1990) 'Regulation of manganese superoxide dismutase by lipopolysaccharide, interleukin-1, and tumor necrosis factor', *The Journal of Biological Chemistry,* 265(5), pp. 2856-2864.

Visser, M.B., Koh, A., Glogauer, M. and Ellen, R.P. (2011) '*Treponema denticola* major outer sheath protein induces actin assembly at free barbed ends by a PIP2-dependent uncapping mechanism in fibroblasts', *PLoS ONE,* 6(8), pp. e23736.

Visser, M.B. and Pollitt, C.C. (2010) 'Characterization of extracellular matrix macromolecules in primary cultures of equine keratinocytes', *BMC Veterinary Research*, 6, pp. 16.

Walker, R.L., Read, D.H., Loretz, K.J. and Nordhausen, R.W. (1995) 'Spirochetes isolated from dairy cattle with papillomatous digital dermatitis and interdigital dermatitis', *Veterinary Microbiology*, 47(3-4), pp. 343-355.

Walker, S.L., Smith, R.F., Routly, J.E., Jones, D.N., Morris, M.J. and Dobson, H. (2008) 'Lameness, activity time-budgets, and estrus expression in dairy cattle', *Journal of Dairy Science,* 91(12), pp. 4552-4559.

Wang, L.T., Lee, F.L., Tai, C.J. Kasai, H. (2007) 'Comparison of *gyrB* gene sequences, 16S rRNA gene sequences and DNA-DNA hybridization in the *Bacillus subtilis* group', *International Journal of Systematic and Evolutionary Microbiology,* 57(Pt8), pp. 1846-1850.

Wang, Q., Ko, K.S., Kapus, A., McCulloch, C.A.G. and Ellen, R.P. (2001) 'A spirochete surface protein uncouples store-operated calcium channels in fibroblasts: a novel cytotoxic mechanism', *The Journal of Biological Chemistry,* 276(25), pp. 23056-23064.

Wang, W., Zhang, W., Han, Y., Chen, J., Wang, Y., Zhang, Z. and Hui, R. (2005) 'NELIN, a new F-actin associated protein, stimulates HeLa cell migration and adhesion', *Biochemical and Biophysical Research Communications,* 330(4), pp. 1127-1131.

Wang, Z., Gerstein, M. and Snyder, M. (2009) 'RNA-Seq: a revolutionary tool for transcriptomics', *Nature Reviews Genetics,* 10(1), pp. 57-63.

Warnick, L.D., Janssen, D., Guard, C.L. and Gröhn, Y.T. (2001) 'The effect of lameness on milk production in dairy cows', *Journal of Dairy Science,* 84, pp. 1988-1997.

Watkins, C.A., Mackellar, A., Frew, D., Mackie, C., George, A., Hopkins, J., Burgess, S.T.G., McNeilly, T.N. and Huntley, J.F. (2009) 'Gene expression profiling of ovine keratinocytes stimulated with *Psoroptes ovis* mite antigen - a preliminary study', *Parasite Immunology,* 31(6), pp. 304-311.

Watt, F.M. (1989) 'Terminal differentiation of epidermal keratinocytes', *Current Opinion in Cell Biology,* 1(6), pp. 1107-1115.

Weinlich, R., Oberst, A., Dillon, C.P., Janke, L.J., Milasta, S., Lukens, J.R., Rodriguez, D.A., Gurung, P., Savage, C. and Kanneganti, T.D. (2013) 'Protective roles for caspase-8 and cFLIP in adult homeostasis', *Cell Reports,* 5(2), pp. 340-348.

Weiser, J.N., and Gotschlich, E.C. (1991) 'Outer membrane protein A (OmpA) contributes to serum resistance and pathogenicity of *Escherichia coli* K-1', *Infection and Immunity,* 59(7), pp. 2252-2258.

Wells, S.J., Garber, L.P. and Wagner, B.A. (1999) 'Papillomatous digital dermatitis and associated risk factors in US dairy herds', *Preventive Veterinary Medicine*, 38(1), pp. 11-24.

Wempe, F., Kuhlmann, J.K., Scheit, K.H. (1994) 'Characterization of the bovine monocyte chemoattractant protein-1 gene', *Biochemical and Biophysical Research Communications,* 202(3), pp. 1272-1279.

Whay, H.R., Main, D.C.J., Green, L.E. and Webster, A.J.F. (2002) 'Farmer perception of lameness prevalence.' In: Shearer, J.K. *Proceedings of the 12th International Symposium on Lameness in Ruminants*. Orlando, Florida, USA, pp. 355-358.

Whay, H.R., Waterman, A.E. and Webster, A.J.F. (1997) 'Associations between locomotion, claw lesions and nociceptive threshold in dairy heifers during the peri-partum period', *The Veterinary Journal,* 154(2), pp. 154-161.

Whay, H.R., Waterman, A.E., Webster, A.J.F. and O'Brien, J.K. (1998) 'The influence of lesion type on the duration of hyperalgesia associated with hindlimb lameness in dairy cattle', *The Veterinary Journal,* 156(1), pp. 23-29.

Wilkinson, J.E., Smith, C., Suter, M. and Lewis, R.M. (1987) 'Long-term cultivation of canine keratinocytes', *Journal of Investigative Dermatology,* 88(2), pp. 202-206.

Willshire, J.A. and Bell, N.J. (2009) 'An economic review of cattle lameness', *Cattle Practice*, 17(2), pp. 136-141.

Woese, C.R. (1987) 'Bacterial evolution', *Microbiological Reviews*, 51(2), pp. 221-271.

Wooten, R.M., Modur, V.R., McIntyre, T.M. and Weis, J.J. (1996) '*Borrelia burgdorferi* outer membrane protein A induces nuclear translocation of nuclear factor-kappa B and inflammatory activation in human endothelial cells', *The Journal of Immunology,* 157(10), pp. 4584-4590.

Wu, Q., Guan, G., Liu, Z., Li, Y., Luo, J. and Yin, H. (2015) 'RNA-Seq-based analysis of changes in *Borrelia burgdorferi* gene expression linked to pathogenicity', *Parasites and Vectors,* 8, pp.155.

Wu, X.B., Tian, L.H., Zou, H.J., Wang, C.Y., Yu, Z.Q., Tang, C.H., Zhao, F.K. and Pan, J.Y. (2013) 'Outer membrane protein OmpW of *Escherichia coli* is required for resistance to phagocytosis', *Research in Microbiology,* 164(8), pp. 848-855.

Wu, Z., Hansmann, B., Meyer-Hoffert, U., Gläser, R. and Schröder, J.M. (2009) 'Molecular identification and expression analysis of filaggrin-2, a member of the S100 fused-type protein family', *PLoS ONE,* 4(4), pp. e5227.

Wufuer, M., Lee, G., Hur, W., Jeon, B., Kim, B.J., Choi, T.H. and Lee, S. (2016) 'Skin-on-a-chip model simulating inflammation, edema and drug-based treatment', *Nature Scientific Reports,* 6 (37471), pp. 1-12.

Wyss, C., Choi, B.K., Schüpbach, P., Guggenheim, B. and Göbel, U.B. (1996) '*Treponema maltophilum* sp. nov., a small oral spirochete isolated from human periodontal lesions', *International Journal of Systematic Bacteriology*, 46(3), pp. 745-752.

Wyss, C., Choi, B.K., Schüpbach, P., Guggenheim, B. and Göbel, U.B. (1997) '*Treponema amylovorum* sp. nov., a saccharolytic spirochete of medium size isolated from an advanced human periodontal lesion', *International Journal of Systematic Bacteriology*, 47(3), pp. 842-845.

Wyss, C., Choi, B.K., Schüpbach, P., Moter, A., Guggenheim, B. and Göbel, U.B. (1999) '*Treponema lecithinolyticum* sp. nov., a small saccharolytic spirochaete with phospholipase A and C activities associated with periodontal disease', *International Journal of Systematic Bacteriology*, 49(Pt4), pp. 1329-1339.

Wyss, C., Dewhirst, F.E., Gmür, R., Thurnheer, T., Xue, Y., Schüpbach, P., Guggenheim, B. and Paster, B.J. (2001) '*Treponema parvum* sp. nov., a small, glucuronic or galacturonic acid-dependent oral spirochaete from lesions of human periodontitis and acute necrotizing ulcerative gingivitis', *International Journal of Systematic and Evolutionary Microbiology*, 51(Pt3), pp. 955-962.

Wyss, C., Moter, A., Choi, B.K., Dewhirst, F.E., Xue, Y., Schüpbach, P., Göbel, U.B., Paster, B.J. and Guggenheim, B. (2004) '*Treponema putidum* sp. nov., a medium-sized proteolytic spirochaete isolated from lesions of human periodontitis and acute necrotizing ulcerative gingivitis', *International Journal of Systematic and Evolutionary Microbiology*, 54(Pt4), pp. 1117-1122.

Wyss, C., Dewhirst, F.E., Paster, B.J., Thurnheer, T. and Luginbühl, A. (2005) *Guggenheimella bovis* gen. nov., sp. nov., isolated from lesions of bovine dermatitis digitalis. *International Journal of Systematic and Evolutionary Microbiology*, 55(Pt2), pp. 667-671.

Xue, F., Zhao, X., Yang, Y., Zhao, J., Yang, Y., Cao, Y., Hong, C., Liu, Y., Sun, L., Huang, M. and Gu, J. (2013) 'Responses to murine and human macrophages to Leptospiral infection: a study using comparative array analysis', *PLoS Neglected Tropical Diseases,* 7(10), pp. e2477.

Yaffe, M.B., Murthy, S. and Eckert, R.L. (1993) 'Evidence that involucrin is a covalently linked constituent of highly purified cultured keratinocyte cornified envelopes', *Journal of Investigative Dermatology,* 100(1), pp. 3-9.

Yamazaki, T., Miyamoto, M., Yamada, S., Okuda, K. and Ishihara, K. (2006) 'Surface protease of *Treponema denticola* hydrolyzes C3 and influences function of polymorphonuclear leukocytes', *Microbes and Infection,* 8(7), pp. 1758-1763.

Yang, D., Chertov, O., Bykovskaia, S.N., Chen, Q., Buffo, M.J., Shogan, J., Anderson, M., Schröder, J.M., Wang, J.M., Howard, O.M.Z. and Oppenheim, J.J. (1999) 'β-defensins: linking innate and adaptive immunity through dendritic and T cell CCR6', *Science,* 286(5439), pp. 525-528.

Yang, P.F., Song, M., Grove, D.A. and Ellen, R.P. (1998) 'Filamentous actin disruption and diminished inositol phosphate response in gingival fibroblasts caused by *Treponema denticola', Infection and Immunity,* 66(2), pp. 696-702.

Yano, S. and Okochi, H. (2005) 'Long-term culture of adult murine epidermal keratinocytes', British Journal of Dermatology, 153(6), pp. 1101-1104.

Yao, C., Oh, J.H., Lee, D.H., Bae, J.S., Jin, C.L., Park, C.H. and Chung, J.H. (2015) 'Toll-like receptor family members in skin fibroblasts are functional and have a higher expression compared to skin keratinocytes', *International Journal of Molecular Medicine,* 35(5), pp. 1443-1450.

Yao, Z., Painter, S.L., Fanslow, W.C., Ulrich, D., Macduff, B.M., Spriggs, M.K. and Armitage, R.J. (1995) 'Human IL-17: a novel cytokine derived from T cells', *The Journal of Immunology,* 155(12), pp. 5483-5486.

Yeh, T.L., Lee, C.Y., Amzel, L.M., Espenshade, P.J. and Bianchet, M.A. (2011) 'The hypoxic regulator of sterol synthesis nro1 is a nuclear import adaptor', *Structure,* 19(4), pp. 503-514.

Yeruham, I. and Perl, S. (1998) 'Clinical aspects of an outbreak of papillomatous digital dermatitis in a dairy cattle herd', *Journal of the South African Veterinary Association*, 69(3), pp. 112-115.

Young, B., Lowe, J.S., Stevens, A. and Heath, J.W. (2006) 'Part 2 Basic Tissue Types: 4. supportive/connective tissues.' In: Wheater's functional histology; A Text and Colour Atlas. 5th edition, London: Elsevier, Churchill Livingstone, pp. 65-81.

Yu, N., Zhang, S., Zuo, F., Kang, K., Guan, M. and Xiang, L. (2009) 'Cultured human melanocytes express functional Toll-like receptors 2-4, 7 and 9', *Journal of Dermatological Science,* 56(2), pp. 113-120.

Zhang, J.R., Hardham, J.M., Barbour, A.G. and Norris, S.J. (1997) 'Antigenic variation in Lyme disease *Borreliae* by promiscuous recombination of VMP-like sequence cassettes', *Cell,* 89(2), pp. 275-285.

Zhang, X., Ibrahimi, O.A., Olsen, S.K., Umemori, H., Mohammadi, M. and Ornitz, D.M. (2006) 'Receptor specificity of the fibroblast growth factor family: the complete mammalian FGF family', *Journal of Biological Chemistry,* 281, pp. 15694-15700.

Zhao, Z., McCloud, B., Fleming, R. and Klempner, M.S. (2007) '*Borrelia burgdorferi*-induced monocyte chemoattractant protein-1 production *in vivo* and *in vitro*', *Biochemical and Biophysical Research Communications,* 358(2), pp. 528-533.

Zhou, Y., Bizzaro, J.W. and Marx, K.A. (2004) 'Homopolymer tract length dependent enrichments in functional regions of 27 eukaryotes and their novel dependence on the organism DNA (G+C)% composition', *BMC Genomics,* 5(95), pp. 1-16.

Zimin, A.V., Delcher, A.L., Florea, L., Kelley, D.R., Schatz, M.C., Puiu, D., Hanrahan, F., Pertea, G., Van Tassell, C.P., Sonstegard, T.S., Marçais, G., Roberts, M., Subramanian, P., Yorke, J.A. and Salzberg, S.L. (2009) 'A whole-genome assembly of the domestic cow, *Bos taurus', Genome Biology,* 10(4), pp. R42.

Zinicola, M., Higgins, H., Lima, S., Machado, V., Guard, C. and Bicalho, R. (2015b) 'Shotgun metagenomic sequencing reveals functional genes and microbiome associated with bovine digital dermatitis', *PLoS ONE,* 10(7), pp. e0133674.

Zinicola, M., Lima, F., Lima, S., Machado, V., Gomez, M., Döpfer, D., Guard, C. and Bicalho, R. (2015a) 'Altered microbiomes in bovine digital dermatitis lesions, and the gut as a pathogen reservoir', *PLoS ONE*, 10(3), pp. e0120504.

Ziolecki, A. (1979) 'Isolation and characterization of large treponemes from the bovine rumen', *Applied and Environmental Microbiology*, 37(1), pp. 131-135.

Ziolecki, A. and Wojciechowicz, M. (1980) 'Small pectinolytic spirochetes from the rumen', *Applied and Environmental Microbiology*, 39(4), pp. 919-922.

Zuerner, R.L., Heidari, M., Elliot, M.K., Alt, D.P. and Neill, J.D. (2007) 'Papillomatous digital dermatitis spirochetes suppress the bovine macrophage innate immune response', *Veterinary Microbiology,* 125(3-4), pp. 256-264.

Appendices

Appendix A: Chemicals and reagents

Table A.1 Formulation and method of preparation for reagents and solutions.

Appendix B: RNA-Seq data analysis (Chapter four)

(1) Quantification and quality control data for RNA-Seq.

Table B.1 Quantification and quality control of total RNA preparations for RNA-Seq.

Figure B.1 The total number of reads obtained for each sample by RNA-Seq.

Table B.2 Mapping rates of sequenced reads to *Bos taurus* genome using TopHat2.

(2) Summary of significantly differentially expressed genes.

Table B.3 Significantly differentially expressed genes (log2 fold change) in bovine fibroblasts stimulated with BDD treponemes, commensal treponeme or control LPS.

(3) Ingenuity pathway analysis

Table B.4 Differentially expressed mRNA transcripts mapping to multiple Ensembl stable bovine gene identifiers.

Table B.5 Differentially expressed genes of bovine foot skin fibroblasts with more than one orthologous human gene.

Figure B.2 The 20 most significantly activated or inhibited canonical pathways, enriched diseases and biological functions in fibroblasts stimulated withcontrol LPS.

Figure B.3 The 20 most significantly activated or inhibited canonical pathways, enriched diseases and biological functions in fibroblasts stimulated with *T. medium* phylogroup sonicate.

Figure B.4 The 20 most significantly activated or inhibited canonical pathways, enriched diseases and biological functions in fibroblasts stimulated with *T. phagedenis* phylogroup sonicate.

Figure B.5 The 20 most significantly activated or inhibited canonical pathways, enriched diseases and biological functions in fibroblasts stimulated with *T. pedis* sonicate.

Figure B.6 The 20 most significantly activated or inhibited canonical pathways, enriched diseases and biological functions in fibroblasts stimulated with *T. ruminis* sonicate.

(4) Analysing the variance between experimental replicates

Figure B.7 Principle component analysis of variance in normalised gene expression data across 17 experimental replicates, excluding three likely outliers, by RNA-Seq.

Appendix C: Investigating the molecular diversity of a putative OMP of DD treponemes (Chapter five)

Publications and supporting papers

Newbrook, K., Staton, G.J., Clegg, S.R., Birtles, R.J., Carter, S.D. and Evans, N.J. (2017) '*Treponema ruminis* sp. Nov., a spirochaete isolated from the bovine rumen', *International Journal of Systematic and Evolutionary Microbiology,* 67, pp. 1349-1354.

Appendix A: Chemicals and reagents

Table A.1 Formulation and method of preparation for all of the reagents and solutions used throughout this thesis.

Reagent or solution	Preparation
Agarose [1% (w/v)]	Dissolved 1 g certified™ molecular biology agarose (Bio-Rad Laboratories Ltd, Hemel Hempstead, UK) in 100 ml 1x Tris-acetate-EDTA (TAE) buffer.
Ammonium chloride [500 mM] [50 mM]	A 500 mM ammonium chloride (NH_4Cl) stock solution was prepared by Miss Lisa Luu by dissolving 13.4g NH_4Cl (Sigma-Aldrich, Poole, UK) in 500 ml Dulbecco's phosphate buffered saline without calcium and magnesium (DPBS-CMF; Sigma-Aldrich, Poole, UK). A 10 ml working solution of 50 mM NH_4Cl was prepared by diluting 1 ml (500 mM) NH_4Cl stock solution in 9 ml DPBS-CMF.
Bovine type I collagen solution [100 µg/ml]	Diluted 33 µl (3 mg/ml) PureCol® purified bovine type I collagen solution (Advanced Biomatrix Inc., Carlsbad, USA) in 967 µl sterile water (Sigma-Aldrich, Poole, UK). A 25 cm^3 tissue culture flask was coated with 1 ml (100 µg/ml) bovine type I collagen solution for 2 hours at 37°C.
Chelex® 100 resin [5% (w/v)]	Dissolved 0.5 g chelex® 100 resin (Bio-Rad Laboratories Ltd, Hemel Hempstead, UK) in 10 ml distilled water.
Cholera toxin from *Vibrio cholerae* [1 mg/ml]	Reconstituted 1 mg cholera toxin from *Vibrio cholerae* (Sigma-Aldrich, Poole, UK) in 1 ml distilled water. The solution was stored at 4°C until use.
Dispase II solution [10 mg/ml]	Resuspended 0.5 g dispase II (Sigma-Aldrich, Poole, UK) in 20 ml isolation media (see Chapter 2.1.1) by gentle vortexing and then filtered through a sterile 0.45 µM syringe filter. Each 10 ml suspension added

	to a further 30 ml isolation media to produce a 10 mg/ml working solution. The solution was prepared as required and stored at 4°C until use.
DNA ladder [100 bp] [1 kb]	Diluted DNA ladders (100 bp or 1 kb; Promega UK, Southampton, UK) with 100 µl blue/orange 6x loading dye (Promega UK, Southampton, UK).
Enrofloxacin [5 µg/ml]	Miss Jennifer Bell prepared the 5 µg/ml solution by dissolving 50 µg enrofloxacin (Sigma-Aldrich, Poole, UK) in 1.0 M potassium hydroxide (Sigma-Aldrich, Poole, UK) and filtering through a 0.22 µM filter. The solution was stored in the dark at 4°C in 500 µl aliquots. Enrofloxacin balancing solution (1M hydrochloric acid, filter sterilised through a 0.22 µM filter; Sigma-Aldrich, Poole, UK) was added alongside Enrofloxacin to balance the culture medium pH.
Ethylene glycol-bis(2-aminoethylether)-N,N,N',N'-tetraacetic acid (EGTA) [100 mM]	Dissolved 0.380 g Ethylene glycol-bis(2-aminoethylether)-N,N,N',N'-tetraacetic acid (EGTA; Sigma-Aldrich, Poole, UK) in 100 ml 1 M sodium hydroxide (NaOH). The solution was filtered through a sterile 0.45 µM filter and stored at room temperature until required.
Foetal bovine serum (FBS)	Foetal bovine serum (FBS; Gibco™ by Life Technologies Ltd, Paisley, UK) was heat inactivated by incubation at 56°C for 30 minutes using a water bath SWB (Stuart Scientific, Staffordshire, UK). Stored at -20°C in sterile 20 ml and 50 ml aliquots.
Formaldehyde solution [4% (w/v)]	Diluted one volume 16% (w/v) formaldehyde solution (Pierce™ by Thermo Fisher Scientific, Loughborough, UK) in three volumes of DPBS-CMF (Sigma-Aldrich, Poole, UK).
IF blocking buffer (containing 10% (v/v) donkey serum, 1% (v/v) Triton™ X-100 and DPBS-CMF)	A 5 ml solution of IF blocking buffer was prepared as required by combining 500 µl donkey serum (Sigma-Aldrich, Poole, UK) and 50 µl Triton™ X-100 (Sigma-

	Aldrich, Poole, UK) in a total volume of 5 ml with DPBS-CMF.
IF washing buffer (containing 1% (v/v) donkey serum, 0.1% (v/v) Triton™ X-100 and DPBS-CMF)	A 50 ml solution of IF washing buffer was prepared as required by combining 500 µl donkey serum (Sigma-Aldrich, Poole, UK) and 50 µl Triton™ X-100 (Sigma-Aldrich, Poole, UK) in a total volume of 50 ml with DPBS-CMF.
Lipopolysaccharides (LPS) from *Salmonella enterica* serotype *typhimurium* [1 mg/ml]	Reconstituted lipopolysaccharides (LPS) from *Salmonella enterica* serotype *typhimurium* (Sigma-Aldrich, Poole, UK) in 1 ml 1x Hank's Balanced Salt Solution (HBSS; Gibco™ by Life Technologies Ltd, Paisley, UK). A 10 µg/ml working solution of LPS was prepared by diluting 100 µl of 1 mg/ml LPS stock solution in 9.9 ml control medium (WME containing 2 mM L-glutamine).
Magnesium chloride ($MgCl_2$) [100 mM]	Dissolved 0.41 g magnesium chloride ($MgCl_2$; Fisher Scientific UK Ltd, Loughborough, UK) in 20 ml phosphate buffered saline (PBS) using a magnetic stirrer hotplate (Stuart Scientific, Staffordshire, UK). The solution was filtered through a sterile 0.45 µM syringe filter and stored at room temperature. A 5 mM working solution of $MgCl_2$ was prepared as required by adding 20 ml 100 mM $MgCl_2$ to 380 ml PBS.
Phosphate buffered saline (PBS) [1x]	Dissolved 5 PBS tablets (Sigma-Aldrich, Poole, UK) in 1 litre (L) distilled water using a magnetic stirrer hotplate (Stuart Scientific, Staffordshire, UK). Stored at room temperature.
Povidone iodine [2.5% (v/v)]	One volume 7.5% (w/w) povidone iodine (Vetasept®; Animalcare Ltd, York, UK) was diluted in two volumes of distilled water to a final concentration of 2.5% (v/v) as required. Povidone

	iodine was transferred to 10 ml aliquots and was stored temporarily at room temperature until use.
Rabbit serum (RS)	Rabbit serum (RS; GE Healthcare Life Sciences, Buckinghamshire, UK) was heat inactivated through incubation at 56°C for 30 minutes using a water bath SWB (Stuart Scientific, Staffordshire, UK) and was then immediately stored at -20°C in sterile 20ml aliquots.
Rat tail collagen type I solution [100 µg/ml]	Diluted 50 µl (2 mg/ml) rat tail collagen type I solution (First Link (UK) Ltd., Wolverhampton, UK) in 950 µl sterile water (Sigma-Aldrich, Poole, UK). A 25 cm^3 tissue culture flask was coated with 1 ml (100 µg/ml) rat tail collagen type I solution for 2 hours at 37°C.
Rifampicin [25 µg/ml]	Dissolved 250 µg rifampicin (Sigma-Aldrich, Poole, UK) in 10 ml methanol (analytical grade) and then filtered through a sterile 0.22 µM syringe filter. Stored in 1ml aliquots at -20°C.
Tris-acetate-ethylenediaminetetraacetic acid (EDTA) (TAE) buffer [x]	Diluted 100 ml 40x TAE buffer (Promega UK, Southampton, UK) in 3.9 litres (L) of distilled water. Stored at room temperature.
Triton™ X-100 [2.5% (v/v)]	Diluted 12.5 ml Triton™ X-100 (Sigma-Aldrich, Poole, UK) in 487.5 ml distilled water.
Trypsin-ethylenediaminetetraacetic acid (trypsin-EDTA) [0.25% (w/v)] [0.025% (w/v)]	One volume of 0.5% (w/v) or 0.05% (w/v) Trypsin-ethylenediaminetetraacetic acid (trypsin-EDTA; Gibco™ by Life Technologies Ltd, Paisley, UK) was diluted in one volume of 1x HBSS. Trypsin-EDTA was transferred into 5 ml aliquots and was stored at -20°C until required.

Appendix B: RNA-Seq data analysis (Chapter 4)

Appendix B: (1) Quantification and quality control data for RNA-Seq.

Table B.1 Quantification and quality control of total RNA preparations for RNA-Seq. *An assessment of the quantity and quality of total RNA preparations from primary bovine foot skin fibroblast cells following co-incubation with either control media, LPS from S. enterica serotype Typhimurium, T. medium phylogroup strain T19 sonicate, T. phagedenis phylogroup strain T320A sonicate, T. pedis strain T3552B^T sonicate or T. ruminis strain Ru1^T sonicate in triplicate experimental and technical replicates. Total RNA samples which underwent RNA-Seq analysis are highlighted in pink, whereby those sample numbers which were* initially submitted (§) but subsequently replaced by poorer quality replacement samples ($^#$) are indicated. A sample that required two rounds of rRNA depletion (*) is also indicated. *Total RNA samples which underwent further quality control (QC) assessment of cellular characterisation and gDNA content are highlighted in green.*

Sample number	Co-incubation treatment	Experimental replicate	Technical replicate	RNA purity		RNA integrity number (RIN)	RNA yield (ng/µl)
				A260:A280	A260:A230		
7	Medium [control]	1	QC	2.06	1.87	9.80	73.07
1	Medium [control]	1	1	2.08	1.74	10.00	112.33
8	Medium [control]	1	2	2.05	1.83	10.00	99.83
14	Medium [control]	1	3	2.07	1.81	10.00	73.47
2$^#$	LPS from *S. enterica* serotype Typhimurium [control]	1	1	2.06	1.83	10.00	75.93
9§	LPS from *S. enterica* serotype Typhimurium [control]	1	2	2.05	1.91	10.00	71.10
15	LPS from *S. enterica* serotype Typhimurium [control]	1	3	2.08	1.91	N/A	57.50
3	*T. medium* phylogroup sonicate	1	1	2.11	0.90	10.00	56.03

10	*T. medium* phylogroup sonicate	1	2	2.06	1.97	9.90	83.50
16	*T. medium* phylogroup sonicate	1	3	2.08	1.82	N/A	57.60
4[§]	*T. phagedenis* phylogroup sonicate	1	1	2.09	1.94	10.00	61.47
11[#]	*T. phagedenis* phylogroup sonicate	1	2	2.05	1.58	9.80	57.93
17	*T. phagedenis* phylogroup sonicate	1	3	2.09	1.52	10.00	65.77
5[§]	*T. pedis* sonicate	1	1	2.10	1.68	10.00	50.77
12	*T. pedis* sonicate	1	2	2.09	0.47	9.60	48.43
18[#*]	*T. pedis* sonicate	1	3	2.08	1.62	10.00	56.87
6	*T. ruminis* sonicate	1	1	2.11	1.79	10.00	63.23
13	*T. ruminis* sonicate	1	2	2.07	1.98	10.00	68.97
19	*T. ruminis* sonicate	1	3	2.08	1.69	9.90	57.33
26	Medium [control]	2	QC	2.09	1.79	10.00	89.50
20	Medium [control]	2	1	2.11	0.75	9.80	41.70
27	Medium [control]	2	2	2.10	1.82	N/A	55.73
33	Medium [control]	2	3	2.10	1.83	10.00	107.67
21	LPS from *S. enterica* serotype Typhimurium [control]	2	1	2.10	1.63	10.00	43.17
28	LPS from *S. enterica* serotype Typhimurium [control]	2	2	2.12	1.88	10.00	59.60

34	LPS from *S. enterica* serotype Typhimurium [control]	2	3	2.09	1.94	10.00	101.67
22	*T. medium* phylogroup sonicate	2	1	2.09	1.67	9.90	62.97
29	*T. medium* phylogroup sonicate	2	2	2.12	1.60	10.00	49.20
35	*T. medium* phylogroup sonicate	2	3	2.08	1.81	10.00	68.10
23	*T. phagedenis* phylogroup sonicate	2	1	2.09	1.89	10.00	79.70
30	*T. phagedenis* phylogroup sonicate	2	2	2.10	1.83	10.00	72.47
36	*T. phagedenis* phylogroup sonicate	2	3	2.08	2.00	10.00	79.50
24	*T. pedis* sonicate	2	1	2.09	1.62	N/A	58.20
31	*T. pedis* sonicate	2	2	2.11	1.92	10.00	64.20
37	*T. pedis* sonicate	2	3	2.10	1.90	10.00	49.77
25	*T. ruminis* sonicate	2	1	2.10	1.80	10.00	61.67
32	*T. ruminis* sonicate	2	2	2.11	1.11	9.80	95.30
38	*T. ruminis* sonicate	2	3	2.09	1.92	10.00	83.07
45	Medium [control]	3	QC	2.06	1.75	N/A	62.73
39	Medium [control]	3	1	2.13	1.15	N/A	39.33
46	Medium [control]	3	2	2.06	1.75	N/A	32.43
52	Medium [control]	3	3	2.07	1.83	10.00	73.60

40	LPS from *S. enterica* serotype Typhimurium [control]	3	1	2.10	1.61	N/A	42.47
47	LPS from *S. enterica* serotype Typhimurium [control]	3	2	2.05	2.02	10.00	73.03
53	LPS from *S. enterica* serotype Typhimurium [control]	3	3	2.07	1.99	10.00	61.97
41	*T. medium* phylogroup sonicate	3	1	2.09	1.76	10.00	90.17
48	*T. medium* phylogroup sonicate	3	2	2.07	1.98	10.00	69.17
54	*T. medium* phylogroup sonicate	3	3	2.07	2.01	10.00	56.10
42	*T. phagedenis* phylogroup sonicate	3	1	2.10	2.12	N/A	58.80
49	*T. phagedenis* phylogroup sonicate	3	2	2.07	1.85	10.00	70.70
55	*T. phagedenis* phylogroup sonicate	3	3	2.08	2.03	10.00	77.80
43	*T. pedis* sonicate	3	1	2.13	0.24	N/A	35.53
50	*T. pedis* sonicate	3	2	2.07	2.03	10.00	62.23
56	*T. pedis* sonicate	3	3	2.07	2.15	10.00	67.40
44	*T. ruminis* sonicate	3	1	2.10	1.80	N/A	58.67
51	*T. ruminis* sonicate	3	2	2.09	1.72	10.00	40.60
57	*T. ruminis* sonicate	3	3	2.08	2.08	N/A	84.33

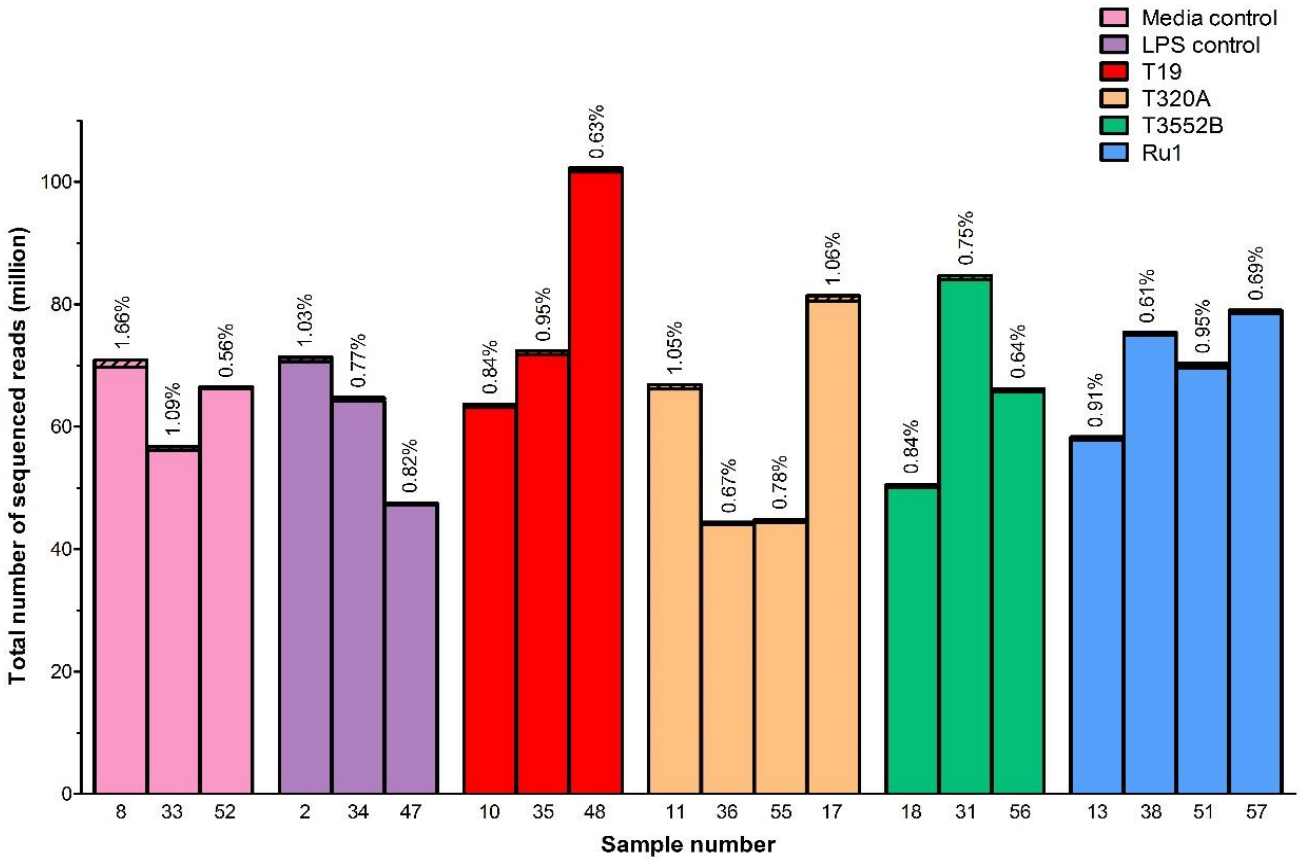

Figure B.1 The total number of reads obtained for each sample by RNA-Seq. *A summary of the total number (in millions) of sequenced reads for each replicate (sample numbers given), both before (plain and hashed sections) and after (plain sections) reads of poor quality were removed. The percentages of total sequenced reads excluded through quality control for each sample are given above each corresponding bar. Samples were primary bovine foot skin fibroblasts co-incubated with either control media (media control), LPS from S. enterica serotype Typhimurium (LPS) or sonicated preparations of T. medium phylogroup (T19), T. phagedenis phylogroup (T320A), T. pedis (T3552B) or T. ruminis (Ru1).*

Table B.2 Mapping rates of sequenced reads to the Bos taurus genome using TopHat2. *Percentage of forward pair (R1), reverse pair (R2) and combined R1 and R2 sequenced reads successfully mapped to the Bos taurus genome (UMD 3.1.1/bosTau8) using TopHat2. Sample numbers are given alongside corresponding co-incubation treatment and the experimental and technical replicate number.*

Sample number	Co-incubation treatment	Experimental replicate	Technical replicate	Percentage of mapped reads (%)		Overall read mapping rate (%)
				Forward pair (R1)	Reverse pair (R2)	
8	Media [control]	1	2	88.1	86.3	87.2
2	LPS from *S. enterica* serotype Typhimurium [control]	1	1	91.0	88.6	89.8
10	*T. medium* phylogroup sonicate	1	2	90.5	88.5	89.5
11	*T. phagedenis* phylogroup sonicate	1	2	80.5	78.6	79.5
17	*T. phagedenis* phylogroup sonicate	1	3	89.2	86.7	87.9
18	*T. pedis* sonicate	1	3	80.3	78.8	79.6
13	*T. ruminis* sonicate	1	2	91.2	89.3	90.3
33	Media [control]	2	3	89.9	88.1	89.0
34	LPS from *S. enterica* serotype Typhimurium [control]	2	3	91.2	89.4	90.3
35	*T. medium* phylogroup sonicate	2	3	89.8	87.4	88.6
36	*T. phagedenis* phylogroup sonicate	2	3	82.5	82.0	82.3
31	*T. pedis* sonicate	2	2	84.0	83.5	83.8
38	*T. ruminis* sonicate	2	3	78.1	77.9	78.0
52	Media [control]	3	3	85.5	85.3	85.4
47	LPS from *S. enterica* serotype Typhimurium [control]	3	2	86.2	85.8	86.0
48	*T. medium* phylogroup sonicate	3	2	86.2	86.0	86.1
55	*T. phagedenis* phylogroup sonicate	3	3	85.2	84.5	84.9
56	*T. pedis* sonicate	3	3	85.1	84.7	84.9
51	*T. ruminis* sonicate	3	2	86.8	86.3	86.6
57	*T. ruminis* sonicate	3	3	85.3	84.9	85.1

Appendix B: (2) Summary of significantly differentially expressed genes.

Table B.3 Summary of significantly differentially expressed genes (p ≤ 0.05, q ≤ 0.05, log2 fold change ≥ 1 or ≤ -1), given as log2 fold change, in primary bovine foot skin fibroblast cells upon stimulation with either sonicated T. medium phylogroup (T19), T. phagedenis phylogroup (T320A), T. pedis (T3552B) or T. ruminis (Ru1) or the LPS control compared to the control medium.

Gene Identifier	Chromosome and locus	Log2 fold change in gene expression compared to the control medium				
		LPS	T19	T320A	T3552B	Ru1
Uniquely expressed genes						
5_8S_rRNA	chr25:32465609-32465762	-2.766	-	-	-	-
ADAMTS3	chr6:89162541-89460195	1.663	-	-	-	-
ADAMTS6	chr20:14008346-14285012	1.106	-	-	-	-
ARHGAP42	chr15:8264443-8359734	1.155	-	-	-	-
ARHGAP6	chrX:137588933-137693777	-1.122	-	-	-	-
ARRDC2	chr7:5101427-5105930	1.054	-	-	-	-
ARTN	chr3:102712153-102713309	-1.829	-	-	-	-
BTG3	chr1:18909511-18928469	1.210	-	-	-	-
C15orf48	chr10:65243194-65246838	1.292	-	-	-	-
CD40	chr13:75563517-75574215	1.559	-	-	-	-
CD83	chr23:42335198-42354922	2.661	-	-	-	-
CDC42EP2	chr29:44189277-44195090	1.077	-	-	-	-
CDKL4	chr11:21526905-21574655	1.370	-	-	-	-
CDKN2B	chr8:22114511-22119419	-1.042	-	-	-	-
CLCN2	chr1:83443168-83457221	-1.468	-	-	-	-
CMPK2	chr11:90042356-90057598	2.959	-	-	-	-
CSRNP1	chr22:12520392-12532806	1.061	-	-	-	-
DHX58	chr19:42877796-42888179	1.044	-	-	-	-
ENSBTAG00000004339	chr21:20422126-20429481	1.305	-	-	-	-
ENSBTAG00000004556	chr5:101896621-101909500	1.336	-	-	-	-

ENSBTAG00000008705	chr24:33687907-33792573	1.149	-	-	-	-
ENSBTAG00000016661	chr5:76375511-76405820	1.059	-	-	-	-
ENSBTAG00000018499	chr28:42288944-42305211	1.007	-	-	-	-
ENSBTAG00000018731	chr1:46322717-46323776	1.414	-	-	-	-
ENSBTAG00000022954	chr3:2630818-2631902	1.184	-	-	-	-
ENSBTAG00000023365	chr18:57927151-57929923	-1.426	-	-	-	-
ENSBTAG00000032265	chr1:80502600-80506904	1.066	-	-	-	-
ENSBTAG00000039524	chr5:74875953-74876802	2.812	-	-	-	-
ENSBTAG00000039861,OAS2	chr17:63611773-63646117	1.331	-	-	-	-
ENSBTAG00000045822	chr15:74915625-74916613	1.097	-	-	-	-
ENSBTAG00000046971	chr11:5754348-5776837	1.062	-	-	-	-
F3	chr3:49110155-49121034	2.234	-	-	-	-
FAM65C	chr13:79329172-79355665	1.056	-	-	-	-
FLT3LG	chr18:56383542-56393411	1.124	-	-	-	-
GBP5	chr3:54253046-54269514	1.430	-	-	-	-
HIST2H3A	chr3:20823725-20824139	-1.237	-	-	-	-
IFNAR2	chr1:1593294-1627137	1.512	-	-	-	-
IL16	chr21:27527683-27606711	2.176	-	-	-	-
IMMP1L	chr15:63034392-63093076	1.014	-	-	-	-
IRAK3	chr5:47796255-47839675	1.095	-	-	-	-
KCNK5	chr23:13057052-13095621	1.301	-	-	-	-
LIF	chr17:71413854-71418166	2.193	-	-	-	-
MEOX2	chr4:23943519-24019359	1.091	-	-	-	-
Metazoa_SRP	chr6:31669691-31669966	1.340	-	-	-	-
Metazoa_SRP	chr8:7983900-8000085	1.192	-	-	-	-
Metazoa_SRP	chrX:17862230-17862527	1.230	-	-	-	-
MOCOS	chr24:21198153-21256992	1.437	-	-	-	-
NCALD	chr14:64875134-64898581	1.034	-	-	-	-
NFKBIE	chr23:17879934-17887291	1.072	-	-	-	-

NLK	chr19:20177846-20307081	1.110	-	-	-	-
NUB1	chr4:114689766-114725191	1.033	-	-	-	-
OSBPL3	chr4:71394902-71488446	1.352	-	-	-	-
PCDH7	chr6:51536862-52007783	1.623	-	-	-	-
PIM1	chr23:11051543-11055416	1.059	-	-	-	-
RELB	chr18:53099824-53127762	1.219	-	-	-	-
RNF125	chr24:25452968-25496186	1.837	-	-	-	-
SAMD9	chr4:10302666-10307412	1.021	-	-	-	-
SLC39A14	chr8:70186538-70237645	1.327	-	-	-	-
SLC9A3R2	chr25:1575648-1589619	-1.025	-	-	-	-
SNAI1	chr13:78766067-78772194	1.372	-	-	-	-
SNORA73	chr2:125499759-125499963	1.576	-	-	-	-
SNORA73	chr2:125501621-125501825	1.430	-	-	-	-
SNORA8	chr29:1065600-1065737	1.669	-	-	-	-
snoU85	chr5:104244558-104272651	1.153	-	-	-	-
SYNJ2	chr9:96023879-96091443	1.654	-	-	-	-
TBC1D9	chr17:17374259-17443063	1.618	-	-	-	-
TICAM1	chr7:20547963-20550264	1.715	-	-	-	-
TMEM100	chr19:6237390-6239838	3.764	-	-	-	-
TMEM121	chr21:71417178-71418135	-1.122	-	-	-	-
TSFM	chr5:56003066-56011109	1.226	-	-	-	-
TSNARE1	chr14:3054762-3171546	-1.601	-	-	-	-
U2	chr19:43829755-43829946	1.108	-	-	-	-
U2	chr19:43833326-43833517	1.277	-	-	-	-
U2	chr19:43876414-43876605	1.198	-	-	-	-
U2	chr19:43901107-43901298	1.240	-	-	-	-
U2	chr19:43912414-43912605	1.249	-	-	-	-
U2	chr19:43923765-43923956	1.241	-	-	-	-
UBALD1	chr25:3744166-3749205	1.047	-	-	-	-

ZBP1	chr13:59099338-59109190	1.174	-	-	-	-
5_8S_rRNA	chr25:32466576-32466729	-	-2.422	-	-	-
5_8S_rRNA	chr25:32469328-32469481	-	-2.917	-	-	-
CRY2	chr15:76753524-76790450	-	1.133	-	-	-
CSF1	chr3:33607138-33621030	-	1.784	-	-	-
ENSBTAG00000007447	chr5:23348067-23364470	-	1.009	-	-	-
ENSBTAG00000010813	chr14:17228478-17229057	-	1.064	-	-	-
ENSBTAG00000013213	chr14:67533221-67540870	-	1.015	-	-	-
ENSBTAG00000023169	chr13:10934395-10992906	-	1.099	-	-	-
ENSBTAG00000046153	chr24:44291871-44292990	-	1.822	-	-	-
ENSBTAG00000046307	chr14:20738813-20740407	-	1.135	-	-	-
FAM105A	chr20:58634393-58664249	-	1.618	-	-	-
FKBP5	chr23:9521253-9637802	-	3.623	-	-	-
GLUL	chr16:64948331-64958885	-	1.731	-	-	-
HMGA1	chr23:8258749-8268920	-	1.133	-	-	-
HRH1	chr22:55929987-55931463	-	2.288	-	-	-
KIAA0408	chr9:24120227-24131671	-	1.033	-	-	-
KLF15	chr22:61283171-61292866	-	2.205	-	-	-
KLF9	chr8:46883355-46907760	-	1.326	-	-	-
MAOA	chrX:105380193-105462564	-	1.182	-	-	-
MEOX1	chr19:44170624-44189417	-	1.049	-	-	-
NEDD9	chr23:44851676-44988907	-	1.144	-	-	-
NMB	chr21:22741476-22744781	-	1.115	-	-	-
PDK4	chr4:12754201-12767677	-	1.517	-	-	-
PFKFB3	chr13:17380742-17406594	-	1.427	-	-	-
PGM5	chr8:44682698-44892128	-	1.629	-	-	-
SESN1	chr9:41555160-41690067	-	1.268	-	-	-
SYBU	chr14:56909761-56997967	-	2.842	-	-	-
TSC22D3	chrX:59707291-59772737	-	1.484	-	-	-

ACAD10	chr17:57648596-57696347	-	-	-1.072	-	-
ARFGEF2	chr13:77822893-77903223	-	-	-1.032	-	-
BAG1	chr8:76352437-76363634	-	-	-1.286	-	-
BTBD19	chr3:101784089-101789519	-	-	-1.056	-	-
CCNF	chr25:1949261-1965512	-	-	-1.006	-	-
CNNM4	chr11:2690659-2725964	-	-	-1.089	-	-
CSNK1D	chr19:51207150-51241060	-	-	-1.119	-	-
DMRTA2	chr3:96451572-96456722	-	-	-1.913	-	-
ENGASE	chr19:53956453-53965180	-	-	-1.135	-	-
ENSBTAG00000012876	chr20:17609459-17610173	-	-	-1.135	-	-
ENSBTAG00000013159	chr12:19150793-19184692	-	-	-1.037	-	-
ENSBTAG00000015432	chr18:2882155-2903093	-	-	-1.086	-	-
ENSBTAG00000045579	chr14:1204507-1204909	-	-	1.400	-	-
ENSBTAG00000046357	chr28:27680679-27685834	-	-	-1.035	-	-
ENSBTAG00000046432	chr10:555201-555884	-	-	1.013	-	-
ENSBTAG00000046620	chr1:140578415-140578628	-	-	-1.013	-	-
FECH	chr24:57298433-57333273	-	-	-1.242	-	-
FZD1	chr4:8490675-8494829	-	-	-1.015	-	-
FZD5	chr2:96470386-96472144	-	-	-1.068	-	-
GADD45A	chr3:77972152-77975265	-	-	-1.066	-	-
GNE	chr8:60873150-60905455	-	-	-1.005	-	-
GPR107	chr11:100432296-100484528	-	-	-1.104	-	-
HIF1AN	chr26:21291075-21300157	-	-	-1.229	-	-
HILS1	chr19:37113476-37122446	-	-	-1.545	-	-
LSS	chr1:147623690-147654154	-	-	-1.258	-	-
LYRM7	chr7:24487321-24508916	-	-	1.024	-	-
MAGED1	chrX:95708019-95714844	-	-	-1.087	-	-
MFSD6	chr2:5752910-5814559	-	-	-1.186	-	-
MXD1	chr11:68232861-68255606	-	-	-1.032	-	-

NR4A2	chr2:39999716-40017015	-	-	-1.088	-	-
OAZ2	chr10:45428931-45433129	-	-	-1.044	-	-
PABPC5	chrX:42008983-42011006	-	-	-1.051	-	-
PLAGL2	chr13:62226993-62236866	-	-	-1.184	-	-
PSKH1	chr18:35521164-35534184	-	-	-1.148	-	-
PURA	chr7:52983070-52984039	-	-	-1.076	-	-
RAD54L2	chr22:49725491-49784000	-	-	-1.004	-	-
RCAN1	chr1:351707-362907	-	-	-1.135	-	-
RHEB	chr4:114803156-114855282	-	-	-1.047	-	-
SGMS1	chr26:8735911-8775858	-	-	-1.049	-	-
SLC35D1	chr3:78601769-78644543	-	-	-1.018	-	-
SSBP3	chr3:92411759-92576787	-	-	-1.134	-	-
SUPT7L	chr11:72021272-72033985	-	-	-1.178	-	-
SYNM	chr21:7768428-7793372	-	-	-1.074	-	-
TMC8	chr19:54633143-54642106	-	-	-1.144	-	-
TNRC6B	chr5:112043300-112172811	-	-	-1.122	-	-
TRA2A	chr4:32250995-32269539	-	-	-1.061	-	-
TTC8	chr10:101571087-101629775	-	-	-1.222	-	-
UBE3B	chr17:65905226-65944588	-	-	-1.036	-	-
UBE3D	chr9:23061429-23228366	-	-	-1.484	-	-
WNT5A	chr22:46096244-46112683	-	-	-1.057	-	-
ZNF526	chr18:51373916-51378873	-	-	-1.144	-	-
AADAT	chr8:1792851-1816770	-	-	-	-1.160	-
ACKR3	chr3:116650277-116662501	-	-	-	-1.872	-
AGPAT1	chr23:27017064-27027205	-	-	-	-1.077	-
ANKS6	chr8:64244149-64293418	-	-	-	-1.074	-
ANXA5	chr6:3542634-3575330	-	-	-	-1.197	-
ASTE1	chr1:140334902-140348547	-	-	-	-1.376	-
BDKRB1	chr21:62760702-62772148	-	-	-	1.050	-

BHLHE40	chr22:21492895-21498539	-	-	-	-1.548	-
BNC2	chr8:27974916-27993276	-	-	-	-1.061	-
C9orf64	chr8:78544395-78556152	-	-	-	-1.220	-
CBFA2T2	chr13:63632326-63670697	-	-	-	-1.267	-
CBLL1	chr4:49037767-49052388	-	-	-	-1.423	-
CCDC6	chr28:15582653-15636803	-	-	-	-1.131	-
CFL1	chr29:44638895-44642280	-	-	-	-1.108	-
CHAMP1	chr12:91100866-91103281	-	-	-	-1.071	-
COPS6	chr25:36893604-36896370	-	-	-	-1.055	-
CSRP2	chr5:6266017-6274473	-	-	-	-1.177	-
DCP1B	chr5:108814603-108857086	-	-	-	-1.048	-
DTL	chr16:73315562-73364134	-	-	-	-1.009	-
EIF3A	chr26:39585657-39616179	-	-	-	-1.303	-
EIF4EBP2	chr28:26764784-26786028	-	-	-	-1.292	-
ENSBTAG00000009359	chr15:38876121-38876667	-	-	-	-1.109	-
ENSBTAG00000009580	chr2:127429584-127431204	-	-	-	-1.871	-
ENSBTAG00000013463	chr16:27161601-27209886	-	-	-	-1.167	-
ENSBTAG00000016174	chr2:120039584-120049214	-	-	-	-1.249	-
ENSBTAG00000017765	chr3:33805753-33816442	-	-	-	-1.018	-
ENSBTAG00000020953	chr16:9512152-9514110	-	-	-	-1.088	-
ENSBTAG00000021574	chr26:33755955-33943059	-	-	-	-2.737	-
ENSBTAG00000022204	chrX:57664212-57664899	-	-	-	-1.725	-
ENSBTAG00000026909	chr10:87344475-87346625	-	-	-	-1.482	-
ENSBTAG00000032764	chr6:323370-323914	-	-	-	-1.049	-
ENSBTAG00000033961	chr9:26441434-26484894	-	-	-	-1.081	-
ENSBTAG00000045937	chr4:17767924-17769016	-	-	-	-1.709	-
ENSBTAG00000046135	chr14:69160053-69161571	-	-	-	-1.671	-
ENSBTAG00000046184	chr10:43871177-43988950	-	-	-	-1.150	-
ENSBTAG00000046314	chrX:56796340-56826755	-	-	-	-1.278	-

ENSBTAG00000047265	chr29:43163336-43163913	-	-	-	1.027	-
F2RL2	chr10:7554264-7867328	-	-	-	-1.390	-
FAM120A	chr8:86200481-86316789	-	-	-	-1.307	-
FAM98A	chr11:16157513-16173332	-	-	-	-1.070	-
FBXO7	chr5:71448943-71469170	-	-	-	-1.025	-
FHL3	chr3:108547856-108555472	-	-	-	-1.065	-
FOXJ2	chr5:102003894-102023009	-	-	-	-1.636	-
FRA10AC1	chr26:15012961-15070687	-	-	-	-1.203	-
FTH1	chr29:41172508-41175112	-	-	-	-1.195	-
GATAD2B	chr3:16633873-16644316	-	-	-	-1.528	-
GNA13	chr19:62550514-62575992	-	-	-	-1.274	-
GPATCH11	chr11:19564810-19578680	-	-	-	-1.053	-
GSPT1	chr25:10622208-10652097	-	-	-	-1.151	-
HACD2	chr1:68464486-68550787	-	-	-	-1.280	-
HNRNPA2B1	chr4:70198052-70207085	-	-	-	-1.195	-
HNRNPAB	chr7:40638056-40643916	-	-	-	-1.157	-
HSPB1	chr25:34858434-34861074	-	-	-	-1.200	-
IL36A	chr11:46569594-46573057	-	-	-	1.549	-
KLF10	chr14:63951757-63957275	-	-	-	-1.314	-
KLF12	chr12:48831951-49108263	-	-	-	-1.100	-
MGEA5	chr26:22390929-22417746	-	-	-	-1.090	-
MPHOSPH8	chr12:36608007-36653042	-	-	-	-1.130	-
NAV1	chr16:49447983-49564506	-	-	-	-1.080	-
NEXN	chr3:66998943-67053966	-	-	-	-1.168	-
NFAT5	chr18:36847729-36898690	-	-	-	-1.012	-
NFATC3	chr18:35640708-35732176	-	-	-	-1.403	-
PARP14	chr1:67613091-67659266	-	-	-	-1.163	-
PCDHGA5	chr7:54130984-54133372	-	-	-	-1.185	-
PDZD8	chr26:37939959-38021120	-	-	-	-1.142	-

PLEKHM1	chr19:45719319-45767382	-	-	-	-1.050	-
PNRC1	chr9:61921604-61925635	-	-	-	-1.366	-
POFUT1	chr13:62237056-62276100	-	-	-	-1.073	-
PPP1R10	chr23:28177337-28192982	-	-	-	-1.115	-
RBPMS	chr27:25637685-25816012	-	-	-	-1.026	-
RHOG	chr15:52061682-52075146	-	-	-	-1.498	-
RIOK1	chr23:47789366-47806517	-	-	-	-1.191	-
RNASEK	chr19:27436502-27438226	-	-	-	-1.361	-
RPAIN	chr19:26730161-26737179	-	-	-	1.017	-
RPRD2	chr3:20254978-20345588	-	-	-	-1.280	-
SGK1	chr9:73305312-73310869	-	-	-	-1.033	-
SLC35A4	chr7:53424461-53426334	-	-	-	-1.141	-
SPTSSA	chr21:45295074-45341768	-	-	-	-1.015	-
SYVN1	chr29:43997380-44003325	-	-	-	-1.098	-
TAF9B	chrX:79269813-79277533	-	-	-	-1.058	-
TBC1D25	chrX:91741936-91755079	-	-	-	-1.165	-
TRAF3IP2	chr9:39309719-39341546	-	-	-	-1.213	-
TRIM14	chr8:63676508-63698768	-	-	-	-1.812	-
UBA1	chrX:90831726-90850346	-	-	-	-1.196	-
UBE2K	chr6:60420295-60496136	-	-	-	-1.020	-
UBE2V1	chr13:78845235-78873171	-	-	-	-1.379	-
WBP11	chr5:95536890-95549925	-	-	-	-1.062	-
WDYHV1	chr14:18015439-18033296	-	-	-	-1.089	-
ZFP3	chr19:26968017-26975114	-	-	-	-1.185	-
ZNF142	chr2:107322276-107338174	-	-	-	-1.181	-
ZNF358	chr7:17610090-17611773	-	-	-	-1.044	-
ZNF462	chr8:98331863-98426787	-	-	-	-1.083	-
ZNF652	chr19:37919481-37932791	-	-	-	-1.545	-
AASDH	chr6:73409451-73435649	-	-	-	-	1.221

ABCB9	chr17:54827285-54851000	-	-	-	-	-1.325
ABCD1	chrX:39869942-39885758	-	-	-	-	-1.199
ABCE1	chr17:13333869-13446148	-	-	-	-	1.069
ABL1	chr11:101118799-101150880	-	-	-	-	-1.327
ABRACL	chr9:77787554-77802592	-	-	-	-	1.090
ACADL	chr2:98416823-98456944	-	-	-	-	1.032
ACAT1	chr15:17999931-18028984	-	-	-	-	1.148
ACIN1	chr10:21598910-21637359	-	-	-	-	-1.052
ACTR3	chr2:65892591-65912704	-	-	-	-	1.172
ADAMTS7	chr21:30835150-30897314	-	-	-	-	-1.056
ADAR	chr3:16033025-16052140	-	-	-	-	-1.017
AEBP1	chr4:77881912-77891706	-	-	-	-	-1.151
AGAP3	chr4:114461158-114517394	-	-	-	-	-1.238
AGPAT5	chr27:4679599-4727246	-	-	-	-	1.241
AGTPBP1	chr8:80235082-80392851	-	-	-	-	1.039
AHI1	chr9:74330946-74544060	-	-	-	-	1.072
AIMP1	chr6:20111149-20138597	-	-	-	-	1.180
AK3	chr8:39930089-40165514	-	-	-	-	1.067
AKAP12	chr9:89558648-89563595	-	-	-	-	-1.083
AKT1S1	chr18:56672751-56680246	-	-	-	-	-1.106
ALCAM	chr1:50332271-50558841	-	-	-	-	1.070
ALDH1A1	chr8:49354206-49408166	-	-	-	-	1.158
ALG10	chr5:76497228-76503464	-	-	-	-	1.116
ALKBH8	chr15:17190070-17323066	-	-	-	-	1.374
ANAPC4	chr6:46471812-46504926	-	-	-	-	1.288
ANGEL2	chr16:72473638-72491699	-	-	-	-	1.018
ANKMY2	chr4:25057922-25097468	-	-	-	-	1.019
ANKRD11	chr18:14371891-14436368	-	-	-	-	-1.690
ANKRD13B	chr19:21409207-21425398	-	-	-	-	-1.790

ANKRD46	chr14:65992658-66033894	-	-	-	-	1.100
ANKRD49	chr15:1732076-1734884	-	-	-	-	1.051
ANKRD9	chr21:68908373-68911835	-	-	-	-	-1.165
ANO8	chr7:5716939-5727054	-	-	-	-	-1.086
ANXA11	chr28:35318689-35360793	-	-	-	-	-1.001
ANXA3	chr6:95065255-95136945	-	-	-	-	1.301
AP1AR	chr6:14425509-14454377	-	-	-	-	1.213
AP4E1	chr10:59578463-59644086	-	-	-	-	1.130
APLF	chr11:66840543-66933742	-	-		-	1.259
APOO	chrX:126397964-126427158	-	-	-	-	1.149
AQP11	chr29:18477127-18488713	-	-	-	-	-1.960
AREL1	chr10:86341462-86384102	-	-	-	-	-1.080
ARFIP1	chr17:4732241-4868678	-	-	-	-	1.089
ARHGAP32	chr29:32874441-33009046	-	-	-	-	-1.255
ARHGAP39	chr14:1563865-1600378	-	-	-	-	-1.135
ARHGEF10	chr27:219419-264986	-	-	-	-	-1.205
ARHGEF11	chr3:13887503-13970875	-	-	-	-	-1.119
ARHGEF17	chr15:53582240-53643983	-	-	-	-	-1.080
ARL14EP	chr15:61834228-61847775	-	-	-	-	1.046
ARL2BP	chr18:25334587-25339259	-	-	-	-	1.036
ARL4A	chr4:20296430-20297969	-	-	-	-	1.064
ARL6	chr1:41640352-41679711	-	-	-	-	1.201
ARL8A	chr16:70894433-70900751	-	-	-	-	-1.049
ARMC4	chr13:36899557-37016058	-	-	-	-	1.130
ARPP19	chr10:57923245-57938671	-	-	-	-	1.193
ARRDC3	chr7:93240418-93253094	-	-	-	-	1.022
ARVCF	chr17:74929358-74945937	-	-	-	-	-1.120
ATF1	chr5:29272371-29336696	-	-	-	-	1.016
ATF3	chr16:72820025-72832974	-	-	-	-	-1.072

ATF4	chr5:111462844-111464936	-	-	-	-	-1.016
ATG16L2	chr15:53137072-53152599	-	-	-	-	-1.018
ATG4C	chr3:83298918-83395090	-	-	-	-	1.475
ATM	chr15:18119200-18265060	-	-	-	-	1.212
ATP11B	chr1:84722367-84818534	-	-	-	-	1.177
ATP11C	chrX:23235985-23324986	-	-	-	-	1.061
ATP13A2	chr2:136162615-136182586	-	-	-	-	-1.080
ATP5S	chr10:43265125-43277198	-	-	-	-	1.330
ATP6AP2	chrX:108396796-108424821	-	-	-	-	1.031
ATP6V1A	chr1:58880057-58940217	-	-	-	-	1.146
ATP6V1C1	chr14:63592783-63632839	-	-	-	-	1.207
ATR	chr1:127485980-127590752	-	-	-	-	1.262
B3GALT6	chr16:52467803-52468793	-	-	-	-	-1.286
BANP	chr18:13425302-13493366	-	-	-	-	-1.052
BCAM	chr18:52965137-52976445	-	-	-	-	-1.032
BCAP29	chr4:48870589-48922462	-	-	-	-	1.243
BCHE	chr1:102337856-102409795	-	-	-	-	1.343
BCKDK	chr25:27468635-27472842	-	-	-	-	-1.147
BCO2	chr15:22838239-22905944	-	-	-	-	1.270
BEND3	chr9:43409749-43424091	-	-	-	-	-1.313
BET1	chr4:11162354-11176872	-	-	-	-	1.003
BHLHE40	chr22:21492895-21498539	-	-	-	-	-1.397
BIRC2	chr15:6585515-6607013	-	-	-	-	1.064
BLOC1S6	chr10:65111942-65126559	-	-	-	-	1.103
BNIP3	chr26:51353457-51357472	-	-	-	-	-1.042
BOD1L1	chr6:113647964-113701414	-	-	-	-	-1.319
BORA	chr12:47782114-47809879	-	-	-	-	1.123
BRD3	chr11:104860031-104880077	-	-	-	-	-1.455
BRD4	chr7:8873858-8906100	-	-	-	-	-1.065

BZW2	chr4:25097883-25161432	-	-	-	-	1.022
C11orf24	chr29:46407486-46417346	-	-	-	-	-1.403
C11orf54	chr29:1032167-1056464	-	-	-	-	1.230
C11orf58	chr15:36224847-36251371	-	-	-	-	1.223
C12orf29	chr5:17892373-17902271	-	-	-	-	1.007
C12orf45	chr5:68866723-68876104	-	-	-	-	1.083
C18orf32	chr24:49610403-49615823	-	-	-	-	1.017
C1QTNF1	chr19:53978216-53984772	-	-	-	-	-1.302
C3orf38	chr1:35753285-35759257	-	-	-	-	1.256
C5orf34	chr20:31324012-31350848	-	-	-	-	1.079
C7orf73	chr4:100261071-100277950	-	-	-	-	1.397
CABIN1	chr17:73332327-73399148	-	-	-	-	-1.271
CACYBP	chr16:57694738-57705495	-	-	-	-	1.094
CALM2	chr20:8066340-8067501	-	-	-	-	1.202
CAND1	chr5:46719649-46753948	-	-	-	-	1.207
CAND2	chr22:56990322-57017221	-	-	-	-	-1.113
CAPZA1	chr3:30810108-30854190	-	-	-	-	1.185
CAPZA2	chr4:51781848-51836823	-	-	-	-	1.130
CARD10	chr5:76287157-76312955	-	-	-	-	-1.097
CARNMT1	chr8:51344226-51383813	-	-	-	-	1.242
CASD1	chr4:11735527-11787909	-	-	-	-	1.147
CASKIN2	chr19:56666536-56679122	-	-	-	-	-1.445
CCDC106	chr18:62342040-62345590	-	-	-	-	-1.051
CCDC117	chr17:70331047-70342078	-	-	-	-	1.001
CCDC125	chr20:10329063-10351647	-	-	-	-	1.067
CCDC126	chr4:32356964-32399552	-	-	-	-	1.260
CCDC43	chr19:45052979-45062313	-	-	-	-	1.080
CCDC58	chr1:67398384-67457625	-	-	-	-	1.102
CCDC8	chr18:54124478-54127099	-	-	-	-	-1.334

CCDC85B	chr29:44671367-44672651	-	-	-	-	-1.073
CCDC9	chr18:54707620-54718292	-	-	-	-	-1.750
CCDC90B	chr29:12460187-12486627	-	-	-	-	1.096
CCNG1	chr7:77249996-77257261	-	-	-	-	1.191
CCT6A	chr25:27985730-27993651	-	-	-	-	1.289
CDC25C	chr7:51313473-51344138	-	-	-	-	1.014
CDC27	chr19:46844173-46901634	-	-	-	-	1.169
CDC40	chr9:40471782-40519845	-	-	-	-	1.205
CDKAL1	chr23:36601289-37218380	-	-	-	-	1.055
CEBPZ	chr11:19659021-19683088	-	-	-	-	1.148
CENPC	chr6:84904998-84998863	-	-	-	-	1.060
CENPW	chr9:25263763-25279586	-	-	-	-	1.016
CEP131	chr19:52110944-52124532	-	-	-	-	-1.284
CEP170B	chr21:70919569-70983506	-	-	-	-	-1.055
CEP19	chr1:71834224-71839862	-	-	-	-	1.070
CEP44	chr8:6449814-6473747	-	-	-	-	1.003
CEP70	chr1:131590398-131658628	-	-	-	-	1.269
CEPT1	chr3:32339826-32376260	-	-	-	-	1.173
CETN2	chrX:35382934-35386969	-	-	-	-	1.261
CETN3	chr7:92290238-92307723	-	-	-	-	1.091
CFAP36	chr11:38066010-38095813	-	-	-	-	1.024
CGRRF1	chr10:67244516-67272546	-	-	-	-	1.029
CHD3	chr19:28185821-28206741	-	-	-	-	-1.173
CHD6	chr13:70727511-70859012	-	-	-	-	-1.316
CHEK1	chr29:29402368-29420344	-	-	-	-	1.213
CHERP	chr7:6408551-6427823	-	-	-	-	-1.625
CHIC2	chr6:71186362-71245780	-	-	-	-	1.089
CHORDC1	chr29:5035801-5057715	-	-	-	-	1.338
CHRNE	chr19:27118516-27123114	-	-	-	-	-1.305

CHURC1	chr10:77359721-77378295	-	-	-	-	1.170
CISD2	chr6:23289383-23302661	-	-	-	-	1.235
CLDN15	chr25:36040354-36045878	-	-	-	-	-1.272
CLHC1	chr11:37787988-37822911	-	-	-	-	1.100
CLIP2	chr25:33571587-33619646	-	-	-	-	-1.019
CLK1	chr2:89920585-89927819	-	-	-	-	1.165
CLN6	chr10:15025857-15041922	-	-	-	-	-1.210
CLSTN1	chr16:44633322-44671659	-	-	-	-	-1.020
CMIP	chr18:8210814-8289563	-	-	-	-	-1.172
CMPK1	chr3:99484968-99521190	-	-	-	-	1.461
CMTM7	chr22:6894654-6942330	-	-	-	-	-1.085
CMTR2	chr18:39902860-39905155	-	-	-	-	1.065
CNIH1	chr10:67176768-67191630	-	-	-	-	1.161
CNNM3	chr11:2730997-2762524	-	-	-	-	-1.277
CNOT7	chr27:19052443-19067489	-	-	-	-	1.107
COL16A1	chr2:122557457-122611951	-	-	-	-	-1.025
COL18A1	chr1:146989243-147040968	-	-	-	-	-1.040
COL4A1	chr12:88876124-89009422	-	-	-	-	-1.602
COL5A1	chr11:106856170-106994803	-	-	-	-	-1.327
COL6A1	chr1:147404395-147423644	-	-	-	-	-1.299
COMMD10	chr7:38949642-39134100	-	-	-	-	1.226
COMMD2	chr1:119344633-119354566	-	-	-	-	1.220
COPB1	chr15:38765049-38800769	-	-	-	-	1.331
COPG1	chr22:59799130-59816732	-	-	-	-	-1.275
COPS4	chr6:99610791-99649394	-	-	-	-	1.186
COX16	chr10:82412751-82426801	-	-	-	-	1.022
COX6C	chr14:66637800-66647721	-	-	-	-	1.034
COX7A2L	chr11:24824244-24836596	-	-	-	-	1.020
CPSF2	chr21:57395845-57429002	-	-	-	-	1.063

CRABP2	chr3:14173129-14178630	-	-	-	-	-1.261
CRAMP1	chr25:1245668-1284542	-	-	-	-	-1.079
CRIPT	chr11:28903111-28914000	-	-	-	-	1.139
CROCC	chr2:136193742-136239981	-	-	-	-	-1.181
CRTAP	chr22:7532625-7565025	-	-	-	-	-1.001
CRTC1	chr7:4363529-4447524	-	-	-	-	-1.728
CRYBB1	chr17:68506966-68519007	-	-	-	-	-1.153
CSTF2	chrX:54633864-54668205	-	-	-	-	1.016
CTNNAL1	chr8:100221979-100277722	-	-	-	-	1.186
CTSB	chr8:7414944-7423429	-	-	-	-	-1.028
CTSF	chr29:45242551-45248115	-	-	-	-	-1.013
CTTN	chr29:48167167-48194210	-	-	-	-	-1.167
CUL5	chr15:17857168-17983781	-	-	-	-	1.077
CWF19L1	chr26:21010621-21035035	-	-	-	-	1.045
CWF19L2	chr15:16346714-16484043	-	-	-	-	1.159
CYB5R3	chr5:114009260-114024565	-	-	-	-	-1.023
CYP51A1	chr4:9306413-9323252	-	-	-	-	1.017
DAB2IP	chr11:92577650-92664126	-	-	-	-	-1.473
DARS	chr2:61722451-61787886	-	-	-	-	1.162
DBF4	chr4:32427569-32454703	-	-	-	-	1.318
DBP	chr18:55722335-55729578	-	-	-	-	-1.660
DBR1	chr1:132002920-132014620	-	-	-	-	1.119
DBT	chr3:43189904-43230271	-	-	-	-	1.130
DCAF13	chr14:63227995-63256229	-	-	-	-	1.080
DDIT4	chr28:28483402-28485410	-	-	-	-	-1.034
DDX31	chr11:102698013-102771662	-	-	-	-	-1.088
DDX52	chr19:14213233-14235863	-	-	-	-	1.234
DENND1A	chr11:94526959-95055931	-	-	-	-	-1.245
DHX34	chr18:54786975-54810524	-	-	-	-	-1.362

DIP2A	chr1:147856756-147977430	-	-	-	-	-1.123
DIS3	chr12:47812800-47837465	-	-	-	-	1.113
DNAJC24	chr15:62935665-63020362	-	-	-	-	1.229
DNAJC28	chr1:1308526-1310072	-	-	-	-	1.103
DNAJC3	chr12:76958977-77024110	-	-	-	-	1.089
DNAL1	chr10:85467721-85504542	-	-	-	-	1.012
DNMT3A	chr11:74030424-74059688	-	-	-	-	-1.058
DOCK6	chr7:16851753-16898876	-	-	-	-	-1.194
DOHH	chr7:21649440-21654927	-	-	-	-	-1.351
DOT1L	chr7:22629691-22680307	-	-	-	-	-1.354
DPH5	chr3:42408613-42448917	-	-	-	-	1.077
DPH6	chr10:30916476-31109121	-	-	-	-	1.037
DPM1	chr13:79580468-79597861	-	-	-	-	1.066
DPY19L4	chr14:71868731-71925891	-	-	-	-	1.214
DPYD	chr3:45563731-46487165	-	-	-	-	1.201
DYNC1I2	chr2:24807356-24860776	-	-	-	-	1.104
DYNLT3	chrX:111023273-111034498	-	-	-	-	1.438
EAPP	chr21:45354861-45371985	-	-	-	-	1.093
ECE1	chr2:131935440-132060210	-	-	-	-	-1.060
ECHDC1	chr9:24240994-24273071	-	-	-	-	1.337
ECT2	chr1:95475797-95536054	-	-	-	-	1.216
EED	chr29:9325135-9355669	-	-	-	-	1.167
EEF1A2	chr13:54623916-54631595	-	-	-	-	-1.309
EEF1B2	chr2:94922838-94926122	-	-	-	-	1.258
EFCAB7	chr3:82334707-82389287	-	-	-	-	1.103
EFS	chr10:21395794-21405291	-	-	-	-	-1.108
EHHADH	chr1:82467816-82521151	-	-	-	-	1.013
EIF1AX	chrX:130307268-130317159	-	-	-	-	1.045
EIF2A	chr1:118495011-118536744	-	-	-	-	1.182

EIF3J	chr10:103984740-104002866	-	-	-	-	1.249
EIF4A2	chr1:81057778-81064090	-	-	-	-	1.156
EIF4E	chr6:27042236-27080766	-	-	-	-	1.135
EIF5	chr21:69638190-69647505	-	-	-	-	1.050
EIF5A2	chr1:97308270-97324962	-	-	-	-	1.046
ELN	chr25:33787888-33820672	-	-	-	-	-1.244
ELP6	chr22:52696726-52708951	-	-	-	-	-1.438
EMX2	chr26:38163824-38170070	-	-	-	-	-1.113
EN1	chr2:70972737-70977033	-	-	-	-	-1.582
ENSBTAG00000000021	chr5:66168585-66227000	-	-	-	-	1.083
ENSBTAG00000000177	chr25:649252-652835	-	-	-	-	-1.082
ENSBTAG00000000562	chr28:7926959-7941655	-	-	-	-	1.007
ENSBTAG00000001575	chr11:29424995-29432052	-	-	-	-	1.284
ENSBTAG00000001648	chr12:32852825-32859542	-	-	-	-	1.001
ENSBTAG00000001840	chr11:10155202-10157927	-	-	-	-	-2.131
ENSBTAG00000001911	chrX:42583761-42621146	-	-	-	-	1.189
ENSBTAG00000001968	chr1:87007532-87017223	-	-	-	-	1.421
ENSBTAG00000002226	chr18:12974879-13009289	-	-	-	-	-1.106
ENSBTAG00000002350	chr7:4987070-4999686	-	-	-	-	-1.588
ENSBTAG00000003747	chr10:85645802-85666323	-	-	-	-	1.167
ENSBTAG00000004243	chr14:23651476-23668800	-	-	-	-	1.027
ENSBTAG00000004459	chr1:45281218-45394335	-	-	-	-	1.111
ENSBTAG00000004861	chr15:45130567-45138822	-	-	-	-	-1.091
ENSBTAG00000005007	chr26:10251023-10251836	-	-	-	-	1.172
ENSBTAG00000005265	chr7:83599488-83607997	-	-	-	-	1.197
ENSBTAG00000005574	chr8:11043940-11061301	-	-	-	-	-1.450
ENSBTAG00000006140	chr21:21523626-21530708	-	-	-	-	1.079
ENSBTAG00000006383	chrX:126048948-126049743	-	-	-	-	1.183
ENSBTAG00000006492	chr6:46355299-46391439	-	-	-	-	1.075

ENSBTAG00000006756	chr7:52218127-52244915	-	-	-	-	1.253
ENSBTAG00000007096	chr18:14830326-14847323	-	-	-	-	-1.050
ENSBTAG00000007394	chr1:97339618-97343997	-	-	-	-	1.133
ENSBTAG00000007546	chr5:110565205-110567190	-	-	-	-	-1.414
ENSBTAG00000007696	chr24:25595236-25652303	-	-	-	-	1.109
ENSBTAG00000008595	chr5:38397359-38571901	-	-	-	-	1.217
ENSBTAG00000008809	chr3:46860031-46910656	-	-	-	-	1.037
ENSBTAG00000008997	chr11:98517161-98541363	-	-	-	-	-1.142
ENSBTAG00000009110	chr17:18734078-18735046	-	-	-	-	1.275
ENSBTAG00000009517	chr2:71561191-71566372	-	-	-	-	1.244
ENSBTAG00000009823	chr4:87410390-87412230	-	-	-	-	1.205
ENSBTAG00000009859	chr2:91155251-91180862	-	-	-	-	1.133
ENSBTAG00000009908	chr17:6703059-6707745	-	-	-	-	1.129
ENSBTAG00000010046	chr18:58212121-58220103	-	-	-	-	1.127
ENSBTAG00000010577	chr6:73448406-73507190	-	-	-	-	1.080
ENSBTAG00000010597	chr4:66204845-66214292	-	-	-	-	1.083
ENSBTAG00000010736	chr2:26800660-26821659	-	-	-	-	1.229
ENSBTAG00000011027	chr8:102666739-102697281	-	-	-	-	1.046
ENSBTAG00000011135	chr7:5794170-5796248	-	-	-	-	-1.309
ENSBTAG00000012803	chr10:1102149-1110236	-	-	-	-	1.118
ENSBTAG00000013650	chr2:133933076-133949856	-	-	-	-	-1.348
ENSBTAG00000014068	chr27:36921291-36933273	-	-	-	-	1.015
ENSBTAG00000014423	chr16:47992812-48000514	-	-	-	-	1.386
ENSBTAG00000014494	chr9:103275248-103292877	-	-	-	-	-1.311
ENSBTAG00000015309	chr15:6917401-6947618	-	-	-	-	1.053
ENSBTAG00000016147	chr17:35347483-35351627	-	-	-	-	1.490
ENSBTAG00000016818	chr2:122784557-122889605	-	-	-	-	1.179
ENSBTAG00000016999	chr1:136207772-136291018	-	-	-	-	1.226
ENSBTAG00000017071	chr20:39760049-39792323	-	-	-	-	1.103

ENSBTAG00000017942	chr3:16535365-16544863	-	-	-	-	-1.350
ENSBTAG00000018046	chr11:60654633-60687730	-	-	-	-	1.060
ENSBTAG00000018052	chr7:20191964-20256722	-	-	-	-	-1.020
ENSBTAG00000019284	chr11:84076853-84078206	-	-	-	-	1.313
ENSBTAG00000019601	chr10:58569061-58646799	-	-	-	-	1.105
ENSBTAG00000019785	chr18:51312807-51336025	-	-	-	-	-2.074
ENSBTAG00000020227	chr16:3836699-3849134	-	-	-	-	1.338
ENSBTAG00000020535	chr25:27541408-27542740	-	-	-	-	-1.013
ENSBTAG00000020756	chr18:51362252-51371564	-	-	-	-	-1.125
ENSBTAG00000020790	chr26:11812675-11813475	-	-	-	-	1.224
ENSBTAG00000021069	chr8:10819982-10852941	-	-	-	-	1.261
ENSBTAG00000021246	chr26:23563110-23764458	-	-	-	-	1.435
ENSBTAG00000021410	chrX:4694746-4698796	-	-	-	-	1.222
ENSBTAG00000022372	chr29:28137004-28137881	-	-	-	-	1.465
ENSBTAG00000022647	chr9:46186208-46187168	-	-	-	-	1.081
ENSBTAG00000022801	chr10:60078423-60128552	-	-	-	-	1.088
ENSBTAG00000023279	chr12:28545677-28560619	-	-	-	-	1.074
ENSBTAG00000023462	chr8:24927467-24930788	-	-	-	-	1.028
ENSBTAG00000023464	chr18:47280907-47330516	-	-	-	-	1.097
ENSBTAG00000023978	chrX:38558144-38559257	-	-	-	-	-1.197
ENSBTAG00000025441	chr23:27331772-27333698	-	-	-	-	-1.221
ENSBTAG00000027412	chr13:51930066-51930888	-	-	-	-	1.158
ENSBTAG00000027809	chr16:56941659-57039130	-	-	-	-	1.012
ENSBTAG00000031572	chr1:107962965-108058677	-	-	-	-	1.067
ENSBTAG00000031785	chr23:31589470-31607791	-	-	-	-	1.011
ENSBTAG00000032609	chr13:10535553-10536828	-	-	-	-	1.281
ENSBTAG00000033381	chr27:32417550-32418888	-	-	-	-	1.220
ENSBTAG00000033563	chr18:47193773-47226339	-	-	-	-	1.091
ENSBTAG00000034185	chr18:2944866-2960921	-	-	-	-	1.098

ENSBTAG00000034662	chr9:18473882-18475244	-	-	-	-	1.056
ENSBTAG00000037516	chr13:16262483-16263567	-	-	-	-	1.008
ENSBTAG00000038079	chr16:66960789-67142414	-	-	-	-	1.019
ENSBTAG00000038931	chr9:50950779-50954323	-	-	-	-	1.311
ENSBTAG00000039130	chr7:14670707-14672994	-	-	-	-	1.089
ENSBTAG00000039462	chr10:45700242-45709247	-	-	-	-	1.192
ENSBTAG00000039493	chr7:15324726-15346774	-	-	-	-	1.084
ENSBTAG00000039671	chr26:37282718-37285100	-	-	-	-	1.222
ENSBTAG00000040334	chr7:45556209-45557580	-	-	-	-	-1.052
ENSBTAG00000040507	chr7:17513880-17565624	-	-	-	-	-1.277
ENSBTAG00000045493	chr28:22419202-24270401	-	-	-	-	-2.848
ENSBTAG00000045678	chrX:78134339-78135016	-	-	-	-	1.480
ENSBTAG00000045867	chrX:110447687-110479469	-	-	-	-	1.107
ENSBTAG00000046566	chr3:27378642-27481821	-	-	-	-	1.049
ENSBTAG00000046690	chr18:35056133-35117221	-	-	-	-	1.267
ENSBTAG00000046700	chr6:99812237-99839387	-	-	-	-	1.116
ENSBTAG00000046828	chr21:71011579-71016820	-	-	-	-	-1.702
ENSBTAG00000047051	chrX:36171713-36172838	-	-	-	-	1.011
ENSBTAG00000047210	chr29:31113680-31114595	-	-	-	-	1.095
ENSBTAG00000047824	chr16:31136170-31137374	-	-	-	-	1.075
ENSBTAG00000048213	chr8:83551681-83581560	-	-	-	-	-1.158
EPHA2	chr2:136525536-136551769	-	-	-	-	-1.160
EPHB4	chr25:36347293-36362877	-	-	-	-	-1.367
ERAL1	chr19:20792194-20796711	-	-	-	-	-1.044
ERGIC2	chr5:80616118-80659407	-	-	-	-	1.402
ERI2	chr25:18657383-18672630	-	-	-	-	1.039
ERN1	chr19:48924510-48971838	-	-	-	-	-1.213
ERO1A	chr10:11438272-11488427	-	-	-	-	1.093
ERP44	chr8:65500572-65597182	-	-	-	-	1.021

ESD	chr12:16771119-16788845	-	-	-	-	1.045
ETAA1	chr11:65813299-65826759	-	-	-	-	1.020
ETV2	chr18:46555942-46558285	-	-	-	-	-1.184
EXOC1	chr6:72941462-72989013	-	-	-	-	1.206
EXOC5	chr10:69862216-69914486	-	-	-	-	1.197
EXOC6	chr26:14268979-14445905	-	-	-	-	1.054
FAIM2	chr5:30155762-30185025	-	-	-	-	-1.072
FAM102B	chr3:34839058-34877721	-	-	-	-	1.140
FAM109A	chr17:57352624-57353599	-	-	-	-	-1.086
FAM111B	chr15:83568473-83582435		-	-	-	1.231
FAM114A2	chr7:67287093-67321469	-	-	-	-	1.144
FAM126A	chr4:31742335-31791212	-	-	-	-	1.181
FAM174A	chr7:102227148-102236125	-	-	-	-	-1.117
FAM193A	chr6:108145917-108198645	-	-	-	-	-1.471
FAM229B	chr9:38816217-38821062	-	-	-	-	1.040
FAM46B	chr2:126799590-126807056	-	-	-	-	-1.093
FAM60A	chr5:79034367-79064677	-	-	-	-	1.049
FANCL	chr11:40656143-40744419	-	-	-	-	1.105
FASN	chr19:51384921-51403614	-	-	-	-	-1.238
FASTKD2	chr2:95499477-95519762	-	-	-	-	1.142
FBRS	chr25:27048342-27051971	-	-	-	-	-1.261
FBRSL1	chr17:45613859-45696523	-	-	-	-	-1.474
FBXL3	chr12:52466039-52477380	-	-	-	-	1.090
FBXL5	chr6:115573480-115610298	-	-	-	-	1.235
FBXO42	chr2:136362254-136444097	-	-	-	-	-1.261
FCF1	chr10:86384168-86394595	-	-	-	-	1.002
FGFR1	chr27:33250533-33291989	-	-	-	-	-1.012
FHOD1	chr18:34977245-34993385	-	-	-	-	-1.215
FKBP14	chr4:66758678-66770727	-	-	-	-	1.121

FLNB	chr22:43674719-43815706	-	-	-	-	-1.457
FNIP1	chr7:23993127-24063506	-	-	-	-	1.059
FOSL1	chr29:44673878-44679325	-	-	-	-	-2.753
FOXF1	chr18:12379749-12382722	-	-	-	-	-1.191
FOXJ2	chr5:102003894-102023009	-	-	-	-	-1.647
FOXO3	chr9:42008605-42118673	-	-	-	-	-1.344
FURIN	chr21:22206516-22213761	-	-	-	-	-1.393
FZD2	chr19:44954981-44956760	-	-	-	-	-1.205
FZD9	chr25:34245428-34247198	-	-	-	-	-1.056
G6PD	chrX:40484794-40500923	-	-	-	-	-1.574
GAB4	chr29:17833136-17887917	-	-	-	-	-1.136
GALNT1	chr24:21687845-21756844	-	-	-	-	1.242
GCLM	chr3:49741374-49759098	-	-	-	-	1.166
GGA3	chr19:56863206-56877029	-	-	-	-	-1.196
GHITM	chr28:39435545-39448963	-	-	-	-	1.055
GINS2	chr18:11687199-11724596	-	-	-	-	-1.075
GLI3	chr4:79444242-79758476	-	-	-	-	-1.173
GLO1	chr23:12483467-12509232	-	-	-	-	1.142
GMFB	chr10:67212807-67226749	-	-	-	-	1.351
GMNN	chr23:32775580-32786297	-	-	-	-	1.083
GNAI1	chr4:41160157-41266152	-	-	-	-	1.084
GNG10	chr8:102784500-102790524	-	-	-	-	1.421
GNPAT	chr28:3378607-3418245	-	-	-	-	1.023
GNPDA2	chr6:64961797-64992219	-	-	-	-	1.281
GNPNAT1	chr10:11332414-11344167	-	-	-	-	1.042
GPN3	chr17:56587852-56607236	-	-	-	-	1.040
GPR89A	chr3:21802388-21847767	-	-	-	-	1.046
GPX8	chr20:23975639-23980445	-	-	-	-	1.176
GRAMD1A	chr18:45932690-45957028	-	-	-	-	-1.174

GTF2IRD1	chr25:33414264-33493476	-	-	-	-	-1.288
GTPBP10	chr4:75013860-75132831	-	-	-	-	1.236
HAT1	chr2:24606879-24646776	-	-	-	-	1.109
HAUS2	chr10:37995371-38008615	-	-	-	-	1.020
HAUS3	chr6:108508716-108523815	-	-	-	-	1.161
HAUS6	chr8:25150279-25191188	-	-	-	-	1.221
HBS1L	chr9:74011378-74096501	-	-	-	-	1.169
HCFC1	chrX:40075765-40095591	-	-	-	-	-1.548
HCN2	chr7:44831439-44850882	-	-	-	-	-1.120
HDAC4	chr3:118937214-119412428	-	-	-	-	-1.013
HERC4	chr28:24587773-24715401	-	-	-	-	1.091
HERC6	chr6:37736137-37793279	-	-	-	-	1.059
HIP1	chr25:34393879-34528240	-	-	-	-	-1.044
HIST3H2A	chr7:2485680-2487189	-	-	-	-	1.023
HLTF	chr1:120013764-120075520	-	-	-	-	1.181
HOMER1	chr10:10350691-10484916	-	-	-	-	1.015
HOXA13	chr4:69297274-69298937	-	-	-	-	-1.081
HPCAL1	chr11:87191214-87307998	-	-	-	-	-1.051
HPS3	chr1:119944593-119985509	-	-	-	-	1.010
HS6ST1	chr2:4111870-4149372	-	-	-	-	-1.007
HSD17B11	chr6:104006455-104056137	-	-	-	-	1.051
HSD17B12	chr15:74652042-74830690	-	-	-	-	1.212
HSD17B7	chr3:6629250-6659067	-	-	-	-	1.119
HSDL2	chr8:103452038-103512716	-	-	-	-	1.406
HSF1	chr14:1806080-1825793	-	-	-	-	-1.179
HSPA14	chr13:29778731-29803330	-	-	-	-	1.265
HSPA8	chr15:34216277-34220705	-	-	-	-	1.021
HSPBAP1	chr1:67664798-67720894	-	-	-	-	1.265
HSPG2	chr2:131517578-131587498	-	-	-	-	-1.317

IARS2	chr16:24285716-24329372	-	-	-	-	1.053
IBTK	chr9:22263094-22343685	-	-	-	-	1.098
IER2	chr7:13543663-13545435	-	-	-	-	-1.098
IFNGR1	chr9:76092203-76116593	-	-	-	-	1.020
IFT20	chr19:20372729-20379655	-	-	-	-	1.148
IFT81	chr17:56311085-56408960	-	-	-	-	1.101
IGF1R	chr21:8208821-8268093	-	-	-	-	-1.136
IL17D	chr12:36076411-36105865	-	-	-	-	-1.116
IL1RAP	chr1:77198181-77343645	-	-	-	-	1.043
IMPACT	chr24:32611657-32646496	-	-	-	-	1.208
INF2	chr21:70827524-70839732	-	-	-	-	-1.100
INPPL1	chr15:52609011-52623088	-	-	-	-	-1.321
INSL6	chr8:39603072-39614295	-	-	-	-	1.186
INTS2	chr19:11401821-11455023	-	-	-	-	1.019
IQCE	chr25:41225569-41256752	-	-	-	-	-1.024
IQSEC1	chr22:59460405-59549010	-	-	-	-	-1.471
IRAK4	chr5:36877862-36905927	-	-	-	-	1.317
IRGQ	chr18:52152025-52155244	-	-	-	-	-1.174
IRS1	chr2:115790539-115794253	-	-	-	-	-1.191
ITFG2	chr5:107426528-107436938	-	-	-	-	-1.248
JAK2	chr8:39632637-39719731	-	-	-	-	1.033
JKAMP	chr10:72005596-72101711	-	-	-	-	1.098
KEAP1	chr7:16235814-16244046	-	-	-	-	-1.044
KHSRP	chr7:19259131-19269635	-	-	-	-	-1.571
KIAA1033	chr5:68979109-69034136	-	-	-	-	1.013
KIAA1107	chr3:51382747-51475663	-	-	-	-	1.135
KIAA1524	chr1:53727495-53754034	-	-	-	-	1.244
KIF27	chr8:78439019-78524275	-	-	-	-	1.134
KIFAP3	chr16:38360034-38502334	-	-	-	-	1.076

KIRREL	chr3:12308302-12326076	-	-	-	-	-1.592
KLC2	chr29:44960929-44970707	-	-	-	-	-1.293
KPNA5	chr9:34316844-34358840	-	-	-	-	1.087
KRBA1	chr4:113378725-113393942	-	-	-	-	-1.139
KYAT3	chr3:55093504-55153828	-	-	-	-	1.226
LACE1	chr9:42153687-42350641	-	-	-	-	1.013
LAMA3	chr24:33072941-33324798	-	-	-	-	-1.103
LAMA5	chr13:55379958-55433278	-	-	-	-	-1.060
LARS	chr7:59319661-59382124	-	-	-	-	1.031
LCORL	chr6:38840893-38992112	-	-	-	-	1.224
LDHB	chr5:88962678-88981219	-	-	-	-	1.063
LENG1	chr18:63421901-63425192	-	-	-	-	-1.028
LENG8	chr18:63107488-63117295	-	-	-	-	-1.050
LIAS	chr6:60215271-60227136	-	-	-	-	1.211
LIN7C	chr15:58994223-59004197	-	-	-	-	1.421
LIN9	chr16:29993987-30067842	-	-	-	-	1.086
LINS1	chr21:6232489-6239168	-	-	-	-	1.146
LIPE	chr18:51216018-51227395	-	-	-	-	-1.043
LLPH	chr5:47901611-47905608	-	-	-	-	1.342
LMNB1	chr7:28414755-28465352	-	-	-	-	1.137
LNPK	chr2:20941573-21011178	-	-	-	-	1.002
LOXL1	chr21:35057677-35082119	-	-	-	-	-1.289
LRFN3	chr18:46818877-46825746	-	-	-	-	-1.662
LRP1	chr5:56562308-56641157	-	-	-	-	-1.488
LRP5	chr29:46485171-46573460	-	-	-	-	-1.035
LRRC34	chr1:98357199-98369907	-	-	-	-	1.321
LRRC8A	chr11:99411392-99437846	-	-	-	-	-1.458
LRRK2	chr5:40703504-40916225	-	-	-	-	1.023
LSM5	chr4:64411818-64415413	-	-	-	-	1.303

LTBP2	chr10:86186699-86294121	-	-	-	-	-1.279
LTBP4	chr18:50173267-50202104	-	-	-	-	-1.370
LY96	chr14:39369424-39402263	-	-	-	-	1.015
LYPLAL1	chr16:23350278-23382370	-	-	-	-	1.102
LYRM2	chr9:61434664-61436740	-	-	-	-	1.028
LZTS2	chr26:21703369-21710503	-	-	-	-	-1.038
M6PR	chr5:101439876-101452407	-	-	-	-	1.060
MAD2L1	chr6:6013171-6020467	-	-	-	-	1.084
MAFG	chr19:51576539-51582086	-	-	-	-	-1.045
MAGT1	chrX:79554828-79602478	-	-	-	-	1.162
MAN1C1	chr2:127888645-128008111	-	-	-	-	-1.089
MAP1A	chr21:55810060-55829462	-	-	-	-	-1.858
MAP3K3	chr19:48570156-48620315	-	-	-	-	-1.029
MAP7D1	chr3:110233981-110243621	-	-	-	-	-1.064
MAPK7	chr19:34687987-34693036	-	-	-	-	-1.233
MAPK8	chr28:43160796-43196195	-	-	-	-	1.060
MAPK8IP3	chr25:1304434-1348409	-	-	-	-	-1.366
MARCH7	chr2:36682215-36729906	-	-	-	-	1.035
MARK2	chr29:42829260-42865910	-	-	-	-	-1.105
MARK4	chr18:53330877-53379087	-	-	-	-	-2.024
MCM8	chr13:48489738-48532765	-	-	-	-	1.285
MCTS1	chrX:4710875-4718733	-	-	-	-	1.177
MED17	chr29:990200-1019330	-	-	-	-	1.030
MED25	chr18:56632967-56646924	-	-	-	-	-1.175
MEN1	chr29:43661746-43668039	-	-	-	-	-1.156
MESDC1	chr21:27346490-27348447	-	-	-	-	-1.206
METAP2	chr5:25255493-25286217	-	-	-	-	1.070
METTL18	chr16:38247529-38249860	-	-	-	-	1.040
MFAP4	chr19:34685356-34687892	-	-	-	-	-1.592

MFSD14A	chr3:43332800-43386388	-	-	-	-	1.019
MFSD8	chr17:30144104-30181831	-	-	-	-	1.221
MICAL3	chr5:109664102-109737010	-	-	-	-	-1.090
MICU2	chr12:35710542-35769962	-	-	-	-	1.215
MICU3	chr27:19168586-19243562	-	-	-	-	1.032
MIER1	chr3:78663150-78730912	-	-	-	-	1.191
MIER2	chr7:44606512-44622229	-	-	-	-	-1.296
MIER3	chr20:22299384-22323643	-	-	-	-	1.075
MINK1	chr19:27123624-27170653	-	-	-	-	-1.695
MKLN1	chr4:95807760-96016756	-	-	-	-	1.002
MKNK2	chr7:22787217-22796782	-	-	-	-	-1.273
MLF1	chr1:109763291-109793739	-	-	-	-	1.004
MLLT6	chr19:39938324-39956916	-	-	-	-	-1.399
MMADHC	chr2:46648516-46664675	-	-	-	-	1.127
MMP11	chr17:73216821-73220883	-	-	-	-	-1.034
MMP17	chr17:46236042-46260184	-	-	-	-	-1.012
MMS22L	chr9:53228693-53352386	-	-	-	-	1.175
MNAT1	chr10:73153516-73363530	-	-	-	-	1.036
MND1	chr17:4212633-4296899	-	-	-	-	1.142
MORC2	chr17:71921349-71961422	-	-	-	-	-1.059
MORF4L2	chrX:57744029-57756166	-	-	-	-	1.090
MORN2	chr11:21226394-21234596	-	-	-	-	1.033
MORN4	chr26:18660894-18665346	-	-	-	-	-1.286
MOSPD1	chrX:18524574-18549242	-	-	-	-	1.084
MPRIP	chr19:35557244-35646258	-	-	-	-	-1.027
MRC2	chr19:47721710-47747246	-	-	-	-	-1.015
MRE11	chr15:1640851-1716775	-	-	-	-	1.092
MRPL1	chr6:94337923-94408905	-	-	-	-	1.358
MRPL13	chr14:84125769-84167593	-	-	-	-	1.046

MRPL19	chr11:43885453-43896122	-	-	-	-	1.084
MRPL3	chr1:139880638-139937339	-	-	-	-	1.015
MRPL35	chr11:48529513-48535995	-	-	-	-	1.010
MRPL51	chr5:104273437-104276752	-	-	-	-	1.210
MRPS21	chr3:20381752-20394664	-	-	-	-	1.415
MRPS35	chr5:82486884-82530466	-	-	-	-	1.001
MTCL1	chr24:41576969-41689810	-	-	-	-	-1.215
MTDH	chr14:68799571-68853740	-	-	-	-	1.112
MTHFD2L	chr6:90842933-90985937	-	-	-	-	1.009
MTIF2	chr11:37826328-37848931	-	-	-	-	1.057
MTPAP	chr13:35533551-35564536	-	-	-	-	1.129
MTSS1L	chr18:1531381-1545901	-	-	-	-	-2.847
MXRA8	chr16:52424101-52428456	-	-	-	-	-1.315
MYBBP1A	chr19:25636460-25650975	-	-	-	-	-1.320
MYBL1	chr14:32840048-32862669	-	-	-	-	1.092
MYBL2	chr13:72939568-72966159	-	-	-	-	-1.373
MYH9	chr5:75094865-75179909	-	-	-	-	-1.454
MYNN	chr1:98377177-98392775	-	-	-	-	1.389
MZF1	chr18:65971579-65980686	-	-	-	-	-1.024
NAA25	chr17:64361787-64413468	-	-	-	-	1.044
NACAD	chr4:77239818-77248648	-	-	-	-	-1.638
NACC1	chr7:13554142-13559771	-	-	-	-	-1.179
NAE1	chr18:34636279-34660241	-	-	-	-	1.039
NAGK	chr11:13405926-13415101	-	-	-	-	-1.045
NAGPA	chr25:4077596-4086314	-	-	-	-	-1.151
NAPA	chr18:54902550-54928520	-	-	-	-	-1.008
NAT1	chr27:38862139-38868825	-	-	-	-	1.037
NCAPG	chr6:38765968-38812051	-	-	-	-	1.226
NCLN	chr7:21870309-21882869	-	-	-	-	-1.351

NCOR1	chr19:33945403-34043863	-	-	-	-	-1.029
NCOR2	chr17:53568326-53708353	-	-	-	-	-1.578
NDFIP2	chr12:54923988-54993756	-	-	-	-	1.065
NDUFB5	chr1:88096666-88111780	-	-	-	-	1.295
NDUFS1	chr2:94893226-94922667	-	-	-	-	1.144
NECAP2	chr2:136252383-136266397	-	-	-	-	-1.073
NECTIN3	chr1:56353744-56378308	-	-	-	-	1.066
NEDD1	chr5:61446534-61498524	-	-	-	-	1.124
NELFCD	chr13:57899211-57909996	-	-	-	-	-1.070
NEPRO	chr1:58170477-58185755	-	-	-	-	1.216
NFKBIB	chr18:48880854-48891485	-	-	-	-	-1.298
NFXL1	chr6:68239349-68299616	-	-	-	-	1.002
NIFK	chr2:73804849-73815299	-	-	-	-	1.082
NLRX1	chr15:30278099-30296544	-	-	-	-	-1.202
NME7	chr16:37568415-37838172	-	-	-	-	1.303
NOG	chr19:7613375-7614074	-	-	-	-	-1.329
NOSTRIN	chr2:27317637-27380506	-	-	-	-	1.017
NOTCH1	chr11:103986873-104030692	-	-	-	-	-1.520
NQO1	chr18:36911357-36924689	-	-	-	-	1.151
NSL1	chr16:72664763-72701047	-	-	-	-	1.076
NSUN3	chr1:37960748-38021040	-	-	-	-	1.177
NT5DC2	chr22:48847445-48909562	-	-	-	-	-1.077
NTN1	chr19:29084418-29269338	-	-	-	-	-1.059
NUDCD1	chr14:57249476-57342028	-	-	-	-	1.437
NUDT8	chr29:46123751-46126289	-	-	-	-	-1.184
NUP107	chr5:45275636-45323760	-	-	-	-	1.319
NUP35	chr2:13455251-13487222	-	-	-	-	1.018
NUP43	chr9:88051511-88066828	-	-	-	-	1.137
NXF1	chr29:41796852-41808165	-	-	-	-	-1.103

OLFML2B	chr3:7528021-7577290	-	-	-	-	-1.296
OPA1	chr1:74383827-74467298	-	-	-	-	1.152
ORC4	chr2:48282735-48377766	-	-	-	-	1.140
ORC6	chr18:15066960-15075288	-	-	-	-	1.037
ORMDL1	chr2:6511309-6523389	-	-	-	-	1.137
OSBPL8	chr5:5823986-5903115	-	-	-	-	1.070
OSGEPL1	chr2:6531524-6542021	-	-	-	-	1.009
OSGIN1	chr18:10294995-10305608	-	-	-	-	-1.189
OSTC	chr6:17789597-17801277	-	-	-	-	1.090
OSTF1	chr8:51440386-51501432	-	-	-	-	1.255
P4HA1	chr28:29229500-29329487	-	-	-	-	1.124
P4HA2	chr7:23480314-23513315	-	-	-	-	-1.269
PACS1	chr29:44920589-44948773	-	-	-	-	-1.237
PAIP2	chr7:52252773-52270426	-	-	-	-	1.003
PAK4	chr18:49160981-49169719	-	-	-	-	-1.149
PALM	chr7:44926930-44939347	-	-	-	-	-1.315
PASK	chr3:120818379-120844640	-	-	-	-	-1.134
PATL1	chr15:84160419-84188567	-	-	-	-	-1.085
OCIAD2	chr6:69175253-69187082	-	-	-	-	1.023
PCIF1	chr13:75404992-75435377	-	-	-	-	-1.240
PCNP	chr1:46355782-46370616	-	-	-	-	1.021
PCNX3	chr29:44462345-44481118	-	-	-	-	-1.202
PDE1A	chr2:14087655-14483437	-	-	-	-	1.077
PDE4A	chr7:16176855-16215655	-	-	-	-	-1.199
PDXP	chr5:110000367-110006138	-	-	-	-	-1.089
PEX13	chr11:43608811-43640302	-	-	-	-	1.060
PEX7	chr9:75813333-75891921	-	-	-	-	1.123
PHC1	chr5:101453053-101472170	-	-	-	-	-1.598
PHF2	chr8:86380912-86424891	-	-	-	-	-1.011

PHOSPHO2	chr2:26660799-26665974	-	-	-	-	1.294
PHRF1	chr29:50887354-50951170	-	-	-	-	-1.085
PIBF1	chr12:47837818-48053497	-	-	-	-	1.003
PIGK	chr3:67687801-67824632	-	-	-	-	1.103
PIGW	chr19:13192528-13194040	-	-	-	-	1.121
PIK3C2B	chr16:1981478-2030002	-	-	-	-	-1.027
PIK3C3	chr24:14182756-14347226	-	-	-	-	1.004
PIK3CA	chr1:88504289-88533061	-	-	-	-	1.048
PKD1	chr25:1627977-1666088	-	-	-	-	-1.029
PLCG1	chr13:70510823-70524389	-	-	-	-	-1.132
PLD3	chr18:49995630-50005033	-	-	-	-	-1.135
PLEC	chr14:2054916-2088261	-	-	-	-	-1.383
PLEKHA8	chr4:66696648-66755780	-	-	-	-	1.020
PLEKHH3	chr19:43366277-43374706	-	-	-	-	-1.194
PLGRKT	chr8:39532017-39568029	-	-	-	-	1.134
PLOD3	chr25:36057471-36065405	-	-	-	-	-1.044
PLXNA1	chr22:60913458-60946157	-	-	-	-	-1.252
PLXNA2	chr16:77046128-77250393	-	-	-	-	-1.134
PMS1	chr2:6395004-6511175	-	-	-	-	1.178
PNPT1	chr11:38161133-38200964	-	-	-	-	1.141
POLR3G	chr7:92404696-92434910	-	-	-	-	1.178
PPARD	chr23:9340954-9353750	-	-	-	-	-1.414
PPID	chr17:41249492-41262410	-	-	-	-	1.008
PPIF	chr28:35167544-35173642	-	-	-	-	-1.650
PPIL2	chr17:74073546-74092409	-	-	-	-	-1.114
PPIP5K2	chr7:104530076-104642552	-	-	-	-	1.026
PPL	chr25:3966799-4014117	-	-	-	-	-1.349
PPP1CC	chr17:56814812-56833870	-	-	-	-	1.093
PPP1R13L	chr18:53432746-53447531	-	-	-	-	-1.318

PPP1R18	chr23:28128193-28137021	-	-	-	-	-1.216
PPP2R2A	chr8:74834627-74913332	-	-	-	-	1.043
PRCC	chr3:14090126-14117838	-	-	-	-	-1.122
PRDM2	chr16:55096210-55154550	-	-	-	-	-1.083
PRDM5	chr6:4491174-4743136	-	-	-	-	1.032
PREX1	chr13:77566189-77671122	-	-	-	-	-1.022
PRKAA1	chr20:33688290-33716677	-	-	-	-	1.015
PRKD2	chr18:54224456-54256892	-	-	-	-	-1.339
PrP	chr13:47400412-47418507	-	-	-	-	1.025
PRPF39	chr21:55289714-55324776	-	-	-	-	1.218
PSMA6	chr21:45974821-45998591	-	-	-	-	1.258
PSMC6	chr10:11401912-11425951	-	-	-	-	1.107
PSMD14	chr2:35076259-35186366	-	-	-	-	1.397
PSPH	chr25:27955044-27977149	-	-	-	-	1.024
PTGES	chr11:100143652-100155090	-	-	-	-	-1.059
PTP4A2	chr2:122350143-122359897	-	-	-	-	1.204
PTPN14	chr16:70619177-70749808	-	-	-	-	-1.123
PTPN23	chr22:52818987-52844833	-	-	-	-	-1.535
PTPRF	chr3:102998561-103067133	-	-	-	-	-1.447
PTPRM	chr24:40768712-41437121	-	-	-	-	-1.068
PTPRU	chr2:124819575-124906896	-	-	-	-	-1.178
PTS	chr15:22912246-22920397	-	-	-	-	1.244
PUS7L	chr5:36909425-36926975	-	-	-	-	1.351
QPCT	chr11:19815844-19846493	-	-	-	-	1.028
QPCTL	chr18:53684729-53690649	-	-	-	-	-1.381
RAB2A	chr14:27864734-27937015	-	-	-	-	1.096
RAB36	chr17:73784638-73796290	-	-	-	-	-1.292
RAD17	chr20:10266267-10300200	-	-	-	-	1.019
RAD18	chr22:17627572-17735891	-	-	-	-	1.166

RAD51C	chr19:9888990-9919367	-	-	-	-	1.026
RALGDS	chr11:103126161-103139619	-	-	-	-	-1.245
RAN	chrX:57523484-57525442	-	-	-	-	1.079
RANBP3	chr7:19640260-19692540	-	-	-	-	-1.043
RAP1B	chr5:45355307-45399175	-	-	-	-	1.043
RARS	chr7:82792842-82822084	-	-	-	-	1.314
RASSF5	chr16:4144348-4218744	-	-	-	-	-1.081
RBM34	chr28:7946839-7966130	-	-	-	-	1.256
RCN2	chr21:32577839-32595997	-	-	-	-	1.076
RDX	chr15:20589673-20650077	-	-	-	-	1.051
REEP3	chr28:19709520-19806763	-	-	-	-	1.133
REXO1	chr7:45765018-45784173	-	-	-	-	-1.113
RGN	chrX:90732501-90747294	-	-	-	-	1.296
RHBDF2	chr19:55893570-55902692	-	-	-	-	-1.190
RHBDL1	chr25:555009-556679	-	-	-	-	-1.038
RIDA	chr14:68412746-68420944	-	-	-	-	1.074
RILPL1	chr17:54358763-54400473	-	-	-	-	-1.392
RIN1	chr29:45029459-45034780	-	-	-	-	-1.211
RINT1	chr4:46919801-46943664	-	-	-	-	1.024
RMDN2	chr11:20388062-20448763	-	-	-	-	1.260
RNase_MRP	chr8:60244065-60244343	-	-	-	-	1.299
RND3	chr2:45800465-45822011	-	-	-	-	1.000
RNF111	chr10:51288676-51380159	-	-	-	-	1.064
RNF13	chr1:119160736-119290651	-	-	-	-	1.051
RNFT1	chr19:11112588-11123128	-	-	-	-	1.288
RNMT	chr24:43942057-43967106	-	-	-	-	1.159
ROM1	chr29:41655046-41657047	-	-	-	-	-1.348
RP2	chrX:90487297-90537534	-	-	-	-	1.033
RPAP2	chr3:51195434-51281129	-	-	-	-	1.104

RPL14	chr22:13336572-13339983	-	-	-	-	1.041
RPS27A	chr11:37823445-37825428	-	-	-	-	1.215
RPS6KA2	chr9:102918981-103074109	-	-	-	-	-1.080
RSL24D1	chr10:55165839-55179463	-	-	-	-	1.353
RSRP1	chr2:128302961-128306994	-	-	-	-	1.166
RUFY2	chr28:24917631-24955300	-	-	-	-	1.040
RUSC2	chr8:60134671-60198469	-	-	-	-	-1.076
RWDD1	chr9:34577931-34595665	-	-	-	-	1.220
SACM1L	chr22:54199065-54252163	-	-	-	-	1.138
SAFB2	chr7:19908340-19936959	-	-	-	-	-1.208
SAP18	chr12:35860635-35868470	-	-	-	-	1.005
SCAF1	chr18:56505737-56516430	-	-	-	-	-1.760
SCFD1	chr21:41692841-41804341	-	-	-	-	1.071
SCP2	chr3:93846488-93968364	-	-	-	-	1.156
SCRN3	chr2:22400873-22432815	-	-	-	-	1.279
SDF2L1	chr17:74104344-74106285	-	-	-	-	-1.202
SDHAF3	chr4:14364654-14452240	-	-	-	-	1.311
SDK1	chr25:39998763-40186702	-	-	-	-	-1.202
SEC23A	chr21:49489516-49555507	-	-	-	-	1.216
SELENOT	chr1:118445767-118476097	-	-	-	-	1.225
SEMA4C	chr11:2784989-2793644	-	-	-	-	-1.199
SEMA4F	chr11:9943905-9969422	-	-	-	-	-1.281
SENP7	chr1:46162637-46317067	-	-	-	-	1.135
SF3B6	chr11:75039680-75047800	-	-	-	-	1.028
SFR1	chr26:24945603-24949627	-	-	-	-	1.240
SGTB	chr20:13805927-13851473	-	-	-	-	1.021
SH3BGR	chr1:141029892-141100984	-	-	-	-	1.226
SH3GL1	chr7:20923761-20951051	-	-	-	-	-1.265
SH3PXD2A	chr26:24413185-24469653	-	-	-	-	-1.174

SH3PXD2B	chr20:4010452-4094221	-	-	-	-	-1.296
SH3RF1	chr8:1025433-1073248	-	-	-	-	-1.560
SHOC2	chr26:31762791-31849699	-	-	-	-	1.137
SHQ1	chr22:28952975-29056982	-	-	-	-	1.046
SIPA1	chr29:44484283-44493549	-	-	-	-	-1.311
SIX2	chr11:27260474-27263699	-	-	-	-	-1.376
SKA2	chr19:10322519-10354258	-	-	-	-	1.173
SKI	chr16:51766101-51819356	-	-	-	-	-1.428
SKIL	chr1:97824478-97843625	-	-	-	-	1.198
SKP1	chr7:47389356-47401412	-	-	-	-	1.120
SLC12A7	chr20:71395141-71420351	-	-	-	-	-1.001
SLC30A6	chr11:14781532-14827970	-	-	-	-	1.050
SLC41A1	chr16:3367786-3384777	-	-	-	-	-1.013
SLC6A17	chr3:33337959-33373481	-	-	-	-	-1.166
SLF1	chr7:96366970-96422024	-	-	-	-	1.195
SMARCB1	chr17:73222639-73239871	-	-	-	-	-1.270
SMIM14	chr6:60277931-60336533	-	-	-	-	1.039
SMNDC1	chr26:31141808-31152181	-	-	-	-	1.003
SMS	chrX:128561585-128591569	-	-	-	-	1.057
SMTN	chr17:72041476-72064312	-	-	-	-	-1.252
SNPH	chr13:60355541-60362412	-	-	-	-	-1.248
SNRPB2	chr13:10734367-10747954	-	-	-	-	1.138
SNRPF	chr5:60556050-60564297	-	-	-	-	1.550
SNX19	chr29:37526200-37555971	-	-	-	-	-1.110
SNX4	chr1:70504977-70557887	-	-	-	-	1.217
SNX6	chr21:45418668-45454655	-	-	-	-	1.189
SOCS4	chr10:67735432-67749358	-	-	-	-	1.030
SP3	chr2:22841313-22888725	-	-	-	-	1.030
SPC25	chr2:27296840-27309226	-	-	-	-	1.197

SPEG	chr2:108089327-108147468	-	-	-	-	-1.290
SREBF1	chr19:35234636-35250672	-	-	-	-	-1.225
SREK1IP1	chr20:14682281-14717765	-	-	-	-	1.054
SRFBP1	chr7:33128259-33152038	-	-	-	-	1.406
SRP54	chr21:45732640-45762266	-	-	-	-	1.380
SRPRB	chr1:136636525-136676796	-	-	-	-	1.012
ST8SIA4	chr7:102456174-102555855	-	-	-	-	1.162
STBD1	chr6:92967766-92971371	-	-	-	-	-1.050
STK26	chrX:15811929-15878198	-	-	-	-	1.219
STRN4	chr18:54263457-54287817	-	-	-	-	-1.075
STX7	chr9:71381756-71455585	-	-	-	-	1.096
SUCLA2	chr12:17884900-17930933	-	-	-	-	1.127
SUCLG2	chr22:33977311-34251728	-	-	-	-	1.031
SUGCT	chr4:80866976-81642046	-	-	-	-	1.128
SUGP1	chr7:3892064-3924127	-	-	-	-	-1.289
SULF2	chr13:76879807-77005009	-	-	-	-	-1.221
SUMO2	chr19:56923423-56931160	-	-	-	-	1.102
SUV39H2	chr13:29813364-29835882	-	-	-	-	1.065
SWT1	chr16:67653940-67759357	-	-	-	-	1.263
SYAP1	chrX:134023362-134039236	-	-	-	-	1.040
TAF1D	chr29:1056626-1062580	-	-	-	-	1.069
TAF7	chr7:54080963-54083194	-	-	-	-	1.329
TATDN3	chr16:72650160-72664647	-	-	-	-	1.085
TBC1D19	chr6:47570061-47723788	-	-	-	-	1.206
TBC1D23	chr1:44199314-44254410	-	-	-	-	1.043
TBCD	chr19:50388666-50536976	-	-	-	-	-1.140
TBL1XR1	chr1:90517078-90605473	-	-	-	-	1.023
TBX2	chr19:11943184-11951411	-	-	-	-	-1.054
TCF20	chr5:113634003-113683472	-	-	-	-	-1.206

TEAD3	chr23:9398810-9422609	-	-	-	-	-1.403
TECPR2	chr21:68837086-68901733	-	-	-	-	-1.115
TEFM	chr19:18400705-18408200	-	-	-	-	1.366
TENM4	chr29:17048262-17489455	-	-	-	-	-1.449
TGDS	chr12:69614374-69634335	-	-	-	-	1.111
THAP12	chr15:56543032-56571783	-	-	-	-	1.035
THEM4	chr3:18881346-18930585	-	-	-	-	1.099
THSD1	chr12:21669545-21697383	-	-	-	-	-1.536
THUMPD2	chr11:22066099-22109204	-	-	-	-	1.030
TM4SF1	chr1:119750362-119758888	-	-	-	-	1.045
TM9SF3	chr26:17712945-17774060	-	-	-	-	1.234
TMCO1	chr3:3166688-3222619	-	-	-	-	1.107
TMEM14A	chr23:24803729-24814237	-	-	-	-	1.250
TMEM161B	chr7:90097693-90176089	-	-	-	-	1.219
TMEM167B	chr3:34401024-34405907	-	-	-	-	1.085
TMEM201	chr16:44775431-44797198	-	-	-	-	-1.110
TMEM220	chr19:30304817-30322098	-	-	-	-	1.287
TMEM263	chr5:70573523-70593134	-	-	-	-	1.053
TMEM38B	chr8:97151937-97211919	-	-	-	-	1.227
TMEM50B	chr1:1324543-1361378	-	-	-	-	1.259
TMTC3	chr5:18010338-18047085	-	-	-	-	1.171
TNC	chr8:105965497-106067887	-	-	-	-	-1.977
TNFAIP8	chr7:35812576-35858617	-	-	-	-	1.074
TMEM119	chr17:66586627-66593115	-	-	-	-	-1.348
TNKS1BP1	chr15:81792137-81813276	-	-	-	-	-1.041
TNRC18	chr25:39430998-39510699	-	-	-	-	-1.341
TNXB	chr23:27083668-27136954	-	-	-	-	-1.469
TOM1L1	chr19:5221506-5283308	-	-	-	-	1.073
TPM1	chr3:16376435-16403812	-	-	-	-	1.086

TPMT	chr23:39209389-39232415	-	-	-	-	1.111
TRAFD1	chr17:64313878-64328239	-	-	-	-	-1.006
TRAPPC6B	chr21:49597595-49608630	-	-	-	-	1.067
TRAPPC9	chr14:4229511-4616552	-	-	-	-	-1.033
TRERF1	chr23:15948726-15988075	-	-	-	-	-1.294
TRIM56	chr25:36233861-36236129	-	-	-	-	-1.149
TRIP6	chr25:36321719-36325556	-	-	-	-	-1.019
TRMT10A	chr6:26444868-26470795	-	-	-	-	1.072
TRMT13	chr3:43251250-43291189	-	-	-	-	1.146
TRRAP	chr25:37807382-37895047	-	-	-	-	-1.252
TSKU	chr15:56961319-56974713	-	-	-	-	-1.145
TSNAX	chr28:3039813-3076657	-	-	-	-	1.373
TSPAN13	chr4:25213087-25251241	-	-	-	-	1.067
TSPAN14	chr28:36077427-36109014	-	-	-	-	-1.320
TSPAN18	chr15:75693436-75843207	-	-	-	-	-1.436
TSPAN4	chr29:50560712-50570675	-	-	-	-	-1.013
TTC37	chr7:97172633-97262280	-	-	-	-	1.027
TUBD1	chr19:11046573-11070490	-	-	-	-	1.334
TVP23B	chr19:33585302-33594740	-	-	-	-	1.000
TWF1	chr5:36847868-36859266	-	-	-	-	1.336
TWSG1	chr24:41986505-42008147	-	-	-	-	1.084
TXNDC12	chr3:94860379-94895914	-	-	-	-	1.090
UBA3	chr22:32583220-32607984	-	-	-	-	1.050
UBA6	chr6:85050209-85137078	-	-	-	-	1.268
UBE2H	chr4:94467622-94565768	-	-	-	-	-1.178
UBE2N	chr5:23370704-23411877	-	-	-	-	1.196
UBE2W	chr14:39233173-39295068	-	-	-	-	1.013
UBR1	chr10:38301492-38447561	-	-	-	-	1.136
UBR3	chr2:26361547-26565226	-	-	-	-	1.012

UCKL1	chr13:54362733-54373970	-	-	-	-	-1.436
UEVLD	chr29:26390465-26444955	-	-	-	-	1.082
UGDH	chr6:60231099-60265819	-	-	-	-	1.234
UHRF1BP1L	chr5:64414614-64481097	-	-	-	-	1.319
UHRF2	chr8:38569326-38636946	-	-	-	-	1.260
UIMC1	chr7:39718678-39856764	-	-	-	-	1.027
UMPS	chr1:69732777-69782823	-	-	-	-	1.074
UNK	chr19:56402886-56450260	-	-	-	-	-1.238
UPF1	chr7:4268128-4299794	-	-	-	-	-1.325
UROC1	chr22:61133593-61160689	-	-	-	-	-1.724
USF2	chr18:46164775-46174400	-	-	-	-	-1.151
USO1	chr6:92297158-92378158	-	-	-	-	1.127
USP15	chr5:51380095-51510100	-	-	-	-	1.182
USP16	chr1:6490670-6517408	-	-	-	-	1.187
USP19	chr22:51470660-51482027	-	-	-	-	-1.441
USP45	chr9:50963544-51013480	-	-	-	-	1.276
USP53	chr6:7151717-7207800	-	-	-	-	1.158
VBP1	chrX:38609346-38633977	-	-	-	-	1.078
VGLL4	chr22:56220083-56290873	-	-	-	-	-1.977
VMA21	chrX:34102419-34112798	-	-	-	-	1.232
VPS29	chr17:56617707-56622846	-	-	-	-	1.312
VPS35	chr18:15038820-15066463	-	-	-	-	1.152
VPS37C	chr29:38034775-38063344	-	-	-	-	-1.585
VPS41	chr4:82705581-82896816	-	-	-	-	1.039
VPS54	chr11:62301308-62377281	-	-	-	-	1.088
WDR12	chr2:91621731-91645548	-	-	-	-	1.276
WDR43	chr11:70851864-70890941	-	-	-	-	1.143
WDR54	chr11:10186101-10189962	-	-	-	-	-1.101
WDR89	chr10:76151141-76198252	-	-	-	-	1.151

WDSUB1	chr2:37167344-37235900	-	-	-	-	1.000
WISP1	chr14:9176078-9187850	-	-	-	-	-1.079
WNK1	chr5:108079509-108207083	-	-	-	-	-1.180
WRN	chr27:26263002-26449795	-	-	-	-	1.151
WRNIP1	chr23:50703506-50714364	-	-	-	-	-1.152
XPC	chr22:58702012-58724435	-	-	-	-	-1.437
XPNPEP2	chrX:13645602-13671526	-	-	-	-	-1.165
XPO1	chr11:60068220-60109922	-	-	-	-	1.040
XRCC4	chr7:85267806-85556934	-	-	-	-	1.278
YAE1D1	chr4:82020143-82024360	-	-	-	-	1.124
YAF2	chr5:38674058-38753871	-	-	-	-	1.204
YEATS4	chr5:44318356-44342854	-	-	-	-	1.040
YIPF5	chr7:57200809-57216549	-	-	-	-	1.237
YPEL5	chr11:69688036-69702229	-	-	-	-	1.022
ZBTB12	chr23:27274033-27275413	-	-	-	-	-1.254
ZBTB4	chr19:27769638-27773345	-	-	-	-	-1.310
ZBTB7A	chr7:21189878-21196263	-	-	-	-	-1.271
ZBTB8OS	chr2:121818176-121830440	-	-	-	-	1.187
ZC3H7B	chr5:112977784-113010230	-	-	-	-	-1.259
ZCCHC10	chr7:46188838-46202621	-	-	-	-	1.187
ZDHHC18	chr2:126937973-126964887	-	-	-	-	-1.255
ZDHHC20	chr12:35781298-35837108	-	-	-	-	1.064
ZFP36L2	chr11:25585492-25587785	-	-	-	-	-1.239
ZFYVE16	chr7:82875304-82908670	-	-	-	-	1.162
ZFYVE26	chr10:80180314-80245861	-	-	-	-	-1.434
ZMIZ1	chr28:35032454-35142181	-	-	-	-	-1.148
ZMPSTE24	chr3:106426044-106468939	-	-	-	-	1.005
ZMYM1	chr3:111180175-111205859	-	-	-	-	1.386
ZNF148	chr1:70287256-70382437	-	-	-	-	1.157

ZNF165	chr23:30332528-30343084	-	-	-	-	1.155
ZNF200	chr25:2675125-2686354	-	-	-	-	1.141
ZNF217	chr13:81854046-81863004	-	-	-	-	-1.089
ZNF268	chr17:45221484-45223845	-	-	-	-	1.057
ZNF335	chr13:75404992-75435377	-	-	-	-	-1.342
ZNF341	chr13:63750158-63790156	-	-	-	-	-1.019
ZNF395	chr8:10188170-10246574	-	-	-	-	-1.660
ZNF45	chr18:52429557-52446106	-	-	-	-	1.013
ZNF469	chr18:13740621-13753849	-	-	-	-	-1.263
ZNF503	chr28:31317208-31320375	-	-	-	-	-1.227
ZNF512B	chr13:54353901-54359471	-	-	-	-	-1.016
ZNF518A	chr26:17367944-17372393	-	-	-	-	1.022
ZNF566	chr18:47237080-47266289	-	-	-	-	1.019
ZNF569	chr18:47619375-47630372	-	-	-	-	1.454
ZNF570	chr18:47656763-47675770	-	-	-	-	1.469
ZNF579	chr18:62393200-62408437	-	-	-	-	-1.547
ZNF599	chr18:45731749-45746037	-	-	-	-	1.009
ZNF639	chr1:88405654-88410920	-	-	-	-	1.097
ZNF644	chr3:52413190-52508199	-	-	-	-	1.329
ZNF665	chr18:58866567-58876003	-	-	-	-	1.177
ZNF770	chr10:30525209-30527276	-	-	-	-	1.245
ZNF777	chr4:113238977-113261531	-	-	-	-	-1.097
ZRANB2	chr3:74448728-74464316	-	-	-	-	1.069
Commonly expressed genes						
C2	chr23:27231724-27243367	1.483	1.085	-	-	-
HAS2	chr14:19703610-19733798	3.381	2.086	-	-	-
PTGS2	chr16:69263775-69271399	2.938	1.107	-	-	-
SLC16A12	chr26:11141010-11161385	3.666	2.870	-	-	-
TMCC3	chr5:24466599-24537335	1.538	1.272	-	-	-

ARL4D	chr19:43945991-43947907	-1.158	-	-1.090	-	-
ISG15	chr16:52714626-52715665	2.573	-	1.221	-	-
PDE4B	chr3:79284892-79823433	1.919	-	1.005	-	-
RASL11B	chr6:70179361-70183823	-1.287	-	-1.209	-	-
TNFAIP2	chr21:69455151-69466051	1.602	-	1.166	-	-
TNIP1	chr7:64295656-64339418	1.698	-	1.129	-	-
U2	chr19:43937801-43937992	1.369	-	-1.342	-	-
ENSBTAG00000006078	chr13:17623241-17639994	1.675	-	-	1.381	-
FBP2	chr8:82396094-82438817	2.296	-	-	1.476	-
PSMB9	chr23:7127078-7133608	1.197	-	-	1.066	-
RARB	chr27:40131404-40235970	1.006	-	-	1.039	-
ADORA2B	chr19:34084459-34104983	1.146	-	-	-	1.092
CLASRP	chr18:53129171-53153714	-1.315	-	-	-	-1.167
COQ10B	chr2:86410859-86427846	1.076	-	-	-	1.175
CRYZL1	chr1:1189227-1222846	1.036	-	-	-	1.199
DNAJC12	chr28:24397287-24447263	1.093	-	-	-	1.283
DRAM1	chr5:66043814-66079316	1.688	-	-	-	1.179
DRAM2	chr3:32376401-32404442	1.148	-	-	-	1.344
EIF3E	chr14:58397834-58445787	1.045	-	-	-	1.308
EMB	chr20:28721654-28743621	1.097	-	-	-	1.239
ENSBTAG00000013284	chr14:33004982-33065711	1.157	-	-	-	1.434
ENSBTAG00000014685	chrX:18120060-18151262	1.020	-	-	-	1.353
ENSBTAG00000017670	chr3:54307499-54323003	1.052	-	-	-	1.170
ENSBTAG00000018854	chr1:3113948-3122613	1.007	-	-	-	1.173
ENSBTAG00000026993	chr5:47877714-47894116	1.044	-	-	-	1.405
ENSBTAG00000031731	chr11:49760291-49761138	1.089	-	-	-	1.075
ENSBTAG00000032914	chr5:28887966-28914607	1.528	-	-	-	1.087
ENSBTAG00000032961	chr24:47304920-47322103	1.096	-	-	-	1.294
ENSBTAG00000034449	chr3:5454660-5455256	1.136	-	-	-	1.215

ENSBTAG00000034676	chr24:8845812-8847179	1.413	-	-	-	1.172
ENSBTAG00000045544	chrX:144159055-144234222	1.037	-	-	-	1.224
ENSBTAG00000046367	chr18:47862387-47883111	1.147	-	-	-	1.102
ENTPD7	chr26:20494068-20524328	1.222	-	-	-	1.054
FAM103A1	chr21:23705959-23711314	1.012	-	-	-	1.158
G2E3	chr21:41640497-41686535	1.122	-	-	-	1.345
GTF2B	chr3:55179368-55210377	1.360	-	-	-	1.092
HERC5	chr6:37683712-37728536	1.301	-	-	-	1.052
HSPA13	chr1:22290119-22300252	1.242	-	-	-	1.300
KATNBL1	chr10:28459344-28509712	1.192	-	-	-	1.316
KCTD12	chr12:52351170-52352151	-1.078	-	-	-	-1.013
MFN1	chr1:88263739-88387147	1.008	-	-	-	1.309
MIS12	chr19:26678019-26682795	1.002	-	-	-	1.071
MITD1	chr11:4290568-4306454	1.259	-	-	-	1.030
MORC3	chr1:150307554-150349311	1.096	-	-	-	1.317
MSANTD4	chr15:1991264-2001671	1.052	-	-	-	1.436
NDUFA5	chr4:88657783-88673594	1.035	-	-	-	1.050
NMI	chr2:44930494-44950481	1.157	-	-	-	1.041
PCGF5	chr26:12879193-12931310	1.008	-	-	-	1.081
PPP2R3C	chr21:45794780-45820504	1.192	-	-	-	1.146
PRELID2	chr7:58900992-59009921	1.189	-	-	-	1.342
PSMA3	chr10:70797327-70822594	1.025	-	-	-	1.204
RAB33B	chr17:18553786-18573502	1.145	-	-	-	1.346
RABGGTB	chr3:69316066-69322906	1.060	-	-	-	1.245
RBM43	chr2:44961706-44973211	1.068	-	-	-	1.066
SCARNA7	chr1:107774352-107834443	1.230	-	-	-	1.235
SLC41A2	chr5:68700932-68813411	1.088	-	-	-	1.191
SLMAP	chr22:43864915-43951804	1.017	-	-	-	1.046
SNORA73	chr2:125500692-125500896	1.472	-	-	-	1.062

SOX4	chr23:36292361-36293944	-1.017	-	-	-	-1.304
STK17B	chr2:85077800-85097107	1.115	-	-	-	1.148
STXBP3	chr3:34681545-34734868	1.026	-	-	-	1.321
TBK1	chr5:49502463-49542968	1.080	-	-	-	1.269
TMEM168	chr4:56459730-56517535	1.040	-	-	-	1.265
TMEM41B	chr15:43901751-43929481	1.080	-	-	-	1.159
TPRKB	chr11:10862326-10869029	1.057	-	-	-	1.016
TRMT11	chr9:25578681-25640399	1.122	-	-	-	1.365
U2	chr19:43889805-43889996	1.430	-	-	-	1.086
U3	chr27:16404736-16404951	2.102	-	-	-	1.334
UTP23	chr14:49706794-49714027	1.047	-	-	-	1.390
YES1	chr24:35973658-36038238	1.028	-	-	-	1.316
PER1	chr19:28390593-28399600	-	2.028	-1.462	-	-
PLSCR4	chr1:123231175-123273104	-	1.007	-	-	1.210
RFX2	chr7:19529295-19622972	-	-1.116	-	-	-1.042
ALG11	chr12:21488036-21498946	-	-	-1.097	-1.372	-
ASH2L	chr27:32989768-33014982	-	-	-1.111	-1.116	-
ATXN2	chr17:57425984-57527920	-	-	-1.123	-1.410	-
CHEK2	chr17:70269591-70305247	-	-	-1.115	-1.230	-
ENSBTAG00000015497	chr9:33546889-33553200	-	-	-1.461	-2.307	-
ENSBTAG00000021367	chr8:63617040-63630082	-	-	-1.011	-1.677	-
ENSBTAG00000047428	chr16:81040750-81042142	-	-	-1.087	-1.222	-
ENSBTAG00000047699	chrX:130065241-130067460	-	-	-1.073	-1.167	-
FMR1	chrX:30922773-30962111	-	-	-1.167	-1.093	-
GAR1	chr6:16747756-16755365	-	-	-1.043	-1.510	-
GLCCI1	chr4:17067021-17141147	-	-	-1.305	-1.671	-
HNRNPU	chr16:33163183-33172676	-	-	-1.002	-1.096	-
KIAA0430	chr25:14138541-14171367	-	-	-1.205	-1.140	-
RGS7	chr16:36195997-36695079	-	-	-1.022	-1.039	-

UBE2J1	chr9:61766992-61782483	-	-	-1.223	-1.311	-
UBE4B	chr16:44263937-44385466	-	-	-1.171	-1.182	-
ABCA3	chr25:1796659-1828217	-	-	-1.310	-	-1.557
ADAMTS1	chr1:8955133-8963815	-	-	-1.223	-	-1.137
ALG6	chr3:82389601-82545184	-	-	1.057	-	1.432
ANTXR1	chr11:67334897-67590481	-	-	-1.254	-	-1.322
APLP1	chr18:46754201-46764958	-	-	-1.367	-	-1.287
APOOL	chrX:75160535-75265102	-	-	1.060	-	1.517
ARID1B	chr9:94882343-95271883	-	-	-1.292	-	-1.012
AXIN2	chr19:62834849-62860774	-	-	-1.395	-	-1.743
B4GALT6	chr24:25770342-25836730	-	-	-1.084	-	-1.054
BRPF3	chr23:10099946-10130409	-	-	-1.095	-	-1.185
BZW1	chr2:89886719-89897574	-	-	1.077	-	1.504
BOC	chr1:58428031-58464999	-	-	-1.063	-	-1.421
CAD	chr11:72383286-72404747	-	-	-1.378	-	-1.367
CALCRL	chr2:8901431-9030989	-	-	1.023	-	1.281
CENPH	chr20:10407094-10425913	-	-	1.177	-	1.403
CENPQ	chr23:21980290-21997926	-	-	1.017	-	1.068
CEP250	chr13:65366075-65405852	-	-	-1.101	-	-1.617
CEP57L1	chr9:41469870-41554001	-	-	1.035	-	1.247
CGN	chr3:19290675-19309322	-	-	-1.049	-	-1.350
CHD4	chr5:104186060-104214563	-	-	-1.152	-	-1.284
CHMP2B	chr1:34970459-35004356	-	-	1.074	-	1.437
CHMP4B	chr13:63817039-63849782	-	-	-1.246	-	-1.362
CHST3	chr28:28254031-28256945	-	-	-1.101	-	-1.572
COL14A1	chr14:83892852-84109620	-	-	-1.212	-	-1.454
COMMD8	chr6:67746951-67761215	-	-	1.285	-	1.625
CPEB1	chr21:23309724-23333820	-	-	-1.610	-	-1.488
CTSZ	chr13:57889706-57899205	-	-	-1.587	-	-2.009

CUL9	chr23:16759131-16794939	-	-	-1.130	-	-1.281
CYR61	chr3:58678778-58681686	-	-	-1.431	-	-1.501
DCTN3	chr8:77322210-77330626	-	-	-1.098	-	-1.224
DHRS1	chr10:20704885-20713840	-	-	-1.008	-	-1.023
DLG5	chr28:33719673-33842951	-	-	-1.164	-	-1.620
DLL1	chr9:105508312-105516028	-	-	-1.066	-	-1.170
DTWD1	chr10:60913314-60924152	-	-	1.131	-	1.349
DYNC1H1	chr21:68507133-68568024	-	-	-1.035	-	-1.487
ECSIT	chr7:17085481-17097271	-	-	-1.110	-	-1.434
EGR1	chr7:51438726-51442500	-	-	-1.061	-	-1.634
ENSBTAG00000003144	chr7:96124691-96354407	-	-	1.053	-	1.067
ENSBTAG00000004240	chr5:63027193-63052820	-	-	1.016	-	1.198
ENSBTAG00000006551	chr8:10859328-10885722	-	-	1.115	-	1.245
ENSBTAG00000009889	chr18:45705246-45717737	-	-	1.196	-	1.506
ENSBTAG00000011072	chr28:30215524-30732444	-	-	1.033	-	1.487
ENSBTAG00000019116	chr2:86464319-86494036	-	-	1.052	-	1.482
ENSBTAG00000022396	chr29:26668046-26671801	-	-	5.792	-	5.076
ENSBTAG00000045619	chr10:79824701-79824857	-	-	1.142	-	1.216
ENSBTAG00000046684	chr10:102020146-102300271	-	-	-1.177	-	-1.031
ETFRF1	chr5:85210769-85217660	-	-	1.149	-	1.161
ETV3	chr3:13743910-13753402	-	-	-1.353	-	-1.401
FABP5	chr14:46644608-46649827	-	-	1.208	-	1.533
FN1	chr2:103881401-103950562	-	-	-1.134	-	-1.538
FOSL2	chr11:71329771-71349193	-	-	-1.411	-	-1.684
GTF2E1	chr1:66042805-66070880	-	-	1.149	-	1.285
HNMT	chr2:59376268-59417330	-	-	1.050	-	1.362
HPS4	chr17:68368660-68396020	-	-	-1.090	-	-1.351
ITGA11	chr10:15103980-15196986	-	-	-1.020	-	-1.768
ITGA5	chr5:25778011-25799053	-	-	-1.020	-	-1.029

KAT6A	chr27:36532981-36636049	-	-	-1.158	-	-1.329
KIAA1549	chr4:103305513-103380070	-	-	-1.038	-	-1.330
KIF13A	chr23:39404302-39501810	-	-	-1.131	-	-1.172
KRR1	chr5:4974614-5034909	-	-	1.025	-	1.429
L2HGDH	chr10:43211977-43265008	-	-	1.024	-	1.320
LAMP1	chr12:90609709-90621680	-	-	-1.187	-	-1.540
LNX2	chr12:32604930-32646201	-	-	-1.115	-	-1.283
LPCAT4	chr10:28331828-28339111	-	-	-1.364	-	-1.080
LRIG1	chr22:35068217-35181384	-	-	-1.239	-	-1.458
LUZP1	chr2:130360071-130363164	-	-	-1.192	-	-1.094
MAFB	chr13:70068209-70069181	-	-	-1.491	-	-1.943
MAP3K10	chr18:49872448-49887851	-	-	-1.022	-	-1.432
MFSD9	chr11:7422150-7432712	-	-	-1.226	-	-1.299
MRPL47	chr1:88111911-88129274	-	-	1.184	-	1.521
NCS1	chr11:100548299-100564121	-	-	-1.007	-	-1.245
NIPAL3	chr2:129041412-129091075	-	-	-1.343	-	-1.241
NUF2	chr3:6033720-6072026	-	-	1.009	-	1.292
NUP214	chr11:101350156-101438043	-	-	-1.101	-	-1.424
NYAP1	chr25:36603210-36609285	-	-	-1.014	-	-1.385
PCBP1	chr11:68383792-68385266	-	-	-1.063	-	-1.139
PCNA	chr13:47788529-47794602	-	-	1.067	-	1.443
PDCD10	chr1:100540219-100587970	-	-	1.027	-	1.342
PFDN4	chr13:82399772-82402817	-	-	1.118	-	1.698
PI4KA	chr17:74200827-74260366	-	-	-1.211	-	-1.916
PIH1D2	chr15:22701524-22707582	-	-	1.022	-	1.229
PLXNB2	chr5:119840725-119854120	-	-	-1.138	-	-1.736
PPP1R15A	chr18:55925890-55929294	-	-	-1.004	-	-1.378
PPP1R35	chr25:36643094-36644330	-	-	-1.034	-	-1.562
PRDM6	chr7:31950212-32058001	-	-	-1.146	-	-1.149

PRPF31	chr18:63443998-63455010	-	-	-1.124	-	-1.635
PRRC2B	chr11:101592545-101644848	-	-	-1.184	-	-1.809
RAB35	chr17:64724243-64742928	-	-	-1.153	-	-1.187
RAPGEF1	chr11:101728371-101793685	-	-	-1.190	-	-1.421
RAVER1	chr7:16073296-16086918	-	-	-1.209	-	-1.231
RBM11	chr1:22455499-22497927	-	-	1.091	-	1.423
RNF44	chr7:39351902-39357420	-	-	-1.234	-	-1.529
RPTOR	chr19:52308518-52629957	-	-	-1.050	-	-1.271
SASS6	chr3:43291332-43331499	-	-	1.083	-	1.412
SEPT7	chr4:61611419-61710127	-	-	1.082	-	1.376
SET	chr11:99223001-99226827	-	-	1.168	-	1.469
SH3BGRL	chrX:70399115-70527059	-	-	1.186	-	1.507
SLC35F5	chr2:65677514-65719366	-	-	1.130	-	1.606
SLC39A10	chr2:84734001-84770814	-	-	1.090	-	1.326
SLC7A1	chr12:31004651-31019183	-	-	-1.319	-	-1.221
SNAPC1	chr10:74148206-74178126	-	-	1.069	-	1.268
SNRNP48	chr23:47647767-47663909	-	-	-1.116	-	-1.363
SPATA2	chr13:78712287-78722796	-	-	-1.022	-	-1.636
SPRY2	chr12:55684000-55685894	-	-	-1.190	-	-1.226
SRRM2	chr25:2286716-2304536	-	-	-1.037	-	-1.151
SRSF4	chr2:124956593-124982238	-	-	-1.570	-	-1.593
SSB	chr2:26582628-26599728	-	-	1.028	-	1.364
TAF1A	chr16:26747505-26779536	-	-	1.080	-	1.324
THBS2	chr9:104735656-104760261	-	-	-1.176	-	-1.418
TMED5	chr3:50448642-50467156	-	-	1.212	-	1.445
TMEM267	chr20:31353135-31372951	-	-	1.117	-	1.418
TNRC6C	chr19:54670557-54721786	-	-	-1.253	-	-1.800
TNS2	chr5:27069112-27082523	-	-	-1.063	-	-1.564
TRMT10C	chr1:46339131-46343357	-	-	1.181	-	1.548

TYW3	chr3:70224344-70246822	-	-	1.058	-	1.098
USP21	chr3:8350179-8356345	-	-	-1.159	-	-1.202
USP30	chr17:66239944-66263958	-	-	-1.361	-	-1.421
VPS50	chr4:10432173-10564199	-	-	1.103	-	1.309
ZBTB14	chr24:39250141-39251488	-	-	-1.152	-	-1.563
ZCCHC3	chr13:61254417-61257121	-	-	-1.295	-	-1.870
ZFAND3	chr23:11712801-12040961	-	-	-1.095	-	-1.382
ZNF532	chr24:58491690-58551186	-	-	-1.102	-	-1.491
ADAMTSL4	chr3:20187038-20195550	-	-	-	-1.290	-1.484
ADRM1	chr13:55433439-55439176	-	-	-	-1.010	-1.247
AHDC1	chr2:126350163-126354957	-	-	-	-1.272	-1.761
ARHGAP1	chr15:77496429-77513093	-	-	-	-1.154	-1.412
ATF6B	chr23:27057895-27067756	-	-	-	-1.111	-1.149
ATP6V0C	chr25:2014228-2019603	-	-	-	-1.969	-1.919
BAG3	chr26:40118555-40141989	-	-	-	-1.004	-1.208
BAHD1	chr10:36180772-36187722	-	-	-	-1.402	-1.798
BCL6	chr1:80179481-80202388	-	-	-	-1.278	-1.143
BGN	chrX:39639905-39653687	-	-	-	-1.431	-1.459
CAMTA2	chr19:27054327-27067739	-	-	-	-1.719	-1.671
CCBE1	chr24:58886143-58924772	-	-	-	-1.693	-1.188
CDCP1	chr22:54717552-54770691	-	-	-	-1.118	-1.028
CHMP4A	chr10:20782272-20785952	-	-	-	-2.076	-2.159
CIZ1	chr11:98806163-98823350	-	-	-	-1.824	-2.132
COPZ2	chr19:39081065-39090187	-	-	-	-2.214	-2.248
CPSF7	chr29:40600719-40616875	-	-	-	-1.726	-1.138
Csnk2b-Ly6g5b	chr23:27447510-27451477	-	-	-	-1.564	-1.178
CTNNBIP1	chr16:44541238-44559715	-	-	-	-1.566	-1.384
DHX37	chr17:53092230-53122446	-	-	-	-1.343	-1.708
DTX3	chr5:56201576-56205117	-	-	-	-1.042	-1.246

DYRK1B	chr18:49650521-49658124	-	-	-	-1.193	-1.396
EHD2	chr18:55071101-55087454	-	-	-	-1.250	-1.788
ELF4	chrX:13915386-13926276	-	-	-	-1.078	-1.824
ELMSAN1	chr10:85517889-85536667	-	-	-	-1.307	-2.017
ENSBTAG00000001538	chr3:117506246-117506811	-	-	-	-2.076	-1.772
ENSBTAG00000001879	chr3:118191440-118206600	-	-	-	-1.725	-2.066
ENSBTAG00000002633	chr19:55118591-55153750	-	-	-	-1.267	-1.366
ENSBTAG00000007443	chr19:5642997-5644194	-	-	-	-1.001	-1.006
ENSBTAG00000008690	chr3:102623729-102659082	-	-	-	-1.313	-1.082
ENSBTAG00000011134	chr7:5800190-5803107	-	-	-	-1.247	-1.200
ENSBTAG00000014417	chr25:33157513-33168430	-	-	-	-2.153	-1.847
ENSBTAG00000015438	chr13:38289296-38317466	-	-	-	-1.306	-1.725
ERCC1	chr18:53449225-53466227	-	-	-	-1.820	-1.588
EVL	chr21:66675973-66738876	-	-	-	-1.230	-1.598
FOXO1	chr12:21915746-22005338	-	-	-	-2.484	-2.255
FOXP4	chr23:15391989-15425174	-	-	-	-1.448	-1.675
GAA	chr19:53100964-53113264	-	-	-	-1.042	-1.351
GIT1	chr19:21391292-21400011	-	-	-	-1.314	-1.516
GLIS2	chr25:3492817-3497250	-	-	-	-1.465	-1.608
GLTSCR1L	chr23:16478579-16509798	-	-	-	-1.079	-1.034
GPS2	chr19:27653443-27656067	-	-	-	-1.316	-1.008
HTRA3	chr6:119387683-119418513	-	-	-	-1.326	-1.694
IFT122	chr22:56881078-56948817	-	-	-	-1.025	-1.425
IMPDH1	chr4:93382311-93399661	-	-	-	-1.026	-1.839
INPP5K	chr19:23193609-23212514	-	-	-	-1.088	-1.224
IRX1	chr20:69472638-69477632	-	-	-	-1.401	-1.743
IRX3	chr18:22692065-22694550	-	-	-	-1.797	-2.581
KAT2A	chr19:42888853-42895399	-	-	-	-1.452	-1.365
KDM2B	chr17:55899387-56017498	-	-	-	-1.109	-1.311

KMT2B	chr18:46620835-46640904	-	-	-	-1.003	-1.482
LHPP	chr26:44431213-44558731	-	-	-	-1.117	-1.125
LRRC3	chr1:145885349-145887681	-	-	-	-1.303	-1.213
MAML2	chr15:14426512-14556383	-	-	-	-1.727	-1.353
MAP1B	chr20:9330174-9419040	-	-	-	-1.079	-1.035
MAP1S	chr7:5335660-5367540	-	-	-	-1.043	-1.613
MAPRE3	chr11:72598139-72653468	-	-	-	-1.179	-1.261
MAST3	chr7:5002381-5033392	-	-	-	-1.585	-1.157
MDH2	chr25:34734995-34779637	-	-	-	-1.568	-1.613
MED12	chrX:84789499-84811761	-	-	-	-1.168	-1.251
MED15	chr17:74425041-74490537	-	-	-	-1.248	-1.778
MEF2D	chr3:14380071-14413740	-	-	-	-1.776	-1.831
MICALL1	chr5:110213000-110240434	-	-	-	-1.154	-1.949
MKL1	chr5:112261805-112372282	-	-	-	-1.858	-2.110
MLXIP	chr17:55472595-55528501	-	-	-	-1.293	-1.611
MRPL18	chr9:97493687-97499407	-	-	-	-1.016	-1.179
MRPL40	chr17:74708564-74711079	-	-	-	-1.126	-2.551
MYL9	chr13:66306259-66314230	-	-	-	-1.597	-1.882
NCKAP5L	chr5:30251224-30262563	-	-	-	-1.214	-1.581
NHSL1	chr9:77233381-77296724	-	-	-	-1.024	-1.141
NKIRAS2	chr19:42812568-42816762	-	-	-	-1.121	-1.802
NLGN2	chr19:27727924-27733393	-	-	-	-1.254	-1.593
NOL6	chr8:76540580-76552661	-	-	-	-1.247	-1.570
NPRL3	chr25:147446-179877	-	-	-	-1.227	-1.328
P3H1	chr3:104065148-104084575	-	-	-	-1.173	-1.661
PCDHGC5	chr7:54152474-54281944	-	-	-	-1.187	-1.369
PFKM	chr5:32312956-32337525	-	-	-	-1.307	-1.530
PLK1	chr25:21587068-21597613	-	-	-	-1.753	-1.624
PMM2	chr25:7700703-7730822	-	-	-	-1.219	-1.040

PNPLA2	chr29:50742385-50747161	-	-	-	-2.192	-1.648
PPP1R13B	chr21:69982290-70077426	-	-	-	-1.264	-1.432
PTCD2	chr20:9179367-9211165	-	-	-	-1.539	-1.264
PTP4A3	chr14:3578345-3586015	-	-	-	-2.271	-3.196
PTPRG	chr22:39175037-40360572	-	-	-	-1.126	-1.213
PXN	chr17:64818099-64833437	-	-	-	-1.801	-1.662
RAB11B	chr7:18249533-18259141	-	-	-	-1.389	-1.580
RAI1	chr19:35252241-35263546	-	-	-	-1.137	-1.631
RCAN2	chr23:19437557-19667184	-	-	-	-1.510	-1.365
RENBP	chrX:40063729-40071014	-	-	-	-1.272	-1.536
RNPS1	chr25:1780539-1789539	-	-	-	-1.123	-1.490
RPS16	chr18:49393724-49396191	-	-	-	-2.200	-1.774
RRAS	chr18:56497093-56501119	-	-	-	-1.683	-1.767
RREB1	chr23:47900594-47959504	-	-	-	-1.113	-1.605
SEC16A	chr11:103939069-103964031	-	-	-	-1.005	-1.720
SELENON	chr2:127851647-127869417	-	-	-	-1.325	-1.066
SERTAD2	chr11:62992907-62993855	-	-	-	-1.666	-1.734
SF1	chr29:43623209-43636775	-	-	-	-1.309	-1.024
SF3A2	chr7:22687236-22695545	-	-	-	-1.807	-1.586
SFSWAP	chr17:46273771-46354749	-	-	-	-1.096	-1.567
SH3BP4	chr3:115210339-115232304	-	-	-	-1.391	-1.363
SIK3	chr15:27942430-28060833	-	-	-	-1.206	-1.480
SLC9A1	chr2:126676549-126727482	-	-	-	-1.785	-2.310
SLX4	chr25:2958709-2977159	-	-	-	-1.038	-1.678
SMIM12	chr3:111426911-111431172	-	-	-	-1.086	-1.253
SORBS3	chr8:70354892-70384759	-	-	-	-1.547	-1.376
SUSD6	chr10:81751603-81800132	-	-	-	-1.733	-1.444
SYNPO	chr7:64020056-64027999	-	-	-	-2.857	-1.934
TBXA2R	chr7:21561178-21569885	-	-	-	-1.133	-1.103

TFG	chr1:45489051-45521372	-	-	-	-1.472	-1.058
TGFB1I1	chr25:27760810-27766954	-	-	-	-1.172	-1.529
TM9SF4	chr13:62165597-62218184	-	-	-	-1.016	-1.112
TMEM94	chr19:56679701-56697953	-	-	-	-1.050	-1.397
TNS1	chr2:106627005-106773157	-	-	-	-1.295	-1.561
TSC2	chr25:1596729-1626967	-	-	-	-1.060	-1.492
TSHZ3	chr18:41991379-41994613	-	-	-	-1.325	-1.477
TUFM	chr25:26225845-26229801	-	-	-	-1.073	-1.024
UBA52	chr7:4535466-4537851	-	-	-	-1.644	-1.098
UBAP2	chr8:76668493-76759843	-	-	-	-1.472	-1.021
ULK1	chr17:46171843-46193233	-	-	-	-1.986	-1.854
VAC14	chr18:1449427-1525767	-	-	-	-1.463	-2.176
WDR62	chr18:46906320-46954817	-	-	-	-1.129	-1.413
WFS1	chr6:104673700-104696495	-	-	-	-1.021	-1.412
WIPF2	chr19:41162357-41177893	-	-	-	-2.811	-1.878
WIZ	chr7:8742335-8750651	-	-	-	-2.003	-2.016
YBX3	chr5:99335507-99360895	-	-	-	-1.665	-1.663
YTHDF2	chr2:125294727-125324175	-	-	-	-1.336	-1.087
ZC3H18	chr18:13879227-13922305	-	-	-	-1.026	-1.994
ZCCHC24	chr28:35189621-35251005	-	-	-	-1.121	-1.095
ZDHHC5	chr15:82336095-82354378	-	-	-	-1.275	-1.772
ZDHHC8	chr17:75039313-75050946	-	-	-	-2.254	-1.241
ZER1	chr11:99255810-99284276	-	-	-	-1.739	-1.902
ZMIZ2	chr4:77432314-77441756	-	-	-	-1.335	-1.356
ZNF414	chr7:18343921-18347588	-	-	-	-2.029	-1.598
ZNF592	chr21:22822828-22871700	-	-	-	-1.095	-1.536
ZYX	chr4:107598855-107607834	-	-	-	-1.163	-1.125
NFKBIA	chr21:46065548-46068942	3.443	1.968	-	1.658	-
OCLN	chr20:10154908-10201157	4.073	1.804	-	1.638	-

RND1	chr5:31090624-31097555	5.399	2.674	-	3.259	-
TNFAIP3	chr9:76766556-76776874	3.830	3.016	-	2.143	-
MCFD2	chr11:29200742-29210371	1.443	1.216	-	-	1.344
ACADM	chr3:69344156-69382504	1.017	-	1.122	-	1.452
ACTR6	chr5:64510373-64529644	1.189	-	1.126	-	1.573
ANXA1	chr8:49624472-49642916	1.171	-	1.145	-	1.404
ATAD1	chr26:9411264-9448494	1.109	-	1.013	-	1.372
C17orf96	chr19:39912108-39913248	-1.460	-	-1.220	-	-1.435
C18orf54	chr24:54209586-54228633	1.160	-	1.143	-	1.505
C1orf54	chr3:20406683-20413546	1.214	-	1.345	-	1.445
CCNC	chr9:50920351-50946139	1.256	-	1.225	-	1.779
CENPI	chrX:54969323-55038292	1.079	-	1.002	-	1.389
CENPK	chr20:13952310-13989063	1.508	-	1.469	-	2.017
COPS2	chr10:61295668-61326360	1.072	-	1.098	-	1.479
CYP7B1	chr14:30982607-31154016	2.273	-	1.284	-	1.498
ELMOD2	chr17:17477249-17506592	1.097	-	1.198	-	1.463
ENSBTAG00000000655	chr21:47852814-48169316	1.037	-	1.199	-	1.262
ENSBTAG00000005722	chr16:52997829-52998556	1.133	-	1.168	-	1.184
ENSBTAG00000006564	chr15:38745760-38758646	1.075	-	1.079	-	1.468
ENSBTAG00000011511	chr3:10821597-10858863	1.524	-	1.137	-	1.012
ENSBTAG00000015741	chr3:9371594-9372444	1.337	-	1.230	-	1.656
ENSBTAG00000019437	chr19:15129225-15141376	1.355	-	1.200	-	1.458
ENSBTAG00000021135	chr8:78599029-78600903	1.013	-	1.148	-	1.462
ENSBTAG00000032872	chr22:37731239-37737102	1.298	-	1.057	-	1.647
ENSBTAG00000046324	chr5:100926602-100938555	1.978	-	1.425	-	1.896
ENSBTAG00000047379	chr25:37125928-37175162	1.847	-	1.535	-	1.559
ERCC8	chr20:18372122-18423094	1.164	-	1.145	-	1.630
FAM171A2	chr19:44782787-44792763	-1.337	-	-1.055	-	-1.506
FASTKD1	chr2:26740842-26776374	1.063	-	1.130	-	1.576

FGF7	chr10:61005652-61068184	1.166	-	1.118	-	1.583
GAS1	chr8:81511016-81512051	-1.114	-	-1.211	-	-1.244
GCNT4	chr10:6432187-6433552	1.256	-	1.103	-	1.166
GMCL1	chr11:68149828-68205598	1.481	-	1.008	-	1.265
GRAMD1C	chr1:58963949-59063256	1.264	-	1.164	-	1.311
GTF2H2	chr20:10127242-10148631	1.024	-	1.044	-	1.439
IL18	chr15:22800426-22826698	1.189	-	1.113	-	1.343
IPMK	chr26:762047-814255	1.606	-	1.064	-	1.554
LINC00998	chr4:55612201-55614012	1.263	-	1.166	-	1.557
NAB1	chr2:5567017-5603683	1.561	-	1.055	-	1.173
NLRP3	chr7:42028058-42075814	1.494	-	1.029	-	1.056
NMD3	chr1:106973279-107009693	1.051	-	1.034	-	1.422
NT5C3A	chr4:64185798-64205027	1.004	-	1.347	-	1.453
NXT2	chrX:62392937-62399511	1.279	-	1.153	-	1.526
OLR1	chr5:100244331-100255640	2.641	-	1.583	-	1.778
OMA1	chr3:88054069-88119290	1.046	-	1.041	-	1.228
PDPN	chr16:55407770-55442826	1.738	-	1.250	-	1.316
PSMA4	chr21:31442648-31450480	1.027	-	1.033	-	1.400
RAB8B	chr10:46837291-46907334	1.096	-	1.037	-	1.438
SCOC	chr17:17627246-17639129	1.036	-	1.150	-	1.476
SLC35A3	chr3:43400345-43444844	1.030	-	1.083	-	1.450
SNRNP27	chr11:68215015-68222914	1.086	-	1.011	-	1.243
SNX16	chr14:83139845-83177274	1.014	-	1.140	-	1.501
SUB1	chr20:41122022-41143914	1.281	-	1.230	-	1.786
TFRC	chr1:71260067-71280648	1.488	-	1.014	-	1.344
TMEM167A	chr7:85222950-85267629	1.197	-	1.261	-	1.689
TNFSF18	chr16:41541498-41552708	1.243	-	1.150	-	1.420
TRIM38	chr23:31693731-31708621	1.338	-	1.021	-	1.260
TXNDC9	chr11:4414188-4424370	1.215	-	1.099	-	1.320

UCHL3	chr12:50948443-50997544	1.024	-	1.009	-	1.322
ZNF277	chr4:55994118-56128665	1.025	-	1.017	-	1.383
ZUFSP	chr9:34364850-34389669	1.018	-	1.019	-	1.475
IL15	chr17:16347924-16363886	2.494	-	-	1.785	1.660
U4	chr17:64874907-64875048	1.485	-	-	-1.461	1.170
MYC	chr14:13769243-13774438	-	1.124	-	-1.739	-1.422
ACBD5	chr13:18047208-18075549	-	-	-1.742	-1.719	-2.022
ACTN1	chr10:81023525-81121590	-	-	-1.065	-1.799	-2.298
ACTN3	chr29:45230681-45242282	-	-	-1.228	-1.084	-1.286
ACVR1B	chr5:28038531-28070153	-	-	-1.821	-1.266	-1.643
AFF1	chr6:103688010-103825580	-	-	-1.263	-1.163	-1.296
ANPEP	chr21:21620138-21637144	-	-	-1.028	-1.050	-1.403
APBB1IP	chr13:18259067-18334728	-	-	-1.144	-1.559	-1.494
B4GAT1	chr29:45043095-45045344	-	-	-1.450	-1.574	-1.748
BANF1	chr29:44759485-44761429	-	-	-1.280	-1.865	-2.002
BAX	chr18:55985201-55989378	-	-	-1.302	-1.959	-1.689
BAZ2A	chr5:57132350-57162026	-	-	-1.046	-1.047	-1.237
BCL9	chr3:22106733-22120933	-	-	-1.077	-1.404	-1.065
C14orf2	chr21:70113044-70118400	-	-	-1.480	-1.894	-1.777
CCDC184	chr5:32277007-32278883	-	-	-1.654	-1.648	-1.565
CCDC92	chr17:54003919-54039850	-	-	-1.220	-1.629	-2.599
CHD8	chr10:25785914-25825625	-	-	-1.348	-1.041	-1.236
CHST1	chr15:76573747-76577430	-	-	-1.003	-1.129	-1.617
CKS2	chr8:90300716-90305611	-	-	-1.372	-1.980	-1.393
CMTM3	chr18:34471578-34475671	-	-	-1.035	-1.278	-1.682
CNOT3	chr18:63425205-63435541	-	-	-1.386	-2.362	-2.343
CREBBP	chr25:3050213-3169185	-	-	-1.079	-1.310	-1.625
DLGAP4	chr13:66204670-66292988	-	-	-1.174	-1.660	-1.622
DPF2	chr29:44205031-44217694	-	-	-1.311	-1.198	-1.483

ECM1	chr3:20228527-20233933	-	-	-1.521	-1.632	-2.857
EIF4ENIF1	chr17:72293385-72332007	-	-	-1.122	-1.061	-1.437
ELK3	chr5:60823239-60891359	-	-	-1.349	-1.865	-1.360
EMC4	chr10:28441592-28445103	-	-	-1.521	-1.638	-1.699
ENO1	chr16:45401694-45416462	-	-	-1.190	-1.136	-1.530
ENSBTAG00000002510	chr29:41730791-41739870	-	-	-1.516	-1.779	-1.793
ENSBTAG00000002950	chr17:49075826-49090245	-	-	-1.950	-1.300	-1.404
ENSBTAG00000012495	chr3:20727609-20731285	-	-	-1.112	-2.408	-1.613
ENSBTAG00000014583	chr18:54169312-54178928	-	-	-1.381	-1.712	-2.417
ENSBTAG00000019739	chr7:57828457-57829687	-	-	-1.634	-1.496	-1.713
ENSBTAG00000019983	chr11:73602729-73638589	-	-	-1.154	-1.406	-1.154
ENSBTAG00000020152	chr3:8395604-8407551	-	-	-1.654	-2.146	-1.716
ENSBTAG00000033543	chr8:25197703-25199286	-	-	-1.084	-1.160	-1.349
ENSBTAG00000046303	chr11:98509473-98513781	-	-	-1.109	-1.296	-1.263
ETV6	chr5:98412842-98468293	-	-	-1.472	-1.427	-1.672
FAM189B	chr3:15437675-15442475	-	-	-1.125	-1.273	-1.251
FBLN5	chr21:57153109-57246389	-	-	-1.049	-1.446	-1.308
FOSB	chr18:53501994-53508395	-	-	-1.401	-1.155	-1.218
FUS	chr25:27523968-27533988	-	-	-1.855	-3.234	-3.107
GPS1	chr19:51422925-51427197	-	-	-1.260	-1.120	-1.731
GSE1	chr18:11655285-11682581	-	-	-1.007	-1.322	-2.279
GTF2H5	chr9:96153559-96167611	-	-	-1.605	-1.616	-1.226
HNRNPA0	chr7:50814952-50815885	-	-	-1.253	-1.030	-2.036
ITGBL1	chr12:81980947-82108529	-	-	-1.408	-1.372	-1.344
ITM2B	chr12:18114552-18139506	-	-	-1.112	-1.542	-1.151
KIF26B	chr16:32381117-32471604	-	-	-1.143	-1.169	-1.543
KLF3	chr6:59593803-59610697	-	-	-1.806	-3.094	-2.752
KSR1	chr19:19548866-19618012	-	-	-1.318	-1.847	-1.391
LMAN2	chr7:40185728-40206355	-	-	-1.318	-1.218	-1.697

LRP4	chr15:77663791-77701236	-	-	-1.086	-1.054	-2.056
MAGEF1	chr1:83090389-83091984	-	-	-1.704	-1.111	-1.382
MAGI1	chr22:36005377-36134917	-	-	-1.003	-1.031	-1.323
MAPRE2	chr24:22193148-22306884	-	-	-1.137	-1.148	-1.109
MFGE8	chr21:20889912-20904968	-	-	-1.166	-1.150	-1.941
MICAL2	chr15:41003242-41107850	-	-	-1.040	-1.022	-1.147
MOB3B	chr8:16745166-16961930	-	-	-1.025	-1.237	-1.055
MYO9B	chr7:5804897-5913540	-	-	-1.235	-1.035	-2.057
NCOA2	chr14:35949384-36126601	-	-	-1.676	-1.437	-2.095
NCSTN	chr3:9453299-9468330	-	-	-1.131	-2.031	-2.183
NDUFAF4	chr9:53673440-53682097	-	-	-1.510	-2.157	-2.019
NR4A1	chr5:27977006-27992869	-	-	-1.202	-1.301	-1.414
NYNRIN	chr10:20590621-20600789	-	-	-1.262	-1.090	-1.310
PEG10	chr4:11912008-11921418	-	-	-1.342	-1.350	-2.142
PICK1	chr5:110346674-110363542	-	-	-1.485	-1.922	-1.883
PITPNA	chr19:23215814-23249410	-	-	-1.179	-1.649	-1.271
PLEKHG2	chr18:49379106-49389351	-	-	-1.411	-1.189	-1.363
PLXND1	chr22:56774466-56824220	-	-	-1.013	-1.220	-2.095
PPRC1	chr26:22677210-22691109	-	-	-1.154	-1.111	-1.515
PQBP1	chrX:92092354-92098095	-	-	-1.160	-1.826	-2.093
PRELP	chr16:1041922-1055957	-	-	-1.150	-1.927	-1.310
PRKACA	chr7:12693767-12711139	-	-	-1.352	-1.059	-1.037
PRR13	chr5:26730146-26733390	-	-	-1.047	-1.557	-1.175
PRR14	chr25:27034799-27038835	-	-	-1.211	-1.243	-1.549
PRRC2A	chr23:27475780-27488753	-	-	-1.032	-1.209	-1.822
PRRX1	chr16:39016044-39091099	-	-	-1.567	-1.399	-1.660
PSMC5	chr19:48728281-48732869	-	-	-2.114	-2.042	-2.475
PSMD11	chr19:18035609-18064853	-	-	-1.616	-1.943	-2.169
PTGDS	chr11:106247576-106250629	-	-	-1.204	-1.584	-2.053

RAB7A	chr22:59862213-59877343	-	-	-1.321	-1.099	-1.525
RBM18	chr11:93101472-93121906	-	-	-1.216	-1.381	-1.493
RFFL	chr19:15378252-15400325	-	-	-1.450	-1.360	-1.932
RPL28	chr18:62547219-62549950	-	-	-1.063	-2.150	-2.112
RUNX1T1	chr14:74642805-74787356	-	-	-1.369	-2.089	-1.613
S100A11	chr3:18768795-18770416	-	-	-1.554	-2.133	-1.557
SEC14L1	chr19:55328988-55376388	-	-	-1.064	-1.037	-1.096
SEMA5A	chr20:64147932-64352311	-	-	-1.076	-1.267	-1.287
SF3A1	chr17:71497414-71517122	-	-	-1.254	-1.798	-1.830
SIN3B	chr7:6104505-6147010	-	-	-1.039	-1.031	-1.497
SLC38A7	chr18:26514590-26525996	-	-	-1.103	-1.292	-1.746
SNAPC3	chr8:28889218-28924567	-	-	-1.073	-1.320	-1.341
SNX15	chr29:43905795-43917298	-	-	-1.170	-1.645	-2.028
ST5	chr15:44335341-44460360	-	-	-1.417	-1.422	-2.157
STIM1	chr15:51845121-52049569	-	-	-1.427	-1.297	-2.052
SUPT5H	chr18:49403803-49430177	-	-	-1.080	-1.462	-1.838
SYNPO2	chr6:7388727-7590933	-	-	-1.257	-1.390	-1.679
TACC2	chr26:42323742-42485654	-	-	-1.482	-1.158	-1.985
TAF15	chr19:14858563-14890086	-	-	-2.143	-1.906	-1.624
TCF7	chr7:47352222-47385009	-	-	-1.170	-1.860	-1.100
TCHP	chr17:65602268-65616737	-	-	-1.237	-1.167	-1.154
TJP1	chr21:28934157-28992880	-	-	-1.341	-1.193	-1.385
TKT	chr22:48264510-48288061	-	-	-1.075	-1.126	-1.638
TOB2	chr5:113060939-113070989	-	-	-1.063	-1.257	-1.385
TSHZ1	chr24:3674812-3678046	-	-	-1.013	-1.701	-2.601
UBAP2L	chr3:16318127-16358192	-	-	-1.090	-1.240	-1.044
UBASH3B	chr15:33944542-33975910	-	-	-1.416	-1.923	-1.847
UBE2D4	chr22:322995-343683	-	-	-1.167	-1.911	-1.168
WASF2	chr2:126399311-126469335	-	-	-1.220	-1.222	-1.371

WBP2	chr19:56394187-56401350	-	-	-1.067	-2.860	-2.056
ZC3H4	chr18:54552425-54588113	-	-	-1.192	-1.164	-2.028
ZEB1	chr13:34063174-34261299	-	-	-1.381	-1.429	-1.282
ZHX2	chr14:18386656-18389173	-	-	-1.566	-1.390	-1.999
ZNF689	chr25:27014539-27018793	-	-	-1.174	-1.215	-1.523
ENSBTAG00000037558	chr6:90822747-90824841	5.972	3.920	4.530	3.860	-
IL-8	chr6:90559881-90563647	7.068	3.378	6.297	5.320	-
MAFF	chr5:110475769-110484826	1.960	1.263	1.339	1.023	-
RGS16	chr16:65128480-65134057	1.294	2.387	1.021	1.269	-
ZC3H12A	chr3:108990073-108999453	1.969	1.209	1.271	1.121	-
ENSBTAG00000023659	chr18:24125365-24126333	2.098	1.875	1.722	-	1.132
FGF18	chr20:3132654-3195021	-1.646	-1.482	-1.661	-	-2.688
BIRC3	chr15:6639727-6654015	2.963	-	2.031	1.888	2.147
CASP4	chr15:3474705-3494168	2.331	-	1.697	1.149	1.917
CASP7	chr26:34457099-34464840	1.946	-	1.036	1.075	1.342
CASP8	chr2:90278154-90301820	1.734	-	1.339	1.030	1.640
CCRL2	chr22:53567796-53569696	2.870	-	1.671	1.989	1.463
ENSBTAG00000001143	chr3:55063829-55075636	2.613	-	1.801	1.554	1.816
GCH1	chr10:67576389-67631089	2.035	-	1.326	1.240	1.490
IRF1	chr7:23235652-23243697	2.144	-	1.443	1.359	1.242
MAP3K8	chr13:35600312-35626614	1.747	-	1.197	1.181	1.085
PLA2G4A	chr16:69443237-69620712	2.282	-	1.273	1.007	1.519
CCL2	chr19:16232967-16234839	6.651	4.772	5.839	5.081	5.091
CDA	chr2:132636461-132657392	4.294	3.281	4.351	2.861	3.810
ENSBTAG00000006523	chr9:97399158-97404522	4.124	3.275	3.073	2.181	2.357
ENSBTAG00000009812	chr6:90645963-90648076	4.727	2.262	3.805	3.089	3.534
ENSBTAG00000027513	chr6:90695493-90697557	7.702	5.766	6.204	5.631	5.019
ENSBTAG00000037778	chr6:90811061-90813079	4.897	2.767	3.351	2.948	2.640
ENSBTAG00000046158	chr23:27225269-27231292	4.763	2.876	3.892	3.275	2.969

IL6	chr4:31578310-31582667	5.726	2.774	4.653	3.892	3.779
Mail	chr1:46543384-46554479	2.439	1.933	1.432	1.037	1.173
TNFSF15	chr8:105725136-105745282	2.745	1.863	2.070	1.812	1.369

Appendix B: (3) Ingenuity Pathway Analysis

Table B.4 Differentially expressed mRNA transcripts mapping to multiple Ensembl stable bovine gene identifiers. *Identifiers furthest to the 5' end consistently mapped to the near-complete or complete mRNA transcript and were subsequently used for IPA. Transcripts with significant differential expression (log2 fold change ≤ -1 or ≥ 1) in bovine foot skin fibroblasts are highlighted in bold and the corresponding co-incubation treatment groups are colour-coded for upregulation (green) or downregulation (red).*

Transcript identifier	Ensembl stable bovine gene identifiers of mapped genes	Ensembl stable bovine gene identifier mapped furthest to the 5' end	Chromosome and locus	Co-incubation treatment in which differential expression identified
XLOC_001707	ENSBTAG00000045492, ENSBTAG00000046668, *RNASE4*	ENSBTAG00000019612	chr10:26423873-26445634	LPS, T19, T320A, T3552B, Ru1
XLOC_002883	ENSBTAG00000015007, ENSBTAG00000047575	ENSBTAG00000047575	chr11:74496691-74590933	LPS, T19, T320A, T3552B, Ru1
XLOC_003689	ENSBTAG00000045555, ENSBTAG00000046276	ENSBTAG00000046276	chr13:50362600-50400983	LPS, T19, T320A, T3552B, Ru1
XLOC_003690	ENSBTAG00000046776, ENSBTAG00000047962	ENSBTAG00000046776	chr13:50362600-50400983	LPS, T19, T320A, T3552B, Ru1
XLOC_003693	ENSBTAG00000046631, ENSBTAG00000046716, ENSBTAG00000047102, ENSBTAG00000048089	ENSBTAG00000048089	chr13:50362600-50400983	LPS, T19, T320A, T3552B, Ru1
XLOC_004183	ENSBTAG00000017475, ENSBTAG00000047223	ENSBTAG00000017475	chr13:58010286-58049012	LPS, T19, T320A, T3552B, Ru1
XLOC_004246	*CPNE1, RBM12*	ENSBTAG00000006955	chr13:65507239-65543175	LPS, T19, T320A, T3552B, Ru1
XLOC_004373	*C8orf82, LRRC24*	ENSBTAG00000046031	chr14:1602473-1609477	LPS, T19, T320A, T3552B, Ru1
XLOC_005491	ENSBTAG00000039307, ENSBTAG00000047406	ENSBTAG00000047406	chr15:6748307-6884549	LPS, T19, T320A, T3552B, Ru1
XLOC_006525	ENSBTAG00000039728, *TMEM88B*	ENSBTAG00000039728	chr16:52240500-52373541	LPS, T19, T320A, T3552B, Ru1
XLOC_006601	ENSBTAG00000037813, *TOR1AIP2*	ENSBTAG00000035230	chr16:62493957-62528817	LPS, T19, T320A, T3552B, Ru1
XLOC_006869	ENSBTAG00000010958, ENSBTAG00000046730	ENSBTAG00000010958	chr17:64230115-64279571	LPS, T19, T320A, T3552B, Ru1

XLOC_007204	**ENSBTAG00000039861, *OAS2***	**ENSBTAG00000014628**	**chr17:63611773-63646117**	**LPS, T19, T320A, T3552B, Ru1**
XLOC_007360	*MON1B, SYCE1L*	ENSBTAG00000015694	chr18:4445955-4468213	LPS, T19, T320A, T3552B, Ru1
XLOC_007520	*CTCF,* ENSBTAG00000008860	ENSBTAG00000008860	chr18:35242380-35333286	LPS, T19, T320A, T3552B, Ru1
XLOC_007741	ENSBTAG00000047345, *NECTIN2*	ENSBTAG00000015318	chr18:52984271-53016520	LPS, T19, T320A, T3552B, Ru1
XLOC_008723	*DPH1, OVCA2*	ENSBTAG00000009376	chr19:23636130-23646338	LPS, T19, T320A, T3552B, Ru1
XLOC_008339	*CEACAM20, ZNF180*	ENSBTAG00000006805	chr18:52638276-52675994	T19
XLOC_010971	*AK6, TAF9*	ENSBTAG00000046192	chr20:10300552-10314075	LPS, T19, T320A, T3552B, Ru1
XLOC_011180	ENSBTAG00000047828, *TRAPPC13*	ENSBTAG00000016900	chr20:13856107-13891297	LPS, T19, T320A, T3552B, Ru1
XLOC_014095	ENSBTAG00000038577, *TSC22D4*	ENSBTAG00000038577	chr25:36614549-36623993	LPS, T19, T320A, T3552B, Ru1
XLOC_014368	ENSBTAG00000010904, ENSBTAG00000046752	ENSBTAG00000010904	chr25:26681933-26689460	LPS
XLOC_015151	ENSBTAG00000016486, ENSBTAG00000047857	ENSBTAG00000016486	chr27:14906505-15022818	LPS, T19, T320A, T3552B, Ru1
XLOC_016145	*BSCL2, LRRN4CL*	ENSBTAG00000010484	chr29:41710700-41724967	LPS, T19, T320A, T3552B, Ru1
XLOC_016789	*LRP8, MAGOH*	ENSBTAG00000000736	chr3:93488722-93580869	LPS, T19, T320A, T3552B, Ru1
XLOC_018299	ENSBTAG00000018909, ENSBTAG00000046308	ENSBTAG00000018909	chr4:67767892-68200912	LPS, T19, T320A, T3552B, Ru1
XLOC_022651	*ALDOB, TMEM246*	ENSBTAG00000015358	chr8:92773691-92865307	LPS, T19, T320A, T3552B, Ru1
XLOC_023775	*ASB12, MTMR8*	ENSBTAG00000035705	chrX:101228032-101492856	LPS, T19, T320A, T3552B, Ru1

Table B.5 Differentially expressed genes of bovine foot skin fibroblasts with more than one orthologous human gene. *Bovine gene identifiers, their equivalent Ensembl stable bovine gene identifiers (where not given) and their corresponding human ortholog, as identified by reciprocal BLAST where possible, using Ensembl Biomart. The co-incubation treatments for which these differentially expressed genes were identified are given, with significant expression highlighted in bold and upregulation (green) or downregulation (red) highlighted as appropriate. -, reciprocal BLAST did not confirm a single orthologous human gene.*

Bovine gene identifier	Ensembl stable bovine gene identifier	Ensembl stable human gene identifier	Co-incubation treatment in which differential expression identified
ENSBTAG00000018278	**ENSBTAG00000018278**	**-**	**LPS, T19, T320A, T3552B, Ru1**
ENSBTAG00000006724	ENSBTAG00000006724	-	LPS, T19, T320A, T3552B, Ru1
PARL	**ENSBTAG00000014460**	**ENSG00000175193**	**LPS, T19, T320A, T3552B, Ru1**
ENSBTAG00000031572	**ENSBTAG00000031572**	**-**	**LPS, T19, T320A, T3552B, Ru1**
ENSBTAG00000022227	**ENSBTAG00000022227**	**ENSG00000188313**	**LPS, T19, T320A, T3552B, Ru1**
TRAPPC10	ENSBTAG00000007100	-	LPS, T19, T320A, T3552B, Ru1
ENSBTAG00000007105	ENSBTAG00000007105	ENSG00000241945	LPS, T19, T320A, T3552B, Ru1
ENSBTAG00000007106	ENSBTAG00000007106	-	LPS, T19, T320A, T3552B, Ru1
SMIM11A	ENSBTAG00000011528	-	LPS, T19, T320A, T3552B, Ru1
ENSBTAG00000019404	ENSBTAG00000019404	-	LPS, T19, T320A, T3552B, Ru1
ENSBTAG00000032684	ENSBTAG00000032684	-	LPS, T19, T320A, T3552B, Ru1
SNORA4	ENSBTAG00000042702	ENSG00000263776	LPS, T19, T320A, T3552B, Ru1
ENSBTAG00000003151	**ENSBTAG00000003151**	**-**	**LPS, T19, T320A, T3552B, Ru1**
SNORA63	ENSBTAG00000047590	ENSG00000201229	LPS
ZNF560	ENSBTAG00000025146	-	LPS, T19, T320A, T3552B, Ru1
ENSBTAG00000000160	ENSBTAG00000000160	-	LPS, T19, T320A, T3552B, Ru1
ENSBTAG00000014880	ENSBTAG00000014880	-	LPS, T19, T320A, T3552B, Ru1
ENSBTAG00000011437	ENSBTAG00000011437	ENSG00000142178	LPS, T19, T320A, T3552B, Ru1
ENSBTAG00000023186	ENSBTAG00000023186	-	LPS, T19, T320A, T3552B, Ru1
ENSBTAG00000002712	ENSBTAG00000002712	-	LPS, T19, T320A, T3552B, Ru1
ENSBTAG00000002709	ENSBTAG00000002709	ENSG00000100926	LPS, T19, T320A, T3552B, Ru1

ENSBTAG00000012723	ENSBTAG00000012723	-	LPS, T19, T320A, T3552B, Ru1
ENSBTAG00000011396	**ENSBTAG00000011396**	**ENSG00000092199**	**LPS, T19, T320A, T3552B, Ru1**
ENSBTAG00000019076	ENSBTAG00000019076	ENSG00000137843	LPS, T19, T320A, T3552B, Ru1
ENSBTAG00000039462	**ENSBTAG00000039462**	**-**	**LPS, T19, T320A, T3552B, Ru1**
DCAF4	ENSBTAG00000008713	-	LPS, T19, T320A, T3552B, Ru1
ENSBTAG00000046814	ENSBTAG00000046814	-	LPS, T19, T320A, T3552B, Ru1
ENSBTAG00000003747	**ENSBTAG00000003747**	**ENSG00000140043**	**LPS, T19, T320A, T3552B, Ru1**
ENSBTAG00000012803	**ENSBTAG00000012803**	**ENSG00000153037**	**LPS, T19, T320A, T3552B, Ru1**
ENSBTAG00000012365	ENSBTAG00000012365	ENSG00000140350	LPS, T19, T320A, T3552B, Ru1
ENSBTAG00000012981	ENSBTAG00000012981	-	LPS, T19, T320A, T3552B, Ru1
ENSBTAG00000005815	ENSBTAG00000005815	ENSG00000092098	LPS, T19, T320A, T3552B, Ru1
ENSBTAG00000017665	ENSBTAG00000017665	-	LPS, T19, T320A, T3552B, Ru1
ENSBTAG00000025664	ENSBTAG00000025664	ENSG00000169397	LPS, T19, T320A, T3352B, Ru1
ENSBTAG00000010365	ENSBTAG00000010365	ENSG00000137767	LPS, T19, T320A, T3552B, Ru1
ENSBTAG00000039950	ENSBTAG00000039950	-	LPS, T19, T320A, T3552B, Ru1
Metazoa_SRP	ENSBTAG00000048139	-	LPS, T19, T320A, T3552B, Ru1
ENSBTAG00000011553	ENSBTAG00000011553	-	LPS, T19, T320A, T3552B, Ru1
ENSBTAG00000038949	**ENSBTAG00000038949**	**-**	**LPS, T19, T320A, T3552B, Ru1**
ENSBTAG00000002105	ENSBTAG00000002105	ENSG00000144043	LPS, T19, T320A, T3552B, Ru1
ENSBTAG00000004168	ENSBTAG00000004168	ENSG00000243244	LPS, T19, T320A, T3552B, Ru1
ENSBTAG00000013589	**ENSBTAG00000013589**	**ENSG00000115561**	**LPS, T19, T320A, T3552B, Ru1**
ENSBTAG00000017330	**ENSBTAG00000017330**	**-**	**LPS, T19, T320A, T3552B, Ru1**
SET	**ENSBTAG00000020959**	**-**	**LPS, T19, T320A, T3552B, Ru1**
ENSBTAG00000019018	ENSBTAG00000019018	ENSG00000142089	LPS, T19, T320A, T3552B, Ru1
ENSBTAG00000001840	**ENSBTAG00000001840**	**ENSG00000115274**	**LPS, T19, T320A, T3552B, Ru1**
ENSBTAG00000002943	ENSBTAG00000002943	-	LPS, T19, T320A, T3552B, Ru1
ENSBTAG00000019458	ENSBTAG00000019458	-	LPS, T19, T320A, T3552B, Ru1
RANBP2	ENSBTAG00000000152	ENSG00000153201	LPS, T19, T320A, T3552B, Ru1
ENSBTAG00000010971	**ENSBTAG00000010971**	**ENSG00000256977**	**LPS, T19, T320A, T3552B, Ru1**

ENSBTAG00000031731	**ENSBTAG00000031731**	**-**	**LPS, T19, T320A, T3552B, Ru1**
GOLGA2	ENSBTAG00000011317	-	LPS, T19, T320A, T3552B, Ru1
SNORA17	ENSBTAG00000042930	-	LPS, T19, T320A, T3552B, Ru1
SNORA17	ENSBTAG00000042482	ENSG00000281808	LPS, T19, T320A, T3552B, Ru1
PTGDS	**ENSBTAG00000015074**	**ENSG00000284341**	**LPS, T19, T320A, T3552B, Ru1**
IFITM1	ENSBTAG00000019017	-	LPS, T19, T320A, T3552B, Ru1
ENSBTAG00000016691	ENSBTAG00000016691	ENSG00000179630	LPS, T19, T320A, T3552B, Ru1
ENSBTAG00000018846	ENSBTAG00000018846	-	LPS, T19, T320A, T3552B, Ru1
ENSBTAG00000014043	ENSBTAG00000014043	-	LPS, T19, T320A, T3552B, Ru1
ENSBTAG00000019645	ENSBTAG00000019645	ENSG00000198176	LPS, T19, T320A, T3552B, Ru1
ENSBTAG00000015584	**ENSBTAG00000015584**	**ENSG00000168283**	**LPS, T19, T320A, T3552B, Ru1**
ENSBTAG00000017244	**ENSBTAG00000017244**	**-**	**LPS, T19, T320A, T3552B, Ru1**
ENSBTAG00000039520	ENSBTAG00000039520	-	LPS, T19, T320A, T3552B, Ru1
ENSBTAG00000021096	ENSBTAG00000021096	-	LPS, T19, T320A, T3552B, Ru1
ENSBTAG00000039208	ENSBTAG00000039208	-	LPS, T19, T320A, T3552B, Ru1
ENSBTAG00000008303	ENSBTAG00000008303	ENSG00000088832	LPS, T19, T320A, T3552B, Ru1
CSNK2A1	ENSBTAG00000012341	-	LPS, T19, T320A, T3552B, Ru1
ENSBTAG00000000598	ENSBTAG00000000598	ENSG00000101439	LPS, T19, T320A, T3552B, Ru1
ENSBTAG00000007213	ENSBTAG00000007213	ENSG00000198053	LPS, T19, T320A, T3552B, Ru1
ENSBTAG00000047150	ENSBTAG00000047150	-	LPS, T19, T320A, T3552B, Ru1
ENSBTAG00000011263	**ENSBTAG00000011263**	**ENSG00000242372**	**LPS, T19, T320A, T3552B, Ru1**
NFS1	ENSBTAG00000006962	ENSG00000244005	LPS, T19, T320A, T3552B, Ru1
ENSBTAG00000000856	ENSBTAG00000000856	ENSG00000182325	LPS, T19, T320A, T3552B, Ru1
ENSBTAG00000015319	ENSBTAG00000015319	ENSG00000189376	LPS, T19, T320A, T3552B, Ru1
ENSBTAG00000013284	**ENSBTAG00000013284**	**-**	**LPS, T19, T320A, T3552B, Ru1**
ENSBTAG00000000632	ENSBTAG00000000632	-	LPS, T19, T320A, T3552B, Ru1
ENSBTAG00000000857	**ENSBTAG00000000857**	**ENSG00000185803**	**LPS, T19, T320A, T3552B, Ru1**
ENSBTAG00000010813	**ENSBTAG00000010813**	**ENSG00000177144**	**LPS, T19, T320A, T3552B, Ru1**
UBE2W	**ENSBTAG00000008260**	**ENSG00000104343**	**LPS, T19, T320A, T3552B, Ru1**

ENSBTAG00000032812	ENSBTAG00000032812	-	LPS, T19, T320A, T3552B, Ru1
SNORA14	ENSBTAG00000042492	ENSG00000207181	LPS, T19, Ru1
CASP4	**ENSBTAG00000020884**	**ENSG00000196954**	**LPS, T19, T320A, T3552B, Ru1**
ENSBTAG00000016266	ENSBTAG00000016266	-	LPS, T19, T320A, T3552B, Ru1
RBM7	**ENSBTAG00000008219**	**ENSG00000255663**	**LPS, T19, T320A, T3552B, Ru1**
ENSBTAG00000007332	ENSBTAG00000007332	ENSG00000167283	LPS, T19, T320A, T3552B, Ru1
ENSBTAG00000006564	**ENSBTAG00000006564**	**-**	**LPS, T19, T320A, T3552B, Ru1**
ENSBTAG00000024657	ENSBTAG00000024657	ENSG00000186660	LPS, T19, T320A, T3552B, Ru1
ENSBTAG00000020279	ENSBTAG00000020279	ENSG00000086848	LPS, T19, T320A, T3552B, Ru1
TIMM10B	ENSBTAG00000003567	ENSG00000132286	LPS, T19, T320A, T3552B, Ru1
ENSBTAG00000037465	ENSBTAG00000037465	-	LPS, T19, T320A, T3552B, Ru1
ENSBTAG00000000025	ENSBTAG00000000025	ENSG00000175582	LPS, T19, T320A, T3552B, Ru1
ENSBTAG00000017352	ENSBTAG00000017352	-	LPS, T19, T320A, T3552B, Ru1
SRGAP2	ENSBTAG00000001483	-	LPS, T19, T320A, T3552B, Ru1
ENSBTAG00000031749	ENSBTAG00000031749	-	LPS, T19, T320A, T3552B, Ru1
ENSBTAG00000010737	ENSBTAG00000010737	-	LPS, T19, T320A, T3552B, Ru1
ENSBTAG00000020227	**ENSBTAG00000020227**	**ENSG00000196550**	**LPS, T19, T320A, T3552B, Ru1**
ENSBTAG00000005835	ENSBTAG00000005835	ENSG00000143811	LPS, T19, T320A, T3552B, Ru1
ENSBTAG00000002219	ENSBTAG00000002219	-	LPS, T19, T320A, T3552B, Ru1
U2	ENSBTAG00000033994	-	LPS, T19, T320A, T3552B, Ru1
ULBP3	ENSBTAG00000026437	-	LPS, T19, T320A, T3552B, Ru1
ENSBTAG00000004203	ENSBTAG00000004203	-	LPS, T19, T320A, T3552B, Ru1
ENSBTAG00000012791	ENSBTAG00000012791	-	LPS, T19, T320A, T3552B, Ru1
DDT	ENSBTAG00000022027	ENSG00000099974	LPS, T19, T320A, T3552B, Ru1
ENSBTAG00000047299	ENSBTAG00000047299	ENSG00000128185	LPS, T19, T320A, T3552B, Ru1
ENSBTAG00000034089	**ENSBTAG00000034089**	**-**	**LPS, T19, T320A, T3552B, Ru1**
PSMD9	ENSBTAG00000004179	-	LPS, T19, T320A, T3552B, Ru1
ENSBTAG00000008743	ENSBTAG00000008743	-	LPS, T19, T320A, T3552B, Ru1
ENSBTAG00000018086	ENSBTAG00000018086	ENSG00000099992	LPS, T19, T320A, T3552B, Ru1

UBE2L3	ENSBTAG00000013038	ENSG00000185651	LPS, T19, T320A, T3552B, Ru1
ENSBTAG00000014646	ENSBTAG00000014646	ENSG00000152082	LPS, T19, T320A, T3552B, Ru1
ENSBTAG00000047676	ENSBTAG00000047676	-	LPS, T19, T320A, T3552B, Ru1
ENSBTAG00000004248	ENSBTAG00000004248	ENSG00000103150	LPS, T19, T320A, T3552B, Ru1
ENSBTAG00000011632	ENSBTAG00000011632	ENSG00000140941	LPS, T19, T320A, T3552B, Ru1
ENSBTAG00000023632	ENSBTAG00000023632	ENSG00000135722	LPS, T19, T320A, T3552B, Ru1
ENSBTAG00000001659	ENSBTAG00000001659	ENSG00000132612	LPS, T19, T320A, T3552B, Ru1
ENSBTAG00000002571	ENSBTAG00000002571	-	LPS, T19, T320A, T3552B, Ru1
ENSBTAG00000009889	**ENSBTAG00000009889**	**ENSG00000197841**	**LPS, T19, T320A, T3552B, Ru1**
ENSBTAG00000018593	ENSBTAG00000018593	-	LPS, T19, T320A, T3552B, Ru1
ENSBTAG00000009078	ENSBTAG00000009078	-	LPS, T19, T320A, T3552B, Ru1
ENSBTAG00000009079	ENSBTAG00000009079	ENSG00000167578	LPS, T19, T320A, T3552B, Ru1
BCKDHA	ENSBTAG00000016037	ENSG00000248098	LPS, T19, T320A, T3552B, Ru1
ENSBTAG00000020756	**ENSBTAG00000020756**	**ENSG00000105723**	**LPS, T19, T320A, T3552B, Ru1**
ENSBTAG00000007070	ENSBTAG00000007070	ENSG00000189114	LPS, T19, T320A, T3552B, Ru1
CYTH2	ENSBTAG00000001498	ENSG00000105443	LPS, T19, T320A, T3552B, Ru1
ZNF665	**ENSBTAG00000017651**	**-**	**LPS, T19, T320A, T3552B, Ru1**
ENSBTAG00000011926	**ENSBTAG00000011926**	**-**	**LPS, T19, T320A, T3552B, Ru1**
ENSBTAG00000038926	ENSBTAG00000038926	ENSG00000204524	LPS, T19, T320A, T3552B, Ru1
ENSBTAG00000017613	ENSBTAG00000017613	ENSG00000152439	LPS, T19, T320A, T3552B, Ru1
ENSBTAG00000039946	ENSBTAG00000039946	-	LPS, T19, T320A, T3552B, Ru1
ENSBTAG00000039453	ENSBTAG00000039453	ENSG00000083812	LPS, T19, T320A, T3552B, Ru1
ENSBTAG00000040000	ENSBTAG00000040000	ENSG00000183196	LPS, T19, T320A, T3553B, Ru1
ENSBTAG00000015432	**ENSBTAG00000015432**	**-**	**LPS, T19, T320A, T3552B, Ru1**
ENSBTAG00000006795	ENSBTAG00000006795	ENSG00000140905	LPS, T19, T320A, T3552B, Ru1
ENSBTAG00000018040	ENSBTAG00000018040	-	LPS, T19, T320A, T3552B, Ru1
ENSBTAG00000001665	ENSBTAG00000001665	-	LPS, T19, T320A, T3552B, Ru1
ENSBTAG00000023610	ENSBTAG00000023610	ENSG00000161265	LPS, T19, T320A, T3552B, Ru1
ENSBTAG00000001780	ENSBTAG00000001780	ENSG00000104835	LPS, T19, T320A, T3552B, Ru1

ENSBTAG00000015644	ENSBTAG00000015644	ENSG00000176396	LPS, T19, T320A, T3552B, Ru1
ZNF112	**ENSBTAG00000040209**	**ENSG00000062370**	**LPS, T19, T320A, T3552B, Ru1**
ENSBTAG00000038735	**ENSBTAG00000038735**	**ENSG00000104826**	**LPS, T19, T320A, T3552B, Ru1**
SIGLEC10	ENSBTAG00000008852	-	LPS, T19, T320A, T3552B, Ru1
ZNF548	ENSBTAG00000011262	ENSG00000188785	LPS, T19, T320A, T3552B, Ru1
ENSBTAG00000019437	**ENSBTAG00000019437**	**ENSG00000154760**	**LPS, T19, T320A, T3552B, Ru1**
ENSBTAG00000009354	ENSBTAG00000009354	-	LPS, T19, T320A, T3552B, Ru1
ENSBTAG00000023970	ENSBTAG00000023970	-	LPS, T19, T320A, T3552B, Ru1
ENSBTAG00000021931	**ENSBTAG00000021931**	**ENSG00000258315**	**LPS, T19, T320A, T3552B, Ru1**
ENSBTAG00000000131	ENSBTAG00000000131	-	LPS, T19, T320A, T3552B, Ru1
ENSBTAG00000000943	ENSBTAG00000000943	-	LPS, T19, T320A, T3552B, Ru1
ENSBTAG00000008010	ENSBTAG00000008010	ENSG00000154803	LPS, T19, T320A, T3552B, Ru1
U2	**ENSBTAG00000045973**	**-**	**LPS, T19, T320A, T3552B, Ru1**
U2	ENSBTAG00000045620	-	LPS, T19, T3552B, Ru1
ENSBTAG00000013529	ENSBTAG00000013529	-	LPS, T19, T320A, T3552B, Ru1
ENSBTAG00000009987	ENSBTAG00000009987	ENSG00000259207	LPS, T19, T320A, T3552B, Ru1
ENSBTAG00000009458	ENSBTAG00000009458	-	LPS, T19, T320A, T3552B, Ru1
SUMO2	**ENSBTAG00000030169**	**-**	**LPS, T19, T320A, T3552B, Ru1**
ENSBTAG00000033298	ENSBTAG00000033298	ENSG00000266202	LPS, T19, T320A, T3552B, Ru1
SPAG5	ENSBTAG00000013100	ENSG00000076382	LPS, T19, T320A, T3552B, Ru1
ENSBTAG00000000829	ENSBTAG00000000829	ENSG00000262304	LPS, T19, T320A, T3552B, Ru1
ENSBTAG00000015258	ENSBTAG00000015258	-	LPS, T19, T320A, T3552B, Ru1
ENSBTAG00000031752	ENSBTAG00000031752	ENSG00000205544	LPS, T19, T320A, T3552B, Ru1
ENSBTAG00000002605	ENSBTAG00000002605	-	LPS, T19, T320A, T3552B, Ru1
ENSBTAG00000006982	ENSBTAG00000006982	ENSG00000108774	LPS, T19, T320A, T3552B, Ru1
PTGES3L-AARSD1	ENSBTAG00000015136	-	LPS, T19, T320A, T3552B, Ru1
U2	**ENSBTAG00000047023**	**-**	**LPS, T19, T320A, T3552B, Ru1**
U2	**ENSBTAG00000048293**	**ENSG00000274585**	**LPS, T19, T320A, T3552B, Ru1**
U2	ENSBTAG00000045916	-	LPS, T19, T320A, T3552B, Ru1

U2	**ENSBTAG00000030306**	**ENSG00000274585**	**LPS, T19, T320A, T3552B, Ru1**
U2	**ENSBTAG00000048183**	**-**	**LPS, T19, T320A, T3552B, Ru1**
U2	**ENSBTAG00000046183**	**-**	**LPS, T19, T320A, T3552B, Ru1**
U2	**ENSBTAG00000039550**	**-**	**LPS, T19, T320A, T3552B, Ru1**
U2	**ENSBTAG00000040600**	**-**	**LPS, T19, T320A, T3552B, Ru1**
ENSBTAG00000015958	ENSBTAG00000015958	ENSG00000262633	LPS, T19, T320A, T3552B, Ru1
ENSBTAG00000000417	ENSBTAG00000000417	-	LPS, T19, T320A, T3552B, Ru1
METTL23	ENSBTAG00000044138	ENSG00000181038	LPS, T19, T320A, T3552B, Ru1
TEN1	ENSBTAG00000044038	-	LPS, T19, T320A, T3552B, Ru1
ENSBTAG00000027694	**ENSBTAG00000027694**	**ENSG00000196659**	**LPS, T19, T320A, T3552B, Ru1**
ENSBTAG00000012289	ENSBTAG00000012289	ENSG00000053371	LPS, T19, T320A, T3552B, Ru1
ENSBTAG00000030340	ENSBTAG00000030340	ENSG00000169991	LPS, T19, T320A, T3552B, Ru1
ENSBTAG00000033523	ENSBTAG00000033523	-	LPS, T19, T320A, T3552B, Ru1
ENSBTAG00000047806	ENSBTAG00000047806	ENSG00000197713	LPS, T19, T320A, T3552B, Ru1
SNORA73	**ENSBTAG00000046050**	**ENSG00000200087**	**LPS, T19, T320A, T3552B, Ru1**
SNORA73	**ENSBTAG00000046681**	**-**	**LPS, T19, T320A, T3552B, Ru1**
SNORA73	**ENSBTAG00000045668**	**-**	**LPS, T19, T320A, T3552B, Ru1**
TCEB3	ENSBTAG00000026585	ENSG00000011007	LPS, T19, T320A, T3352B, Ru1
ENSBTAG00000013085	ENSBTAG00000013085	-	LPS, T19, T320A, T3552B, Ru1
ENSBTAG00000005140	ENSBTAG00000005140	-	LPS, T19, T320A, T3552B, Ru1
ENSBTAG00000026758	ENSBTAG00000026758	ENSG00000162482	LPS, T19, T320A, T3552B, Ru1
CALM2	**ENSBTAG00000032705**	**-**	**LPS, T19, T320A, T3552B, Ru1**
ENSBTAG00000034360	ENSBTAG00000034360	ENSG00000172058	LPS, T19, T320A, T3552B, Ru1
COX8A	ENSBTAG00000004920	-	LPS, T19, T320A, T3552B, Ru1
ENSBTAG00000017071	**ENSBTAG00000017071**	**ENSG00000082196**	**LPS, T19, T320A, T3552B, Ru1**
ENSBTAG00000034598	ENSBTAG00000034598	ENSG00000145919	LPS, T19, T320A, T3552B, Ru1
GTF2H2	**ENSBTAG00000027983**	**-**	**LPS, T19, T320A, T3552B, Ru1**
ENSBTAG00000009682	**ENSBTAG00000009682**	**-**	**LPS, T19, T320A, T3552B, Ru1**
ENSBTAG00000018708	ENSBTAG00000018708	ENSG00000253797	LPS, T320A, T3552B, Ru1

UBR7	ENSBTAG00000004310	ENSG00000012963	LPS, T19, T320A, T3552B, Ru1
ENSBTAG00000031834	ENSBTAG00000031834	-	LPS, T19, T320A, T3552B, Ru1
ENSBTAG00000004272	ENSBTAG00000004272	-	LPS, T19, T320A, T3552B, Ru1
ENSBTAG00000003152	ENSBTAG00000003152	-	LPS, T19, T320A, T3552B, Ru1
YY1	ENSBTAG00000020819	-	LPS, T19, T320A, T3552B, Ru1
WDR20	ENSBTAG00000007007	ENSG00000140153	LPS, T19, T320A, T3552B, Ru1
ENSBTAG00000027059	ENSBTAG00000027059	-	LPS, T19, T320A, T3552B, Ru1
CPEB1	**ENSBTAG00000000623**	**ENSG00000214575**	**LPS, T19, T320A, T3552B, Ru1**
ENSBTAG00000020023	**ENSBTAG00000020023**	**ENSG00000136371**	**LPS, T19, T320A, T3552B, Ru1**
ENSBTAG00000038020	ENSBTAG00000038020	ENSG00000129480	LPS, T19, T320A, T3552B, Ru1
ATXN3	ENSBTAG00000005786	ENSG00000066427	LPS, T19, T320A, T3552B, Ru1
ENSBTAG00000003155	ENSBTAG00000003155	-	LPS, T19, T320A, T3552B, Ru1
ENSBTAG00000047229	**ENSBTAG00000047229**	**ENSG00000213145**	**LPS, T19, T320A, T3552B, Ru1**
ENSBTAG00000032954	ENSBTAG00000032954	ENSG00000180389	LPS, T19, T320A, T3552B, Ru1
ENSBTAG00000011344	ENSBTAG00000011344	-	LPS, T19, T320A, T3552B, Ru1
SNORA7	ENSBTAG00000042863	ENSG00000207088	LPS
ENSBTAG00000038640	**ENSBTAG00000038640**	**-**	**LPS, T19, T320A, T3552B, Ru1**
ENSBTAG00000019479	ENSBTAG00000019479	ENSG00000157014	LPS, T19, T320A, T3552B, Ru1
ENSBTAG00000007966	ENSBTAG00000007966	ENSG00000214021	LPS, T19, T320A, T3552B, Ru1
ENSBTAG00000032304	ENSBTAG00000032304	ENSG00000114786	LPS, T19, T320A, T3552B, Ru1
ENSBTAG00000019163	ENSBTAG00000019163	ENSG00000114395	LPS, T19, T320A, T3552B, Ru1
ENSBTAG00000000387	ENSBTAG00000000387	-	LPS, T19, T320A, T3552B, Ru1
ENSBTAG00000030915	ENSBTAG00000030915	-	LPS, T19, T320A, T3552B, Ru1
ENSBTAG00000038916	ENSBTAG00000038916	ENSG00000124593	LPS, T19, T320A, T3552B, Ru1
ENSBTAG00000038619	ENSBTAG00000038619	-	LPS, T19, T320A, T3552B, Ru1
ENSBTAG00000024176	ENSBTAG00000024176	-	LPS, T19, T320A, T3552B, Ru1
H2BFS	ENSBTAG00000038173	-	LPS, T19, T320A, T3552B, Ru1
ENSBTAG00000031771	ENSBTAG00000031771	-	LPS, T19, T320A, T3552B, Ru1
ENSBTAG00000031738	ENSBTAG00000031738	-	LPS, T19, T320A, T3552B, Ru1

ENSBTAG00000002534	**ENSBTAG00000002534**	**-**	**LPS, T19, T320A, T3552B, Ru1**
TAP2	ENSBTAG00000003038	-	LPS, T19, T320A, T3552B, Ru1
ENSBTAG00000003037	ENSBTAG00000003037	-	LPS, T19, T320A, T3552B, Ru1
ENSBTAG00000012451	ENSBTAG00000012451	-	LPS, T19, T320A, T3552B, Ru1
7SK	ENSBTAG00000042716	-	LPS, T19, T320A, T3552B, Ru1
PPT2	ENSBTAG00000004436	-	LPS, T19, T320A, T3552B, Ru1
ENSBTAG00000046158	**ENSBTAG00000046158**	**ENSG00000243649**	**LPS, T19, T320A, T3552B, Ru1**
ENSBTAG00000025441	**ENSBTAG00000025441**	**ENSG00000204389**	**LPS, T19, T320A, T3552B, Ru1**
ZKSCAN4	ENSBTAG00000003575	ENSG00000187626	LPS, T19, T320A, T3552B, Ru1
ENSBTAG00000024183	ENSBTAG00000024183	ENSG00000196747	LPS, T19, T320A, T3552B, Ru1
HIST1H2AI	ENSBTAG00000040378	-	LPS, T19, T320A, T3552B, Ru1
ENSBTAG00000039492	ENSBTAG00000039492	-	LPS, T19, T320A, T3552B, Ru1
ENSBTAG00000031766	ENSBTAG00000031766	-	LPS, T19, T320A, T3552B, Ru1
ENSBTAG00000005808	**ENSBTAG00000005808**	**-**	**LPS, T19, T320A, T3552B, Ru1**
CDYL	ENSBTAG00000016397	-	LPS, T19, T320A, T3552B, Ru1
SCARNA17	ENSBTAG00000045039	ENSG00000251992	LPS, T19, T320A, T3552B, Ru1
ENSBTAG00000034676	**ENSBTAG00000034676**	**-**	**LPS, T19, T320A, T3552B, Ru1**
ENSBTAG00000032961	**ENSBTAG00000032961**	**-**	**LPS, T19, T320A, T3552B, Ru1**
ENSBTAG00000016571	**ENSBTAG00000016571**	**-**	**LPS, T19, T320A, T3552B, Ru1**
TBC1D24	ENSBTAG00000005458	ENSG00000162065	LPS, T19, T320A, T3552B, Ru1
AMDHD2	ENSBTAG00000001022	-	LPS, T19, T320A, T3552B, Ru1
ENSBTAG00000002189	ENSBTAG00000002189	-	LPS, T19, T320A, T3552B, Ru1
ENSBTAG00000017759	ENSBTAG00000017759	ENSG00000103512	LPS, T19, T320A, T3552B, Ru1
ENSBTAG00000008632	ENSBTAG00000008632	-	LPS, T19, T320A, T3552B, Ru1
ENSBTAG00000013917	ENSBTAG00000013917	ENSG00000080603	LPS, T19, T320A, T3552B, Ru1
ENSBTAG00000007934	ENSBTAG00000007934	ENSG00000239789	LPS, T19, T320A, T3552B, Ru1
TYW1	ENSBTAG00000008446	-	LPS, T19, T320A, T3552B, Ru1
ENSBTAG00000026286	ENSBTAG00000026286	ENSG00000174428	LPS, T19, T320A, T3552B, Ru1
ENSBTAG00000005448	ENSBTAG00000005448	ENSG00000170667	LPS, T19, T320A, T3552B, Ru1

ENSBTAG00000020440	ENSBTAG00000020440	-	LPS, T19, T320A, T3552B, Ru1
ENSBTAG00000003288	ENSBTAG00000003288	ENSG00000122674	LPS, T19, T320A, T3552B, Ru1
RBAK	ENSBTAG00000010291	ENSG00000146587	LPS, T19, T320A, T3552B, Ru1
SNORD60	ENSBTAG00000042751	ENSG00000206630	LPS, T19, T320A, T3552B, Ru1
ENSBTAG00000009201	ENSBTAG00000009201	ENSG00000262246	LPS, T19, T320A, T3552B, Ru1
ENSBTAG00000008222	ENSBTAG00000008222	-	LPS, T19, T320A, T3552B, Ru1
ENSBTAG00000006543	ENSBTAG00000006543	ENSG00000205609	LPS, T19, T320A, T3552B, Ru1
ENSBTAG00000018000	ENSBTAG00000018000	-	LPS, T19, T320A, T3552B, Ru1
ENSBTAG00000048253	ENSBTAG00000048253	ENSG00000176476	LPS, T19, T320A, T3552B, Ru1
ENSBTAG00000008635	ENSBTAG00000008635	-	LPS, T19, T320A, T3552B, Ru1
ENSBTAG00000008633	**ENSBTAG00000008633**	**ENSG00000132207**	**LPS, T19, T320A, T3552B, Ru1**
ENSBTAG00000010904	ENSBTAG00000010904	ENSG00000280789	LPS, T19, T320A, T3552B, Ru1
ENSBTAG00000018082	ENSBTAG00000018082	-	LPS, T19, T320A, T3552B, Ru1
ENSBTAG00000000405	ENSBTAG00000000405	-	LPS, T19, T320A, T3552B, Ru1
ENSBTAG00000020535	**ENSBTAG00000020535**	**ENSG00000103490**	**LPS, T19, T320A, T3552B, Ru1**
ENSBTAG00000015314	ENSBTAG00000015314	-	LPS, T19, T320A, T3552B, Ru1
SCARNA20	ENSBTAG00000044466	-	LPS, T19, T320A, T3552B, Ru1
ENSBTAG00000047379	**ENSBTAG00000047379**	**-**	**LPS, T19, T320A, T3552B, Ru1**
ARPC1A	ENSBTAG00000004242	ENSG00000284292	LPS, T19, T320A, T3552B, Ru1
ENSBTAG00000002010	ENSBTAG00000002010	ENSG00000249967	LPS, T19, T320A, T3552B, Ru1
ENSBTAG00000021246	**ENSBTAG00000021246**	**ENSG00000166275**	**LPS, T19, T320A, T3552B, Ru1**
ENSBTAG00000040427	ENSBTAG00000040427	-	LPS, T19, T320A, T3552B, Ru1
NDUFB8	ENSBTAG00000000091	-	LPS, T19, T320A, T3552B, Ru1
ENSBTAG00000020304	ENSBTAG00000020304	-	LPS, T19, T320A, T3552B, Ru1
ENSBTAG00000012416	ENSBTAG00000012416	ENSG00000198546	LPS, T19, T320A, T3552B, Ru1
ENSBTAG00000008584	**ENSBTAG00000008584**	**-**	**LPS, T19, T320A, T3552B, Ru1**
ENSBTAG00000018960	ENSBTAG00000018960	ENSG00000196693	LPS, T19, T320A, T3552B, Ru1
ENSBTAG00000011694	ENSBTAG00000011694	-	LPS, T19, T320A, T3552B, Ru1
SNORA74	ENSBTAG00000043162	ENSG00000212402	LPS, T19, T320A, T3552B, Ru1

FAM21A	ENSBTAG00000018915	ENSG00000099290	LPS, T19, T320A, T3552B, Ru1
TSNAX	**ENSBTAG00000047434**	**ENSG00000116918**	**LPS, T19, T320A, T3552B, Ru1**
SNORA14	ENSBTAG00000043324	-	LPS, T19, T320A, T3552B, Ru1
ENSBTAG00000012664	ENSBTAG00000012664	ENSG00000166507	LPS, T19, T320A, T3552B, Ru1
GLUD1	ENSBTAG00000007540	ENSG00000148672	LPS, T19, T320A, T3552B, Ru1
ENSBTAG00000018499	**ENSBTAG00000018499**	**ENSG00000265190**	**LPS, T19, T320A, T3552B, Ru1**
ENSBTAG00000018188	ENSBTAG00000018188	-	LPS, T19, T320A, T3552B, Ru1
SDHAF2	ENSBTAG00000015266	ENSG00000167985	LPS, T19, T320A, T3552B, Ru1
ENSBTAG00000020147	**ENSBTAG00000020147**	**-**	**LPS, T19, T320A, T3552B, Ru1**
CTSD	**ENSBTAG00000007622**	**ENSG00000117984**	**LPS, T19, T320A, T3552B, Ru1**
IFITM3	ENSBTAG00000019015	-	LPS, T19, T320A, T3552B, Ru1
MED17	**ENSBTAG00000003552**	**ENSG00000284057**	**LPS, T19, T320A, T3552B, Ru1**
ENSBTAG00000011846	ENSBTAG00000011846	ENSG00000149016	LPS, T19, T320A, T3552B, Ru1
ENSBTAG00000010465	ENSBTAG00000010465	-	LPS, T19, T320A, T3552B, Ru1
ENSBTAG00000002510	**ENSBTAG00000002510**	**ENSG00000214753**	**LPS, T19, T320A, T3552B, Ru1**
ENSBTAG00000017951	ENSBTAG00000017951	-	LPS, T19, T320A, T3552B, Ru1
ENSBTAG00000000103	ENSBTAG00000000103	ENSG00000276345	LPS, T19, T320A, T3552B, Ru1
ENSBTAG00000005796	ENSBTAG00000005796	-	LPS, T19, T320A, T3552B, Ru1
ENSBTAG00000011511	**ENSBTAG00000011511**	**-**	**LPS, T19, T320A, T3552B, Ru1**
SCARNA15	ENSBTAG00000045209	ENSG00000280466	LPS, T19, T320A, T3552B, Ru1
ENSBTAG00000045596	ENSBTAG00000045596	ENSG00000116580	LPS, T19, T320A, T3552B, Ru1
ENSBTAG00000020356	ENSBTAG00000020356	ENSG00000163374	LPS, T19, T320A, T3552B, Ru1
ENSBTAG00000001143	**ENSBTAG00000001143**	**ENSG00000117228**	**LPS, T19, T320A, T3552B, Ru1**
ENSBTAG00000020037	ENSBTAG00000020037	ENSG00000215883	LPS, T19, T320A, T3552B, Ru1
snoU2_19	ENSBTAG00000042358	-	LPS
ENSBTAG00000030337	ENSBTAG00000030337	-	LPS, T19, T320A, T3552B, Ru1
ENSBTAG00000026114	ENSBTAG00000026114	-	LPS, T19, T320A, T3552B, Ru1
HIST2H2AC	ENSBTAG00000046003	ENSG00000203812	LPS, T19, T320A, T3552B, Ru1
ENSBTAG00000008592	**ENSBTAG00000008592**	**ENSG00000198019**	**LPS, T19, T320A, T3552B, Ru1**

ENSBTAG00000013910	ENSBTAG00000013910	ENSG00000121851	LPS, T19, T320A, T3552B, Ru1
GPR89A	**ENSBTAG00000005809**	**ENSG00000188092**	**LPS, T19, T320A, T3552B, Ru1**
ENSBTAG00000032057	ENSBTAG00000032057	-	LPS, T19, T320A, T3552B, Ru1
ENSBTAG00000031788	ENSBTAG00000031788	-	LPS, T19, T320A, T3552B, Ru1
ENSBTAG00000017765	**ENSBTAG00000017765**	**-**	**LPS, T19, T320A, T3552B, Ru1**
ENSBTAG00000016472	ENSBTAG00000016472	-	LPS, T19, T320A, T3552B, Ru1
ENSBTAG00000037673	ENSBTAG00000037673	-	LPS, T19, T320A, T3552B, Ru1
MFSD14A	**ENSBTAG00000015776**	**ENSG00000156875**	**LPS, T19, T320A, T3552B, Ru1**
KIAA1107	**ENSBTAG00000006167**	**ENSG00000069712**	**LPS, T19, T320A, T3552B, Ru1**
ENSBTAG00000017670	**ENSBTAG00000017670**	**-**	**LPS, T19, T320A, T3552B, Ru1**
ENSBTAG00000017595	**ENSBTAG00000017595**	**-**	**LPS, T19, T320A, T3552B, Ru1**
ENSBTAG00000009603	ENSBTAG00000009603	ENSG00000173660	LPS, T19, T320A, T3552B, Ru1
ENSBTAG00000007746	ENSBTAG00000007746	ENSG00000106546	LPS, T19, T320A, T3552B, Ru1
ENSBTAG00000010597	**ENSBTAG00000010597**	**ENSG00000006625**	**LPS, T19, T320A, T3552B, Ru1**
STEAP1	**ENSBTAG00000015749**	**ENSG00000164647**	**LPS, T19, T320A, T3552B, Ru1**
ENSBTAG00000000990	**ENSBTAG00000000990**	**ENSG00000106588**	**LPS, T19, T320A, T3552B, Ru1**
ENSBTAG00000017770	**ENSBTAG00000017770**	**ENSG00000146963**	**LPS, T19, T320A, T3552B, Ru1**
ENSBTAG00000007983	ENSBTAG00000007983	ENSG00000196456	LPS, T19, T320A, T3552B, Ru1
ACTR3B	ENSBTAG00000008032	ENSG00000133627	LPS, T19, T320A, T3552B, Ru1
ENSBTAG00000005475	ENSBTAG00000005475	-	LPS, T19, T320A, T3552B, Ru1
ENSBTAG00000012271	ENSBTAG00000012271	ENSG00000258064	LPS, T19, T320A, T3552B, Ru1
ENSBTAG00000007447	**ENSBTAG00000007447**	**ENSG00000173598**	**LPS, T19, T320A, T3552B, Ru1**
ENSBTAG00000005863	ENSBTAG00000005863	ENSG00000170653	LPS, T19, T320A, T3552B, Ru1
ENSBTAG00000004374	ENSBTAG00000004374	ENSG00000257727	LPS, T19, T320A, T3552B, Ru1
ENSBTAG00000016661	**ENSBTAG00000016661**	**-**	**LPS, T19, T320A, T3552B, Ru1**
ENSBTAG00000015092	ENSBTAG00000015092	-	LPS, T19, T320A, T3552B, Ru1
ENSBTAG00000047582	ENSBTAG00000047582	ENSG00000213923	LPS, T19, T320A, T3552B, Ru1
ENSBTAG00000004876	ENSBTAG00000004876	-	LPS, T19, T320A, T3552B, Ru1
7SK	ENSBTAG00000043299	-	LPS, T19, T320A, T3552B, Ru1

ENSBTAG00000031950	ENSBTAG00000031950	-	LPS, T19, T320A, T3552B, Ru1
ENSBTAG00000011918	ENSBTAG00000011918	ENSG00000135441	LPS, T19, T320A, T3552B, Ru1
ENSBTAG00000039524	**ENSBTAG00000039524**	**-**	**LPS**
ALG10	**ENSBTAG00000030632**	**ENSG00000139133**	**LPS, T19, T320A, T3552B, Ru1**
ENSBTAG00000004556	**ENSBTAG00000004556**	**ENSG00000173262**	**LPS, T19, T320A, T3552B, Ru1**
ENSBTAG00000013126	ENSBTAG00000013126	-	LPS, T19, T320A, T3552B, Ru1
ENSBTAG00000005465	ENSBTAG00000005465	-	LPS, T19, T320A, T3552B, Ru1
MGC127055	ENSBTAG00000026501	-	LPS, T19, T320A, T3552B, Ru1
SCO2	ENSBTAG00000012609	ENSG00000130489	LPS, T19, T320A, T3552B, Ru1
ENSBTAG00000016050	ENSBTAG00000016050	ENSG00000100288	LPS, T19, T320A, T3552B, Ru1
Metazoa_SRP	**ENSBTAG00000046888**	**-**	**LPS, T19, T320A, T3552B, Ru1**
ENSBTAG00000006492	**ENSBTAG00000006492**	**ENSG00000281028**	**LPS, T19, T320A, T3552B, Ru1**
PDGFRA	**ENSBTAG00000007173**	**ENSG00000134853**	**LPS, T19, T320A, T3552B, Ru1**
ENSBTAG00000009812	**ENSBTAG00000009812**	**-**	**LPS, T19, T320A, T3552B, Ru1**
ENSBTAG00000027513	**ENSBTAG00000027513**	**ENSG00000081041**	**LPS, T19, T320A, T3552B, Ru1**
ENSBTAG00000037778	**ENSBTAG00000037778**	**ENSG00000163734**	**LPS, T19, T320A, T3552B, Ru1**
ENSBTAG00000037558	**ENSBTAG00000037558**	**-**	**LPS, T19, T320A, T3552B**
U7	ENSBTAG00000047521	-	LPS
ENSBTAG00000020923	ENSBTAG00000020923	ENSG00000130283	LPS, T19, T320A, T3552B, Ru1
SMIM7	ENSBTAG00000013613	-	LPS, T19, T320A, T3552B, Ru1
ENSBTAG00000005312	ENSBTAG00000005312	ENSG00000105085	LPS, T19, T320A, T3552B, Ru1
MAN2B1	**ENSBTAG00000006241**	**ENSG00000104774**	**LPS, T19, T320A, T3552B, Ru1**
ENSBTAG00000039493	**ENSBTAG00000039493**	**ENSG00000270011**	**LPS, T19, T320A, T3552B, Ru1**
ENSBTAG00000012745	ENSBTAG00000012745	ENSG00000130810	LPS, T19, T320A, T3552B, Ru1
ENSBTAG00000040507	**ENSBTAG00000040507**	**ENSG00000268861**	**LPS, T19, T320A, T3552B, Ru1**
ENSBTAG00000019025	ENSBTAG00000019025	-	LPS, T19, T320A, T3552B, Ru1
ENSBTAG00000024450	ENSBTAG00000024450	ENSG00000126934	LPS, T19, T320A, T3552B, Ru1
SLC39A3	ENSBTAG00000017706	ENSG00000141873	LPS, T19, T320A, T3552B, Ru1
ENSBTAG00000000682	ENSBTAG00000000682	-	LPS, T19, T320A, T3552B, Ru1

ENSBTAG00000010735	ENSBTAG00000010735	ENSG00000146066	LPS, T19, T320A, T3552B, Ru1
SNORA74	ENSBTAG00000042256	ENSG00000200959	LPS, T19, T320A, T3552B, Ru1
ENSBTAG00000010871	ENSBTAG00000010871	ENSG00000131503	LPS, T19, T320A, T3552B, Ru1
ENSBTAG00000011642	ENSBTAG00000011642	ENSG00000091009	LPS, T19, T320A, T3552B, Ru1
U2	ENSBTAG00000043747	-	LPS, T19, T320A, T3552B, Ru1
ENSBTAG00000012184	ENSBTAG00000012184	ENSG00000164611	LPS, T19, T320A, T3552B, Ru1
ENSBTAG00000002350	**ENSBTAG00000002350**	**ENSG00000268173**	**LPS, T19, T320A, T3552B, Ru1**
SNORA68	ENSBTAG00000043512	ENSG00000207166	LPS
ENSBTAG00000012587	ENSBTAG00000012587	ENSG00000105393	LPS, T19, T320A, T3552B, Ru1
RAVER1	**ENSBTAG00000015721**	**ENSG00000161847**	**LPS, T19, T320A, T3552B, Ru1**
ENSBTAG00000046319	ENSBTAG00000046319	-	LPS, T19, T320A, T3552B, Ru1
VMAC	ENSBTAG00000006067	ENSG00000267314	LPS, T19, T320A, T3552B, Ru1
RAD50	ENSBTAG00000011252	ENSG00000113522	LPS, T19, T320A, T3552B, Ru1
ENSBTAG00000008692	ENSBTAG00000008692	-	LPS, T19, T320A, T3552B, Ru1
SKP1	**ENSBTAG00000025191**	**ENSG00000113558**	**LPS, T19, T320A, T3552B, Ru1**
DHFR	ENSBTAG00000007681	-	LPS, T19, T320A, T3552B, Ru1
MFSD14B	ENSBTAG00000003124	ENSG00000148110	LPS, T19, T320A, T3552B, Ru1
ENSBTAG00000000269	ENSBTAG00000000269	-	LPS, T19, T320A, T3552B, Ru1
ENSBTAG00000047389	ENSBTAG00000047389	-	LPS, T19, T320A, T3552B, Ru1
ENSBTAG00000048226	ENSBTAG00000048226	-	LPS, T19, T320A, T3552B, Ru1
IL11RA	ENSBTAG00000014907	ENSG00000137070	LPS, T19, T320A, T3552B, Ru1
ENSBTAG00000030960	ENSBTAG00000030960	ENSG00000059769	LPS, T19, T320A, T3552B, Ru1
RNASEH1	ENSBTAG00000016235	-	LPS, T19, T320A, T3552B, Ru1
7SK	ENSBTAG00000043171	-	LPS, T19, T320A, T3552B, Ru1
ENSBTAG00000025929	ENSBTAG00000025929	-	LPS, T19, T320A, T3552B, Ru1
ENSBTAG00000032777	**ENSBTAG00000032777**	**-**	**LPS, T19, T320A, T3552B, Ru1**
ENSBTAG00000014936	**ENSBTAG00000014936**	**ENSG00000122696**	**LPS, T19, T320A, T3552B, Ru1**
SHB	ENSBTAG00000014922	ENSG00000107338	LPS, T19, T320A, T3552B, Ru1
SNORA8	ENSBTAG00000043103	-	LPS

ENSBTAG00000000885	ENSBTAG00000000885	-	LPS, T19, T320A, T3552B, Ru1
ENSBTAG00000038335	ENSBTAG00000038335	ENSG00000266826	LPS, T19, T320A, T3552B, Ru1
ENSBTAG00000003921	ENSBTAG00000003921	ENSG00000214338	LPS, T19, T320A, T3552B, Ru1
7SK	ENSBTAG00000042601	-	LPS, T19, T320A, T3552B, Ru1
ENSBTAG00000032163	**ENSBTAG00000032163**	**-**	**LPS, T19, T320A, T3552B, Ru1**
ENSBTAG00000024751	ENSBTAG00000024751	-	LPS, T19, T320A, T3552B, Ru1
ENSBTAG00000038112	**ENSBTAG00000038112**	**-**	**LPS, T19, T320A, T3552B, Ru1**
CNKSR3	**ENSBTAG00000012674**	**ENSG00000153721**	**LPS, T19, T320A, T3552B, Ru1**
ENSBTAG00000014494	**ENSBTAG00000014494**	**-**	**LPS, T19, T320A, T3552B, Ru1**
ENSBTAG00000013671	ENSBTAG00000013671	ENSG00000156697	LPS, T19, T320A, T3552B, Ru1
ENSBTAG00000038228	ENSBTAG00000038228	-	LPS, T19, T320A, T3552B, Ru1
ENSBTAG00000019548	ENSBTAG00000019548	ENSG00000196972	LPS, T19, T320A, T3552B, Ru1
ENSBTAG00000047518	ENSBTAG00000047518	ENSG00000197620	LPS, T19, T320A, T3552B, Ru1
ENSBTAG00000023978	**ENSBTAG00000023978**	**ENSG00000277203**	**LPS, T19, T320A, T3552B, Ru1**
ENSBTAG00000009959	ENSBTAG00000009959	ENSG00000130821	LPS, T19, T320A, T3552B, Ru1
ENSBTAG00000001911	**ENSBTAG00000001911**	**-**	**LPS, T19, T320A, T3552B, Ru1**
ENSBTAG00000022204	**ENSBTAG00000022204**	**ENSG00000184905**	**LPS, T19, T320A, T3552B, Ru1**
MAGED4B	ENSBTAG00000048077	ENSG00000187243	LPS, T19, T320A, T3552B, Ru1
ENSBTAG00000008911	ENSBTAG00000008911	-	LPS, T19, T320A, T3552B, Ru1
ENSBTAG00000010922	**ENSBTAG00000010922**	**-**	**LPS, T19, T320A, T3552B, Ru1**
ENSBTAG00000006034	ENSBTAG00000006034	ENSG00000125352	LPS, T19, T320A, T3552B, Ru1
ENSBTAG00000039434	ENSBTAG00000039434	-	LPS, T19, T320A, T3552B, Ru1
ENSBTAG00000039890	ENSBTAG00000039890	ENSG00000203950	LPS, T19, T320A, T3552B, Ru1
IDS	ENSBTAG00000011056	ENSG00000010404	LPS, T19, T320A, T3552B, Ru1
ENSBTAG00000033167	ENSBTAG00000033167	-	LPS, T19, T320A, T3552B, Ru1
ENSBTAG00000036028	ENSBTAG00000036028	ENSG00000133134	LPS, T19, T320A, T3552B, Ru1
ENSBTAG00000006878	ENSBTAG00000006878	-	LPS, T19, T320A, T3552B, Ru1
KIF4A	ENSBTAG00000012861	-	LPS, T19, T320A, T3552B, Ru1
ENSBTAG00000007797	ENSBTAG00000007797	ENSG00000089289	LPS, T19, T320A, T3552B, Ru1

ENSBTAG00000031523	ENSBTAG00000031523	ENSG00000198455	LPS, T19, T320A, T3552B, Ru1
ENSBTAG00000008124	ENSBTAG00000008124	ENSG00000198814	LPS, T19, T320A, T3552B, Ru1,
ZFY	ENSBTAG00000007730	ENSG00000005889	LPS, T19, T320A, T3552B, Ru1
ENSBTAG00000007866	ENSBTAG00000007866	-	T19, T320A, T3552B
ENSBTAG00000017946	ENSBTAG00000017946	-	T19, T3552B
HS3ST3A1	ENSBTAG00000031107	-	T19
ENSBTAG00000039618	ENSBTAG00000039618	-	T19
ENSBTAG00000044125	ENSBTAG00000044125	-	T19, T3552B
ULBP21	ENSBTAG00000047902	-	T19
snoU2_19	ENSBTAG00000042837	-	T320A
5S_rRNA	ENSBTAG00000045518	-	T320A
ENSBTAG00000011961	ENSBTAG00000011961	-	T3552B
7SK	ENSBTAG00000042618	-	Ru1
SNORD33	ENSBTAG00000043197	-	Ru1

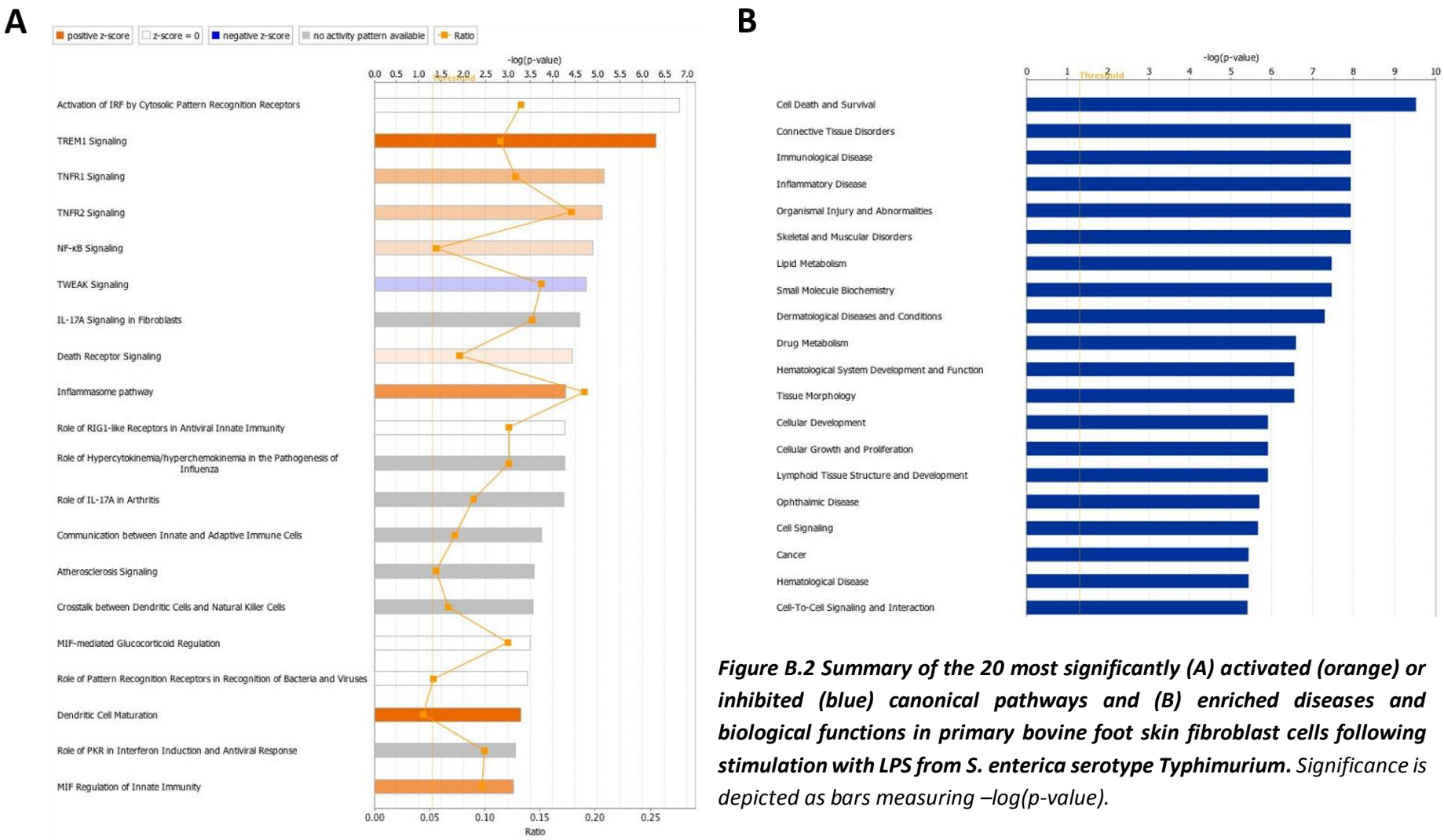

Figure B.2 Summary of the 20 most significantly (A) activated (orange) or inhibited (blue) canonical pathways and (B) enriched diseases and biological functions in primary bovine foot skin fibroblast cells following stimulation with LPS from S. enterica serotype Typhimurium. *Significance is depicted as bars measuring –log(p-value).*

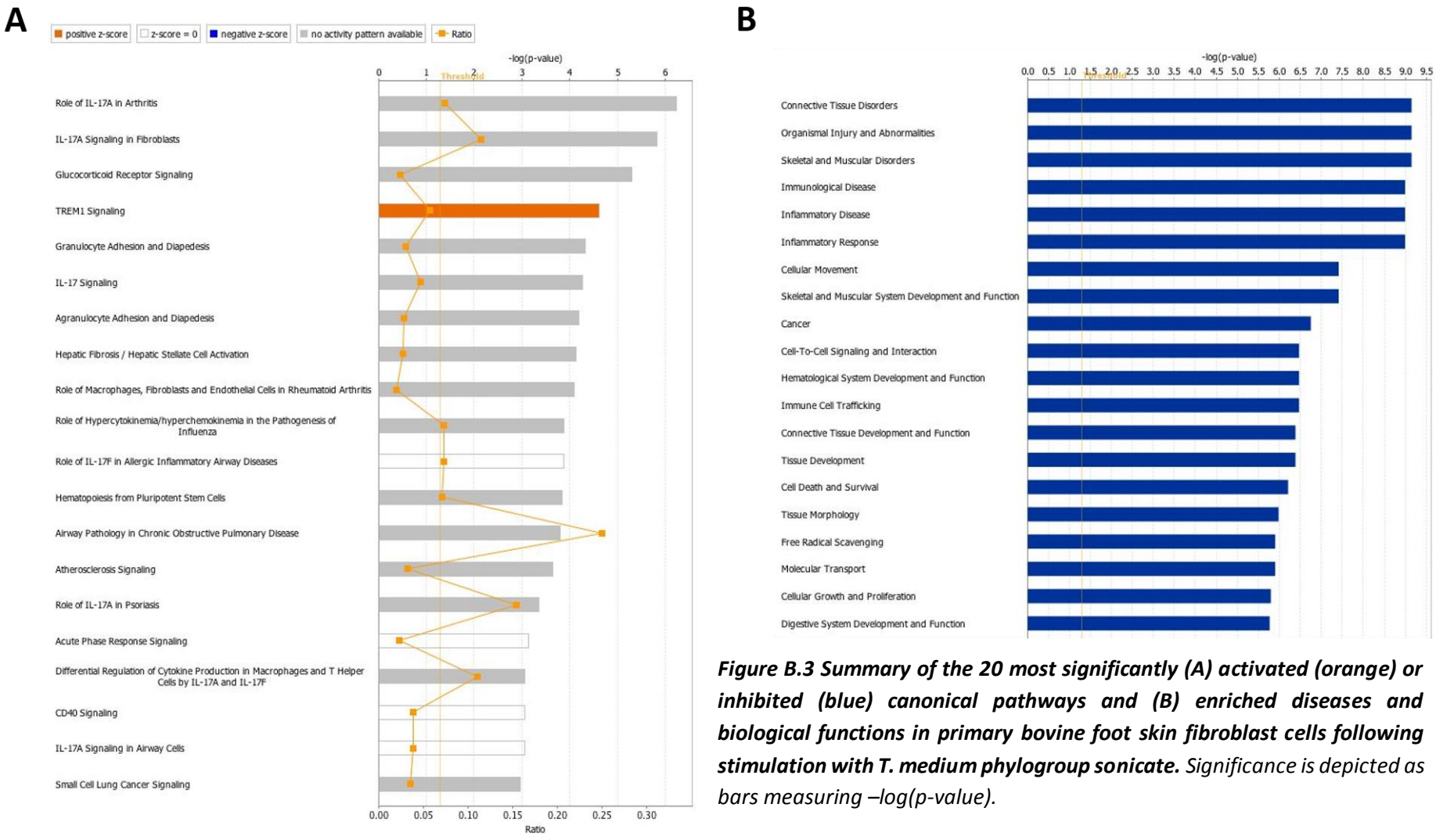

Figure B.3 Summary of the 20 most significantly (A) activated (orange) or inhibited (blue) canonical pathways and (B) enriched diseases and biological functions in primary bovine foot skin fibroblast cells following stimulation with T. medium phylogroup sonicate. *Significance is depicted as bars measuring –log(p-value).*

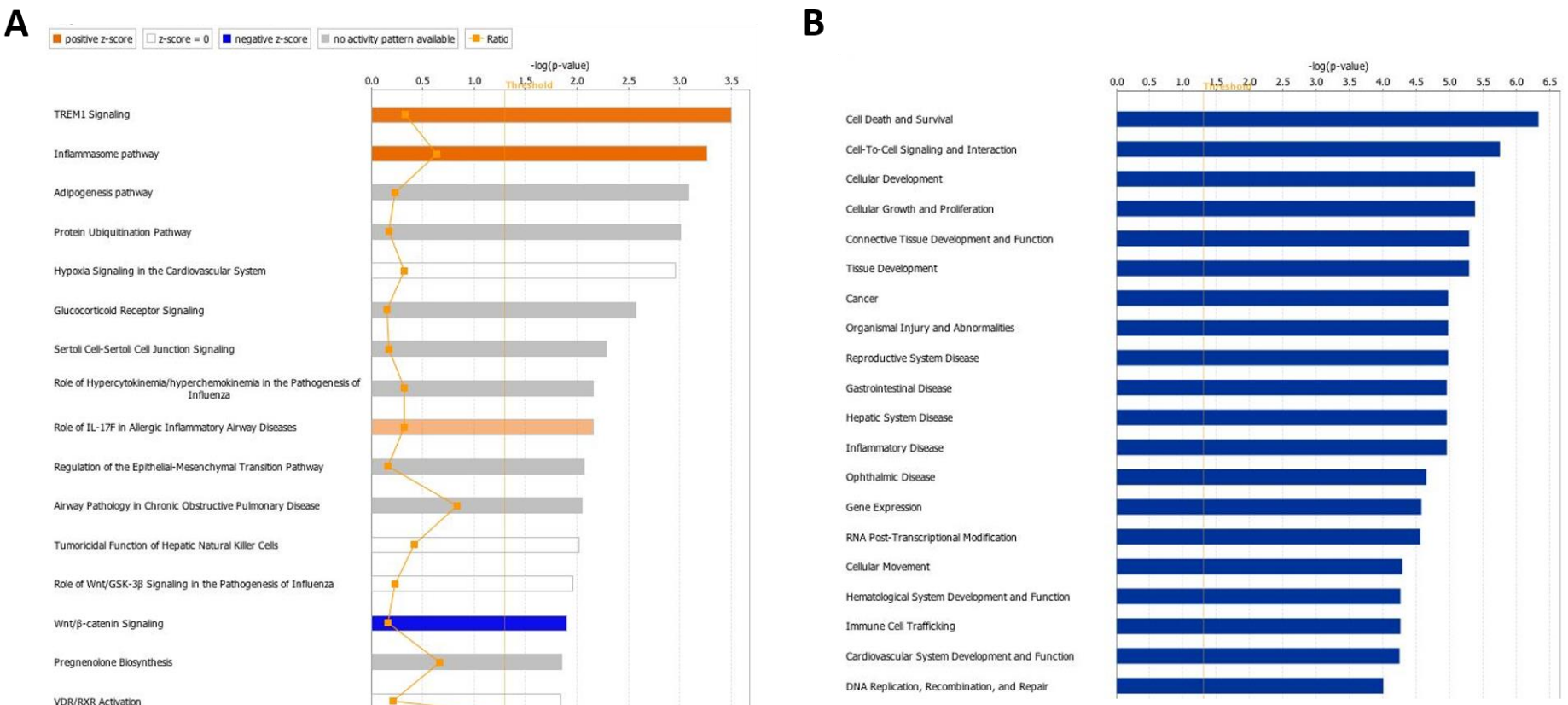

Figure B.4 Summary of the 20 most significantly (A) activated (orange) or inhibited (blue) canonical pathways and (B) enriched diseases and biological functions in primary bovine foot skin fibroblast cells following stimulation with T. phagedenis phylogroup sonicate. *Significance is depicted as bars measuring –log(p-value).*

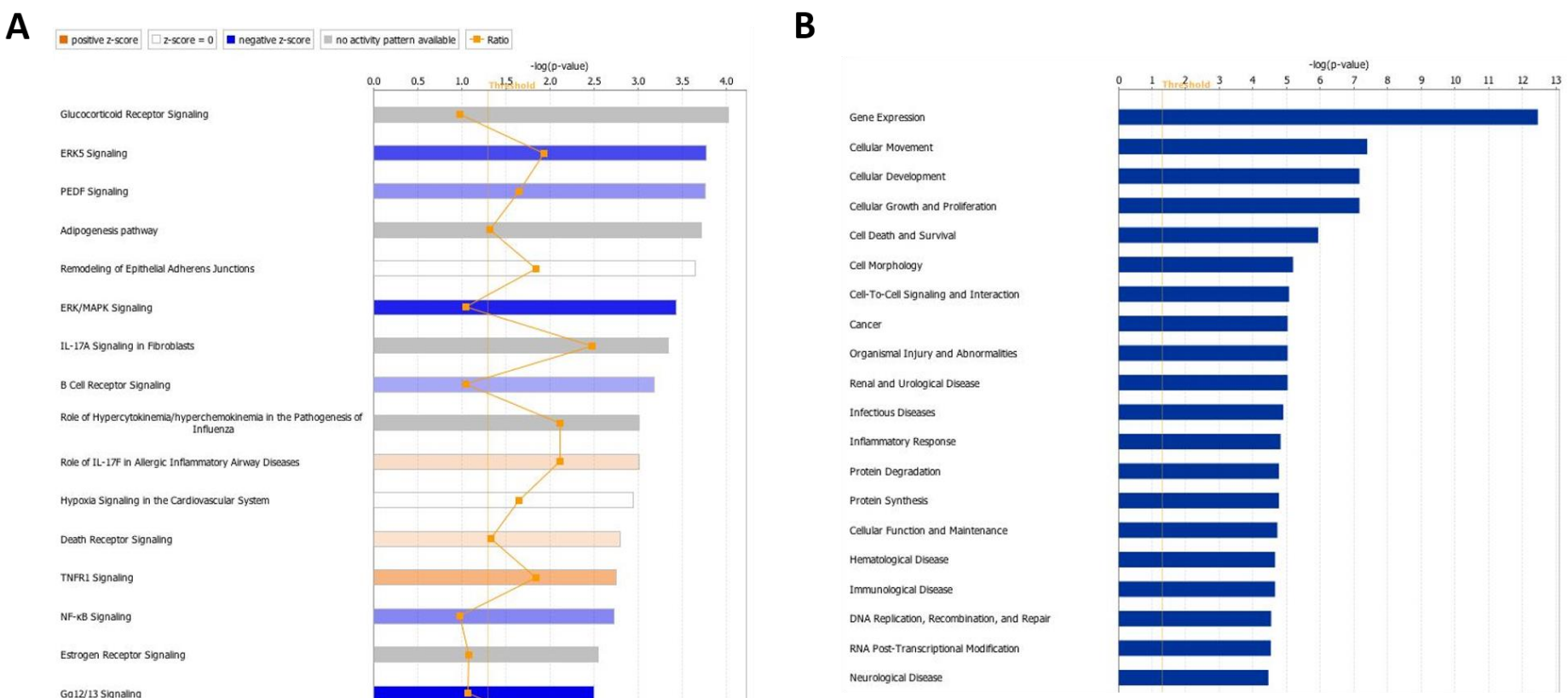

Figure B.5 Summary of the 20 most significantly (A) activated (orange) or inhibited (blue) canonical pathways and (B) enriched diseases and biological functions in primary bovine foot skin fibroblast cells following stimulation with T. pedis sonicate. *Significance is depicted as bars measuring –log(p-value).*

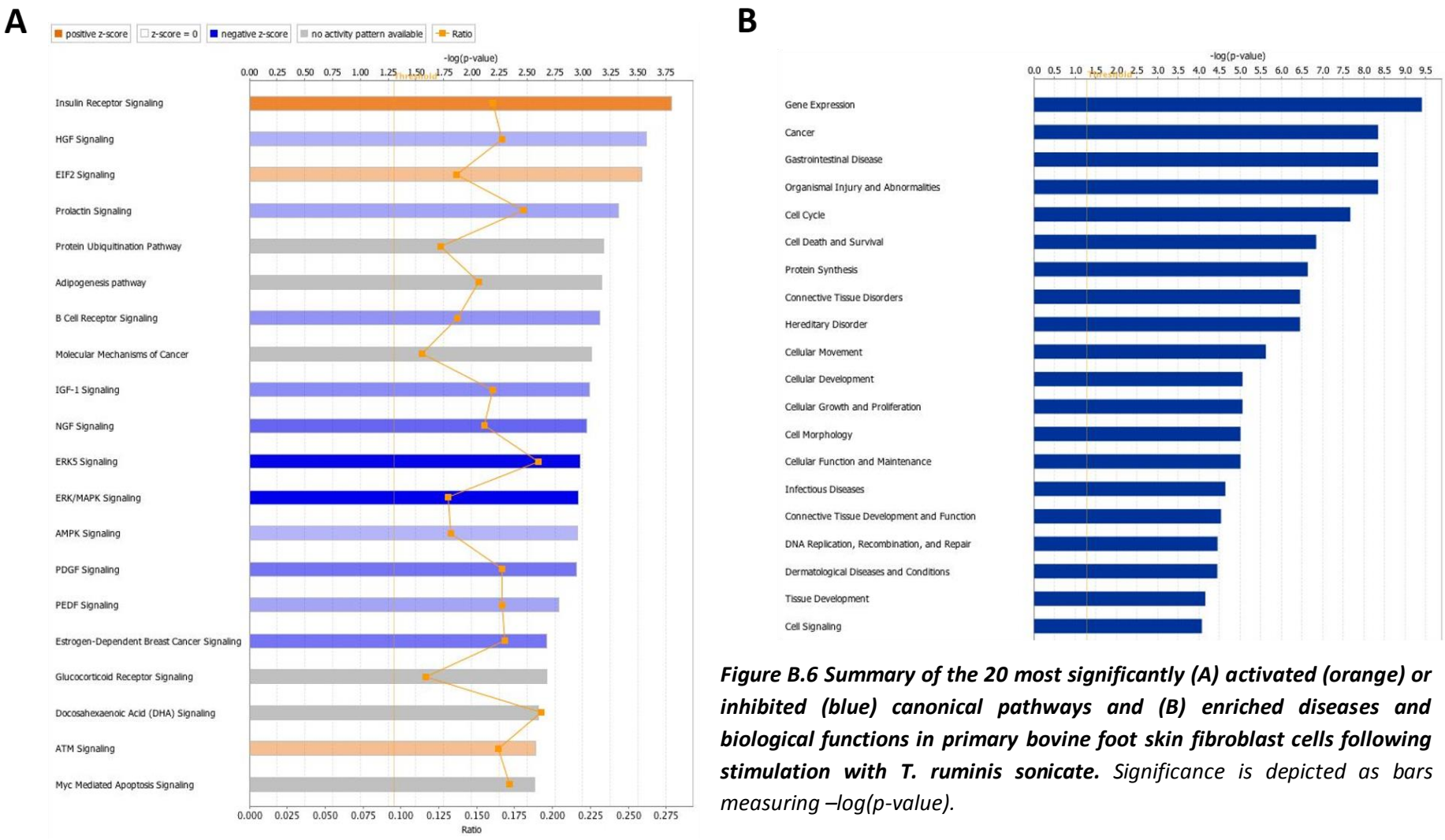

Figure B.6 Summary of the 20 most significantly (A) activated (orange) or inhibited (blue) canonical pathways and (B) enriched diseases and biological functions in primary bovine foot skin fibroblast cells following stimulation with T. ruminis sonicate. *Significance is depicted as bars measuring –log(p-value).*

Appendix B: (4) Analysing the variance between experimental replicates

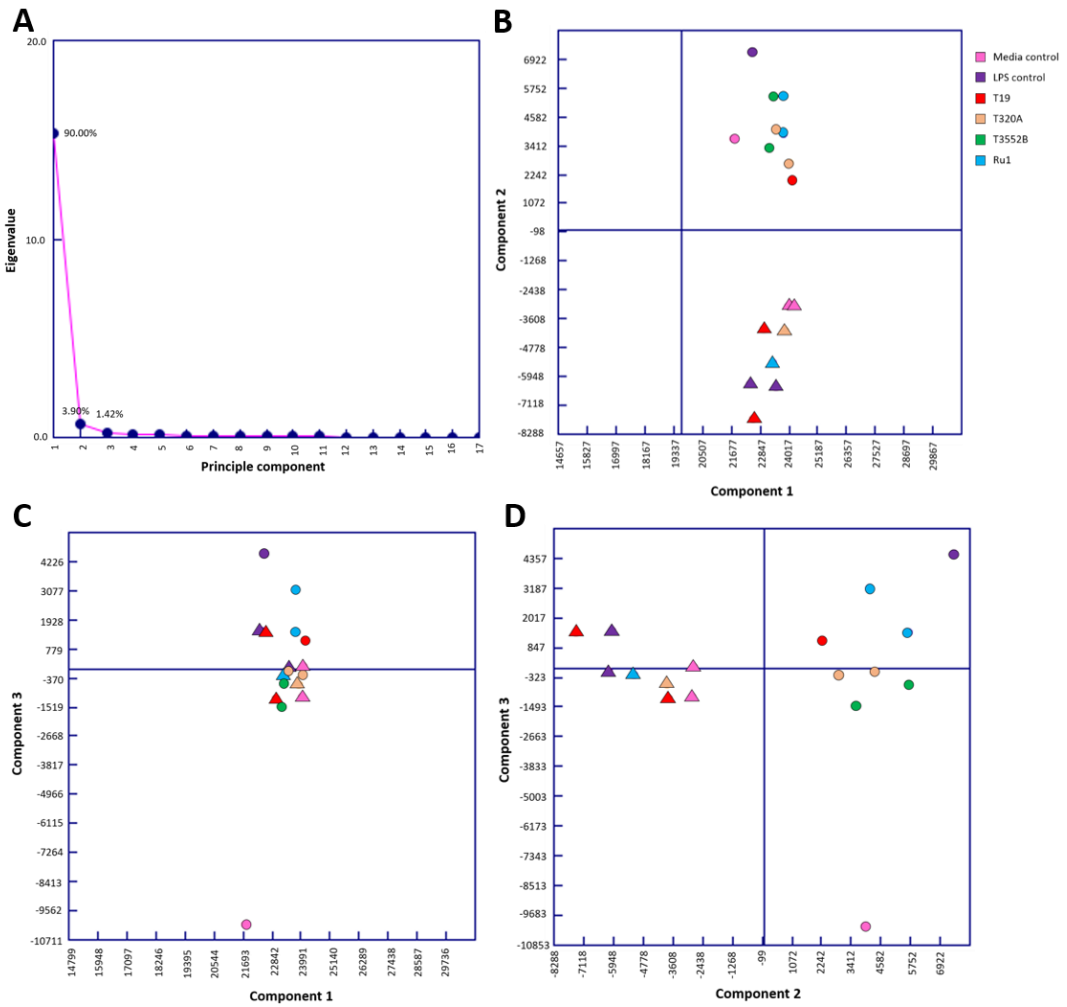

Figure B.7 Principle component analysis demonstrating variance in normalised gene expression data across 17 experimental replicates, excluding three likely outliers, by RNA-Seq. *Normalised gene expression (FPKM) data, from bovine fibroblast cells following co-incubation with various control (media and LPS from S. enterica serotype typhimurium) or treatment (T. medium phylogroup sonicate, T. phagedenis phylogroup sonicate, T. pedis sonicate, T. ruminis sonicate) groups, underwent further normalisation and subsequent principle component analysis (PCA) to determine the quality and variation in experimental replicates, excluding three likely outliers (as identified and discussed in Chapter 5.3.4.5). Graphical representation of PCA plots illustrating (A) the percentage (%) of variation explained by each of the 17 principle components, variation observed by comparison of (B) principle component 1 and principle component 2, (C) principle component 1 and principle component 3, (D) principle component 2 and principle component 3. The circular nodes represent the first pool of cDNA libraries, whereas the triangular nodes represent the second pool of cDNA libraries.*

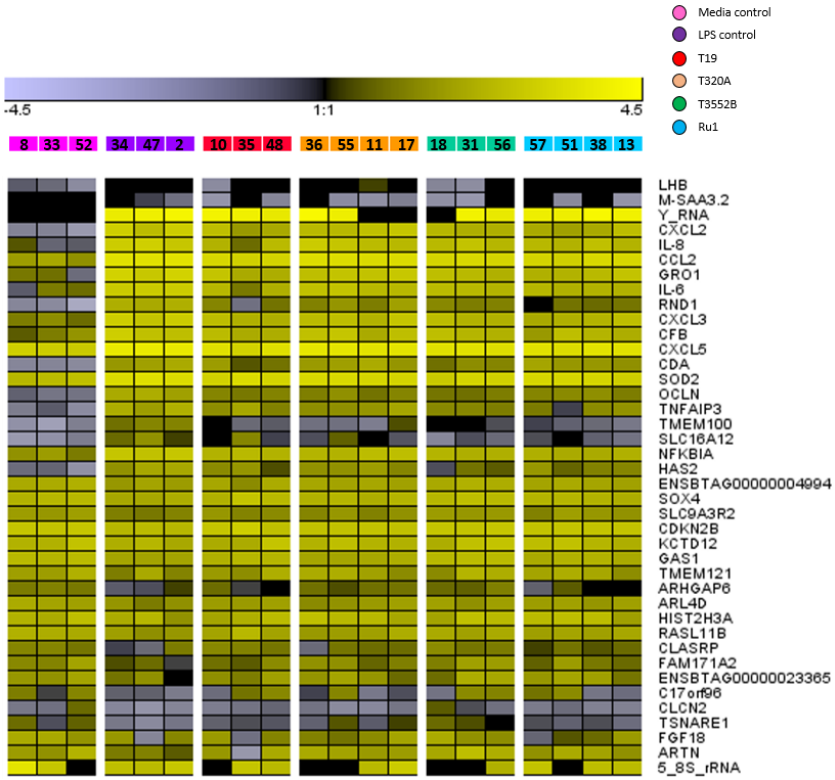

Figure B.8 Normalised expression heatmap demonstrating variation across experimental replicates for the 20 most upregulated and downregulated genes in bovine foot skin fibroblast cells upon stimulation with LPS from S. enterica serotype Typhimurium. *Normalised gene expression is shown as FPKM for each experimental sample, with sample numbers shown in corresponding treatment group colours.*

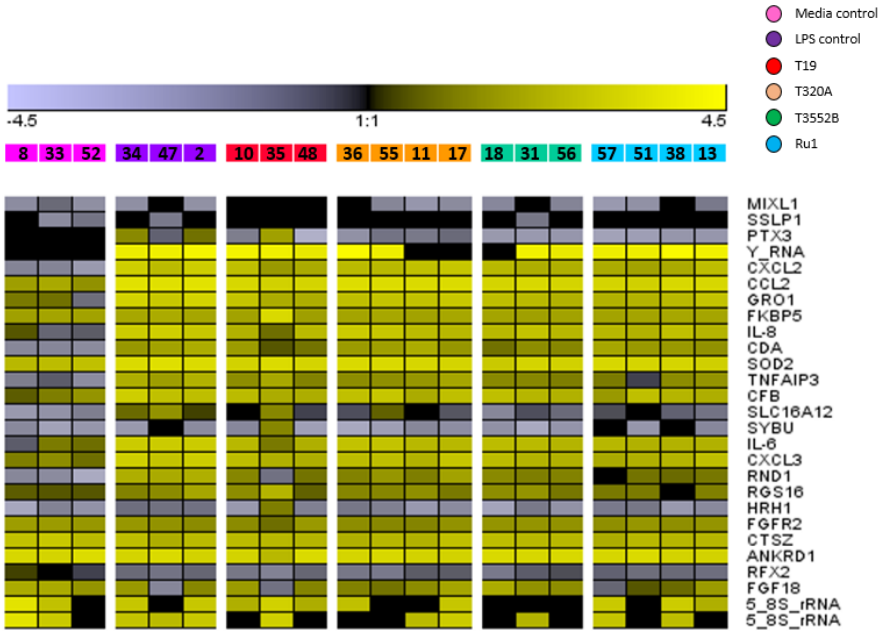

Figure B.9 Normalised expression heatmap demonstrating variation across experimental replicates for the 20 most upregulated and 7 downregulated genes in bovine foot skin fibroblast cells upon stimulation with T. medium phylogroup sonicate. *Normalised gene expression is shown as FPKM for each experimental sample, with sample numbers shown in corresponding treatment group colours.*

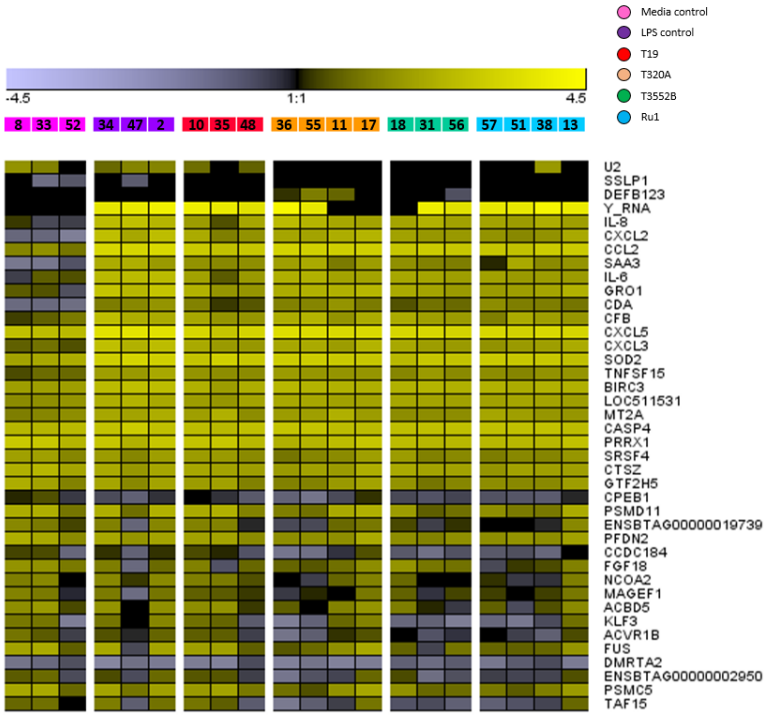

Figure B.10 Normalised expression heatmap demonstrating variation across experimental replicates for the 20 most upregulated and downregulated genes in bovine foot skin fibroblast cells upon stimulation with T. phagedenis phylogroup sonicate. *Normalised gene expression is shown as FPKM for each experimental sample, with sample numbers shown in corresponding treatment group colours.*

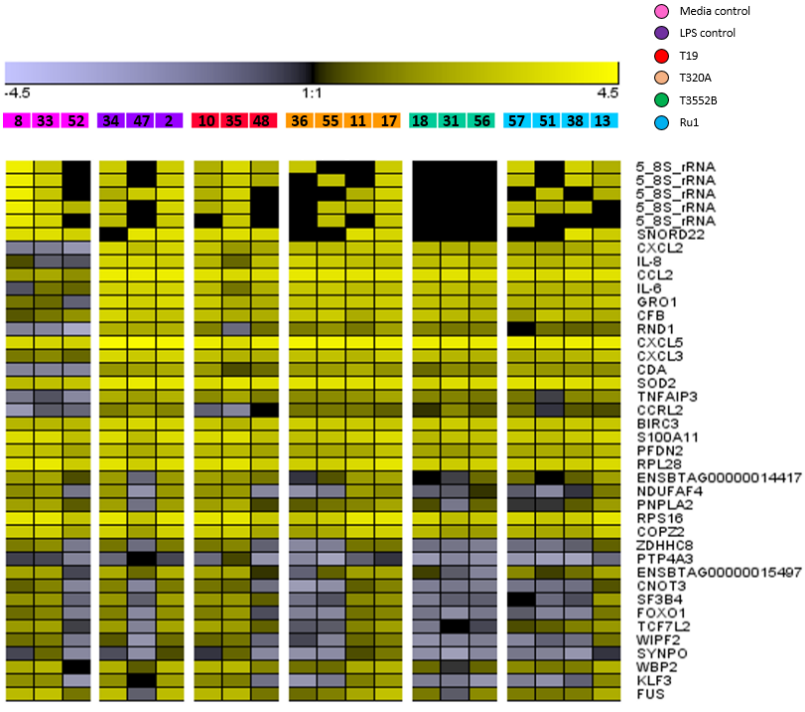

Figure B.11 Normalised expression heatmap demonstrating variation across experimental replicates for the 20 most upregulated and downregulated genes in bovine foot skin fibroblast cells upon stimulation with T. pedis sonicate. *Normalised gene expression is shown as FPKM for each experimental sample, with sample numbers shown in corresponding treatment group colours.*

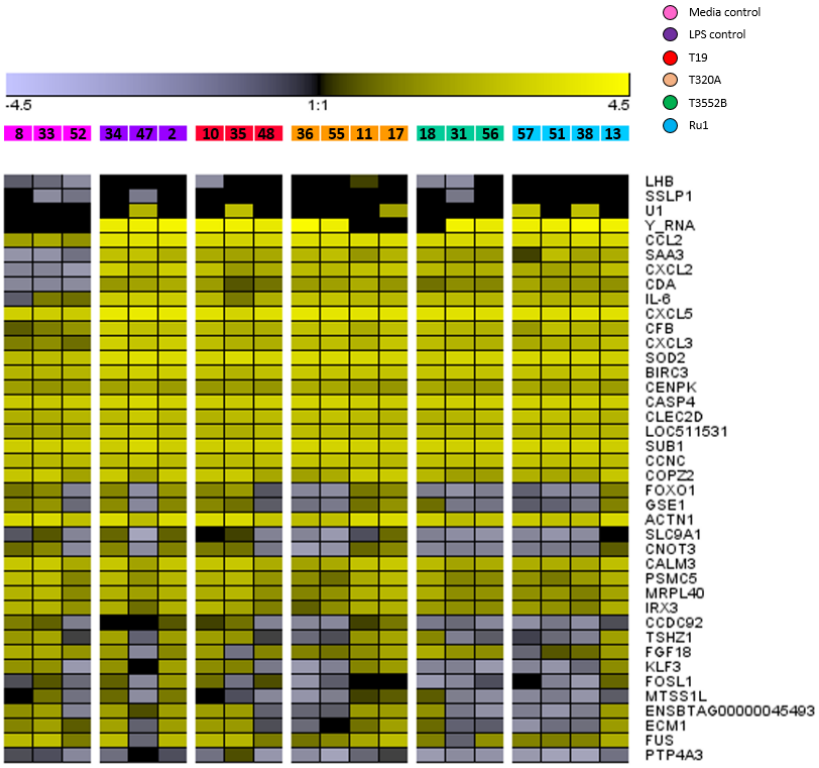

Figure B.12 Normalised expression heatmap demonstrating variation across experimental replicates for the 20 most upregulated and downregulated genes in bovine foot skin fibroblast cells upon stimulation with T. ruminis sonicate. *Normalised gene expression is shown as FPKM for each experimental sample, with sample numbers shown in corresponding treatment group colours.*

Appendix C: Investigating the molecular diversity of a putative Omp of DD treponemes (Chapter 5)

Table C.1. Details of the T. medium phylogroup isolates. *Treponeme isolate designations are provided alongside details of the host from which they were originally isolated, the year of isolation, their farm and geographic provenance, their allele designation for a putative Omp gene (as determined during this study; Chapter 5.3.4), ‡their ST and allele designation for each of the 7 genes (groEL, recA, glpK, adk, gdh, pyrG and rplB) previously assessed by MLST (Clegg et al., 2016d), their 16S rRNA gene GenBank accession number and associated references.*

Isolate name	**Host**	**Year**	**Farm and geographic provenance**	**Omp allele**	**MLST ST‡**	**MLST allele‡**							***16S rRNA* gene GenBank Accession Number**	**Reference**
						groEL	***recA***	***glpK***	***adk***	***gdh***	***pyrG***	***rplB***		
T19	Dairy	2003	Farm A, Merseyside, England, UK	1	1	1	1	1	1	1	1	1	EF061249	Evans *et al.*, 2008
G12F2	Sheep	2013	Farm B, Conwy, Wales, UK	1	1	1	1	1	1	1	1	1	KP063172	Sullivan *et al.*, 2015d
ST27 (1)	Sheep	2013	Farm C, Conwy, Wales, UK	2	1	1	1	1	1	1	1	1	KR025808	Clegg *et al.*, 2016d
g1F7c5	Sheep	2013	Farm C, Conwy, Wales, UK	1	1	1	1	1	1	1	1	1	KP063152	Sullivan *et al.*, 2015d
g1F9c27	Sheep	2013	Farm C, Conwy, Wales, UK	1	1	1	1	1	1	1	1	1	KP063153	Sullivan *et al.*, 2015d
g16F2	Sheep	2013	Farm B, Conwy, Wales, UK	1	1	1	1	1	1	1	1	1	KP063174	Sullivan *et al.*, 2015d

T56	Dairy	2003	Farm A, Merseyside, England, UK	1	1	1	1	1	1	1	1	1	EF061251	Evans *et al.*, 2008
T54	Dairy	2003	Farm A, Merseyside, England, UK	1	1	1	1	1	1	1	1	1	EF061250	Evans *et al.*, 2008
T184Y (RLUH-1)	Dairy	2003	Farm A, Merseyside, England, UK	1	1	1	1	1	1	1	1	1	AY387410	Evans *et al.*, 2008
T18A	Dairy	2003	Farm A, Merseyside, England, UK	1	1	1	1	1	1	1	1	1	EF061252	Evans *et al.*, 2008
T35B1	Dairy	2003	Farm A, Merseyside, England, UK	1	1	1	1	1	1	1	1	1	KR025809	Clegg *et al.*, 2016d
ST12	Sheep	2013	Farm B, Conwy, Wales, UK	2	1	1	1	1	1	1	1	1	KR025810	Clegg *et al.*, 2016d
T200BA2	Dairy	2004	Farm E, Shropshire, England, UK	2	1	1	1	1	1	1	1	1	KR025811	Clegg *et al.*, 2016d
T. medium ATCC 700293[§]	Human	1972	Japan	3	2	2	2	2	2	2	2	2	D85437	Umemoto *et al.*, 1997
7.45 G	Goat	2013	Farm F, Lancashire, England, UK	2	3	1	1	3	4	1	1	3	KR025812	Clegg *et al.*, 2016d
T136E	Dairy	2004	Farm G, Shropshire, England, UK	1	4	1	1	1	3	1	1	1	FJ204242	Evans *et al.*, 2009a

T52B	Dairy	2004	Farm G, Shropshire, England, UK	1	5	1	1	1	1	3	1	1	FJ204241	Evans *et al.*, 2009a
OV11F	Sheep	2009	Farm H, Gloucestershire, England, UK	1	6	1	1	1	1	1	3	1	KR025813	Clegg *et al.*, 2016d
EL023 aR	Elk	2013	Washington State, USA	3	6	1	1	1	1	1	3	1	KM586669	Clegg *et al.*, 2015
G2S2R	Sheep	2009	Farm I, Cheshire, England, UK	2	6	1	1	1	1	1	3	1	KP063164	Sullivan *et al.*, 2015d
T200BA1	Dairy	2004	Farm G, Shropshire, England, UK	2	7	1	1	1	4	1	1	1	KR025814	Clegg *et al.*, 2016d
EL022R	Elk	2013	Washington State, USA	3	7	1	1	1	4	1	1	1	KM586668	Clegg *et al.*, 2015
DD3F (1)	Dairy	2009	Farm J, Merseyside, England, UK	3	7	1	1	1	4	1	1	1	KR025815	Clegg *et al.*, 2016d
2c	Beef	2012	Farm K, Gloucestershire, England, UK	2	7	1	1	1	4	1	1	1	KP859546	Clegg *et al.*, 2016d
2D	Beef	2012	Farm K, Gloucestershire, England, UK	1	7	1	1	1	4	1	1	1	KP859544	Clegg *et al.*, 2016d
T296	Dairy	2004	Farm L, Cheshire, England, UK	1	8	1	1	1	1	1	1	3	KR025816	Clegg *et al.*, 2016d
T380	Dairy	2004	Farm J, Merseyside, England, UK	1	8	1	1	1	1	1	1	3	KR025817	Clegg *et al.*, 2016d

T3551	Dairy	2004	Farm J, Merseyside, England, UK	1	8	1	1	1	1	1	1	3	KR025818	Clegg *et al.*, 2016d
T3202F	Dairy	2004	Farm J, Merseyside, England, UK	1	8	1	1	1	1	1	1	3	KR025819	Clegg *et al.*, 2016d
3E	Beef	2012	Farm K, Gloucestershire, England, UK	1	9	1	1	1	4	1	3	1	KP859545	Clegg *et al.*, 2016d
G1OV11	Sheep	2009	Farm H, Gloucestershire, England, UK	1	9	1	1	1	4	1	3	1	KP063154	Sullivan *et al.*, 2015d
EL024 R	Elk	2013	Washington State, USA	3	10	1	1	1	4	1	3	3	KM586673	Clegg *et al.*, 2015
T. vincentii OMZ 838[§]	Human	1998	China	4	11	3	3	4	5	4	4	4	CP009227	Chan *et al.*, 2014

[§]Denotes treponeme isolates for which the putative Omp gene sequence was obtained from a complete genome sequence available from the NCBI nucleotide database.

Table C.2. Details of the T. phagedenis phylogroup isolates. *Treponeme isolate designations are provided alongside details of the host from which they were originally isolated, the year of isolation, their farm and geographic provenance, their allele designation for a putative Omp gene (as determined during this study; Chapter 5.3.4), ‡their ST and allele designation for each of the 7 genes (groEL, recA, glpK, adk, gdh, pyrG and rplB) previously assessed by MLST (Clegg et al., 2016d), their 16S rRNA gene GenBank accession number and associated references.*

Isolate name	Host	Year	Farm and geographic provenance	Omp allele	MLST ST‡	MLST allele‡							*16S rRNA* gene GenBank Accession Number	Reference
						groEL	*recA*	*glpK*	*adk*	*gdh*	*pyrG*	*rplB*		
T320A	Dairy	2004	Farm J, Merseyside, England, UK	1	1	1	1	1	1	1	1	1	EF061261	Evans *et al.*, 2008
G2F3	Sheep	2013	Farm B, Conwy, Wales, UK	1	1	1	1	1	1	1	1	1	KP063156	Sullivan *et al.*, 2015d
EL022 F	Elk	2013	Washington State, USA	2	1	1	1	1	1	1	1	1	KM586667	Clegg *et al.*, 2015
EL023 F	Elk	2013	Washington State, USA	1	2	1	9	1	1	1	1	1	KM586670	Clegg *et al.*, 2015
G187	Dairy	2004	Farm M, Gloucestershire, England, UK	1	2	1	9	1	1	1	1	1	EF061266	Evans *et al.*, 2008
G23F1	Sheep	2013	Farm N, Anglesey, Wales, UK	1	2	1	9	1	1	1	1	1	KP063178	Sullivan *et al.*, 2015d
1498 MED AG	Dairy	1994	Farm D, California, USA	1	2	1	9	1	1	1	1	1	KR025851	Walker *et al.*, 1995
T122A	Dairy	2005	Farm L, Cheshire, England, UK	1	2	1	9	1	1	1	1	1	FJ204238	Evans *et al.*, 2009a
C2R (1)	Sheep	2009	Farm I, Cheshire, England, UK	1	3	3	9	1	1	4	1	1	KR025821	Clegg *et al.*, 2016d

C2F	Sheep	2009	Farm I, Cheshire, England, UK	1	3	3	9	1	1	4	1	1	KR025822	Clegg *et al.*, 2016d
10C	Beef	2012	Farm K, Gloucestershire, England, UK	1	3	3	9	1	1	4	1	1	KP859543	Clegg *et al.*, 2016d
C2RA	Dairy	2009	Farm L, Cheshire, England, UK	1	3	3	9	1	1	4	1	1	KR025820	Clegg *et al.*, 2016d
T167LAB2	Dairy	2003	Farm L, Cheshire, England, UK	1	3	3	9	1	1	4	1	1	EF061253	Evans *et al.*, 2008
T100A	Dairy	2005	Farm L, Cheshire, England, UK	1	3	3	9	1	1	4	1	1	FJ204239	Evans *et al.*, 2009a
T323C F1	Dairy	2004	Farm A, Merseyside, England, UK	1	4	3	9	1	1	5	1	1	EF061263	Evans *et al.*, 2008
T2723	Dairy	2004	Farm A, Merseyside, England, UK	1	4	3	9	1	1	5	1	1	FJ204237	Evans *et al.*, 2009a
T2721A	Dairy	2004	Farm A, Merseyside, England, UK	1	5	3	9	1	1	5	1	2	EF061260	Evans *et al.*, 2008
DD3F (2)	Dairy	2009	Farm J, Merseyside, England, UK	1	6	1	9	1	2	4	1	1	KR025823	Clegg *et al.*, 2016d
T. phagedenis Reiter[§]	Human	1926	Germany	2	7	3	8	4	3	4	3	1	KR025824	Wallace *et al.*, 1967
G169A	Dairy	2004	Farm M, Gloucestershire, England, UK	1	8	3	9	1	1	2	1	1	EF061265	Evans *et al.*, 2008
ST27 (2)	Sheep	2013	Farm B, Conwy, Wales, UK	1	9	3	9	1	1	1	1	1	KR025825	Clegg *et al.*, 2016d
G26F1	Sheep	2013	Farm O, Denbighshire, Wales, UK	1	9	3	9	1	1	1	1	1	KP063180	Sullivan *et al.*, 2015d

DD4F	Dairy	2009	Farm J, Merseyside, England, UK	1	9	3	9	1	1	1	1	1	KR025826	Clegg *et al.*, 2016d
S4R	Sheep	2009	Farm I, Cheshire, England, UK	1	9	3	9	1	1	1	1	1	KR025827	Clegg *et al.*, 2016d
T136	Dairy	2004	Farm G, Shropshire, England, UK	1	10	3	9	1	2	3	1	1	EF061255	Evans *et al.*, 2008
T119A	Dairy	2004	Farm G, Shropshire, England, UK	1	10	3	9	1	2	3	1	1	EF061256	Evans *et al.*, 2008
T354B	Dairy	2004	Farm L, Cheshire, England, UK	1	10	3	9	1	2	3	1	1	EF061259	Evans *et al.*, 2008
T35	Dairy	2004	Farm J, Merseyside, England, UK	1	10	3	9	1	2	3	1	1	-	Clegg *et al.*, 2016d
SL4	Sheep	2013	Farm N, Anglesey, Wales, UK	1	11	3	2	1	1	4	1	1	KR025828	Clegg *et al.*, 2016d
G2S4F	Sheep	2009	Farm I, Cheshire, England, UK	1	11	3	2	1	1	4	1	1	KP063166	Sullivan *et al.*, 2015d
SL2	Sheep	2013	Farm N, Anglesey, Wales, UK	1	12	1	2	1	1	4	1	1	KR025829	Clegg *et al.*, 2016d
G2SL1	Sheep	2013	Farm N, Anglesey, Wales, UK	1	12	1	2	1	1	4	1	1	KP063167	Sullivan *et al.*, 2015d
G10JD	Goat	2013	Farm F, Lancashire, England, UK	1	13	1	1	1	1	4	1	1	KJ206532	Sullivan *et al.*, 2015a
T645C3	Dairy	2004	Farm A, Merseyside, England, UK	1	14	3	1	1	1	5	1	1	FJ204236	Evans *et al.*, 2009a
6LD	Beef	2013	Farm P, Anglesey, Wales, UK	1	15	3	1	1	1	4	1	1	KP859539	Clegg *et al.*, 2016d
2LC	Beef	2013	Farm P, Anglesey, Wales, UK	1	15	3	1	1	1	4	1	1	KP859540	Clegg *et al.*, 2016d

G2S1F	Sheep	2009	Farm Q, Cheshire, England, UK	1	16	2	1	1	1	4	1	1	KP063163	Sullivan *et al.*, 2015d
S2321	Sheep	2009	Farm Q, Cheshire, England, UK	1	16	2	1	1	1	4	1	1	KR025830	Clegg *et al.*, 2016d
S5R	Sheep	2009	Farm Q, Cheshire, England, UK	1	16	2	1	1	1	4	1	1	KR025831	Clegg *et al.*, 2016d
G2S3R1	Sheep	2009	Farm Q, Cheshire, England, UK	1	16	2	1	1	1	4	1	1	KP063165	Sullivan *et al.*, 2015d
S32R	Sheep	2009	Farm I, Cheshire, England, UK	1	16	2	1	1	1	4	1	1	KR025832	Clegg *et al.*, 2016d
S3R	Sheep	2009	Farm I, Cheshire, England, UK	1	16	2	1	1	1	4	1	1	KR025833	Clegg *et al.*, 2016d
11A	Beef	2012	Farm K, Gloucestershire, England, UK	1	17	3	9	1	1	2	1	1	KP859541	Clegg *et al.*, 2016d
1A	Beef	2012	Farm K, Gloucestershire, England, UK	1	17	3	9	1	1	2	1	1	KP750188	Clegg *et al.*, 2016d
T296A	Dairy	2004	Farm L, Cheshire, England, UK	1	17	3	9	1	1	2	1	1	EF061258	Evans *et al.*, 2008
T257	Dairy	2004	Farm L, Cheshire, England, UK	1	17	3	9	1	1	2	1	1	EF061257	Evans *et al.*, 2008
T380 A2F45	Dairy	2004	Farm A, Merseyside, England, UK	1	17	3	9	1	1	2	1	1	EF061262	Evans *et al.*, 2008
T. phagedenis ATCC Kazan 8	Human	1984	Russia	2	18	3	6	4	3	2	3	1	KR025835	Smibert, 1984

T. phagedenis CIP	Human	1962	France	2	19	3	5	3	3	2	2	1	KR025834	Evans *et al.*, 2008
P	Dairy	2000	Farm A, Cheshire, England, UK	1	20	3	9	1	2	2	1	1	KR025836	Clegg *et al.*, 2016d
K	Dairy	2000	Farm A, Cheshire, England, UK	1	20	3	9	1	2	2	1	1	KR025837	Clegg *et al.*, 2016d
DD2R	Dairy	2009	Farm J, Merseyside, England, UK	1	21	3	9	1	1	1	1	1	KR025838	Clegg *et al.*, 2016d
DD2F	Dairy	2009	Farm J, Merseyside, England, UK	1	22	1	9	1	2	1	1	1	KR025839	Clegg *et al.*, 2016d
EL022a F	Elk	2013	Washington State, USA	1	23	1	7	1	1	1	1	1	KM586666	Clegg *et al.*, 2015
W35	Dairy	2004	Farm L, Cheshire, England, UK	1	24	1	9	1	1	1	1	2	EF061264	Evans *et al.*, 2008
DD1R	Dairy	2009	Farm J, Merseyside, England, UK	1	25	1	9	2	1	1	1	1	KR025840	Clegg *et al.*, 2016
DD5F	Dairy	2009	Farm J, Merseyside, England, UK	1	25	1	9	2	1	1	1	1	KR025841	Clegg *et al.*, 2016d
T200	Dairy	2004	Farm G, Shropshire, England, UK	1	26	3	4	1	1	1	1	1	FJ204240	Evans *et al.*, 2009a
T52	Dairy	2004	Farm G, Shropshire, England, UK	1	27	3	1	1	1	1	1	1	EF061254	Evans *et al.*, 2009a
3F2	Sheep	2014	Farm N, Anglesey, Wales, UK	1	27	3	1	1	1	1	1	1	KR025842	Clegg *et al.*, 2016d
T116B	Dairy	2005	Farm A, Merseyside, England, UK	1	28	1	3	1	1	1	1	1	FJ204237	Evans *et al.*, 2009a
G2SL5	Sheep	2013	Farm N, Anglesey, Wales, UK	1	29	1	2	1	1	1	1	1	KP063168	Sullivan *et al.*, 2015d

ST25	Sheep	2013	Farm B, Conwy, Wales, UK	1	30	1	2	1	1	2	1	1	KR025843	Clegg *et al.*, 2016d
ST26	Sheep	2013	Farm B, Conwy, Wales, UK	1	31	1	2	1	1	2	1	1	KR025844	Clegg *et al.*, 2016d
G2ST24	Sheep	2013	Farm B, Conwy, Wales, UK	1	31	1	2	1	1	2	1	1	KP063169	Sullivan *et al.*, 2015d
DD1F	Dairy	2009	Farm J, Merseyside, England, UK	1	32	1	9	2	1	2	1	1	KR025845	Clegg *et al.*, 2016d
T. phagedenis 4A[§]	Dairy	unknown	Iowa, USA	1	33	3	9	1	1	4	1	3	AQCF00000000	Wilson-Welder *et al.*, 2013
T. phagedenis F0421[§]	Human	unknown	USA	2	34	3	7	5	3	4	3	1	NZ_AEFH00000000	Wilson-Welder *et al.*, 2013
T. phagedenis V1[§]	Dairy	unknown	Sweden	1	35	1	9	1	1	2	1	1	CDNC01000001-CDNC01000051	Mushtaq *et al.*, 2015

[§]Denotes treponeme isolates for which the putative Omp gene sequence was obtained from a complete genome sequence available from the NCBI nucleotide database.

Table C.3. Details of the T. pedis isolates. *Treponeme isolate designations are provided alongside details of the host from which they were originally isolated, the year of isolation, their farm and geographic provenance, their allele designation for a putative Omp gene (as determined during this study; Chapter 5.3.4), ‡their ST and allele designation for each of the 7 genes (groEL, recA, glpK, adk, gdh, pyrG and rplB) previously assessed by MLST (Clegg et al., 2016d), their 16S rRNA gene GenBank accession number and associated references.*

Isolate name	Host	Year	Farm and geographic provenance	Omp allele	MLST ST‡	MLST allele‡							*16S rRNA* gene GenBank Accession Number	Reference
						groEL	*recA*	*glpK*	*adk*	*gdh*	*pyrG*	*rplB*		
T3552B^T	Dairy	2004	Merseyside, England, UK	1	1	1	1	1	1	1	1	1	EF061268	Evans *et al.*, 2008
T136P2	Dairy	2004	Farm E, Shropshire, England, UK	1	1	1	1	1	1	1	1	1	FJ204243	Evans *et al.*, 2009b
G3ST1	Sheep	2014	Farm R, Shropshire, England, UK	2	2	4	5	4	5	5	5	4	KP063171	Sullivan *et al.*, 2015d
G3T1	Sheep	2014	Farm R, Shropshire, England, UK	1	2	4	5	4	5	5	5	4	KR025846	Clegg *et al.*, 2016d
G9JD	Goat	2013	Farm F, Lancashire, England, UK	2	2	4	5	4	5	5	5	4	KJ206531	Sullivan *et al.*, 2015a
9185 Med Ag 2	Dairy	1994	Farm D, California, USA	3	4	2	2	2	2	2	2	3	KR025852	Walker *et al.*, 1995
T184F2	Dairy	2003	Farm A, Merseyside, England, UK	4	5	3	6	3	4	4	4	3	KR025848	Clegg *et al.*, 2016d
T18D2 (T18B)	Dairy	2003	Farm A, Merseyside, England, UK	4	5	3	6	3	4	4	4	3	EF061270	Evans *et al.*, 2008
T354A	Dairy	2004	Farm L, Cheshire, England, UK	4	5	3	6	3	4	4	4	3	EF061267	Evans *et al.*, 2008

G819CB	Dairy	2004	Farm M, Gloucestershire, England, UK	4	5	3	6	3	4	4	4	3	EF061269	Evans *et al.,* 2008
Ovine (G179)	Sheep	2006	Farm S, Northern Ireland, UK	4	5	3	6	3	4	4	4	3	AF363634	Demirkan *et al.,* 2006
T3551C	Dairy	2004	Farm A, Merseyside, England, UK	1	6	1	1	1	5	1	1	1	KR025850	Clegg *et al.,* 2016d
T. pedis T A4[§]	Pig	2013	Sweden	5	7	1	3	2	3	3	3	2	CP004120	Svartström *et al.,* 2013

[§]Denotes treponeme isolates for which the putative Omp gene sequence was obtained from a complete genome sequence available from the NCBI nucleotide database.

A

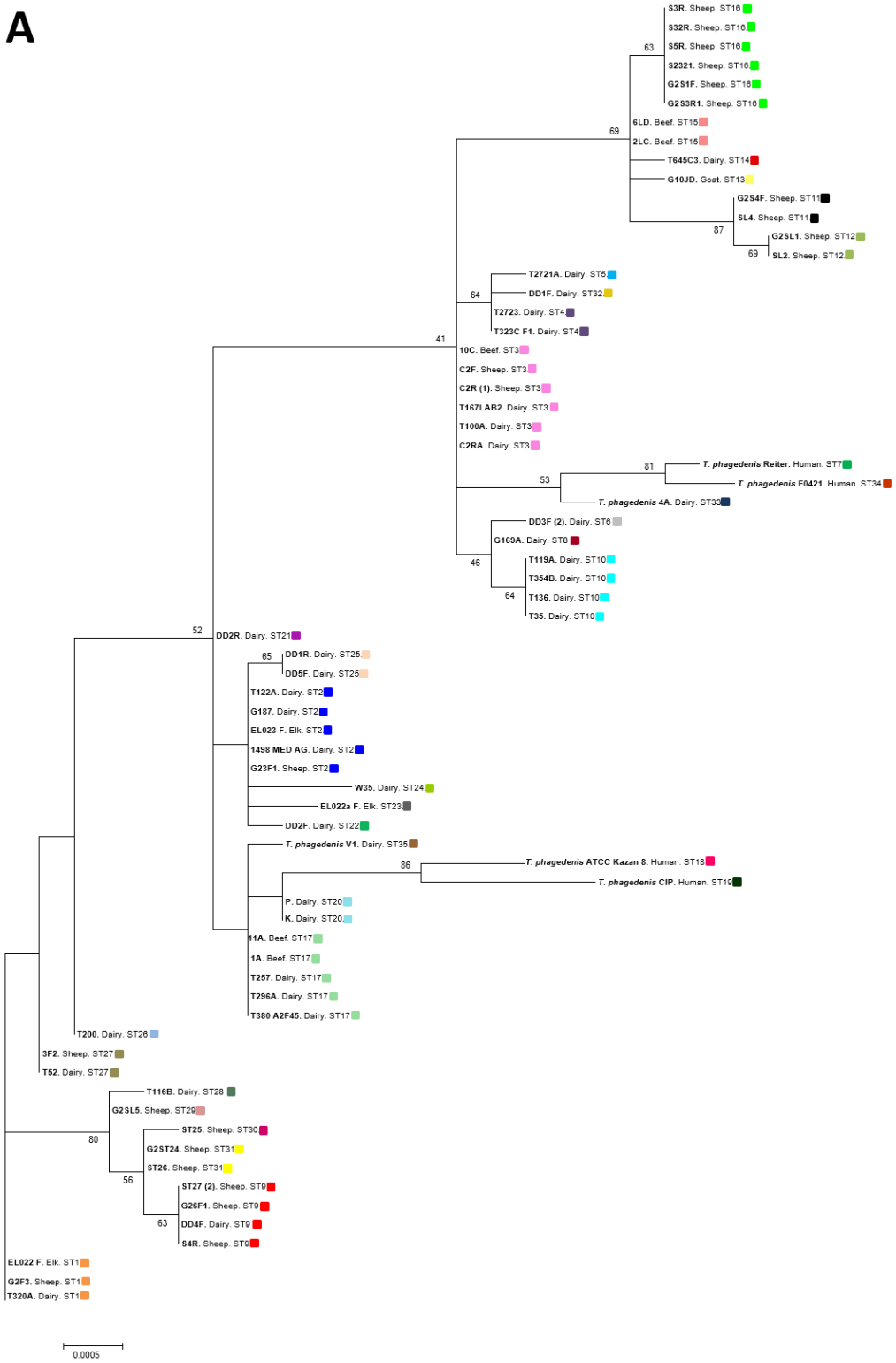
S3R. Sheep. ST16
S32R. Sheep. ST16
S5R. Sheep. ST16
S2321. Sheep. ST16
G2S1F. Sheep. ST16
G2S3R1. Sheep. ST16
6LD. Beef. ST15
2LC. Beef. ST15
T645C3. Dairy. ST14
G10JD. Goat. ST13
G2S4F. Sheep. ST11
SL4. Sheep. ST11
G2SL1. Sheep. ST12
SL2. Sheep. ST12
T2721A. Dairy. ST5
DD1F. Dairy. ST32
T2723. Dairy. ST4
T323C F1. Dairy. ST4
10C. Beef. ST3
C2F. Sheep. ST3
C2R (1). Sheep. ST3
T167LAB2. Dairy. ST3
T100A. Dairy. ST3
C2RA. Dairy. ST3
T. phagedenis Reiter. Human. ST7
T. phagedenis F0421. Human. ST34
T. phagedenis 4A. Dairy. ST33
DD3F (2). Dairy. ST6
G169A. Dairy. ST8
T119A. Dairy. ST10
T354B. Dairy. ST10
T136. Dairy. ST10
T35. Dairy. ST10
DD2R. Dairy. ST21
DD1R. Dairy. ST25
DD5F. Dairy. ST25
T122A. Dairy. ST2
G187. Dairy. ST2
EL023 F. Elk. ST2
1498 MED AG. Dairy. ST2
G23F1. Sheep. ST2
W35. Dairy. ST24
EL022a F. Elk. ST23
DD2F. Dairy. ST22
T. phagedenis V1. Dairy. ST35
T. phagedenis ATCC Kazan 8. Human. ST18
T. phagedenis CIP. Human. ST19
P. Dairy. ST20
K. Dairy. ST20
11A. Beef. ST17
1A. Beef. ST17
T257. Dairy. ST17
T296A. Dairy. ST17
T380 A2F45. Dairy. ST17
T200. Dairy. ST26
3F2. Sheep. ST27
T52. Dairy. ST27
T116B. Dairy. ST28
G2SL5. Sheep. ST29
ST25. Sheep. ST30
G2ST24. Sheep. ST31
ST26. Sheep. ST31
ST27 (2). Sheep. ST9
G26F1. Sheep. ST9
DD4F. Dairy. ST9
S4R. Sheep. ST9
EL022 F. Elk. ST1
G2F3. Sheep. ST1
T320A. Dairy. ST1
0.0005

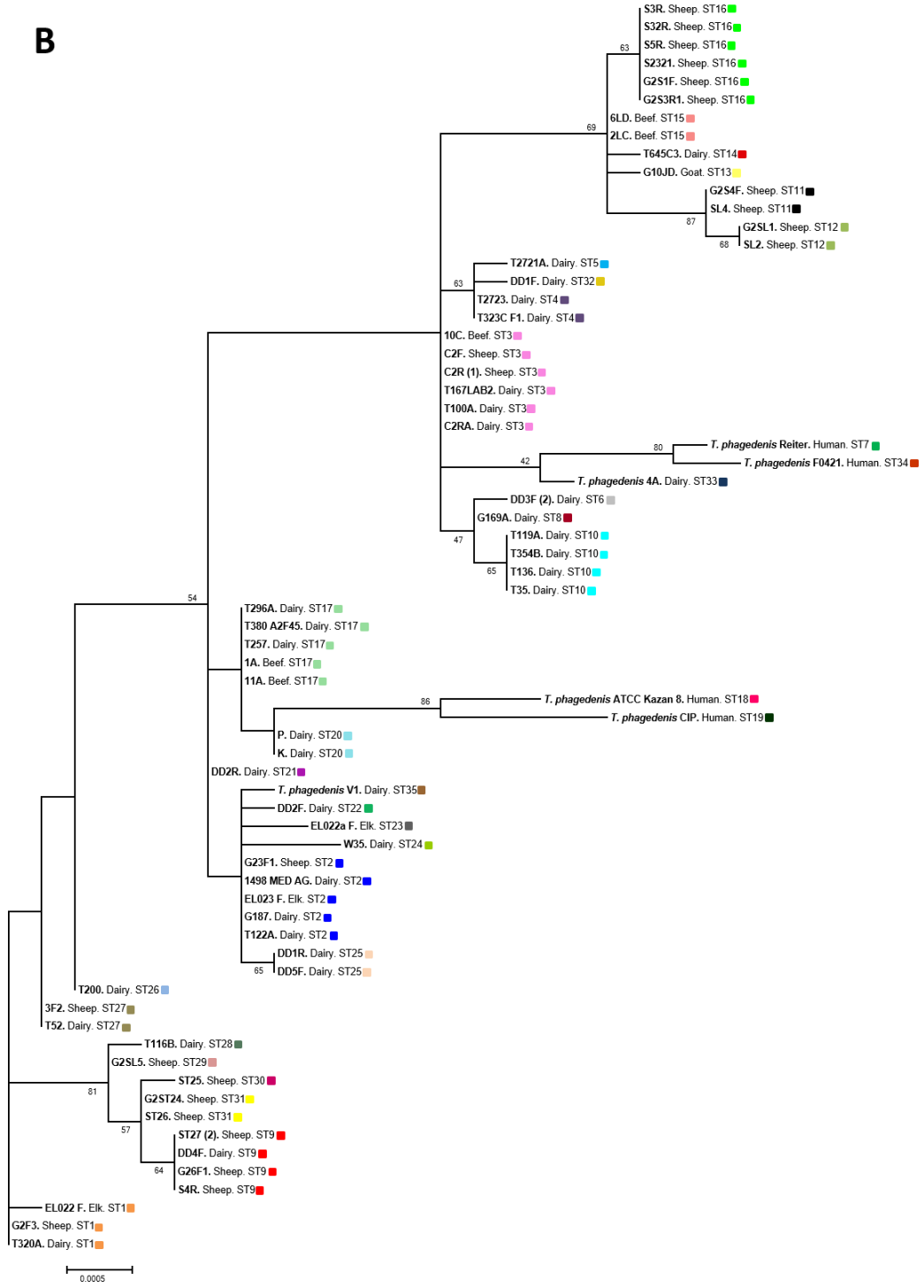

Figure C.1 Phylogenetic tree of maximum-likelihood comparing concatenated gene sequences of (A) seven housekeeping genes alone with (B) the further addition of putative Omp gene across 3402 and 3949 aligned bases respectively for 69 T. phagedenis phylogroup isolates. *Treponeme isolate names are given in bold type, alongside the host from which they were isolated (dairy cow, beef cow, sheep, goat, elk or human) and their respective ST (with colour-coded blocks). Isolates with an altered relationship based upon the addition of putative Omp_694 are highlighted in blue. Bootstrap confidence intervals, based on 10,000 reiterations, are shown as percentages at the nodes. Bar, 0.0005 nucleotide substitutions per site*

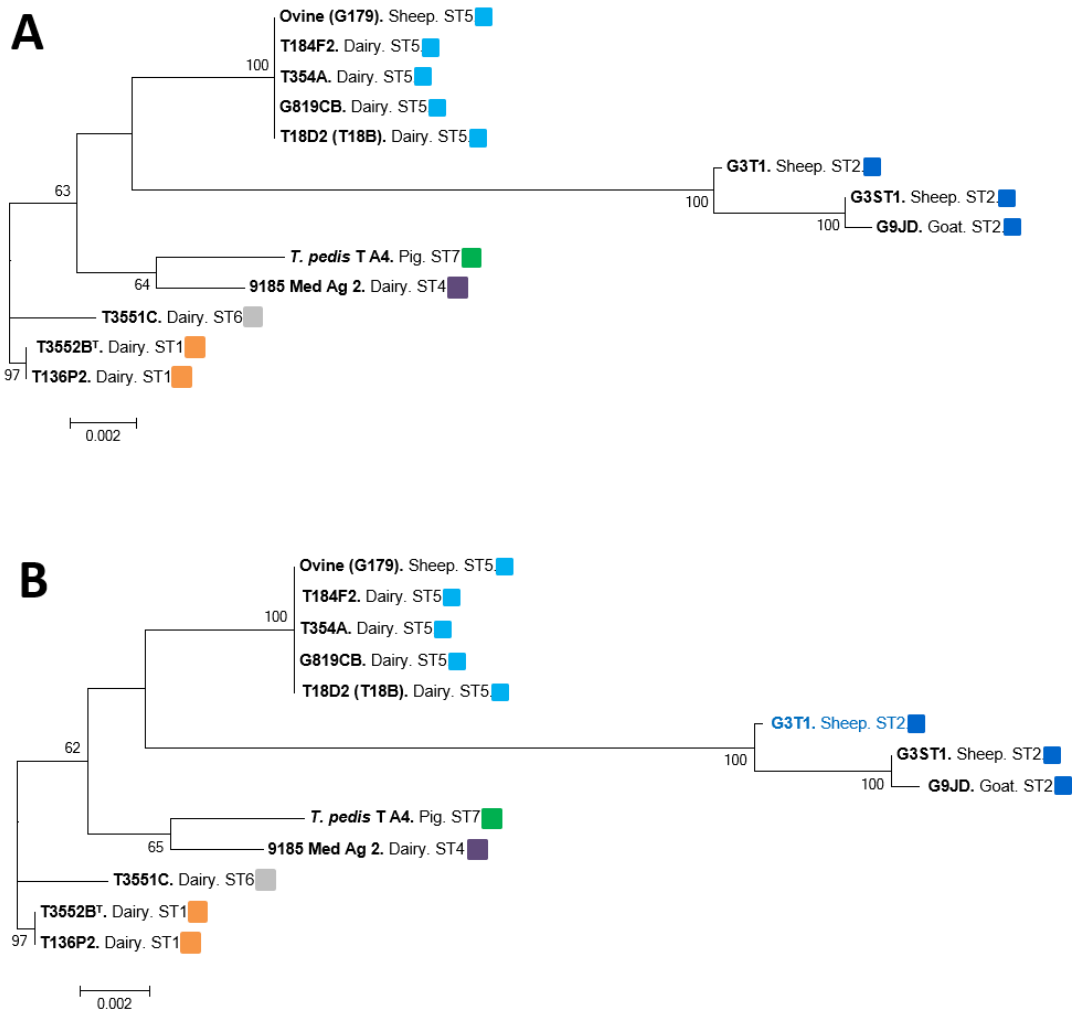

Figure C.2 Phylogenetic tree of maximum-likelihood comparing concatenated gene sequences of (A) seven housekeeping genes alone with (B) the further addition of putative Omp gene across 3366 and 3846 aligned bases respectively for 13 T. pedis isolates. *Treponeme isolate names are given in bold type, alongside the host from which they were isolated (dairy cow, sheep, goat, or pig) and their respective ST (with colour-coded blocks). Isolates with an altered ST based upon the addition of putative Omp_2390 are highlighted in blue. Bootstrap confidence intervals, based on 10,000 reiterations, are shown as percentages at the nodes. Bar, 0.002 nucleotide substitutions per site.*

Table C.4 Amino acid sequence identities between the putative Omps of T. medium phylogroup strain T19 (Omp_34), T. phagedenis phylogroup (Omp_694) strain T320A and T. pedis strain T3552B^T (Omp_2390) and homologous proteins of other recognised Treponema isolates.

***Treponema* species**	**Predicted protein**	**Accession number**	**Amino acid sequence identity (%) to putative Omp**		
			Omp_34	**Omp_694**	**Omp_2390**
***T. medium* phylogroup strain T19**	**Putative Omp (Omp_34)**	-	-	**59.3**	**54.8**
T. vincentii	Hypothetical protein	WP_016519005.1	96.2	60.9	54.0
T. vincentii	Hypothetical protein	WP_006188345.1	96.2	60.9	54.0
Treponema sp. OMZ 838	Hypothetical protein	WP_044014042.1	96.2	59.3	53.3
T. medium	Hypothetical protein	WP_016522898.1	96.2	57.8	54.0
***T. phagedenis* phylogroup strain T320A**	**Putative Omp (Omp_694)**	-	**59.3**	-	**60.0**
T. phagedenis	Hypothetical protein	WP_024752876.1	59.3	100.0	60.0
T. phagedenis	Hypothetical protein	WP_002700634.1	59.3	99.2	60.0
T. phagedenis	Hypothetical protein	WP_044634708.1	59.3	100.0	60.0
***T. pedis* strain T3552B^T**	**Putative Omp (Omp_2390)**	-	**54.8**	**60.0**	-
T. pedis strain T A4	Hypothetical protein TPE_1550	AGT44045.1	54.8	60.0	100.0
T. pedis	Hypothetical protein	WP_024465290.1	54.8	60.0	100.0
T. putidum	Hypothetical protein	WP_044978399.1	56.2	57.0	74.0
T. denticola	Hypothetical protein	WP_002666925.1	58.5	58.5	74.0
T. denticola	Hypothetical protein	WP_002673392.1	57.7	57.7	73.3
T. denticola	Hypothetical protein	WP_002680870.1	57.7	57.7	72.5
T. denticola	Hypothetical protein	WP_010689345.1	57.7	57.7	73.3

T. denticola	Hypothetical protein	WP_010698236.1	57.7	57.7	74.0
T. denticola	Hypothetical protein	WP_010694487.1	55.5	57.7	72.5
T. pallidum	Hypothetical protein	WP_095214048.1	39.5	47.0	41.4
T. pallidum	Hypothetical protein	WP_014342554.1	39.5	47.0	41.4
T. pallidum	Hypothetical protein	WP_015613235.1	39.5	47.0	41.4
T. pallidum	Hypothetical protein	WP_010882178.1	38.8	46.2	42.2
T. pallidum	Hypothetical protein	WP_069029652.1	38.8	46.2	42.2
T. pallidum	Hypothetical protein	WP_039487322.1	39.5	47.0	41.4
T. pallidum	Hypothetical protein	WP_014342713.1	30.8	26.1	26.6
T. pallidum	Hypothetical protein	WP_014342777.1	28.3	28.3	27.5
T. pallidum	Hypothetical protein	WP_014342291.1	28.3	28.3	27.5
T. pallidum	Uncharacterised protein TP_0126	O83163.1	30.8	26.1	26.6
T. pallidum subsp. *pallidum*	Hypothetical protein TPSea814_000134a	AHN66838.1	28.3	28.3	27.5
T. pallidum subsp. *pallidum*	Hypothetical protein A4W95_00019	ANA41867.1	28.3	28.3	27.5
T. pallidum subsp. *pertenue*	Conserved hypothetical protein	ADR64330.1	30.8	26.1	26.6
T. pallidum subsp. *pertenue* strain SamoaD	Putative membrane protein	AEZ57246.1	30.8	26.1	26.6
T. pallidum subsp. *endemicum*	Hypothetical protein TEND11qi_0733	AQX44394.1	39.5	47.0	41.4
T. pallidum subsp. *endemicum*	Hypothetical protein TEND11qj_0134b	AQX44371.1	28.3	28.3	27.5
T. paraluiscuniculi	Hypothetical protein	WP_013945334.1	38.8	46.2	41.4
T. paraluiscuniculi	Hypothetical protein	WP_013944828.1	30.8	26.1	26.6
T. paraluiscuniculi	Hypothetical protein	ABO37094.1	27.7	30.4	28.1
T. paraluiscuniculi	Truncated hypothetical protein	ABO37086.1	30.8	26.1	26.6

T. paraluiscuniculi Cuniculi A	Hypothetical protein TPCCA_0133b	AEH40091.1	27.7	30.4	28.1
T. maltophilum	Hypothetical protein	WP_016526235.1	39.5	38.8	37.0
T. lecithinolyticum	Hypothetical protein	WP_084604402.1	36.5	34.3	34.8
T. lecithinolyticum ATCC 700332	Hypothetical protein HMPREF9193_01878	ERJ91871.1	36.5	34.3	34.8
T. socranskii	Hypothetical protein	WP_016520556.1	33.3	33.3	30.1
T. socranskii	Hypothetical protein	WP_021495717.1	35.5	35.5	30.8
T. socranskii subsp. *socranskii* ATCC 35536	Hypothetical protein	ERF60913.1	35.5	35.5	30.8
T. brennaborense	Hypothetical protein	WP_013757786.1	39.5	35.0	34.0
T. rectale strain CHPA^{T}	Hypothetical protein	-	32.3	34.5	32.1
T. ruminis strain Ru1^{T}	Hypothetical protein	-	35.8	31.3	31.8
T. saccharophilum	Hypothetical protein	WP_002702954.1	32.8	33.5	35.5
T. bryantii	Hypothetical protein	WP_074931452.1	28.2	28.9	25.8
T. bryantii	Hypothetical protein	WP_022931999.1	28.3	33.5	27.4
T. bryantii	Hypothetical protein	WP_074642314.1	26.2	26.8	23.9
Treponema sp. JC4	Hypothetical protein	WP_009103113.1	24.6	29.1	25.9
T. berlinense	Hypothetical protein	WP_078931408.1	38.8	35.8	36.2
T. porcinum	Hypothetical protein	WP_078933417.1	31.6	33.0	35.0
T. succinifaciens	Hypothetical protein	WP_013701705.1	32.1	29.9	25.3
T. azonutricium	Hypothetical protein	WP_015711592.1	34.0	37.0	34.5
T. primitia	Hypothetical protein	WP_015707785.1	33.5	33.5	28.8
T. primitia	Hypothetical protein	WP_010255538.1	31.3	30.5	27.4
Treponema sp. CETP13	Hypothetical protein BKP49_03910	OJF77012.1	42.5	38.0	35.5

Treponema caldarium	Hypothetical protein	WP_013968589.1	38.5	39.2	33.8
Treponema sp. endosymbiont	Hypothetical protein	WP_062377456.1	35.8	33.5	32.5
Treponema sp. GWC1_61_84	Hypothetical protein A2001_07840	OHE67046.1	34.0	35.5	31.6
Treponema sp. C6A8	Hypothetical protein	WP_027728611.1	26.1	31.3	25.1